Imaging Acute Abdomen in Children

Fred E. Avni · Philippe Petit
Editors

Springer

Imaging Acute Abdomen in Children

Fred E. Avni • Philippe Petit
Editors

Imaging Acute Abdomen in Children

Springer

Editors
Fred E. Avni
Department of Pediatric Imaging
Jeanne de Flandre Hospital
Lille Cedex, France

Philippe Petit
Department of Prenatal and
Pediatric Imaging
Hospital Timone-Enfants
Marseille Cedex 05, France

ISBN 978-3-319-63699-3 ISBN 978-3-319-63700-6 (eBook)
https://doi.org/10.1007/978-3-319-63700-6

Library of Congress Control Number: 2017957596

Printed on acid-free paper

This Springer imprint is published by Springer Nature
The registered company is Springer International Publishing AG
The registered company address is: Gewerbestrasse 11, 6330 Cham, Switzerland

Contents

Part IV Any Age: Digestive Tract

Part V Any Age: The Uro-Genital Tract

Part VI Any Age: General Overviews

Part I

Introduction

Paediatric Emergencies: What Is It about? What Approach?

1

François Dubos

Contents

1.1 Introduction

Abdominal pain or symptoms related to the gastrointestinal, urinary or genital tract are common complaints and frequent reason for admission of children in the emergency department (ED) [1]. Despite the relatively benign nature of the most common diseases treated in the paediatric ED, there are some clinical entities that can have adverse outcomes.

How high is the index of suspicion among clinicians for such serious pathologies and how well aware are they of recent advances in their diagnosis and treatment? What are the clinical pitfalls to be avoided? One issue is to detect the child with a rare and potentially severe condition among all children with more common diagnoses in the ED. A second issue is the management of abdominal diseases in very young children, who often present with less specific signs. A third issue is more and more often the admission of children soon after the onset of the first symptoms. In this situation, the repetition of initially normal examinations could be necessary.

The mechanisms of intra-abdominal diseases can be of vascular, obstructive or infectious origin. The causes vary with the age of the child, although almost all causes can be seen at any age. For example, intussusception usually occurs in children 2 months to 2 years of age. When it is described (rarely) in older children, an underlying disease has to be searched [2].

F. Dubos
Paediatric Emergency Unit and Infectious Diseases, Lille University and Lille University Hospitals, 59037 CHRU Lille, France
e-mail: francois.dubos@chru-lille.fr

F.E. Avni, P. Petit (eds.), *Imaging Acute Abdomen in Children*,
https://doi.org/10.1007/978-3-319-63700-6_1

The causes also vary according to the duration of the symptoms and the associated signs. Recurrent abdominal pain (>3 episodes of pain over a period of at least 3 months) suggests a functional cause (in 80% of cases). On the other hand, a surgical cause must be suggested first in case of acute pain. The radiologist must therefore be vigilant in seeking first the urgent causes, usually surgical. He/She must also be able to search for rare or unusual causes when the clinical presentation is atypical.

1.2 Team Approach

In this situation of abdominal emergency with uncertainty on the definitive diagnosis, the importance of a team approach is crucial: nurses, emergency clinicians, radiologists, anaesthesiologists, surgeons, etc. The role of the radiologists within the team, particularly for acutely ill appearing children, is a key factor for the success of a good management. Several generic skills are expected of all health professionals involved with the care of sick children [3, 4]. These are:

1. To recognise the critically sick or injured child;
2. To initiate appropriate initial treatment;
3. To work as part of a team for a rapid and appropriate management;
4. To know how to challenge oneself and maintain/enhance skills;
5. To be aware of issues/pitfalls around some uncommon presentations;
6. To verify and continuously ensure children safety;
7. To communicate effectively with children and parents/carers.

When the physician asks for the realisation of abdominal imaging in the ED, the non-urgent medical causes have usually been previously eliminated by the history of the disease and by the clinical examination.

The demand is usually motivated by a surgical hypothesis suggested by the clinician, which may require urgent surgery (peritonitis, appendicitis, intestinal obstruction, etc.). It can also be motivated by a medical hypothesis justifying the implementation of an urgent or rapid treatment (foreign body, rheumatoid vasculitis, pancreatitis, abdominal tumour, etc.).

1.3 Clinical Presentation

The causes that can be raised will vary according to the main anamnestic signs reported by the parents or the child. These main symptoms are listed in Table 1.1 with the diseases most frequently related and the causes that should not be missed. Abdominal surgical causes should be sought as first line. Regurgitation with pain is usually of medical benign origin but can be related to surgical causes such as intussusception, volvulus and incarcerated hernia. In case of vomiting, gastrointestinal surgery should be given priority, particularly in case of bilious vomiting in infants, which is an alarming symptom that necessitates exclusion of midgut volvulus. In case of abdominal mass, think of acute urinary retention, abdominal tumour (nephroblastoma, neuroblastoma, lymphoma, hepatic tumour (hepatoblastoma, cyst, abscess, etc.)), tumour of the female genital tract (cyst/ovarian tumour), splenomegaly (erythroblastopenia, kala azar, etc.). Haematemesis is rarely a sign that justifies emergency imaging. When additional investigation is necessary in this case, it is usually an oesogastroduodenal endoscopy. Children with abdominal trauma are usually well identified. A careful screening of those children is needed to detect trauma of the gut or solid organs. The growing expansion of fast ultrasound at the bedside should be a factor to improve this interaction between physicians.

Table 1.2 provides a classification of the causes responsible for abdominal diseases by age group.

Table 1.1 Main symptoms potentially associated with an abdominal emergency in children

Symptoms	Think/Main causes	Causes not to be missed
Regurgitation with pain	Gastro-oesophageal reflux Oesophagitis Allergy to cow's milk proteins	– Volvulus – Intussusception – Inguinal hernia – Missed diaphragmatic hernia
Vomiting	Acute gastroenteritis Ketosis Food allergy Other infections	– Abdominal surgical causes – Neurosurgical causes – Meningitis – Other medical NS causes: angiocholitis, pancreatitis
Abdominal pain with fever	Acute gastroenteritis Urinary tract infection Hepatitis Other infections	– Abdominal surgical causes: peritonitis, abscess, tumour – Gastrointestinal NS causes: angiocholitis, pancreatitis
Abdominal pain without fever	Infantile colic Ketosis Constipation/Functional pain Food intolerance Acute cystitis Lymphadenitis Henoch–Schönlein purpura	– Intussusception, volvulus, appendicitis, intestinal obstruction – Testicular/ovarian torsion – Intra-abdominal mass – Trauma – Diabetes mellitus
Lumbar pain	Acute pyelonephritis	– Urinary lithiasis – Hydronephrosis – Trauma
Abdominal mass	Think acute urinary retention	– Nephroblastoma, neuroblastoma, lymphoma – Hepatic or peri-hepatic tumour, splenomegaly
Jaundice	Hepatitis	– Angiocholitis
Haematemesis	Mallory–Weiss syndrome Epistaxis	– Gastric or duodenal ulcer – Oesophageal varices
Blood in stool	Anal fissure Invasive gastroenteritis Secondary to medications	– Intussusception – Meckel's diverticulosis – Complicated Henoch–Schönlein purpura – Haemolytic uremic syndrome – IBD
Haematuria	Acute cystitis Renal lithiasis	– Renal lithiasis – Vesical tumor – Renal tumor – Nephrologic diseases

NS non-surgical, *IBD* Inflammatory bowel diseases

Table 1.2 Causes of abdominal symptoms that justify abdominal imaging in emergency in children, by age group

Age	Causes to search[a]	Rare causes to think	Differential diagnoses
Newborns (≤28 days)	– Inguinal hernia – Volvulus[b] – Enterocolitis – Testicular/ovarian torsion	– Testicular/ovarian torsion – Meckel's diverticulitis – Meconium related ileus – Rare congenital malformations – Post-surgical complications	– GER – Oesophagitis – Cow's milk proteins allergy – Constipation[b]
Infants (29 days–2 years)	– Pyloric stenosis – Inguinal hernia – Intussusception – Volvulus[b] – Digestive duplication	– Testicular/ovarian torsion – HUS – Appendicitis – Meckel's diverticulitis – Ovarian tumour – Abdominal tumour – Cystic lymphangioma – Acute urinary retention[b] – Obstructive foreign body – Rare congenital malformations	– GER – Oesophagitis – Cow's milk proteins allergy – AGE – ENT, respiratory or urinary tract infection – Constipation[b] – Ketosis – Periodic fever (FMF) – Pseudo-obstruction intestinal chronic
Children (2–10 years)	– Appendicitis – Intestinal obstruction[b] – Testicular/ovarian torsion – Junction syndrome – Renal lithiasis – Digestive duplication – Henoch–Schönlein purpura/complication? – Pancreatitis[b]	– Abdominal tumour – Meckel's diverticulitis – Secondary intussusception[b] – Acute urinary retention[b] – Medical peritonitis/ nephrotic syndrome – Falciform anaemia with crisis ± complication?[b] – Cystic lymphangioma	– Cystitis/Acute nephritis – Gastritis/Peptic ulcer – Diabetes ketoacidosis – Other metabolic diseases – Pneumonia – Pleural effusion – Constipation[b] – Cranial hypertension – Functional digestive pain – Ketosis – Migraine
Adolescents (>10 years)	– Appendicitis – IBD – Intestinal obstruction[b] – Testicular/ovarian torsion – Renal lithiasis – Abdominal abscess – Pancreatitis[b]	– Abdominal tumour – Ovarian tumour/Cyst – Falciform anaemia with crisis ± complication – Extra-uterine pregnancy – Pregnancy	– Cystitis/PNA – Lymphadenitis – Gastritis/Peptic ulcer – Functional digestive pain – Hepatitis/Angiocholitis[b] – Pneumonia – Pleural effusion[b] – Dysmenorrhea

[a]Emergency that requires a rapid management
[b]Underlying cause to look for
AGE acute gastroenteritis, *FMF* familial Mediterranean fever, *GER* gastro-oesophageal reflux, *HUS* haemolytic uremic syndrome, *IBD* inflammatory bowel diseases

Conclusion

A close collaboration between the clinicians and the radiologists in the ED and a good confidence between each other is a necessary condition to provide the best management of children with abdominal complaints in the emergency department.

References

1. Smith J, Fox SM. Pediatric abdominal pain. An emergency medicine perspective. Emerg Med Clin North Am. 2016;34:341–61.
2. van Heurn LWE, Pakarinen MP, Wester T. Contemporary management of abdominal surgical emergencies in infants and children. Br J Surg. 2014;101:e24–33.
3. Yang W-C, Chen C-Y, Wu H-P. Etiology of non-traumatic acute abdomen in pediatric emergency departments. World J Clin Cases. 2013;1:276–84.
4. McDougall RJ. Paediatric emergencies. Anaesthesia. 2013;68(Suppl 1):61–71.

Surgical Pediatric Imaging: What is It About? What Approach?

2

Rony Sfeir

Content

In the majority of cases, emergency department pediatric surgeons deal with classic and frequent surgical pediatric diseases. Before the development of radiology, throughout time, pain semiology with some specific signs was described like the "Blumberg's sign" in peritonitis [1], "Rovsing's sign" in appendicitis [2], "Murphy's sign" in cholecystitis [3], or other signs or association of signs for intestinal obstruction or lesions with vascular damage. Progressively, imaging techniques first helped the clinicians to understand the clinical symptoms and degrees of severity before becoming for some diseases, the only way to obtain an exact diagnosis. Therefore, today, a good pediatric surgeon in the emergency suite is someone with good experience (in as much as many fields of pediatrics), for sure a physician examining himself his patients before asking for complementary imaging; a physician calling the radiologist himself to discuss the case; choosing together the best exam to perform, being present with the radiologist during complex examinations and finally discussing the optimal treatment with all specialists involved.

In the pediatric population, there is a clear split between two categories defined as before and after acquired language where physical exam is completed by children expressing precisely their pain and their history. Often, pediatric diseases are age-related. Therefore, in order to obtain the correct diagnosis, a strong knowledge

R. Sfeir
Department of Pediatric Surgery, Jeanne de Flandre Hospital, 59037 Lille-Cedex, France
e-mail: rony.sfeir@chru-lille.fr

F.E. Avni, P. Petit (eds.), *Imaging Acute Abdomen in Children*,
https://doi.org/10.1007/978-3-319-63700-6_2

of the potential diseases both by the clinician and by the radiologist is mandatory. This would also optimize the subsequent management and care. Furthermore, in infants particularly, symptoms are delayed or misinterpreted and a wandering diagnosis is frequent. Imaging techniques should be used rapidly but adequately.

In appendicitis, the statement reported in Rowe saying, "The PHYSICAL EXAMINATION is the most important single diagnostic determinant in children with acute abdominal conditions" should be maintained as a primary objective in teaching pediatric surgery [4]. For instance, one important predictor in the clinical diagnosis of acute appendicitis is the classic *migration of pain* described by Murphy in 1905 [5]. According to the medical literature, this specific sign has a diagnostic accuracy of up to 95% [6, 7]. Yet, this sign is not found constantly and depends on age, level of experience of the physician, previous treatments, or medical conditions, the diagnosis may be difficult to ascertain. In daily practice, clinical findings are missed or insufficiently searched by doctors with lack of sufficient experience in about 40% of cases; this could potentially lead to a higher perforation rate due to a delayed diagnosis [8]. Laboratory findings are not discriminatory and the aim of imaging should be to reduce the rate of missed diagnoses. Imaging techniques are also very helpful in infants where appendicitis is frequently seen in a more advanced stage with signs of septic and intestinal obstruction. In these patients, the contribution of physical examination is very limited and many of them have a history of recent antibiotherapy. In these young patients, imaging will frequently find abscesses due to perforation. To be noted, abscesses may also be post-operative findings and imaging is needed to find them and eventually to allow drainage under CT or US guidance. Not to forget, appendicitis in neonates or infants with a long history of constipation or abdominal distention could be a symptom of Hirschsprung disease.

In intussusception, clinical findings are usually typical; still, imaging is the key for the diagnosis. As reported extensively, in children under 3 years, US studies in the setting of acute abdominal pain have a nearly 100% sensitivity for the detection of intussusception and should be performed as soon as possible (at least in stable or stabilized) patients. If the diagnosis is confirmed, it should be followed, in the absence of signs of major sepsis or peritonitis, by therapeutic air contrast enema (or any other suitable radiological technique) as first line treatment; Surgery is indicated in case of failure of the therapeutic enema, or in case of intestinal perforation with general sepsis in an unstable infant.

In *malrotation complications*, Doppler study of the superior mesenteric vascular axis is very helpful to prove vascular torsion with pathognomonic ultrasound signs [9]. Surgery must be urgently performed after a rapid and accurate diagnosis since any delay in detorsion will lead to extensive intestinal vascular damage and final loss of a segment of the intestine. If imaging is not available, urgent surgery must be performed based on the clinical suspicion.

In case of (suspected) *acute intestinal obstruction*, the initial treatment should always include gastric aspiration, hydration, and antibiotherapy. Whenever a vascular damage is suspected, surgery should be immediate in order to prevent intestinal necrosis and loss. The surgeon may be helped by clinical and historical findings but radiological findings are more accurate and contributive in order to discriminate between all potential etiologies. When the patient has a history of previous abdominal surgery, *adhesions* are the presumed diagnosis. Imaging should help identifying the level of the obstruction and studying the vascular supplies to the bowel loops in order to determine the need for rapid surgery. Classically, free intraabdominal fluid is a frequent associated non-specific finding; on the other hand, the demonstration of free intraabdominal air confirms perforation and the need to operate.

In girls, *adnexal masses and their complications* are frequently encountered after or around the beginning of puberty. *Ovarian torsion* can occur with or without tumoral lesions of the

ovary. Ultrasound with color flow Doppler is the first line imaging modality for any suspected adnexal torsion [10]. In case of *neoplastic tumor,* which is less frequent than benign lesions, pelvic US is the main examination; the demonstration of a heterogeneous cyst should lead to perform MR imaging and evaluate tumoral markers [11]. Information from the radiologic evaluation should include description of the tumor and of any extra ovarian extension—not only in the abdomen but also in the lungs.

Imaging should never delay surgery whenever an ovarian torsion is suspected.

In case of an *inguinal hernia*, the clinical findings are sufficient in most cases. Imaging techniques can be useful in hernia recurrence or in obese children.

In *conclusion*, pediatric imaging in an emergency department is crucial for numerous diseases. Experienced pediatric radiologists are needed to provide the optimal care in close collaboration with pediatric surgeons and pediatricians. In front of difficult cases, surgeons need the best imaging techniques and highly precise diagnoses. This cannot be obtained without a continuous and friendly interaction between the different specialists. Specificity of the pediatric population is that their potential diseases are numerous even if they are rare for many among them.

References

1. Blumberg JM. Ein neues diagnostisches Symptom bei Appendicitis. Münch Med Wochenschr. 1907;54:1177–8.
2. Rovsin NT. Indirektes Hervorrufen des typischen Schmerzes an McBurney's Punkt. Ein Beitrag zur diagnostik der Appendicitis und Typhlitis. Zentralbl Chir. 1907;34:1257–9.
3. Murphy JB. Five diagnosis methods of John B. Murphy. Surg Clin J. B. Murphy. 1912;1:459–66.
4. Rowe MI. Essentials in pediatric surgery. Maryland Heights: Mosby; 1995. p. 899.
5. Murphy JB. Appendicitis with original report, histories, and analysis of 141 laparotomies for that disease. JAMA. 1984;22:302–8.
6. Birnbaum BA, Wilson SR. Appendicitis at the millennium. Radiology. 2000;215:337–48.
7. Ferrarese A, Falcone A, Solej M, Bono D, Moretto P, Dervishi N, et al. Surgeon's clinical valuation and accuracy of ultrasound in the diagnosis of acute appendicitis: a comparison with intraoperative evaluation. Five years' experience. Int J Surg. 2016;33(Suppl 1):S45–50.
8. Bickell NA, Aufses AH Jr, Rojas M, et al. How time affects the risk of rupture in appendicitis. J Am Coll Surg. 2006;202:401–6.
9. Gale HI, Gee MS, Westra SJ, Nimkin K. Abdominal ultrasonography of the pediatric gastrointestinal tract. World J Radiol. 2016;8(7):656–67.
10. Kives S, Gascon S, Dubuc É, Van Eyk N. Diagnosis and management of adnexal torsion in children, adolescents, and adults. J Obstet Gynaecol Can. 2017;39(2):82–90.
11. Pienkowski C, Kalfa N. Presumed benign ovarian tumors of childhood and adolescent. J Gynecol Obstet Biol Reprod. 2013;42(8):833–41.

Imaging and Emergency: What Modalities? What Strategies?

3

Philippe Petit and Fred E. Avni

Content

In children, acute abdominal complaints are common presentation in the emergency department. The etiologies, presentations, diagnosis and management vary widely and establishing (rapidly) a precise diagnosis is often challenging. Imaging techniques are increasingly important to sort out between all possible diagnoses in order to differentiate cases necessitating acute management from those where the management can be organized more "quietly". A close collaboration with our paediatric colleagues is mandatory in order to define the panel of differential diagnosis to be considered and the degree of emergency before applying imaging. Familial history, history of the disease, clinical and biological data are all of upmost importance.

The imaging work-up will surely be oriented by this information. Among them one of the most important data is the age of the patient that will help to categorize it. This is the way we have chosen to organize the book.

The armamentarium of imaging techniques is wide. In the setting of emergency suits, US and CT are clearly the imaging techniques mostly performed and highly accurate for the work-up of paediatric abdominal emergencies.

Except for polytrauma where body-CT is the imaging exploration of choice, any work-up of an abdominal "drama" has to start by a highly detailed and complete US examination. US has many advantages: it is highly accurate, harmful, easily and rapidly performed (at bedside if necessary) and is repeatable. Newer equip-

P. Petit (✉)
Department of Pediatric and Prenatal Imaging, Hôpital Timone Enfants, 264 Rue St Pierre, 13385, Marseille Cedex 05, France
e-mail: ppetit@ap-hm.fr

F.E. Avni (✉)
Department of Pediatric Imaging, Jeanne de Flandre—Lille University Hospitals, Lille-Cedex 59037, France
e-mail: Freddy.Avni@chru-lille.fr

F.E. Avni, P. Petit (eds.), *Imaging Acute Abdomen in Children*,
https://doi.org/10.1007/978-3-319-63700-6_3

ment, higher resolution transducers are well adapted for children. The technique provides information on any organ of the abdomen when abnormal. The drawbacks of the technique are that it is more operator-dependent than CT, its performances are low among obese patients and too widely aerated abdomen. The technique has proven essential in the wide spectrum of anomalies that can involve the abdomen. In selected indications, Color Doppler, hydrosonography, elastography and the use of contrast enhanced US increase its efficiency.

Unenhanced and contrast enhanced CT (CE-CT) have gained popularity in the emergency departments especially among those dealing with both children and adults. It is well known that the numbers of CT examinations have increased markedly these last years to an unexpected summit. Fortunately, several organizations have arouse a deep reflection reactions about this "overuse" and this has led to a somewhat more limited and more focused use of the technique. CT has many advantages such as rapidity, a better reproducibility than US and accuracy in demonstrating abnormalities in any part of the abdomen. The drawbacks are the irradiation burden, the need for contrast injection and sometimes a need for sedation. So, whenever indicated, the technique (mAS, KvP, position of the patient and all surrounding potential artifacts, etc.) should be optimized to the type of disease and to the morphology of the patient.

Other techniques can be useful and provide diagnostic information. MR imaging has been used for many years now and is highly appreciated for the work-up of children. Yet, it is more difficult to perform MR imaging in the setting of abdominal emergencies as the examination is long, sedation might be needed as well as contrast injection. Faster imaging protocols already exist which give diagnostic clues in less than 15′. Its use will surely increase in forthcoming years.

Not to forget, the more ancient imaging techniques such as plain radiograph, upper GI tract opacification or contrast enema may provide additional information in selective cases.

Whatever the technique used, every effort should be made to optimize its contribution and to lower the burden that can be provoked taking into account the vulnerability of those little and young patients.

The aim of the book is to provide to the readers an overview of acute diseases affecting the paediatric abdomen. The book is organized through sections related to age, starting from prematurely born till adolescent. The chapters are also divided into digestive tract, uro-genital tract and global diseases affecting all or some parts of the abdomen. Several diseases are described within different chapters, since their presentation may be variable and they have to be considered from these various approaches. The readers are encouraged to consult the different chapters as referred in order to have a global overview.

Suggested Readings

1. Boluyt N, Lincke CR, Offringa M. Quality of evidence-based pediatric guidelines. Pediatrics. 2005;115:1378–91.
2. Kim HJ, Sang HS, Han KH, et al. Systemic classification for new diagnostic approach to acute abdominal pain in children. Pediatr Gastroenterol Hepatol Nutr. 2014;17:223–31.
3. van Heurn LWE, Pakarinen MP, Wester T. Contemporary management of abdominal surgical emergencies in infants and children.
4. Homme JL, Foster AA. Recurrent severe abdominal pain in the pediatric patient. J Emerg Med. 2014;46:627–31.
5. Saliakellis A, Borelli O, Thapar N. Pediatric GI emergencies. Best Pract Res Clin Gastroenterol. 2013;27:799–817.
6. Trompane T, Leong CW, Bush R, et al. Appropriateness of radiology procedures performed in children with GI symptoms and conditions. Clin Gastroenterol Hepatol. 2014;12:970–7.
7. Ramarajan N, Krishnamoorthi R, Barth R, et al. An interdisciplinary initiative to reduce radiation exposure: evaluation of appendicitis in a pediatric emergency department with clinical assessment supported by a staged US and CT pathway. Acad Emerg Med. 2009;16:1258–65.
8. Williams CH, Frush DP. Compendium of national guidelines for imaging of the pediatric patient. Pediatr Radiol. 2012;42:82–94.

9. Arthurs OJ, Bjorkum AA. Safety in pediatric imaging: an update. Acta Radiol. 2013;54:983–90.
10. Hryhorczuk AL, Mannix RC, Taylor GA. Pediatric abdominal pain: use of imaging in the US from 1999-2007. Radiology. 2012;263:778–85.
11. Cogley JR, O'Connor SC, Houshyar R, et al. Emergent Pediatr US: what every radiologist should know. Radiographics. 2012;32:661–5.
12. Young C, Owens C. Pediatric CT imaging guideline. Acta Radiol. 2013;54:998–1005.
13. Menoch MJA, Hirsh DA, Khan NS, et al. Trends in CT utilization in the pediatric emergency department. Pediatrics. 2012;129:e690–7.
14. Macias CG, Sahouria JJ. The appropriate use of CT: quality improvement and clinical decision-making in pediatric emergency medicine. Pediatr Radiol. 2011;41(suppl):S498–504.
15. Goske MJ, Strauss KJ, Mandel KE, et al. Diagnostic reference ranges for pediatric abdominal CT. Radiology. 2013;268:208–18.

Part II

The Prematurely Born

Abdominal Complications in the Premature Infant

4

Fred E. Avni, Annie Lahoche, Laurent Storme, and Veronica Donoghue

Contents

F.E. Avni (✉)
Department of Pediatric Imaging, Jeanne de Flandre Hospital, Av Eugène Avinée, 2, 59037 Lille-Cedex, France
e-mail: Freddy.Avni@chru-Lille.fr

A. Lahoche
Department of Pediatric Nephrology, Jeanne de Flandre Hospital, Av Eugène Avinée, 2, 59037 Lille-Cedex, France

L. Storme
Department of Neonatology, Jeanne de Flandre Hospital, Av Eugène Avinée, 2, 59037 Lille-Cedex, France

V. Donoghue
Radiology Department, The National Maternity Hospital, Holles Street, Dublin 2, Ireland

4.1 General Considerations

There are 13 million preterm babies worldwide. The incidence ranges from 5 to 12% in developed countries and is increasing. The risk factors for prematurity and growth restriction are multiple, including maternal stress (socio-economic adversity, psychosocial stress), premature membrane rupture, maternal co-morbidities, chorioamnionitis, decidual hemorrhage, placental dysfunction, and some fetal conditions (such as polyhydramnios). Although the causes of prematurity are heterogeneous, a suboptimal environment during the perinatal period is a common factor that may play a major role in the development of later morbidity in adulthood. It is well known that preterm birth, especially very preterm birth, is a major cause of neonatal mortality and morbidity [1]. There is growing evidence that prematurity is associated with an increased risk of developing non-communicable diseases in adulthood such as obesity and the metabolic syndrome, type 2 diabetes, dyslipidemia, and hypertension. In addition preterm babies are also at increased risk of developing neurologic and psychiatric morbidity [2, 3].

Morbidity and mortality in the premature infant during the neonatal period is related to brain injury,

F.E. Avni, P. Petit (eds.), *Imaging Acute Abdomen in Children*,
https://doi.org/10.1007/978-3-319-63700-6_4

to the consequences of respiratory distress, and to acute abdominal complications. The latter includes necrotizing enterocolitis (NEC), hepatobiliary consequences mainly related to the parenteral nutrition, meconium ileus—like obstruction and vascular damage especially to the kidneys. Iatrogenic diseases usually related to therapeutic measures have also to be considered. Furthermore, short- and long-term consequences of prematurity related diseases should be taken into account when considering acute abdominal symptoms in older prematures [1, 4].

In most instances, the plain film of the abdomen is the main imaging modality used in the neonatal intensive care unit. However, ultrasound (US) including Doppler evaluation is a useful tool especially when considering the abdomen, as it can easily be used at the bedside; in some instances (e.g., intestinal obstruction), opacification of the bowel through radio-opaque enema or upper gastro-intestinal (GI) follow-through will be necessary. Very rarely, a CT scan will be performed to monitor specific abdominal complications. Whenever imaging is being performed in the radiology department, everything should be done to maintain comfort, warmth, and an aseptic environment for these vulnerable patients.

The unpredictable nature of the various abdominal complications will require vigilant surveillance via clinical, laboratory, and imaging examinations. Therefore, affected neonates will be exposed to significant amounts of radiation. It is impossible to predict whether or not an individual will experience the consequences of radiation; it is therefore important to reduce radiation whenever possible at each exposure. Decreasing the need for imaging, for instance, by imaging only the indicated region and avoiding (or shielding) radiosensitive zones are important measures to consider [5, 6].

4.2 Intestinal Complications

4.2.1 Necrotizing Enterocolitis

NEC is the most common neonatal gastrointestinal (GI) emergency; it affects 5–7% of preterm infants each year. The mortality continues to be high varying from 16 to 42%. Its origin remains unclear as intestinal immaturity, abnormal bacterial colonization of the intestine, exaggerated inflammatory response, and immature vascular supply to the intestine are considered as risk factors [4]. The most typical initial symptoms of NEC are feeding intolerance, abdominal distension and bloody stools after 10 days of life. The role of imaging is to help to confirm the diagnosis, to monitor its evolution, and to detect complications that would lead to surgical management. However, indications for surgery may be difficult to determine and are sometimes non-consensual; therefore, imaging findings will be of utmost importance.

Spontaneous intestinal perforation in prematures (see below) constitutes the main differential diagnosis. To be noted, NEC-like symptoms may occur in term neonates; they are usually associated with specific problems such as maternal use of drugs, congenital heart disease, intestinal anomalies, or perinatal stress [7, 8].

4.2.1.1 Plain Film of the Abdomen

Plain film of the abdomen constitutes the corner stone of the diagnosis of NEC. The radiograph should be performed by positioning the patient supine, as straight as possible, and by removing lines and catheters from the abdomen as much as possible in order to avoid artifacts and misinterpretation.

Based mainly on imaging findings on the plain film, three stages of the disease have been defined as (1) Suspected NEC, (2) Definite medical NEC, and (3) Surgical NEC.

- *In stage 1*, bowel distension occurs without any sign of further anomalies as encountered in stages 2 or 3. The distension affects localized areas of the abdomen or more globally the entire abdomen. The distance between the aerated bowel loops is increased due to edema and/or effusion; the bowel loops can be displaced due to free fluid (Fig. 4.1a)
- *In stage 2*, bowel loops distension progresses with visible intestinal pneumatosis, portal venous gas, or both. Intestinal pneumatosis

appears as clusters of linear or bubbly pouches of air paralleling the intraluminal air (Fig. 4.1b). (The linear fat surrounding the colon should not be misinterpreted as pneumatosis.) There may be associated fixed dilated loops of intestine.

– *In stage 3,* free intraperitoneal air (pneumoperitoneum) indicates bowel perforation; it will appear on abdominal radiograph after initial stage 1 or 2 (or sometimes being inaugural) and will be coupled with deteriorating clinical and laboratory values. Intraperitoneal free air typically collects on the midline at the level of the xiphoid process (determining the so-called rugby sign) (Fig. 4.1c), the falciform ligament will also appear enhanced by free air; when more marked, the air will collect in front of the liver and decrease globally the hepatic density. Extra-digestive bubbles indicating early perforation may be difficult to visualize on the plain film of the abdomen and a shoot—through lateral supine view of the abdomen should be obtained in case of clinical suspicion. Free air will then appear as round, bubbly, or triangular air separating bowel loops (Telltale sign).

Each stage will be managed accordingly through close observation, bowel decompression, or exploratory laparotomy [7].

4.2.1.2 Ultrasound

US is considered as a complementary imaging tool to the plain film of the abdomen. Its main advantages are that it is a radiation free technique, it can be performed at the bedside, and it can be repeated in order to monitor unstable clinical evolution. Its role in assessing NEC remains somewhat controversial but the technique does provide some additional information complementary to the findings on the plain abdominal radiograph. US provides direct images of the bowel and peritoneal cavity and may help to predict the need for surgery. High resolution transducers with 8–15 MHz frequency should be used. The use of a linear-array transducer is preferable for evaluating the bowel and a sectorial transducer can be used to detect free fluid or free abdominal air.

The examination is intended to assess bowel wall thickness, wall echogenicity, bowel peristalsis, intestinal pneumatosis, portal venous gas, free abdominal air or free fluid, and abscesses. Color Doppler US can be helpful to evaluate blood flow in the superior mesenteric artery and to verify bowel wall perfusion.

Bowel wall thickness greater than 2 mm should be considered as suspicious for NEC and is thought to correspond to mucosal edema and hemorrhage. It may represent the first feature of the disease. Conversely, thickness below 1 mm indicates abnormal thinning resulting from ischemia that may lead to perforation. Typically intestinal peristalsis is reduced. Some authors monitor abnormal and reduced peristalsis through color Doppler.

Intestinal pneumatosis or intramural gas corresponds to the presence of air within the serosal and submucosal layers. It is due to the passage of intramural gas into the injured intestinal wall. It corresponds to the passage from stage 1 to stage 2. It is most commonly observed in the distal ileum and colon. On US, intestinal pneumatosis appears as highly echogenic dots within the bowel wall. The amount of gas is variable, sometimes only a few foci, but sometimes it encircles the entire wall determining the "circle sign" (Fig. 4.2a). Intestinal pneumatosis should be differentiated from intraluminal air that usually moves within the bowel whereas pneumatosis tends to remain unchanged with time.

Portal venous gas possibly originates from the venous absorption of intestinal pneumatosis; its finding in the appropriate clinical setting should raise the suspicion of intestinal pneumatosis and of NEC of stage 2. On US, it appears as echogenic dots distributed within the distal portal branches (Fig. 4.2b). It can appear within a segmental area or the entire liver can appear dotted due to the presence of air. Portal venous gas should be differentiated from intrahepatic calcifications, presenting in asymptomatic neonates and related to different entities (e.g., congenital infections) or to air observed after the placement of intrahepatic umbilical catheters. Portal venous gas seems to be demonstrated earlier on US than on the plain film of the abdomen.

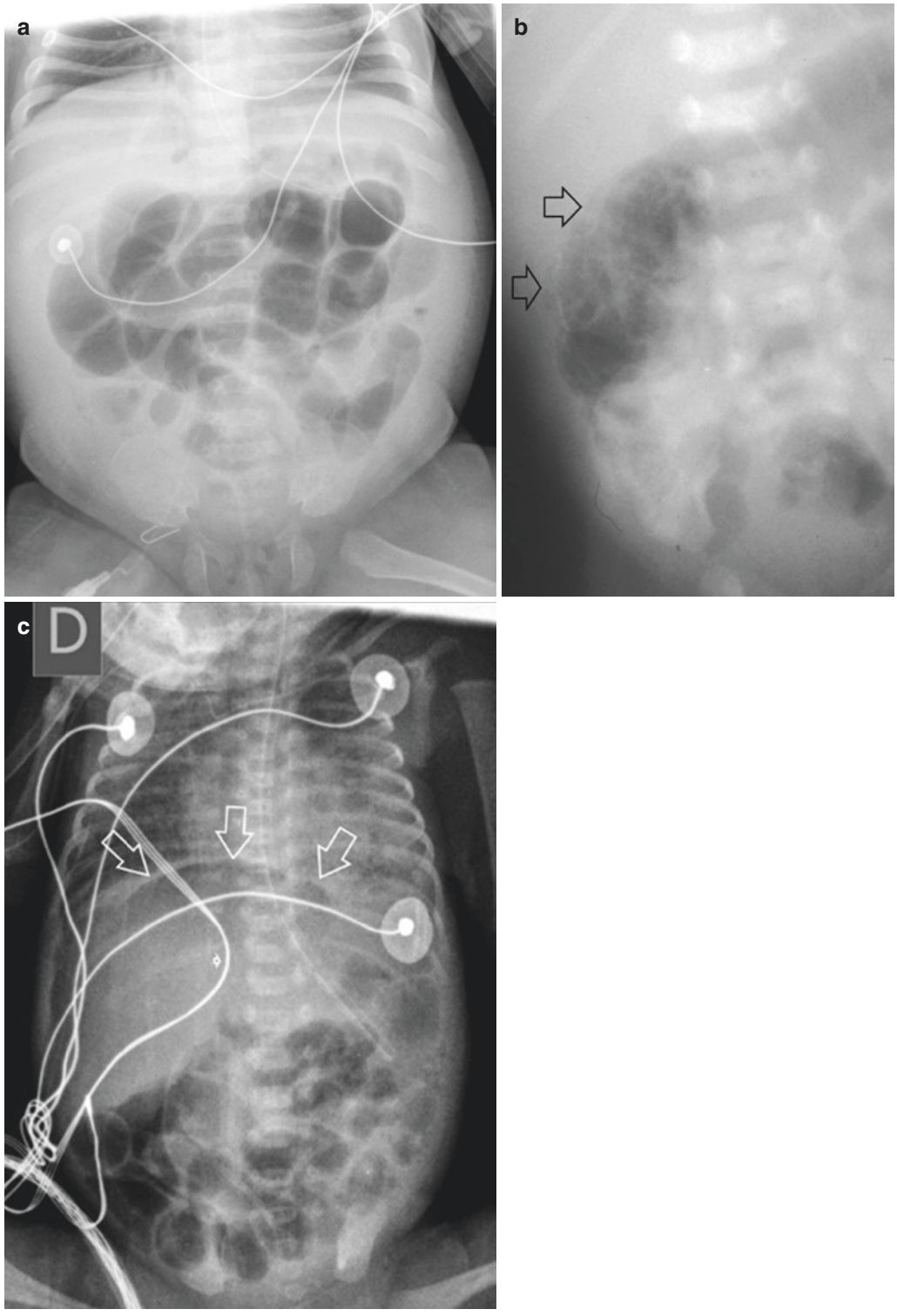

Fig. 4.1 NEC—Various stages on plain abdominal radiograph. (**a**) Stage 1. Plain radiograph of the abdomen showing distended bowel loops. The distance between some bowel loops is increased suggesting bowel wall thickening and/or effusion. (**b**) Stage 2. Focused plain radiograph of the abdomen showing pneumatosis in the bowel loops of the right flank (*arrows*). (**c**) Stage 3. A pneumoperitoneum can be observed as an area of radiolucency below the diaphragm and superimposed to the liver (*arrows*)

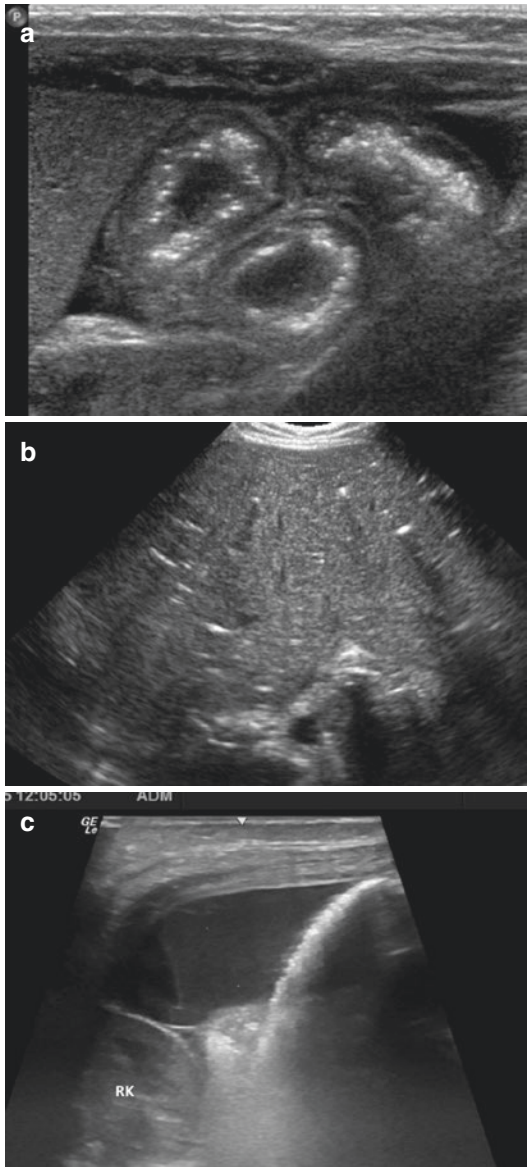

Fig. 4.2 NEC—US features. (**a**) Pneumatosis. Transverse scan in the midline below the liver. Bubbly hyperechogenicities can be observed within all bowel loops wall (determining the "*circle sign*"). They corresponding to pneumatosis. (**b**) Portal air. Oblique scan of the liver. Scattered hyperechogenic dots can be seen throughout the liver parenchyma corresponding to air bubbles within the portal system. (**c**) Effusion. Transverse scan of the right flank, echogenic fluid (in front of the right kidney (RK)) displaces the bowel loops to the midline

Free abdominal fluid and abscesses are common complications of NEC. Free abdominal fluid is a non-specific finding unless present in large amounts. Echogenic fluid or organized collections are more suspicious of complicated NEC and of bowel perforation. The presence of air within the collection is even more suspicious. Clearly, US is better than a plain film of the abdomen to demonstrate these complications (Fig. 4.2c).

Free abdominal air indicating bowel perforation can be observed on abdominal US as the reverberating artifact. However, this is more easily visualized on the plain film of the abdomen.

(Color) Doppler of the superior mesenteric artery is considered by some authors as useful in the evaluation of NEC. The mean diameter of the artery is 3 mm; the mean peak velocity is 57 ± 3 cm/s. However, during daily work Doppler evaluation of the artery is difficult due to abdominal air distension and to surrounding artifacts from various supporting equipment [9–13].

4.2.1.3 Late Complications of NEC (Presenting as Acute Abdominal Symptoms)

Intestinal strictures are a complication that occurs in up to 40% of neonates with a history of NEC. Strictures develop in patients with both medical and surgical management of their disease. The strictures may be symptomatic or asymptomatic (and discovered incidentally). They appear 4–6 weeks after the acute event. In symptomatic patients, a progressive distension of the abdomen, confirmed by a plain film of the abdomen, will raise the suspicion of a stricture and a contrast enema should be performed. In the absence of suspicion of perforation, a barium enema should be preferred as it might show more accurately the strictures. Water soluble enema should be preferred whenever there is a risk for perforation.

The strictures, defined as areas of persistent narrowing of the lumen on contrast enema with distension of the more proximal bowel, are typically observed at the splenic flexure or on the transverse colon; but may occur anywhere within the entire colon and small bowel (Fig. 4.3). Small bowel localization may be more difficult to demonstrate but is quite frequent. Upper GI

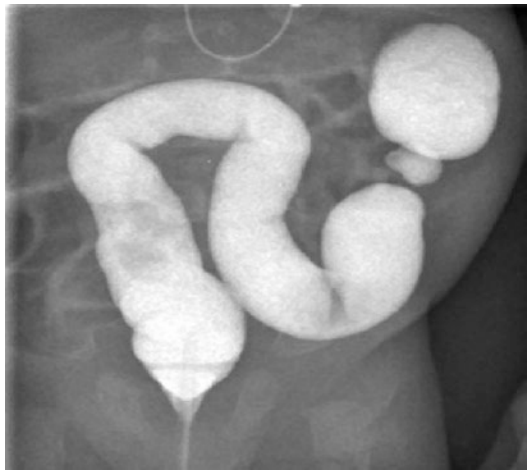

Fig. 4.3 Post-NEC colonic strictures. Contrast enema showing a double stenosis at the junction between the descending colon and the sigmoid

opacification is very rarely performed in these patients as it is a time and radiation consuming technique [14, 15]. Conservative or surgical management will be decided on the basis of the clinical symptoms and the degree of narrowing on imaging.

4.2.2 Meconium: Ileus Equivalent of the Premature

A thick and sticky inspissated meconium can cause bowel obstruction as demonstrated in patients with cystic fibrosis or in the meconium plug syndrome. Intestinal obstruction due to intraluminal inspissated meconium is recognized as a distinct clinical entity affecting very low birth prematures and is known as the "meconium obstruction of the prematurity." Its origin is unclear. Favoring factors include immature motility (with delayed passage of meconium), increased viscosity of the meconium, maternal diabetes, fetal hypoglycemia, and prenatal intestinal hypoperfusion. Sepsis and respiratory distress syndrome (with tracheal intubation) contribute to the intestinal dysmotility. If left untreated, ischemia of the distal bowel and subsequent perforation may occur [16, 17].

4.2.2.1 Imaging at Clinical Suspicion

Typically there is progressive abdominal distension in a baby that did pass some meconium at birth. Plain film of the abdomen will show, around the second week of life, multiple dilated loops suggestive of distal intestinal mechanical obstruction (Fig. 4.4a). In contrast to NEC, no associated pneumatosis is observed.

4.2.2.2 Confirmative Imaging and Management

Contrast enema with iso-osmolar or slightly hyperosmolar water soluble enema under fluoroscopic control is the gold standard procedure. This agent is not only radio-opaque but would also dilute and mobilize the thick meconium. When performed, the contrast enema should reach the ileo-cecal valve and opacify the small bowel proximal to the site of obstruction (Fig. 4.4b). During and after the examination, hydration and fluid and electrolyte balance should be closely monitored.

Contrast enema may be difficult to organize and achieve in low birth or extremely low birth prematurely born and therefore alternative treatments can be proposed. First, contrast enema in the NICU had been advocated by some while others have tried to remove the obstruction under US guidance. Both methods encompass a higher risk of perforation and should be undertaken with extreme caution and only in exceptional cases. Finally, medications like N-Acetylcysteine have been used with variable rates of successes. Attempts at reduction should not be performed in case of suspected sepsis or perforation [18, 19].

4.2.3 "Spontaneous" Digestive Tract Perforation

Spontaneous intestinal perforation does occur (rarely) in full-term neonates. It is a distinct clinical entity from NEC. Its origin is unclear; associations have been reported with the maternal use of antibiotics, maternal chorioamnionitis, postnatal use of corticosteroids, indomethacin, and positive neonatal blood

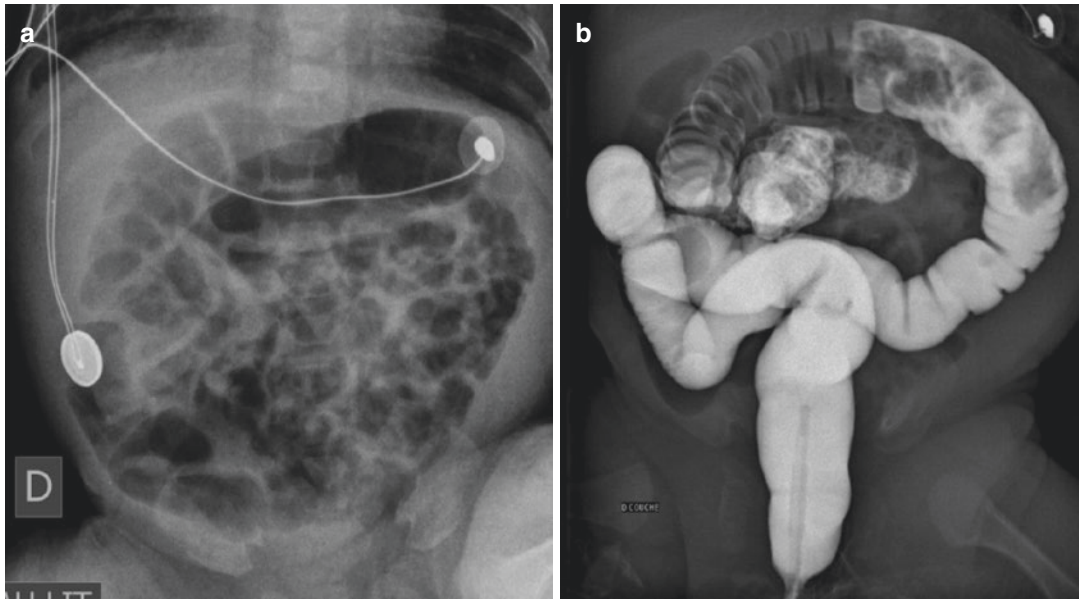

Fig. 4.4 Meconium ileus equivalent in a 4-week-old premature. (**a**) Plain film of the abdomen showing increased intestinal distension, especially in the right flank. (**b**) Water soluble enema showing persisting meconium in the colon. A filling of the terminal ileum is achieved indicating that the plug has been removed, thanks to the enema

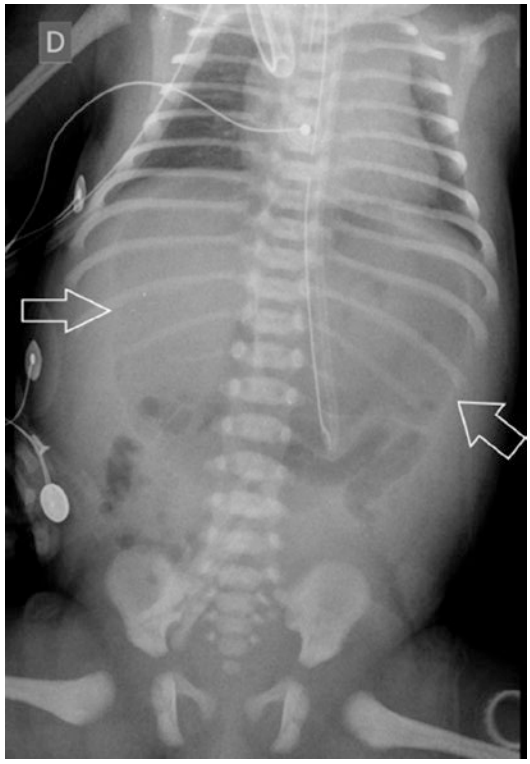

Fig. 4.5 Spontaneous pneumoperitoneum in 34 weeks premature on its second day of life. Plain film of the abdomen. A large area of radiolucency (*arrows*) is visible superimposed to the upper abdomen. The origin of the perforation was not found at exploratory surgery. Follow-up was uneventful

culture sepsis (staphylococcus). Spontaneous perforation also occurs as an early manifestation of Hirschsprung disease (see below). Perforation may occur either early within the first days of life or later within the two first weeks of life. The diagnosis is suspected, in the appropriate clinical setting, on the basis of early occurring pneumoperitoneum as demonstrated on the plain radiograph of the abdomen (Fig. 4.5). No other sign of NEC should be present. In cases of a gasless abdomen, extradigestive air will be more difficult to demonstrate and in these circumstances US has been shown to provide additional information by demonstrating intraperitoneal echogenic free fluid [20, 21].

4.2.4 Hirschsprung Disease in the Premature

Previous reports have stated that Hirschsprung disease (HD) is uncommon in premature patients. More recent reports contradict these ancient data and show that the prevalence of HD is similar to that of full-term neonates. The diagnosis is based on the same imaging features as those described in full-term (Fig. 4.6): persistent abdominal

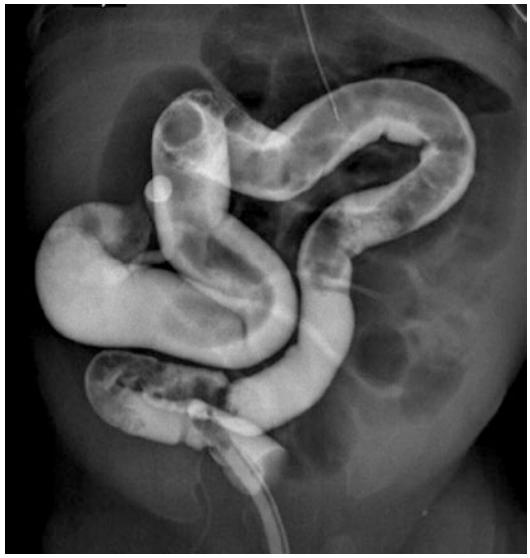

Fig. 4.6 Total Hirschsprung disease in a prematurely born (25 weeks at birth) aged 2 months. Contrast enema shows a relatively short colon without haustra (and without peristalsis at fluoroscopy). The small bowel loops are dilated as well (biopsy confirmed the involvement of the ileum as well)

distension on the abdominal radiograph and a transitional zone on radio-opaque enema. The diagnosis may be delayed due to intestinal dysmotility observed in the premature and to a delay in passing meconium (related to prematurity). Spontaneous pneumoperitoneum has been reported as the primary feature of HD in prematures [22, 23].

4.3 Hepato-Biliary Complications

Hepatobiliary complications in the premature infant are mainly related to hepatic immaturity, to the consequences of total parenteral nutrition, to the consequences of the insertion of umbilical catheters, and to sepsis.

Ultrasound examination is the main imaging procedure performed to detect and follow these complications. In very few selected cases, CT may be used in order to confirm a large hematoma or abscess [24].

4.3.1 Complications of Total Parenteral Nutrition

Parenteral nutrition (PN) related liver disease develops in about 50% of infants with birth weight < 1000 g but falls to 7% in patients > 1500 g. Its prevalence is directly related to the duration of the parenteral nutrition (PN). The hepatic dysfunction may be related to immaturity of the neonatal liver. The components of the PN are the main causative factor in the development of liver disease.

Acalculous cholecystitis (see below), biliary sludge, gallbladder distension, and gallstones have been reported in neonates on long-term PN.

On US, the main sign of liver disease is nonspecific hepatomegaly.

Echogenic sludge within the gallbladder may be visualized as early as 1 week after the starting of the PN (Fig. 4.7a). This sludge can disappear once the infant is fed orally. Yet, if the PN is continued, sludge may transform into sludge balls and into gallstones thereafter. These appear on US as echogenic masses within the gallbladder and acoustic shadowing is not the rule due to the soft nature of the balls. The sludge balls or gallstones may eventually migrate and induce (transient) biliary obstruction (Fig. 4.7b). Treatment will be conservative in most cases [25].

4.3.2 Acute Cholecystitis and Other Biliary Anomalies

Acute neonatal acalculous and calculus cholecystitis are uncommon events in neonates and premature infants, and their prevalence is unknown. Prematurity itself, some antibiotics, ischemia, and sepsis are favoring factors. On US, the gallbladder appears enlarged and non-depressible; its wall may appear thickened and edematous with fluid in the peri-vesicular space (Fig. 4.8). The differential diagnosis should include heart failure that causes a transient non-inflammatory wall thickening.

It should be noted that septic cholecystitis may induce secondary portal vein thrombosis (see below) [26, 27].

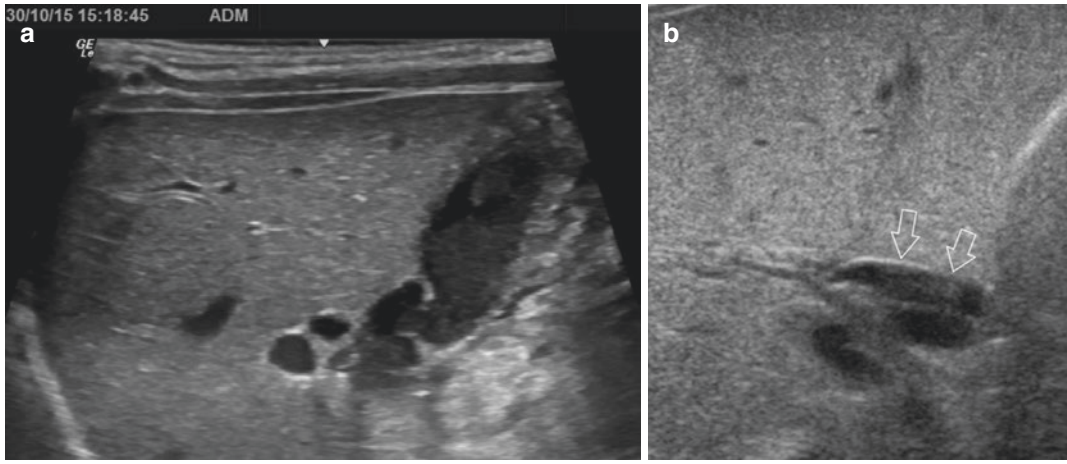

Fig. 4.7 Biliary tract obstruction by sludge in a premature under total PN displayed on US. (**a**) Sludge within the gallbladder. Sagittal scan of the liver and the gallbladder displaying echogenic sludge. (**b**) Sludge within the distended common bile duct (*arrows*). Sagittal scan through the bile duct and portal vein. Echogenic sludge is obstructing the common bile duct. The treatment was conservative and the dilatation resumed on follow-up

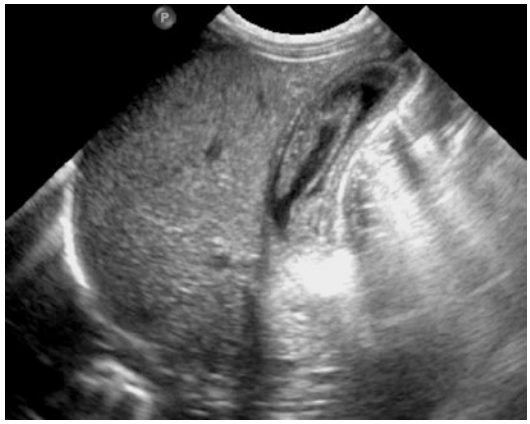

Fig. 4.8 Cholecystitis seen on US. Sagittal scan through the gallbladder. The gallbladder wall appears thickened with irregular interrupted layers. Some effusion is visible around it

4.3.3 Hepatic Complications of Umbilical Catheters

Venous umbilical catheters (UC) are widely used during the neonatal care especially in premature infants. The UC enters the abdomen following the course of the umbilical vein, then joins the ductus venosus at the junction with the left portal vein. The optimal position of the catheter tip is at the level of the inferior vena cava just below the right atrium (Fig. 4.9). Any position more proximal, any malposition within the right or left liver (Fig. 4.10a) (intra- or extravascular) can lead to administration of fluids and drugs into the portal system or even into the parenchyma. UC is also a potential source of infection and sepsis. Complications include intrahepatic hematoma, intrahepatic abscesses, portal vein thrombosis, and retrograde omphalitis. It should be noted that the catheter tip may be misplaced in other vessels (e.g., inferior vena cava). Whenever an antero-posterior view of the abdomen is obtained to check for the UC position, too proximal, too distal, or lateral insertions of the UC are easily demonstrated. However, as the course of the ductus venous runs obliquely, the antero-posterior view alone can miss a frontal malposition of the UC.

Systematic US is advocated by several authors in order to determine the exact position of the UC. US can easily demonstrate the umbilical vein course and the tip of the UC when it lies next to the right atrium; the course within the ductus venosus is more difficult to visualize because of acoustic shadowing. Some free intrahepatic air bubbles can be observed for a few days within the liver after an UC insertion. These air bubbles should be differentiated from portal air (more peripheric) associated with NEC or from intrahepatic calcification due to a prenatal

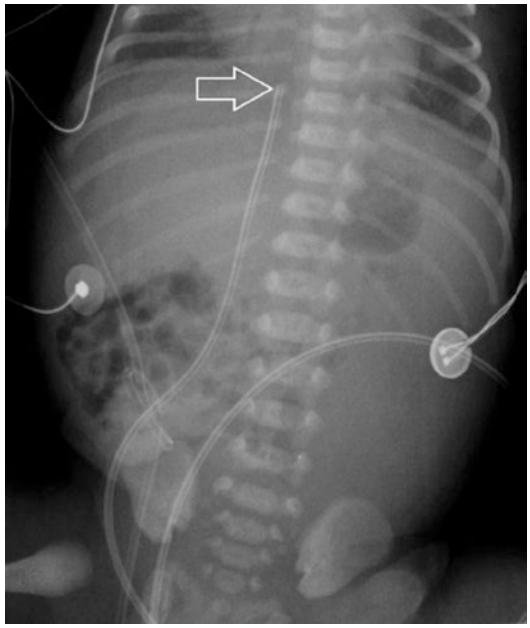

Fig. 4.9 Well-positioned umbilical catheter. Plain film of the abdomen. The extremity of the UC lies just below the heart (*arrow*)

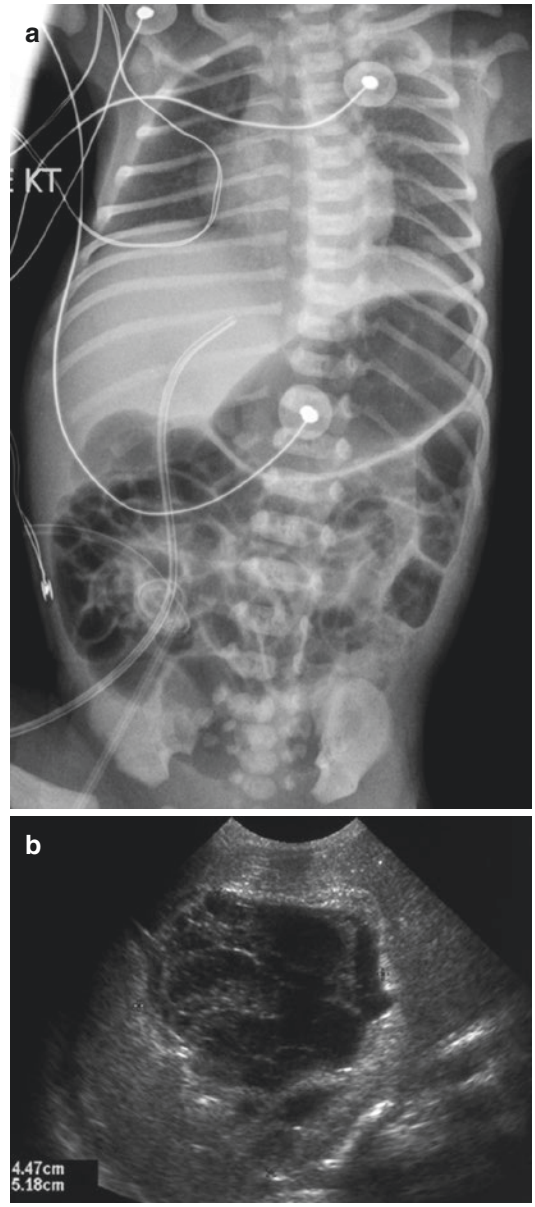

Fig. 4.10 Hematoma due to a misplaced UC—(**a**) Plain film of the abdomen at birth. The tip of the UC lies within the liver. (**b**) US of the liver at 10 days—Oblique view through the liver showing a large hypoechoic hematoma. It calcified first and then progressively disappeared on long-term follow-up

event, for instance, congenital CMV infection (in the latter, the hyperechogenicity will persist for a longer time).

A hematoma may result from intrahepatic parenchymal insertion of the UC and subsequent extravasation. This will appear as an intrahepatic collection or pseudo mass with areas of varying echogenicity. In some instances, the hematoma will be very large or determine a sub-capsular collection (Fig. 4.10b). The diagnosis is sometimes not straightforward and a CT scan rather than MR imaging may be useful in order to provide features confirming the hemorrhagic nature of the collection. Intrahepatic perfusion of drugs and fluids may also induce areas of hepatic ischemia or necrosis that might eventually calcify. Color Doppler analysis is helpful in determining areas of poor vascularization. As mentioned, infection or sepsis may complicate UC insertion. This may lead to omphalitis appearing as a thickened hypoechoic course of the umbilical vein and adjacent portal vein. Secondary intrahepatic vascular complications may occur. Portal vein thrombosis and intrahepatic abscesses may occur. It should be noted that a history of UC insertion can be found in over 50% of children with complete portal thrombosis associated with a cavernoma. Thrombosis of other vessels used for vascular access can also occur (Fig. 4.11a, b) [28–31].

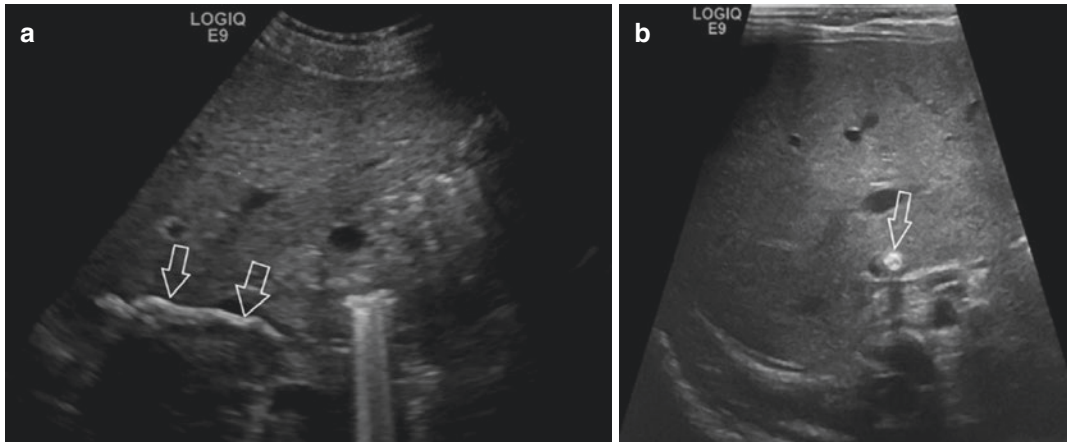

Fig. 4.11 Calcified thrombus within the IVC (previous IVC catheter removed few weeks ago). (**a**) Sagittal scan through the right flank showing a linear thick calcification (*arrows*) within the IVC (that was partially patent on color Doppler). (**b**) Transverse scan through the mid abdomen with a calcification within the IVC (*arrow*)

4.4 Uro-Nephological Complications of Prematurity

4.4.1 Renal Failure (See Also Chap. 6)

Acute renal failure (ARF) affects approximatively 8% of severely ill newborns—especially prematurely infants—treated in intensive care units. ARF is classified as pre-renal, intrinsic renal, and post-renal (in association with an obstructive uropathy). In pre-renal failure, ARF is due to decrease renal perfusion related to hypovolemia, hypotension, and hypoxemia. Decreased renal perfusion can lead first to acute transitory tubular necrosis and consequently to permanent renal lesions and necrosis in case of severe insults. Vasomotor nephropathy (VN) is the term used to describe the renal damage resulting from permanent or severe reduced renal perfusion. Septicemia, hypothermia, umbilical catheters, nephrotoxic drugs (antibiotics, non-steroidal anti-inflammatory drugs (NSAID)), and any disturbances of the renin–angiotensin system (RAS) (starting for some patients in utero) may also contribute or induce intrinsic ARF. The twin-twin-transfusion syndrome typically illustrates secondary disturbances of the RAS starting in utero with consequent post-natal ARF. Post-renal ARF is much rarer in the premature and can be related to bladder retention (see below).

Morbidity and mortality among premature infants with ARF is still very high.

Renal US may provide information on the status of the kidneys and on the consequences of the VN. The changes on US of the kidneys are frequently non-specific; still, in some cases the changes observed are more characteristic and allow a precise diagnosis. Doppler analysis is difficult especially in ventilation assisted premature infants; however, it should be used as often as possible [32–36].

4.4.1.1 Imaging Ischemic Renal Changes

Renal cortical necrosis, medullary necrosis, or combined cortical-medullary necrosis result from renal ischemia with or without vascular occlusion. In the premature infant, these conditions are associated with hypoxic/ischemic insults secondary to respiratory distress, perinatal anoxia, or are consequences of prenatal events such as twin-twin-transfusion syndrome or placental abruption.

On US, during the acute phase, the renal size will usually remain normal, the renal cortex will appear hyperechoic and the cortico-medullary

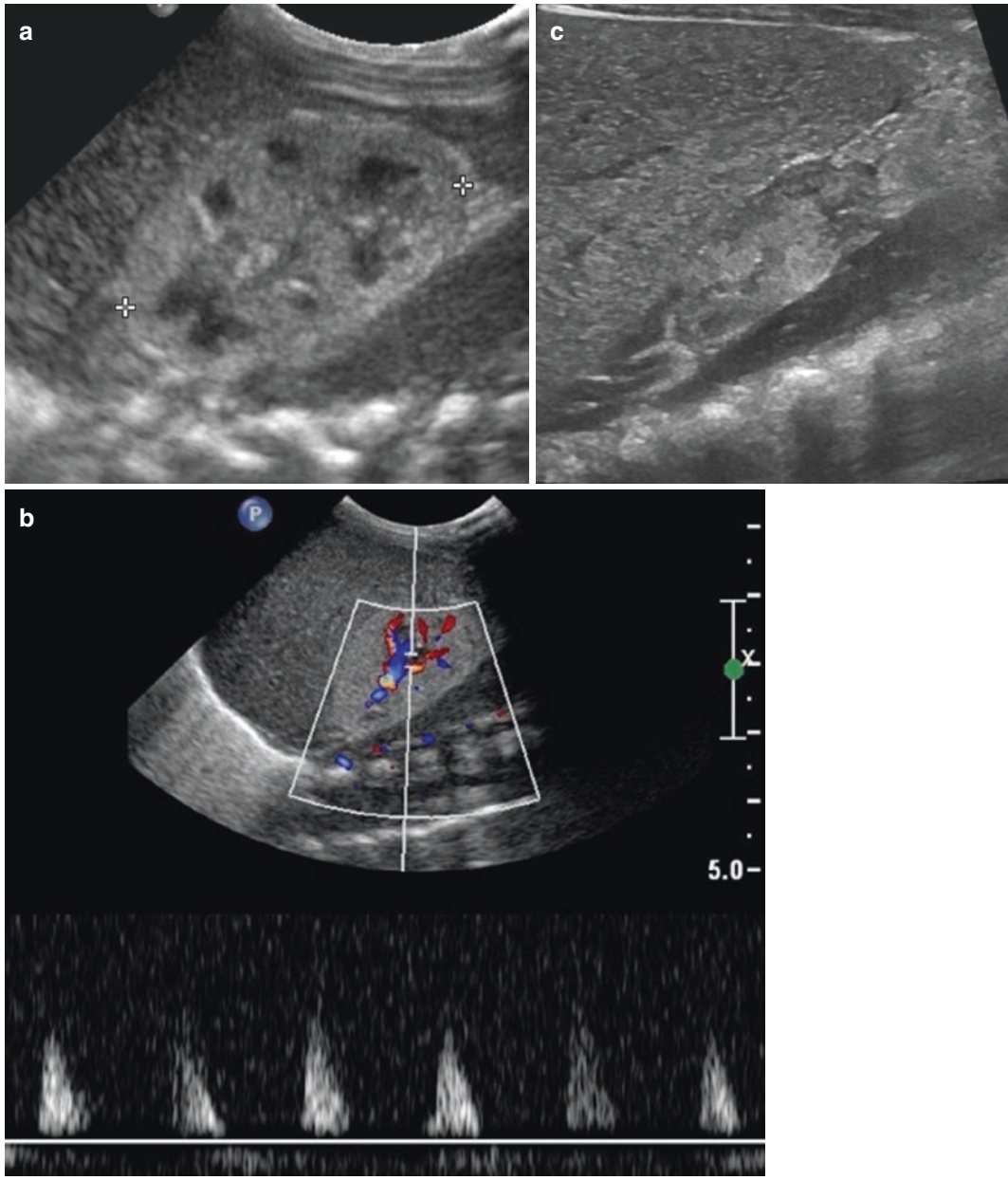

Fig. 4.12 Global renal ischemia—Ultrasound. (**a**) Sagittal scan of the right kidney (between the crosses). The renal cortex appears hyperechoic. (**b**) Duplex Doppler assessment—High resistive arterial flow with absent diastolic flow. (**c**) US follow-up, at age 3 months: the kidney has completely shrunken

differentiation is usually preserved (Fig. 4.12a, b). On duplex Doppler, the diastolic flow will be absent or reversed.

In case of permanent cortical ischemia, the cortical layer will rapidly shrink; in case of medullary ischemia, the pyramids may appear transitorily hyperechoic (Fig. 4.13); their size and echogenicity will decrease progressively. Cortical or medullar calcifications may develop within 2 weeks. Whenever the necrosis involves the entire kidney, the whole kidney may shrink or stop growing (Fig. 4.12c). A radionucleotide renal scan will show decreased or no uptake of radiopharmaceutical [32, 37].

4.4.1.2 Imaging Thrombotic Events

Renal artery thrombosis or renal vein thrombosis will result in renal failure if bilateral.

Renal artery thrombosis is typically associated with UC complications. Standard US may appear normal. Doppler evaluation may show absent flow in the renal artery or one of its branches. An aortic thrombus may be an associated finding [38].

In cases of renal vein thrombosis (see also Chap. 6), US will show an enlarged swollen kidney with lack of cortico-medullary differentiation and patchy areas of increased echogenicity (Fig. 4.14). Associated findings include direct visualization of the renal vein or inferior vena cava thrombus as well as homolateral adrenal hemorrhage [32, 39, 40].

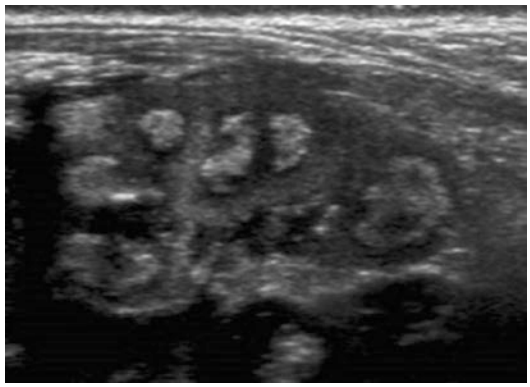

Fig. 4.13 Diffused renal medulla ischemia—Ultrasound. Sagittal scan through the right kidneys displaying hyperechoic pyramids due to hemorrhage

4.4.2 Acute Bladder Retention

Bladder distension and urinary tract dilatation may occur in ventilated premature infants after morphine administration. This dilatation is reversible once the medication is stopped. It is probable that immaturity of the musculature and interstitial tissue of the urinary tract may play an important role in the excessive dilatation of the urinary tract.

On US, the bladder appears markedly enlarged; and dilatation of the renal tracts is mild but obvious (Fig. 4.15) [41, 42].

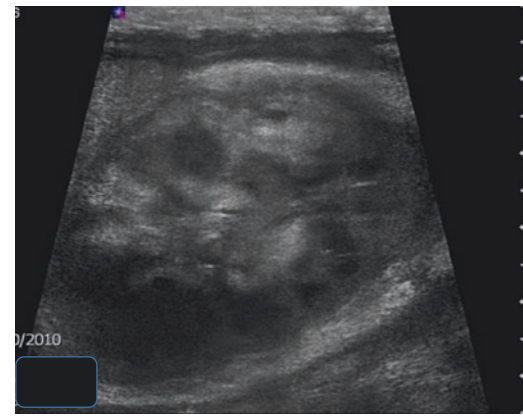

Fig. 4.14 Renal vein thrombosis—Ultrasound. Sagittal scan through the right kidney—The kidney appears swollen. The kidney echogenicity is completely distorted alternating areas of hyper- and hypo-echogenicities

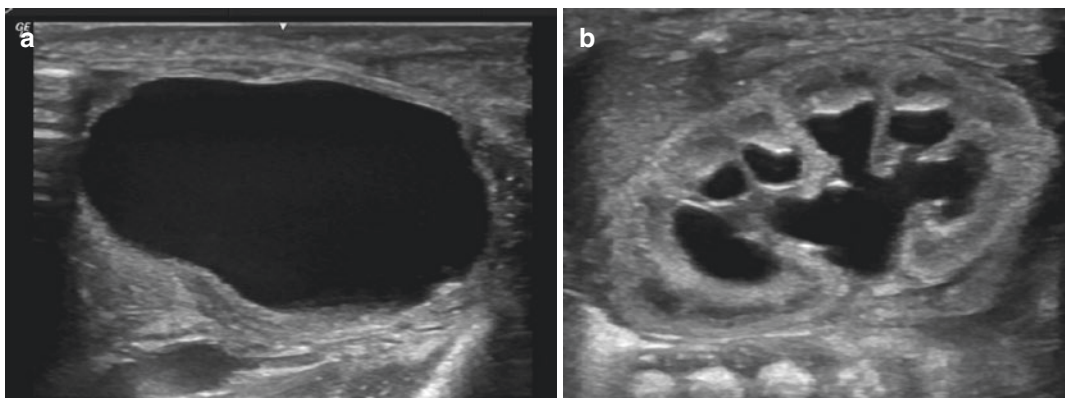

Fig. 4.15 Bladder retention due to morphinoid drugs. (**a**) US—Sagittal scan of the bladder. Massively enlarged bladder (5 cm length). (**b**) US—Sagittal scan of the right kidney (the *left* had a similar appearance). Dilated pyelocaliceal system

Conclusions

Many events and complications occur in premature infants with insults to the bowel, hepato-biliary tract, and kidneys. Plain film of the abdomen, US, and in some specific instances, bowel opacification will help to evaluate the anomalies and optimize the management.

References

1. Anderson JG, Baer RJ, Partridge JG, et al. Survival and major morbidity of extremely premature infants: a population based study. Pediatrics. 2016;138:e20154434.
2. Rossi P, Tauzin L, Marchand E. Respective roles of preterm birth and fetal growth restriction in blood pressure and arterial stiffness in adolescence. J Adolesc Health. 2011;48:520–2.
3. Hack M, Flannery DJ, Schluchter M, et al. Outcomes in young adulthood for very-low-birth-weight infants. N Engl J Med. 2002;346:149–57.
4. Yee W, Soraisham A, Shah V, et al. Incidence and timing of presentation of NEC in preterm infants. Pediatrics. 2012;129:2011–22.
5. Baird R, Tessier R, Guilbault M, et al. Imaging, radiation exposure, and attributable cancer risk for neonates with necrotizing enterocolitis. J Pediatr Surg. 2013;48:1000–5.
6. Puch-Kapst K, Juran R, Stoever B, et al. Radiation exposure in 212 VL and ELBW infants. Pediatrics. 2009;124:1556–64.
7. Neu J, Walker A. NEC. NEJM. 2011;364:255–64.
8. Chu A, Chiu HK. NEC in the full-term infant. Pediatr Ann. 2015;44:e 237–e242.
9. Bohnhorst B. Usefulness of abdominal US in diagnosing NEC. Arch Dis Child Fetal Neonatal Ed. 2013;98:F445–50.
10. Dördemann M, Rau GA, Bartels D, et al. Evaluation of portal venous gas detected by US examination for diagnosis of NEC. Arch Dis Child Fetal Neonat Ed. 2009;94:F183–7.
11. Muchantef K, Epelman M, Darge K, et al. US and radiographic imaging features of the neonates with NEC: correlating findings with outcomes. Pediatr Radiol. 2013;43:1444–52.
12. Yikilmaz A, Hall NJ, Daneman A, et al. Prospective evaluation of the impact of US in the management and surgical intervention in neonates with NEC. Pediatr Surg Int. 2014;30:1231–40.
13. He Y, Zhong Y, Yu J, et al. US and radiography findings predicted the need for surgery in patients with NEC without pneumoperitoneum. Acta Paediatr. 2016;105:e151–5.
14. Gaudin A, Farnoux C, Bonnard A, et al. NEC and the risk of intestinal stricture: the value of the C-reactive protein. PLoS One. 2013;8:e76858C.
15. Wiland EL, South AP, Kraus SJ, et al. Utility of GI fluoroscopic studied in detecting stricture after neonatal NEC. J. Pediatr. Gastroenterol. Nutr. 2014;59:789–94.
16. Garza-Cox S, Keeney SE, Angel CA, et al. Meconium obstruction in the VLBW premature infant. Pediatrics. 2004;114:285–90.
17. Siddiqui MMF, Drewett M, Burge DM. Meconium obstruction of prematurity. Arch Dis Child Fetal Neonatal Ed. 2010;97:F147–50.
18. Cho HH, Cheon J, Choi YH, et al. US guided contrast enema for meconium obstruction in VLBW infants: factors that affect treatment success. Eur J Radiol. 2015;84:2024–11.
19. Koshinaga T, Inoue M, Ohashi K, et al. Therapeutic strategies of meconium obstruction of the small bowel in VLBW neonates. Pediatr Int. 2011;53:338–44.
20. Khan TR, Rawat JD, Ahmed I, et al. Neonatal pneumoperitoneum: a critical appraisal of its causes and subsequent management from a developing country. Pediatr Surg Int. 2009;25:1093–7.
21. Fischer A, Vachon L, Durand M, et al. US to diagnose spontaneous intestinal perforation in infants weighing < 1000 g at birth. J Perinatol. 2015;35:104–9.
22. Duess JW, Hofman AD, Puri P. Prevalence of HD in the premature: a systematic review. Pediatr Surg Int. 2014;30:791–5.
23. Downey EC, Hughes E, Putnam AR, et al. HD in the premature newborn: a population based study and 40-year single center experience. J Pediatr Surg. 2015;50:123–5.
24. Kelly DA. Preventing parenteral nutrition liver disease. Early Hum Dev. 2010;86:683–7.
25. Jawahweer C, Pierro A, Lloyd TA, et al. Gall bladder contractility in neonates effect of parenteral and enteral nutrition. Arch Dis Child. 1995;72:F200–F 202.
26. Mateos-Corral D, Garza-Luna U, Gutierez-Martin A. Two reports of acute neonatal acalculous cholecystitis in a 2 week-old premature infant and term neonate. J Pediatr Surg. 2006;41:E3–5.
27. Herzog D, Bouchard G. High rate complicated idiopathic gallstone disease in pediatric patients of a north American tertiary care center. World J Gastroenterol. 2008;14:1544–8.
28. Simanovsky N, Ofek-Schlomai N, Rozovsky K, et al. Umbilical venous catheter position: evaluation by US. Eur Radiol. 2011;21:1882–6.
29. Sherwani P, Vire A, Anand R, et al. Umbilical venous catheterization gone wrong: hepatic complications. Indian J Radiol Imaging. 2016;26:40–3.
30. Morag I, Epelman M, Daneman A, et al. Portal vein thrombosis in the neonate: risk factors, course, and outcome. J Pediatr. 2006;148:735–9.
31. Demirel N, Aydin M, Zenciroglu A, et al. Neonatal thrombo-embolism: risks factors, clinical features and outcome. Ann Trop Paediatr. 2009;29:271–9.

32. Andreoli SP. Acute renal failure in the newborn. Semin Perinatol. 2004;28:112–23.
33. Arcinue R, Kantak A, Elkhwad M. Acute kidney injury in ELBW infants (< 750 gr) and its associated risk factors. J Neonatal-Perinatal Med. 2015;8:349–57.
34. Gouyon JB, Guignard JP. Management of ARF in newborns. Pediatr Nephrol. 2000;14:1037–44.
35. Waisman D, Kessel I, Ish-Shalom N, et al. The anuric preterm newborn infant with normal US: a diagnostic and ethical challenge. Prenat Diagn. 2006;26:350–3.
36. Mahieu-Caputo D, Muller F, Joly D, et al. Pathogenesis of the TTTS: the renin-angiotensin system hypothesis. Fetal Diagn Ther. 2001;16:241–4.
37. Lerner GR, Kurnetz R, Bernstein J, et al. Renal cortical and renal medullary necrosis in the first 3 months of life. Pediatr Nephrol. 1992;6:516–8.
38. Lam HS, Chu WCW, Lee CH, et al. Renal artery thrombosis and ischemia presenting as severe neonatal hypertension. Arch Dis Child. 2007;92:F264.
39. Wright NB, Blanch G, Walkingshaw S, et al. Antenatal and neonatal RVT: new US features with high resolution transducers. Pediatr Radiol. 1996;26:686–9.
40. Winyard PJ, Bharucha T, de Bruyn R, et al. Perinatal RVT: presenting renal length predicts outcome. Arch Dis Child Fetal Neonatal Ed. 2006;91:F273–8.
41. Gatti JM, Perez-Brayfield M, Kirsch AJ, et al. Acute urinary retention in children. J Urol. 2001;165:918–21.
42. Bengtsson B-O, Wootton-Georges SL, Poulain FR, et al. Urinary effects of morphine in preterm infants. Acta Paediatr. 2003;92:251–3.

Part III

The Newborn Including The Impact of Antenatal Diagnosis

Abdominal Neonatal Emergencies Considering Prenatal Diagnosis

5

Marie Cassart and Fred E. Avni

Contents

M. Cassart (✉)
Department of Fetal and Pediatric Imaging,
Iris Hospitals, Brussels, Belgium
e-mail: marie.cassart@icloud.com

F.E. Avni
Department of Medical Imaging,
Edith Cavell Institute, Brussels, Belgium

Department of Pediatric Imaging,
Jeanne de Flandre Hospital, University Hospital,
Lille-Cedex, France

5.1 Introduction

Nowadays, due to prenatal diagnosis, many newborns have already a "medical history." In most cases, the anomaly discovered prenatally allows to adapt the neonatal care. After birth, whatever the antenatal diagnosis, the first step is to confirm the anomaly, thereafter to precise the diagnosis (in classical and less classical cases) and third to determine the emergency status (medical or surgical emergency) in order to optimize the treatment strategy.

Throughout the chapter, we will discuss the management of various neonatal abdominal emergencies highlighted by the antenatal data differentiating the most classical presentations from the atypical potentially acute ones.

5.2 Newborns with Prenatally Diagnosed Abdominal-Pelvic Masses

5.2.1 Introduction

In the neonatal period, a fetus with a history of abdominal mass should have a neonatal US in order to better characterize the lesion and confirm or precise the prenatal diagnosis [1, 2]. According to the suspected US diagnosis and the clinical status of the baby, complementary customized immediate or programmed imaging (MR Imaging, plain radiographs, etc.) will be proposed. We will

F.E. Avni, P. Petit (eds.), *Imaging Acute Abdomen in Children*,
https://doi.org/10.1007/978-3-319-63700-6_5

mostly focus on the work-up considering classical and less classical presentations of the different types of abdomino-pelvic masses.

5.2.2 Cystic Masses

5.2.2.1 Duplication Cysts

Duplication cysts are classical but rare malformations (1/10000 life birth) that can be observed all along the digestive tract from the esophagus to the rectum. The small bowel localization is the most common (30%) whereas colonic duplication occurs from 3 to 20% of cases [3]. They can be unique or multiple, round or tubular, communicating or non-communicating with the normal digestive tract. Various theories have tried to explain their origin: failure of recanalization, split notochord anomalies, defect of spontaneous regression of diverticular structures, etc. There is no unique theory that can explain the large variety of these malformations and their various clinical presentations. Their clinical history may depend on their location, size, and anatomical aspect (communicating or not with the digestive tract) [4].

Classical presentation: On US, a duplication cyst presents a multilayered pattern of its wall (muscular and epithelial linings: the "gut signature sign") and possibly intermittent peristalsis (Fig. 5.1). They are located close to digestive loops. Calcifications may be present. The aims of the neonatal US are to confirm the prenatal suspicion and to exclude complications. Noteworthy, most of these cysts remain clinically silent for months or years, still, programmed surgical resection is the most frequent treatment adviced nowadays.

Potential complications are: bleeding due to the presence of ectopic gastric mucosa, torsion (in cases of pediculate lesions), intussusception, and occlusion responsible for acute abdominal pain and vomiting.

These complications may lead to *abdominal emergencies*.

For instance, *major neonatal distension* may be encountered in communicating duplication cysts. The lesion that appeared cystic in utero will progressively and sometimes massively get inflated due to the progressive digestive tract aeration. In such situation, a plain radiograph of the abdomen (potentially associated with an opacification of specific parts of the digestive tract to confirm the presence of a communication) (Fig. 5.2) will establish the diagnosis and confirm the need for immediate surgery.

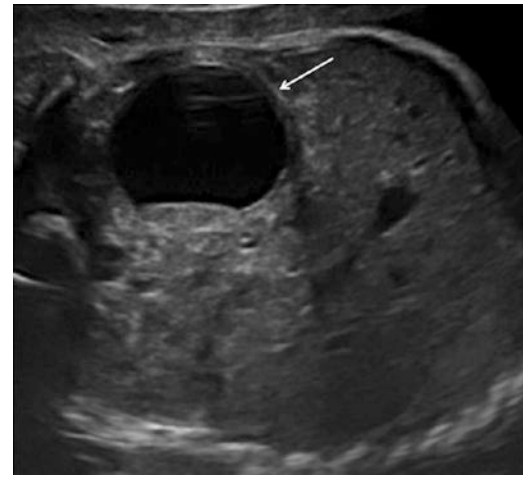

Fig. 5.1 Typical prenatal US aspect of a duplication cyst. Axial US scan on the abdomen of a 30-week-old fetus, showing a cystic right pelvic structure with a multilayered wall (*arrow*)

In some other cases, the lesion may be responsible for acute abdominal distension due to *intestinal occlusion* secondary to digestive tract compression [5–7] (Fig. 5.3). Sometimes, the duplication cyst (even small) can also be the leading point of a secondary *intussusception*. These complications are generally diagnosed at surgery.

In very rare cases, rectal duplication may prolapse through the perineum and appear like a large external *mass* developing in the buttocks potentially diagnosed in utero (Fig. 5.4). As usual, a prenatal detection has the advantage of inducing the consideration of all differential diagnosis including other pelvic and external masses such as teratomas and prompting neonatal management and surgery.

In most of these uncommon situations, thanks to the prenatal diagnosis, the neonatal investigations are limited to abdominal plain radiograph and US. Still, in more complex or rare cases, opacification or MR Imaging can be useful [8, 9].

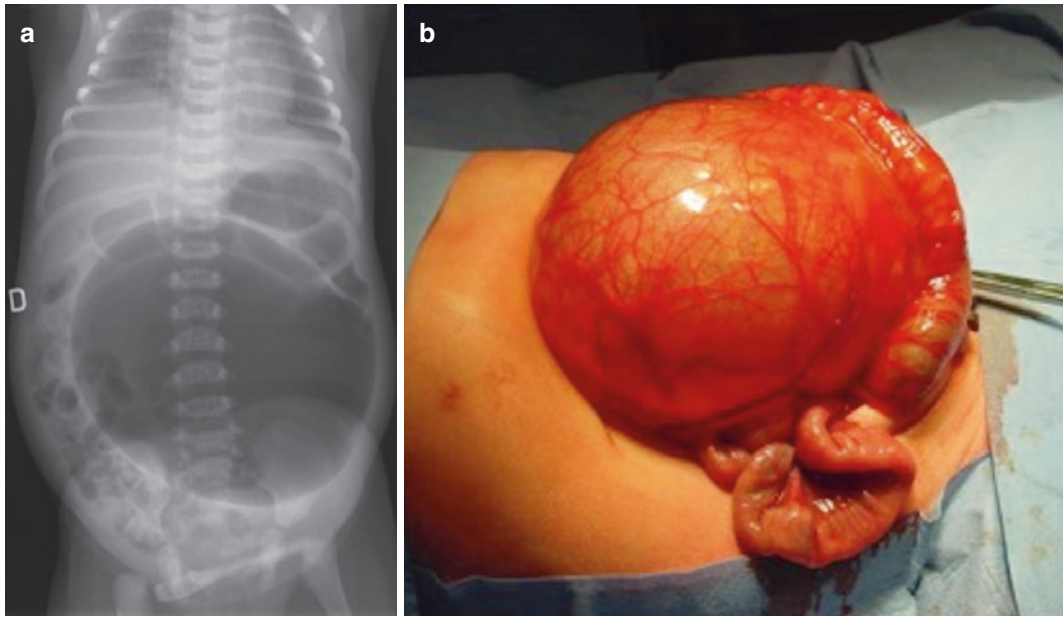

Fig. 5.2 Acute neonatal distension of a communicating duplication cyst. (**a**) Abdominal radiograph showing a large distended digestive structure, which corresponds to an acute aeration of a communicating duplication cyst. (**b**) Surgery confirms the presence of a distended duplication cyst (Courtesy P. Lingier MD)

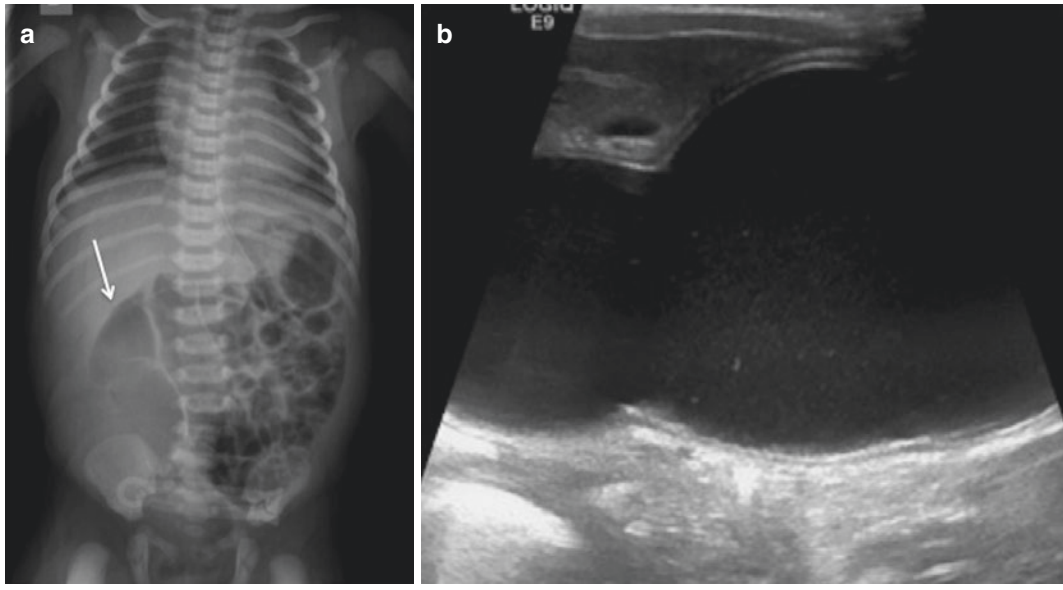

Fig. 5.3 Neonatal digestive occlusion by a tubular duplication cyst. (**a**) Abdominal radiograph shows a distended loop in the right flank (*arrow*) and evidence for intestinal occlusion. (**b**) The US performed at the same time shows a typical multilayered walled cystic structure corresponding to a duplication cyst responsible for the occlusion

5.2.2.2 Ovarian Cysts

Ovarian cysts are the most common pelvic cystic masses encountered in female fetuses. They occur in 1/2600 pregnancies. These cysts would classically appear in the third trimester in relation with the hormonal environment associated with the gestation. Most appear as a unilocular thin walled cystic structure with anechoic con-

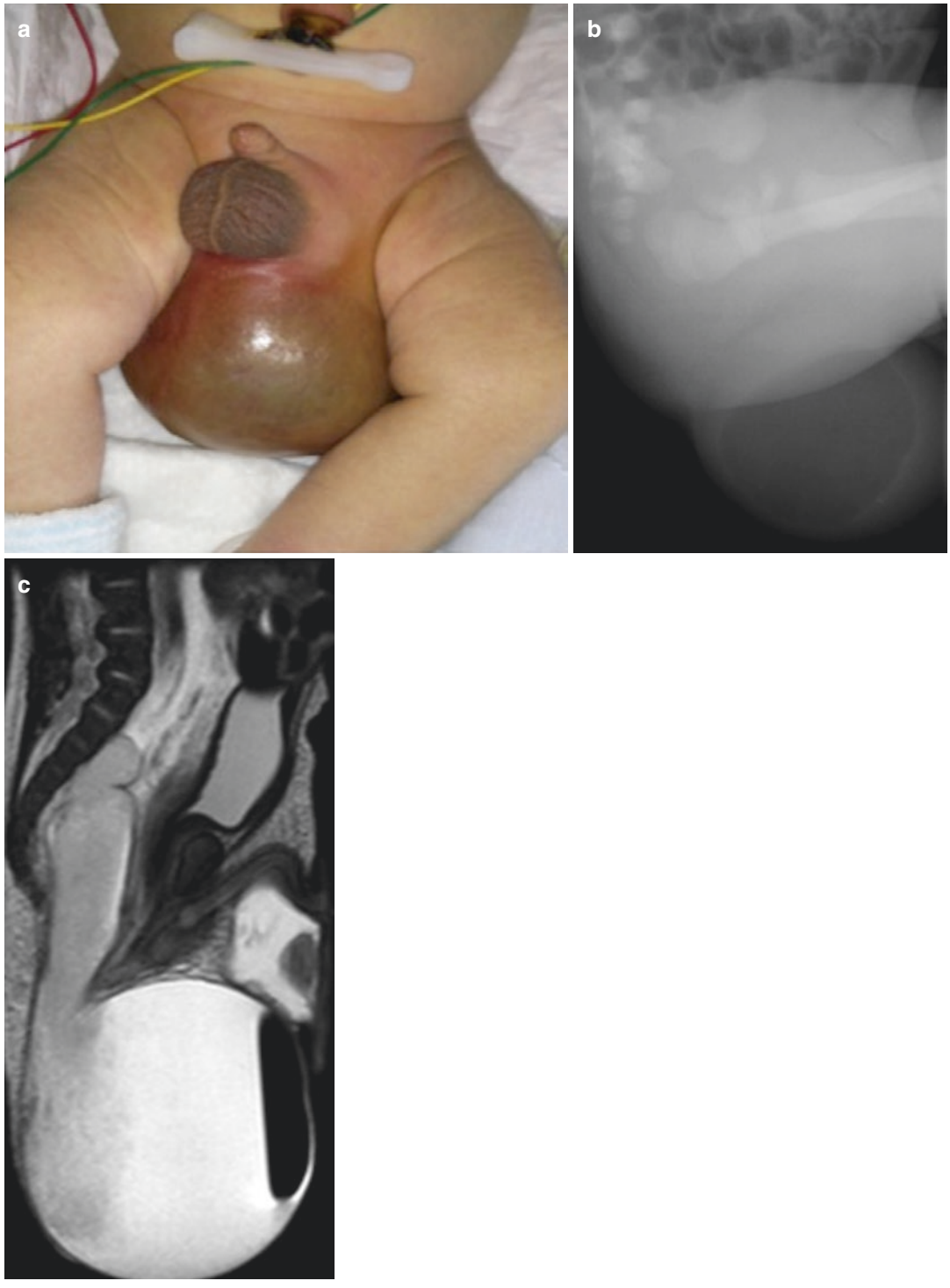

Fig. 5.4 Neonatal large external mass corresponding to a rectal duplication diagnosed prenatally (Courtesy C. Fayard MD). (**a**) Large extraperineal soft mass. (**b**) The left lateral decubitus radiograph shows a partially aerated mass. (**c**) The sagittal T2 weighted MR imaging confirms that the mass corresponds to a duplicated rectum prolapsed through the perineum

tent developed within the fetal pelvis. Rarely the cysts may appear during the second trimester or develop bilaterally. After birth, the influence of maternal hormones decreases rapidly leading to spontaneous progressive involution of the cyst. Sometimes, the cyst can persist a few months in particular in case of breast-feeding. Still, most commonly, it should have disappeared before the age of 6 months. Complications like bleeding or torsion can occur in utero or after birth and modify the aspect of the content of the cyst which then would appear more echogenic with possible sedimentation confirming the blood content.

No therapeutic procedure or early delivery is advised in case of prenatal diagnosis.

Classical presentation: In the neonate, ovarian cysts detected in utero should be imaged by US only. The examination confirms the diagnosis mostly by identifying peripheral small daughter cysts that are pathognomonic for the ovarian origin of the cystic lesion (Fig. 5.5). If the cyst measures less than 4 cm, a simple monthly US monitoring is advised because many cysts will stay clinically silent and will regress spontaneously. In some cases, neonatal complications can occur leading to urgent (celioscopic) surgery.

Noteworthy, an ovarian hemorrhagic lesion can appear like an echogenic "solid type" mass with worrisome differential diagnosis. A rapid postnatal involution would favor the diagnosis of a (complicated) ovarian cyst [10].

An ovarian cyst is rarely an *abdominal emergency* in the neonate. Yet, acute bleeding, torsion, or mass effect can occur in the neonatal period. In such case, an important increase in size or ischemic insult (torsion) is responsible for acute abdominal pain. Complications occur more frequently in big cysts (larger than 5 cm) and therefore cyst aspiration has been advocated to reduce the risk of torsion. In such presentation, US is the best diagnostic tool to confirm the ovarian origin of the lesion and exclude other causes of acute abdominal symptoms. Complicated ovarian cysts appear like heterogeneous structures with intracystic echogenic clots or debris, fluid/fluid levels, and septations (Fig. 5.6) [11]. The presence of vascular flow on Doppler imaging does not exclude ovarian torsion or auto-amputation [12], as the presence of flow may be secondary to vascular proliferation in the fibrotic walls. Urgent surgery or celioscopic cystectomy/fenestration is required in order to preserve functional ovarian

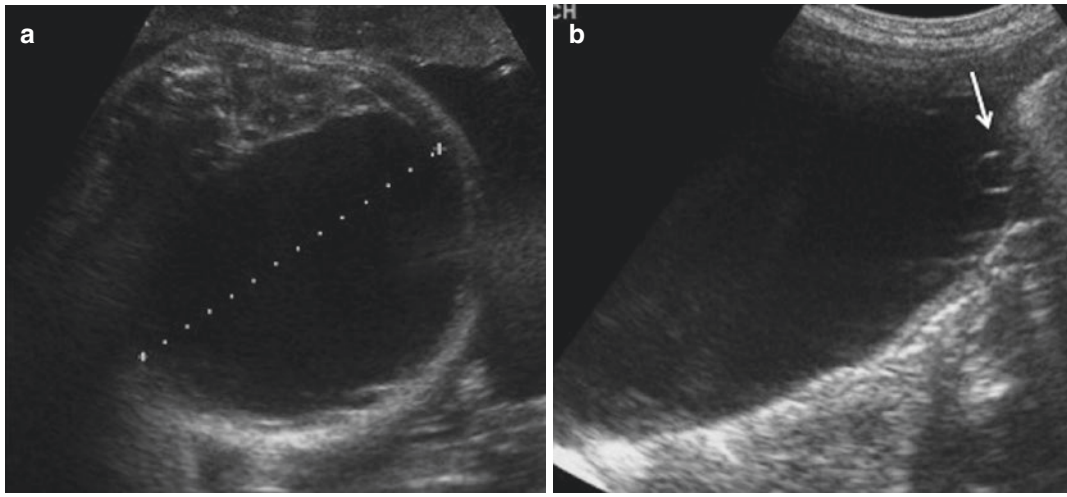

Fig. 5.5 Very large ovarian cyst. (**a**) Axial US abdominal scan of a third trimester fetus showing a large cystic mass filling almost entirely the abdomen. The differential diagnosis with other etiologies is difficult because of the size of the cyst. (**b**) The postnatal US is pathognomonic of an ovarian cyst, thanks to the demonstration of peripheral daughter follicle (*arrow*)

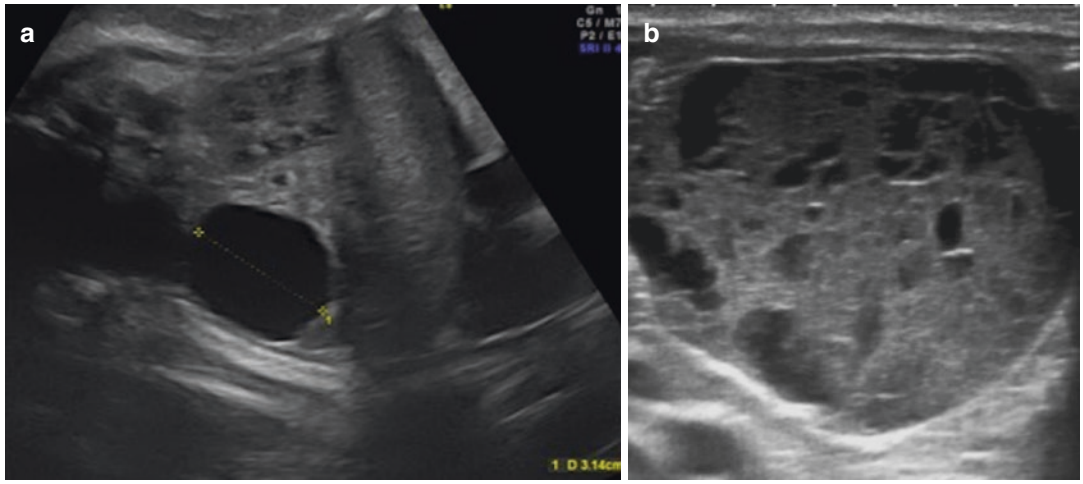

Fig. 5.6 Acute neonatal hemorrhage in an ovarian cyst. (**a**) Prenatal US abdominal sagittal scan of a 36-week-old fetus displaying a completely hypoechoic ovarian cyst. (**b**) The neonatal (Day 1) abdominal US shows a complex echogenic content corresponding most probably to hemorrhage within the cyst

tissue [13]. Cases of ovarian cysts associated with bowel obstruction have been described as well (Fig. 5.7). Two mechanisms are suggested: adhesions caused by twisted necrotic ovary or mass compression in case of large cysts [14]. In this context, immediate surgery is also required. When calcifications are present, even if they may suggest auto-amputation, the differential diagnosis with a teratoma should be raised. In this context, evaluation by MR imaging can be useful.

5.2.2.3 Choledocal Cyst (See Also Chap. 8)

Choledocal cyst is a difficult prenatal diagnosis. Only 15% of the cases are accurately diagnosed in utero. In fetuses with subhepatic cysts, the differential diagnoses are hepatic cysts, cystic biliary atresia, and duodenal duplication cyst. In the fetus, the demonstration of intrahepatic biliary ducts dilatation connected with the cyst is the only sign ascertaining choledochal cyst. When this sign is absent, there is no absolute criterion to exclude intrahepatic biliary atresia with intrahilar cyst.

The etiologies suggested for such a malformation are an abnormal bilio-pancreatic junction-leading to biliary reflux and secondary distension of the common bile duct- or a failure of bile duct recanalization during the embryologic development.

Classical presentation: A prenatal suspicion of choledochal cyst requires a neonatal US to confirm the nature of and exact localization of the cyst. An MR Imaging can also help to rule out biliary atresia by showing other specific malformations and to classify the type of the cyst [15]. In case of persisting neonatal cholestasis or inconclusive examinations, exploratory surgery is needed and peri-operative cholangiogram should be performed. If a conservative approach is decided, in early life. The newborns are carefully followed up clinically, biologically, and by means of US; 50% of the patients will be free of symptoms. Still, the prognosis is uniformly poor if left untreated (cholangitis, obstructive jaundice, liver dysfunction, pancreatitis, etc.) progressing to biliary cirrhosis and portal hypertension. The surgical treatment in asymptomatic patients should optimally be planned within the first 6 months in order to avoid progressive hepatic fibrosis [16].

Rarely, *acute complications* such as stomach outlet compression or cyst rupture may occur leading to vomiting and feeding difficulties [17, 18]. In this context, the newborn presents acute abdominal discomfort and peritoneal fluid due to biliary ascites. The diagnosis relies on the previous prenatal diagnosis of a subhepatic cyst and on the biological analysis of the peritoneal

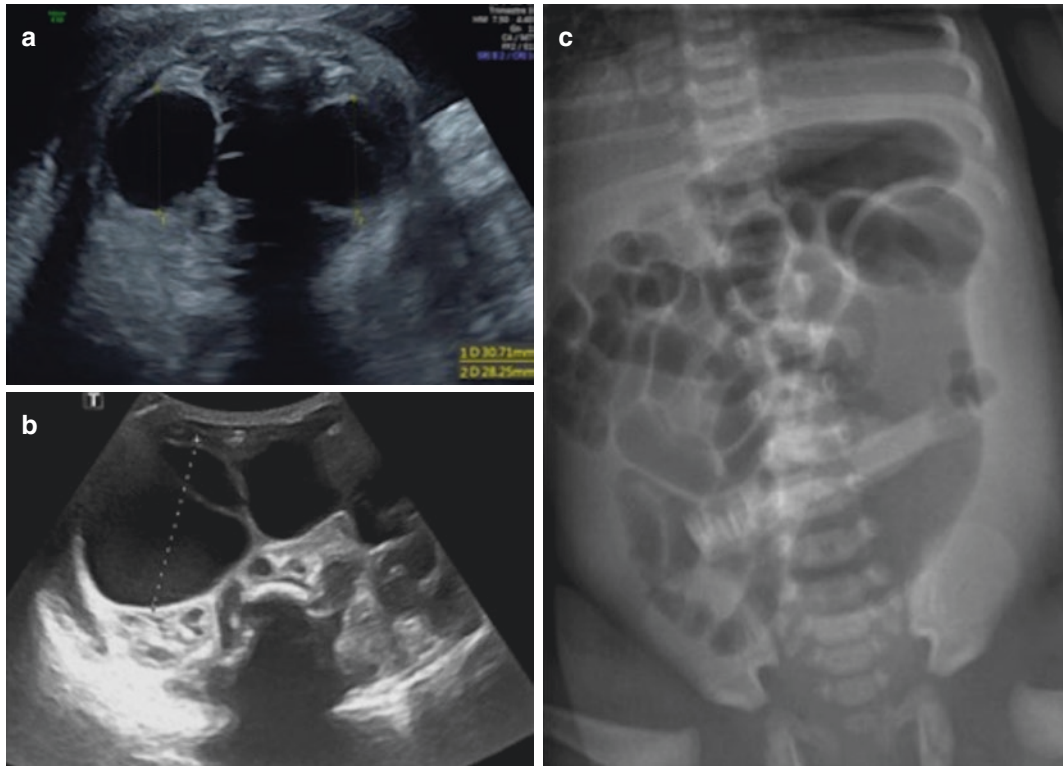

Fig. 5.7 Acute intestinal obstruction secondary to compression by bilateral ovarian cysts. (**a**) Prenatal US at 33 weeks demonstrating bilateral huge ovarian cysts (between crosses) (Courtesy C. Coulon MD). (**b**) Neonatal abdominal US confirming the prenatal diagnosis of bilateral ovarian cysts. (**c**) Abdominal radiograph (Day 1) shows an intestinal obstruction that was confirmed to be secondary to external compression of the small bowel by the bilateral ovarian cysts

fluid. The treatment is urgent surgery with cyst resection peritoneal lavage and Roux en Y hepatico-jejunostomy.

5.2.3 Solid Masses

5.2.3.1 Renal Masses

Renal masses are rare in the fetus. The most common mass is mesoblastic nephroma. It appears on US like a solid or mixed type well-circumscribed mass of the kidney and is associated with polyhydramnios [19] (Fig. 5.8). The differential diagnoses include rare Wilms' tumor and intrarenal neuroblastoma [20], the final diagnosis relies on histological data.

Classical presentation: In newborns with prenatal diagnosis of a renal mass, a clinical and biological close monitoring has to be performed with regular evaluation of blood pressure and calcemia [21]. An abdominal US is performed to confirm the mass, its limits, and content. Renal masses are usually well delineated. If adenopathies or calcifications are present, a diagnosis of neuroblastoma should be raised [20]. An abdominal MR imaging examination or CE-CT is mandatory to better define the extension of the lesion before surgery.

Mesoblastic nephroma has an excellent oncological outcome but a high risk of perinatal *life-threatening complications*. Besides the hemodynamic instability (hypertension), and the respiratory distress, these tumors may induce unusual acute clinical complications due to tumor rupture and massive hematuria leading to hemorrhagic shock [22, 23]. Furthermore, the mass effect of very large tumors on the digestive tract can lead to (sub)occlusion and vomiting. These

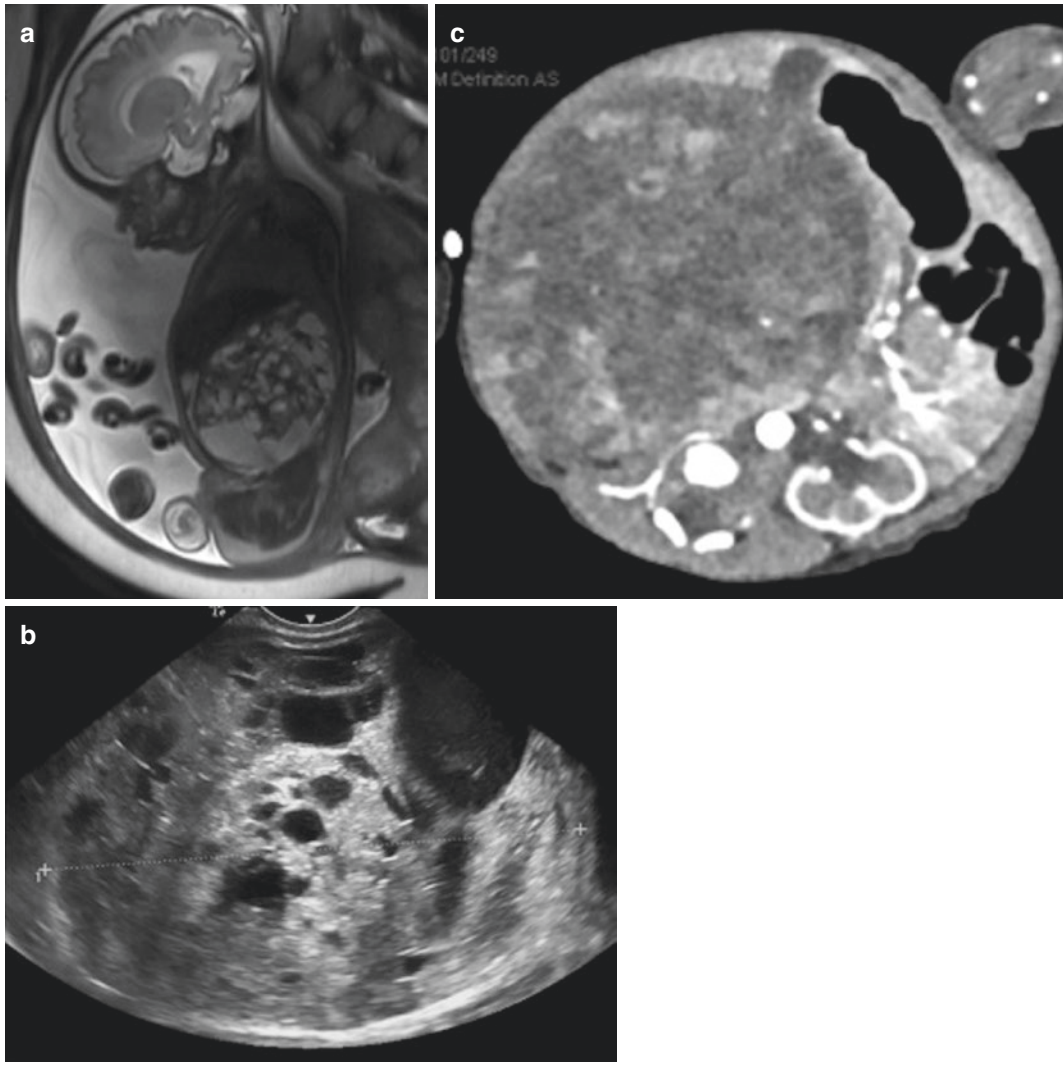

Fig. 5.8 Pre- and postnatal assessment of a mesoblastic nephroma. (**a**) Sagittal T2 weighted MR imaging of a 35-week-old fetus with hydramnios demonstrating a very large heterogeneous abdominal mass. (**b**) Neonatal US confirms the heterogeneous mass that almost completely fills the abdominal cavity. (**c**) Axial enhanced CT scan of the newborn demonstrates more accurately the limits of the mass and the relation with the displaced abdominal vessels

exceptional situations lead to urgent surgical resection of the affected kidney, and this can be anticipated, thanks to the prenatal diagnosis.

5.2.3.2 Suprarenal Masses

Suprarenal masses may be of variable origins. They are very often detected in the fetus. The main diagnoses are infradiaphragmatic sequestration, adrenal hemorrhage, and neuroblastoma. Infradiaphragmatic extralobar pulmonary sequestration is rare [24]; it corresponds to non-functional lung without any connection with the bronchial tree; its blood supply derives from systemic vessels. The prenatal diagnosis is generally made in the second trimester and relies on a well-circumscribed lesion with similar echogenicity compared to the lung parenchyma. The demonstration of the systemic vascular supply, which is not always obvious, confirms the diagnosis. The vessel may be more evident on fetal MR imaging.

Adrenal hemorrhage and the suprarenal neuroblastoma are most often depicted in the third trimester like heterogeneous or solid suprarenal masses. Their differential diagnosis may be difficult, both can present with cystic components. The main differentiating criterion is the rapid changes of echogenicity in cases of hemorrhage (Fig. 5.9). Noteworthy, both may involute spontaneously. MR imaging may help in detecting blood within the lesion, which is more in favor of a hemorrhage.

Classical presentation: In newborns with prenatal diagnosis of a suprarenal mass, a neonatal ultrasound is performed to confirm the diagnosis. The US criteria are the same as in the fetus. In case of sequestration (in the absence of clinical symptoms), a CE-CT scan is performed preferably between the third and sixth month of life in order to precise the vascular anatomy before surgery. In case of the suspicion of a neuroblastoma, MR imaging is the most useful imaging modality for the staging; it shows bone marrow infiltration and intraspinal extension much more accurately than CE-CT. Urinary catecholamines levels and I-MIBG scintigraphy are also mandatory in this context.

Very rarely, a suprarenal lesion may be life threatening and represent a *neonatal emergency*. A sequestration with high blood flow may lead to neonatal cardiac failure (Fig. 5.10), a cardiac support therapy should be initiated before surgery. Cases of severe respiratory distress have been reported; they are related to the upward displacement of the diaphragm secondary to huge bilateral adrenal cystic neuroblastoma requiring urgent debulking surgical procedure. This abdominal involvement can be rapidly confirmed by abdominal US [25].

5.2.3.3 Hepatic Masses

(See Also Chap. 8)

Hepatic masses are rare in the perinatal period. The three most frequent are hemangioendothelioma, mesenchymal hamartoma, and hepatoblastoma. Many are detected in utero. Hemangioendothelioma is a benign vascular tumor. Prominent US features include an intrahepatic mass with a complex heterogeneous pattern associated with dilated hepatic artery and veins indicating intratumoral arteriovenous shunting. Mesenchymal hamartomas are also complex intraparenchymal lesions that can be mostly cystic or with a mixed pattern but without vascular components demonstrable on US examination. Hepatoblastoma, the most common malignant liver tumor of infancy, appears like a solid hepatic mass.

Classical presentation: After birth, these lesions will be confirmed by an US with Doppler

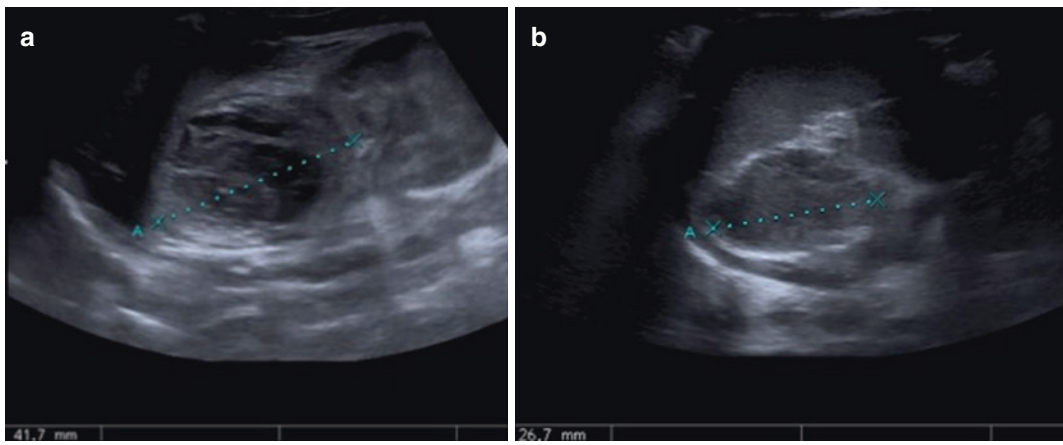

Fig. 5.9 Suprarenal neonatal mass. (**a**) Axial US neonatal scan on the left kidney showing a heterogeneous suprarenal mass that could correspond to a suprarenal hemorrhage or to a neuroblastoma. (**b**) US performed at 1 month shows the partial involution of the lesion favoring the diagnosis of a hemorrhage

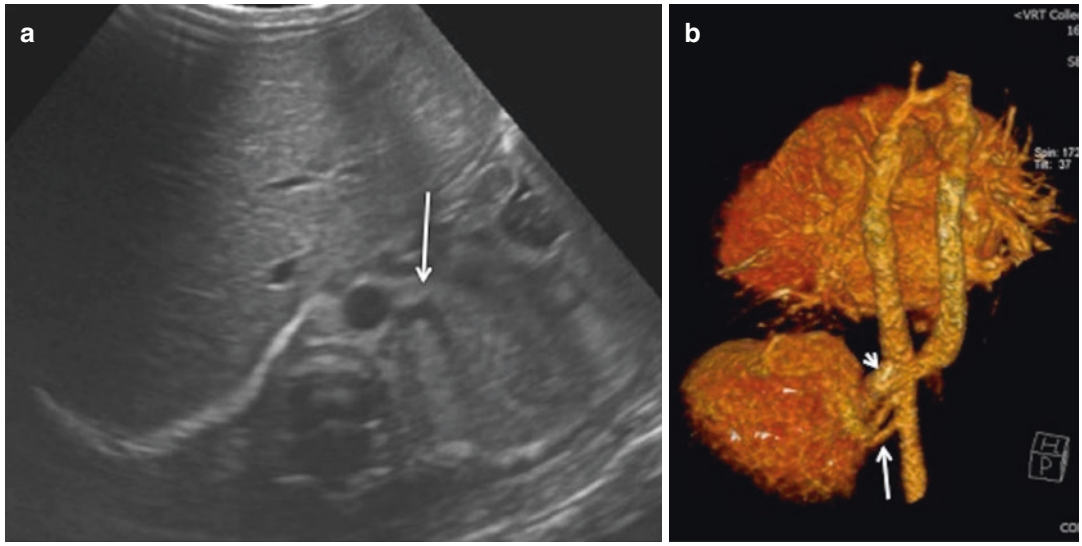

Fig. 5.10 Sequestration (the lesion was detected antenatally). (**a**) Axial neonatal US scan on the upper abdomen showing hyperechogenic mass with a systemic feeding vessel (*arrow*) confirming the diagnosis of sequestration. (**b**) 3D reconstruction of the CE-CT scanner performed after birth shows the highly vascularized lesion with two arterial feeding pedicles (*arrow*) arising from the aorta and one large vein draining in the dilated azygos vein. This vascular shunting has been responsible for a transitory cardiac failure

analysis. An associated abdominal MR Imaging or CE-CT is required in order to better characterize the lesion and precise its topography within the liver. A raised alpha-fetoprotein level is suggestive of hepatoblastoma. In case of massive hemangioendothelioma, corticotherapy generally leads to progressive involution of the tumor. Mesenchymatous hamartoma should be operated as these tumors do not regress spontaneously. Hepatoblastoma should be treated by chemotherapy and surgery as appropriated. A Beckwith-Wiedemann syndrome has to be excluded in babies with hepatoblastoma or mesenchymal hamartoma, as they can be associated features.

On rare occasions, these hepatic lesions may induce *acute neonatal complications*. The hemangioendothelioma may lead to cardiac failure and hydrops due to the important vascular intratumoral shunting (Fig. 5.11). Cases of rupture and hemorrhage in case of large mesenchymatous hamartoma or hepatoblastoma leading to hypovolemic shock have also been reported [26–28]. In cases of very large masses, babies may present with jaundice and respiratory distress, respectively, due to hepatic infiltration and upward displacement of the diaphragm [29].

It is important to differentiate vascular tumors from vascular malformations like portosystemic shunts (Fig. 5.12). The latter correspond to abnormal communications between the ombilicoportal and caval system and can be intra or extrahepatic (see Chap. 15) [30]. Most of them will close spontaneously but possible high vascular flow may lead to cardiac failure. Therefore, a close hemodynamic follow-up should be initiated before and after birth. In some cases, embolization will be necessary to prevent cardiac and hepatic failure (see also Chap. 8).

5.2.3.4 Congenital Sacrococcygeal Teratomas

Sacrococcygeal teratoma (SCT) is the most common location for teratoma. The tumor arises from the anterior part of the coccyx and may extend externally or within the pelvis and abdomen. It originates from Hensen' nodes and comprises all cell layers. Most fetal teratomas are benign; consequently, their prognosis relies mainly on their intrapelvic/abdominal extension and spinal canal

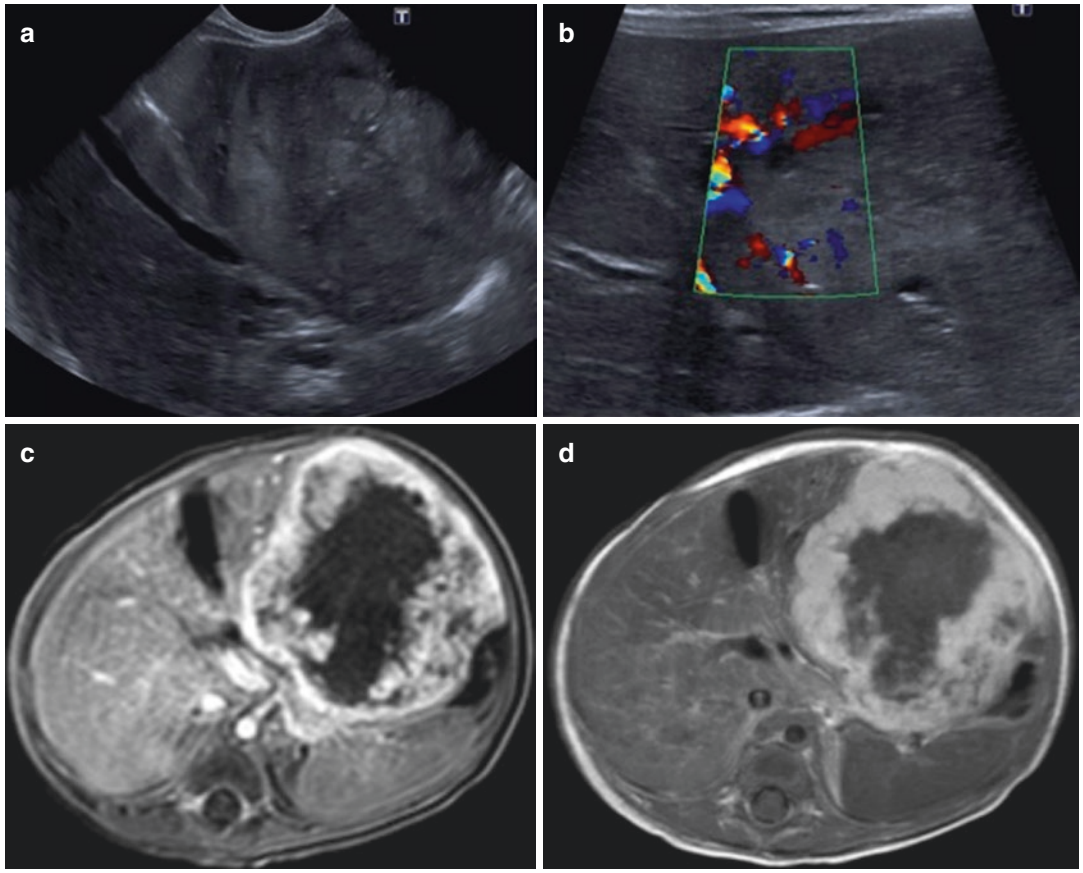

Fig. 5.11 Hepatic mass. (**a**) Axial US scan of the abdomen of a 20-day-old neonate presenting abdominal deformation without prenatal diagnosis. It shows a huge solid aspect lesion of the left hepatic lobe. (**b**) The lesion seems moderately vascularized on Doppler imaging. (**c**, **d**) The enhanced T1 weighted MR sequences show characteristic progressive centipede filling of a vascular tumor: hemangioendothelioma

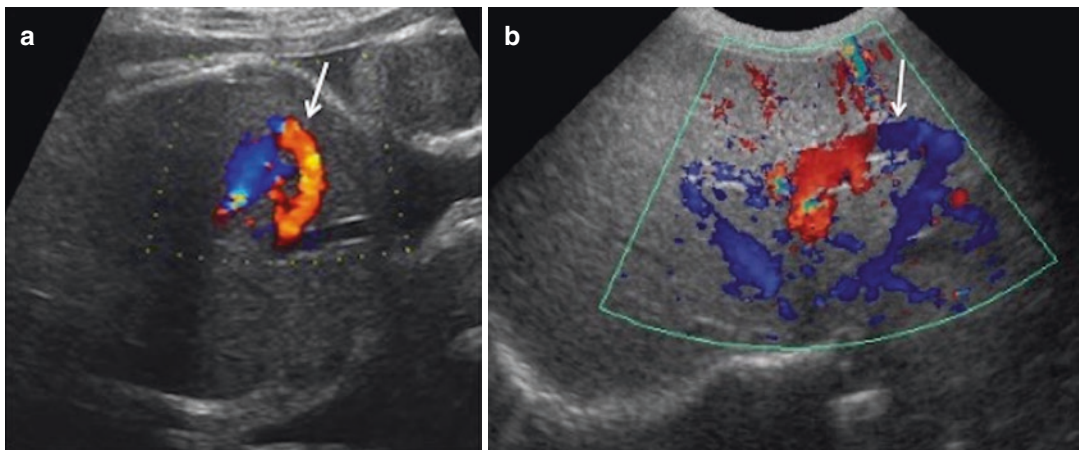

Fig. 5.12 Intrahepatic portosystemic shunt. (**a**) Axial US scan of the liver of a 36-week-old fetus showing the wide anastomosis between the left portal and one suprahepatic vein (*arrow*). (**b**) The same aspect is observed at birth; the shunt closed spontaneously within the first month of life

invasion [31]. Therefore, fetal MR imaging is performed as a complementary tool to US to better define the topography of the lesion and its impact on adjacent organs [32]. Some tumors can be huge, necessitating drainage of their large cystic components before delivery to prevent tumor or uterine rupture. The tissular part of the tumor is also important for the prognosis, as it can be highly vascularized and responsible for blood shunting leading to cardiac failure and hydrops. Fetal hemodynamic status should be carefully monitored.

Classical presentation: The postnatal management consists in neonatal US and MR imaging in order to define the tumoral extent before surgery. The prognosis relies on the consequences of the mass on the surrounding organs and on the hemodynamic and respiratory status of the newborn. It should be carefully monitored in specialized neonatal units.

Sometimes, an SCT can present, already in utero, *acute symptoms* necessitating urgent C-section and rapid surgical management [33]. Fetal cardiac failure secondary to high vascular output or to massive bleeding increases perinatal morbidity and mortality. Furthermore, the compressive tumor may interfere with renal or digestive tract function. Tumoral bladder outlet compression may lead to urinary retention and secondary renal failure (Fig. 5.13). Intramedullar

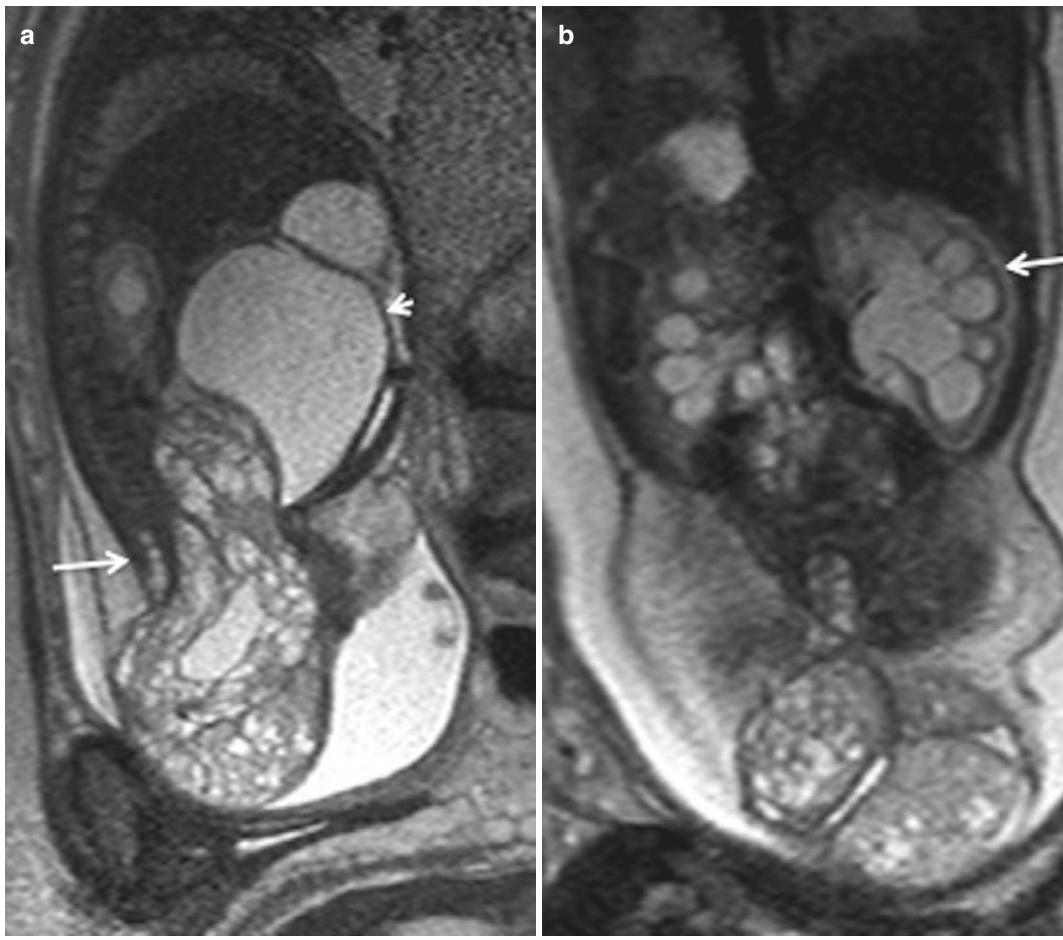

Fig. 5.13 Sacrococcygeal teratoma with intrapelvic development. (**a**) Sagittal T2 weighted MR imaging on a third trimester fetus showing a large mostly solid mass with microcysts infiltrating the spinal canal (*arrow*) and responsible for the distension of the genital tract (*arrow head*). (**b**) The coronal T2 weighted image shows the compression of the urinary tract by the pelvic mass that induces bilateral hydronephrosis (*arrow*)

infiltration may also be responsible for irreversible damage to the splanchnic or hypogastric nerves with the potential associated consequences as neurogenic bladder and fecal incontinence as well as reduced lower limbs mobility. All these complications render a rapid neonatal management mandatory.

5.2.3.5 Lymphatic Malformations

Lymphatic malformations are not real neoplasms. They are composed of distended cystic lymphatic channels and are generally diagnosed in the second or third trimester of pregnancy. They are mainly located in the cervico-facial and mediastinal regions but some can develop in the chest or abdomen. They appear as heterogeneous cystic and septated masses (Fig. 5.14a). The cystic components appear anechoic but sometimes they display an echogenic content suggesting intracystic hemorrhage. These lesions typically infiltrate or displace the surrounding organs.

Classical presentation: The postnatal management includes neonatal US and MR imaging in order to better define the loco-regional extension (Fig. 5.14b) and to differentiate intra- from retroperitoneal lymphangioma as well as to define the relation of the malformation with the intra-abdominal vessels. The treatment may generally

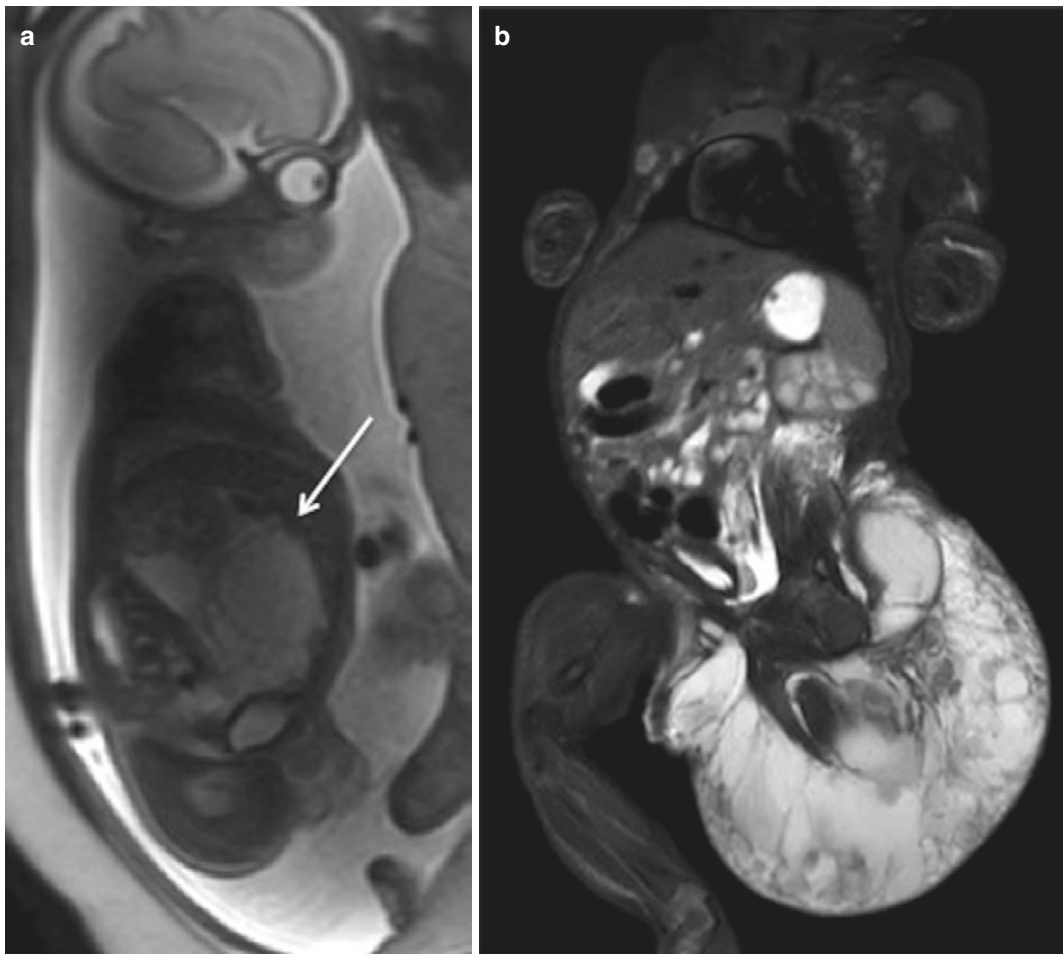

Fig. 5.14 Lymphatic malformation. (**a**) Sagittal T2 weighted MR image performed on a 29-week-old fetus showing a massive retroperitoneal lymphatic malformation presenting the typical cystic and septated aspect. (**b**) Post-natal T2 weighted coronal image demonstrates the extraabdominal extension with pelvic and left limb infiltration. The newborn died of acute sepsis

be delayed except in cases with important compression of intraabdominal organs and vessels. Whenever elected, surgery should be as complete as possible as these tumors may recur.

Uncommonly, it can happen that these lesions bleed and become therefore a *surgical emergency* for obvious hemodynamic reasons. They may also be infected and lead to acute septic situations. Some other will need rapid surgery because of infiltration of adjacent structures (Fig. 5.14). Rarely, like every large intraperitoneal mass, lymphatic malformations may interfere with digestive tract transit and lead to acute situations like (sub)occlusion or even volvulus [34].

5.3 Newborns with (Suspected) Antenatal Intestinal Occlusion

5.3.1 Introduction

Thanks to prenatal diagnosis, many neonatal digestive tract occlusions can be anticipated and the neonatal work-up is therefore simplified. In a newborn presenting signs of occlusion such as abdominal distension, bilious vomiting, delayed or absent meconium emission, it is mandatory to first refer to the prenatal data (hydramnios, digestive tract distension, colonic content, associated malformations, etc.) and second to be informed about the family history (cystic fibrosis, maternal diabetes, etc.).

Imaging will include a supine abdominal radiograph to confirm the obstruction. An US is performed to detect ascites, digestive tract wall damage, position of mesenteric vessels, abdominal masses and to precise as much as possible the etiology of abdominal distension. Thereafter, the newborn can rapidly be oriented either to the medical (ileus) or surgical management (atresia).

5.3.2 Upper Gastrointestinal Tract

5.3.2.1 Esophageal Atresia

Esophageal atresia (EA) is encountered in 1/3500 live births. The sensitivity of prenatal diagnosis is still quite poor (40%). It relies mostly on indirect signs like polyhydramnios and small or absent stomach. These signs are mainly encountered in EA type I. The proximal esophageal pouch can sometimes be demonstrated confirming the diagnosis. The most common type is the type III with a distal fistula between the airways and the distal esophagus leading to less obvious indirect signs (presence of a small stomach, discrete polyhydramnios). Fetal MR imaging increases the diagnosis sensibility being able to demonstrate more frequently the proximal pouch using dynamic acquisitions (Fig. 5.15).

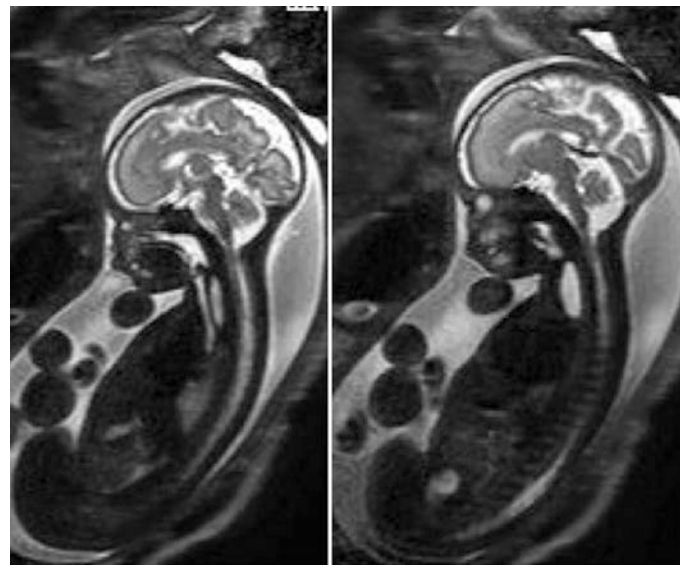

Fig. 5.15 Esophageal atresia—prenatal diagnosis. Dynamic MR sagittal T2 weighted images focused on the esophagus of a third trimester fetus showing the progressive filling of the proximal esophageal pouch establishing a diagnosis of esophageal atresia

Classical presentations: The neonatal diagnosis (even more if suspected/diagnosed prenatally) is very easy, thanks to the systematic introduction of a nasogastric tube. The surgical intervention can rapidly be planned and consists in a direct end-to-end suture of both esophageal extremities when the gap is short (less than one vertebral body) or to a gastrostomy allowing feeding before more invasive surgery is performed to compensate the gap with colonic interposition. However, associated anomalies, low birth weight, and long gap influence the therapeutic schedule and may render the treatment more difficult [35].

Less frequently, if there is neither prenatal diagnosis nor neonatal diagnosis, the newborn may present with respiratory distress at first feeding due to fluid leak within the airways in case of proximal fistula; pulmonary inhalation, infections, and sepsis may occur in case of the upper blind esophageal pouch. EA is therefore always a *surgical emergency* because this malformation is still responsible for significant morbidity and mortality [36]. The only imaging procedure required is a thoracic radiograph with a catheter in the proximal pouch and eventually an abdominal US to visualize the distal esophagus. In case of urgent gastrostomy, a gastric opacification and provoked esophageal reflux can be performed in order to approximate the length of the blind gap (Fig. 5.16).

To be noted, in rare cases, no stomach is seen in fetal abdomen and instead an intrathoracic cystic structure can be observed that should raise the differential diagnoses of hiatal hernia versus esophageal duplication (see above). At birth, a chest plain radiograph and a barium opacification may be necessary for this differentiation. Complicated hiatal hernia like gastric kinking or volvulus will necessitate urgent surgery.

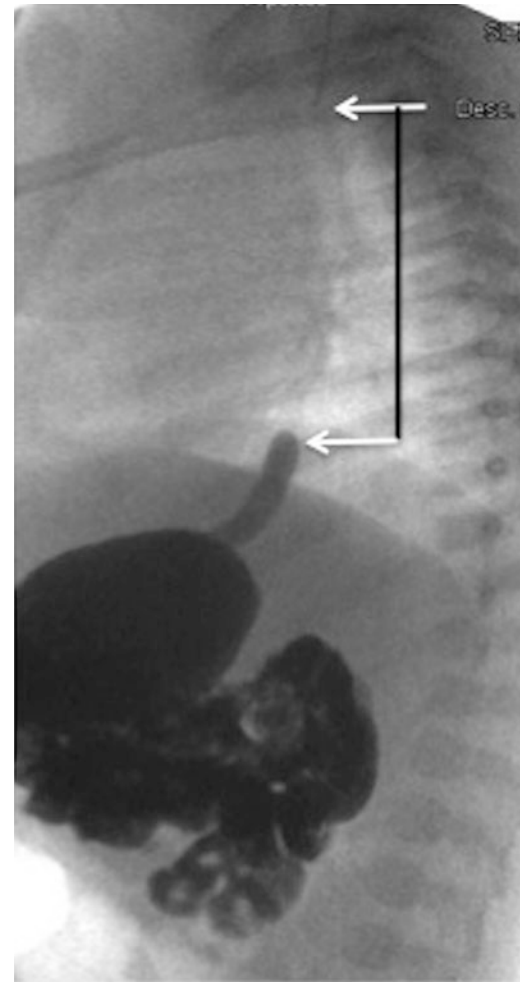

Fig. 5.16 Esophageal atresia: post-natal work-up. Lateral X-ray shows the end of the proximal pouch as limited by the catheter (*upper arrow*). The distal esophagus is opacified by reflux secondary to gastric filling by a gastrostomy (*lower arrow*). The gap between the two-blind ends is measured between the arrows (*black line*)

5.3.2.2 Duodenal Obstruction

The incidence of duodenal obstruction is 1–2 out of 10,000 live births. It is the commonest cause of neonatal intestinal obstruction. The prenatal US diagnosis has a very high sensitivity around 90–95% with the typical association of the double bubble sign (gastric and duodenal pouches) and hydramnios secondary to atresia, stenosis, or intraluminal web. The main prognostic factor is determined by the association with trisomy 21, which should be ruled out by chromosomal analysis.

Classical presentation: The prenatal diagnosis leads to surgical management at birth. In case of absent prenatal diagnosis, the newborn will present with vomiting and epigastric fullness and the abdominal radiograph will show the typical double bubble sign (Fig. 5.17). No complementary imaging is needed for the

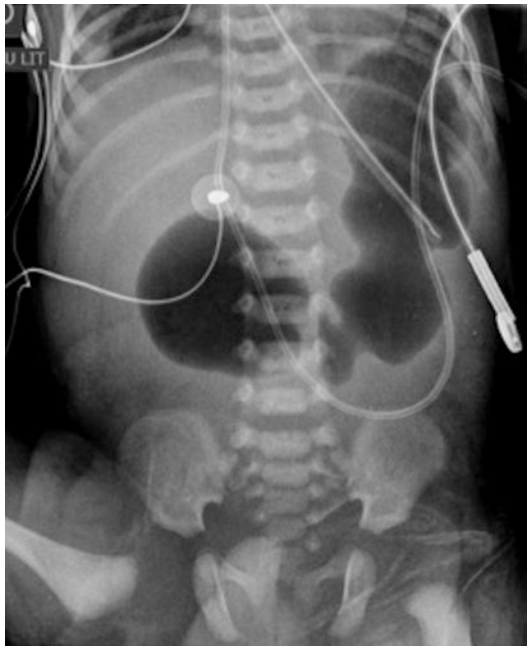

Fig. 5.17 Neonatal abdominal radiograph of a baby showing the typical double bubble sign pathognomonic of duodenal atresia

diagnosis; an abdominal US can be performed to rule out associated annular pancreas [37]. The prognosis seems to be unrelated to the exact location of the obstacle (infra- or supra-ampullary) or to a complete or incomplete obstruction.

Duodenal obstruction represents a surgical emergency in order to allow normal feeding. The complicated cases are mostly due to associated prematurity, associated malformations, and possible multiple atresias (which are usually discovered at surgery), [38].

5.3.3 Small Bowel Occlusion

5.3.3.1 Small Bowel Atresia

Small bowel atresia occurs in 1 in 4000 births. Different theories have been proposed to explain digestive tract atresia: lack of vacuolization of the solid cord stage of intestinal development or ischemic insult to the midgut due to mesenteric vascular occlusion [39, 40]. The atresia can be isolated but may also be multiple and associated with other locations that lead to more complex cases such as apple peel atresia [41]. Cystic fibrosis should always be considered, as it is an associated condition in 7–40% of cases. The diagnosis of atresia is generally performed in the third trimester and the proximal jejunum and distal ileum are the more commonly affected sites. The US signs in the prenatal period are dilatation of intestinal loops above 10 mm associated with polyhydramnios in case of proximal occlusion. Digestive wall damage can be suspected when there is wall thickening, ascites, or heterogeneous bowel content. Fetal MR imaging is a good complementary tool in order to better localize the site of occlusion (Fig. 5.18).

Classical presentation: A prenatal diagnosis leads to immediate neonatal gastric aspiration and subsequent surgery. It is always an emergency because of the important risk of perforation, meconium peritonitis, or volvulus secondary to the intestinal distension. The clinical symptoms are vomiting, delayed meconium emission, and distended abdomen. A supine abdominal radiograph can be performed to confirm obstruction, still it will not be always possible to differentiate proximal from distal obstruction (Fig. 5.19). An abdominal US may provide additional information about the viability of the bowel walls, evaluate the amount of ascites, analyze the position of the mesenteric vessels, and detect meconium pseudocysts. A contrast water-soluble enema might be performed before surgery to confirm the presence of the classical associated unused microcolon.

In any case, small bowel atresia is a *surgical emergency* that leads usually to the resection of the atretic segment, ileo- or jejunostomy and colostomy in order to allow feeding and the emptying of the colon. In the absence of complications, mostly due to a delayed diagnosis, the prognosis is good.

Noteworthy, *complications* do occur either in utero—circumstance that would prompt a cesarean section—or after birth [42]. Classical

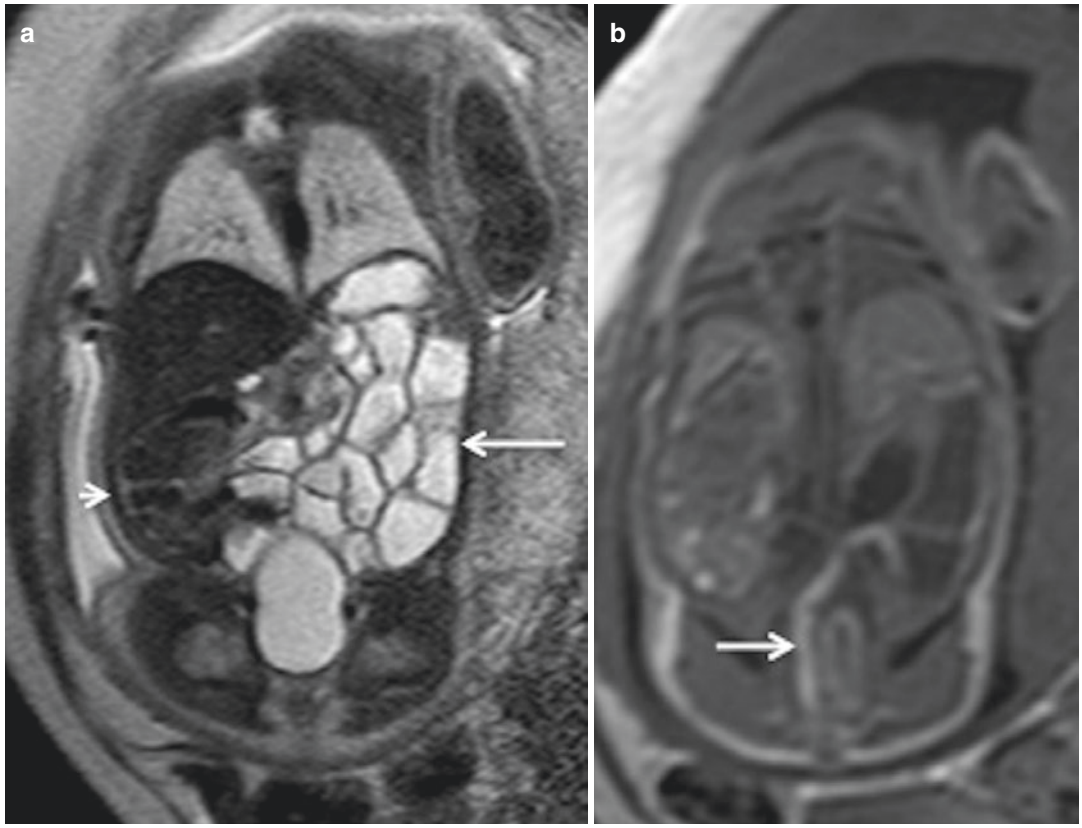

Fig. 5.18 Small bowel occlusion—prenatal diagnosis (Courtesy A. Massez MD). (**a**) Coronal T2 weighted MR imaging of a 32-week-old fetus (intestinal distension was observed on US). Thanks to the hypersignal content of the distended proximal loops (filled with amniotic fluid) and the collapsed distal loops filled with meconium (that appear in *black* (*arrow head*)); we suspected a mid-intestinal occlusion. (**b**) Coronal T1 weighted image demonstrates the classically associated microcolon (*arrow*)

complications are *volvulus*, due to the twisting of the dilated loop around the vascular pedicle showing the typical « whirlpool » sonographic sign and *perforation* leading to meconium peritonitis or to a meconium pseudocyst. The pseudocyst corresponds to a meconium collection walled by adhesions between the loops and the omentum which constitute a pseudocapsule. The pseudocyst appears on US like a heterogeneous collection with thin progressively calcifying wall (Fig. 5.20). Both situations require immediate surgery. Imaging should be limited to abdominal US to avoid delaying surgical treatment [43].

5.3.3.2 Meconium Related Occlusions: Meconium Ileus (See Also Chap. 7)

Most often, meconium ileus is associated with cystic fibrosis. The abnormal and sticky meconium gets impacted in the distal ileum and progressively dehydrates getting harder and obstructive. The bowel loops uphill dilate progressively and the final result is the same as in an atresia, with distended distal ileal loops and increased risk of volvulus and perforation. The prenatal pattern is the same that in atresia and the differential diagnosis is difficult except in cases with known cystic fibrosis. In neonatal

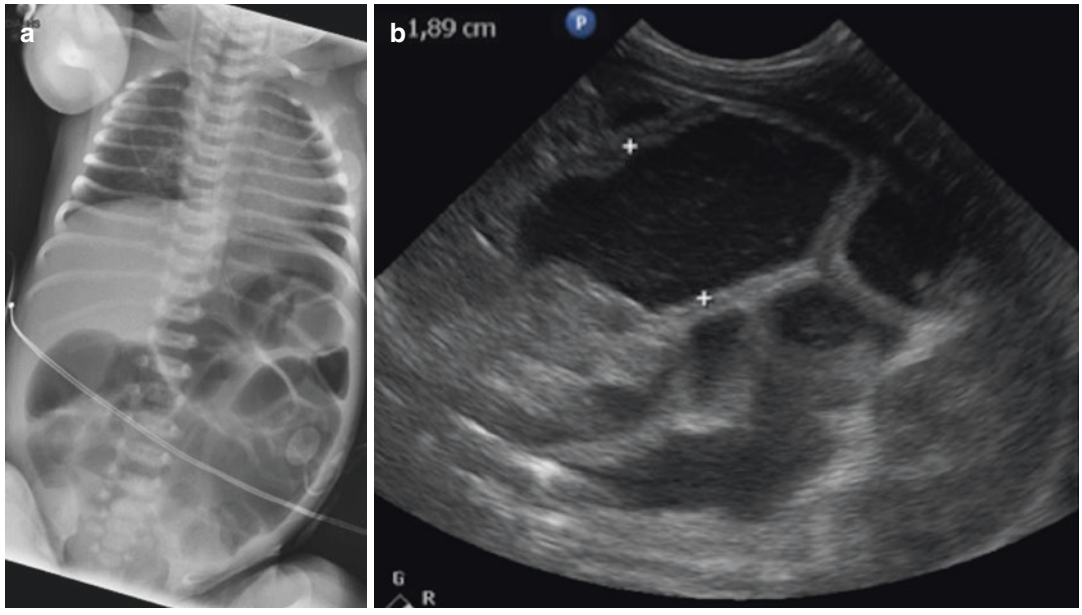

Fig. 5.19 Small bowel occlusion: neonatal work-up (Courtesy A. Massez MD). (**a**) Neonatal supine X-ray of the same baby as in Fig. 5.18 shows distended loops. (**b**) Abdominal US confirms the proximal small bowel distension. These data associated with the prenatal findings (Fig. 5.18) confirms the obstruction and the need for urgent surgery. Occlusion was confirmed, histology diagnosed an extended Hirschsprung disease

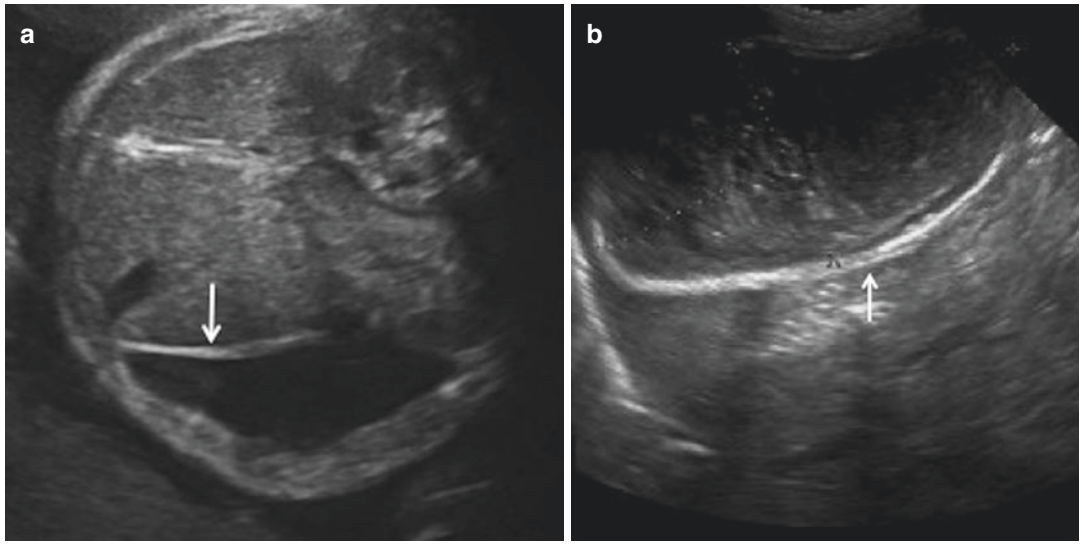

Fig. 5.20 Meconium peritonitis. (**a**) Axial US scan of the abdomen in a 32-week-old fetus showing a meconium pseudocyst. The collection presents hyperechoic walls secondary to calcifications (*arrow*). (**b**) Neonatal abdominal US performed at birth on the same baby shows a similar aspect. The newborn was subsequently (and rapidly) operated

cases without prenatal diagnosis, clinical symptoms develop around the third day of life by bilious vomiting and abdominal distension (see Chap. 7). A water soluble enema using diluted hyperosmolar contrast confirms the diagnosis by showing an unused microcolon without passage of contrast further than the ileocecal junction. On the contrary, in ileal atresia, the contrast would pass the ileocecal junction and opacify the distal nonobstructed ileum. Sometimes, the ileal reflux of contrast may lead to meconium evacuation and release of the mechanical obstruction obviating the need for surgery [44].

5.3.4 Colonic Occlusion

5.3.4.1 Colonic Atresia and Stenosis

Colonic atresia is a very rare condition, it represents 2–15% of digestive tract atresia; very few cases have been reported in the literature [45]. At prenatal US, the fetus presents dilated small bowel loops and distended proximal part of the colon above the atretic segment. Fetal MR imaging may help to localize the atretic site (Fig. 5.21a, b). The prenatal diagnosis may be difficult; on fetal MR imaging, some cases of small bowel occlusions may be mistaken for colonic atresia because of the confusing hyperintense content of the dilated loops, which are due to intraluminal hemorrhage within the small bowel and not to meconium content. To be noted, there may be multiple levels of stenosis leading to more difficult/impossible diagnosis and more complex surgical management.

Classical presentation: Newborns with colonic atresia present with delayed meconium passage, distended abdomen and bilious vomiting. Surgery should be performed without delay based on prenatal diagnosis. Postnatal imaging evaluation should be restricted to abdominal X ray, US, and/or colonic opacification (Fig. 5.21c, d).

In any case, colon atresia is a *surgical emergency* [46], consisting in resection of the atretic segment and colostomy for decompression or colo-colic anastomosis with covering ileostomy [47]. Later anastomosis is recommended to allow bowel length preservation. Like in all cases of bowel occlusion, acute complications like perforation or volvulus can occur.

5.3.4.2 Anorectal Malformations, Urogenital Sinus, and Genital Malformations

Abnormal progression of the urorectal septum leads to incomplete separation of the digestive from the urogenital tracts. Different types have been described and in each case, a complete anatomical mapping should be obtained after birth. The anomaly can include (or be limited) to anorectal malformations that occur in 1/2500 to 5000 live births. In some cases only the urinary and genital tracts are both abnormal leading to various forms of urogenital sinus (Fig. 5.22). These anomalies must be differentiated from cases where the malformation is limited to the genital tract with distention of the vagina (hydrocolpos). In such cases, prenatal diagnosis relies mostly on the detection of a cystic pelvic lesion behind the bladder and/or to the detection of an abnormal colonic content with enterolithiasis due to mixed urine and meconium. Fetal MR imaging is useful to clarify the anatomy of the malformation. Interruption of pregnancy can be proposed in complex cases (cloaque) because of the poor functional outcome of such malformations.

Classical presentation: At birth, the diagnoses of anorectal malformation or cloaque are clinically obvious. There might be a digestive perineal fistula allowing meconium evacuation, corresponding most probably to a low anorectal malformation. No imaging is required before surgery. In other more complex cases (for example with one perineal hole or meconium evacuation through the vagina or the urethra), complementary imaging is mandatory and should include abdominal US, cystography, and pelvic MR imaging (Fig. 5.23) in order to assess the complexity of the malformation. Surgery is not an emergency except in case of absent digestive tract evacuation pathway; in this context, urgent ileostomy and colostomy are performed.

Many patients will not be detected in utero. As mentioned, the diagnosis will usually be rapid

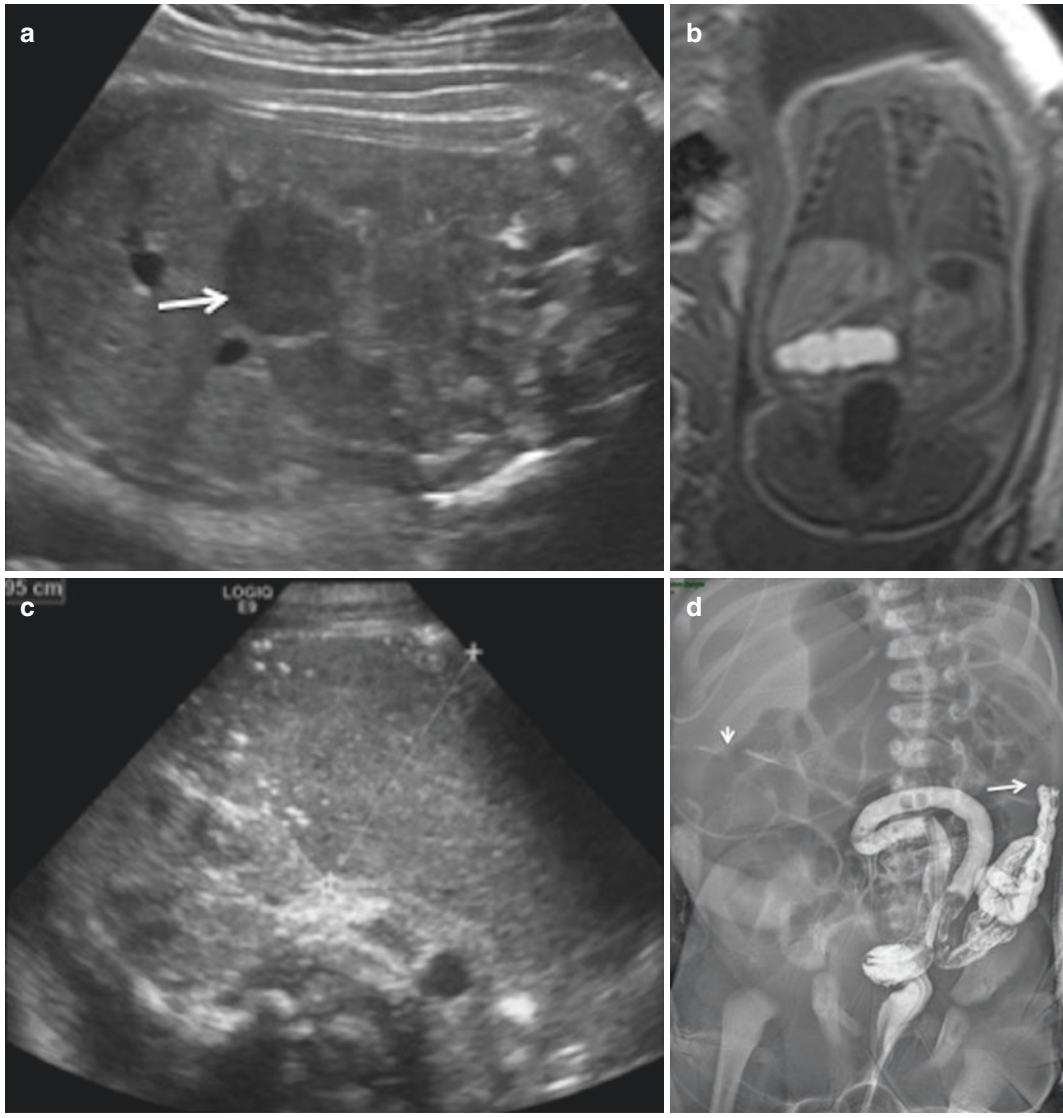

Fig. 5.21 Colonic atresia (Courtesy A. Massez MD). (**a**) Axial US scan of the abdomen of a 35-week-old fetus presenting a distended digestive loop with echogenic content (*arrow*). The differential diagnosis between dilated small bowel and colon is difficult. (**b**) MR imaging: coronal T1 weighted sequence shows that the dilated hyperintense loop corresponds to the colon filled with meconium. Only the right and transverse parts of the colon were visualized suggesting a rare diagnosis of left colic atresia. (**c**) On post-natal US, the right colon was extremely dilated (*crosses*). (**d**) Radiopaque enema demonstrates the complete atresia of the left colon at the splenic angle (*arrow*) and the distended proximal colon (*arrow head*)

after birth, thanks to clinical examination. As mentioned, imaging, mainly US, cystography, and colonic opacification will help to determine the type of anomaly. Cystography and colonic opacification will diagnose the presence of fistula. Surgery will be performed rapidly [48]. It is obviously also urgent to initiate a prophylactic antibiotherapy to prevent urinary tract infections. Assuring meconium evacuation and preventing infections are the two urgent measures to be taken.

In some cases, US will demonstrate an isolated distended vagina and potentially uterus which can be encountered in congenital imperforate hymen accompanied with hydro/metrocolpos (Fig. 5.24). Marked distended vagina can induce interlabial swelling and cause urinary tract obstruction and

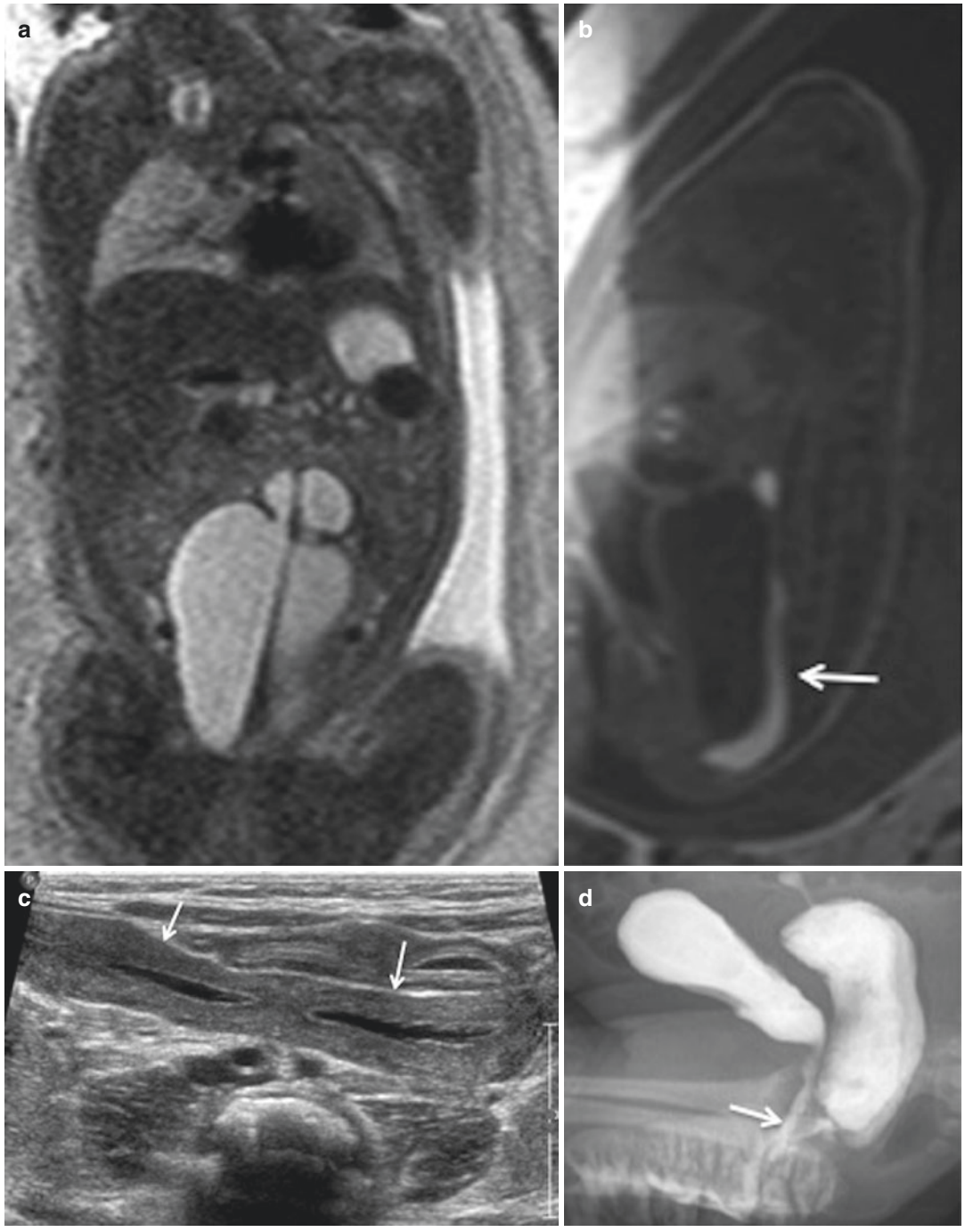

Fig. 5.22 Urogenital sinus. (**a**) Fetal MR imaging: coronal T2 weighted image performed at 33 weeks to evaluate a cystic pelvic mass seen at obstetrical US. The "mass" appears septated and corresponds to a duplicated genital tract distended by fluid suggesting a complex malformation with a urogenital fistula. (**b**) Sagittal T1 weighted sequence shows a normal colon (*arrow*) attesting that the digestive tract is not involved in the malformation. (**c**) Neonatal pelvic US confirms the duplicated genital tract with two vaginal and two uterine cavities (*arrows*). (**d**) Neonatal retrograde opacification of the bladder outlines the fistula and the genital tract (*arrow*)

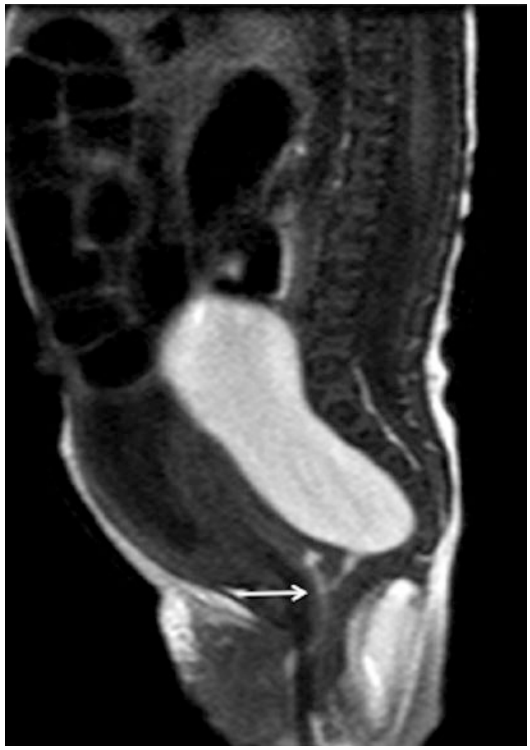

Fig. 5.23 Recto-ureteral fistula—MR imaging. Sagittal T1 weighted image performed on a newborn showing a distended rectal pouch filled with meconium. The hyperintense meconium fills the fistula connecting the rectum with the proximal urethra (*arrow*)

bladder retention. Perforating the hymen will usually be sufficient to remove the obstruction, prevent pain and retrograde flow [49].

5.4 Newborns with Dilated Urinary Tract

5.4.1 Introduction

Emergencies in relation with urinary tract anomalies are mainly related to enlarged bladder, or massive upper urinary tract dilatation. The latter is most frequent malformation as it represents 0.2–2% of the fetal malformations. They need to be carefully evaluated and treated because of the potential risk of renal damage secondary to the obstruction, reflux, or infection. They are mainly detected in utero but sometimes, the etiology of the dilatation (obstruction or reflux) is unclear before birth. The main role of prenatal diagnosis is to detect the cases with poorer outcome. The prenatal (indirect) markers of the renal function are the patterns of the renal parenchyma (renal size, parenchymal thickness, corticomedullary differentiation, presence of cysts, etc.) and the amniotic fluid volume.

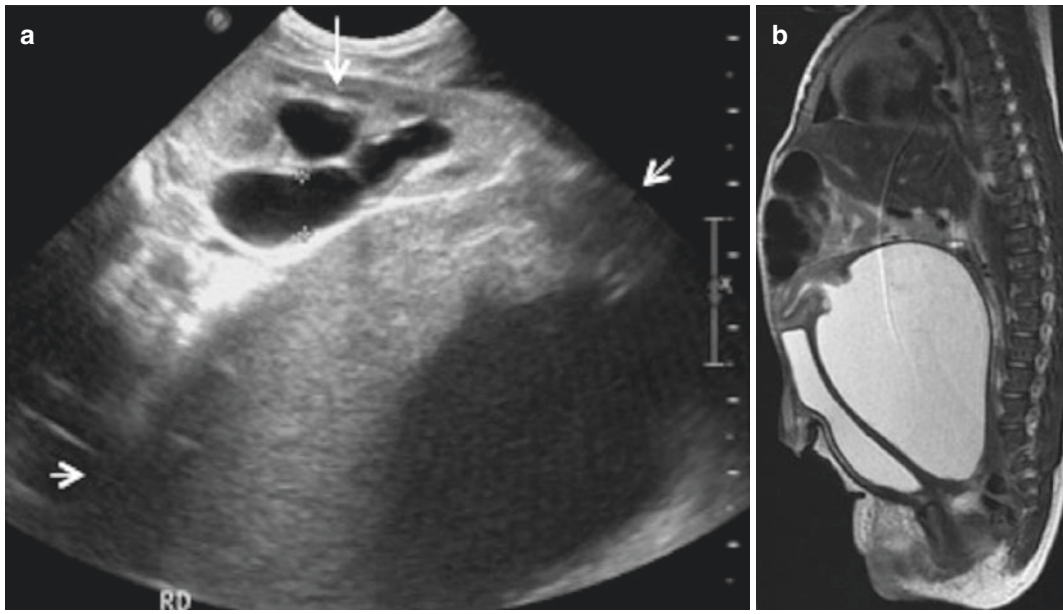

Fig. 5.24 Neonatal hydrocolpos. (**a**) Parasagittal US performed on a 4-day-old newborn showing a distended pelvic structure with fine echogenic sedimentation (*arrow heads*) causing hydronephrosis (*arrow*). (**b**) Sagittal T2 weighted MR imaging confirmed the diagnosis of hydrocolpos

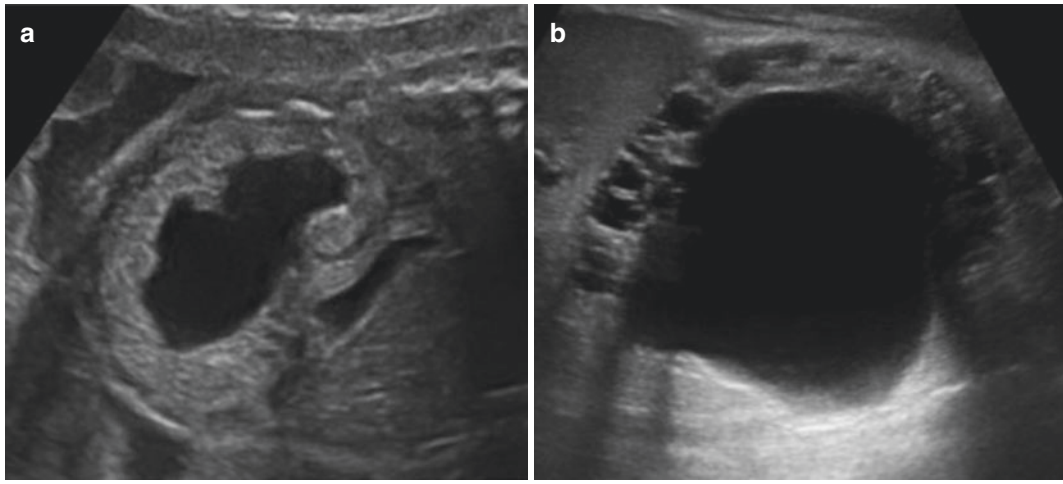

Fig. 5.25 Renal dysplasia secondary to obstruction. (**a**) Obstetrical US: Sagittal US scan of the left kidney in a 23 -week-old fetus. The pyelocaliceal system is dilated and the renal parenchyma appears without differentiation and hyperechoic. No cysts were visible at that age. (**b**) Neonatal US of the same kidney shows persistent marked dilatation of the renal pelvis secondary to a (probable) pyeloureteral obstruction. Multiple cysts are present in a thin and undifferentiated renal parenchyma attesting of obstructive renal dysplasia. No reflux was seen on cystography

5.4.2 Upper Urinary Tract Dilatation

Upper urinary tract dilatation is considered when the pelvicalyceal cavities are enlarged and the renal pelvis anteroposterior diameter is superior to 7 mm in the third trimester of the pregnancy or in the neonatal period. Most dilatations are mild or moderate and do not necessitate urgent postnatal management. When the dilatation is massive (above 30 mm), the work-up should be more immediate. Such dilatations can compress the digestive tract and induce digestive symptoms. These huge dilatations may also jeopardize the renal function. Such findings can be encountered in high grade reflux, ureteropelvic junction obstruction, and ureterovesical obstruction. In the latter, there can be an associated dilated ureter or renal duplication. The diagnoses are mostly suspected in utero but the newborns will need complementary neonatal investigations to clarify the etiology of the dilatation.

Classical presentation: A sonographic examination should be performed in neonates with a prenatal history of upper urinary tract dilatation to measure the renal cavities, rapidly after birth in case of massive dilatation, within two weeks in milder cases. Signs suggestive of obstruction are dilated renal pelvis, urinoma, and possible renal parenchymal hyperechogenicity with cysts (Fig. 5.25). Signs suggestive of reflux are fluctuating renal pelvic diameter, parietal wall thickening, dilated ureter, enlarged bladder, etc. [50]. However, none of these signs is specific and the only way to confirm reflux is by a cystography.

Preventing infection is of upmost importance. Newborns with significantly dilated renal cavities or confirmed high grade reflux should beneficiate of antibiotic prophylaxis. In cases of very huge (giant) dilatation due to proximal ureteropelvic junction obstruction, renal external drainage should be placed [51].

5.4.3 Megabladder

In utero, a megabladder is defined in the second and third trimester as a bladder with a long axis on a midsagittal US scan of more than 30 and 50 mm, respectively. The main point is to differentiate between an obstructive megabladder secondary to posterior ureteral valves or to a prolapsed ureterocele (in case of duplication) from a megabladder associated with high grade reflux. The neonatal work-up should be adapted accordingly. Dysplastic megabladders as encountered in Prune Belly syndrome or megabladder-microcolon-intestinal-hypoperistalsis syndrome are generally diagnosed earlier in pregnancy due

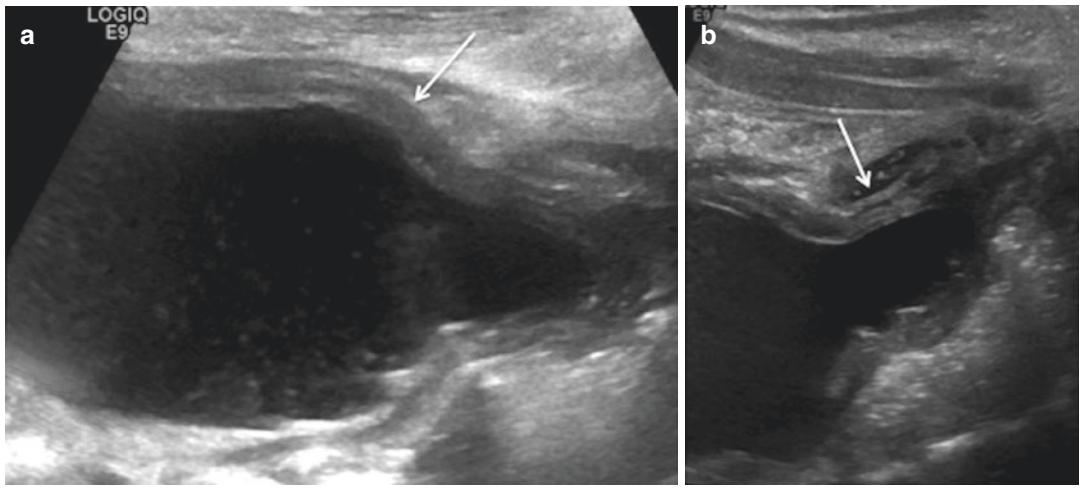

Fig. 5.26 Neonatal megabladder and PUV. (**a**) Neonatal US pelvic scan performed in a newborn with a fetal history of megabladder. US shows an enlarged bladder with thickened wall (*arrow*). (**b**) Perineal approach: The posterior urethra is dilated (*arrow*)

to associated findings and often lead to medical interruption of the pregnancy because of their poor prognosis.

Classical presentation: In newborns with a prenatal history of megabladder, an US should be performed rapidly after birth. The US investigation should analyze the entire urinary tract. Bladder wall thickening and dilated proximal urethra in a male fetus will orient the diagnosis towards a urethral obstruction such as posterior urethral valves (Fig. 5.26). The upper urinary tract should be analyzed in detail to exclude renal duplication, megaureter, or renal dysplasia that will worsen the prognosis (Fig. 5.27) [52]. The main difficulty is that obstructive bladders may be associated with uni- or bilateral reflux (that will resolve after valves resection). The final diagnosis is established on cystography that should be performed in the neonatal period whenever the diagnosis of megabladder is confirmed.

Relieving uphill hyperpressure due to the obstruction is a *neonatal emergency*. Once the diagnosis is confirmed, endoscopic treatment in cases of PUV or antibiotic prophylaxis in cases of high grade reflux can be applied.

5.5 Newborns with Congenital Anomalies Necessitating Early Neonatal Work-Up

5.5.1 Congenital Adrenal Hyperplasia

Neonatal endocrine emergencies are rare, however, stabilizing endocrine disorders may be challenging. Several different systems can be affected and clinical presentation can be subtle. Again, prenatal diagnosis may in some cases help in the neonatal care of newborns with prenatally detected pathologies associated with metabolic acute disorders.

Such a situation can be encountered in congenital adrenal hyperplasia. It is a disorder associating impaired adrenal cortisol biosynthesis and androgen excess. The diagnosis is suspected in utero in cases of virilized female fetuses. The suprarenal glands present a typical “cerebriform” pattern (Fig. 5.28), which along with the biological data leads to the diagnosis. The classical 21-hydroxylase deficiency, the commonest cause of adrenal hyperplasia, may lead to life-threatening neonatal salt wasting. The diagnosis is ascertained

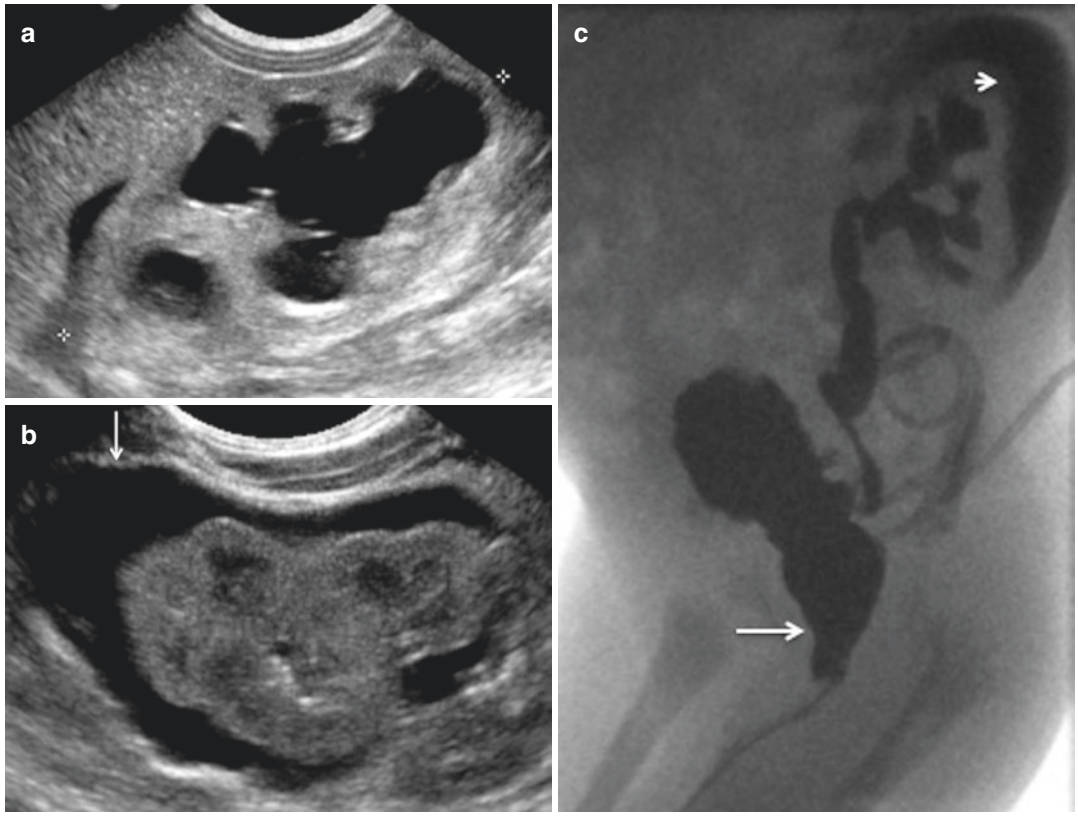

Fig. 5.27 Neonatal renal dysplasia and PUV (Courtesy C. Dimitriou MD). (**a**, **b**) Sagittal US scans of the kidneys performed on a newborn presenting clinically with distended abdomen. There was massive ascites on US (not shown) and the kidneys appear bilaterally dysplastic, with associated urinoma on the left side (*arrow*). (**c**) A retrograde cystography was performed showing the distended posterior urethra (*arrow*), the left associated reflux and the urine leak into the abdomen (*arrow head*)

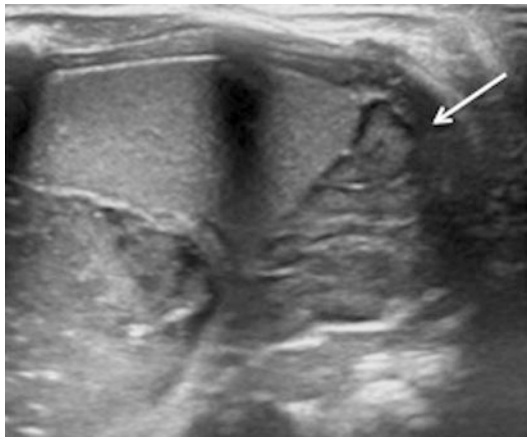

Fig. 5.28 Neonatal US in a newborn with congenital adrenal hyperplasia. The suprarenal glands present a typical "cerebriform" aspect (*arrow*)

by demonstrating high serum 17 hydroxyprogesterone levels [53]. In the absence of prenatal diagnosis, which mostly occurs in male newborns (who have normal external genital aspect), the situation can be life threatening because of delayed electrolyte compensation.

Conclusion

Prenatal diagnosis allows a more rapid and adequate neonatal work-up for newborns with anomalies or malformations. It may involve the digestive or the urinary tracts and medical or surgical emergencies. In each situation, the appropriate hospital, medical care unit, and medical team can be chosen according to the

pathology. The parents can also be better prepared to this stressful beginning in life of their baby.

References

1. Marchitelli G, Stimmermann J, Acanfora MM, et al. Prenatal diagnosis of intra-abdominal cystic lesions by fetal ultrasonography: diagnostic agreement between prenatal and postnatal diagnosis. Prenat Diagn. 2015;35(9):848–52.
2. Catania VD, Briganti V, Di Giacomo V, et al. Fetal intra abdominal cysts: accuracy and predictive value of prenatal ultrasound. J Matern Fetal Neonatal Med. 2016;29(10):1691–9.
3. Temiz A, Oguzkurt P, Serin Ezr S, et al. Differential clinical presentations, diagnostic difficulties and management of cecal duplication. J Pediatr Surg. 2013;48:550–4.
4. Puligandla PS, Nguyen LT, St. Vil D, et al. Gastrointestinal duplications. J Pediatr Surg. 2003;38:740–4.
5. Puraligegowda AK, Mohanty PK, Razak A, et al. Neonatal intestinal obstruction secondary to a small bowel duplication cyst. BMJ Case Rep. 2014;8:bcr2014204187. doi:10.1136/bcr-2014-204187.
6. Tawil KA, Crankson S, Emam S, et al. Cecal duplication cyst: a cause of intestinal obstruction in a newborn infant. Am J Perinatol. 2005;22(1):49–52.
7. Patel RV, Brown LM, More B, et al. Neonatal perforated appendix forming antibioma masquerading as duodenal duplication. BMJ Case Rep. 2013;2013(jul29 1):bcr2013200067. doi:10.1136/bcr-2013-200067.
8. Hur J, Choon-sik Y, Myung-Joon K. Imaging features of gastrointestinal tract duplications in infants and children: from oesophagus to rectum. Pediatr Radiol. 2007;37:691–9.
9. Laskowska K, Galaska P, Daniluk-matras I, et al. Use of diagnostic imaging in the evaluation of gastro intestinal tract duplications. Pol J Radiol. 2014;79:243–50.
10. Trinh TW, Kennedy AM. Fetal ovarian cysts: review of imaging spectrum, differential diagnosis, management and outcome. Radiographics. 2015;35(2):621–35.
11. Kim HS, Yoo SY, Cha MJ, et al. Diagnosis of neonatal ovarian torsion: emphasis on prenatal and postnatal sonographic findings. J Clin Ultrasound. 2016;44(5):290–7.
12. Ozca HN, Balci S, Ekinci S, et al. MR imaging findings of fetal-neonatal ovarian cysts complicated with ovarian torsion and autoamputation. AJR. 2015;205:185–9.
13. Papic JC, Billmire DF, Rescorla FJ, et al. Management of neonatal ovarian cysts and its effect on ovarian preservation. J Pediatr Surg. 2014;49(6):990–3.
14. Jeanty C, Frayer EA, Page R, et al. Neonatal ovarian torsion complicated by intestinal obstruction and perforation, and review of the literature. J Pediatr Surg. 2010;45(6):e5–9. doi:10.1016.
15. Kim MJ, Park YN, Han SJ, et al. Biliary atresia in neonates and infants: triangular area of high signal intensity in the porta hepatis at T2-weigted MR cholangiography with US and histopathologic correlation. Radiology. 2000;215(2):395–401.
16. Okada T, Sasaki F, Ueki S, et al. Postnatal management of prenatally diagnosed choledochal cysts. J Pediatr Surg. 2004;39:1055–8.
17. Chardot C, Debray D. Biliary atresia: a condition requiring urgent diagnosis and treatment. Arch Pediatr. 2011;18(4):476–81.
18. Siddiqui MM, Grier D, Cusick E. Postnatal rupture of an antenatally diagnosed choledochal cyst: first case report. Acta Paediatr. 2006;95(1):115–7.
19. Do AY, Kim JS, Choi SJ, et al. Prenatal diagnosis of congenital mesoblastic nephroma. Obstet Gynecol Sci. 2015;58(5):405–8.
20. Garnier S, Maillet O, Haouy S, et al. Prenatal intrarenal neuroblastoma mimicking a mesoblastic nephroma: a case report. J Pediatr Surg. 2012;47(8):e21–3.
21. Soheilipour F, Ashrafi M, Hashemipour M, et al. Pamidronate therapy for hypercalcemia and congenital mesoblastic nephroma: a case report. Cases J. 2009;2:9315.
22. Hu JM, Wu TT, Chan SW, et al. Congenital mesoblastic nephroma presenting with massive hematuria and hemorrhagic shock: report of one case. Acta Paediatr Taiwan. 2006;47(3):135–8.
23. Leclair MD, El-Ghoneimi A, Audry G, et al. The outcome of prenatally diagnosed renal tumors. J Urol. 2005;173(1):186–9.
24. Kalenahalli KV, Garg N, Goolahally LN, et al. Infradiaphragmatic extralobar pulmonary sequestration: masquerading a supra renal mass. J Clin Neonatol. 2013;2(3):146–8.
25. Avanzini S, Conte M, Granata C, et al. Life threatening bilateral cystic neuroblastoma in an infant. J Pediatr Hematol Oncol. 2009;31(12):963–4.
26. Esteves E, Goraib JA, Martins JL. Hepatic mesenchymal hamartoma in neonates. J Pediatr. 1997;73(5):345–8.
27. Wan P, Susman J, Kandel J, et al. Neonatal hepatic mesenchymal hamartoma causing cardiac failure and disseminated intravascular coagulopathy. Am J Perinatol. 2009;26(8):601–4.
28. Lai M, Burjonrappa S. Perinatal haemorrhage complicating neonatal hepatoblastoma: case report. J Pediatr Surg. 2012;47(10):e29–32.
29. Chattopadhyay S, Mukherjee S, Boler A, et al. Hepatoblastoma in the neonatal period: an unusual presentation. J Cytol. 2012;29(4):252–4.
30. Jerabek-Klestil S, Brantner C, Nehoda R, et al. Prenatal sonographic diagnosis of intrahepatic portosystemic shunts. J Ultrasound Med. 2014;33:543–6.
31. Jelin E, Jelin AC, Lee H. Sacrococcygeal teratoma with spinal canal invasion prenatally diagnosed. J Pediatr Surg. 2009;44(4):E9–11. doi:10.1016.
32. Avni F, Guibaud L, Robert Y, et al. MR imaging of fetal sacrococcygeal teratoma: diagnosis and assessment. AJR. 2002;178(1):179–83.

33. Fadler KM, Askin DF. Sacrococcygeal teratoma in the newborn: a case study of prenatal management and clinical intervention. Neonatal Netw. 2008;27(3):185–91.
34. Solari V, Mullassery D, Lansdale N, et al. Laparoscopic excision of a retroperitoneal lymphatic malformation in a newborn. J Pediatr Surg. 2011;46(2):e 15–7.
35. Hannon EJ, Billington J, Kiely EM, et al. Oesphageal atresia is correctable and survivable in infants less than 1kg. Pediatr Surg. 2016;32(6):571–6.
36. Fall M, Mbaye PA, Horace HJ, et al. Oesophageal atresia: diagnosis and prognosis in Dakar, Senegal. Afr J Pediatr Surg. 2015;12(3):187–90.
37. Rattan KN, Singh J, Dalal P. Neonatal duodenal obstruction: a 15-year experience. J Neonatal Surg. 2016;5(2):13.
38. Gharpure V. Duodenal atresia. J Neonatal Surg. 2014;3(1):14.
39. Werler MM, Sheehan JE, Mitchell AA. Association of vasoconstrictive exposures with risks of gastroschisis and small intestinal atresia. Epidemiology. 2003;14:349–54.
40. Louw JH, Barnard CN. Congenital intestinal atresia: observations on its origin. Lancet. 1955;2:1065–7.
41. Onofre LS, Maranhao RF, Martins EC, et al. Apple-peel atresia: enteroplasty for intestinal lengthening and primary anastomosis. J Pediatr Surg. 2013;48(6):E5–7.
42. Lee SH, Cho HN, Kim HY, et al. Clinical experience of complex jejunal atresia. Pediatr Surg Int. 2012;28(11):1079–83.
43. Sinha S, Sarin YK. Outcome of jejuno-ileal atresia associated with intraoperative finding of volvulus of small bowel. J Neonatal Surg. 2012;1(3):37.
44. Carlyle BE, Borowitz DS, Glick PL. A review of pathophysiology and management of fetuses and neonates with meconium ileus for the pediatric surgeon. J Pediatr Surg. 2012;47(4):772–81.
45. Elisa Z, Cinzia C, Sergio S, et al. Multiple congenital colonic stenosis: a rare gastrointestinal malformation. Case Rep Pediatr. 2016;2016:1–4. article ID 6329793.
46. Etensel B, Temir G, Karkiner A, et al. Atresia of the colon. J Pediatr Surg. 2005;40(8):1258–68.
47. Mirza B, Iqbal S, Ijaz L. Colonic atresia and stenosis : our experience. J Neonatal Surg. 2012;1(1):4.
48. Maletha M, Khan TR, Gupta A, et al. Presentation of high ano-rectal malformation beyond neonatal period. Pediatr Surg Int. 2009;25(4):373–5.
49. Ozturk H, Yazici B, Kucuk A, et al. Congenital imperforate hymen with bilateral hydronephrosis, polydactyly and laryngocele: a rare neonatal presentation. Fetal Pediatr Pathol. 2010;29(2):89–94.
50. Ismaili K, Hall M, Piepsz A, et al. Primary vesicoureteral reflux detected among neonates with a history of fetal renal pelvis dilatation: a prospective clinical and imaging study. J Pediatr. 2006;148:222–7.
51. Shimada K, Matsumoto F, Kawagoe M, et al. Urological emergency in neonates with congenital hydronephrosis. Int J Urol. 2007;14(5):388–92.
52. Hochart V, Lahoche A, Priso RH, et al. Posterior uretral valves: are neonatal imaging findings predictive of renal function during early childhood ? Pediatr Radiol. 2016;10:1418–23.
53. Sharma R, Seth A. Congenital adrenal hyperplasia: issues in diagnosis and treatment in children. Indian J Pediatr. 2014;81(2):178–85.

(Acute) Renal Failure in the Full Term Neonate

6

Fred E. Avni and Annie Lahoche

Contents

F.E. Avni (✉)
Department of Pediatric Imaging,
Jeanne de Flandre Hospital,
Avenue Eugène Avinée, 59037 Lille-Cedex, France
e-mail: Freddy.Avni@chru-lille.fr

A. Lahoche
Department of Pediatric Nephrology,
Jeanne de Flandre Hospital,
Avenue Eugène Avinée, 59037 Lille-Cedex, France

6.1 General Considerations

Acute renal failure (ARF) is a quite common problem in the neonate and there are many different etiologies. ARF is classified as pre-renal, intrinsic renal, and post-renal. It is characterized by an increase in the blood concentration of creatinine and nitrogenous waste product, a decrease in the glomerular filtration rate and by the inability of the kidney to appropriately regulate fluid and electrolytes homeostasis. Noteworthy, directly after birth and up to the fifth day, the serum creatinine of the newborn is the reflection of maternal renal function. Therefore, its use should be cautious as evidence for renal failure. A decline of urine output is a common clinical manifestation of ARF (less than 0.5–1.0 mL/kg/h); yet, many forms of ARF are associated with normal urine output. ARF will be clearly confirmed when the creatinine level raises above 30 μmol/L after the fourth or the fifth day.

The precise incidence and prevalence of ARF in the newborn is uncertain. Studies in NICU (neonatal intensive care units) have shown that this incidence ranges from 6 to 24% of newborns. Neonates who have undergone cardiac surgery, prematures (see also Chap. 4), newborns with sepsis, and newborns with severe asphyxia are particularly vulnerable. Nephrotoxic medications may increase the renal damage. Other studies have shown that some newborns have genetic risk

F.E. Avni, P. Petit (eds.), *Imaging Acute Abdomen in Children*,
https://doi.org/10.1007/978-3-319-63700-6_6

factors for ARF (in relation with alteration of the renin-angiotensin system). Furthermore, ARF may have a prenatal origin associated with IUGR, congenital diseases such as renal dysplasia and CAKUT (congenital anomalies of the kidney and urinary tract), renal cystic diseases or diseases secondary to maternal intake of some medications. US is the main imaging technique able to provide some useful information able to precise the diagnosis [1–3].

6.2 Imaging Approach: The Central Role of US

Because of its advantages of portability and lack of ionizing radiation, US is the primary (and usually only) imaging modality used to determine the origin of the ARF. High frequency transducers allow precise evaluation of the renal parenchyma. Doppler, color, and duplex may provide useful additional information. The US appearance of the kidneys in neonates is characteristic and different than in older children. The renal cortex is quite echogenic as compared to the liver and spleen and the cortico-medullary differentiation (CMD) is particularly obvious (Fig. 6.1). The resistive index (RI around 0.9) is especially high in the neonatal period. In several conditions, the renal changes will enable to provide useful information to approach the etiology of the ARF [2–4].

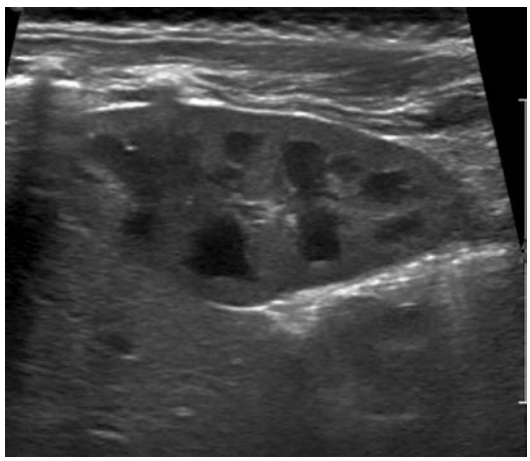

Fig. 6.1 Normal kidney Sagittal scan - Note the obvious Cortico-medullary differentiation

6.2.1 RF from Antenatal Origin

As mentioned, in the newborn, renal failure may have a prenatal onset in a wide spectrum of diseases such as renal congenital bilateral uropathies, hypodysplasia, and hereditary renal cystic diseases or as a result of maternal diseases and treatments. Anomalies may already have been detected in utero during obstetrical US [5] and transmission of this type of information will be essential for the proper management of the patients. For others, the anomaly will be detected immediately after birth due to renal (oligoanuria) or extrarenal symptoms (associated malformation as in Potter's syndrome or spontaneous massive pneumothorax—see below). Finally, in some patients, ARF will be diagnosed during the work-up of failure to thrive or urinary tract infection.

6.2.1.1 Congenital Uropathies (see Also Chap. 5)

Congenital anomalies of the kidney and urinary tract (CAKUT) are frequently detected in utero and in up to 5% of the neonates. If CAKUT occurs unilaterally, the prognosis is usually good. *Bilateral renal disease* (Fig. 6.2) with oligohydramnios in utero indicates global renal dysfunction and potentially pulmonary hypoplasia with respiratory distress after birth and increased risk of pneumothorax (Fig. 6.2a). Typically, posterior urethral valves (PUV) with marked urinary tract dilatation and severe renal dysplasia, bilateral renal dysplasia associated with massive vesicoureteric reflux will potentially be associated with neonatal RF (that would evolve towards chronic renal failure) (Fig. 6.2b, c). Similarly, anomalies (obstruction, or massive reflux) occurring on a single kidney will also induce neonatal RF (Fig. 6.3).

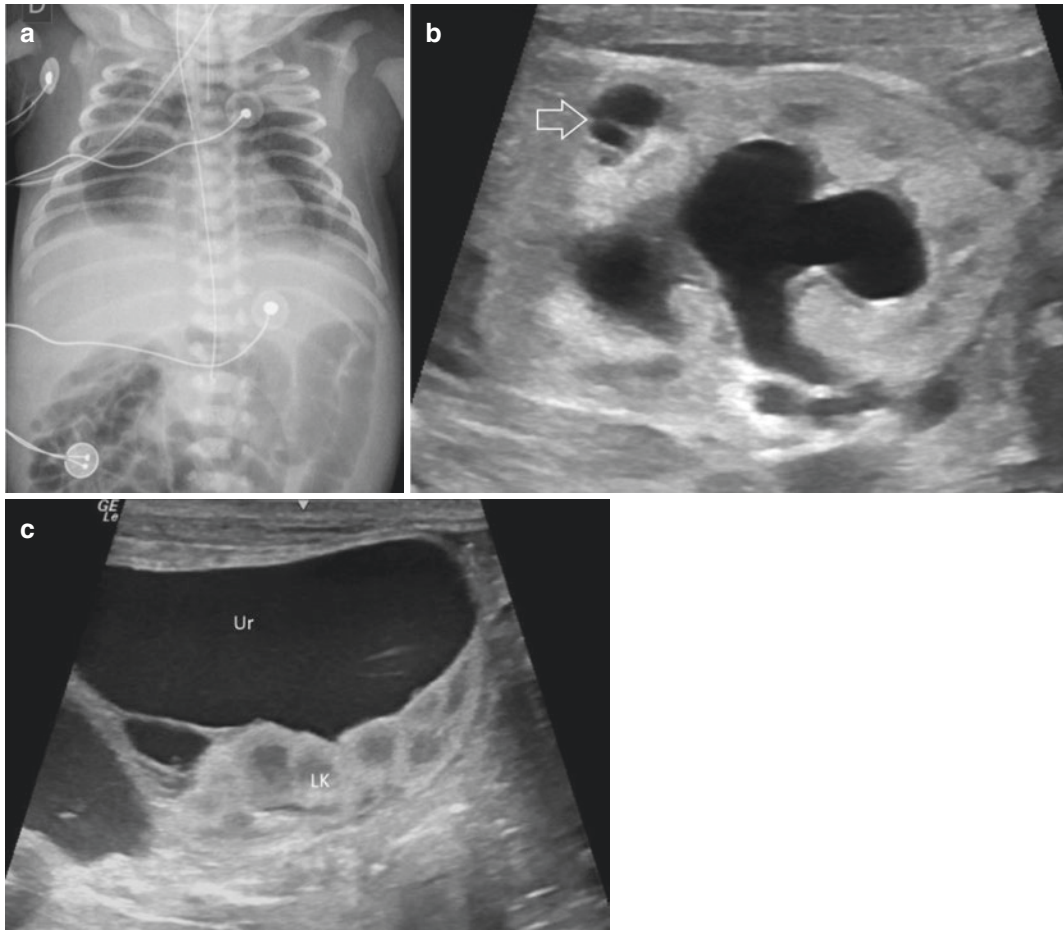

Fig. 6.2 (LK Fig 6.2 A Case of PUV (CAKUT) (**a**) Chest X ray showing massive pneumothorax and pneumomediastinum. (**b**) US - sagittal scan of the right kidney - urinary tract dilatation is obvious; cystic obstructive dysplasia is visible (*arrow*). (**c**) US - sagittal scan of the left kidney - A large urinoma (U) is displacing the kidney (k)

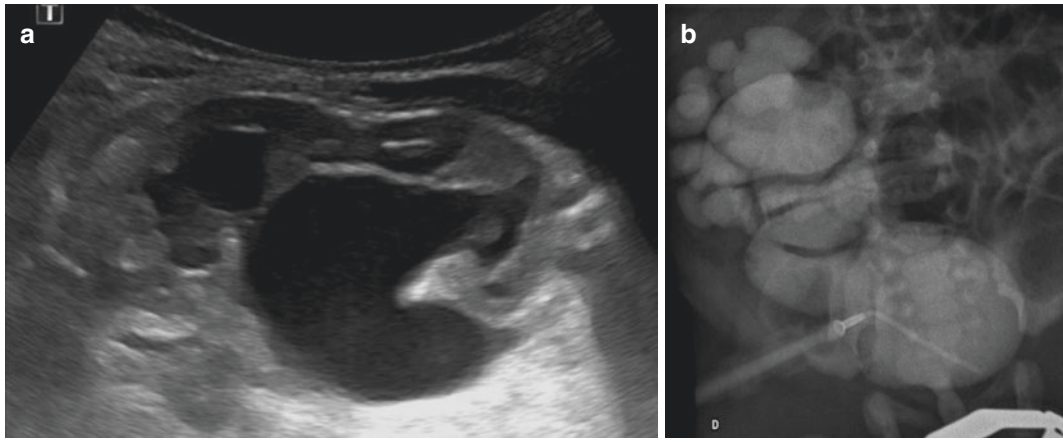

Fig. 6.3 Hypodysplasia and vesico-ureteric reflux. (**a**) Ultrasound sagittal scan of the right kidney showing marked dilatation, loss of CMD in a small kidney (3 cm). (**b**) VCUG: massive grade V r right reflux into the right kidney

Any significant antenatal data and any clinical suspicion of complex CAKUT should lead to rapid postnatal ultrasound examination in order to confirm and characterize the anomaly. The examination should start by an evaluation of the bladder and urethra (including using the perineal access): enlarged thickened bladder in a male neonate would suggest PUV whereas enlarged thinned bladder would suggest VUR. In case of VUR and PUV, the urinary tract may or may not be dilated uni- or bilaterally. Small kidneys, echogenic renal parenchyma, absent CMD, cortical or medullary cysts (Fig. 6.2b) are all features indicating renal (hypo)dysplasia. Perirenal urinoma appearing as a fluid collection (Fig. 6.2c) around the kidney may be present as well. To be noted, the kidneys in PUV may appear normal and conversely highly dysplastic kidneys do not necessarily imply RF.

A voiding cystourethrogram should be performed whenever the US examination raises a suspicion of PUV or massive VUR in order to confirm the anomaly. Functional assessment by scintigraphy should be delayed till the age of 6 months, waiting for the kidneys physiological maturation [5–10].

6.2.1.2 The Imaging Approach to Congenital Renal Hypodysplasia

When obstetrical and/or perinatal ultrasound demonstrate small kidneys (<2SD to the mean), a suspicion of *hypodysplastic kidneys* should be raised. The etiologies of hypodysplastic kidneys are numerous; familial and maternal history and genetic studies are essential in order to precise the diagnosis. While hypodysplasia is a histologic diagnosis (hypoplasia = reduction of the number of nephrons; dysplasia = architectural disorganization of the kidney), in selected cases, the sonographic characteristics of the kidneys may orient the diagnosis [1–4, 11, 12].

First, and mentioned above, *bladder outlet obstruction* (as in PUV) and *VUR* may be associated with renal hypodysplasia in fetuses and newborns (Fig. 6.3). Fetal vesical sphincter hypertonicity induces hyperpression uphill inducing tubular dysfunction. Glomerular and renal development is negatively affected.

On US, the kidneys will usually appear small, hyperechoic, and without CMD [13].

Genetic mutations may induce hypodysplastic kidneys. Major progresses have been made for understanding the implication of various genes in the development of the kidney, especially in the interaction between the ureteral bud and the metanephric blastema. It has been demonstrated that any event interfering with this interaction in relation with genetic mutations would induce perturbations of the renal development and typically hypodysplasia. Several specific genetic mutations have been characterized. Some will present an RF already at birth. Mutations of transcription factor TCF2 and gene HNF1β have been described several years ago. These mutations determine among others a spectrum of renal anomalies, partial pancreatic agenesis, and genital anomalies. Hypodysplastic kidneys are among the phenotypic expressions that can be encountered in association with such mutations. On ultrasound, the kidneys of HNF1β mutation may appear small (or asymmetric in size), hyperechoic, without CMD; small subcapsular cysts may be visible as well (Fig. 6.4) [14–16]. Other mutations

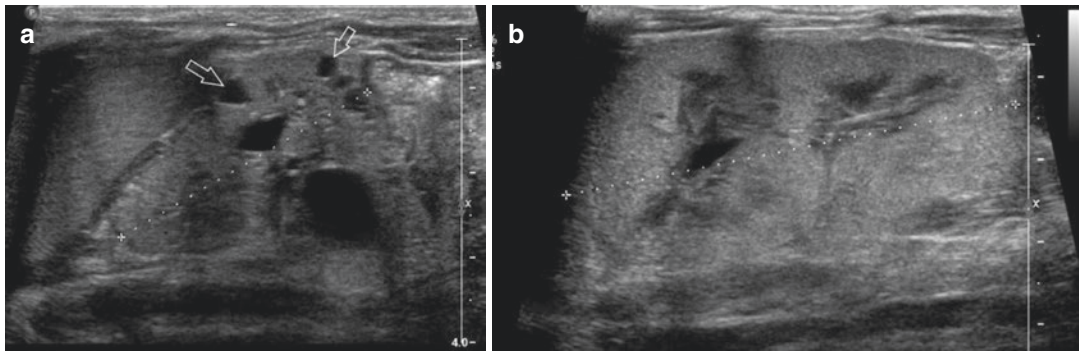

Fig. 6.4 Case of HNF1β mutation with asymmetric kidneys. (**a**) Left kidney appearing small, hyperechoic without CMD and tiny peripheral cysts (*arrows*). (**b**) Right kidney appearing larger, hyperechoic, without CMD and no cysts

(such as genes PAX 2, SALL1 or EYA 1) may be involved as etiology for hypodysplastic kidneys as well; the US characteristics seem less specific.

Congenital tubular dysgenesis (CTD) related to a dysfunction of the renin-angiotensin system (RAS) is another cause of renal hypodysplasia. On histology, CTD is characterized by the absence of the proximal renal tubules. Oligohydramnios is observed in utero due to decreased urine output; death may occur already in utero. If the patient survives, respiratory distress and massive pneumothorax develop at birth due to pulmonary hypoplasia. The newborns will remain oligo-anuric and consequently their mortality is high. CTD can be genetically transmitted but also acquired. The genetic disease is transmitted as autosomal recessive trait. Acquired CTD appears secondary to twin-twin-transfusion syndrome (TTTS), to congenital hemochromatosis and secondary to several maternal medications that are susceptible to block the RAS. Clinically, the symptoms are similar to those observed in the hereditary type of CTD. In all these entities, the kidneys may appear small and highly echogenic on US (Fig. 6.5a); other patterns can be observed as well (Fig. 6.6). Furthermore, the kidneys may appear normal. The most typical cases will show marked delay in ossification of the cranial vault (Fig. 6.5b) [17–22].

6.2.1.3 Hereditary Cystic Diseases

Hereditary renal cystic diseases include various entities classified as ciliopathies (and the so-called

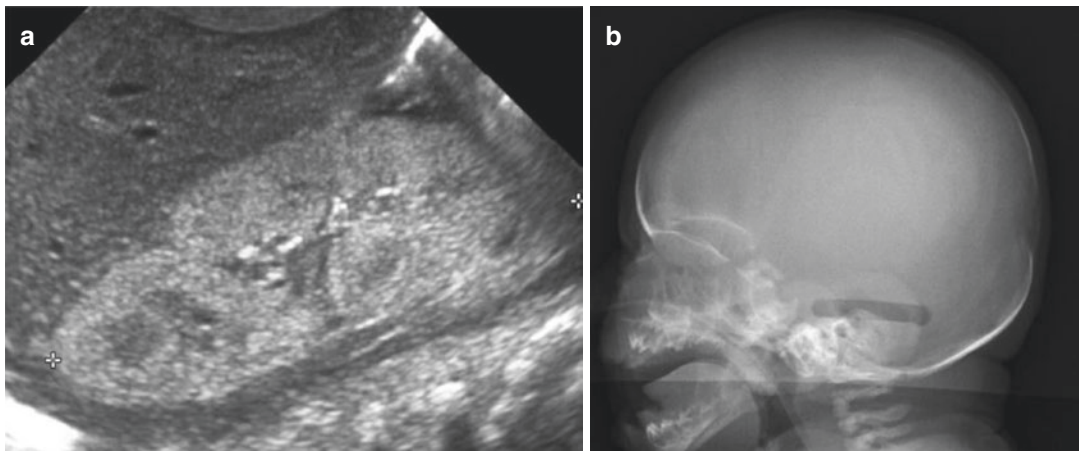

Fig. 6.5 Congenital tubular dysgenesis (Courtesy M Cassart MD). (**a**) Neonatal US of the right kidney (the left appeared equal): striking hyeprechogenicity without CMD. (**b**) Xray of the skull : marked delayed ossification typical in the syndrome

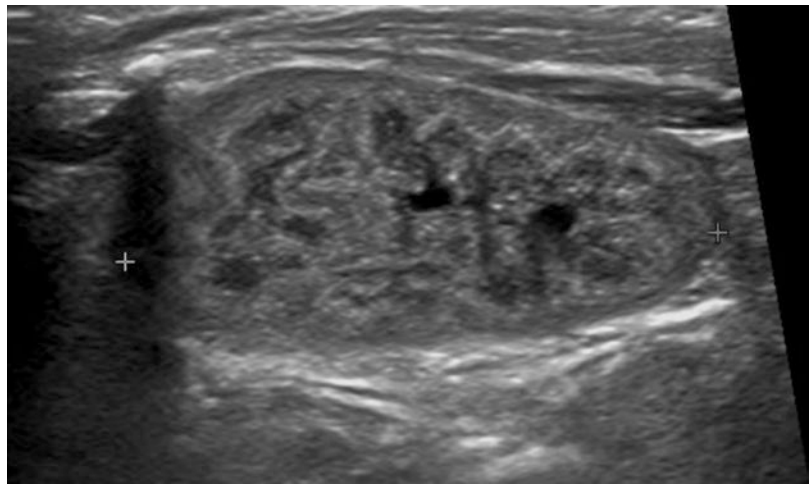

Fig. 6.6 Case of maternal intake of antihypertensive medication leading to hypodysplasia of the kidneys - sagittal scan of the left kideny (the right appeared equal). Abnormal pyramids with irregular margins

hepato-renal fibro-cystic diseases). Therefore, it should be stressed again that the US examination should include not only the urinary tract but also the liver, the spleen, the pancreas and the internal genital organs in order to look for associated malformations. A few among the renal cystic diseases will display RF already at birth progressing into CRF. Still, for the majority of patients, RF will develop later in infancy or childhood.

Autosomal recessive polycystic kidney disease (ARPKD) is related to a mutation of the gene PKHD1 (cases with truncated mutations have a poorer perinatal outcome). This mutation causes fusiform dilatation of the renal collecting ducts to a variable extent. There are variable phenotypes in relation with the extent of the tubular anomalies. Cases with extensive tubular anomalies will usually be detected in utero *a very large kidneys (8–10 cm) with hyperechoic kidney, poor or reversed CMD*; oligohydramnios will develop. Large medullary cysts may already be visible (Fig. 6.7). At birth, these patients may present spontaneous pneumothorax and oligoanuria. Mortality is high in such early presentation [5, 23].

Autosomal dominant polycystic kidney disease (ADPKD) is the most common genetically transmitted renal cystic disease. Mutations of the gene PKD1, PKD2, and PKD3 have been reported. In most cases, the disease is clinically silent up to adolescence or adulthood; in some instances, the disease will be symptomatic at birth with hypertension and ARF. In such cases, the kidneys will appear enlarged (6–7 cm), hyperechoic, without CMD but with subcapsular cysts (Fig. 6.8) (the so-called glomerulocystic type of ADPKD) [5, 23].

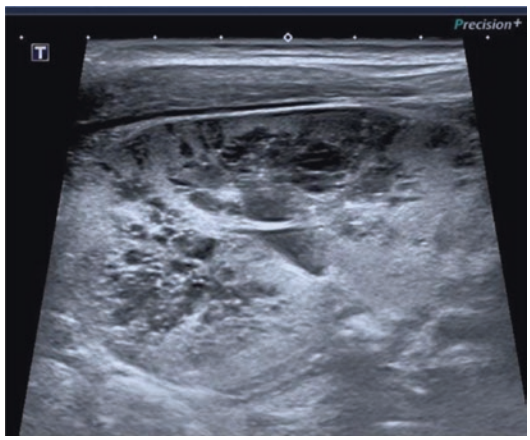

Fig. 6.7 Case of Autosomal recessive polycystic kidney disease. Sagittal scan of the kidneys that appear enlarged with cystic changes within the pyramids

Glomerulocystic kidneys, or kidneys with glomerular cysts, represent a third group of hereditary kidneys diseases. On histology, the peri-glomerular Bowman space will be distended and appear cystic. On US, the cysts will be typically located in the periphery of the cortex and in the subcapsular area. The rest of the kidneys will appear hyperechoic, and without CMD. Glomerulocystic kidneys are typically encountered in the autosomal dominant familial glomerulocystic diseases, in HNF1β mutation, in various syndromes (e.g., Melas syndrome). Furthermore, glomerular cysts can be found in association with obstructive dysplasia. AS mentioned above, HNF1β mutation encoding the TCF2 factor has been shown to correspond to the most common cause of hyperechoic kidneys in the fetus. Various phenotypes may appear in relation with this mutation. Most typically, on US the kidneys will appear normal sized, with a CMD and with subcapsular cysts (Figs. 6.4 and 6.8). Other patterns can be encountered: small kidneys, absent CMD, asymmetric kidneys, renal agenesis, multicystic kidney, urinary tract dilatation, etc. The cysts may also develop postnatally or within the medulla. Infrequently, a RF may be present at birth already. Noteworthy, a pancreatic hypoplasia may also be a neonatal feature of the disease [5, 15, 23].

The complex nephronophthisis/medullary cystic dysplasia will display typically cysts at the cortico-medullary boundaries within a kidney without CMD. It can be an isolated renal disease or included in a polymalformative syndrome (e.g., Joubert syndrome). Rarely a neonatal RF will be present [5, 23].

6.2.1.4 Congenital Nephrotic Syndromes

In nephrotic syndromes (NS), there is a massive leakage of proteins in the urine potentially inducing hypovolemia, hypercoagulability, and infections. They are defined by the association of edema, proteinuria > 50 g/L, protidemia < 50gr/L, and serum albumin level < 20 g/L.

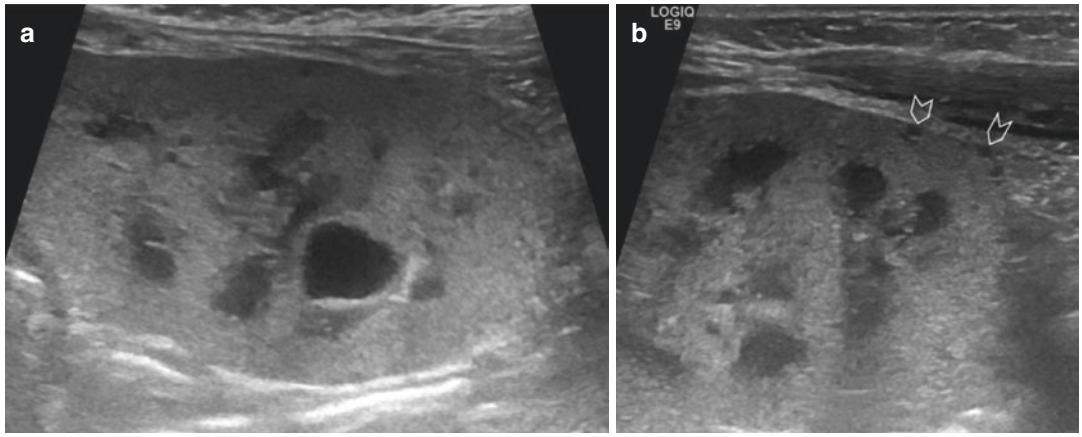

Fig. 6.8 Autosomal dominant polycystic kidney disease in a neonate. (**a**) Sagittal scan of the left kidney : hyperechoic cortex, one cyst is visible. (**b**) Sagittal scan of the right kidney: hyperechoic cortex with tiny peripheral subcapsural cysts (*arrows*)

Congenital nephrotic syndromes (CNS) is a NS diagnosed in utero or during the first 3 months of life. More and more genetic defects are detected in the different types of CNS. Some CNS present as an isolated renal disease while others are part of a polymalformative syndrome. In several CNS, US is able to demonstrate anomalies that would facilitate the diagnosis. Furthermore, for some CNS, symptoms will start already in utero and obstetrical US might detect some anomalies (e.g., echogenic kidneys, IUGR, polyhydramnios, thick placenta, etc.) [6, 24].

Mutation in NPHS1 gene causes CNS of the Finnish type that represents the commonest type of CNS. On post-natal US, the kidneys appear enlarged with echogenic cortex; the pyramids appear small and irregular (Fig. 6.9). They will progressively "disappear" and no CMD will be apparent after several weeks of evolution due to progressive fibrosis. In CNS with diffuse mesangial sclerosis (DMS), the renal parenchyma will appear heterogeneous and patchy. The CMD will be absent in some areas. Noteworthy, DMS can be part of the Denys-Drash syndrome resulting from a mutation of the gene WT1 and that includes increased risk for Wilm's tumor and disorders of the sexual differentiation [24, 25].

A CNS can be secondary to maternal disease (e.g., maternal deficiency in neutral endopeptidase). On US, already in utero, the renal cortex will appear thick and hyperechoic; this pattern will persist transiently after birth as well as a transient ARF; the clinical and US anomalies will resolve progressively [26].

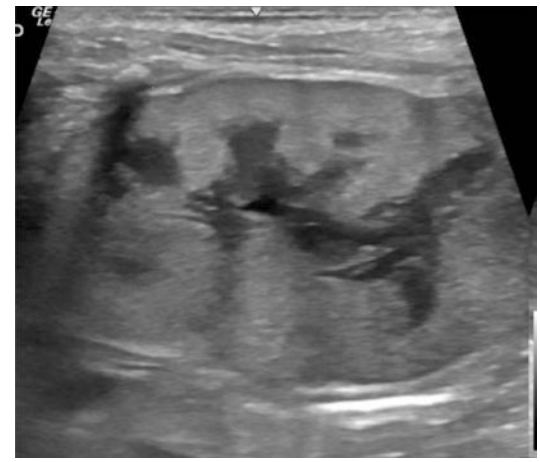

Fig. 6.9 Congenital nephrotic syndrome (Finnish type) - Sagittal scan. Enlarged hyperechoic cortex with irregular shape of the pyramids

Noteworthy, in the neonatal period, a transient proteinuria may develop and is associated with precipitates of urate in the renal tubules leading to a transient oligoanuric episode. The prevalence is unknown but has been reported in as many as 50% of healthy neonates. It has been reported by some as the Tamm-Horsfall proteinuria. In such cases, on US, a transient hyperechogenicity of the entire or of the tips of the pyramids will be observed (Fig. 6.10a). Echogenic debris may be present in

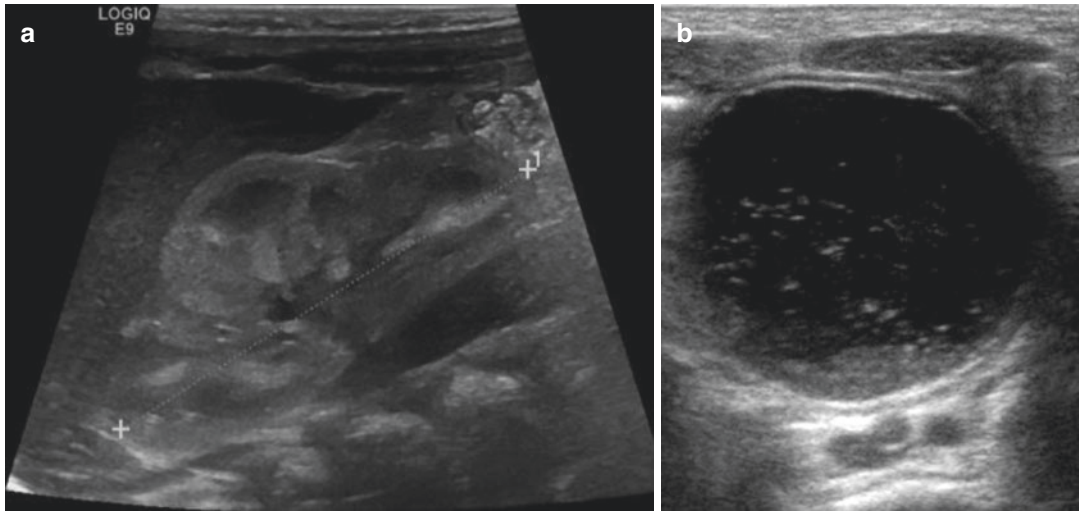

Fig. 6.10 Tamm- Horsfall proteinuria in a neonate (**a**) sagittal scan of the right kidney; some clusters of hyperechogenicities appear within the pyramids (the same was observed on the left kidney) (**b**) transverse scan of the bladder - echogenic deposits within the bladder

the bladder as well (Fig. 6.10b). As mentioned, this finding is transient and the hyperechogenicities disappear as the urine output increases [27].

6.2.1.5 Metabolic Diseases with Neonatal RF

Some metabolic disease may become symptomatic very rapidly after birth including renal symptoms. It is the case for some cases of congenital tyrosinemia and for the neonatal form of primitive hyperoxaluria of type I. Both may determine changes on ultrasound. Tyrosinemia will appear with medullary nephrocalcinosis and hypereflective liver whereas hyperoxaluria will rather determine very highly echogenic cortical nephrocalcinosis (Fig. 6.11) [28, 29].

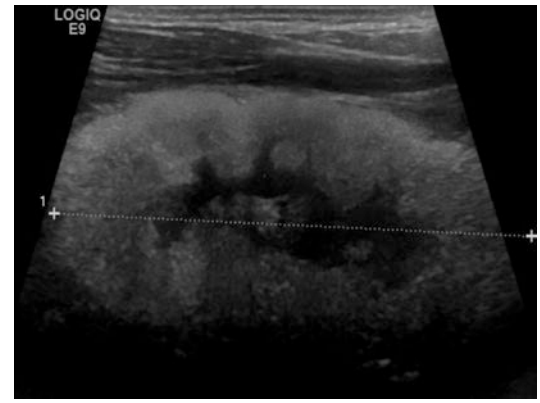

Fig. 6.11 Neonatal hyperoxaluria of type I 15 days old neonate Sagittal scan of the kidney (both appeared equally) Striking hyperechogenicity of the cortex - lack of CMD

6.2.2 Postnatally Acquired ARF

6.2.2.1 Asphyxia and Shock

Renal failure is commonly associated with neonatal shock or asphyxia. In such conditions, there is a clear reduction of the perfusion of the kidneys. Vasomotor nephropathy (VN) is the term indicating renal dysfunction with or without renal damage. On US, the renal cortex may appear hyperechoic but this finding is neither constant nor specific. Some effusion may appear around the kidney (corresponding to fluid in the third space). On duplex Doppler, the RI may increase and the diastolic flow will disappear or even the entire vascular spectrum may become irregular [1, 30–32].

In severe cases especially in prematurely born patients, reduced renal flow may lead to necrosis (medullary, cortical, or global) (see chapter on prematures) [33–34].

6.2.2.2 Renal Vein Thrombosis

Renal vein thrombosis (RVT) is the main form of venous thrombosis in neonates and when

bilateral, can cause ARF and long-term renal dysfunction. The classical presentation includes a palpable abdominal mass, gross hematuria, and thrombocytopenia as well as hypertension. Predisposing factors include maternal diabetes, macrosomia, dehydration, sepsis, neonatal asphyxia, and umbilical catheterization. Several prothrombin deficiency conditions (Factor V Leiden, protein C & S deficiency, etc.) have been shown to be supplementary favoring factors [35, 36].

In neonates, thrombosis starts in the peripheral veins gradually progressing to the central veins. Ultrasound is the central imaging technique allowing a rapid diagnosis. On US, the kidney will appear swollen, the echogenicity becomes heterogeneous, without CMD. Hyperechoic areas appear either as patchy areas or as echogenic interlobar stripes (Fig. 6.12a). These hyperechoic areas correspond most probably to zones of bleeding. On Doppler US, there is evidence of increased vascular resistance with high RI and disappearing (sometimes reversed) diastolic flow (Fig. 6.12d). The renal vein thrombus as well as its extension within the inferior vena cava can usually be demonstrated (Fig. 6.12b, c). An associated homolateral adrenal hemorrhage can be classically demonstrated (Fig. 6.13a) [37, 38].

MR imaging is able to demonstrate the features of RVT, still, it is rarely indispensable or feasible (Fig. 6.13b).

6.2.2.3 Infection

Some infections (usually E. coli) may induce secondary ARF. The kidneys may display a range of patterns from normal kidneys to focal abscesses

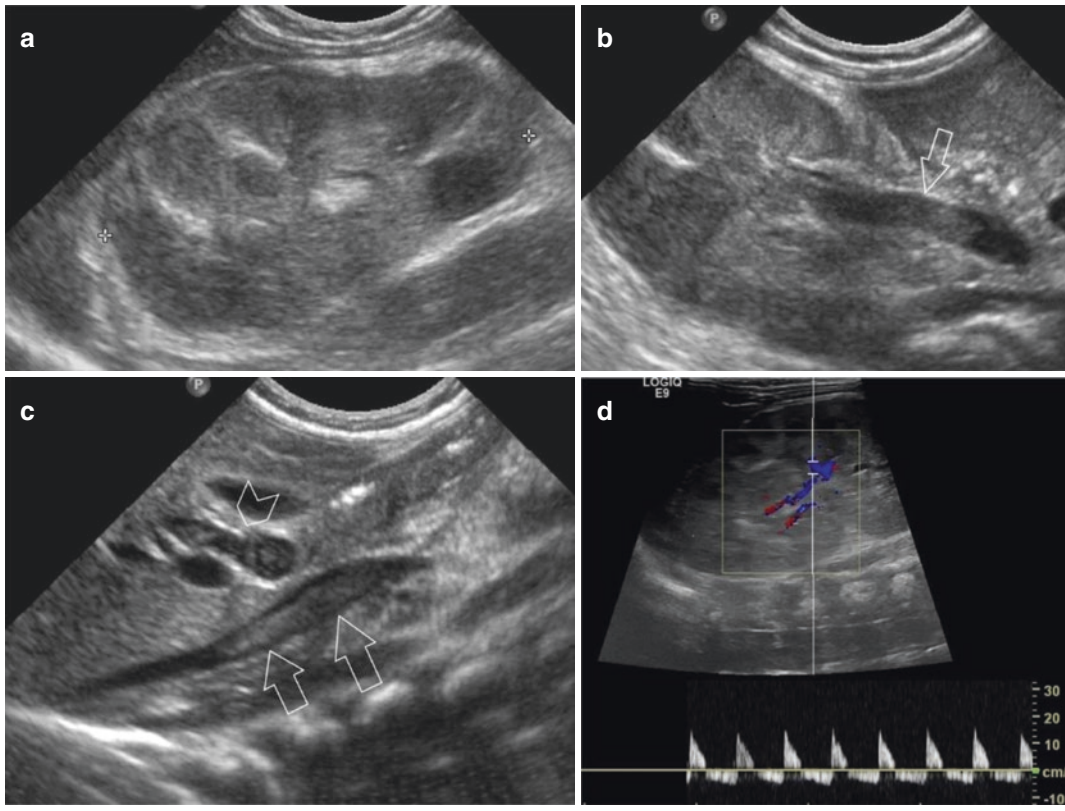

Fig. 6.12 Renal vein thrombosis in a neonate. (**a**) Sagittal scan of the left kidney: enlarged kidney, lack of CMD, some hyperechoic stripes are visibles. (**b**) Transverse scan - a thrombus is visible within the renal vein (*arrow*). (**c**) Right parasagittal scan of the abdomen showing an extension of the thrombus within the IVC (*arrows*) - some sludge is visible within the dilated main bile duct. (**d**) (Color) Doppler analysis showing reversed diastolic flow

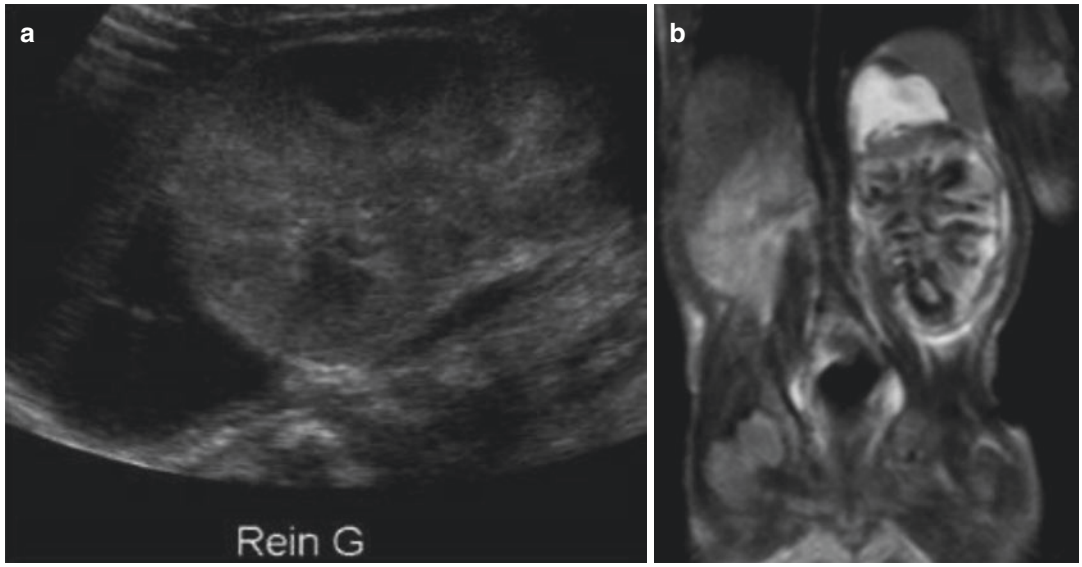

Fig. 6.13 Left RVT with associated adrenal hemorrage. (**a**) US of the left kidney. Typical US anomalies at the level of the kidney - a triangular hypoechoic lesion is visible on top of the kideny corresponding to adrenal hemorrhage. (**b**) MR imaging confirming the hemorrhagic nature of the adrenal mass as well as vascular anomalies at the level of the kidney

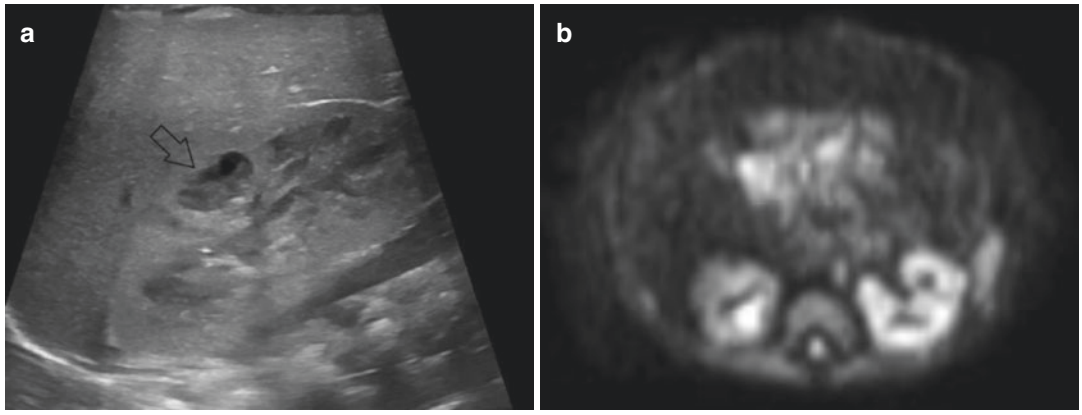

Fig. 6.14 Case of Neonatal pyelonephritis with abscess. (**a**) US of the right kidney displating a cortical abscess (*arrow*). (**b**) MR imaging, axial diffusion weighted sequence showing bilateral inflammatory involvement

(Fig. 6.14). Furthermore, candidiasis may affect neonatal kidneys and induce RF. In such a case, the kidneys would appear hyperechoic or with sludge or sludge balls appearing in the renal cavities [2].

Conclusions

Neonatal RF has numerous causes: hereditary diseases, antenatal insults, and postnatal asphyxia are among the commonest causes. US is usually sufficient for the assessment and follow-up.

References

1. Andreoli PS. Acute renal failure in the newborn. Semin Neonatal. 2004;28:112–23.
2. Mercado-Deane M, Beeson JE, John SD. US of renal insufficiency in neonates. Radiographics. 2002;22:1429–38.

3. Riccabona M. Renal failure in neonates, infants and children: the role of US. Ultrasound Clin. 2000;1:457–69.
4. Andriani G, Persico S, Tursini S, et al. The renal-resistive index from the last 3 months of pregnancy to 6 months old. BJU Intern. 2001;87:562–4.
5. Avni F. Renal and adrenal abnormalities. In: Kline-Fath B, Bahado-Singh R, editors. Fetal imaging. Philadelphia, PA: Wolters Kluwer; 2015. p. 668–700.
6. Klaassen I, Neuhaus TJ, Mueller-Wiefel DE, et al. Antenatal oligohydramnios of renal origin: long term model. Nephrol Dial Transplant. 2007;22:432–9.
7. Quirino IG, Dias CS, Vasconcelos MA, et al. A predictive model of CKD in patients with CAKUT. Pediatr Nephrol. 2014;29:2357–64.
8. Melo BF, Aguiar MB, Bouzada MCF, et al. Early risk factors for neonatal mortality in CAKUT: analysis of 524 affected newborns. Pediatr Nephrol. 2012;27:965–72.
9. de Bruyn R, Marks SD. Postnatal investigation of fetal renal disease. Semin Fetal Neonat Med. 2008;13:133–41.
10. Hochart V, Lahoche A, Priso RH, et al. PUV: are neonatal imaging findings predictive of renal function during early childhood? Pediatr Radiol. 2016;46(10):1418–23.
11. Woolf AS. Renal hypoplasia and dysplasia: starting to put the puzzle together. J Am Soc Nephrol. 2006;17:2647–9.
12. Yosypiv IV. CAKUT: a genetic disorder? Int J Nephrol. 2012;2012:909083.
13. Peters C, Rushton HG. VUR associated renal damage: congenital reflux nephropathy and acquired renal scarring. J Urol. 2012;184:265–73.
14. Weber S, Moriniere V, Knuppel T, et al. Prevalence of mutations in renal development genes in children with renal hypodysplasia: results of the ESCAPE study. J Amer Soc Nephrol. 2006;17:2864–70.
15. Avni FE, Lahoche A, Langlois C, et al. Renal involvement in children with HNF1β mutation: early sonographic appearance and long term follow-up. Europ Radiol. 2015;25:1479–86.
16. Thomas R, Sanna-Cherchi S, Waradi BA, et al. HNF1β and PAX2 mutations are a common cause of renal hypodysplasia in the CKiD cohort. Pediatr Nephrol. 2011;28:897–903.
17. Gribouval O, Moriniere V, Pawtowski A, et al. Spectrum of mutations in the renin angiotensin system genes in autosomal recessive tubular dysgenesis. Hum Mutat. 2012;33:316–26.
18. Gubler MC. Renal tubular dysgenesis. Pediatr Nephrol. 2014;29:51–9.
19. Mahieu-Caputo D, Muller F, Joly D, et al. Pathogenesis of TTTS: the RAS hypothesis. Fetal Diagn Ther. 2001;16:241–4.
20. Boubred F, Vendemmia M, Garcia-Meric P, et al. Effects of maternally administred drugs on the fetal and neonatal kidney. Drug Saf. 2006;29:397–419.
21. Schreuder MF, Bueters RR, Huigen MC, et al. Effects of drugs on renal development. Clin J Amer Soc Nephrol. 2011;6:212–7.
22. Vendemmia M, Garcia-Meric P, Rizzotti A, et al. Fetal and neonatal consequences of antennal exposure to type I angiotensin II receptor- antagonists. J Matern Fetal Neonat Med. 2005;18:137–40.
23. Avni FE, Garel C, Cassart M, et al. Imaging and classification of congenital cystic renal diseases. Amer J Roentgenol. 2012;198:1004–13.
24. Davin JC, Ruties NW. Nephrotic syndromes in children: from bench to treatment. Int J Nephrol. 2011;2011:372304. doi:10.4061/2011/372304. Epub 2011 Aug 28
25. Avni EF, Vandenhoute K, Devriendt A, et al. Update on CNS and the contribution of US. Pediatr Radiol. 2011;41:76–81.
26. Nortier JL, Debiec H, Tournay Y, et al. Neonatal disease in NEP allo-immunisation lessons for immunological monitoring. Pediatr Nephrol. 2006;21:1399–405.
27. Daneman A, Navarro OM, Somers GR, et al. Renal pyramids: focused US of normal and pathological processes. Radiographics. 2010;30:1287–307.
28. Mayorandan S, Meyer U, Gokcay G, et al. Cross-sectional study of 168 patients with hepatorenal tyrosinaemia and implications for clinical practice. Orphanet J of Rare Dis. 2014;9:107.
29. Diallo O, Janssens F, Hall M, Avni EF. Type 1 primary hyperoxaluria in pediatric patients: renal US patterns. Am J Roentgenol. 2004;183:1767–70.
30. Tot-Heyn P, Drucker A, Guignard JP. The stressed neonatal kidney: from pathophysiology to clinical management of neonatal vasomotor nephropathy. Pediatr Nephrol. 2000;14:227–39.
31. Streitman K, Toth A, Horvath I, et al. Renal injury in perinatal hypoxia: US and changes in renal function. Eur J Pediatr. 2001;160:473–7.
32. Luciano R, Gallini F, Romagnoli C, et al. Doppler evaluation of renal blood flow velocity as a predictive index of ARF in perinatal asphyxia. Eur J Pediatr. 1998;157:656–60.
33. Lerner GR, Kurnetz R, Bernstein J, et al. Renal cortical and medullary necrosis in the first 3 months of life. Pediatr Nephrol. 1992;6:516–8.
34. Lam HS, Chu WCW, Lee CH, et al. Renal artery thrombosis and ischaemia presenting as severe neonatal hypertension. Arch Dis Child. 2007;92:F264.
35. Lau KK, Stoffman JM, Williams S, et al. Neonatal RVT: review of the English-language literature between 1992 and 2006. Pediatrics. 2007;120:e1278–83.
36. Winyard PJD, Bharucha T, de Bruyn R, et al. Perinatal RVT: presenting renal length predicts outcome. Arch Dis Child Fetal Neonat. 2006;91:F273–8.
37. Wright NB, Blanch G, Walkinshaw S, et al. Antenatal and neonatal RVT: new US features with high frequency transducers. Pediatr Radiol. 1996;26:686–9.
38. Errington ML, Hendry GM. The rare association of right adrenal hemorrhage and RVT with duplex US. Pediatr Radiol. 1995;25:1191–4.

7 Acute Presentation of Anomalies of the Digestive Tract During the Neonatal Period

Elisa Amzallag-Bellenger, Rony Sfeir, Veronica Donoghue, and Fred E. Avni

Contents

E. Amzallag-Bellenger (✉) • F.E. Avni
Department of Pediatric Imaging,
Jeanne de Flandre Hospital, CHRU Lille,
Avenue Eugène Avinee 2, 59037 Lille-Cedex, France
e-mail: elisa.bellenger@chru-lille.fr

R. Sfeir
Department of Pediatric Surgery,
Jeanne de Flandre Hospital, CHRU Lille,
Avenue Eugène Avinee 2, 59037 Lille-Cedex,
France

V. Donoghue
Radiology Department, The National Maternity
Hospital, Holles Street, Dublin 2, Ireland

7.1 Introduction

During the neonatal period, obstruction of the digestive tract often represents a surgical emergency and therefore, a rapid and accurate diagnosis is mandatory. In the era of obstetrical US and antenatal diagnosis, some pathologies will be detected in utero and managed immediately after birth (see Chap. 5). Yet, the rate of antenatal diagnosis of digestive tract anomalies is still low (30–50%) and many diagnoses will be achieved after birth only mainly on the basis of acute abdominal symptoms. Furthermore, several among the malformations—e.g., Hirschsprung disease—are only exceptionally suspected in utero and most

F.E. Avni, P. Petit (eds.), *Imaging Acute Abdomen in Children*,
https://doi.org/10.1007/978-3-319-63700-6_7

cases will be discovered after birth. Some others will present symptoms only after birth (e.g., small left colon).

Some entities, such as volvulus, are classical in this age group. Several other diseases that occur mostly in childhood may unexpectedly occur in the neonatal period (e.g., appendicitis) and should be considered even in this age group (see also Chap. 9).

The basis of postnatal management is the clinical examination and potential acute symptoms. An esophageal atresia or anal atresia will be clinically obvious and will be treated surgically as required. Furthermore, several clinical symptoms will orient towards acute abdominal conditions. Abdominal distension, delayed meconium emission, or (bilious) vomiting would be the most classical symptoms encountered.

7.2 Imaging: General Approach

The couple "plain film of the abdomen and abdominal US" constitutes the basis of imaging for a neonate suspected of intestinal obstruction. These two could be followed by radiopaque enema or upper GI tract opacification as indicated by initial findings. The plain film of the abdomen demonstrates the pattern of abdominal aeration, evidence for intestinal perforation, and the presence of calcifications. Still, it will rarely be possible to differentiate between a proximal and a distal intestinal obstruction. Noteworthy, skeletal anomalies, e.g. associated vertebral malformations will be potentially visualized.

US is most useful in order to exclude or confirm midgut volvulus. The examination is also useful in demonstrating intestinal loops dilatation, abdominal effusions, and localized (calcified) collections.

Enema, usually with water soluble contrast will demonstrate the size of the colon (unused vs used colon) and the presence of reflux into the distal ileal loops. Upper GI tract opacification would be performed very cautiously in case of proximal obstruction or suspicion of malrotation related anomalies.

7.3 Upper GI Tract Obstruction

7.3.1 Esophageal Anomalies

Esophageal atresia is amenable to antenatal diagnosis especially thanks to the adjunction of fetal MR imaging [1] (See Chap. 5). If undiagnosed during the fetal life, it will be discovered rapidly after birth when the nasogastric tube will be introduced. Some other esophageal anomalies will be diagnosed after birth only.

7.3.1.1 Esophageal Stenosis

Congenital stenosis of the esophagus is much rarer than esophageal atresia with an incidence estimated from 1/25,000 to 50,000 births [2]. Noteworthy, both atresia and stenosis can be associated [3]. Three types of congenital esophageal stenosis have been described [2] (Fig. 7.1):

- Segmental stenosis with loss of esophageal elasticity due to muscular and submucosal thickening
- Tracheobronchial remnant within the esophageal wall
- Intraluminal membranous diaphragm

Clinically, a congenital stenosis may go unrecognized up to the introduction of solid type food; dysphagia, vomiting, and regurgitation may be the main symptoms [2]. It may also be discovered during the post-operative opacification of an esophageal atresia.

Upper GI tract opacification is the diagnostic procedure of choice as it will demonstrate the narrowing in the upper or middle esophagus in case of muscular thickening or diaphragm (Fig. 7.1); in the inferior part in case of tracheobronchial remnant. The most frequent localization of esophageal stenosis is the lower esophagus.

The initial treatment will be endoscopic dilatation followed by surgery in case of failure.

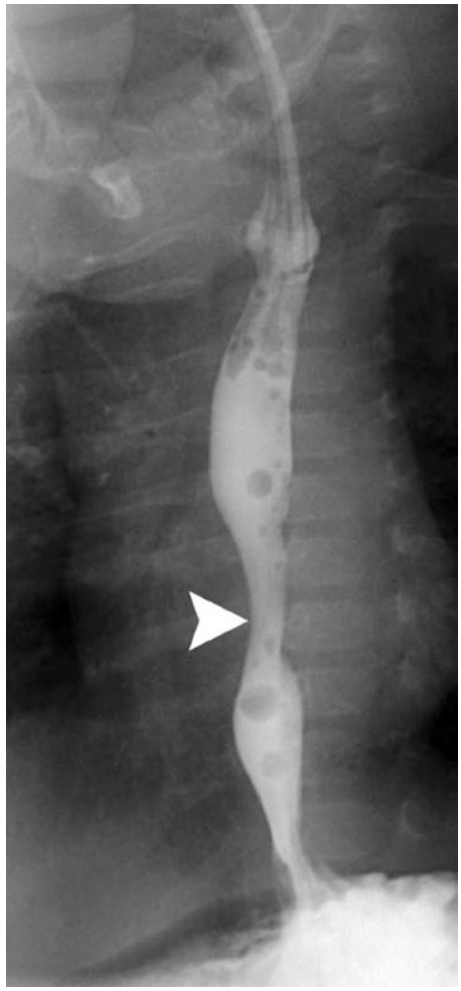

Fig. 7.1 Esophageal stenosis: esophageal opacification showing a stenosis (*arrowhead*) in the *middle portion* of the esophagus

7.3.1.2 Esophageal Bronchus

Esophageal bronchus is a rare anomaly. It is characterized by a lobar bronchus branching from the esophagus. It may be associated with an esophageal atresia, a cardiovascular malformation or be part of a VACTERL syndrome. This malformation will rarely be diagnosed in utero [4]. It will be suspected postnatally, in case of a persistent basal atelectasis on a chest X-ray associated with recurrent infection and repeated coughing during feeding. Cautious esophageal opacification may visualize the bronchus within the atelectatic lung (Fig. 7.2). The (partially) aerated bronchus may be visualized on a chest CT usually performed during the workup of cardiovascular malformation or recurrent pulmonary infections [5].

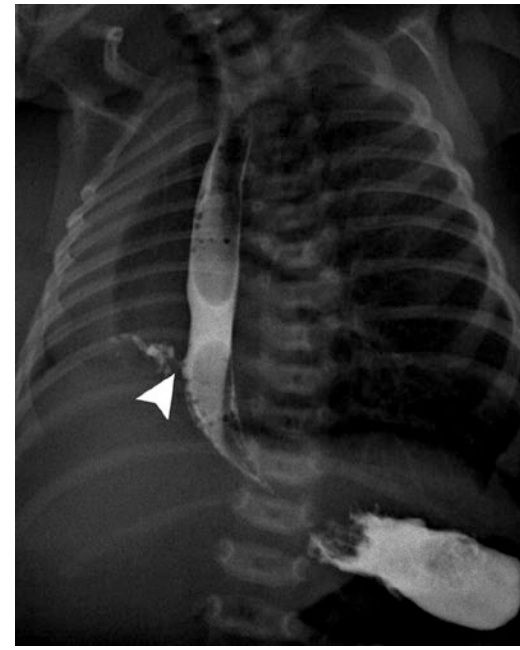

Fig. 7.2 Esophageal bronchus: esophageal opacification showing lobar bronchus opacification branching from the esophagus (*arrowhead*)

7.4 Esogastric Anomalies: Congenital Hiatal Hernia

Hiatal hernia corresponds to the presence of the esogastric junction and of the stomach (partially or completely) within the chest. There are three types of hernia [6]: paraesophageal, sliding hernia, and hernia associated with congenitally short esophagus. This last type is the true congenital hiatal hernia and prenatal diagnosis is usually possible. It is a differential diagnosis of diaphragmatic hernia. When unrecognized in utero, symptoms, both digestive and respiratory, may develop rapidly after birth especially when the distended stomach remains in the chest. Symptoms may

become even more acute when axial volvulus of the stomach occurs leading to gastric outlet obstruction. Noteworthy, hiatal hernia may be associated with intestinal malrotation.

On chest X-ray, the normally aerated pouch of the stomach will not be visible within the abdomen, conversely a distended air-filled structure will be seen above the diaphragm. An upper GI tract opacification will demonstrate the intrathoracic stomach and eventually the volvulus [6] (Fig. 7.3).

The treatment is surgical.

7.5 Gastroduodenal Anomalies

7.5.1 Congenital Microgastria

Congenital microgastria is rare [7]. It is characterized by a very small stomach; its extreme form is total agastria. It can be part of heterotaxia syndromes, Di George syndrome or VACTERL syndrome and long gap esophageal atresia. It should be suspected in case of intractable esophageal reflux and vomiting.

Microgastria will be ascertained through upper GI tract opacification by the demonstration of a small stomach (less than 25% of a normal stomach) lacking peristalsis with massive esophageal reflux with a distended esophagus [7] (Fig. 7.4).

7.5.2 Early Onset Pyloric Stenosis

Early onset hypertrophic pyloric stenosis has been reported in the neonatal period [8–9] and even suspected in utero. Vomiting would be the main diagnostic feature.

On US, the pylorus appears long (>15 mm) with a muscular layer measuring >4 mm. No passage of liquid will be visualized through the hypertrophied pylorus. A cockade image will be visible on the transverse scan.

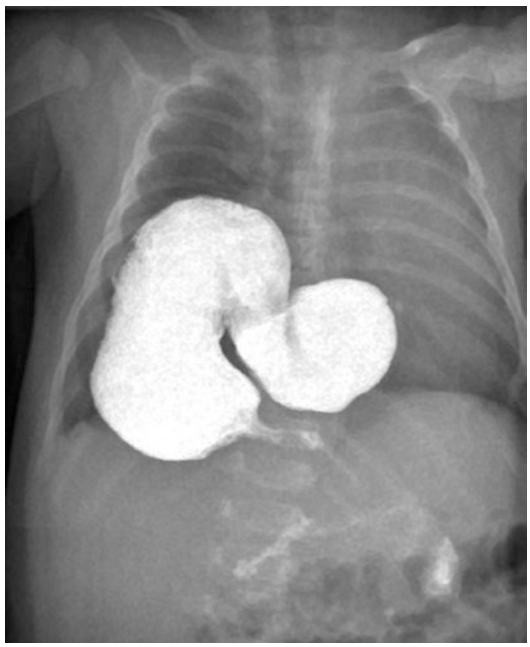

Fig. 7.3 Congenital hiatal hernia: Upper gastrointestinal tract opacification showing the intrathoracic position of the stomach

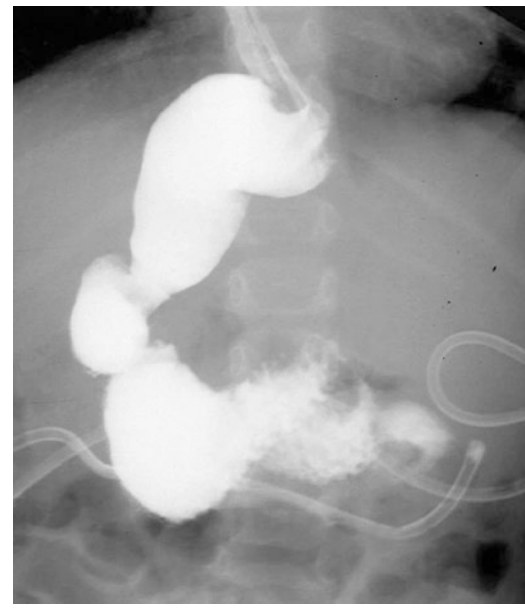

Fig. 7.4 Congenital microgastria: *Frontal view* of an upper gastrointestinal tract opacification with a nasogastric tube demonstrates a small stomach and a distended duodenum

7.5.3 Duodenal Stenosis and Duodenal Web

Neonatal duodenal obstructions encompass a wide spectrum of anomalies related to intrinsic (e.g., duodenal atresia) and extrinsic (Ladd bands) causes [10]. Duodenal atresia is amenable to (an easy) antenatal diagnosis; if not, neonatal diagnosis will be rapid due to neonatal vomiting and confirmation by a plain film of the abdomen that will display the characteristic of double bubble [10]. The diagnosis of duodenal stenosis or web may be more challenging and delayed depending on the clinical symptoms. When suspected, plain film of the abdomen will demonstrate a distended stomach and proximal duodenum but with aeration of the downhill bowel; the partial obstruction/stenosis will be confirmed by upper GI opacification (Fig. 7.5) [10]. Rarely the web will be imaged by US [11]. Duodenal obstruction as in atresia, or subobstruction as in stenosis and web are classical findings of trisomy 21.

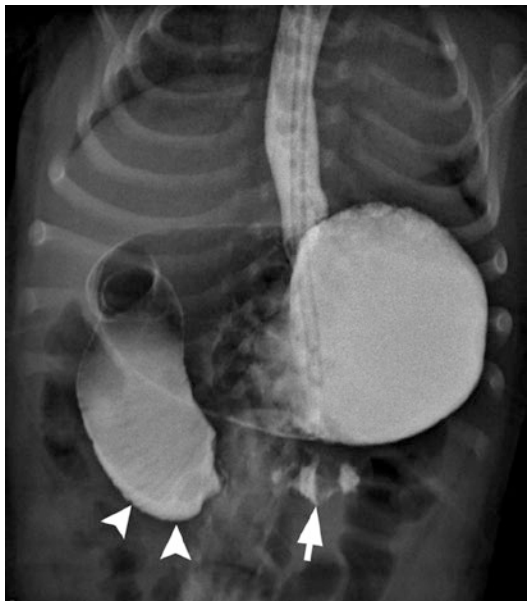

Fig. 7.5 Duodenal stenosis: Upper gastrointestinal tract opacification showing dilated proximal duodenal (*arrowheads*) with partial progression into the distal duodenum (*arrow*)

7.5.4 Duodenal Duplication Cyst

A duodenal duplication cyst is a common cause of bilious vomiting in the neonate. A cystic mass with a stratified wall will be visualized on US. An internal extrinsic compression of the duodenal bulb will be demonstrated on upper GI opacification [10].

7.6 Duodeno-Jejunal Obstructions: Midgut Volvulus and Ladd's Band Related Obstruction

Midgut volvulus and obstruction secondary to Ladd's band are both related to some degree of incomplete rotation. They determine acute symptoms and constitute surgical emergencies. Few cases will be discovered in utero [12] through obstetrical US but most will become symptomatic during the first days of life.

Color Doppler US should be performed very rapidly in order to search for the whirlpool sign so characteristic of midgut volvulus (Fig. 7.6) [11–13]. US may also demonstrate distended bowel loops and peritoneal effusion confirming intestinal obstruction. In doubtful cases, an upper GI tract opacification can be performed cautiously in order to verify the position of the duodeno-jejunal junction (Fig. 7.7).

7.7 Mid and Lower GI Tract (Sub) Obstructions

In the neonatal period, distal intestinal obstruction will determine abdominal distension and delayed passage of meconium. The role of imaging will be to differentiate between small and large bowel obstructions. This will be achieved mainly on the basis of the size of the colon and

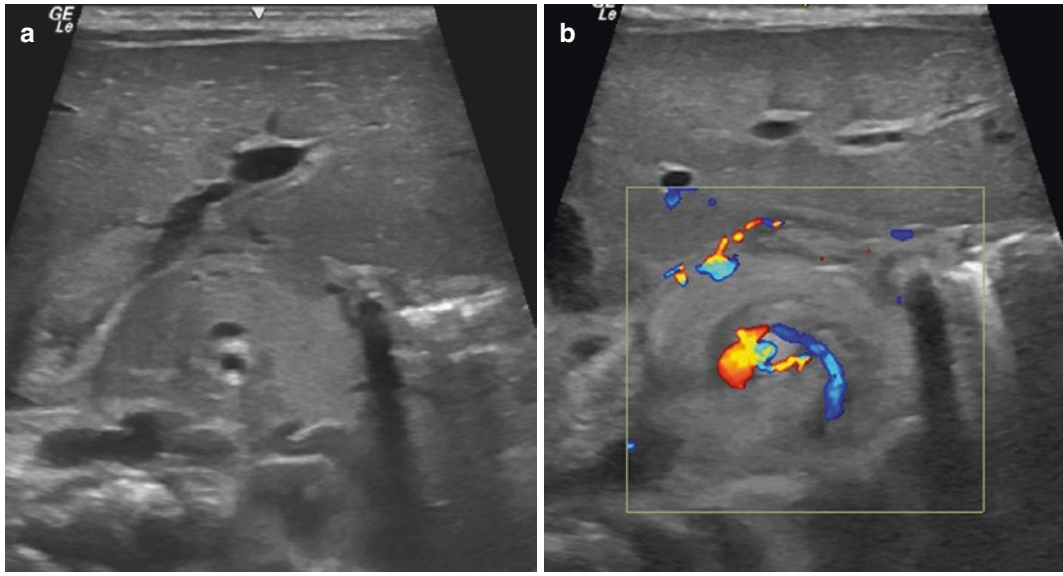

Fig. 7.6 Midgut volvulus: (**a**) Transverse US scan of the epigastric area showing the displaced mesenteric vein (*arrowhead*). (**b**) Showing a typical color Doppler whirlpool sign

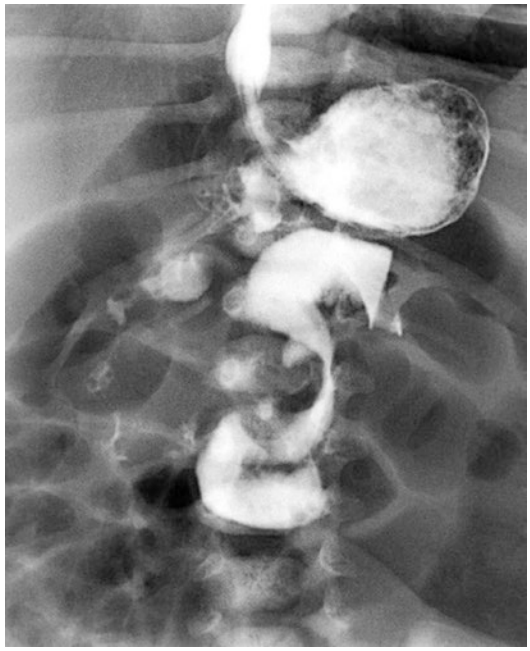

Fig. 7.7 Midgut volvulus: Upper gastrointestinal tract opacification showing the abnormal position of the duodeno-jejunal junction (Note the dilated loops behind indicating intestinal obstruction)

the presence or absence of retrograde filling of the terminal ileal loops.

7.7.1 Jejunal and Ileal Atresia

Jejunal and ileal atresia are potentially diagnosed in utero [14]. Cases undiagnosed will become rapidly evident after birth due to abdominal distension and will necessitate rapid surgical management (Fig. 7.8).

7.7.2 Meconium Related Anomalies

Meconium related anomalies include diseases acquired in utero or developing after birth only.

7.7.2.1 Meconium Ileus

Meconium ileus corresponds to accumulation of thick meconium in the terminal ileum determining uphill dilatation. The condition is mainly diagnosed in utero through the demonstration of

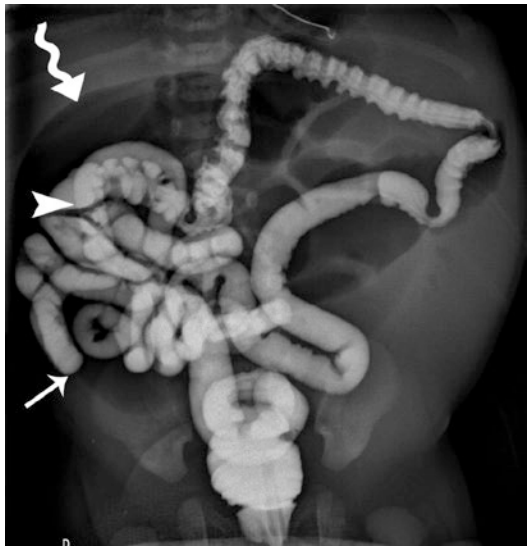

Fig. 7.8 Intestinal atresia: radiopaque enema showing a micro-colon with passage of the ileocecal junction (*arrowhead*). Some distal ileal loops are opacified (*arrow*); the rest of the loops appear distended (*curve arrow*)

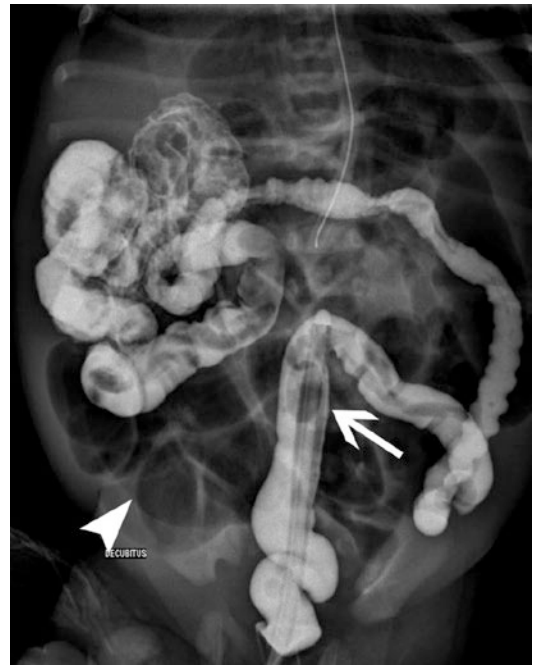

Fig. 7.9 Meconium ileus: radiopaque enema showing a micro-colon (*arrow*) with meconium and dilated intestinal (*arrowhead*). Thick meconium is visualized within the distal ileum loops

dilated digestive tract (see Chap. 5). The condition is often associated with cystic fibrosis. After birth, there will be no passage of meconium and progressive abdominal distension. Radio-opaque enema with hydrosoluble contrast will demonstrate an unused microcolon and usually no passage through the terminal ileum (Fig. 7.9) [13]. If no passage is obtained, the treatment will be surgical.

7.7.2.2 Meconium Peritonitis

Meconium peritonitis corresponds to antenatal perforation of the small bowel probably related to ischemia of the bowel wall and spilling of meconium within the peritoneal cavity. At birth, an intestinal obstruction will be obvious with distended loops and peritoneal calcifications. An organized meconium pseudocyst may be visible on US [11]. Opacification will show an unused microcolon but partial retrograde filling of the distal ileum potentially up to the area of atresia.

7.7.2.3 Meconium Plug

Meconium plug is acquired postnatally and is secondary to accumulation of dried meconium after birth blocking the terminal ileum. The colon will display a normal size on enema and will be partially filled with meconium (Fig. 7.10). The water-soluble radiopaque enema will allow a passage of contrast to the terminal ileum and resolution of the plug [15].

7.7.3 Small Left Colon

Small left colon results from an abnormal peristalsis pattern of the colon in neonates. Small left colon is preferably seen in VLBW prematures (<1500 grs) (see also Chap. 4) or among children born to diabetic mothers [16]. The appearance will be characteristic on the radiopaque enema

showing a pseudo-stenotic left colon (Fig. 7.11) with otherwise normal remaining colon and rectum. The condition resolves spontaneously.

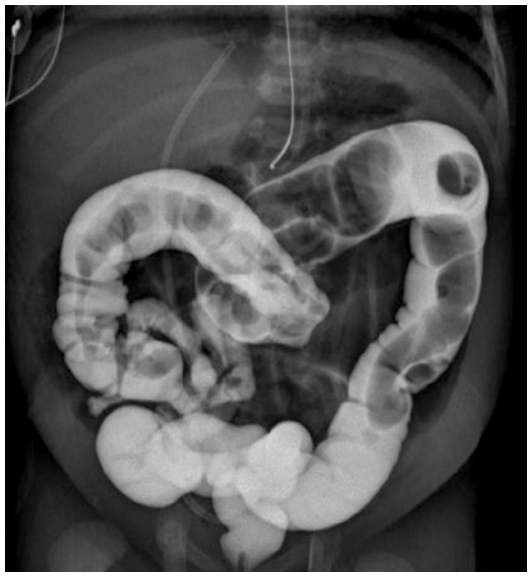

Fig. 7.10 Meconium plug: radiopaque enema showing a colon with a normal caliber and meconium throughout on the colon

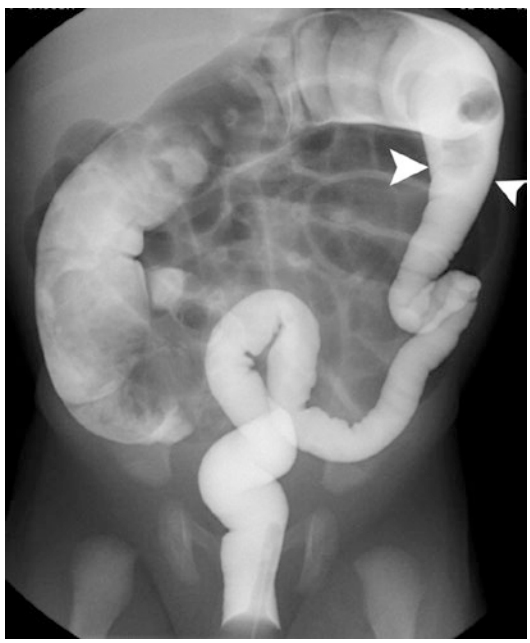

Fig. 7.11 Small left colon: Radiopaque enema showing pseudo-stenotic left (*arrowheads*) colon with otherwise normal colon and rectum

7.7.4 Hirschsprung Disease (HD)

Hirschsprung disease is related to defective innervation of the bowel due to the lack of migration of the plexuses of Meissner and Auerbach that are conducting the intestinal peristalsis. Hirschsprung disease represents the second cause of neonatal obstructions (after bowel atresia) [17]. The disease will be diagnosed in the neonatal period in 80% of cases. HD can be associated to other anomalies (T21, mutation of the RET gene, Williams and Beuren syndrome, etc.). Classically there will be a delay to pass meconium and abdominal distension. Radiopaque enema (preferably using barium) will suggest the diagnosis that will be ascertain by biopsies and histology. The aim of the enema will be to demonstrate the transitional zone (Fig. 7.12) [13]. The normally innervated segments will appear peristaltic and distended above the abnormal aperistaltic and narrowed segment. The disease may be ultrashort, affecting only the distal rectum or ultralong, affecting the entire colon and even the entire digestive tract.

7.7.5 Internal Hernia

Internal hernia corresponds to an outpouching of part of the digestive tract within (acquired or) congenital holes within the peritoneum. Most internal hernias in the neonatal period correspond to congenital trans-mesocolic hernia.

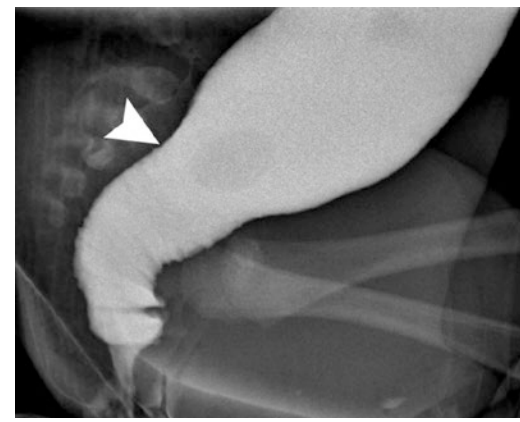

Fig. 7.12 Hirschsprung disease: Radiopaque enema showing the transitional zone (*arrowhead*)

These hernias can be associated with bowel atresia and malrotation. Secondary obstruction may occur. The diagnosis is rarely achieved preoperatively (see also Chap. 14).

7.8 Appendicitis in the Neonatal Period

Neonatal appendicitis is extremely rare [18]. About 50 cases have been reported. Boys are more frequently affected than girls (3:1). NEC, CMV enterocolitis, chorioamnionitis are favoring conditions. Symptoms are non-specific (mainly high temperature, anorexia, vomiting, abdominal distension, and respiratory distress) and the diagnosis can therefore be delayed. The risk of perforation and peritonitis is very high. The diagnosis is rarely obtained pre-operatively unless US demonstrates the dilated inflamed appendix (Fig. 7.13) and evidence of subsequent peritonitis. Noteworthy, the inflamed appendix can be the cause of acute intestinal intussusception (see also Chap. 10).

7.9 Neonatal Intussusception

In the neonatal period, acute intestinal intussusception is more usually secondary and related to a leading cause such as Meckel diverticulum, intestinal duplication, inflamed appendix, or a tumor [19–21].

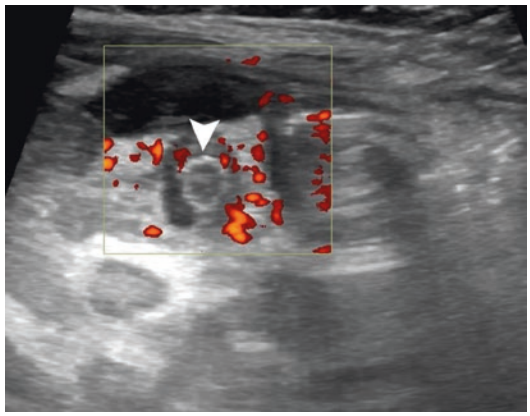

Fig. 7.13 Neonatal appendicitis: Transversal US imaging showing a thickened appendix (*arrowhead*) with hyperhemia on color Doppler

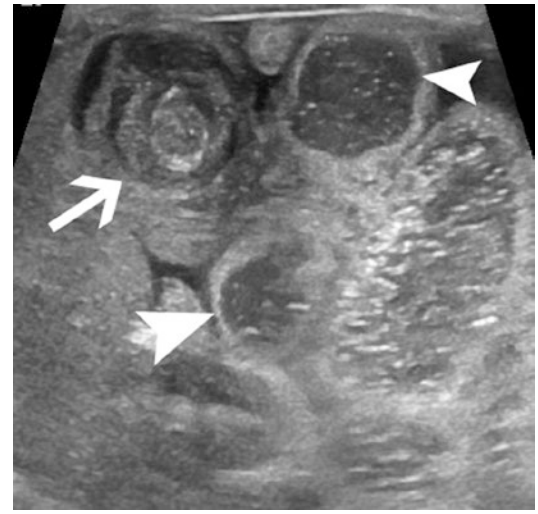

Fig. 7.14 Neonatal intussusception: transversal US imaging of the right flank showing intestinal intussusception (*arrow*) with dilated small bowel loops (*arrowheads*)

The clinical presentation would be that of an intestinal obstruction confirmed by a plain film of the abdomen. US will typically demonstrate the cockade or target appearance corresponding to the intussusception. The size might be lower than for older children. Evidence for secondary obstruction (dilated bowel loops, thickened walls, free fluid) will also be demonstrated (Fig. 7.14). Treatment will be most often surgical (see also Chap. 13).

7.10 Meckel Diverticulitis

Meckel diverticulum is one of the most frequent congenital malformations of the gastrointestinal tract and most patients are asymptomatic. The diagnosis of Meckel diverticulum is very difficult in the neonatal period and few cases have been reported in the literature [22]. Most cases will be diagnosed at surgery. In neonate the most frequent presentation of Meckel diverticulum is bowel obstruction (Fig. 7.15) [22] secondary to an intussusception [20], a volvulus or obstruction by congenital bands [23]. Rupture with secondary peritonitis are common complications [24]. Very

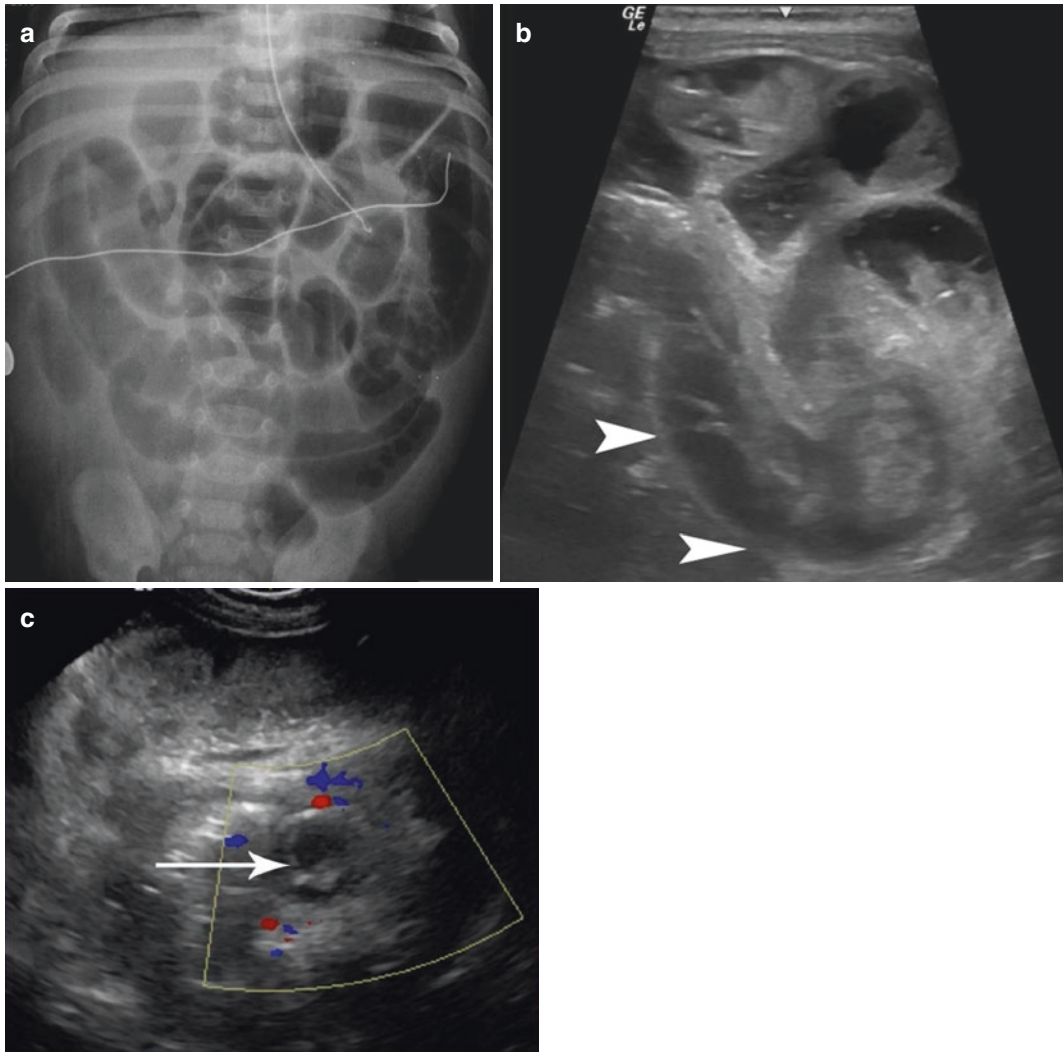

Fig. 7.15 Meckel diverticulum: (**a**) *Frontal view* of an abdomen X-ray showing intestinal dilated loops. (**b**) Transverse US scan showing intestinal dilated loops (*arrowheads*). (**c**) Transverse US scan showing blind ending oval structure containing distended by fluid corresponded to the Meckel diverticulum (*arrow*)

rarely US would orient the diagnosis by demonstrating the inflamed distended diverticulum as a blind ending oval structure containing some fat and distended by fluid (see also Chap. 11).

7.11 Chronic Intestinal Pseudoobstruction (CIPO)

CIPO is defined by a dilatation of the digestive tract without a mechanical etiology. It encompasses various diseases including anomalies of the enteric nervous system or of the intestinal smooth muscles. The main symptom is an intestinal dysmotility. In case of primary CIPO, symptoms may develop during the first months. Forty percent before the first month and 65% before the first year. Neonates and infants affected will present episodes of vomiting, constipation alternating with episodes of diarrhea and abdominal pain. On plain film of the abdomen, the intestinal loops will appear dilated and on enema, the colon markedly enlarged (megacolon). Secondary CIPO may develop associated

with systemic diseases such as mitochondrial diseases or fetal alcohol syndrome [25].

Conclusion

Anomalies of the digestive tract in the neonatal period are common and many will necessitate rapid surgical management. A correct and complete diagnosis is therefore highly desirable. Imaging is the cornerstone of the workup. Opacification of the upper or lower digestive tract coupled to US will provide clues for the diagnosis.

References

1. Hochart V, Verpillat P, Langlois C, et al. The contribution of fetal MR imaging to the assessment of oesophageal atresia. Eur Radiol. 2015;25(2):306–14.
2. Lee NK, Kim S, Jeon TY, et al. Complications of congenital and developmental abnormalities of the gastrointestinal tract in adolescents and adults: evaluation with multimodality imaging. Radiographics. 2010;30(6):1489–507.
3. Yoo HJ, Kim WS, Cheon JE, et al. Congenital esophageal stenosis associated with esophageal atresia/tracheoesophageal fistula: clinical and radiologic features. Pediatr Radiol. 2010;40(8):1353–9.
4. Partridge EA, Victoria T, Coleman BG, et al. Prenatal diagnosis of esophageal bronchus- first report of a rare foregut malformation in utero. J Pediatr Surg. 2015;50(2):306–10.
5. Colleran GC, Ryan CE, Lee EY, Sweeney B, Rea D, Brenner C. Computed tomography and upper gastrointestinal series findings of esophageal bronchi in infants. Pediatr Radiol. 2017;47(2):154–60.
6. Chavhan GB, Babyn PS, Cohen RA, Langer JC. Multimodality imaging of the pediatric diaphragm: anatomy and pathologic conditions. Radiographics. 2010;30(7):1797–817.
7. Sharma SC, Menon P. Congenital microgastria with esophageal stenosis and diaphragmatic hernia. Pediatr Surg Int. 2005;21(4):292–4.
8. Ali KI, Haddad MJ. Early infantile hypertrophic pyloric stenosis: surgery at 26 hours of age. Eur J Pediatr Surg. 1996;6(4):233–4.
9. Zenn MR, Redo SF. Hypertrophic pyloric stenosis in the newborn. J Pediatr Surg. 1993;28(12):1577–8.
10. Brinkley MF, Tracy ET, Maxfield CM. Congenital duodenal obstruction: causes and imaging approach. Pediatr Radiol. 2016;46(8):1084–95.
11. Veyrac C, Baud C, Prodhomme O, Saguintaah M, Couture A. US assessment of neonatal bowel (necrotizing enterocolitis excluded). Pediatr Radiol. 2012;42(Suppl 1):S107–14.
12. Leopold S, Al-Qaraghouli M, Hussain N, Finck C. Magnetic resonance imaging diagnosis of volvulus through mesenteric defect in neonate. AJP Rep. 2016;6(2):e239–42.
13. Vinocur DN, Lee EY, Eisenberg RL. Neonatal intestinal obstruction. Am J Roentgenol. 2012;198(1):W1–10.
14. Furey EA, Bailey AA, Twickler DM. Fetal MR imaging of gastrointestinal abnormalities. Radiographics. 2016;36(3):904–17.
15. Berrocal T, Lamas M, Gutieérrez J, Torres I, Prieto C, del Hoyo ML. Congenital anomalies of the small intestine, colon, and rectum. Radiographics. 1999;19(5):1219–36.
16. Ellis H, Kumar R, Kostyrka BJ. Neonatal small left colon syndrome in the offspring of diabetic mothers-an analysis of 105 children. J Pediatr Surg. 2009;44(12):2343–6.
17. Verma A, Rattan KN, Yadav R. Neonatal intestinal obstruction: a 15 year experience in a tertiary care hospital. J Clin Diagn Res. 2016;10(2):SC10–3.
18. Mammou S, Ayadi I, Ben Hamida E, Marrakchi Z. Acute neonatal appendicitis in a preterm. Afr J Paediatr Surg. 2015;12(4):294–5.
19. Charles T, Penninga L, Reurings JC, Berry MC. Intussusception in children: a clinical review. Acta Chir Belg. 2015;115(5):327–33.
20. Das DK, Majumdar PK, Shukla S. Meckel's diverticulum causing intussusception in a newborn. J Neonatal Surg. 2015;4(4):46.
21. Bruno C, Caliari G, Zampieri N, Segala D, Pozzi-Mucelli R. Congenital fibrosarcoma of the bowel: sonographic description of a rare case of neonatal intestinal obstruction. J Clin Ultrasound. 2014;42(6):363–6.
22. Bertozzi M, Melissa B, Radicioni M, Magrini E, Appignani A. Symptomatic Meckel's diverticulum in newborn: two interesting additional cases and review of literature. Pediatr Emerg Care. 2013;29(9):1002–5.
23. Kunitsu T, Koshida S, Tanaka K, et al. Neonatal Meckel diverticulum: obstruction due to a short mesodiverticular band. Pediatr Int. 2015;57(5):1007–9.
24. Masuko T, Tanaka Y, Kawashima H, Amano H. Diagnostic laparoscopy for neonatal perforated Meckel's diverticulum. J Minim Access Surg. 2016;12(1):71–2.
25. Berger S, Ziebell P, Offsler M, et al. Congenital malformations and perinatal morbidity associated with intestinal neuronal dysplasia. Pediatr Surg Int. 1998;13:474–9.

Obstructive Cholestasis and Acute Hepatobiliary Diseases in the Neonate

8

Stéphanie Franchi-Abella and Danièle Pariente

Contents

S. Franchi-Abella (✉) • D. Pariente
Department of Paediatric Radiology, Hôpital Bicêtre-Hôpitaux Universitaires Paris-Sud-Assistance Publique Hôpitaux de Paris, 78 rue du General Leclerc, 94275 Le Kremlin-Bicêtre, France
e-mail: stephanie.franchi@aphp.fr; daniele.pariente@aphp.fr

8.1 Introduction

Liver and biliary disorders may present shortly after birth or even be suspected or diagnosed during fetal life. Emergency management may be required due to life-threatening conditions such as acute liver failure or cardiac failure related to hypervascularized tumors or vascular malformations. An early diagnosis is of upmost importance in order to increase the chances of success of treatment as in biliary atresia or in case of liver tumor.

In utero, fetuses may present with cystic lesions of the hepatic area, a hepatic mass, an abnormal size of the liver, vascular malformation, calcifications, or ascites. These anomalies may be symptomatic during pregnancy or only after birth.

In neonates (see also Chap. 5), hepatobiliary disorders may present with clinical symptoms—abdominal mass, cardiac or liver failure or infection—and/or biological disorders such as cholestatic jaundice, abnormal coagulation tests, hypoglycemia, hyperammonemia, or hypergalactosemia. According to the disease and its severity, patients may develop acute symptoms.

Early and accurate diagnosis of the causative disease is mandatory for adapting treatment and improving the prognosis. Imaging has a key role for assessing the anatomy of the liver, the biliary tract, abdominal vessels, and other organs and subsequently establishing the diagnosis.

F.E. Avni, P. Petit (eds.), *Imaging Acute Abdomen in Children*,
https://doi.org/10.1007/978-3-319-63700-6_8

8.2 Imaging Work-Up

Imaging should start with ultrasound (US) using linear high frequency transducers in neonates and adapted transducers for fetal imaging including high frequency probes. The real-time capacity of US associated with the high spatial resolution of this technic allows very high quality and detailed demonstration of the anatomical structures. The use of color and duplex Doppler provides important information on hemodynamics and helps to differentiate small cysts from normal or abnormal vessels. In case of obstructive cholestasis, the examination should be performed after 4 h of fasting.

The aims of US are to assess:

- *The liver:* size, margins, parenchyma (homogeneous/heterogeneous), presence of nodules,
- *The biliary tract:* dilatation of intrahepatic and/or extrahepatic bile ducts, aspect of the gallbladder (size, wall, content), presence of cyst(s) (unilocular/multilocular, location of the cysts—intraparenchymal/along the intra- or extra-hepatic biliary tract, size, and content),
- *The vascular network:* hepatic veins and inferior vena cava, main portal vein and portal branches, hepatic artery, ductus venosus, and umbilical vein in the fetus,
- *The spleen*: unique, polyspenia/asplenia, size,
- *The kidneys*: size and echogenicity
- All other intraabdominal organs and vessels.

In selected cases, MR imaging of the liver will be informative, particularly if the bile ducts are dilated, in case of suspected hemochromatosis, in the context of liver failure or for the work-up of a liver mass. The smallest available coils adapted to the size of the abdomen of the newborn should be used in order to increase spatial resolution. Classical T2- and T1-weighted sequences in the axial and coronal planes should be performed. If the biliary tract anatomy needs to be assessed, 2D and 3D MR cholangio-pancreatography (MRCP) has to be performed. To be noted, MRCP should not be considered reliable for the diagnosis of biliary atresia because of its lack of spatial resolution [1]. If a neonatal hemochromatosis is suspected, T2*-weighted sequence in the axial plane is mandatory to study the signal of the pancreatic gland [2]. Sequences obtained after gadolinium injection will be mandatory in case of a liver mass.

In case of vascular malformations or tumors, Computed Tomography (CT) and MR imaging of the liver will provide essential information before interventional radiology or surgery by confirming the diagnosis and establishing vascular mapping.

8.3 Classical Presentations

8.3.1 Prenatal Diagnosis of Hepatobiliary Disorders

8.3.1.1 Fetal Biliary Abnormalities

The two major US features suggesting biliary disorders during fetal life are the absence of visualization of the gallbladder and the presence of a cyst along the portal vein pedicle.

In case of non-visualization of the gallbladder, the prognosis will be determined by the presence or absence of associated malformations (such as heterotaxia, polysplenia syndrome, bowel malformation, etc.). If the absence of the gallbladder is isolated, the prognosis is favorable with over 90% normal neonates. In most cases, the gallbladder will be demonstrated on post-natal imaging. On the contrary, if the absent gallbladder is associated with other disorders, then the prognosis is poorer with more than 95% of severe diseases (cystic fibrosis, biliary atresia, syndromes with multiple malformations, etc.) [3–6].

Thanks to the improvement of fetal imaging, the prenatal detection of cysts in the area of the liver is increasing. The aim of the workup should be to determine the exact location of the cyst: within the liver parenchyma or along the hepatic pedicule (main portal vein and hepatic artery). If the cyst lies within the liver parenchyma and far from the hepatic pedicule, the most probable diagnosis is that of a simple hepatic cyst; most will disappear spontaneously after birth without any symptom. The main problem is to characterize hepatic pedicular cysts that may be related to two major diagnoses: the cystic form of biliary atresia and choledochal cyst.

The only way to differentiate between them before birth is to search for intrahepatic bile ducts dilatation that would favor the diagnosis of choledochal cyst. Conversely, the demonstration of gallbladder anomalies or associated malformations such as polysplenia would favor a biliary atresia (BA) variant. In most cases, the differential diagnosis is not feasible before birth. A complete re-evaluation including clinical examination, biological tests, and liver ultrasound should therefore be performed at birth. If the baby has acholic stools, cholestasis on liver tests and no bile duct dilatation on US, then BA is highly probable. If the bile ducts are dilated on US, then BA can be ruled out and a choledochal cyst is the diagnosis (Fig. 8.1). Whenever the stools are normal at birth, as discoloration of the stools related to BA may develop later during the first 2 months of life, a new clinical and US evaluation should be obtained every 2 weeks in order not to miss progressing BA. For further neonatal presentations and management see below (Sects. 8.3.2 and 8.4.2).

8.3.1.2 Fetal Hepatic Mass

Hepatic masses can develop prenatally. Hemangioma is the most frequent liver tumor in fetuses (and neonates) and represented up to 60% of the lesions encountered in Isaacs's series [7]. The two major differential diagnoses for hemangioma are cystic mesenchymal hamartoma that was encountered in about 23% and hepatoblastoma in 16% of his series. The purpose of the imaging work-up should be to:

- Confirm the intrahepatic location of the lesion,
- Determine whether the mass is unique or whether there are multiple lesions,
- Demonstrate whether the lesion is mostly solid or cystic,
- Study the vascularization searching for signs of hypervascularization on color Doppler; whenever possible record the systolic speed of the hepatic artery and evaluate the size of the hepatic veins looking for their dilatation.

If the mass is solid, heterogeneous with multiple vessels within it, a liver hemangioma should be suspected. Dilated hepatic artery and hepatic veins, cardiomegaly or cardiac failure are associated signs highly suggestive of this diagnosis. They are related to hypervascularization of the tumor. Constant evaluation of the cardiac status is very important as high inflow in the hemangioma may lead to high output cardiac failure.

If the mass is solid without hypervascularization, it may still be a hemangioma or more rarely a hepatoblastoma.

If the mass is mainly cystic and multilocular, a mesenchymal hamartoma should be suspected.

In case of a fetal tumor, a close follow-up during pregnancy should monitor modifications of the size of the tumor and evaluate cardiac com-

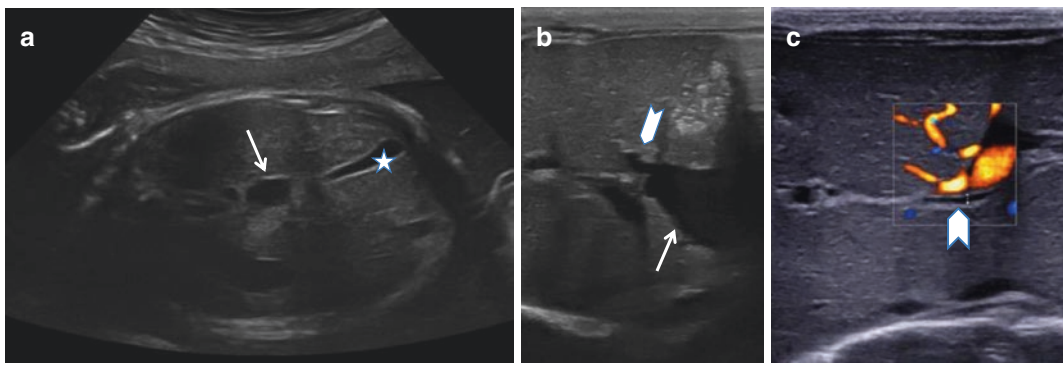

Fig. 8.1 Choledochal cyst: (**a**) Prenatal ultrasound at 32 W GA showing the large cyst located in the liver pedicle (*arrow*) with a normal gallbladder (*star*). (**b**, **c**) Postnatal liver US shows the cyst in the hepatic pedicle that communicates with dilated intrahepatic bile ducts. Dilatation of intrahepatic bile ducts allows to rule out biliary atresia and in the absence of intrinsic or extrinsic obstacle is in favor of a cholechodal cyst

plications [8]. For neonatal presentation and management, see below Sects. 8.3.4 and 8.4.3.

8.3.1.3 Hepatic Vascular Malformations

Vascular malformations involving the hepatic vessels can be diagnosed during pregnancy; in most cases, they are fortuitously discovered.

They appear in utero as umbilico-porto-systemic shunts and as porto-systemic shunts after birth. They may be complicated by intrauterine growth retardation, cardiomegaly, or cardiac failure.

In exceptional cases, an aberrant umbilical vein connects directly with the extrahepatic portal system (mesenteric vein, portal vein, or main portal vein) determining an extrahepatic umbilico-portal shunt. No fetal complications occur (most usually).

Arteriovenous fistulas can also be detected during pregnancy but have been very exceptionally described.

For neonatal presentation and management, see below in Sects. 8.3.5 and 8.4.3.

8.3.2 Obstructive Cholestasis in the Neonate

Cholestatic jaundice is characterized by the elevation of serum-conjugated bilirubin and may be related to serious conditions already in neonates. It affects approximately 1 in every 2500 infants. The most common causes of cholestatic jaundice in the first months of life are biliary atresia and neonatal hepatitis that can be associated with infectious, metabolic and syndromic disorders. The list of causes is summarized in Table 8.1.

The main goal of initial imaging is to assess the aspect of the bile ducts and of the gallbladder and to search for signs suggestive of biliary atresia (BA) (that affects 1 in 10,000–19,000 infants). Early diagnosis of BA is mandatory to perform early surgery and improve the prognosis.

If the intrahepatic bile ducts are dilated, BA can be ruled out. The cause of the dilatation must be rapidly determined: bile plug syndrome, where sludge obstructs the main bile duct, malformation mainly choledochal cyst or extrinsic compression by a tumor or a malformation (Fig. 8.2).

Table 8.1 Causes of neonatal cholestasis

Type of lesion	Cause	Type of cause
Extrahepatic bile duct obstruction (about 5%)	Cholelithiasis Choledochal cyst Spontaneous bile duct perforation Duodenal duplication Bile duct compression by a mass, etc.	Surgical
Extra and intrahepatic obstruction	Biliary atresia	Surgical
Intrahepatic bile ducts lesions and hepatocytes dysfunction	Sclerosing cholangitis Transient neonatal cholestasis Paucity of interlobular bile ducts (Alagille syndrome and the nonsyndromic forms) Progressive familial intrahepatic cholestasis (PFIC) Alpha-1-antitrypsin deficiency Infections Cystic fibrosis Parenteral nutrition Niemann-Pick disease, type C tyrosinemia, galactosemia, mitochondrial respiratory chain disorders, etc.	Medical

If *the bile ducts are not dilated*, the sonologist should search for the various signs quite specific of BA including

- The triangular cord sign (TCS),
- A small gallbladder (<15 mm)
- Thickening and/or irregularity of the gallbladder wall,
- Microcyst(s) of the porta hepatis or macrocyst of the liver pedicle
- Any evidence of the polysplenia syndrome: polysplenia or asplenia and/or preduodenal main portal vein and/or abnormal inferior vena cava (IVC) and/or heterotaxia (Fig. 8.3) [9].

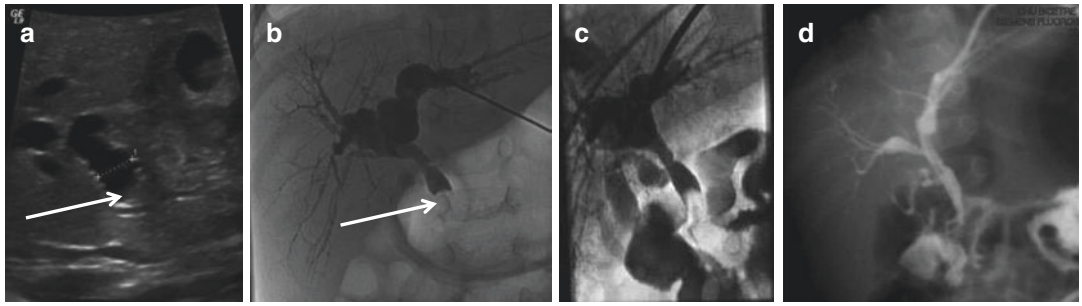

Fig. 8.2 Bile plug syndrome. Two-month-old baby without medical history, presenting with fever, discomfort, and acholic stools for a few hours. (**a**) US shows a biliary stone. Because of the fever and the complete obstruction and dilatation of bile ducts upstream, percutaneous transhepatic (PTC) was performed. (**b**) Opacification shows the major dilatation of intrahepatic and extrahepatic bile ducts with complete obstruction of the common bile duct. (**c**) Serum saline injection allows the progression of the calculus through the papilla. Note intraparenchymal extravasation due to the high intra-biliary pressure during injection. The baby was receiving antibiotics for the treatment of the cholangitis complicating the obstruction at the time of the procedure. (**d**) External drainage is kept in place. Opacification a few days later shows the complete normalization of the aspect of the biliary tree

High diagnostic performances have been reported in most studies, using combination of these signs. *However, very importantly: a normal hepatobiliary ultrasonography does not rule out BA.*

As for the other imaging modalities, neither liver CT nor MR imaging allows the direct diagnosis of BA [1].

MR cholangiography is indicated in cases with bile duct dilatation and suspicion of malformation. The technique will assess the exact anatomy of the bile ducts and of the biliopancreatic junction that may be abnormally long (>5 mm). It may also demonstrate other malformations or a mass compressing the biliary tree.

8.3.3 Neonatal Acute Liver Failure

Acute neonatal liver failure is very rare. Classical causes are neonatal hemochromatosis, hematological malignancies, viral infections, and liver-based metabolic defects [10]. The aim of imaging is to look for:

- Evidence for chronic liver disease that may suggest neonatal cirrhosis related to neonatal hemochromatosis, mitochondrial disease, or tyrosinemia,
- Involvement of other organs indicative of some specific diagnosis: for instance, large echogenic kidneys associated with tyrosinemia or enlarged lymph nodes suggestive of a hemopathy,
- Signs of portal hypertension such as porto-systemic shunt and alteration of portal flow. Prolonged patency of the ductus venosus beyond the age of 1 month is a precocious sign of portal hypertension (Fig. 8.4) [11].

Neonatal hemochromatosis may appear as a cirrhotic multinodular liver. Diagnosis relies on MR imaging that demonstrates the presence of iron overload in the pancreas as well as in the liver but the absence of siderosis in the spleen. On T2*-weighted images the signal intensity of the liver and the pancreas is markedly decreased compared to the signal of paravertebral muscles whereas it is normal in the spleen (Fig. 8.4). To be noted, in the absence of extrahepatic iron overload, marked hepatic siderosis is physiological in the perinatal period [2, 12].

Multilocular liver tumors are exceptionally associated with liver failure; therefore, a multinodular liver associated with liver failure is highly suggestive of a metabolic disorder (hemochromatosis, mitochondrial respiratory chain disorder, tyrosinemia, etc.).

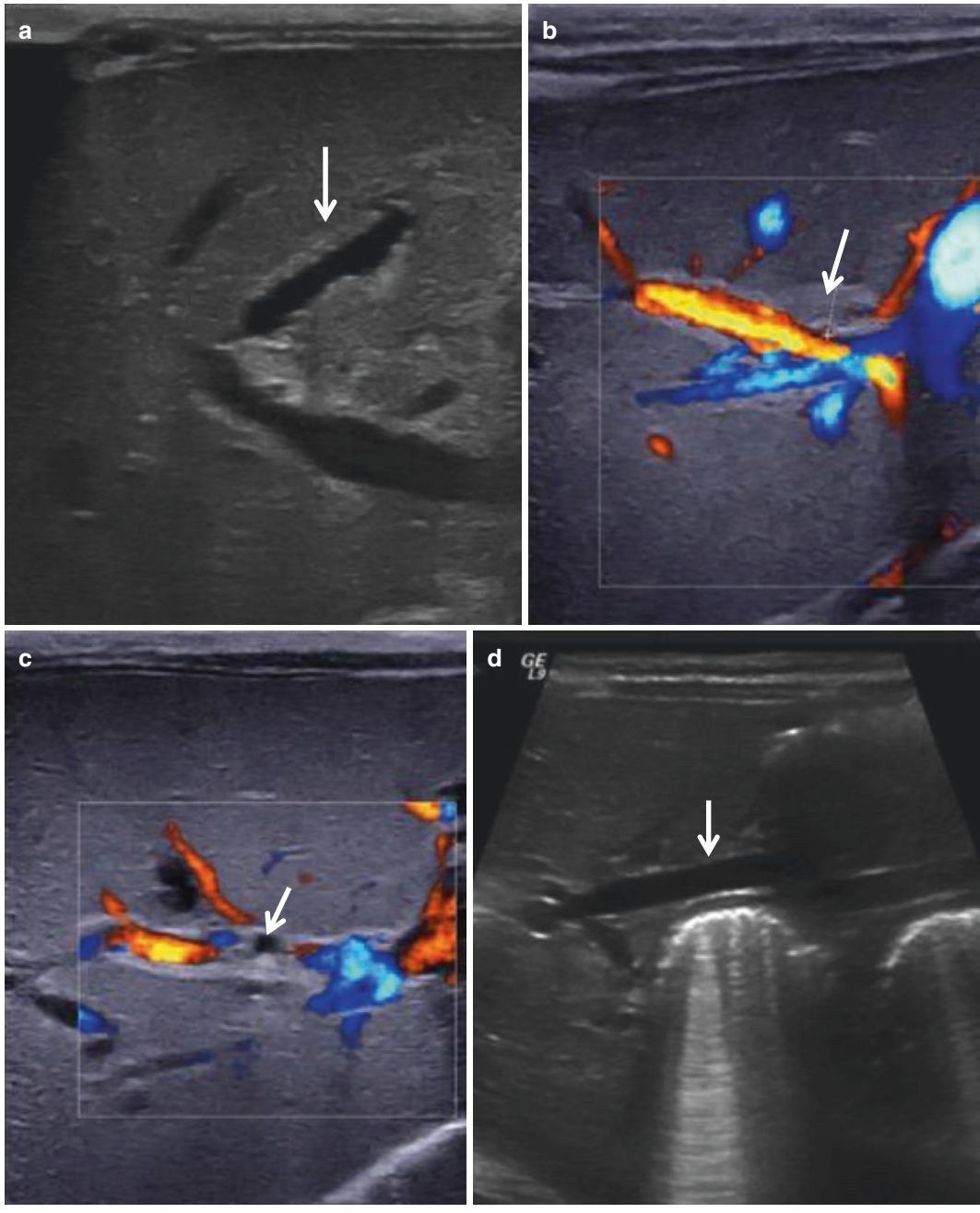

Fig. 8.3 Biliary atresia, suggestive sonographic signs in different patients. (**a**) Small gallbladder with thickened hyperechoic irregular wall. (**b**) Hyperechoic area at the porta hepatis located just anterior to the *right portal* vein corresponding to the triangular cord sign. (**c**) Porta hepatis microcyst. (**d**) Preduodenal main portal vein

8.3.4 Neonatal Liver Mass

The most frequent neonatal liver mass is hemangioma that may be congenital or infantile. It consists in an endothelial proliferation of vessels; it may present as a solitary mass, as multiple masses, or as a diffuse infiltration of the liver without visibility of any normal, non-tumoral,

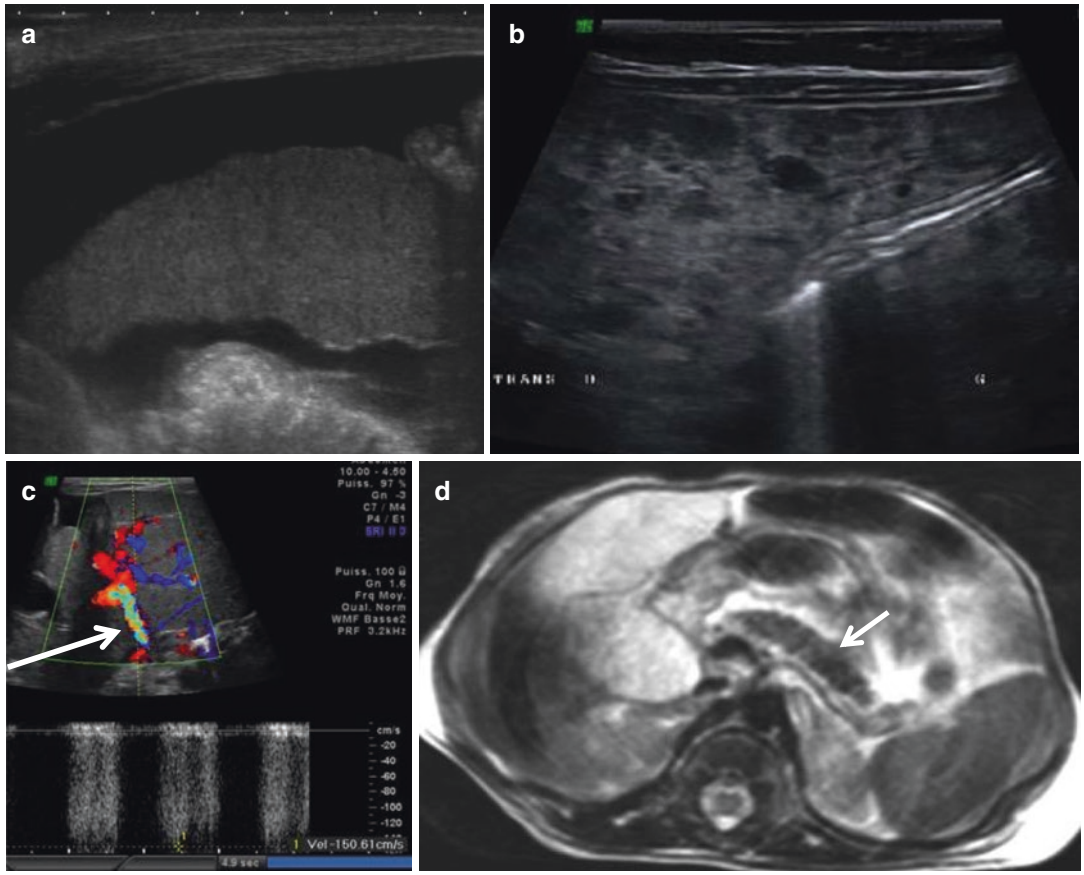

Fig. 8.4 Causes of neonatal liver failure: a, b, and c mitochondrial cytopathy. d and e: neonatal hemochromatosis. (**a**) Perihepatic ascites allows to depict clearly the irregular margins of the liver. (**b**) Multinodular liver. (**c**) Patent ductus venosus at 1 month in a context of liver failure is suggestive of portal hypertension. (**d**) MR Imaging on the axial plan T2* weighted images shows the very low signal of the pancreas highly suggestive of the diagnosi

liver tissue. Most are asymptomatic but some may be life threatening because of the huge hepatomegaly determining the so-called *compartmental syndrome*; high output cardiac failure, consumption coagulopathy, failure to thrive, and /or hypothyroidism (typically associated with multiple or diffuse hemangiomas)**.** Establishing the diagnosis is usually easy with US and is based on the detection of a well-defined, usually heterogeneous mass with multiple vessels within it (Figs. 8.5 and 8.6). However, the pattern may vary in terms of degrees of echogenicity and heterogeneity. Intratumoral calcifications can be observed. Dilated hepatic artery and hepatic veins, cardiomegaly, or cardiac failures are associated findings confirming the diagnosis; they are related to the high vascularization of the tumor. Porto-hepatic fistulas can be associated with hemangiomas (and rarely arteriovenous shunting). If the diagnosis is obvious on US and if there is no significant clinical complication, neither MR imaging nor CT is necessary. In case of ambiguous diagnosis or complication, additional exploration with MR imaging or CE-CT with dynamic acquisitions is necessary to demonstrate the typical pattern. Hemangiomas appear with a high signal on T2-weighted sequences and strong peripheral enhancement during the arterial phase with progressive filling at the portal phase (Figs. 8.5 and 8.6). CE-CT or MR imaging may also provide useful vascular mapping prior to embolization [13, 14]. In symptomatic forms, the

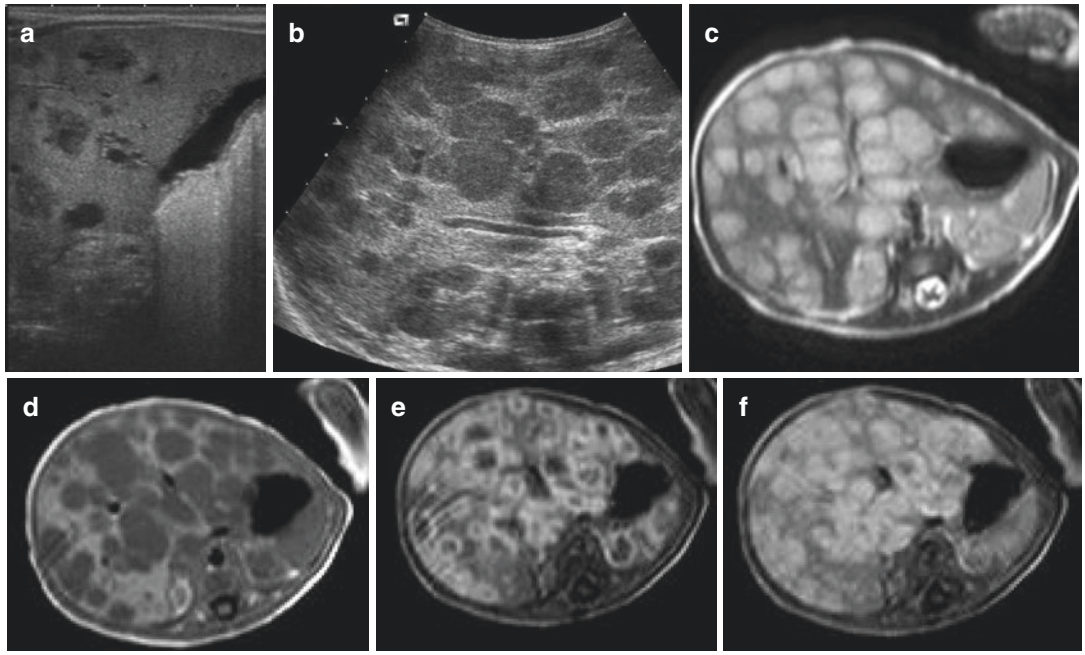

Fig. 8.5 Neonatal multiple liver hemangiomas: various aspects on US and typical MRI patterns. (**a**) In one infant, well delimited multiple hypoechoic nodules with peripheral hyperechoic rim. (**b**) In an other infant with multiple hepatic hemangiomas: On US, multiple well-delimited hypoechoic nodules. (**c**) Multiple nodules with high signal intensity in T2-weighted images. (**d**) The nodules have a low signal on T1-weighted images. (**e**) There is a strong peripheral enhancement at the arterial phase after gadolinium injection. (**f**) A filing-up of the nodule with contrast at the portal phase

treatment is controversial. It includes supportive treatment, medications such as propranolol, arterial embolization, and rarely surgical resection [14, 15].

Mesenchymal hamartoma is much rarer but represents the second most frequent neonatal hepatic tumor. It is considered to be a tumor rather than a developmental anomaly because of the presence of somatic genetic changes common with embryonal sarcoma [16]. Most infants present with an asymptomatic abdominal mass. On imaging, mesenchymal hamartomas are typically multicystic, displaying the association of macro- and microcysts and a tissular contingent of variable size. The multicystic aspect is easily demonstrated on US. If useful, MR imaging will demonstrate the cystic component that will appear hypointense on T1-weighted images and hypersignal on T2-weighted sequences. After contrast injection, enhancement of the septa and of the solid parts is visible. The treatment is usually surgical because of the potential growth of the lesion and of the possible associations with embryonal sarcoma. Associations with hepatic hemangiomas or with the Beckwith-Wiedemann syndrome have also been reported [17].

In exceptional cases, hepatoblastoma will be detected during prenatal US but in most cases, it will be diagnosed after birth because of a neonatal abdominal mass. Most often, it will appear as a solid type mass, quite homogeneous, with no strong enhancement after contrast injection on CT or MR imaging. A marked raised level of α-fetoprotein is frequent. As the α-fetoprotein is physiologically elevated in the neonatal period, in case of levels close to normal values, the level should be re-evaluated by a control examination 2 weeks later. To be noted, a rhabdoid liver tumor may present as a solid mass without elevation of α-fetoprotein. A biopsy of the tumor is usually performed. Chemotherapy followed by surgical resection represents the usual management.

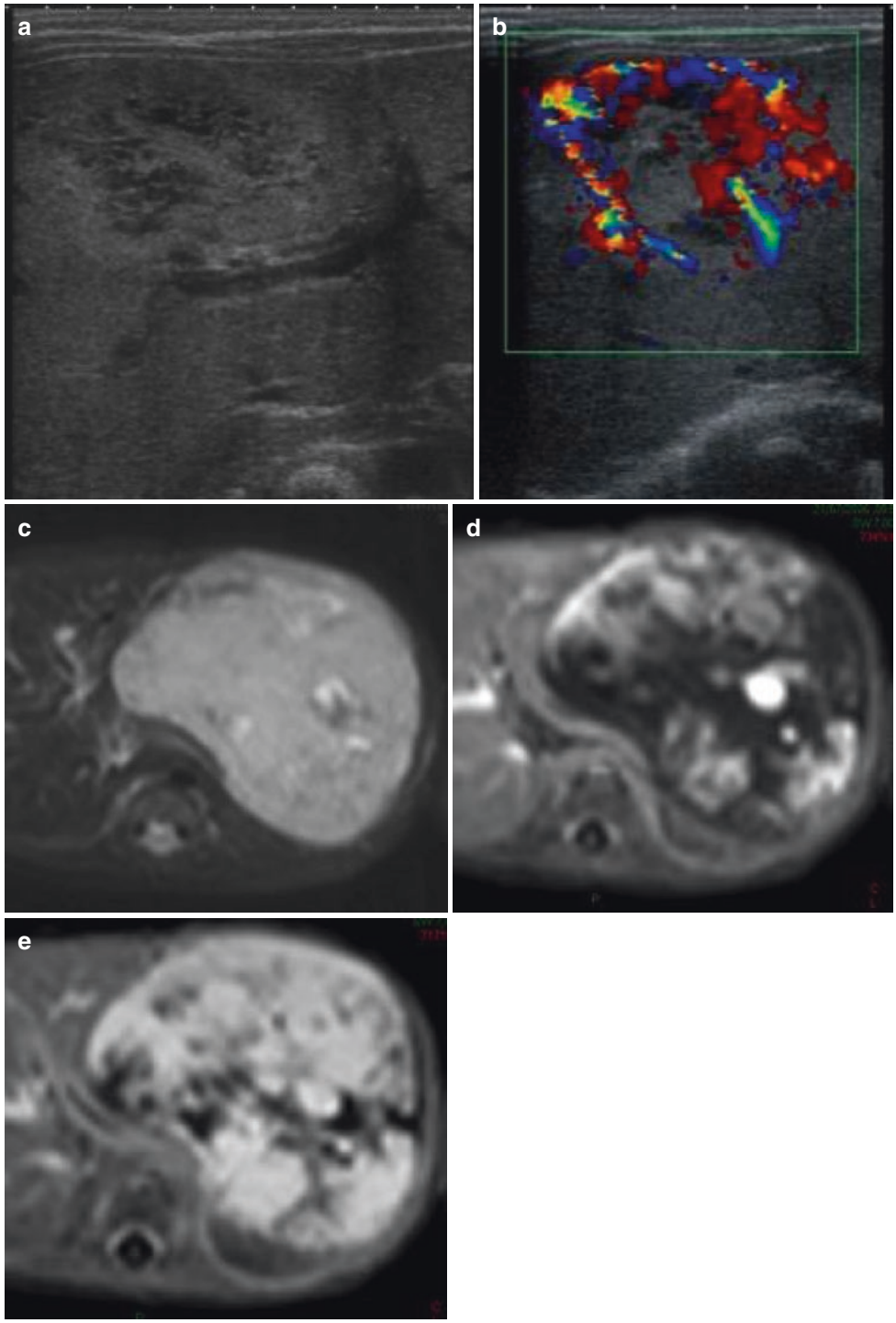

Fig. 8.6 Neonatal liver solitary hemangioma in two different patients: On US: (**a**) Well-delimited heterogeneous mass with anechoic vascular spaces on US. (**b**) Numerous vessels on color Doppler especially at the periphery of the mass. Typical aspect of multiple or solitary hepatic hemangiomas on MRI with: (**c**) hyperintensity of the mass in T2-weighted images, (**d**) strong peripheral enhancement at the arterial phase, and (**e**) filling up at the portal phase

A particular neonatal liver pseudo-mass should be mentioned and is related to umbilical vein catheter (UVC) malposition followed by extravasation in the liver parenchyma. It will appear as a heterogeneous pseudo-mass in the left lobe and/or segment 4, close to the left portal vein. The echogenicity of the pseudo-mass is variable. It is sometimes possible to see the abnormal UVC tract in the parenchyma reaching the pseudo-mass. The neonate may display clinical and/or biological signs of infection. If the UVC is still in place, it must be removed. When infection is present, an adapted treatment should be installed. In the absence of complication, a follow-up by US is sufficient (see also Chap. 4) [18].

8.3.5 Neonatal Vascular Malformation

Vascular malformations are very rare and may be diagnosed either on prenatal imaging (Sect. 8.3.1.3) or because of neonatal complications such as cardiac (cardiomegaly, cardiac failure) or metabolic complications (hypoglycemia, hypergalactosemia, hyperammonemia) or because of portal hypertension (in case of arterio-portal shunt).

Three groups of vascular malformations can be encountered: porto-systemic shunts, arterio-portal fistula, and exceptionally abnormal connection of the umbilical vein or pulmonary veins to the portal system.

Among these rare entities, the most frequent are congenital porto-systemic shunts (CPSS); CPSS consists in an abnormal connection between one or several vein(s) of the portal system and one or several systemic vein(s) inside or outside the liver parenchyma. More than half of these CPSS are porto-hepatic shunts (direct connection(s) of portal branches and hepatic veins) (Fig. 8.7). In our unpublished experience, 8/10 infants have experienced spontaneous closure of the shunts at a median age of 3 months and the majority before 1 year. CPSS may be associated with cardiac failure, abnormal pulmonary hypertension, hypoglycemia, hyperammonemia and hypergalactosemia or thrombopenia. These disorders are usually transient. In rare instances, when the abnormal shunt is located before or just at the beginning of the main portal

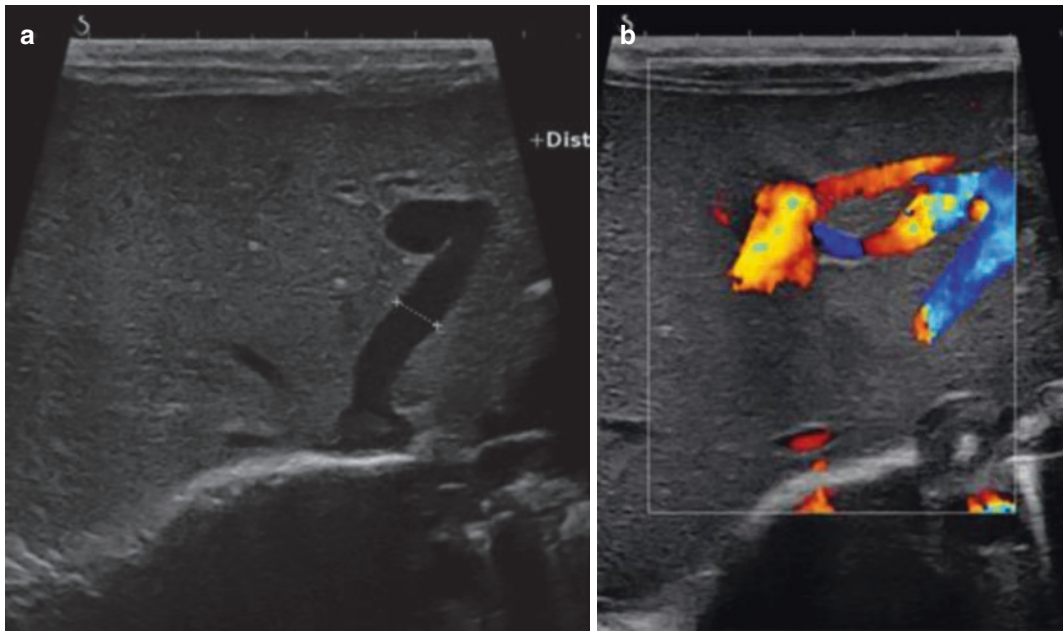

Fig. 8.7 Porto-hepatic fistula between the left portal branch and the left hepatic vein on (**a**) B-mode, (**b**) Color Doppler

vein, early surgical or radiological closure may be necessary to avoid progressive thrombosis or hypoplasia of the portal system downstream the shunt. In other anatomical forms, a US follow-up is recommended and closure of the shunt will be discussed only after 1 year in the absence of spontaneous closure [19].

Congenital arterio-portal fistulas are very rare. In the neonatal period they may present with severe portal hypertension and high cardiac output failure. The diagnosis is achieved on US that will demonstrate the communication between one or several hepatic arteries and one or several portal vein branches. The severity of the shunt is expressed by the reversed and arterialized portal flow displayed in the main portal vein and the extrahepatic portal system. Splenomegaly is associated with the more severe forms. In case of portal hypertension, if the anatomical form is favorable (only few feeding arteries), then embolization of the feeding arteries can be performed percutaneously. If the arterio-portal fistulas are too numerous and complex, with a large part of the liver being involved, a surgical resection can be proposed.

Two very rare malformations may lead to portal thrombosis in the neonatal period with a risk of portal hypertension. First, the umbilical vein may connect directly to an extrahepatic portal system (superior mesenteric vein, left gastric vein, main portal vein, etc.). There is no complication from this connection during fetal life; yet, after birth, there is a possibility of an extension of the physiological thrombosis of the umbilical vein towards the portal system, leading to portal obstruction and portal hypertension. When diagnosed prenatally, close neonatal US follow-up is necessary. In case of thrombosis of "normal" veins, anticoagulation should be started to limit the risk of portal thrombosis [20, 21]. Second, in exceptional cases, an infradiaphragmatic anomalous pulmonary venous return collector may connect directly to a vein of the portal system. After surgical correction of the abnormal venous return, extension of the thrombosis from the collector to the vein of the portal system may lead to portal thrombosis and portal hypertension. Once again, close US follow-up to search for portal thrombosis should be obtained and anticoagulation should be started in case of portal thrombosis.

8.4 The Role of Interventional Radiology

Interventional radiology plays an important role for the diagnosis and the management of different neonatal hepatic disorders.

8.4.1 Neonatal Liver Biopsy

Percutaneous liver biopsy can be performed in neonates in the absence of coagulation disorder. The biopsy will be performed by transjugular approach in case of coagulation disorders or in case of perihepatic ascites in babies weighting more than 2500 g. We usually use an adult biopsy set (Labs-100, William Cook Europe, Bjaervoskov, Denmark) because it allows us to obtain cores with an 18-gauge needle. In all cases, a continuous sonographic guidance is mandatory to avoid complications. Percutaneous liver biopsy should be performed using 18-gauge biopsy needles. Biopsy specimen will be fixed according to the pathologist's recommendations.

8.4.2 Neonatal Biliary Interventions

Biliary interventions in neonates have two main indications: diagnosis of neonatal cholestasis using cholecystography and treatment of the bile plug syndrome.

8.4.2.1 Cholecystography in Neonatal Cholestasis

In neonates with cholestasis and acholic stools, but no other specific patterns of BA (on clinical, biological and non invasive imaging examinations), opacification of the biliary tract via the gallbladder using transhepatic cholecystography may contribute to the diagnosis. It will also allow biochemical analysis of the bile for the diagnosis of rare medical cholestasis.

Cholecystography is performed under general anesthesia. Transhepatic puncture of the gallbladder is performed under US guidance using a 25-gauge needle. Opacification may reveal absence of opacification of intrahepatic bile ducts highly suggestive of BA, very irregular and thin intrahepatic bile ducts suggestive of neonatal cholangitis, or a normal anatomy of intra- and extrahepatic bile ducts that allows to rule out the two previous diagnosis [22].

8.4.2.2 Percutaneous Treatment of Bile Plug Syndrome

Bile plug syndrome is related to the obstruction of the bile ducts by sludge in neonates and infants.

In case of complete obstruction associated with sepsis or prolonged during more than 2 weeks, cholecystography or percutaneous cholangiography with saline flushing may be necessary to push the obstructing sludge into the bowel and relieve the obstacle. When necessary, a small balloon can be inflated at low pressure (1 atm) to push the stones into the duodenum through the Oddi's sphincter. An external drainage is performed at the end of the procedure and repeated saline flushing may be necessary. In case of failure of percutaneous treatment, surgery will be performed [22] (Fig. 8.2).

8.4.3 Neonatal Vascular Interventions

Neonatal vascular interventions are rare but may be necessary in case of complicated vascular tumor (hemangiomas) or malformation.

During the first days of life, the umbilical vein and umbilical arteries may be used as vascular access for endovascular procedures.

8.4.3.1 Endovascular Treatment of Liver Hemangioma

The treatment of hepatic hemangioma remains controversial. Endovascular treatment using arterial embolization can be performed in symptomatic cases with high output cardiac failure or consumptive coagulopathy resisting to medical treatment, as well as in case of life-threatening abdominal compartmental syndrome due to the tumoral volume. The aim of the procedure is to reduce significantly the arterial feeding of the lesion (even if not completely). The efficacy of the procedure can be confirmed very quickly on the cardiac complications but may be delayed on other complications [14, 23].

8.4.3.2 Endovascular Treatment of Vascular Malformations

In exceptional cases, early treatment of vascular malformation may be necessary when complications are not controlled with medical treatment.

Procedures consist in the embolization of abnormal vessels or shunts using adapted devices.

Conclusion

Imaging plays a key role for the diagnosis of fetal and neonatal liver disorders. US using high frequency probe is mandatory in order to provide the best quality exams. Liver-MR imaging and MRCP will be performed in case of suspicion of neonatal hemochromatosis, for the diagnosis work-up of liver tumors, if the diagnosis of hemangioma is not obvious on US or in complicated forms and in suspicion of biliary malformations or obstruction with bile ducts dilatation. Liver CT will be performed mostly for liver tumors and vascular malformations. In exceptional cases, interventional radiology will be performed for treatment.

References

1. Siles P, Aschero A, Gorincour G, Bourliere-Najean B, Roquelaure B, Delarue A, et al. A prospective pilot study: can the biliary tree be visualized in children younger than 3 months on magnetic resonance cholangiopancreatography? Pediatr Radiol. 2014;44(9):1077–84.
2. Hayes AM, Jaramillo D, Levy HL, Knisely AS. Neonatal hemochromatosis: diagnosis with MR imaging. AJR. 1992;159(3):623–5.
3. Blazer S, Zimmer EZ, Bronshtein M. Nonvisualization of the fetal gallbladder in early pregnancy: comparison with clinical outcome. Radiology. 2002;224(2):379–82.

4. Dreux S, Boughanim M, Lepinard C, Guichet A, Rival J-M, de Becdelievre A, et al. Relationship of non-visualization of the fetal gallbladder and amniotic fluid digestive enzymes analysis to outcome. Prenat Diagn. 2012;32(5):423–6.
5. Hertzberg BS, Kliewer MA, Maynor C, McNally PJ, Bowie JD, Kay HH, et al. Nonvisualization of the fetal gallbladder: frequency and prognostic importance. Radiology. 1996;199(3):679–82.
6. Shen O, Rabinowitz R, Yagel S, Gal M. Absent gallbladder on fetal ultrasound: prenatal findings and postnatal outcome. Ultrasound Obstet Gynecol. 2011;37(6):673–7.
7. Isaacs H. Fetal and neonatal hepatic tumors. J Pediatr Surg. 2007;42(11):1797–803.
8. Franchi-Abella S, Gorincour G, Avni F, Guibaud L, Chevret L, Pariente D, et al. Hepatic haemangioma-prenatal imaging findings, complications and perinatal outcome in a case series. Pediatr Radiol. 2012;42(3):298–307.
9. Koob M, Pariente D, Habes D, Ducot B, Adamsbaum C, Franchi-Abella S. The porta hepatis microcyst: an additional sonographic sign for the diagnosis of biliary atresia. Eur Radiol. 2017;27(5):1812–21.
10. Shanmugam NP, Bansal S, Greenough A, Verma A, Dhawan A. Neonatal liver failure: aetiologies and management—state of the art. Eur J Pediatr. 2011;170(5):573–81.
11. Farrant P, Meire HB, Karani J. Ultrasound diagnosis of portocaval anastomosis in infants—a report of eight cases. Br J Radiol. 1996;69(821):389–93.
12. Oddone M, Bellini C, Bonacci W, Bartocci M, Toma P, Serra G. Diagnosis of neonatal hemochromatosis with MR imaging and duplex Doppler sonography. Eur Radiol. 1999;9(9):1882–5.
13. Christison-Lagay ER, Burrows PE, Alomari A, Dubois J, Kozakewich HP, Lane TS, et al. Hepatic hemangiomas: subtype classification and development of a clinical practice algorithm and registry. J Pediatr Surg. 2007;42(1):62–7. discussion 67–8
14. Kassarjian A, Zurakowski D, Dubois J, Paltiel HJ, Fishman SJ, Burrows PE. Infantile hepatic hemangiomas: clinical and imaging findings and their correlation with therapy. AJR. 2004;182(3):785–95.
15. Léauté-Labrèze C, Voisard J-J, Moore N. Oral propranolol for infantile hemangioma. N Engl J Med. 2015;373(3):284–5.
16. Mathews J, Duncavage EJ, Pfeifer JD. Characterization of translocations in mesenchymal hamartoma and undifferentiated embryonal sarcoma of the liver. Exp Mol Pathol. 2013;95(3):319–24.
17. Stringer MD, Alizai NK. Mesenchymal hamartoma of the liver: a systematic review. J Pediatr Surg. 2005;40(11):1681–90.
18. Hagerott HE, Kulkarni S, Restrepo R, Reeves-Garcia J. Clinical-radiologic features and treatment of hepatic lesions caused by inadvertent infusion of parenteral nutrition in liver parenchyma due to malposition of umbilical vein catheters. Pediatr Radiol. 2014;44(7):810–5.
19. Bernard O, Franchi-Abella S, Branchereau S, Pariente D, Gauthier F, Jacquemin E. Congenital portosystemic shunts in children: recognition, evaluation, and management. Semin Liver Dis. 2012;32(4):273–87.
20. Benoist G, Gauthier F, Belloy F, Laloum D, Herlicoviez M, Dreyfus M. Antenatal sonographic features of aneurysmal dilatation of a vitelline vein. Ultrasound Obstet Gynecol. 2007;29(6):708–11.
21. Héry G, Quarello E, Gorincour G, Franchi S, Gauthier F, de Lagausie P. Extrahepatic vitelline vein aneurysm: prenatal diagnosis and follow up. J Pediatr Surg. 2013;48(8):e1–4.
22. Franchi-Abella S, Cahill AM, Barnacle AM, Pariente D, Roebuck DJ. Hepatobiliary intervention in children. Cardiovasc Intervent Radiol. 2014;37(1):37–54.
23. Draper H, Diamond IR, Temple M, John P, Ng V, Fecteau A. Multimodal management of endangering hepatic hemangioma: impact on transplant avoidance: a descriptive case series. J Pediatr Surg. 2008;43(1):120–5. discussion 126

Part IV

Any Age: Digestive Tract

Acute and Subacute Intestinal Obstructions

9

Eléonore Blondiaux and Winnie Mar

Contents

9.1 Introduction

In children, bowel obstruction can be due to a variety of congenital and acquired causes that slightly differs from causes of bowel obstruction in fetuses and neonates (see also Chaps. 5 and 7). In infants and adolescents, the clinical signs of intestinal obstruction are similar to those seen in adults, such as abdominal pain, distension, and vomiting. The vomiting is bile stained when the obstruction occurs below the ampulla of Vater

E. Blondiaux (✉)
Department of Radiology, HUEP – APHP, Hôpital Armand-Trousseau, Faculté de Médecine Pierre et Marie Curie, 26 Avenue du Dr Netter, 75012 Paris, France
e-mail: eleonore.blondiaux@trs.aphp.fr

W. Mar
Department of Radiology, University of Illinois at Chicago, 1740 W. Taylor St., Room 2483 (MC 931), Chicago, IL 60612, USA

F.E. Avni, P. Petit (eds.), *Imaging Acute Abdomen in Children*,
https://doi.org/10.1007/978-3-319-63700-6_9

and clears when the obstruction is supra-ampullary (Fig. 9.1). Other clinical signs that may help elucidate the cause of intestinal obstructions are summarized in Table 9.1. In most cases, intestinal obstruction in a child requires imaging to determine its cause, location, and extent [1].

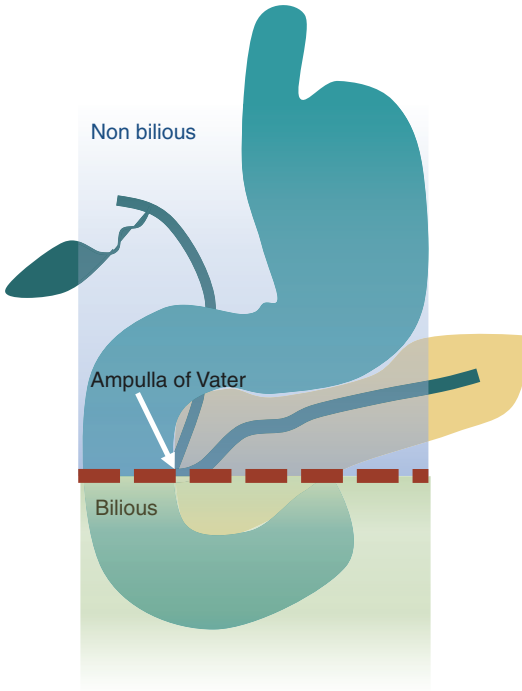

Fig. 9.1 Non-bilious or bilious vomiting according to the location of obstruction above or below the ampulla of Vater

Table 9.1 Summary of clinical signs that may lead to a cause of intestinal obstruction

Clinical sign	Cause of intestinal obstruction
Bilious vomiting	Sub-vaterian obstacle
Fever	Appendicitis or infected Meckel diverticulum
Chronic diarrhea	Inflammatory disease (Crohn's disease, ulcerative colitis)
History of surgery	Post-operative adhesions
Rash involving the legs	Henoch-Schönlein purpura
Posttraumatic abdominal pain	Intestinal wall contusion, acquired diaphragmatic hernia
Recent viral infection	Intestinal intussuception

9.2 Imaging Specificities and Recommendations, Strategies, Controversies, Evidence Based Data

Imaging of acute and subacute obstruction in children consists of a combination of ultrasound and fluoroscopy. Plain abdominal radiography and abdominal computed tomography (CT) are only occasionally performed.

9.2.1 Plain Abdominal Radiographs

In adults, the indications for abdominal radiography have dramatically decreased, as it has been largely if not completely replaced by CT. This is not the case in pediatric radiology where abdominal radiographs are still indicated in (1) Intestinal obstruction; (2) Ingested foreign body or suspected intraabdominal calcification; (3) Suspected perforation. Of note, in children, abdominal radiographs should not be performed to investigate chronic abdominal pain or constipation.

Abdominal radiographs can be limited to one supine film in most cases. In children, differentiating between small and large bowel loops is sometimes possible when the haustra are visible. In neonates, this differentiation is not possible in most cases.

In case of intestinal obstruction, analysis of bowel gas dilatation and distribution on supine abdominal radiograph helps to determine the type of obstruction: functional or mechanical. In older children and adults, small bowel loop diameter does not usually exceed 20–25 mm. In neonates and infants, the upper limit changes according to the age. Obstruction should be considered when the loop diameter exceeds the diameter of a vertebrae. Normal large bowel diameter does not exceed 60 mm. In case of functional obstruction (gastroenteritis, post-operative paralytic ileus), general dilatation of small and large bowel loops is observed on the supine view and air-fluid levels of varying lengths are found on the upright view. In mechanical obstruction, small bowel dilatation with decreased or absent colon or rectal gas can be found on the supine view and air-fluid levels in

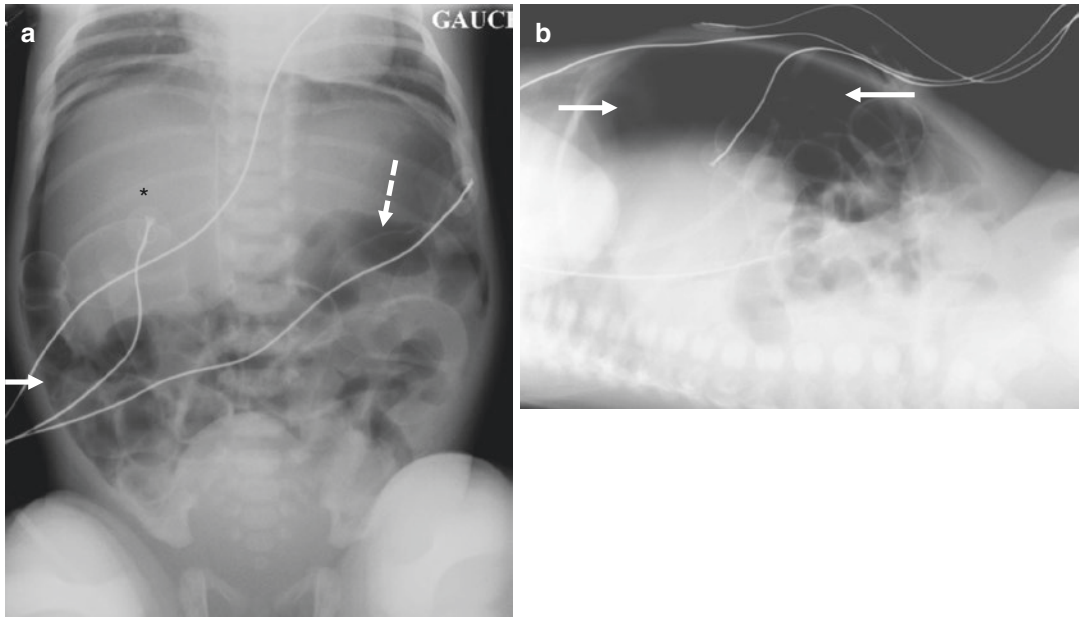

Fig. 9.2 Pneumoperitoneum in a 3-day-old boy with suspicion of Hirschsprung disease complicated with perforation. (**a**) Supine abdominal radiograph shows area of lucency over the liver and right upper quadrant (*asterisk*), triangle sign (*arrow*), and double-wall sign (or Rigler sign) (*dotted arrow*). (**b**) Supine abdominal radiograph with horizontal beam shows a large amount free intraperitoneal gas (*arrows*)

dilated loops can help localize the level of obstruction on a standing film.

Pneumoperitoneum, pneumatosis and in some cases the etiology of the intestinal obstruction (foreign body, abdominal mass) can be detected on abdominal radiographs. If intestinal perforation is suspected, upright position, lateral decubitus with horizontal beam or cross table lateral views depending on patients' age might be necessary to confirm the presence of extraluminal air (Fig. 9.2).

Still, the diagnostic yield of abdominal radiograph is low, as it is inconclusive in 25–35% of intestinal obstructions. Therefore, abdominal radiographs should not be performed if ultrasound or contrast examination finds the cause.

9.2.2 Contrast Examination

Indications for upper gastrointestinal (UGI) series, small-bowel follow-through (SBFT), or contrast enema in acute or subacute intestinal obstruction are summarized in Table 9.2. Iso-osmolar iodinated water-soluble contrast is generally preferred in children with signs of acute intestinal obstruction. The use of barium sulfate should be limited to the evaluation of non-complicated internal hernia or suspected malrotation without midgut volvulus. Air can be administered as natural contrast to reduce ileocolic intussusception [2].

9.2.3 Ultrasound

In most cases of suspected intestinal obstruction, ultrasound should be the first imaging modality performed as it is a noninvasive and radiation free technique. It may localize the level of transition between dilated (>35 mm in older children) and normal loops. US can distinguish functional and mechanical obstruction [3] (Fig. 9.3). Moreover, US can depict the cause of the obstruction (appendicitis, Meckel diverticulum, malrotation, duplication cyst, etc.) and its related complications.

Table 9.2 Indications for contrast examination in acute or subacute intestinal obstruction in children

Contrast examination	Indication	Contrast media
UGI	Gastric volvulus	Low osmolar water soluble
	Small-bowel volvulus	Low osmolar water soluble
	Superior mesenteric artery syndrome	Low osmolar water soluble
UGI with SBFT	Internal hernia (in absence of small-bowel obstruction)	Barium sulfate suspension
	Chronic intestinal pseudo-obstruction syndrome	Barium sulfate suspension
Therapeutic SBFT	Post-operative adhesions	Low osmolar water soluble
Diagnostic enema	Hirschsprung disease	Low osmolar water soluble
	Colonic volvulus	Low osmolar water soluble
Therapeutic enema	Intussusception	Dilute low osmolar water soluble or air
	Distal intestinal obstruction syndrome or meconium ileus	Dilute high osmolar water soluble

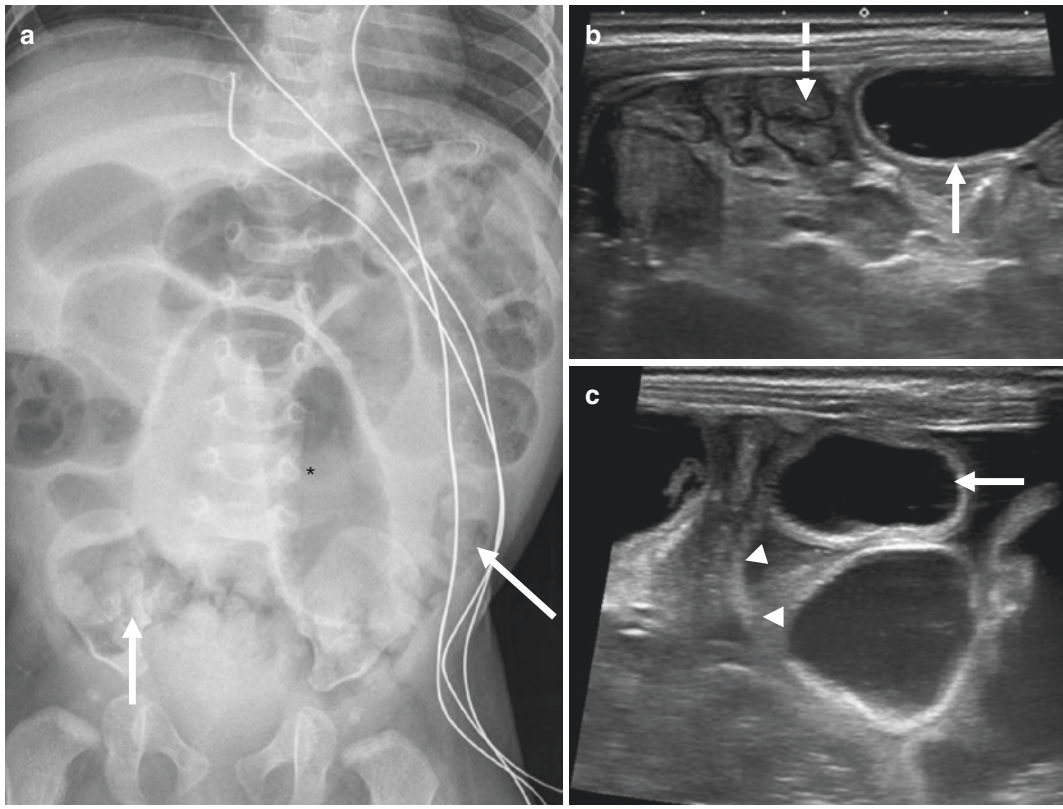

Fig. 9.3 Mechanical obstruction in an 8-month-old boy with history of laparotomy for irreducible intussusception. (**a**) Supine abdominal radiograph shows dilated bowel loops in the umbilical region (*asterisk*) and paucity of gas in colon (*arrow*). (**b**, **c**) Abdominal ultrasound with high-frequency probe images shows dilated small-bowel loops (*arrows*) with normal cecum (*dotted arrow*). The level of transition between normal and dilated loops is seen in the right lower quadrant (*arrowheads*). Note the wall thickening of the small-bowel loops and free intraperitoneal fluid (courtesy Doctor F. Chalard)

The different organs and vascular landmarks can be evaluated with US. The abnormal relative position of the superior mesenteric artery (SMA) and vein (SMV) is observed in small-bowel volvulus by Doppler ultrasound [4]. Finally, US can depict signs of severity such as bowel wall thickness >4 mm,

absence of peristalsis, pneumatosis, intraperitoneal free fluid, or portal venous gas.

US has a lower specificity compared to CT for the diagnosis of pneumoperitoneum and for the assessment of bowel wall ischemia.

9.2.4 CT

CT is usually not the initial radiologic examination in intestinal obstruction in children. In children under 2 years, the small amount of abdominal fat limits the distinction between the different digestive structures [5]. In older children and adolescents, the amount of fat increases and CE-CT allows an accurate evaluation of the localization and cause of the obstruction as well as the degree of severity. Therefore, CE-CT may be recommended when US is inconclusive especially in cases of volvulus, internal hernias, and complicated Meckel diverticulum. Precontrast imaging is not useful in most cases. An optimization of the CT settings according to the child age and weight is mandatory.

9.2.5 MR Imaging

MR imaging is rarely performed to establish a diagnosis of acute intestinal obstruction. MR enterography may be useful for the diagnosis of obstruction related to intestinal stricture/fibrosis in patients with Crohn's disease (see Chap. 13).

9.3 Stomach and Duodenum

9.3.1 Gastric Volvulus

Compared with adults, gastric volvulus is rare in infants and children. The obstruction may be acute (43%) or chronic (57%) [6]. Two types of gastric volvulus have been described:

- Organo-axial (OA) volvulus, in which the stomach rotates on a longitudinal axis. Rotation along this axis causes the greater curvature of the stomach to be situated superior to the lesser curvature, resulting in an "upside-down" stomach [6].
- Mesentero-axial (MA) volvulus, in which the stomach rotates along an axis perpendicular to its longitudinal axis. The antrum and the pylorus rotate anteriorly and superiorly to the gastroesophageal junction.

Mixed-type volvulus corresponds to the presence of features of both OA and OM volvulus.

Clinically, the most common signs of acute gastric volvulus in children are nonbilious vomiting, epigastric distension, and abdominal pain. Less common signs include acute respiratory distress, cyanosis, and hematemesis. In case of chronic gastric volvulus, symptoms may last for a longer time and include: nonbilious emesis, failure to thrive, growth retardation, gastroenteric reflux disease, and dyspnea [6]. In both types, it may be impossible to pass a nasogastric tube into the stomach or its course may be unusual [7]. Neurologic abnormalities, postsurgical interruption of the gastric ligaments following liver transplantation, Nissen fundoplication, heterotaxy syndrome with polysplenia can predispose to gastric volvulus. The mortality rate is relatively high in both acute and chronic gastric volvulus (6.5% and 2.7% respectively); more than two thirds of reported deaths are due to a delayed surgery [6].

Plain supine radiographs show a single large spherical gas bubble in the left upper abdomen or mid-abdomen (Fig. 9.4). It may contain an air-fluid level (one in OA, two in MA) on erect film. Elevation of the left diaphragm may be seen. A paucity of distal bowel gas is also seen in acute volvulus.

Contrast opacification will demonstrate the type of volvulus. In MA volvulus, the greater and lesser curvature maintain their normal relationship. The pylorus is abnormally placed close to and anterior and above the gastroesophageal junction (Fig. 9.4). In OA volvulus, the greater curvature lies above and to the right of the lesser curvature.

CT is not necessary in children and may delay the surgery. It is usually performed when the diagnosis is missed on initial plain radiographs [7].

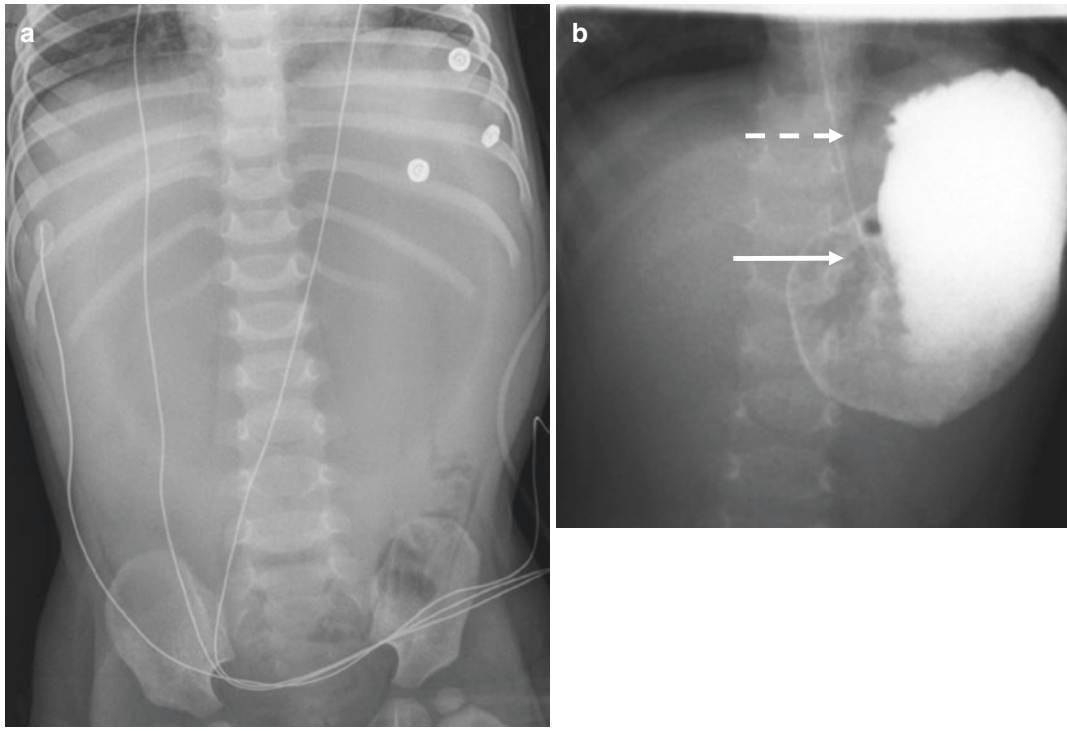

Fig. 9.4 Mesenteroaxial volvulus in a 16-month-old girl with nonbilious vomiting for 48 h and abdominal distension. (**a**) Supine abdominal radiograph shows a marked spherical distension of the stomach and paucity of distal bowel gas. (**b**) UGI series shows the abnormal position of pylorus (*arrow*) which is too close to the gastroesophageal junction (*dotted arrow*)

Gastric distension, gastric pneumatosis, and patterns of heterotaxy may be demonstrated with CT.

As mentioned, the treatment is surgical.

9.3.2 Gastric Bezoars

Bezoars correspond to intraluminal accumulation in the stomach or small bowel of ingested material that cannot be digested due to its particular composition. They may be composed of vegetable fibers (phytobezoar), hair (trichobezoar), or milk (lactobezoar). Trichobezoar is more frequent in children compared with phytobezoar. Lactobezoar is more common in lactating newborns. Initial symptoms are pain, vomiting, anemia, enteric and pancreaticobiliary obstructions. A left upper abdominal mass is usually palpable.

Ultrasound may demonstrate an endoluminal highly echogenic arc of air with a posterior acoustic shadowing whose appearance does not change with the position of patient or with different transducers [8]. The main differential diagnosis is a heavily calcified tumor or a mass of impacted feces [8]. In this case, UGI or CT might be required (Fig. 9.5).

Sensitivity and specificity of CT for diagnosing an ileus induced by a bezoar are 90% and 57%, respectively [9]. The presence of a round, mottled intraluminal mass associated with dilated intestinal loops is a good sign suggestive of bezoar [10]. CT is also effective for excluding other causes of intestinal obstruction.

The removal of the bezoar can be performed by open or laparoscopic surgery [9].

9.3.3 Pyloric Stenosis

Hypertrophic pyloric stenosis occurs usually during the first 3 weeks to the end of the second month of life. Males are more frequently affected than

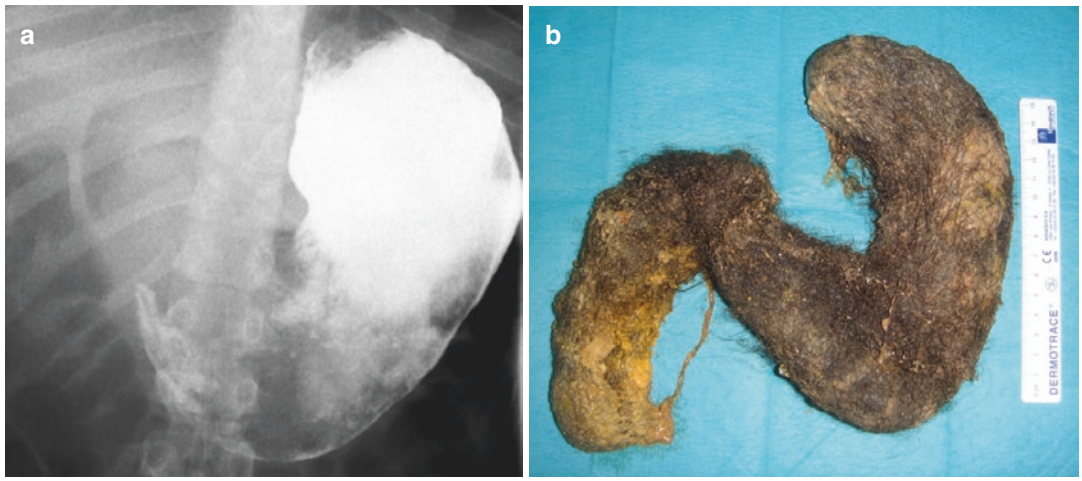

Fig. 9.5 Gastric trichobezoar. Left upper abdominal mass in a 12-year-old girl with vomiting and abdominal pain. (**a**) UGI series showing irregular shaped and mottled gas pattern in the stomach. (**b**) Removal of the trichobezoar at surgery that extended from the stomach to the second duodenum (courtesy Dr Larroquet)

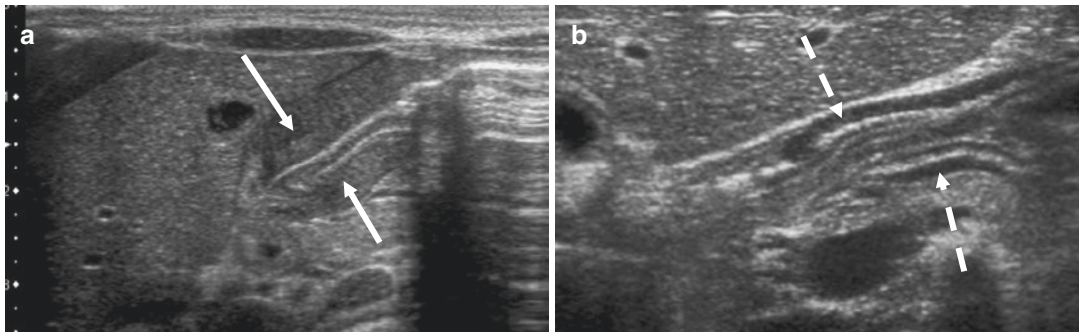

Fig. 9.6 Hypertrophic pyloric stenosis in a 24-day-old girl with projectile non-bilious vomiting. (**a**) Ultrasound with high frequency probe shows the hyperechoic thickening of the pylorus muscle (*arrows*). (**b**) Normal thin and hypoechoic appearance of pyloric muscular layer (*dotted arrows*) in a normal baby for comparison

females. Vomiting is usually projectile and non-bilious, as the obstruction is located above the ampulla of Vater. US shows the muscular thickening, the gastric stasis, and the absence of pylorus opening (Fig. 9.6). US is the only useful examination. The muscle wall thickness is above 3 mm and the pyloric channel length is above 14 mm. Parietal pneumatosis may rarely occur. Pyloric hypertrophy may rarely be diagnosed in utero. Symptoms of hypertrophic pyloric stenosis can also appear after administration of prostaglandin E in patients with cyanotic congenital heart disease. In this case, pyloric stenosis is not secondary to muscular thickening but to mucosal hypertrophy often with polypoid or lobular appearance at US (Fig. 9.7). Subsequent progressive thickening of the antropyloric muscle may develop [11].

Treatment consists first in correcting the dehydration and second in surgical pyloromyotomy.

9.3.4 Duodenal Duplication

Duodenal duplication cysts represent approximately 5% of all gastrointestinal duplication [12]. The cyst is always located on the mesenteric side of the second portion of the duodenum. The cyst is located either within the wall or inside the lumen of the duodenum. The differential diagnosis includes duodenal atresia in the neonatal period

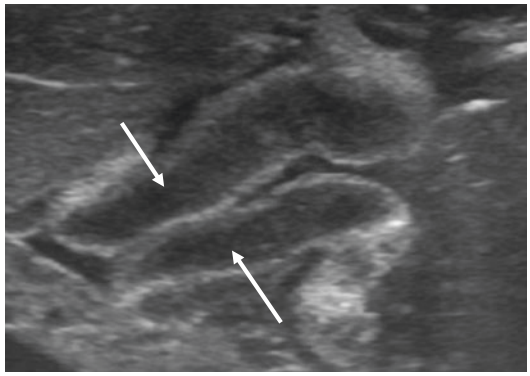

Fig. 9.7 Prostaglandin-induced antral mucosal hypertrophy in a 23-day-old boy post cure of a left diaphragmatic hernia. Ultrasound with high frequency probe shows marked antral mucosal thickening (*arrows*) without thickening of the pyloric muscle

and duodenal stenosis and duodenal web in later life.

US is helpful in demonstrating a round hypoechoic structure with a characteristic multilayered wall with hyperechoic inner mucosal layer and hypoechoic outer muscular layer. Cross-sectional imaging may reveal an intraluminal cyst in the second portion of the duodenum, with a shared medial wall between the cyst and the duodenum (Fig. 9.8).

Another differential diagnosis of intraluminal duodenal duplication cyst is a choledochocele: the former is located distal to the papilla, whereas the latter is located proximal to the papilla [13]. Clinically, children have symptoms of duodenal obstruction or palpable abdominal obstruction. The most common complication is pancreatitis [14].

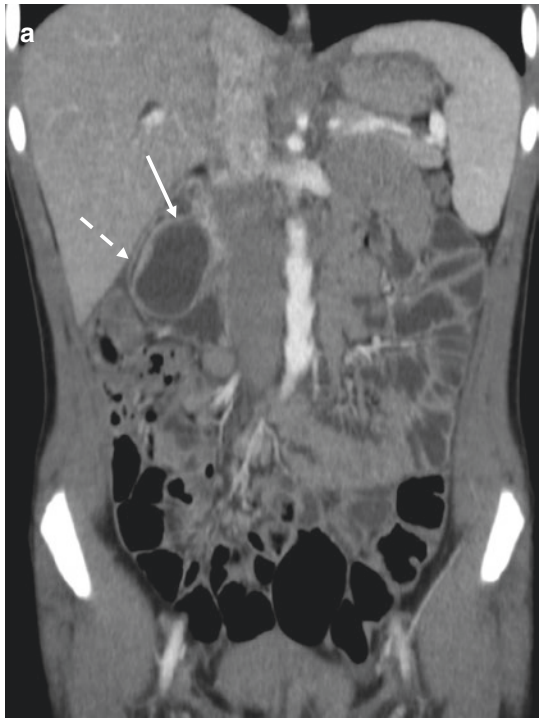

Fig. 9.8 Duodenal duplication cyst in a 10-year-old girl with abdominal pain, fever, vomiting, and elevated pancreatic enzymes. (**a**) CE-CT coronal reformatted image shows an intraluminal cyst (*arrow*) in the second portion of the duodenum (*dotted arrow*). (**b**) MRCP coronal MIP reconstruction shows that the cyst (*arrow*) is located distal to the papilla (*dotted arrow*)

The management includes either complete surgical resection of the duplication cyst or, in selected cases, endoscopic marsupialization.

9.3.5 Superior Mesenteric Artery Syndrome

Superior mesenteric artery syndrome is defined by the compression of the third portion of the duodenum between the aorta and the superior mesenteric artery (SMA). The prevalence of this syndrome is between 0.1 to 0.3%. The most common clinical presentation is vomiting, nausea, epigastric pain/distention, postprandial discomfort, and weight loss. It may be secondary to significant weight loss such as in anorexia nervosa, malabsorption syndrome, malignancy or following any severe injury. Correction of scoliosis (1–3 weeks after surgery) [15], rapid linear growth without compensatory weight gain particularly during the adolescence are other causes of superior mesenteric artery syndrome.

On UGI series, a dilatation of first and second portions of the duodenum with an abrupt narrowing of the third portion is observed (Fig. 9.9). The stomach may be distended as well. When the patient is positioned in a left lateral or ventral decubitus position, the obstruction resolves. However, a study comparing CT to fluoroscopy has a reported false-negative rate of 18.6% for barium studies [16].

On CE-CT with sagittal oblique reconstructions, the two key signs are: aortomesenteric angle below 22° and aortomesenteric distance of less than 8–10 mm [17] (Fig. 9.10). The SMA normally forms an angle of 45° with the aorta, with the normal angle ranging from 25° to 60° [18]. Associated imaging features include gastric and duodenal dilatation up to the aortomesenteric space where a sharp narrowing of the third portion of the duodenum can be seen.

The management is first conservative. It includes insertion of a nasojejunal tube to decompress the stomach and duodenum and enteral feeding. If conservative treatment is unsuccess-

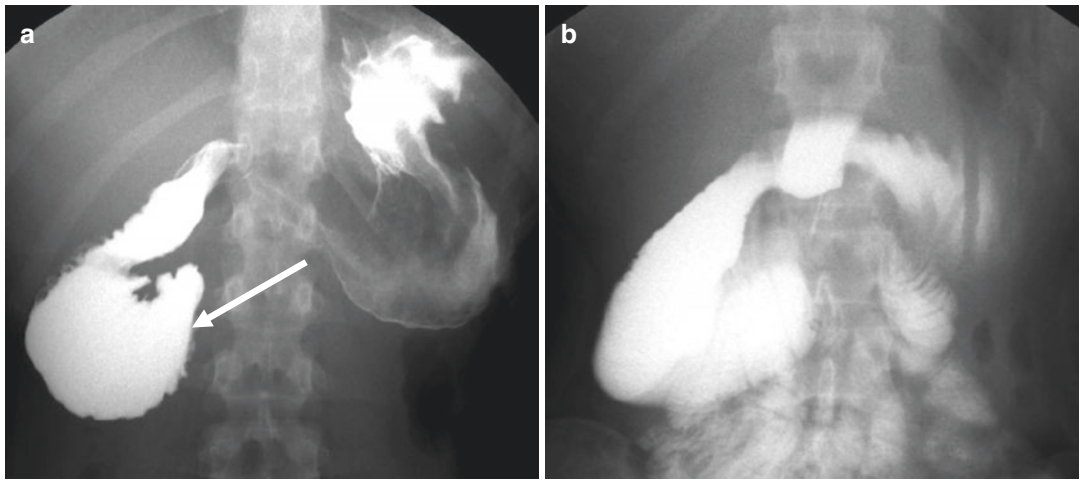

Fig. 9.9 Superior mesenteric artery syndrome in a 17-year-old girl with vomiting. (**a**) UGI series shows an abrupt compression of the third duodenum (*arrow*) and proximal dilatation of the second portion of the duodenum. (**b**) Prone view shows narrowing of third portion of duodenum from vascular compression but also a partial relief of the obstruction

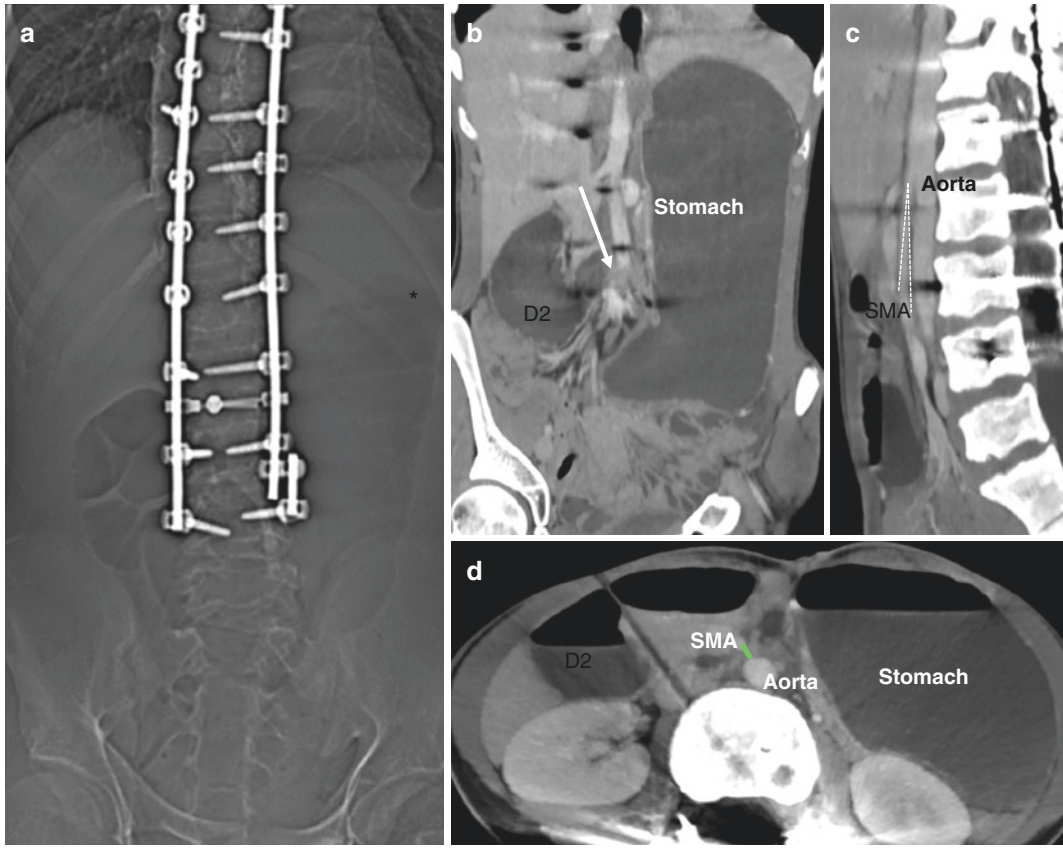

Fig. 9.10 Superior mesenteric artery syndrome in a 15-year-old patient with bilious vomiting and abdominal pain one month after scoliosis surgery. (**a**) Post-operative CT scout-view showing posterior arthrodesis and distended stomach (*asterisk*). (**b**) Oblique coronal image shows the distended stomach and second portion of the duodenum with abrupt narrowing of the third portion (*arrow*). (**c**) Obliquely oriented sagittal reconstruction of the superior mesenteric artery shows a decreased aorto-mesenteric angle (<22°). (**d**) Axial view demonstrates the distended stomach and duodenum as well as a narrowing of the aortomesenteric distance (<8 mm)

ful, laparoscopic or open duodenojejunostomy should be considered.

9.4 Small Bowel Obstructions

9.4.1 Malrotation and Small Bowel Volvulus

Malrotation anomalies occur in approximately 1 in 500 live births [19]. Duodenal obstruction is due to extrinsic compression from Ladd's bands (extending from the cecum to the lateral abdominal wall) or to small-bowel volvulus. Malrotation related volvulus (midgut volvulus) occurs within the first year of life in 90% of cases (75% in neonates), however acute cases can be diagnosed at any age. Midgut volvulus can lead to intestinal ischemia and irreversible necrosis and is potentially fatal.

The most common clinical presentation is bilious vomiting during the first weeks of life. Vomiting may be accompanied by abdominal distension or rectal bleeding, as a late sign. Beyond the first months of life, symptoms are less typical. They range from acute abdominal pain and vomiting to recurrent abdominal pain or simply failure to thrive. In some cases, these signs are wrongly attributed to gastroesophageal reflux or to anorexia in adolescents.

On US, the characteristic finding of midgut volvulus is the so-called "whirlpool sign" [20] (Fig. 9.11). This sign is produced by the clockwise twisting of the bowel, mesentery and superior mesenteric vein (SMV) around the axis of the superior mesenteric artery (SMA) [20]. The SMV, normally located at the right of the SMA, wraps around the SMA and is abnormally located on the left side of the SMA (Fig. 9.11). The presence of dilated bowel loops, thickened bowel walls, aperistaltic loops, and peritoneal fluid suggest intestinal ischemic damage. However, the absence of these signs at US cannot exclude intestinal ischemia.

On abdominal radiographs, air is visible in the stomach with a paucity of or lack of gas in the distal bowel. However, in some cases, the bowel gas pattern is normal. Therefore, normal abdominal radiograph cannot completely exclude malrotation and even volvulus [21].

At UGI series, in children with malrotation, the duodenal-jejunal junction is abnormally located to the right of the spine (or at least on the right side of the left pedicle), below the level of the duodenal bulb and anteriorly on the lateral view. In children with midgut volvulus, the proximal twisted segment has a characteristic corkscrew-like appearance (Fig. 9.12). Obstruction due to Ladd bands produce a Z-shaped configuration of the duodenum [22]. In malrotation (without signs of intestinal obstruction), barium enema is performed to document the position of the cecum.

Older children, like adults, with suspected small bowel volvulus secondary to malrotation, are more likely to undergo CT than any other imaging modality. CE-CT may demonstrate the whirlpool sign and signs of small-bowel ischemia.

Children with midgut volvulus should be immediately referred to surgery. The curative surgical treatment consists in a Ladd's procedure (i.e., untwisting the intestine, dividing congenital bands and widening the mesenteric attachments).

9.4.2 Congenital Inguinal Hernias

Congenital inguinal hernias affect between 1 to 2% of children and approximately 10% of these may be complicated by incarceration and bowel obstruction [1]. Males are more commonly affected than females. If incarceration has occurred, pain and vomiting are associated at physical examination with a localized inguinal lump that may or may not be reducible. In most

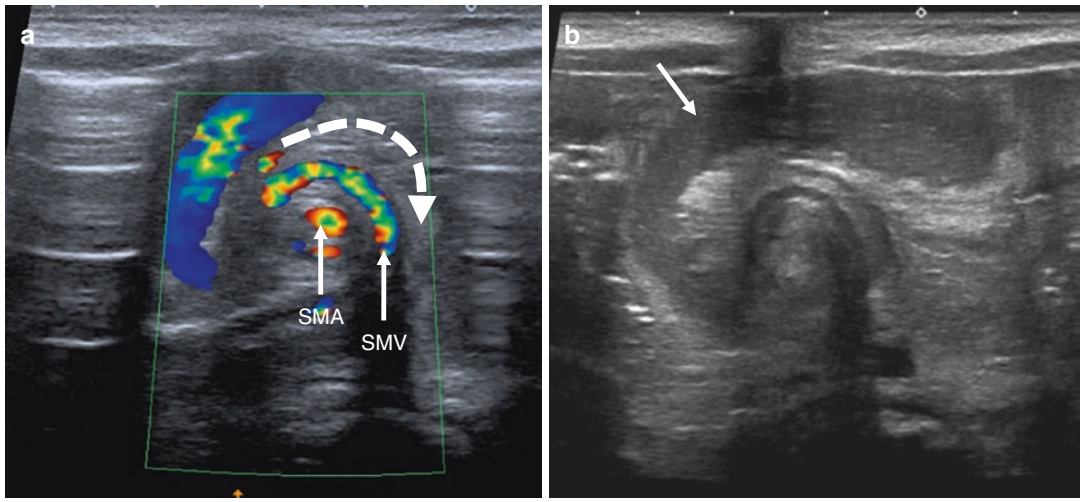

Fig. 9.11 Midgut volvulus in a 3-month-old boy with bilious vomiting and history of operated congenital diaphragmatic hernia. (**a**) Color Doppler ultrasound of the upper abdomen, axial image, shows twisting of the superior mesenteric vein (SMV) around the axis of the superior mesenteric artery (SMA). (**b**) US axial view shows a dilated proximal loop (*arrow*)

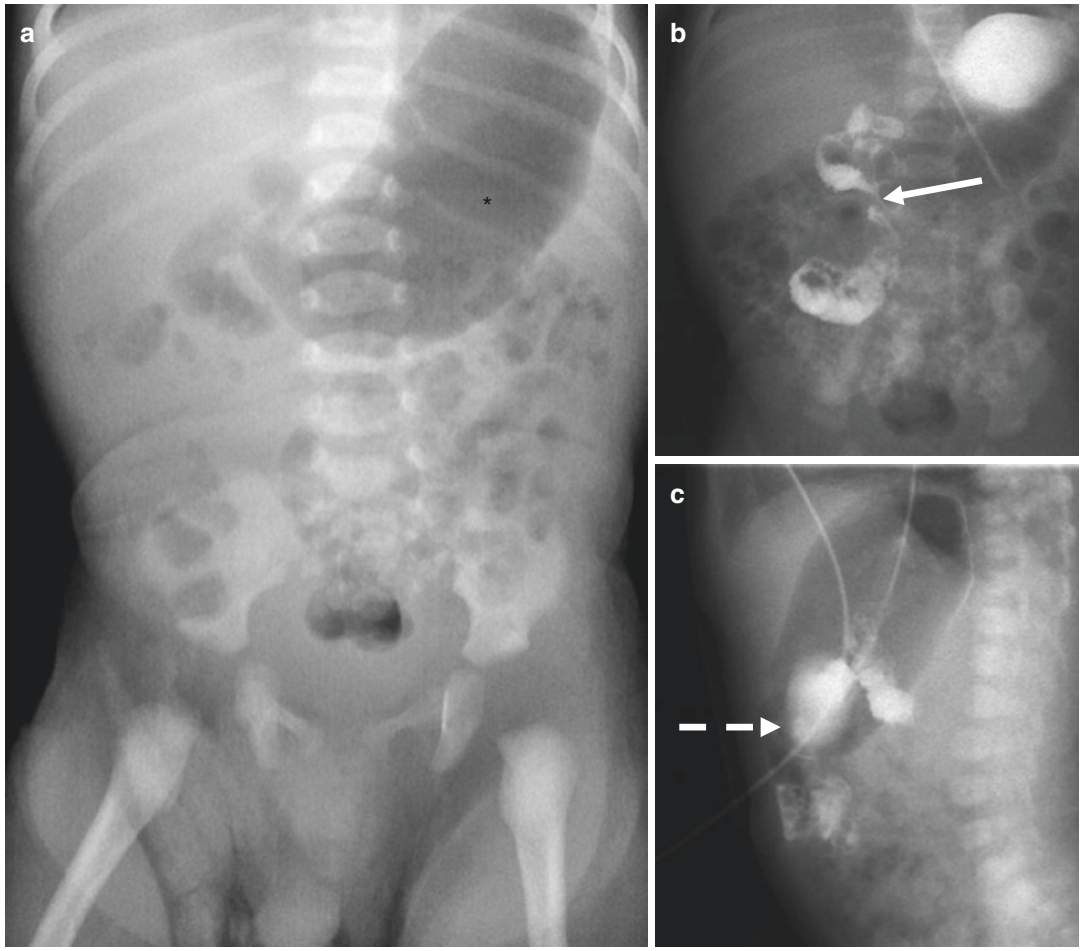

Fig. 9.12 Midgut volvulus on malrotation in a 2-day-old boy with bilious vomiting. (**a**) Supine abdominal radiograph shows the dilated stomach (*asterisk*) with normal pattern of distal bowel gas. (**b**) UGI series, frontal view, shows the abnormal location of the duodeno-jejunal junction to the right of the spine and below the duodenal bulb (*arrow*) with typical corkscrew appearance of the proximal segment. The obstruction is incomplete. (**c**) True lateral view; the duodenal junction projects in an anterior direction (*dotted arrow*)

cases, imaging is not necessary as inguinal hernia is a clinical diagnosis managed with manual reduction or surgery [1]. However, imaging might be required if the differential diagnosis includes hydrocele or if the hernia is not fully reduced.

Abdominal radiographs may show small bowel dilatation and bowel gas in the inguinal region (Fig. 9.13). However, this sign may not be seen if the bowel contains only fluid. US is the preferred modality as it can show the defect in the inguinal canal and the herniated omentum and bowel loops (Fig. 9.14).US is also helpful to demonstrate herniated ovaries in female patients (see also Chap. 30)

9.4.3 Internal Hernias

Internal hernia is defined as a herniation of viscera through a normal or abnormal aperture within the peritoneal cavity. The incidence of complication (volvulus or bowel ischemia) of congenital or acquired internal hernia is not known. Congenital internal hernias are classified

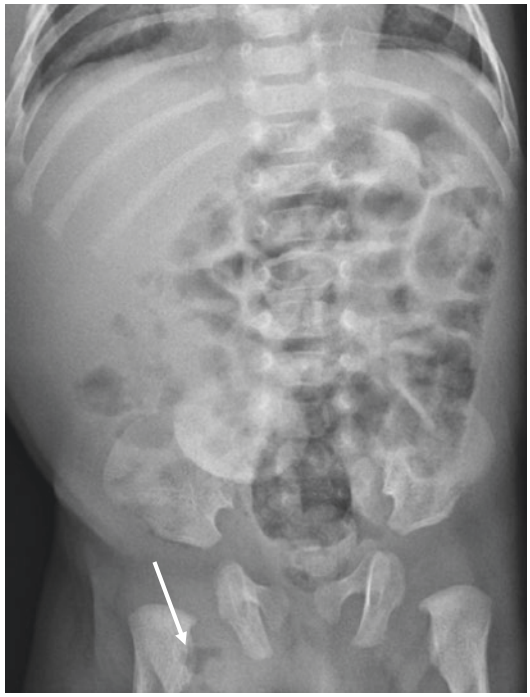

Fig. 9.13 Complicated inguinal hernia in a 1-month-old boy with vomiting and swelling in the inguinal region. Supine abdominal radiograph shows gas in the right inguinal region (*arrow*). There is a only moderate dilatation of the small bowel

as: paraduodenal, through the foramen of Winslow, transmesenteric, transomental, pericecal, and intersigmoid [23]. In a recent study, Tang et al. demonstrated that, though rare in pediatrics, typical presentation of internal hernia can be divided into two age groups [24]. In their series, 100% of neonatal cases (age <1 year) had congenital transmesenteric hernias, and 71% of older children (ages 1–17 years) had paraduodenal hernias [24]. The symptoms of complicated internal hernia are non-specific, including abdominal distension, sudden onset of abdominal pain and bilious vomiting in neonates and in infants. Symptoms of intestinal obstruction or, in older children, history of chronic abdominal pain with history of surgery (liver transplant, gastric bypass surgery) should lead to careful search for internal hernia.

The preoperative diagnosis of internal hernia is challenging. In adults, investigation of internal hernias relies mainly on CE-CT [25, 26], which can be transposed in older children. In symptomatic internal hernia, the following features are observed at CT: (1) Presence of bag-shaped mass or a cluster of dilated small-bowel loops at an abnormal anatomic location; (2) Presence of stretched and displaced mesenteric vascular pedicle with converging vessels at the hernia orifice; and (3) Engorged mesenteric vessels with mesenteric soft-tissue infiltration [26]. Moreover, CE-CT may demonstrate signs of bowel ischemia (Fig. 9.15). However, in neonates and infants, CT may be less contributive than in older children. In such cases, abdominal radiographs and ultrasound can be useful in assessing the mechanical bowel obstruction. In the absence of signs of acute small-bowel obstruction, evaluation of internal hernias in children relies on UGI series or SBFT. Transmesenteric hernias are difficult to appreciate on contrast examinations, probably due to the absence of a hernia sac [27]. In contrast, paraduodenal hernias in UGI series with SBFT are identified as a cluster of bowel loops with loss of normal interdigitation between the loops [24].

The treatment is surgical.

9.4.4 Acquired Diaphragmatic Hernia

Traumatic diaphragmatic hernia occurs in 4–6% in children with blunt thoracoabdominal trauma, but is often associated with other severe injuries [28]. Clinical signs can be an acute presentation in the context of multiorgan injury or a delayed presentation with respiratory distress or intestinal obstruction [29]. As in congenital diaphragmatic hernia, traumatic diaphragmatic hernia is more frequent on the left side.

Chest radiograph findings include the presence of air-filled viscera or visualization of the tip of the nasogastric tube above the diaphragm [30]. The diaphragm is elevated and pleural effusion may be present. In our experience, US, associated with a chest radiograph can identify intra thoracic intestinal loops and pleural fluid in

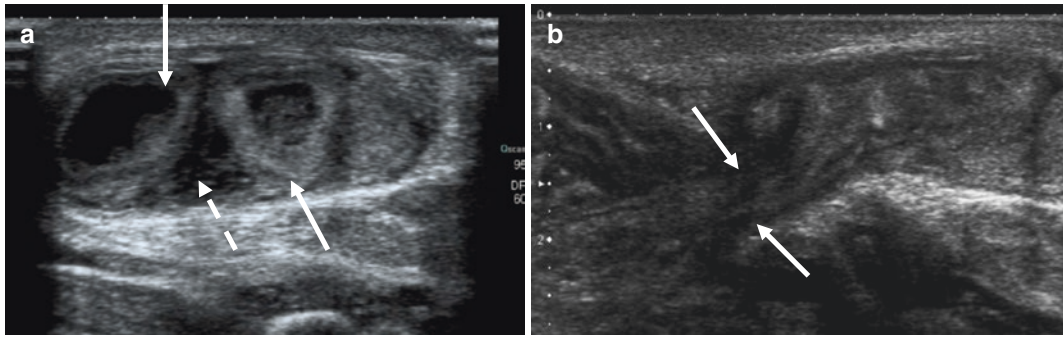

Fig. 9.14 Complicated right inguinal hernia a 22-month-old boy with abdominal pain and vomiting. After a first unsuccessful attempt to reduce the hernia, the surgeon asked for an ultrasound. (**a**) Axial image of the inguinal hernia containing bowel loops with thickened wall (*plain arrow*) and peritoneal fluid (*dotted arrow*). (**b**) sagittal image shows the defect in the inguinal canal (*arrows*)

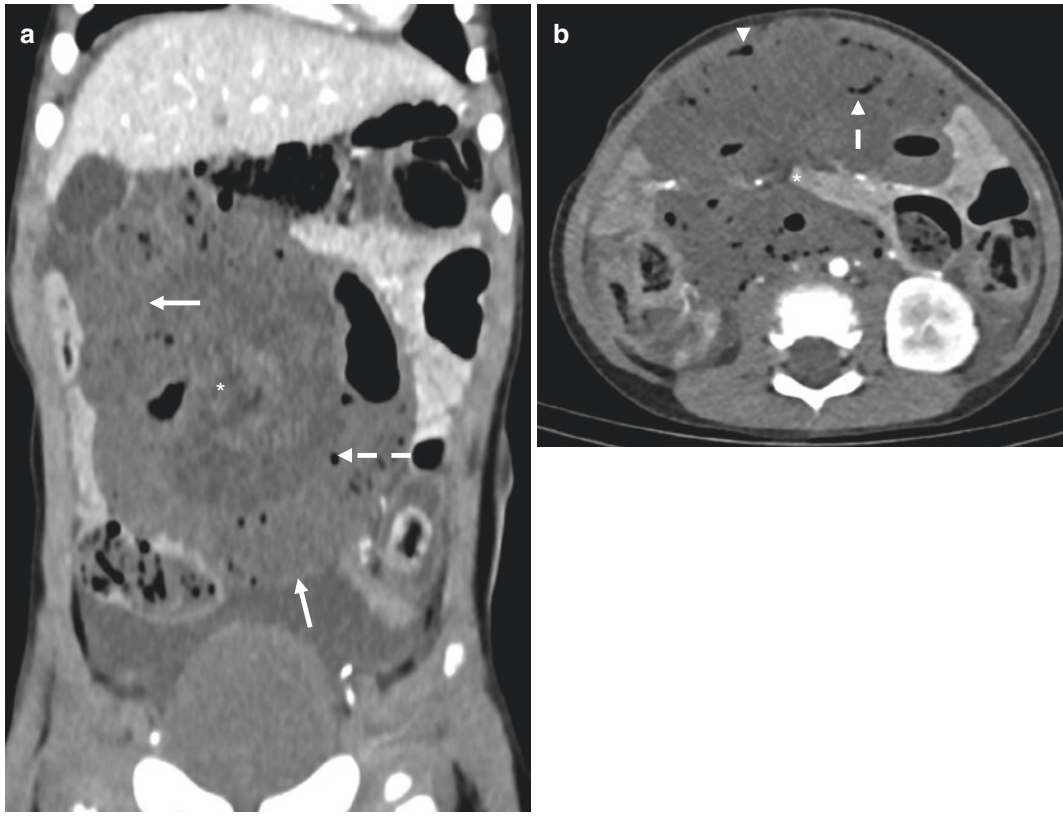

Fig. 9.15 Acquired transmesenteric hernia in a 2-year-old boy with abdominal pain, vomiting and previous history of operated anorectal malformation. (**a**) CE-CT of the abdomen shows on coronal reconstruction and (**b**) axial images signs of bowel ischemia with decreased wall enhancement (*arrows*), pneumatosis (*dotted arrows*), and pneumoperitoneum (*arrowhead*) and ascites in favor of small bowel strangulation. Whirl of the obstructed bowel and beaklike narrowing at the transition zone helped (*asterisk*) localizing the site of volvulus leading to the preoperative diagnosis of distal segmental small-bowel volvulus. Surgery revealed herniated ischemic bowel through mesenteric defect. The child did well after small-bowel loops resection with a 5-year follow-up

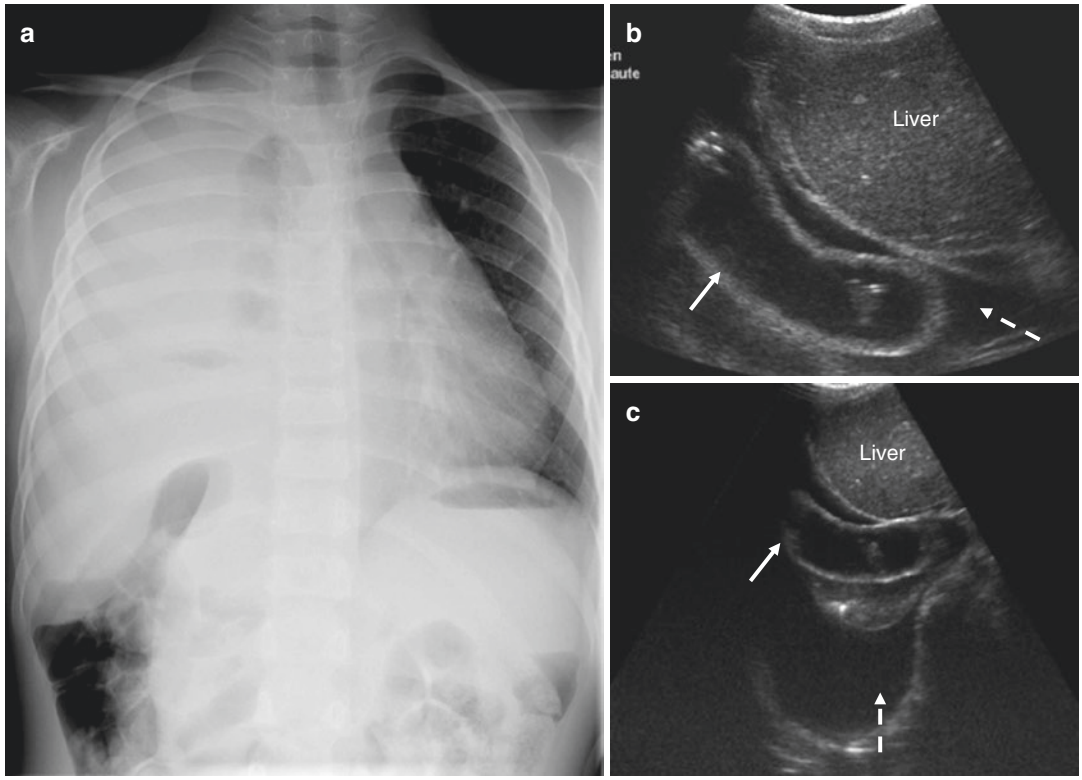

Fig. 9.16 Strangulated traumatic diaphragmatic hernia in a 4-year-old boy after a fight at school. On examination, the child complained of abdominal pain and vomiting and at first, US and abdominal radiograph were normal. After 12 h, the child developed respiratory distress. (**a**) Chest radiograph shows opacity of the right hemithorax with mediastinal shift to the left and air behind the right hemidiaphragm. (**b**, **c**) Ultrasound sagittal images showing dilated intestinal loops within the chest (*arrows*) above the liver associated with pleural effusion (*dotted arrows*)

children with delayed presentation (Fig. 9.16). In children with hemodynamic instability or suspicion of multi-organ traumatic lesions, CE-CT increases the sensitivity and specificity by demonstrating the diaphragmatic rupture, along with abdominal and intrathoracic injury.

Surgical management includes thoracoscopy and thoracotomy.

9.4.5 Post-Operative (Bariatric Surgery)

With the worldwide increase of adolescent obesity and the failing outcome of the conventional treatment of obesity in adolescents, bariatric surgery is emerging as a potential option [31]. There are supporting and opposing arguments for bariatric surgery in adolescents, considering that 2 (sleeve gastrectomy and Roux-en-Y bypass) out of 3 (gastric banding) surgical options are irreversible. There is an increasing incidence of acquired internal hernias after gastric bypass surgery in adult patients, related to mesenteric defects created by Roux-en-Y anastomoses. Though such complications have not yet been described in children, radiologists should be aware that there may be an increase of acquired internal hernias (see Sect. 9.4.3), anastomotic stricture or leak and band slippage, erosion or deflation, in the pediatric population as well [24].

9.5 Masses and Pseudo-Masses

9.5.1 Meckel Diverticulum

In children, the most common presentation of a symptomatic Meckel diverticulum is obstruction, caused by volvulus or intussusception (See Chap. 11).

9.5.2 Lymphatic Malformation

Lymphatic malformations arising in the mesentery are rare. Clinically, the symptoms are abdominal pain, vomiting, and increased abdominal girdle [32] and in one-third of cases, the mass is palpable [33]. In complicated cases, the patient can present signs of obstruction due the direct mass effect, intussusception, or intestinal volvulus [33].

US demonstrates a large multiloculated lesion arising in the peritoneal space. The content may be cystic or hemorrhagic. In case of volvulus, CE-CT will demonstrate more easily than US, the relationship between the superior mesenteric artery and vein and the whirlpool sign [33].

9.5.3 Lymphoma and Intestinal Tumors

Burkitt lymphoma may present as an abdominal mass with intestinal obstruction caused by direct compression or intussusception [34]. In up to 18% of patients with Burkitt lymphoma, intussusception is the presenting feature [35, 36]. In the study by Gupta et al, the median age of patients with lymphoma and intussusception was 10 years. Therefore, an intussusception occurring in an older child should be viewed differently because of its frequent association with a pathologic lead point such as lymphoma (see also Chap. 13) [36].

On US, in addition to the typical signs of intussusception (see Chap. 13), the presence of a hypoechoic mass or thickened hypoechoic small bowel, appendix or colon associated with large lymph nodes is in favor of intestinal location of a lymphoma (Fig. 9.17). Solid organ involvement (kidneys, spleen, and liver) can also be detected.

Signs on contrast abdominal CT of intestinal lymphoma are symmetric or slightly asymmetric circumferential thickening of the bowel wall [37].

As Burkitt lymphoma is frequently revealed by intussusception, it is recommended that hydrostatic reduction should be performed prior to chemotherapy and/or tumor complete surgical resection [36].

9.5.4 Infectious and Inflammatory Causes

9.5.4.1 Inflammatory Bowel Diseases: See also Chap. 12

In children with Crohn's disease, intestinal obstructions are common and approximately 25% of patients will undergo surgery for this reason [38]. Obstruction can be caused by gradual fibrosis and/or inflammatory stricture. Cross-sectional imaging is essential for selecting the appropriate therapeutic strategy as strictures due to inflammation are first managed with medical treatment whereas fibrotic lesions are managed via endoscopic or surgical approaches [39].

9.5.4.2 Tuberculosis

Abdominal tuberculosis may present as subacute intestinal obstruction in children [40]. It is caused by adhesions or gastric outlet obstruction by periduodenal lymphadenopathy [40]. Intestinal tuberculosis may be difficult to differentiate from Crohn's disease, at clinical, pathologic or endoscopic examination as well as at cross-sectional imaging [41]. On CE-CT, the presence of short segment involvement and necrotic lymph nodes is in favor of intestinal tuberculosis, as well as the presence of ascites and pulmonary involvement.

9.5.5 Post-Operative Adhesions

The overall incidence of small bowel obstruction secondary to adhesions is estimated around 6.2% following neonatal open abdominal surgery and

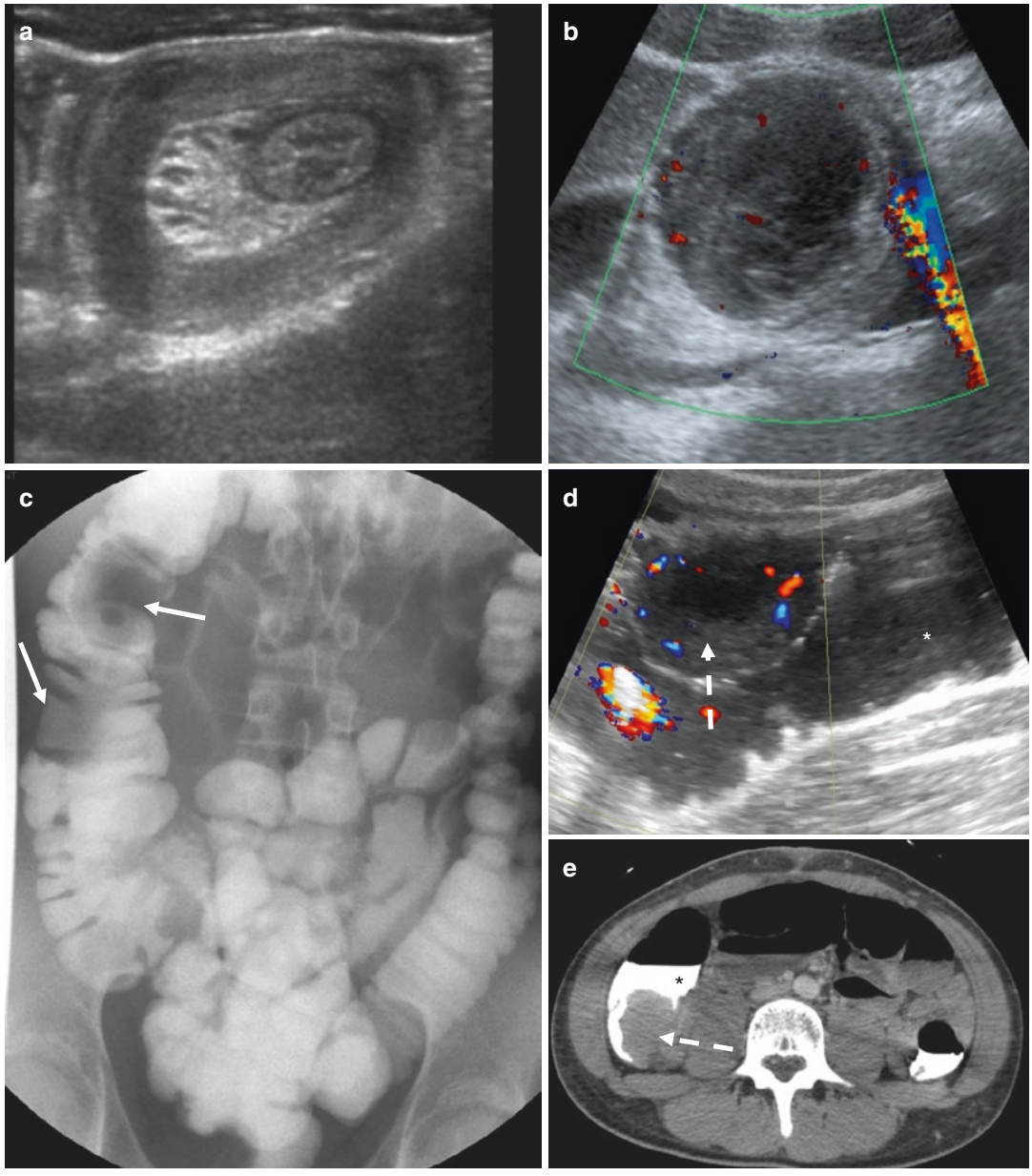

Fig. 9.17 Intestinal Burkitt lymphoma in a 13-year-old boy with abdominal pain since a month and weight loss. (**a**) Initial ultrasound demonstrates an ileocolic intussusception. (**b**) Large hypoechoic masses in the right upper and lower quadrants. (**c**) Radiograph obtained after therapeutic water-soluble enema; two endoluminal masses are still visible (*arrows*). Subsequent ultrasound (**d**) and CE-CT (**e**) showed multiple masses (*dotted arrows*) developed on the right colon wall and protruding inside the colonic lumen (*asterisk*)

4.7% following major abdominal surgery in infants and children [42]. The nature of surgical interventions increases the risk of post-operative adhesions. In neonates, adhesions complicate surgery in (in order of frequency): malrotation (14.2%), gastroschisis (12.6%), necrotizing enterocolitis (10.4%), omphalocele (8.6%), Hirschsprung disease (8.1%), congenital diaphragmatic hernia (6.2%) and intestinal atresia (5.7%). In infants and children, the incidence

according to the nature of surgery varies as well: colorectal surgery (14%), open fundoplication (8.2%), small bowel surgery (5.7%), cancer surgery (5.5%), choledochal cyst (3.1%), appendectomy (1.4%), and pylorotomy (0.1%). These complications can occur at any time, with a highest incidence during the first year after surgery.

The most common clinical presentation is abdominal pain, vomiting, constipation, and abdominal distension. Peritoneal signs, tachycardia, fever, leukocytosis or lactic acidosis are signs of severity indicating of bowel ischemia.

US is useful in neonates and in infants as it can also demonstrate the level of obstruction by showing dilated small-bowel loops and collapsed distal bowel loops (Fig. 9.18). Peritoneal fluid, small-bowel wall thickening can also be identified. Color Doppler may also show a whirlpool pattern of the mesenteric vessels if a mesenteric volvulus is associated.

Supine abdominal radiographs show bowel dilatation proximal to the adhesions and paucity or absence of distal bowel gas depending on the degree of obstruction. On an upright abdominal film, the number and location of air-fluid levels may help to locate the level of obstruction.

Studies on the sensitivity and specificity of CT small bowel obstruction in infants and children due to adhesions are lacking [43]. The sensitivity of CT for the diagnosis of small bowel obstruction in general in children has been reported between 87 and 91.5% [5, 44]. In our experience, CT is useful in children for identifying the site and cause of obstruction. In infants and children, CE-CT may help identify signs of severity such as bowel wall thickening and peritoneal fluid, signs of ischemia with reduced bowel-wall enhancement and pneumatosis that should prompt surgical management [44]. Moreover, CT may be helpful in differentiating an ileus secondary to intraabdominal abscess (such as after perforated appendicitis or peritonitis) versus adhesive bowel obstruction. CT may also guide radiology drainage of intraperitoneal abscess [43].

Conservative treatment, including nasogastric tube insertion and parenteral fluid and correction of electrolyte and fluid balance is an effective mean of managing children without signs of bowel ischemia [45].

Though controversial, the administration of a hyperosmotic water-soluble contrast agent (Gastrografin®, Telebrix® 35, Omnipaque® 350) can be effective in the conservative management of post-adhesion small-bowel obstruction in children [46], reducing the hospital stay by more than 3 days and accelerating feeding by 2 days. The principle is that administration of pure contrast agent has a hyperosmotic effect. The hyperosmotic contrast agent is administrated through the nasogastric tube and an abdominal radiograph is obtained 4–6 h later. If contrast is seen in the

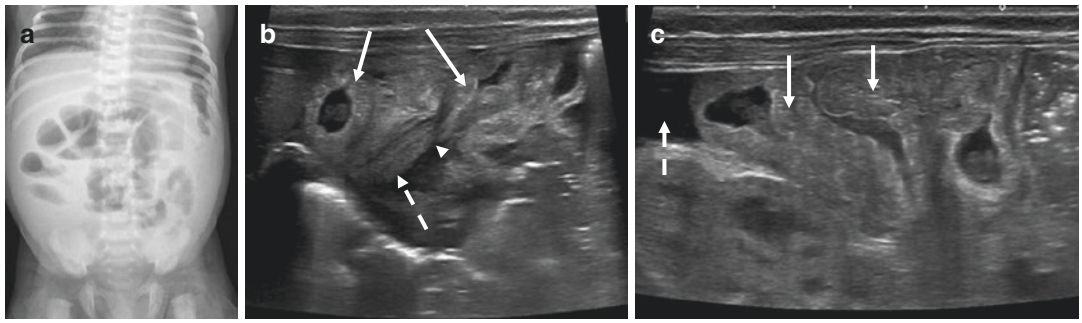

Fig. 9.18 Post-operative adhesion obstruction in a 1-month-old boy with vomiting for 48 h and history of operated congenital diaphragmatic hernia with small bowel placed in the right side and colon on the left side. (**a**) Upright plain radiograph shows multiple air-fluid levels in the right upper and middle quadrants, with paucity of gas in the pelvis. (**b**) Ultrasound shows the level of obstruction in the right middle quadrant with proximal dilated loops (*plain arrows*) and collapsed distal loops (*dotted arrow*) and the level of strangulation (*arrowhead*). (**c**) Ultrasound demonstrates also small-bowel wall thickening (*arrows*) and peritoneal fluid (*dotted arrow*)

cecum, first feeding can be initiated, otherwise, surgery should be performed [46].

Surgical exploration should be performed in children with signs or symptoms suggesting strangulation irrespective of age, nature of operation, or number of previous obstructions [43].

9.6 Varia

9.6.1 Distal Intestinal Obstruction Syndrome

Distal intestinal obstruction syndrome (DIOS) is defined by the complete or incomplete obstruction by viscous thick intestinal content in the terminal ileum and proximal colon. The most frequent cause of this syndrome is cystic fibrosis (so-called ileus-meconium equivalent). However, DIOS is also found in patients with Hirschsprung disease and has been described in association with prematurity (see also Chap. 4) [47]. Its incidence is 5–12 episodes per 1000 patients per year in Europe [48]. It is more frequent in adults than in children, in patients with pancreatic insufficiency, history of meconium ileus, and history of DIOS. It is also more frequent after organ transplantation, particularly after lung transplantation [49]. Dehydration may induce DIOS. Symptoms include acute onset of abdominal pain and vomiting. A palpable mass in the right lower quadrant may be present.

Abdominal radiograph shows air/fluid levels or small-bowel dilatation, their location and severity depends upon the degree of obstruction. Furthermore, a mottled appearance due to inspissated bowel content in the distal ileum and right colon may be present. Abdominal US or CT is only required in case of atypical symptoms or failure of treatment [49]. On US, DIOS is suggested by the presence of packed and hyperechoic distal ileum and right colon content [50]. The proximal small-bowel loops appear dilated. US can also demonstrate an associated intussusception. CT will show abundant feces in the distal ileum and proximal small-bowel dilatation (Fig. 9.19).

Water-soluble enema with hyperosmotic contrast agent is applied and will create a rapid fluid shift that facilitates the expulsion of inspissated material (Fig. 9.19). It must be combined with rehydration.

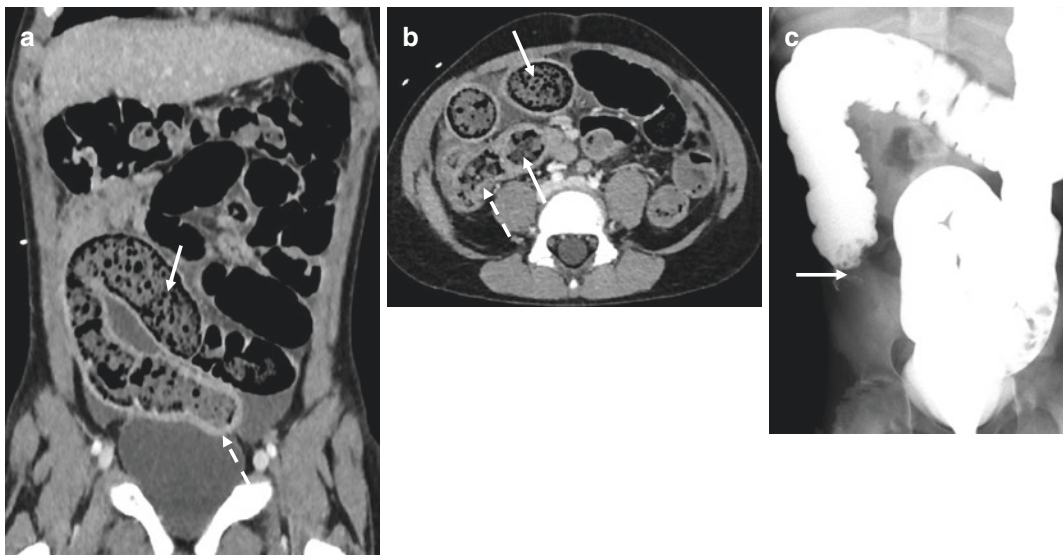

Fig. 9.19 Distal intestinal occlusion syndrome in a 10-year-old girl with abdominal pain and vomiting in a context of cystic fibrosis. CE-CT of the abdomen with: coronal reformatted (**a**) and axial (**b**) views shows feces in the distal ileum (*arrows*), wall thickening due to inflammation (*dotted arrows*), and ascites. (**c**) Contrast enema with hyperosmotic contrast agent shows the filling defect in the cecum (*arrow*)

9.6.2 Chronic Intestinal Pseudo-Obstruction Syndrome

Chronic intestinal pseudo-obstruction syndrome (CIPOS) is described as a permanent or recurrent intestinal obstruction without identifiable organic cause [51]. Its etiology remains unknown, but it always involves alterations of smooth muscle contractile function, leading to abnormal intestinal peristalsis and in some cases, associated abnormal urinary tract peristalsis [51]. In children, clinical manifestations include abdominal distension, bilious vomiting, growth retardation, and episodes of constipation and diarrhea. Episodes of urinary tract infections and an enlarged bladder are also common findings of this syndrome. In neonates, the most common clinical presentation is late meconium evacuation.

Abdominal radiograph shows diffusely dilated large and/or small bowel loops or air/fluid levels. Contrast enema may show microcolon (mostly in neonates), colon of normal caliber but with loss of normal colonic contractions or dilatation of the entire colon without stenosis or caliber disparity [51]. SBFT can be useful in this indication as it may show, in older children delayed contrast progression, abnormal peristalsis with phases of contrast reflux and distension of duodenal and small-bowel loops. Transit time to the cecum is markedly increased.

The medical treatment includes stimulation of intestinal motility with prokinetic drugs and mechanical methods (massage, abdominal muscles strengthening and lavage), a strict diet rich in lipids and poor in fibers and in some cases, parenteral nutrition. Surgical treatment consists of decompression surgery (ileostomy rather than colostomy).

9.7 Large Bowel Obstruction

9.7.1 Volvulus

Colonic volvulus is rare in children. The bowel obstruction is due to a change in the configuration of the colon with twisting or kinking of the mesentery and possible alteration of colonic blood supply. Colonic dysmotility and neurological disorders are predisposing factors. The sigmoid is most commonly affected [52], though a recent study found that cecal volvulus was more frequent in children [53]. Symptoms are nonspecific, including abdominal pain, vomiting, and abdominal distension.

Abdominal radiograph is often the initial imaging study and can lead to a fluoroscopic enema or abdominal CT [53]. On abdominal radiograph, the most common findings are absence of rectal gas and focal dilated colonic loop [53]. The typical "coffee-bean" sign is seen in sigmoid volvulus. However, these various signs are not always recognized on plain radiographs in children. Fluoroscopic enema may show a beaked appearance of the sigmoid colon associated with complete or incomplete obstruction. Abdominal CE-CT may show swirling of the mesentery, twisted distal colon, and dilated colonic loops. CT may also demonstrate signs of bowel wall ischemia [52].

The enema may result in a detorsion of the twisted bowel segment during the examination. In patients with bowel wall ischemia, recurrence of colonic volvulus or absence of resolution after enema, operative treatment is required. This consists of detorsion, resection, and colopexy [52].

9.7.2 Appendicitis (see Chap. 10)

Reflex functional bowel obstruction is well-known consequence of appendicitis. However, mechanical bowel obstruction has been reported in the literature as well. Mechanical obstruction can occur with or without strangulation, in the acute or subacute phase of appendicitis. It results from entrapment of small bowel loops by the inflamed appendix and surrounding mesentery with subsequent adhesions [54].

9.7.3 Hirschsprung Disease (Delayed Diagnosis)

Hirschsprung disease is diagnosed in 80% of cases in the neonatal period (see Chap. 7). However, the diagnosis may be delayed and therefore, Hirschsprung disease should be considered in any child with severe constipation. Patients with Hirschsprung disease are at risk for

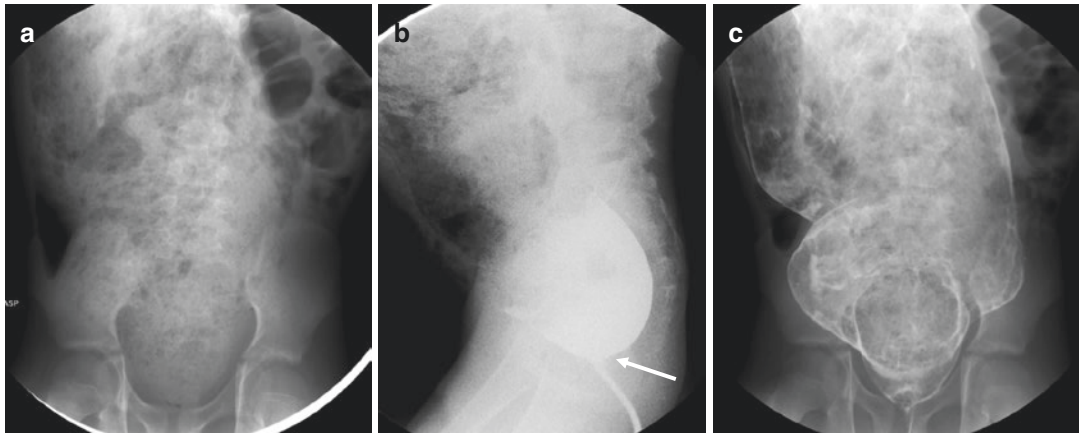

Fig. 9.20 Hirschsprung disease in a 12-year-old boy with history of severe constipation. Chronic intestinal obstruction was suspected. The diagnosis of Hirschsprung disease was achieved based on water-soluble contrast enema. (**a**) Abdominal radiograph demonstrates fecal impaction despite repeated enema and manual extraction. (**b**) Contrast enema shows cone-shaped distal rectum (*arrow*) on lateral view. (**c**) A mega colon is demonstrated on the frontal view

intestinal perforation [55]. The differential diagnosis in children includes chronic intestinal pseudo obstruction, distal intestinal obstruction in patient with cystic fibrosis, and conditions that cause ganglioneuromatosis (as in multiple endocrine neoplasia type 2) [55].

Contrast enema is preferably performed using water-soluble contrast agent since barium contrast agent is known to have a constipating effect. Funnel-like transition zone between the proximal dilated bowel (cone-shaped) and distal non-dilated large bowel is best demonstrated on lateral view. Moreover, recto-anal inhibitory reflex is more commonly absent in children with Hirschsprung disease [56]. However, these typical signs may be absent in ultra-short segment disease (Fig. 9.20) or in long segment disease [57].

In older children, Duhamel procedure is the operation of choice.

9.8 Functional Obstruction

Functional ileus is an occlusion with no mechanical obstruction etiology. The causes are multiple and may be either abdominal or extraabdominal (Table 9.3). Abdominal radiograph demonstrates moderate intestinal dilatation with normal-sized colon containing gas on supine film. On upright film, air-fluid levels of varying lengths are visible

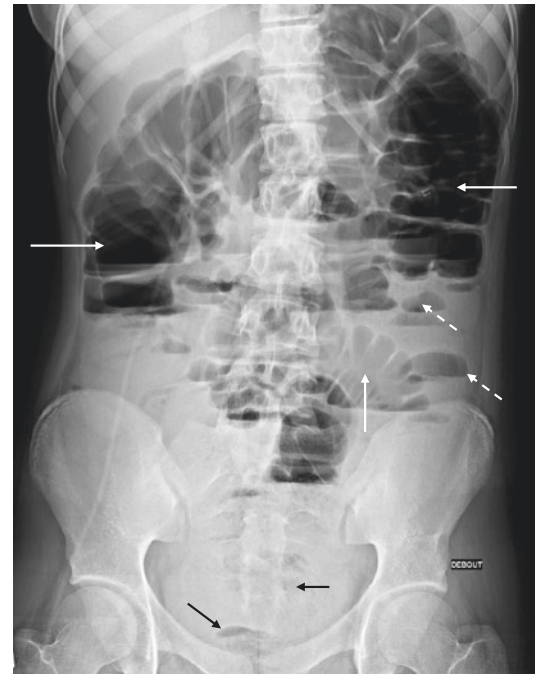

Fig. 9.21 Functional intestinal obstruction in a 14-year-old girl with abdominal pain and distension after gastrostomy catheter insertion. Upright abdominal radiograph shows multiple air/fluid levels of various lengths in the large-bowel (*arrows*) and small-bowel (*dotted arrows*). Air is visible in projection of the rectum (*black arrows*)

(Fig. 9.21). On US, aperistaltic bowel loops and absence of transition zone may help differentiating with mechanical obstruction.

Table 9.3 Common causes of intestinal functional obstruction in children

Causes of intestinal functional obstruction
Appendicitis
Acute pancreatitis, cholecystitis
Abdominal trauma
Anal fissure
Fecaloma
Gastroenteritis
Post-operative

Conclusion

Obstruction and subobstruction of the digest tract is a common and sometimes life-threatening condition in children. The causes are numerous, congenital and acquired.

Imaging has a central position for the work-up. Imaging must be adapted to the clinical conditions and suspected diagnosis. US, plain radiograph of the abdomen will usually be combined to achieve the diagnosis.

CT may be used as a complementary tool whenever US is inconclusive or whenever the condition seems complicated and that a rapid decision must be obtained.

References

1. Hryhorczuk A, Lee EY, Eisenberg RL. Bowel obstructions in older children. Am J Roentgenol. 2013;201(1):W1–8.
2. Callahan MJ, Talmadge JM, MacDougall RD, Kleinman PL, Taylor GA, Buonomo C. Selecting appropriate gastroenteric contrast media for diagnostic fluoroscopic imaging in infants and children: a practical approach. Pediatr Radiol. 2017;47(4):372–81.
3. Wale A, Pilcher J. Current Role of Ultrasound in Small Bowel Imaging. Semin Ultrasound CT MR. 2016;37(4):301–12.
4. Esposito F, Vitale V, Noviello D, Di Serafino M, Vallone G, Salvatore M, et al. Ultrasonographic diagnosis of midgut volvulus with malrotation in children. J Pediatr Gastroenterol Nutr. 2014;59(6):786–8.
5. Jabra AA, Eng J, Zaleski CG, Abdenour GE Jr, Vuong HV, Aideyan UO, et al. CT of small-bowel obstruction in children: sensitivity and specificity. Am J Roentgenol. 2001;177(2):431–6.
6. Cribbs RK, Gow KW, Wulkan ML. Gastric volvulus in infants and children. Pediatrics. 2008;122(3):e752–62.
7. Oh SK, Han BK, Levin TL, Murphy R, Blitman NM, Ramos C. Gastric volvulus in children: the twists and turns of an unusual entity. Pediatr Radiol. 2008;38(3):297–304.
8. Mathai J, Chacko J, Kumar TS, Scott JX, Agarwal I, Varkki S. Rapunzel syndrome: a diagnosis overlooked. Acta Paediatr. 2007;96(1):135–7.
9. Dikicier E, Altintoprak F, Ozkan OV, Yagmurkaya O, Uzunoglu MY. Intestinal obstruction due to phytobezoars: an update. World J Clin Cases. 2015;3(8):721–6.
10. Gayer G, Jonas T, Apter S, Zissin R, Katz M, Katz R, et al. Bezoars in the stomach and small bowel–CT appearance. Clin Radiol. 1999;54(4):228–32.
11. Callahan MJ, McCauley RG, Patel H, Hijazi ZM. The development of hypertrophic pyloric stenosis in a patient with prostaglandin-induced foveolar hyperplasia. Pediatr Radiol. 1999;29(10):748–51.
12. Macpherson RI. Gastrointestinal tract duplications: clinical, pathologic, etiologic, and radiologic considerations. Radiographics. 1993;13(5):1063–80.
13. Antaki F, Tringali A, Deprez P, Kwan V, Costamagna G, Le Moine O, et al. A case series of symptomatic intraluminal duodenal duplication cysts: presentation, endoscopic therapy, and long-term outcome (with video). Gastrointest Endosc. 2008;67(1):163–8.
14. Chen JJ, Lee HC, Yeung CY, Chan WT, Jiang CB, Sheu JC. Meta-analysis: the clinical features of the duodenal duplication cyst. J Pediatr Surg. 2010;45(8):1598–606.
15. Louie PK, Basques BA, Bitterman A, Shah S, Patel K, Abramchayev I, et al. Superior mesenteric artery syndrome as a complication of scoliosis surgery. Am J Orthop. 2017;46(2):E124–E30.
16. Lee TH, Lee JS, Jo Y, Park KS, Cheon JH, Kim YS, et al. Superior mesenteric artery syndrome: where do we stand today? J Gastrointest. 2012;16(12):2203–11.
17. Fong JK, Poh AC, Tan AG, Taneja R. Imaging findings and clinical features of abdominal vascular compression syndromes. Am J Roentgenol. 2014;203(1):29–36.
18. Bhagirath Desai A, Sandeep Shah D, Jagat Bhatt C, Umesh Vaishnav K, Salvi B. Measurement of the distance and angle between the aorta and superior mesenteric artery on CT scan: values in indian population in different BMI categories. Indian J Surg. 2015;77(Suppl 2):614–7.
19. Strouse PJ. Disorders of intestinal rotation and fixation ("malrotation"). Pediatr Radiol. 2004;34(11):837–51.
20. Pracros JP, Sann L, Genin G, Tran-Minh VA, Morin de Finfe CH, Foray P, et al. Ultrasound diagnosis of midgut volvulus: the "whirlpool" sign. Pediatr Radiol. 1992;22(1):18–20.
21. Applegate KE. Evidence-based diagnosis of malrotation and volvulus. Pediatr Radiol. 2009;39(Suppl 2):S161–3.
22. Applegate KE, Anderson JM, Klatte EC. Intestinal malrotation in children: a problem-solving approach to the upper gastrointestinal series. Radiographics. 2006;26(5):1485–500.
23. Meyers MA. Paraduodenal hernias. Radiologic and arteriographic diagnosis. Radiology. 1970;95(1):29–37.
24. Tang V, Daneman A, Navarro OM, Miller SF, Gerstle JT. Internal hernias in children: spectrum of clinical and imaging findings. Pediatr Radiol. 2011;41(12):1559–68.
25. Martin LC, Merkle EM, Thompson WM. Review of internal hernias: radiographic and clinical findings. Am J Roentgenol. 2006;186(3):703–17.

26. Takeyama N, Gokan T, Ohgiya Y, Satoh S, Hashizume T, Hataya K, et al. CT of internal hernias. Radiographics. 2005;25(4):997–1015.
27. Mathieu D, Luciani A, GERMAD Group. Internal abdominal herniations. Am J Roentgenol. 2004;183(2):397–404.
28. Rattan KN, Narang R, Rohilla S, Maggu S, Dhaulakhandi DB. Thirteen years'experience of diaphragmatic injury in children from the Post Graduate Institute of Medical Sciences (PGIMS), Rohtak, India. Malays J Med Sci. 2011;18(1):45–51.
29. Ghionzoli M, Bongini M, Piccolo RL, Martin A, Persano G, Deaconu DE, et al. Role of thoracoscopy in traumatic diaphragmatic hernia. Pediatrics. 2016;58(7):601–3.
30. Gelman R, Mirvis SE, Gens D. Diaphragmatic rupture due to blunt trauma: sensitivity of plain chest radiographs. Am J Roentgenol. 1991;156(1):51–7.
31. Beamish AJ, Reinehr T. Should bariatric surgery be performed in adolescents? Eur J Endocrinol. 2017;176(4):D1–D15.
32. Kosir MA, Sonnino RE, Gauderer MW. Pediatric abdominal lymphangiomas: a plea for early recognition. J Pediatr Surg. 1991;26(11):1309–13.
33. Traubici J, Daneman A, Wales P, Gibbs D, Fecteau A, Kim P. Mesenteric lymphatic malformation associated with small-bowel volvulus–two cases and a review of the literature. Pediatr Radiol. 2002;32(5):362–5.
34. England RJ, Pillay K, Davidson A, Numanoglu A, Millar AJ. Intussusception as a presenting feature of Burkitt lymphoma: implications for management and outcome. Pediatr Surg Int. 2012;28(3):267–70.
35. Sorantin E, Lindbichler F. Management of intussusception. Eur Radiol. 2004;14(Suppl 4):L146–54.
36. Gupta H, Davidoff AM, Pui CH, Shochat SJ, Sandlund JT. Clinical implications and surgical management of intussusception in pediatric patients with Burkitt lymphoma. J Pediatr Surg. 2007;42(6):998–1001.
37. Balthazar EJ, Noordhoorn M, Megibow AJ, Gordon RB. CT of small-bowel lymphoma in immunocompetent patients and patients with AIDS: comparison of findings. Am J Roentgenol. 1997;168(3):675–80.
38. Kim S. Surgery in pediatric Crohn's disease: indications, timing and post-operative management. Pediatr Gastroenterol Hepatol Nutr. 2017;20(1):14–21.
39. Bettenworth D, Nowacki TM, Cordes F, Buerke B, Lenze F. Assessment of stricturing Crohn's disease: current clinical practice and future avenues. World J Gastroenterol. 2016;22(3):1008–16.
40. Malik R, Srivastava A, Yachha SK, Poddar U, Lal R. Childhood abdominal tuberculosis: disease patterns, diagnosis, and drug resistance. Indian J Gastroenterol. 2015;34(6):418–25.
41. Limsrivilai J, Shreiner AB, Pongpaibul A, Laohapand C, Boonanuwat R, Pausawasdi N, et al. Meta-analytic Bayesian model for differentiating intestinal tuberculosis from Crohn's disease. Am J Gastroenterol. 2017;112(3):415–27.
42. Lakshminarayanan B, Hughes-Thomas AO, Grant HW. Epidemiology of adhesions in infants and children following open surgery. Semin Pediatr Surg. 2014;23(6):344–8.
43. Lautz TB, Barsness KA. Adhesive small bowel obstruction–acute management and treatment in children. Semin Pediatr Surg. 2014;23(6):349–52.
44. Wang Q, Chavhan GB, Babyn PS, Tomlinson G, Langer JC. Utility of CT in the diagnosis and management of small-bowel obstruction in children. Pediatr Radiol. 2012;42(12):1441–8.
45. Lin LH, Lee CY, Hung MH, Chen DF. Conservative treatment of adhesive small bowel obstruction in children: a systematic review. BMJ Open. 2014;4(9):e005789.
46. Bonnard A, Kohaut J, Sieurin A, Belarbi N, El Ghoneimi A. Gastrografin for uncomplicated adhesive small bowel obstruction in children. Pediatr Surg Int. 2011;27(12):1277–81.
47. Agrons GA, Corse WR, Markowitz RI, Suarez ES, Perry DR. Gastrointestinal manifestations of cystic fibrosis: radiologic-pathologic correlation. Radiographics. 1996;16(4):871–93.
48. Houwen RH, van der Doef HP, Sermet I, Munck A, Hauser B, Walkowiak J, et al. Defining DIOS and constipation in cystic fibrosis with a multicentre study on the incidence, characteristics, and treatment of DIOS. J Pediatr Gastroenterol Nutr. 2010;50(1):38–42.
49. Colombo C, Ellemunter H, Houwen R, Munck A, Taylor C, Wilschanski M, et al. Guidelines for the diagnosis and management of distal intestinal obstruction syndrome in cystic fibrosis patients. Journal of Cystic. 2011;10(Suppl 2):S24–8.
50. Haber HP. Cystic fibrosis in children and young adults: findings on routine abdominal sonography. Am J Roentgenol. 2007;189(1):89–99.
51. Goulet O, Jobert-Giraud A, Michel JL, Jaubert F, Lortat-Jacob S, Colomb V, et al. Chronic intestinal pseudo-obstruction syndrome in pediatric patients. Eur J Pediatr Surg. 1999;9(2):83–9.
52. Tannouri S, Hendi A, Gilje E, Grissom L, Katz D. Pediatric colonic volvulus: a single-institution experience and review. J Pediatr Surg. 2017;52:1062–6.
53. Marine MB, Cooper ML, Delaney LR, Jennings SG, Rescorla FJ, Karmazyn B. Diagnosis of pediatric colonic volvulus with abdominal radiography: how good are we? Pediatr Radiol. 2017;47(4):404–10.
54. Maly O, Paral J. Appendicitis as a rare cause of mechanical small-bowel obstruction: a literature review of case reports. Int J Surg Case Rep. 2016;29:180–4.
55. Parisi MA. Hirschsprung disease overview. In: Pagon RA, Adam MP, Ardinger HH, Wallace SE, Amemiya A, LJH B, et al., editors. GeneReviews. Seattle, WA: University of Washington; 1993.
56. Vult von Steyern K, Wingren P, Wiklund M, Stenstrom P, Arnbjornsson E. Visualisation of the rectoanal inhibitory reflex with a modified contrast enema in children with suspected Hirschsprung disease. Pediatr Radiol. 2013;43(8):950–7.
57. Jamieson DH, Dundas SE, Belushi SA, Cooper M, Blair GK. Does the transition zone reliably delineate aganglionic bowel in Hirschsprung's disease? Pediatr Radiol. 2004;34(10):811–5.

Appendicitis

10

Alexia Dabadie and Philippe Petit

Contents

A. Dabadie • P. Petit (✉)
Department of Pediatric Imaging,
Hôpital Timone Enfants,
264 rue St Pierre, 13385 Marseille, Cedex 05, France
e-mail: adabadie@ap-hm.fr; ppetit@ap-hm.fr

10.1 Introduction

Appendicitis is the first surgical emergency in childhood. Obstruction of the lumen of the appendix is considered as the main causal mechanism of this pathology. It creates an increased intraluminal pressure leading to ischemia, congestion, and transmural infiltration by neutrophil granulocytes. Appendicitis may occur at any age and its diagnosis can be challenging especially among infants. Multiple factors may explain these difficulties.

Anatomically the appendix is usually located in the right iliac fossa. However, the variable position of the cecum, the direction of the appendix itself, and its length may dramatically modify the site and type of symptoms. Furthermore, the clinical expression of appendicitis may be very variable, including diarrhea, fever or even absence of fever.

The first challenge is to recognize early appendicitis before it gets complicated (perforation, abscess, peritonitis). The second challenge is to avoid negative appendectomies which will carry their own surgical risk for the future (e.g., adhesions causing small bowel obstruction).

F.E. Avni, P. Petit (eds.), *Imaging Acute Abdomen in Children*,
https://doi.org/10.1007/978-3-319-63700-6_10

A clinical examination by a senior pediatric surgeon is extremely efficient for the diagnosis, still the overall negative appendectomy rate ranges between 10 to 30% [1]. Laboratory tests (white blood cell count, C-reactive protein) are unable to reliably distinguish between patients with or without acute appendicitis, even if normal tests render this diagnosis very unlikely [2]. Thanks to imaging, the negative rate has been significantly reduced between 3 and 7% without an increase in perforation rate [1].

10.2 Imaging Strategies and Controversies

US, CT, and MR imaging are all excellent tools for the diagnosis of appendicitis. Numerous articles, meta-analysis [3, 4] have been published and controversies do persist [5–7] as to determine which imaging modality is the most accurate and the most adapted to the pediatric health care. Overall the choice between the different imaging techniques appears depending on the type of imaging unit available on site and on the experience of the local radiologists.

10.3 Ultrasound (US)

10.3.1 Classical Presentations

Linear high frequency probes 7 up to 15 MHz are needed to optimize the evaluation of a patient suspected of appendicitis. Convex probes with low frequency 3.5–6 MHz are also useful in order to provide a good overview of the inflammatory process, to look for its extension to the surrounding structures (such as associated abscesses) as well as to exclude differential diagnoses.

Appendicitis can be ruled out when a normal appendix is visualized in all its length (Fig. 10.1). For Wiersma and all it can be demonstrated in 82% of asymptomatic children [8].

On US, signs to be considered as evidence (with different positive and negative predictive values) for appendicitis include:

- *The visualization of an enlarged and blind bowel-type structure connected to the cecum.* The diameter considered as a significant abnormal enlargement is debated. Normal appendix diameter has been reported as below 6 mm [8–10] independently of the patient's age. Above 6 mm, the diameter is usually considered abnormal but this by itself is not a highly specific sign [11]. A diameter up to 7 mm can be a normal finding [12, 13] or associated with asymptomatic lymphoid hyperplasia (thickening of the lamina propria) (Fig. 10.2) [14]. Still, a diameter equal or superior to 7 mm increases the specificity of this sign for diagnosing appendicitis [13].
- In our experience, *the thickness of the appendiceal wall* is a more reliable sign than the diameter itself since it is less dependent on the lumen content which may increase the whole diameter of the appendix. There are

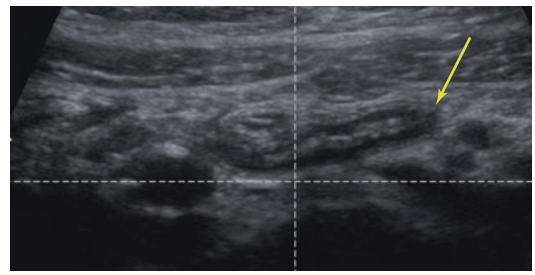

Fig. 10.1 Normal appendix on US in an 8-year-old-boy. The multilayered structure measures 5 mm in diameter and presents a blind ending (*yellow arrow*). It has to be demonstrated all along up to the cecum to establish its normality

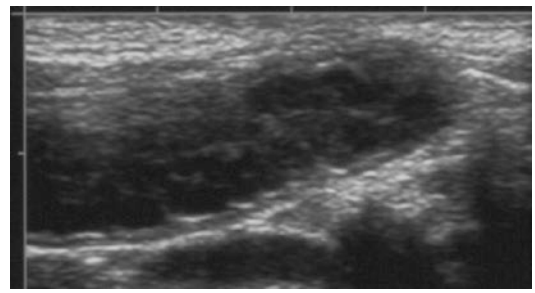

Fig. 10.2 Lymphoid hyperplasia of the appendix in US in an asymptomatic 6-year-old patient: the appendix is enlarged only on the mucosal layer with preservation of the multilayer differentiation

controversies whether this wall thickness is age dependent [8, 9]. Above 3 mm, the wall thickening is definitely abnormal.

- *Peri-appendiceal fat inflammation* appearing as increased hyperechogenicity is an important positive sign even if it can be found in other all inflammatory processes surrounding the appendix or even rarely in normal children. Its specificity increases when this echogenic fat surrounds circumferentially the appendix [11].
- The *presence of an appendicolith* has a low predictive value. Indeed, it can be visualized in asymptomatic patients [15, 16].
- A small amount of fluid within the lumen of the appendix [17].
- An *increased flow in the appendiceal wall* as demonstrated by color Doppler US is a non-specific sign. However, its absence associated with the previous described positive signs would favor a perforation.
- *Lack of compressibility* of the appendix has a poor positive predictive value. It has been reported to be the most commonly false-positive finding (80%) [11].
- Local sonographic tenderness, presence of gas within the lumen of the appendix and lymph nodes within the root of the mesentery are not considered as accurate positive diagnosis signs.

In summary, the association of several different US signs increases the accuracy of US and ascertains the diagnosis (Fig. 10.3). Once confirmed, it becomes mandatory to search for potential complications.

Of course, if an alternative diagnosis is identified during the US exploration, it rules out the diagnosis of appendicitis.

10.3.2 Complications

Perforation of the appendix is a major pejorative stage in the evolution of appendicitis; its frequency increases as the age at presentation decreases since the classic clinical signs and symptoms tend to be absent. Therefore, the diagnosis might be delayed in youngest patients [18].

The prevalence of perforation has been reported to range from 23 to 88% [19]. Perforation opens the way to the two most major life-threatening complications, abscesses and peritonitis. Noteworthy, the therapeutic options have recently evolved and there is a wide discussion regarding the optimal treatment (medical vs surgical treatment) of a simple acute appendicitis [20]. Even perforation with abscesses would now be treated with antibiotics first [21]. In order to decrease surgical complications,

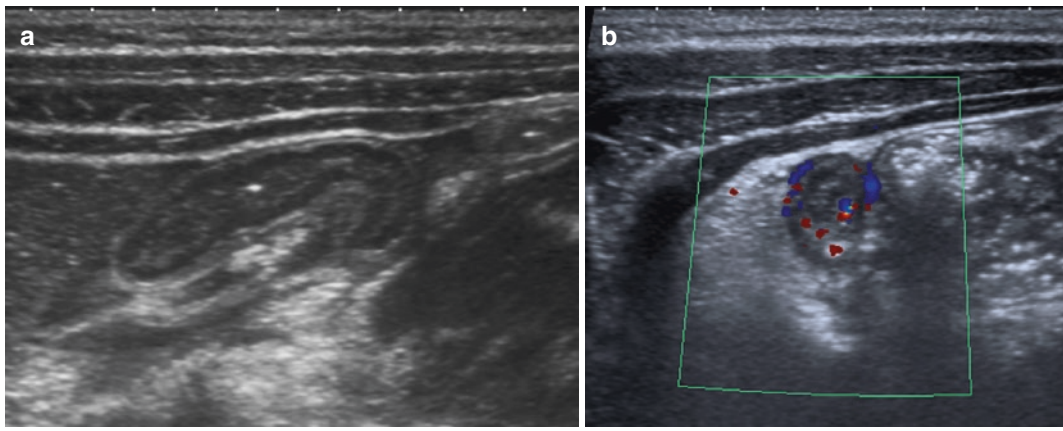

Fig. 10.3 Non-perforated acute appendicitis on US-Color Doppler in a 12-year-old-girl. (**a**) US sagittal scan: The appendix is enlarged surrounded by an increased echogenic fat. (**b**) Color Doppler: Hypervascularization is demonstrated within the appendix wall

an appendectomy will be performed in a second stage after disappearance of infection and inflammation. A clinical, biological, and ultrasound follow-up will confirm the regression of the abscesses. In case of absence of response to the antibiotic treatment, a percutaneous drainage can be performed before to finally consider a surgical option.

US features suggesting *perforation* (isolated or complicated) include [19, 22–24] (Fig. 10.4):

- A focal loss of differentiation of the appendix wall.
- An appendicolith outside the lumen of the appendix.
- The absence of appendiceal hyperhemia on color Doppler.
- A hypoechoic and hyperhemic ill-defined fatty infiltration surrounding the abnormal appendix (=*phlegmon*)
- A well-limited heterogeneous collection containing or not air bubbles (with comet-type hyperechogenicities) and surrounded by a hyperemic capsule of variable thickness (=*abscess*)
- Due to the peritonitis, US may demonstrate several associated features
  - Loculated echogenic fluid collection(s) within the peritoneum
  - A hyperechogenicity of the periportal space
  - A diffuse increase of thickness and echogenicity of the peritoneal fat
  - A diffuse thickening of the outer layers (serosa, muscularis propria) of the small bowel
  - A small bowel ileus
  - Free air bubble(s) in the peritoneal cavity (=pneumoperitoneum). These bubbles appear as hyperechoic isolated spots and must be searched within the surrounding inflammatory fat, close to the anterior liver capsule and under the anterior peritoneal surface.

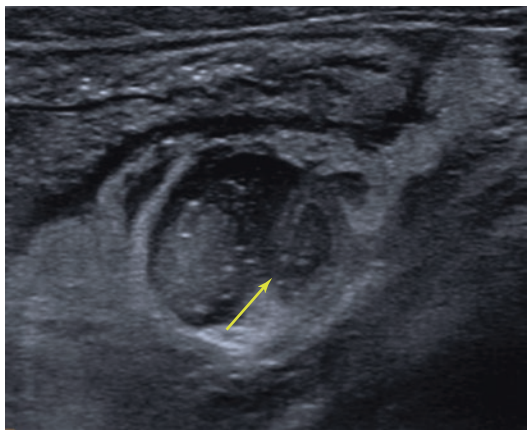

Fig. 10.4 US of a perforated appendix in an 11-year-old-boy: a heterogeneous well-limited fluid collection surrounds an inflamed appendix; part of the perforated appendix wall is not visible anymore (*yellow arrow*). The adjacent mesenteric fat is inflamed and hyperechoic

The complexity of appendicitis and its complications highlights once again the need for the exploration of the entire abdomen when performing US.

10.4 Appendicitis and CT

The lack of peritoneal fat in children younger than 10 years is an important limitation to visualize the appendix on CT [25]. A normal appendix is demonstrated on CT in 55.6% of patients older than 10-year but only in 38.7% in younger patients [25]. However, the absence of the visualization of the appendix has been reported to have a very high negative predictive value up to 98.7% as for the diagnosis of appendicitis [26].

CT has numerous advocates and has demonstrated in a meta-analysis high sensitivity and specificity, respectively 94 and 95%—for the diagnosis of appendicitis in children [3].

Yet, there is a raising concern in relation with the potential radiation risk associated with the use of CT. It has been calculated that 10,000 CT scans would increase the risk of cancer in 13 children; but conversely, not performing these 10,000 CT would lead to 280 missed diagnoses of appendicitis [3].

Whatever the arguments leading to perform CT, an optimized dose reduction strategy needs to be applied in order to minimize the patient's exposure while maintaining a diagnostic level quality of images. The aim is being to obtain the best diagnosis accuracy.

There is no well-established CT protocol in the literature to explore a child with suspected appendicitis.

- Adaptation of the tube current (mA) to the child body weight has been proposed by Donnelly et al. [27]. For instance, in a patient between 27 and 36 kg, 100 mA is sufficient while between 45.1 and 70 kg the mA can range between 140 and 150 mA.
- Recommendations from the SFIPP society propose for a 10-year-old child, 32 kg weight, a CTDI of 7 ± 3 mGy for exploring a body of 35 cm (www.sfip-radiopediatrie.org).
- Some authors prefer to limit the exploration from the lower pole of the right kidney [28] down to the pubic symphysis while others start the acquisition at the level of the diaphragm in order to consider all possible differential diagnoses [6].
- Agreement does exist to perform the acquisition after IV contrast injection contrast media during the portal phase (1.5–2 cm^3/kg with a maximum of 140 cm^3).
- No oral or rectal opacification is usually recommended [29].
- Slice thickness varies in the literature from 1.5 to 5 mm [26].
- Coronal and sagittal reconstructions are recommended mostly to increase the level of confidence for the diagnosis.

10.4.1 Classical Presentation

Diagnosis criteria's include the following [30]

- An appendiceal caliber >6 mm: This measurement has been questioned in the literature since normal caliber of the appendix may raise above 7 mm and increases from birth till 6–7 years [31].
- An increased appendiceal wall enhancement.
- A peri-appendicular fat stranding.
- An appendicolith. However, Lowe et al. [32] report the presence of such finding in 3% of completely asymptomatic children.
- The presence of fluid of more than 2.6 mm of thickness within the lumen of the appendix [33].
- A focal symmetric thickening of the ceco-appendiceal junction (arrowhead sign) or a mass effect on the cecum [34].

None of these signs are highly specific, but the accuracy of diagnosis increases when a combination of signs is observed (Fig. 10.5).

Noteworthy, the presence of gas within the lumen of the appendix does not exclude acute inflammation.

As mentioned, the visualization of a normal appendix on its whole length excludes the diagnosis of appendicitis.

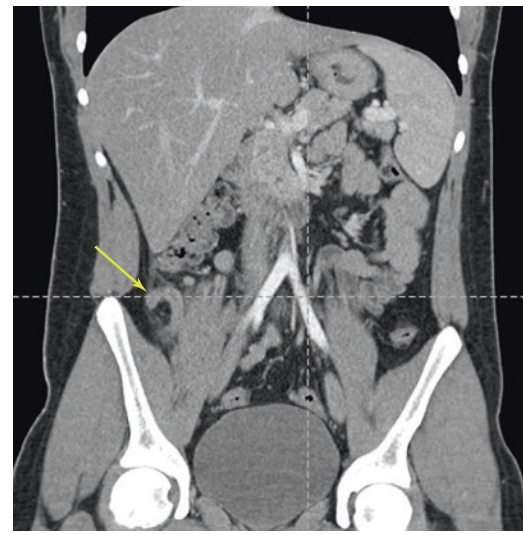

Fig. 10.5 Retro-cecal sub-hepatic appendicitis (*yellow arrow*) on coronal reformatted CE-CT in a 16-year-old-boy

10.4.2 Complications

Peritonitis is more frequent in children due to more rapid perforation than in adults.

Arguments for perforation include:

- Focal loss of enhancement of the wall of the appendix; this sign has the best accuracy
- The demonstration of a phlegmon: ill-defined inflammatory mass of heterogeneous density with an increased volume of inflamed fat associated with a various amount of fluid.
- The presence of an abscess: well-limited fluid collection of various densities surrounded by an enhancing wall of variable thickness (Fig. 10.6).
- Extra-luminal air
- Appendicolith outside the appendix

Using these criteria the overall accuracy of CT is reported as higher than 96% [35].

10.5 MR Imaging and Appendicitis

In order to avoid irradiation hazards, MR imaging has gained acceptance for the evaluation of suspected appendicitis as a first line imaging exploration or when the contribution US is limited especially in obese children [36–39].

Using either a 1.5 or a 3 T unit magnet, a fast MR imaging protocol is performed without the need for IV injection. Three Tesla allows shorter examination time and higher resolution images. The MR imaging examination time ranges from 8 to 35 min.

The use of multi-channel phased array coils with large coverage and parallel processing is mandatory.

Three-plans single-shot turbo spin-echo sequences associated with axial T2-weighted fat saturation acquisitions are obtained with free breathing. Alternative protocols replace the sagittal single-shot TSE by a coronal T2-weighted fat saturation sequence [38, 39].

A respiratory triggering may be used. Slice thickness can range from to 3 to 5 mm.

In more complex cases, the use of DWI sequences and Gadolinium IV injection T1 Fat-Saturation sequences may be required.

The normal appendix in asymptomatic patient can be demonstrated in 48% [40] to 86% [41] of patients while using an upper limit diameter of 7 mm [40].

10.5.1 Classical Presentation

MR imaging signs for appendicitis include: (Fig. 10.7)

- Markedly hyperintense T2-weighted thickened wall of the appendix
- Markedly hyperintense T2-weighted periappendicular tissues

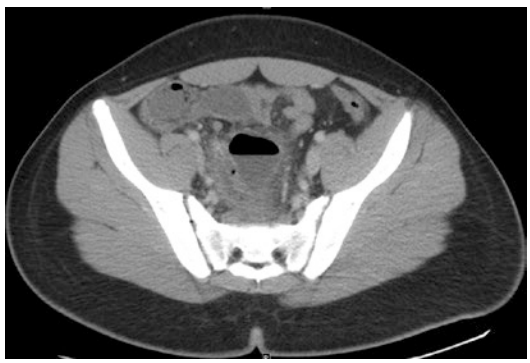

Fig. 10.6 CE-CT on a 15-year-old-boy. Perforated appendicitis surrounded by an abscess (large air fluid level collection on the midline)

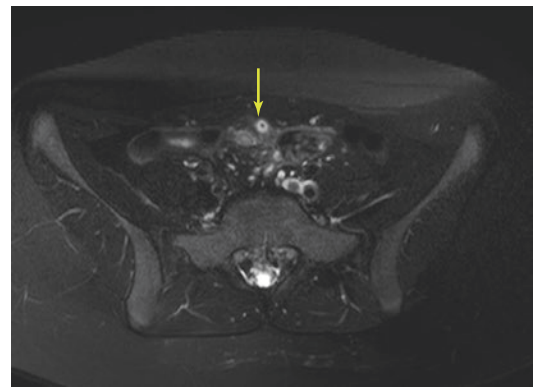

Fig. 10.7 MR imaging Axial T2-weighted fat saturation sequence: Enlarged inflamed appendix (*yellow arrow*) with a small appendicolith in a 12-year-old obese patient

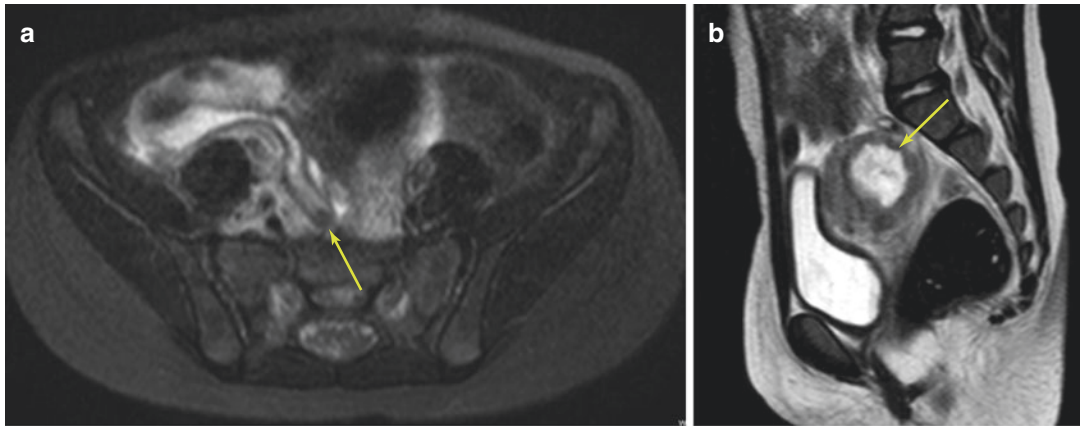

Fig. 10.8 Perforated appendix in a 5-year-old girl: MR imaging T2-weighted sequences. (**a**) Deep perforated appendicitis (*yellow arrow*). (**b**) Associated pelvic abscess (*yellow arrow*)

- Dilated appendix >6 mm
- Presence of an appendicolith appearing as a focal signal void in T2-weighted sequences in a dependent position.
- Free fluid in the pelvis

10.5.2 Complications

Perforation must be considered in case of [37] (Fig. 10.8):

- Localized fluid collection(s): they appear as hypersignal on T2-weighted sequences with or without heterogeneous content, with or without air fluid level or entrapped air within a thick fluid. The collections being surrounded by a hyposignal rim of various thicknesses.
- Free peritoneal air appearing as a signal void outside the bowel lumen in a non-dependent position.
- Direct visualization of the perforation of the appendicular wall

10.6 Unusual Presentations

10.6.1 Appendicitis in Infant and Neonates

Less than 3% of appendicitis occur in children younger than 3 years. Symptoms are non-specific, including abdominal pain, diarrhea, vomiting, abdominal distension, and fever. Due to a delayed diagnosis, the perforation rate is higher and the perforation occurs more rapidly in this age group.

10.6.2 Ectopic Locations

Due to wide variation in its length and position and due to the variable positions of the cecum itself, the symptoms related to appendicitis may be very atypical.

- Retrocecal appendix: it is the second most frequent appendix location [42]. Due to this anatomical position, symptoms may mimic cholecystitis or pyelonephritis. Perforation may lead to abscesses in the pararenal space and/or in the perihepatic spaces.
- Left side appendix: it can be associated with malrotation, situs inversus, or mobile cecum.
- Amyand hernia: It is defined by the presence of the appendix within the inguinal canal. The appendix can be located in the inguinal canal in 1% of children but less than 0.1% will be complicated by an inflammation [43].
- De Garangeot hernia: It is referred to an appendicitis within the femoral canal.
- Intrathoracic appendix is associated with a diaphragmatic hernia

10.6.3 Pylephlebitis

Pylephlebitis refers to a septic thrombophlebitis of the portal vein system. The diagnosis of this rare complication of appendicitis in children is often delayed. Prolonged fever and abdominal pain of unknown origin are the main clinical signs. Even if they have not yet been reported in children, the potential risks are bowel ischemia, liver abscesses, and late portal hypertension. CE-CT is the method of choice recommended for such diagnosis [44]. It will reveal the extent of the hypodense thrombus within the lumen of the portal system and the signs of appendicitis. US-Doppler may potentially achieve this diagnosis but the technique will rather be used to follow up the resolution of the thrombosis. Anticoagulation associated with the adapted antibiotic treatment is advised by most authors to prevent bowel ischemia after appendectomy [45].

10.6.4 Uretero-Hydronephrosis

Uretero-hydronephrosis may occur secondarily to adjacent inflammatory reaction associated with the appendicitis and therefore, it could be mistaken for a urinary tract infection.

10.6.5 The Concepts of Spontaneously Resolving, Recurrent, and Chronic Appendicitis

Interestingly, 7–30% of patients that are operated for appendicitis have sustained one or more episodes of right iliac fossa pain [46–48].

– *Resolving appendicitis* is defined by the association of clinical, biological (possible elevation of the WBC count but no elevation of the erythrocyte sedimentation rate) and imaging signs of appendicitis that disappear spontaneously within less than 48 h. The frequency of such entity has been reported to be at least 8% [48]. In this group of patients, lymphoid hyperplasia may play a major role. US shows an isolated thickening of the lamina propria (but not of the others layers) which can create a transient obstruction of the appendix lumen that will become symptomatic.
– *Recurrent appendicitis* is defined as multiple subtle episodes of right iliac fossa pain, confirmed by histology to be related to appendicitis. Recurrences has been shown to occur between 19 and 38% of cases, most of them within a year [17, 48]. An initial thickness of the appendix above 8 mm [48], a residual intraluminal fluid within the appendix [17] or an appendicolith are features predicting recurrence [49].
– *Chronicity* is defined as continuous symptoms affecting the right iliac fossa lasting for more than several weeks and associated with chronic inflammatory or fibrotic changes of the appendix at histology [50].

The imaging features of the entities described above are identical to those observed in the classical acute appendicitis [46, 50].

10.6.6 Stump Appendicitis

Recurrent episode of acute appendicitis may occur after appendectomy, when the residual stump is too long, usually above 0.5 cm. It can occur either after laparotomy or coelioscopy [51]. The challenge is to consider this diagnosis knowing the past surgical history. Only a few cases have been described in pediatric patients [52]. They occur after a few days or even years post appendicectomy. Imaging findings are similar to classical acute appendicitis.

10.6.7 Infection on an Appendicolith (Fig. 10.9)

When left after appendectomy, an appendicolith may become infected and clinically symptomatic including high fever and abdominal pain. It can be localized anywhere in the peritoneal cavity but usually in the most dependent part of the abdomen and pelvis (Morison's pouch, Douglas cul-

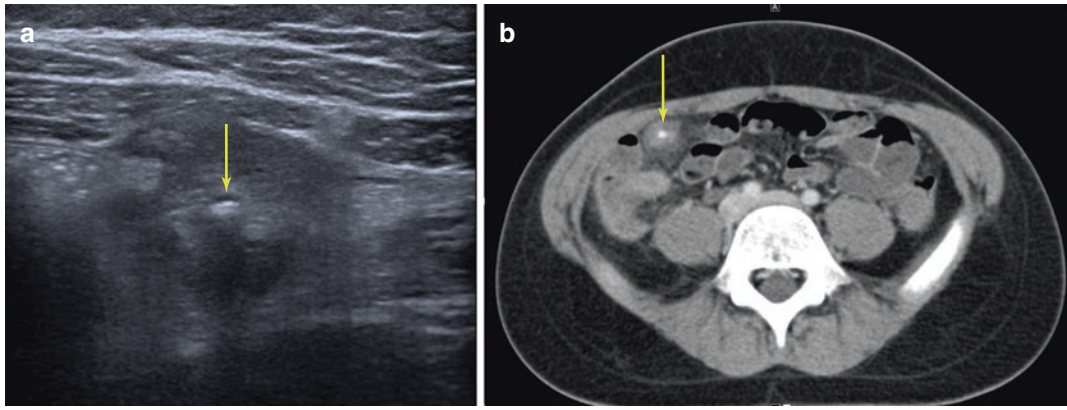

Fig. 10.9 Infection on a left-behind appendicolith. (**a**) US: hyperechoic foci (*yellow arrow*) with posterior shadowing surrounded by a hypoechoic tissue reaction. (**b**) CT: small calcification (*yellow arrow*) surrounded by hyperdense tissue and inflamed fat

de-sac). It has also been reported to be located within the pleural cavity [53]. CT is the modality of choice to search for this lost and infected calcified left-over which can be associated with an abscess. Percutaneous retrieval under CT guidance has been published but the usual treatment remains surgical [54].

10.6.8 Fistula

Fistulas developing during an episode of acute appendicitis have been exceptionally reported [55–58]. The fistulous tract can form between the appendix and the skin, the umbilicus, the rectum, the vagina, or the bladder. The latter has never been reported in pediatric patients [58]. Imaging will search for the inflammation and contact between the appendix and any of these sites. Air bubbles may be seen within the fistulous tract.

10.7 Differential Diagnoses of Acute Bacterial Appendicitis

One has to keep in mind that in the daily practice of an emergency department, when appendicitis is suspected on the basis of clinical evidence, the final diagnosis will be different in one out of 2 patients.

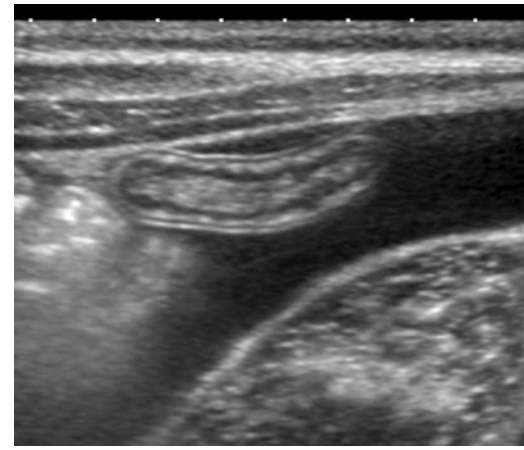

Fig. 10.10 Increased thickness of a normal appendix on US in a 5-year-old boy. The luminal content and the associated ascites are responsible for this increased diameter

10.7.1 Differential Diagnoses Which Directly Involve the Appendix [59]

- Ascites such as in the setting of nephrotic syndrome may increase the diameter of the appendix (Fig. 10.10).
- Transient inflammatory bowel disease:
  - *Lymphoid hyperplasia of the appendix* [14]: The presence of lymphoid tissue within the mucosa and the submucosa of the appendix is a normal finding. It may be responsible

for an increased diameter of the appendix during a transient viral inflammatory process (gastroenteritis, mesenteric adenitis). Other findings, especially, peri-appendiceal fat inflammation, hyperhemia of the appendiceal wall must be present to consider a diagnosis of appendicitis.

- Any kind of *terminal ileitis* may mimic appendicitis and can involve the appendix. This includes infectious ileitis and neutropenic colitis. The most frequent pathogens agents being *E. coli*, Salmonella, Shigella, Campylobacter, and Yersiniosis.
- *Chronic inflammatory bowel diseases*: The appendix can be inflamed in patients with Crohn disease. The correct diagnosis of Crohn can be achieved only when associated terminal ileum and the cecum are even more thickened and inflamed than the appendix itself. Furthermore, the fistulous tracts that are seen within the adjacent inflamed fat will confirm the diagnosis of Crohn. The diagnosis is much more difficult when the Crohn's disease is limited to the appendix or when appendix is involved in case of ulcerative colitis [60].
- *Mucocele*: finding a large appendix over 6 mm of diameter is frequent in cystic fibrosis. Interestingly, acute appendicitis is less frequent in this population [61] (Fig. 10.11). Mucocele without underlying cystic fibrosis has been reported in adolescents [59].

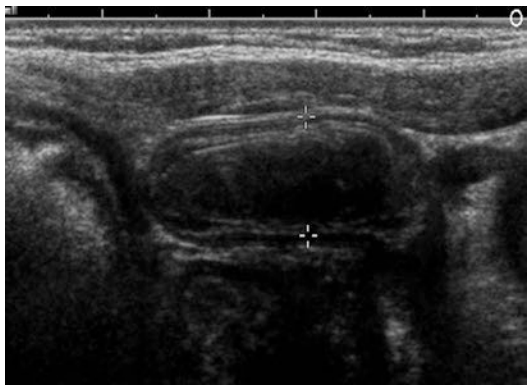

Fig. 10.11 Mucocele in 4-year-old-child with cystic fibrosis

- *Tumor of the appendix*:
  - Carcinoid of the appendix: This rare tumor is considered more aggressive in children than in adults. Due to its small size, this lesion is usually discovered at histology or may appear on imaging as a focal thickening of the appendix layers.
  - Lymphoma: Burkitt lymphoma is the most frequent subtype of lymphoma that can affect the appendix. The appendix is grossly enlarged and there is loss of wall differentiation. Associated tumoral bowel infiltration and large lymph nodes are usually present.
  - Inflammatory pseudo-tumor has exceptionally been described to involve the appendix in pediatric patients [62].

- *Foreign bodies* may be visualized on imaging within the lumen of an inflamed appendix (see also Chap. 26).
- *Worms*: *Obstruction* of the appendiceal lumen by ascaris lumbricoides is a common tropical problem that may mimic appendicitis. The diagnosis is achieved by ultrasound. It shows the worm's alimentary canal as a simple or double hyperechoic bands with a hypoechoic center associated with curling movements, alone or within a complex echogenic mass [63].
- *Torsed appendicitis*: Torsion of the appendix has been rarely reported in pediatric patients [64]. On US, a target like appearance at the base of the appendix is the clue for diagnosis. The other findings are similar to those present in classical appendicitis.

10.7.2 Differential Diagnoses Which Do Not Directly Involve the Appendix

These will be only mentioned. Readers will find their imaging description in the related chapters.

- Ileitis
- Meckel diverticulitis
- Epiploic appendagitis

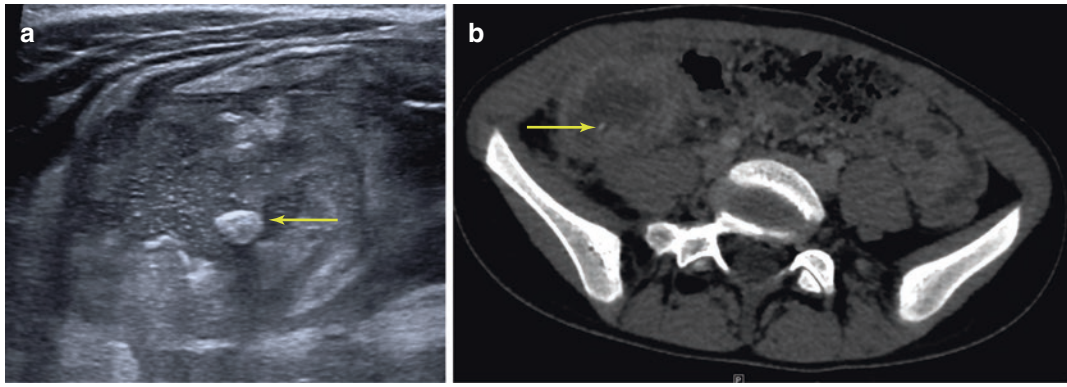

Fig. 10.12 Large post-appendicectomy abscess containing a tiny appendicolith treated with antibiotics. (**a**) US shows a hyperechoic structure with posterior shadowing (*yellow arrow*) surrounded by a well-limited heterogeneous fluid collection. (**b**) CE-CT demonstrated a well-limited enhancing thickened wall and hypodense contents with a tiny calcification (*yellow arrow*)

- Omental infarction
- Cholecystitis
- Acute pyelonephritis, renal or ureteral stones
- Ovarian disease (ovarian torsion, hemorrhagic cyst, abscess) or fallopian inflammation (salpingitis, pyosalpinx, tubo-ovarian abscess)
- Right inferior pulmonary infection

10.8 Post-Operative Complications

Apart from the left behind appendicolith (Fig. 10.12) and stump appendicitis already mentioned, the most frequent post-operative complication is abscess formation (without these underlying causes).

Recurrent abscesses after initial or delayed appendicectomies performed for perforated appendicitis with abscesses have been reported to range from 1 to 24% of cases [65]. Noninvasive treatment, with or without antibiotics, or invasive (surgical or drainage under radiological guidance) treatment remains debated.

Conclusion

Appendicitis due to its numerous presentations and mimickers remains a clinical challenge. Ultrasound, MR, or CT are all highly valuable techniques to look for this diagnosis and search for its differential diagnoses as well as assess complications. The choice of the type of imaging is under the responsibility of the radiologist. When CT is used, an optimized strategy, including IV injection and dose reduction need to be used.

References

1. Rosendahl K, Aukland SM, Fosse K. Imaging strategies in children with suspected appendicitis. Eur Radiol. 2004;14(Suppl 4):L138–45.
2. Lietzén E, Ilves I, Salminen P, et al. Clinical and laboratory findings in the diagnosis of right lower quadrant abdominal pain: outcome analysis of the APPAC trial. Clin Chem Lab Med. 2016;54(10):1691–7.
3. Doria AS, Moineddin R, Kellenberger CJ, et al. US or CT for diagnosis of appendicitis in children and adults? A meta-analysis. Radiology. 2006;241(1):83–94.
4. van Randen A, Bipat S, Zwinderman AH, et al. Acute appendicitis: meta-analysis of diagnostic performance of CT and graded compression US related to prevalence of disease. Radiology. 2008;249(1):97–106.
5. Martin AE, Vollman D, Adler B, et al. CT scans may not reduce the negative appendectomy rate in children. J Pediatr Surg. 2004;39(6):886–90.
6. Kaiser S, Finnbogason T, Jorulf HK, et al. Suspected appendicitis in children: diagnosis with contrast-enhanced versus non enhanced helical CT. Radiology. 2004;231(2):427–33.
7. Kim SH, Choi YH, Kim WS, et al. Acute appendicitis in children: ultrasound and CT findings in negative appendectomy cases. Pediatr Radiol. 2014;44(10):1243–51.

8. Wiersma F, Srámek A, Holscher HC. US features of the normal appendix and surrounding area in children. Radiology. 2005;235(3):1018–22.
9. Coyne SM, Zhang B, Trout AT. Does appendiceal diameter change with age? A sonographic study. Am J Roentgenol. 2014;203(5):1120–6.
10. Ozel A, Orhan UP, Akdana B, et al. Sonographic appearance of the normal appendix in children. J Clin Ultrasound. 2011;39(4):183–6.
11. Trout AT, Sanchez R, Ladino-Torres MF. Reevaluating the sonographic criteria for acute appendicitis in children: a review of the literature and a retrospective analysis of 246 cases. Acad Radiol. 2012;19(11):1382–94.
12. Telesmanich ME, Orth RC, Zhang W, et al. Searching for certainty: findings predictive of appendicitis in equivocal ultrasound exams. Pediatr Radiol. 2016;46:1539–45.
13. Rettenbacher T, Hollerweger A, Macheiner P, et al. Outer diameter of the vermiform appendix as a sign of acute appendicitis: evaluation at US. Radiology. 2001;218(3):757–62.
14. Xu Y, Jeffrey RB, DiMaio MA, et al. Lymphoid hyperplasia of the appendix: a potential pitfall in the sonographic diagnosis of appendicitis. Am J Roentgenol. 2016;206(1):189–94.
15. Rollins MD, Andolsek W, Scaife ER, et al. Prophylactic appendectomy: unnecessary in children with incidental appendicoliths detected by computed tomographic scan. J Pediatr Surg. 2010;45:2377–80.
16. Aljefri A, Al-Nakshabandi N. The stranded stone: relationship between acute appendicitis and appendicolith. Saudi J Gastroenterol. 2009;15:258–60.
17. Koike Y, Uchida K, Matsushita K, et al. Intraluminal appendiceal fluid is a predictive factor for recurrent appendicitis after initial successful non-operative management of uncomplicated appendicitis in pediatric patients. J Pediatr Surg. 2014;49(7):1116–21.
18. Nance ML, Adamson WT, Hedrick HL. Appendicitis in the young child: a continuing diagnostic challenge. Pediatr Emerg Care. 2000;16(3):160–2.
19. Sivit CJ, Siegel MJ, Applegate KE, et al. When appendicitis is suspected in children. Radiographics. 2001;21(1):247–62.
20. Salminen P, Paajanen H, Rautio T, et al. Antibiotic therapy vs appendectomy for treatment of uncomplicated acute appendicitis: the APPAC randomized clinical trial. JAMA. 2015;313(23):2340–8.
21. Simillis C, Symeonides P, Shorthouse AJ, et al. A meta-analysis comparing conservative treatment versus acute appendectomy for complicated appendicitis (abscess or phlegmon). Surgery. 2010;147(6):818–29.
22. Quillin SP, Siegel MJ, Coffin CM. Acute appendicitis in children: value of sonography in detecting perforation. AJR Am J Roentgenol. 1992;159(6):1265–8.
23. Blumfield E, Nayak G, Srinivasan R, et al. Ultrasound for differentiation between perforated and non perforated appendicitis in pediatric patients. Am J Roentgenol. 2013;200(5):957–62.
24. Tulin-Silver S, Babb J, Pinkney L, et al. The challenging ultrasound diagnosis of perforated appendicitis in children: constellations of sonographic findings improve specificity. Pediatr Radiol. 2015;45(6):820–30.
25. Grayson DE, Wettlaufer JR, Dalrymple NC, et al. Appendiceal CT in pediatric patients: relationship of visualization to amount of peritoneal fat. Am J Roentgenol. 2001;176(2):497–500.
26. Garcia K, Hernanz-Schulman M, Bennett DL, et al. Suspected appendicitis in children: diagnostic importance of normal abdominopelvic CT findings with non visualized appendix. Radiology. 2009;250(2):531–7.
27. Donnelly LF, Emery KH, Brody AS, et al. Minimizing radiation dose for pediatric body applications of single-detector helical CT: strategies at a large children's hospital. Am J Roentgenol. 2001;176(2):303–6.
28. Fefferman NR, Bomsztyk E, Yim AM, et al. Appendicitis in children: low-dose CT with a phantom-based simulation technique–initial observations. Radiology. 2005;237(2):641–6.
29. Kharbanda AB, Taylor GA, Bachur RG. Suspected appendicitis in children: rectal and intravenous contrast-enhanced versus intravenous contrast-enhanced CT. Radiology. 2007;243(2):520–6.
30. Krishnamoorthi R, Ramarajan N, Wang NE, et al. Effectiveness of a staged US and CT protocol for the diagnosis of pediatric appendicitis: reducing radiation exposure in the age of ALARA. Radiology. 2011;259(1):231–9.
31. Trout AT, Towbin AJ, Zhang B. Journal club: the pediatric appendix: defining normal. Am J Roentgenol. 2014;202(5):936–45.
32. Lowe LH, Penney MW, Scheker LE, et al. Appendicolith revealed on CT in children with suspected appendicitis: how specific is it in the diagnosis of appendicitis? Am J Roentgenol. 2000;175(4):981–4.
33. Moteki T, Ohya N, Horikoshi H. Computed tomography criterion for the diagnosis of appendicitis without periappendiceal inflammation in children using the maximum depth of intraluminal appendiceal fluid. J Comput Assist Tomogr. 2010;34(6):907–14.
34. Rao PM, Wittenberg J, McDowell RK, et al. Appendicitis: use of arrowhead sign for diagnosis at CT. Radiology. 1997;202(2):363–6.
35. Tsuboi M, Takase K, Kaneda I, et al. Perforated and non-perforated appendicitis: defect in enhancing appendiceal wall–depiction with multi-detector row CT. Radiology. 2008;246(1):142–7.
36. Johnson AK, Filippi CG, Andrews T, et al. Ultrafast 3-T MRI in the evaluation of children with acute lower abdominal pain for the detection of appendicitis. Am J Roentgenol. 2012;198(6):1424–30.
37. Moore MM, Brian JM, Methratta ST, et al. MRI for clinically suspected pediatric appendicitis: case interpretation. Pediatr Radiol. 2014;44(5):605–12.
38. Kulaylat AN, Moore MM, Engbrecht BW, et al. An implemented MRI program to eliminate radiation

from the evaluation of pediatric appendicitis. J Pediatr Surg. 2015;50(8):1359–63.
39. Dillman JR, Gadepalli S, Sroufe NS, et al. Equivocal pediatric appendicitis: unenhanced mr imaging protocol for non sedated children-A clinical effectiveness study. Radiology. 2016;279(1):216–25.
40. Baldisserotto M, Valduga S, da Cunha CF. MR imaging evaluation of the normal appendix in children and adolescents. Radiology. 2008;249:278–84.
41. Hörmann M, Puig S, Prokesch SR, et al. MR imaging of the normal appendix in children. Eur Radiol. 2002;12(9):2313–6.
42. Ong EMW, Venkatesh SK. Ascending retrocecal appendicitis presenting with right upper abdominal pain: utility of computed tomography. World J Gastroenterol. 2009;15(28):3576–9.
43. D'Alia C, Lo Schiavo MG, Tonante A, et al. Amyand's hernia: case report and review of the literature. Hernia. 2003;7:89–91.
44. Balthazar EJ, Gollapudi P. Septic thrombophlebitis of the mesenteric and portal veins: CT imaging. J Comput Assist Tomogr. 2000;24:755–60.
45. Gatibelza ME, Gaudin J, Mcheik J, et al. Pylephlebitis in the child: a challenging diagnosis. Arch Pédiatr. 2010;17:1320–4.
46. Rao PM, Rhea JT, Novelline RA, et al. The computed tomography appearance of recurrent and chronic appendicitis. J Emerg Med. 1998;16(1):26–33.
47. Migraine S, Atri M, Bret PM, et al. Spontaneously resolving acute appendicitis. Clinical and sonographic documentation. Radiology. 1997;205:55–8.
48. Cobben LPJ, de Mol van Otterloo A, Puylaert JBCM. Spontaneously resolving appendicitis: Frequency and natural history in 60 patients. Radiology. 2000;215(2):349–52.
49. Ein SH, Langer JC, Daneman A. Nonoperative management of pediatric ruptured appendix with inflammatory mass or abscess: presence of an appendicolith predicts recurrent appendicitis. J Pediatr Surg. 2005;40:1612–5.
50. Checkoff JL, Wechsler RJ, Nazarian LN. Chronic inflammatory appendiceal conditions that mimic acute appendicitis on helical CT. AJR. 2002;179(9):731–4.
51. Subramanian A, Liang MK. A 60-year literature review of stump appendicitis: the need for a critical view. Am J Surg. 2012;203(4):503–7.
52. Tang XB, Qu RB, Bai YZ, et al. Stump appendicitis in children. J Pediatr Surg. 2011;46(9):233–6.
53. Betancourt SL, Palacio D, Bisset GS. The 'wandering appendicolith'. Pediatr Radiol. 2015;45(1):1091–4.
54. Singh AK, Hahn PF, Gervais D, et al. Dropped appendicolith: CT findings and implications for management. AJR. 2008;190(3):707–11.
55. Alloo J, Gerstle T, Shilyansky J, et al. Appendicitis in children less than 3 years of age: a 28-year review. Pediatr Surg Int. 2004;19(12):777–9.
56. Park WH, Choi SO, Woo SK, et al. Appendicoumbilical fistula as a sequela of perforated appendicitis. J Pediatr Surg. 1991;26(12):1413–6.
57. Deorah S, Seenu V, Pradeep KK, et al. Spontaneous appendico-cutaneous fistula: a rare complication of acute appendicitis. Trop Gastroenterol. 2005;26(1):48–50.
58. Alis D, Samanci C, Namdar Y, et al. A very rare complication of acute appendicitis: appendico-vesical fistula. Case Rep Urol. 2016;2016:4517029.
59. Dietz KR, Merrow AC, Podberesky DJ, et al. Beyond acute appendicitis: imaging of additional pathologies of the pediatric appendix. Pediatr Radiol. 2013;43(1):232–42.
60. Perry WB, Opelka FG, Smith D, et al. Discontinuous appendiceal involvement in ulcerative colitis: pathology and clinical correlation. J Gastrointest Surg. 1999;3:141–4.
61. Chaudry G, Navarro OM, Levine DS, et al. Abdominal manifestations of cystic fibrosis in children. Pediatr Radiol. 2006;36:233–40.
62. Sanders BM, West KW, Gingalewski C, et al. Inflammatory pseudotumor of the alimentary tract: clinical and surgical experience. J Pediatr Surg. 2001;36(1):169–73.
63. Malde HM, Chadha D. Roundworm obstruction: sonographic diagnosis. Abdom Imaging. 1993;18(3):274–6.
64. Perger L, Muensterer OJ. Laparoscopic appendectomy for torsed appendix presenting as an acute abdomen in an infant female. JSLS. 2011;15:565–7.
65. Gorter RR, Meiring S, van der Lee JH, et al. Intervention not always necessary in post-appendectomy abscesses in children; clinical experience in a tertiary surgical center and an overview of the literature. Eur J Pediatr. 2016;175(9):1185–91.

Meckel's Diverticulum

11

Brigitte Bourlière and Philippe Petit

Contents

11.1 Introduction

Meckel's diverticulum (MD) is a remnant of the omphalomesenteric canal and represents more than 90% of these remnants malformations [1]. This canal connects the yolk sac to the midgut and whenever its ileal end does not close, a MD is formed. It is the most frequent bowel congenital abnormality found during autopsy, in around 2% of cases. Only a small percentage of MD will become symptomatic during lifetime and most of them before the age of 2 years [2]. The frequency of complications decreases with age. Contrary to intestinal duplication, a MD develops on the anti-mesenteric border of the ileum. St Vil et al. have published a series of 164 children; they report that the presence within the MD of gastric mucosa, pancreatic mucosa or both were as frequent as respectively 88%, 7%, and 3% of cases [3]. The size of a MD may vary from a few millimeters up to 25 cm. Giant diverticulum is considered above 5 cm. MD is equally found in both sexes but males are more prone to be symptomatic.

In decreasing frequency, acute MD complications appears as, bowel obstruction, rectal bleeding and diverticulitis [3].

11.2 Imaging Specificities

Only a few percentage of MD (6–10%) are diagnosed preoperatively by imaging.

B. Bourlière • P. Petit (✉)
Department of Pediatric Imaging,
Hôpital Timone Enfants, 264 rue St Pierre,
13385 Marseille, Cedex 05, France
e-mail: ppetit@ap-hm.fr

F.E. Avni, P. Petit (eds.), *Imaging Acute Abdomen in Children*,
https://doi.org/10.1007/978-3-319-63700-6_11

- Tc-99m pertechnetate scintigraphy searching for gastric mucosa is considered as the best technique to diagnose MD; its sensitivity and specificity are reported above 85% but false negative and false positive results due to various entities (such as abscesses, appendicitis, intussusception, volvulus, angiodysplasia, any kind of colitis or neoplasm) are frequent [1, 2]. In case of acute bleeding, Tc-99m erythrocytes labeled scintigraphy appears more accurate [2]. However, these examinations are rarely available in an emergency setting.
- Angiography is not performed anymore. Historically, the presence of a remnant vessel arising from the mesenteric artery (vitelline artery) was the accepted diagnostic criteria. Still, therapeutic angiography has been reported in an infant for life-threatening bleeding from a MD [4].
- Whatever the imaging modality and whatever the clinical presentation, the visualization of a segment of bowel with a blind ending, distinct from the appendix, between the right iliac fossa and the umbilicus, is characteristic for a MD.

As already mentioned, ultrasound is the imaging procedure of choice to explore acute abdomen in children. Uncomplicated MD is extremely difficult to diagnose due to its appearance similar to a normal segment of the small bowel. Thickening due to inflammation or a MD inducing intestinal obstruction may lead to its preoperative recognition. Contrast enhanced sonography has been proposed in order to increase confidence in diagnosis [5].

A few articles have also reported the efficacy of CT for such pathology. Yet, among 16 children with proven complicated Meckel's diverticulum, CT exploration was normal in 12% [6].

MR imaging has been only scarcely used for this pathology [7]. However, the same MR imaging protocol used for acute appendicitis [8] could be used for the evaluation of a complicated MD as well. Entero-MR imaging exploration may potentially demonstrate uncomplicated MD.

11.3 Clinical Presentations

11.3.1 Bowel Obstruction

11.3.1.1 Intussusception

MD may serve as a lead point for intussusception either ileo-ileal, ileocolic or ileoileocolic. In a series of 43 children with secondary intussusceptions, 28% were due to MD [9]. In case of inverted MD, the typical imaging appearance is the presence of mesenteric fat at the top or around the serosal surface of the intussusceptum that is well differentiated from the mesenteric fat included in the intussuscipiens (Fig. 11.1). This fat in MD represents stromal remnants of the omphalomesenteric duct [10] and may be seen either on US, on CT or on MR imaging. An uncommon differential diagnosis would be the presence of a lipoma within the intussusceptum. The inverted MD may lose its layered bowel wall signature due to edema or ischemic changes. A multilayered intussusceptum may also be seen, not easily distinguishable from an ileoileal intussuception [11].

11.3.1.2 Mesodiverticular Band

A mesodiverticular band can be responsible for strangulation and volvulus of an adjacent bowel loop or of the MD itself (Fig. 11.2). This remnant band is located at the top of the MD and is linked to the umbilicus or to any structure in the abdominal cavity or may even float freely in the peritoneal cavity. Its visualization is uncommon [1]. Imaging examinations would demonstrate a small bowel obstruction with no obvious reason or related to an associated MD diverticulitis [12].

11.3.2 Diverticulitis

This complication is mostly secondary to ulceration in relation with the presence of gastric mucosa. It has been exceptionally responsible for an associated pseudo-tumor [13].

Other causes of obstruction of a MD in pediatric practice include volvulus by a mesodiverticular band, torsion around its own pedicle, Burkitt's lymphoma [14], enterolith [15], phytobezoar [16], foreign bodies [17], and ascaris [18].

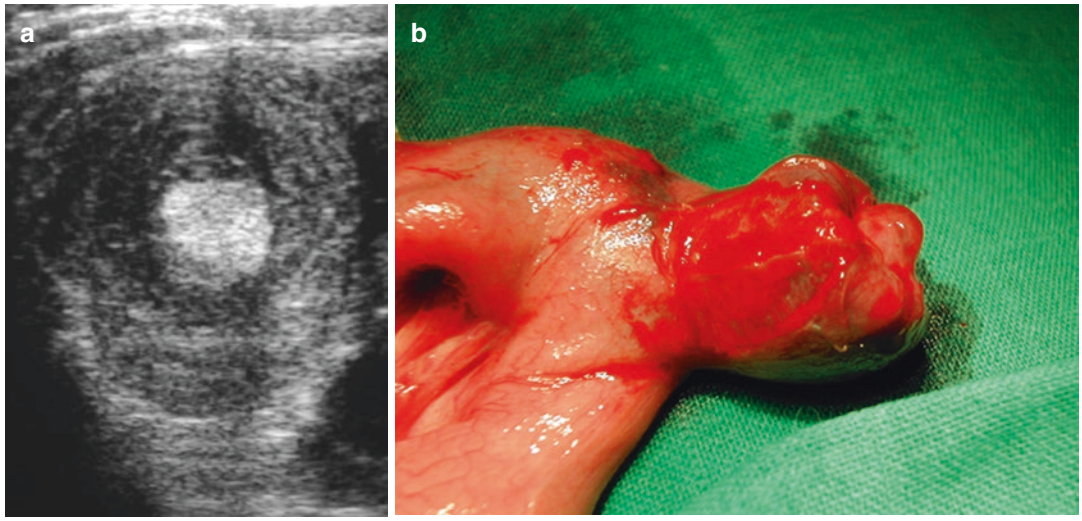

Fig. 11.1 Intussusception in a 2-year-old child. (**a**) Ultrasound reveals a multilayered structure with a hyperechoic center corresponding to fatty stromal remnant of the omphalomesenteric duct. (**b**) Post-operative resected MD after reduction of the intussusception and eversion of the MD (Courtesy, Pr K. Chaumoitre - Pr T. Merrot)

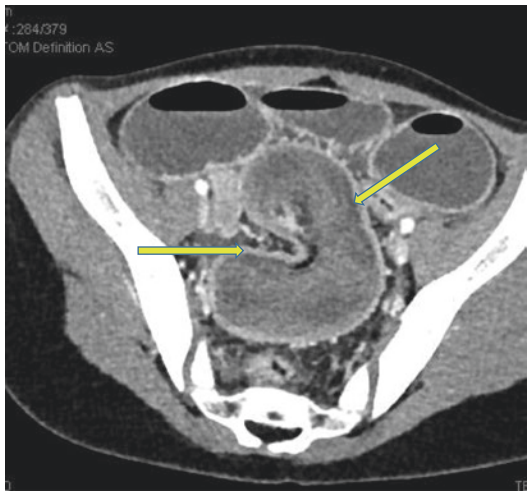

Fig. 11.2 Twelve-year-old child. CE-CT: small bowel obstruction related to a MD volvulus. The MD is distended (*yellow arrows*), its wall is thickened but remains vascularized

In the majority of cases, the clinical symptoms are masquerading as an acute appendicitis. Less likely melena or bloody stools may be the revealing clinical symptoms.

– On ultrasound [19, 20] or on CT [6], the inflamed MD appears as a blind bowel structure with no connection to the cecum. The diverticulitis will appear either tubular or like a pouch-like structure, sometimes very large. Its wall is thickened and the amount adjacent inflammatory fat appears increased and hypervascularized (Fig. 11.3)**.** A cystic mass is present in 50% (Fig. 11.4) of cases that may mimic a duplication cyst; in the latter, a more regular wall can usually be displayed [19]. An associated enterolith is rarely present (Fig. 11.5). The visualization of an adjacent normal appendix helps to orient the differential diagnoses. These include besides appendicitis, Crohn's disease, complicated lymphatic malformation and whenever located close to the umbilicus, inflammation of an urachal remnant.

11.3.3 Hemorrhage

Hemorrhage is mainly secondary to peptic ulceration due to the presence of gastric mucosa within the diverticulum. Hemorrhage may also be a complication of diverticulitis. Such complications are reported to be more severe during childhood [21]; however, severe hemorrhagic presentations have been only scarcely reported [4, 22]. Tc-pertechnetate scintigraphy (Fig. 11.6) is considered as the gold standard procedure to

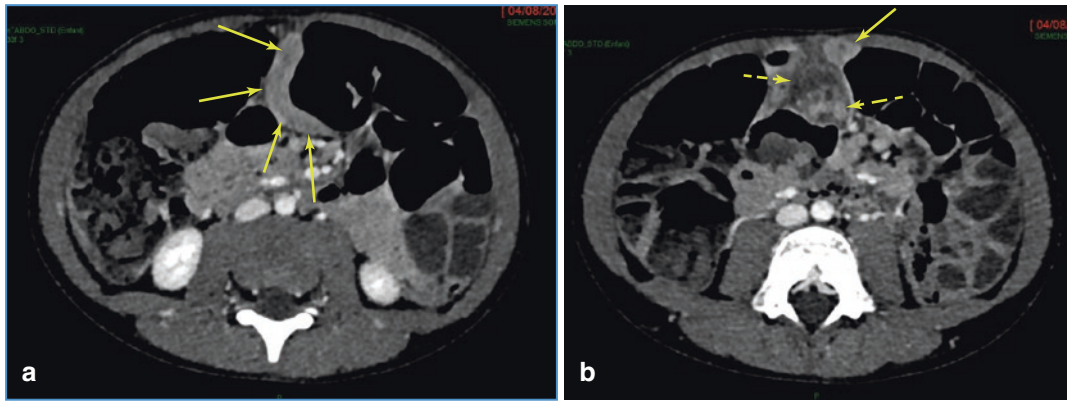

Fig. 11.3 Diverticulitis in a 7-year-old boy explored on CE-CT. (**a**) An inflamed tubular bowel structure is present on the midline (*yellow arrows*). (**b**) The tubular structure connected to the umbilicus (*yellow arrow*) is associated with an adjacent increased amount of fat (*dashed arrows*)

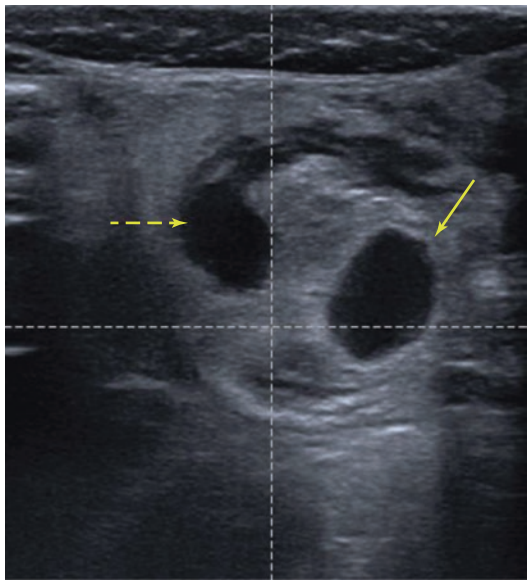

Fig. 11.4 Four-year-old boy complaining of acute onset of abdominal pain. US reveals a cystic structure surrounded by a hyperechoic wall (*yellow arrow*) and hyperechoic fatty infiltration with some free fluid (*dashed yellow arrow*). Surgery and histology confirmed the presence of an inflamed MD

detect gastric mucosa but its negative predictive value is low (0.74) especially when the hemoglobin level in the serum is lower than 11 g/dL [23]. In case of acute bleeding, 99mTc-erythrocytes labeled scintigraphy is described more accurate [24]. SPECT/CT is recommended to avoid false result due to the physiological uptake of the kidney. Scintigraphy can be falsely positive due to intestinal duplication cysts containing heterotopic gastric mucosa, intussusception or significant bowel wall inflammation [7]. CT and US have not proven to be useful in such presentations.

11.3.4 Perforation

Perforation is exceptionally described in pediatric patients. Kotecha et al. reported multiple mechanisms for this complication such as inflammation, ulceration, ischemia, occlusion by parasites or foreign bodies, post-traumatic perforation, and volvulus [2].

11.4 Unusual Presentation

11.4.1 Littre Hernia

Littre Hernia refers to a small bowel obstruction secondary to the incarceration of a MD within a hernia. The specificity in children is the higher prevalence of the umbilical localization of the hernia (85%) [25] and a more frequent "acute" presentation than in adults. Other sites of hernia include the inguinal canal, any post-operative orifice, and even the diaphragm [26].

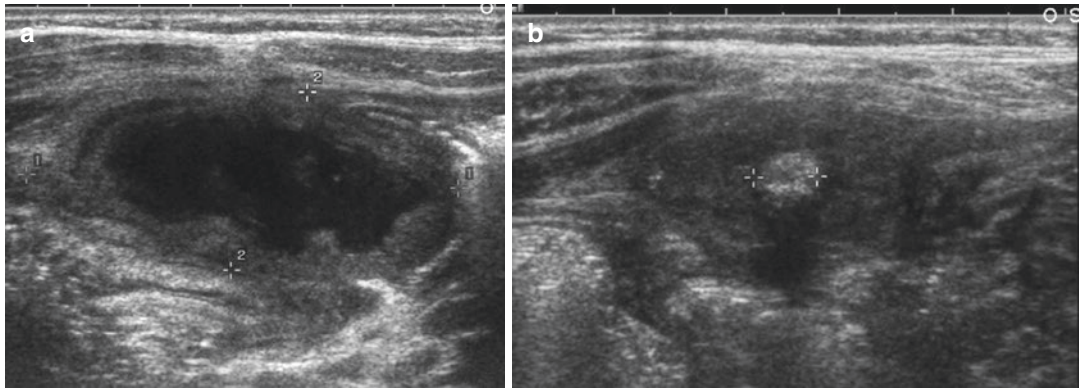

Fig. 11.5 Meckel's diverticulitis in a 3-year-old girl. (**a**) US transverse sections. US demonstrates on the right side of the umbilicus presence of an oval shape cystic structure on the antimesenteric side of an ileal loop. This lesion presents with a thick surrounding wall without bowel layer differentiation. (**b**) The mass is filled with fluid and contains in its distal part a hyperechoic shadowing structure corresponding to an enterolith

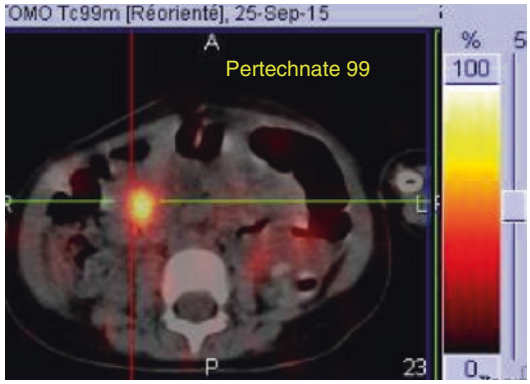

Fig. 11.6 Chronic abdominal pain secondary to MD ulceration in a 4-year-old girl. Tc-99m pertechnetate scintigraphy: A hyperintense activity is identified on the right iliac fossa corresponding to gastric mucosa uptake. (Courtesy G Petyt, MD)

11.5 The Differential Diagnoses of Complicated MD Include

- Appendicitis
- Duplication
- Urachus remnant complications
- Crohn's disease

The readers should refer to the specific chapters.

Conclusion

Meckel Diverticulum displays a wide spectrum of acute abdominal presentations (hemorrhage, obstruction, inflammation, perforation). The frequency of complications decreases with age. The goal of the pediatric radiologist is to consider MD as a potential diagnosis during the child's exploration of acute abdomen and to search for some specific findings (tubular or pouch-like blind bowel structure connected to the terminal ileum, fatty material at or around the tip of an intussusceptum).

References

1. Levy AD, Hobbs CM. From the archives of the AFIP. Meckel diverticulum: radiologic features with pathologic correlation. Radiographics. 2004;24(2):565–87.
2. Kotecha M, Bellah R, Pena AH, et al. Multimodality imaging manifestations of the Meckel diverticulum in children. Pediatr Radiol. 2012;42(1):95–103.
3. St-Vil D, Brandt ML, Panic S, Bensoussan AL, et al. Meckel's diverticulum in children: a 20-year review. J Pediatr Surg. 1991;26(11):1289–92.
4. Bevernage C, Maleux G, De Hertogh G, et al. Life-threatening lower gastrointestinal bleeding in a 2-year-old boy treated by transcatheter embolization: uncommon features of a complicated Meckel diverticulum. Pediatr Radiol. 2010;40(10):1702–5.

5. Hamada T, Tanaka M, Hashimoto Y, et al. Contrast-enhanced sonographic findings of gangrenous meckel diverticulitis. J Ultrasound Med. 2006;25(9): 1227–31.
6. Olson DE, Kim YW, Donnelly LF. CT findings in children with Meckel diverticulum. Pediatr Radiol. 2009;39(7):659–63.
7. Hegde S, Dillman JR, Gadepalli S, et al. MR enterography of perforated acute Meckel diverticulitis. Pediatr Radiol. 2012;42(2):257–62.
8. Navarro O, Dugougeat F, Kornecki A, et al. The impact of imaging in the management of intussusception owing to pathologic lead points in children. A review of 43 cases. Pediatr Radiol. 2000;30(9):594–603.
9. Dillman JR, Gadepalli S, Sroufe NS, et al. Equivocal pediatric appendicitis: unenhanced MR imaging protocol for nonsedated children-a clinical effectiveness study. Radiology. 2016;279(1):216–25.
10. Black ML, Ros PR, Smirniotopoulos JG, et al. Intussuscepted Meckel diverticulum: radiologic-pathologic correlation. Comput Radiol. 1987;11(5–6): 245–8.
11. Daneman A, Myers M, Shuckett B, et al. Sonographic appearances of inverted Meckel diverticulum with intussusception. Pediatr Radiol. 1997;27(4): 295–8.
12. Gaisie G, Curnes JT, Scatliff JH, et al. Neonatal intestinal obstruction from omphalomesenteric duct remnants. AJR Am J Roentgenol. 1985;144(1): 109–12.
13. Lemale J, Boudjemaa S, Parmentier B, et al. A pseudotumoral lesion revealing Meckel's diverticulum. Arch Pediatr. 2016 Nov;23(11):1157–60.
14. Al-Dabbagh AI, Salih SA. Primary lymphoma of Meckel diverticulum: a case report. J Surg Oncol. 1985 Jan;28(1):19–20.
15. Lai HC. Intestinal obstruction due to Meckel's enterolith. Pediatr Neonatol. 2010;51(2):139–40.
16. Mares AJ, Finaly R, Mordechai J, et al. "Pantaloon" phytobezoar: an unusual cause of intestinal obstruction associated with Meckel's diverticulum. Isr J Med Sci. 1993;29(11):683–5.
17. Redmond P, Sawaya D, Nowicki M. Bowel obstruction due to multiple retained foreign bodies in a Meckel diverticulum. J Pediatr. 2014;165(3): 639–639.e1.
18. Wani I, Snábel V, Naikoo G, et al. Encountering Meckel's diverticulum in emergency surgery for ascaridial intestinal obstruction. World J Emerg Surg. 2010;5:15.
19. Daneman A, Lobo E, Alton DJ, et al. The value of sonography, CT and air enema for detection of complicated Meckel diverticulum in children with nonspecific clinical presentation. Pediatr Radiol. 1998;28: 928–32.
20. Baldisserotto M, Maffazzoni DR, Dora MD. Sonographic findings of Meckel's diverticulitis in children. AJR Am J Roentgenol. 2003;180(2):425–8.
21. Elsayes KM, Menias CO, Harvin HJ, et al. Imaging manifestations of Meckel's diverticulum. AJR Am J Roentgenol. 2007;189(1):81–8.
22. Esposito C, Giurin I, Savanelli A, et al. Meckel's diverticulum causing severe hemorrhage. Eur J Pediatr. 2012;171(4):733–4.
23. Swaniker F, Soldes O, Hirschl RB. The utility of technetium 99m pertechnetate scintigraphy in the evaluation of patients with Meckel's diverticulum. J Pediatr Surg. 1999;34(5):760–4.
24. Grady E. Gastrointestinal bleeding scintigraphy in the early 21st century. J Nucl Med. 2016;57(2):252–9.
25. Skandalakis PN, Zoras O, Skandalakis JE, et al. Littre hernia: surgical anatomy, embryology, and technique of repair. Am Surg. 2006;72:238–43.
26. Pampal A, Aksakal ED. Littre hernia in childhood: a case report with a brief review of the literature. Afr J Paediatr Surg. 2011;8(2):221–4.

Inflammatory Bowel Disease

12

Nathalie Colavolpe, Stuart Taylor,
and Philippe Petit

Contents

12.1 Introduction

Inflammatory bowel disease (IBD) is a term which encompasses three different entities: Crohn's disease (CD), ulcerative colitis (UC), and indeterminate colitis. All three may manifest as an acute clinical episode, either at first presentation or secondary to a complication in established disease. The diagnosis of IBD can be difficult and is based on clinical, endoscopic, biological, histological, and imaging findings. Blood and stool markers of inflammation, notably C-reactive protein and fecal calprotectin assist in diagnosis and disease follow-up, but are nonspecific and have limitations.

The phenotype of pediatric IBD may differ from that of adult disease, which in turn impacts on imaging findings.

- Specifically, CD may be limited to the terminal ileum or colon in up to 20% of children [1]. Isolated jejunal involvement is reported to occur in 5–6%, a disease pattern which is more frequent in younger children and that in itself is associated with an increased risk of a complicated course for the disease [2]. Auvin et al. [3] reported small bowel involvement in 80% of pediatric IBD, with less frequent involvement of the terminal ileum compared to the adult population.
- In UC the classical contiguous involvement of the bowel from the rectum to cecum is less consistent in pediatric practice. Macroscopic

N. Colavolpe • P. Petit (✉)
Department of Pediatric Imaging,
Hôpital Timone Enfants, 264 rue St Pierre,
13385 Marseille, Cedex 05, France
e-mail: ncolavolpe@ap-hm.fr; ppetit@ap-hm.fr

S. Taylor
Centre for Medical Imaging,
University College London, 250 Euston Road,
London NW1 2BU, UK
e-mail: Stuart.taylor@uclh.nhs.uk;
csytaylor@yahoo.co.uk

F.E. Avni, P. Petit (eds.), *Imaging Acute Abdomen in Children*,
https://doi.org/10.1007/978-3-319-63700-6_12

rectal sparing is reported from 5 to 30% and the absence of continuous disease from rectum to cecum (cecal patch) described in 2% of children. Transmural inflammation can be severe and the terminal ileum may be inflamed without granulomata (backwash ileitis) [4].

12.2 Epidemiology

The prevalence of IBD has increased in recent years [5], although less than 25% of cases occur in children below 18 years of age [4]. CD is twice as frequent as UC in the pediatric age group, and specific phenotypic and genotypic subtype of IBDs occur in younger children. Early onset (EO) disease, i.e. occurring before 5 years of age, concerns 11% of childhood IBD [6], and UC and indeterminate colitis is more frequent in this age group. EO CD exhibits more frequent isolated colonic and upper gastrointestinal involvement than later-onset disease, in which the disease involves predominantly the colon and terminal ileum. Very EO-IBD, before the age of 1 year, has a strong association with a genetic defect related to interleukin-10 and is associated with frequent peri-anal fistulae [7].

12.3 Presentations on Imaging

12.3.1 Ultrasound

Due to its proven diagnostic accuracy, availability, and high acceptability in children, US is the first-line imaging modality performed in the setting of acute abdominal pain or suspected bowel obstruction, both of which are common presentations of IBD. US, however, may be limited in severe obesity, and overlying bowel gas may hide underlying bowel loops. Full interrogation of the bowel may also be difficult, particularly the jejunum and rectosigmoid.

A child presenting with an acute abdomen should undergo a full abdominal and pelvic examination with a low frequency probe, followed by analysis with a high frequency linear probe. More specifically low frequency convex probes provide a good overview of the spatial relationship between potentially abnormal bowel loops, and facilitate evaluation of associated mesenteric fat reaction, fluid collections, uncommon complications such as mesenteric or portal vein thrombosis [8] or associated biliary disease (cholangitis, biliary stones). The high frequency probe better delineates the structure of the bowel wall itself and the adjacent mesenteric fat.

Differentiation of the small bowel from the colon is of paramount importance both for the diagnosis and for guiding subsequent treatment. The anatomical position of these respective structures is of great help: the small bowel lying centrally and the colon in periphery. Linear high frequency transducers also help distinguishing small bowel from colon, particularly if the bowel is not over distended. The normal small bowel displays peristalsis and has a regular external surface with visible intestinal folds within its lumen. Conversely the colon has an irregular external surface due to haustrations and no or little peristalsis during the ultrasound examination. The high frequency probes facilitate detailed evaluation of the bowel wall (thickness, differentiation of layers, vascularization), surrounding mesenteric fat (volume, echogenicity, homogeneity, presence of fistulous and sinus tracts), the presence and nature of associated collections (for example, echogenicity, presence of gas, etc.) and the presence of a pneumoperitoneum. A major advantage of US is its ability to dynamically interrogate underlying structures using graded compression, providing useful information on elasticity and mobility of the bowel. Harmonic imaging may be used to increase image resolution and decrease artifacts.

In the context of emergency, US is performed without specific diet restriction but when the patient is not an immediate candidate for surgery, ingestion of plain water or non-carbonated fruit juice is recommended [9].

Additional US techniques have application in children, although not in an emergency setting, and are usually used in an attempt to better quantify the disease activity. For instance, hydrosonograpy distends the bowel using specific oral agents (mannitol, sorbitol, polyethylene glycol,

etc.) to better evaluate bowel wall structure. Contrast-enhanced ultrasound and dynamic contrast-enhanced ultrasound (contrast agent is currently off-label in children) [10] and elastography are also advocated for the evaluation of disease activity [11]; initial encouraging results need confirmation [12].

12.3.1.1 Positive US Diagnosis

The first objective is to ascertain the presence of an abnormal bowel segment and precise its location (small bowel and/or colon). IBD typically alters bowel wall thickness and the differentiation of the normal 5-layer pattern

- *Thickness of the wall*: A thickness over 3 mm is considered abnormal by most authors [13–15]. Thickening can be graded as mild (3–6 mm), moderate (6–9 mm), or severe (over 9 mm) [14] (Fig. 12.1).
- *Parietal differentiation*: Advanced CD is more prone than UC to result in loss of differentiation of the normal layered bowel wall and subsequently, the hyperechoic submucosa will no longer be visible between the hypoechoic mucosa and the muscularis mucosa (Fig. 12.2). Ulceration and fissures may be visible as small hyperechoic spots perpendicular to the bowel lumen. Loss of haustrations (in the colon), loss of peristalsis (for the small bowel), and loss of compressibility are important associated findings [14].

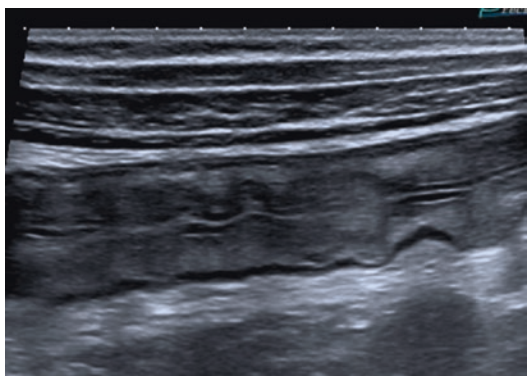

Fig. 12.1 Fourteen-year-old girl treated for UC. Sagittal US section visualizes a mild thickening of the left colon wall with preserved bowel signature

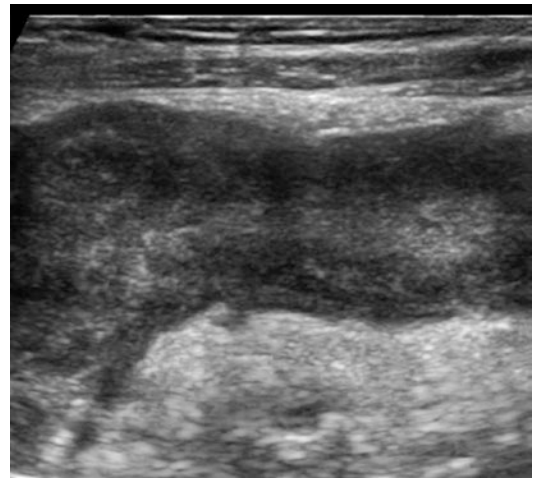

Fig. 12.2 Twelve-year-old boy known for CD. Sagittal US section reveals a severe thickening of the bowel wall and loss of the layered pattern

An abnormal bowel loop often appears fixed with increased Doppler flow within the wall, and is frequently separated from other loops by an increased volume of mesenteric fat (fat wrapping).

In a recent meta-analysis, including both adult and pediatric patients, Calabrese et al. [16] reported that US has a 79.7% sensitivity and a 96.7% specificity for the diagnosis of suspected CD, and 89% sensitivity and 94.3% specificity for initial assessment in established patients with CD. Ileal CD was identified with 92.7% sensitivity, 88.2% specificity, and colonic CD with 81.8% sensitivity and 95.3% specificity, with lower accuracy for detecting proximal lesions. The absence of bowel wall thickening had a high negative predictive value for rapidly excluding CD [17, 18]. Concordance between US and MRE for bowel thickening and vascularization has been reported to be excellent and fairly good, respectively [19], but reliability of US is lower in the mid and proximal portions of the small bowel [20]. Furthermore, in recent study, the utility US for assessing response to medical therapy in CD or detecting and following disease-related complications has been questioned [21].

Other common findings on US in patients with CD include isolated hyperemia of the appendix (73%) and appendiceal involvement in 21% [22].

Enlarged and numerous mesenteric lymph nodes are frequent associated findings, although they are nonspecific. As noted above, some data suggests administration of oral contrast agent (hydrosonography) may improve sensitivity and specificity in identifying CD, and in assessing location and disease extent [16].

12.3.1.2 Complications

Complications are less frequent in children than in the adult population.

- *Stenosis* (Fig. 12.3) presents as a rigid and thickened bowel associated with a dilated upstream normal loop, often with preserved peristalsis. The diagnosis of stenosis is easier in the small bowel than in the colon. Associated hyperemia within the area of the stenosis is helpful in differentiating potentially reversible inflammation from a fixed fibrotic lesion which will usually require surgery. Low vascularization with retraction of the adjacent loops towards the stenosis supports a fibrotic phenotype [23]. However, fibrosis and inflammation frequently coexist within the same segment of stenosed bowel and distinction between these pathological entities using US remains controversial [10–12]. In general, increased bowel wall thickness, loss of mural stratification, and increased fibrofatty proliferation may predict patients who might require surgical treatment [24]. Across adult and pediatric populations, US has sensitivity of 79.7% and specificity of 94.7% in diagnosing stenosis [16].
- *A fistula* (Fig. 12.4) expresses as a hypoechoic tract, for instance, between a bowel loop and another bowel loop, between a bowel loop and the bladder or skin. Detection of mobile hyperechoic gas bubbles within this tract facilitates the diagnosis, and video clips are a useful for their detection. US performs as well as MR imaging for the diagnosis of enteric fistula, with a sensitivity approaching 80%, in adults [25]. A sinus is a blind tract and manifests in a similar way, although does not communicate with another organ.
- *An abscess* is typically a thick walled ill-defined collection, often with increased Doppler signal in the wall. The echogenicity of the central core is variable and depends on the content (gas, debris, blood, pus) (Fig. 12.5). In a recent meta-analysis [16], US has comparable sensitivity (79.7%) and specificity (94.7%) with CT or MR imaging for the detection of CD abscesses in adults and children.

Disease activity: US has been advocated as an efficient tool to monitor disease progression and response to medical therapy [16], although others have questioned its utility [21], for example due to its limited reproducibility and restricted evaluation of some bowel segments such as the jejunum and rectum.

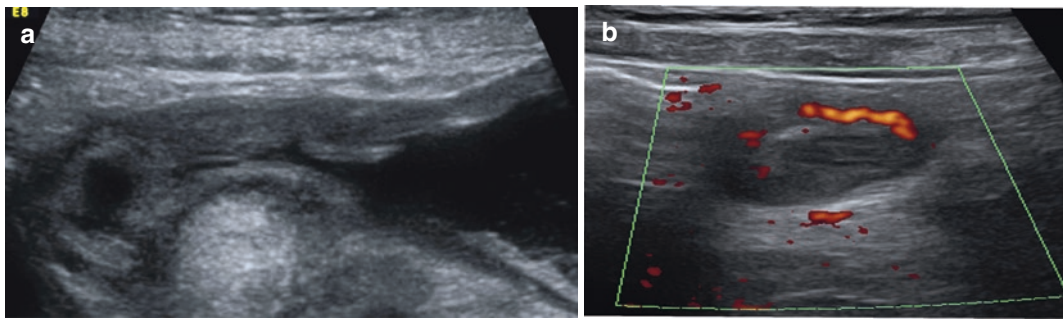

Fig. 12.3 Sixteen-year-old boy known for CD presenting an ileal stenosis. (**a**) Sagittal US section visualizes thickening of the wall and loss of bowel signature. The bowel lumen is not visible anymore and there is a distension of the upstream loop. The aspect of both segments did not modify during the entire examination. (**b**) Transverse Doppler US at the stenosis site demonstrates associated hyperemia of the thickened bowel wall

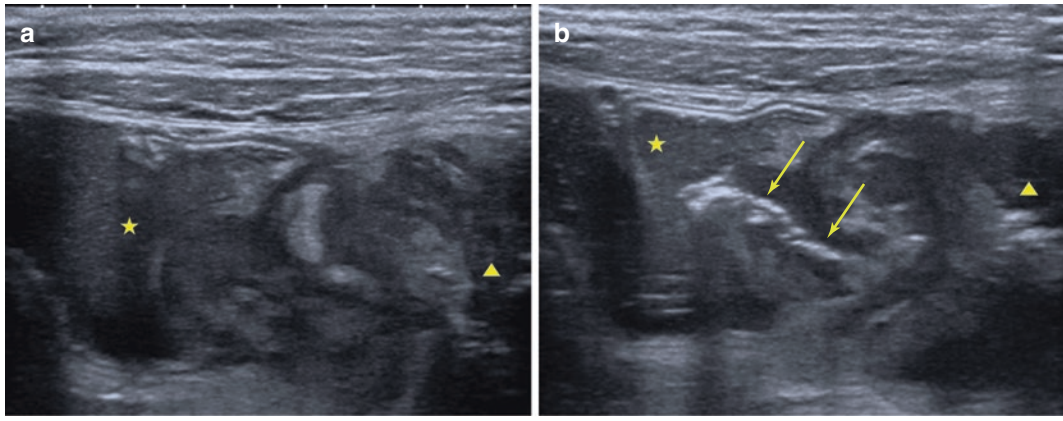

Fig. 12.4 Eleven-year-old boy explored by US; follow-up of a known ileal CD. (**a**) Markedly heterogeneous ill-defined hypoechoic area between the transverse colon (*yellow star*) and the diseased ileal loop (*yellow triangle*). (**b**) A flow of hyperechoic air bubbles (*yellow arrows*) was seen during the examination coming from the ileum towards the transverse colon establishing the presence of a fistulous tract between these two loops

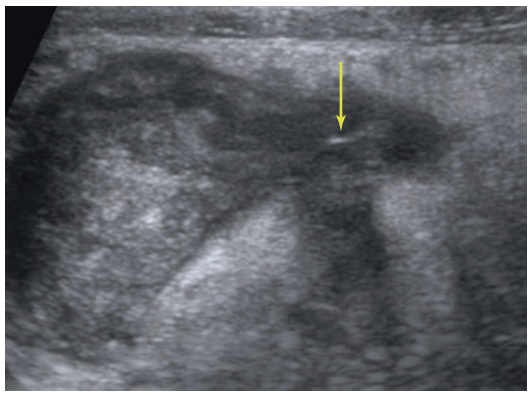

Fig. 12.5 Eleven-year-old boy known for active ileal CD. US demonstrates an ill-defined hypoechoic area surrounded by a hyperechoic fat infiltration adjacent to a thickened ileal loop. The presence of air bubbles (*yellow arrow*) within this hypoechoic area ascertains the diagnosis of abscess

- Increased vessel density and hyperemia (Fig. 12.6) on Color Doppler [26] is a validated marker of disease activity. However, the correlation is weak against the Crohn Disease Activity Index (CDAI) [16] and is not in itself able to precisely map the severity of disease [13, 27].
- Contrast-US may provide additional diagnostic information [28]. Rosembaum et al. [24] have reported that the US findings most often demonstrate in children operated for CD include: bowel wall thickness above 4.3 mm (mean, 6.1 mm), more frequent loss of mural stratification, and fibrofatty proliferation.

There is a high concordance between US and endoscopy (90%) for the extension evaluation of UC. Multiple regression analysis shows that US measurement of increased bowel wall thickness, increased vascularity, loss of haustra, and loss of stratification of the bowel wall were all independent predictive value of severity at endoscopy. A US score based on these parameters strongly correlates with clinical and endoscopic activity of disease [29].

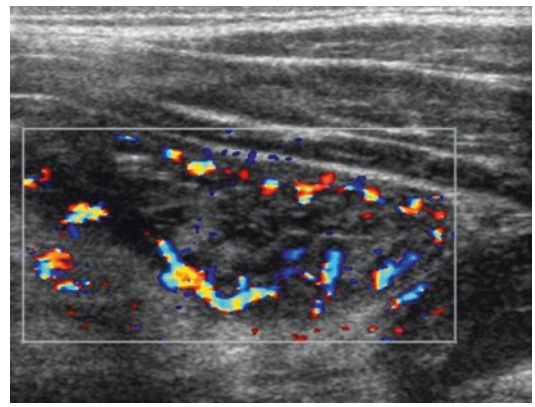

Fig. 12.6 Twelve-year-old boy followed for CD. US Doppler demonstrates thickening and hyperemia of a jejunal loop associated with hyperechoic fat thickening (sclerolipomatosis)

12.3.2 Magnetic Resonance Enterography (MRE)

Thanks to its high contrast resolution, multiplanar capability, absence of radiation exposure and ability to evaluate both the bowel and extra-bowel diseases with high accuracy, MRI is increasingly used to evaluate IBD. Furthermore, the images are in general more easily understood than US by referring clinicians.

12.3.2.1 Technique

A consensus statement on an optimized MRE protocol has been recently published by the ESGAR and the ESPR Societies [9], and is summarized below.

Preparation:
Depending on their age, children should avoid solid oral intake from 2 to 6 h prior to the examination. Fluid restriction is not recommended, although carbonated drinks are best avoided.

Many hyperosmolar contrast agents are acceptable in order to achieve bowel distension including polyethylene glycol, methylcellulose, sorbitol, mannitol, lactose, psyllium fiber, 0.1% low-density barium sulfate suspension, with none proven superior to the others. The ingestion should commence 45–60 min prior to MRE. The recommended volume in children is 20 mL/kg, up to a maximum up to 25 mL/kg. A full explanation of the drinking requirements to both the child and parents is important prior to MRE, and the use of a flavoring to the oral contrast agent will facilitate the child's compliance.

The use of spasmolytic agents is considered optional in children. Whilst image quality may be improved by reducing peristaltic artifact and improving distention, to date there is no strong evidence this translates into improved diagnostic accuracy [30, 31]. Furthermore, use of spasmolytics may prolong the examination time and such agents attract side effects such as nausea and vomiting [30]. If a spasmolytic is employed, the recommended first-line spasmolytic agent is i.v. hyoscine butylbromide (0.5 mg/kg i.v.). The recommended second-line agent is i.v. glucagon 0.5 mg (<24.9 kg) and 1 mg (>24.9 kg), given as a slow infusion with i.v. saline at an infusion rate at 1 mL/s).

A rectal contrast enema is not required.

MRE can be performed at either at 1.5 or 3 T, although the use of higher magnetic field strength can increase chemical shift and susceptibility artifacts.

Scanning in the prone position has been demonstrated to improve small bowel distension, compared to supine although there is no evidence that this translate into improved lesion detection [31, 32]. Large multi-elements coils are needed to cover from the perineum up to the left colonic flexure, in high resolution.

Sequences:
Both steady state free precession gradient echo and 2D—T2-weighted images should be performed in the axial and coronal planes. Fat saturation in one of these planes is recommended. A maximal slice thickness of 5 mm is also recommended.

Currently the use of pre- and post-gadolinium contrast 3D T1-Fat saturation weighted sequences is recommended with a slice thickness does not exceed 3 mm. The post contrast sequence should be acquired at the portal phase of injection.

Additional sequences are also widely used but are currently considered optional whilst supporting evidence accumulates [9]:

- Diffusion-weighted imaging. Recommended values range from 0 or 50 up to 600–900. The slice thickness should be 5 mm. Motion artifacts are problematic due to the length of acquisition but can be reduced with appropriate gating, fast imaging techniques (i.e., echo-planar imaging or parallel imaging), and the use of intravenous antiperistaltic agents before image acquisition. The axial plane may be less prone to artifact than the coronal plane.
- Dynamic cine steady-state motility images [33, 34] are useful, particularly in suspected luminal stenosis. A better appreciation of the upstream distension and real time opening of

the lumen of the abnormal bowel loop are possible using cine imaging.
- Magnetization transfer sequences may have utility in quantifying fibrosis, but currently remain a research tool.

The total scan duration should equal to or be less than 45 min.

Given the success of limited sequences rapid MR protocols for suspected appendicitis [35], a *fast MR IBD* protocol has been proposed as an alternative to emergency US for investigating the acute pediatric abdomen [36]. This fast MR protocol is limited to a morphologic T2 sequence in two planes associated with a DWI sequence to allow identification of IBD and its complications, including diagnosis of bowel stenosis, abscess, and fistula. In the absence of bowel obstruction (which provides intrinsic bowel distension), one of the limiting factors for the use of MRI in the acute setting could be the need for an oral contrast agent in a potential surgical patient. However, it has been established in the adult literature that neither oral or rectal preparation is mandatory in order to exclude UC [37] or CD [38]. Another potential limiting factor for acute MRI is the time taken for the examination. However, rapid MRI protocols can be very short (less than 10 min), do not require spasmolytics or gadolinium chelates and can be performed with easy patient positioning such as dorsal decubitus [32].

The utility of enteric MRI performed without spasmolytics or gadolinium contrast is debated [9, 36, 39–47] but skipping medication and contrast injection reduces examinations time and increases test acceptability in children. Furthermore, there is an increasing evidence base supporting the use of DWI as an alternative to gadolinium enhanced imaging. Shenoy et al. [39] have recently reported in a cohort of 27 pediatric patients that although DWI in isolation does not perform as well as standard MRE for detection of active Crohn disease, a combination of DWI and MRE increases imaging accuracy for disease activity compared with either technique alone. In 44 young adults, Seo et al. [40] found that DWI MRE was at least equal to contrast-enhanced MRE for the evaluation of inflammation in CD, and in a large study of 130 adults and children with CD, DWI was also found to be sufficiently accurate to replace gadolinium administration [14]. Some authors have reported that DWI may indeed be even superior to contrast enhanced imaging. Sirin et al. [41] reported that in a cohort of 37 children, DWI revealed lesions not detected with MRE performed with gadolinium injection. Similarly, both Dubron et al. [42] and Neubauer et al. [36] reported superior performance of DWI in comparison to gadolinium enhanced imaging in cohorts of 48 children, and 33 children and young adults, respectively. Avoiding IV injection and spasmolytics, together with a reduction of repeated breath holds acquisitions are strong motivations for the further development and validation of rapid and "noninvasive" MRI protocols.

12.3.2.2 Disease Phenotype

MRE is a powerful tool in characterizing the underlying phenotype of IBD. Classically, multifocal bowel affecting the colon and the terminal ileum are typical of CD [48] whereas contiguous abnormal bowel wall from the rectum to the cecum is typical of UC. However, as noted above, atypical presentations of IBD exist in pediatric practice and so caution is required when making a final diagnosis.

12.3.2.3 Positive Findings

The ability to evaluate the bowel wall is significantly enhanced by luminal distension. Collapsed bowel can both hide disease and mimic pathology, generating false positive diagnosis. Wall thickening with luminal restriction is typical of CD, although in the absence of significant bowel wall thickening, abnormal DWI signal, for example, should raise the possibility of early mucosal disease (Fig. 12.7).

In parallel with US, abnormal wall thickness is usually defined as greater than 3 mm. Bowel wall signal changes is usually assessed by comparing to a nearby normal bowel loop, or fixed

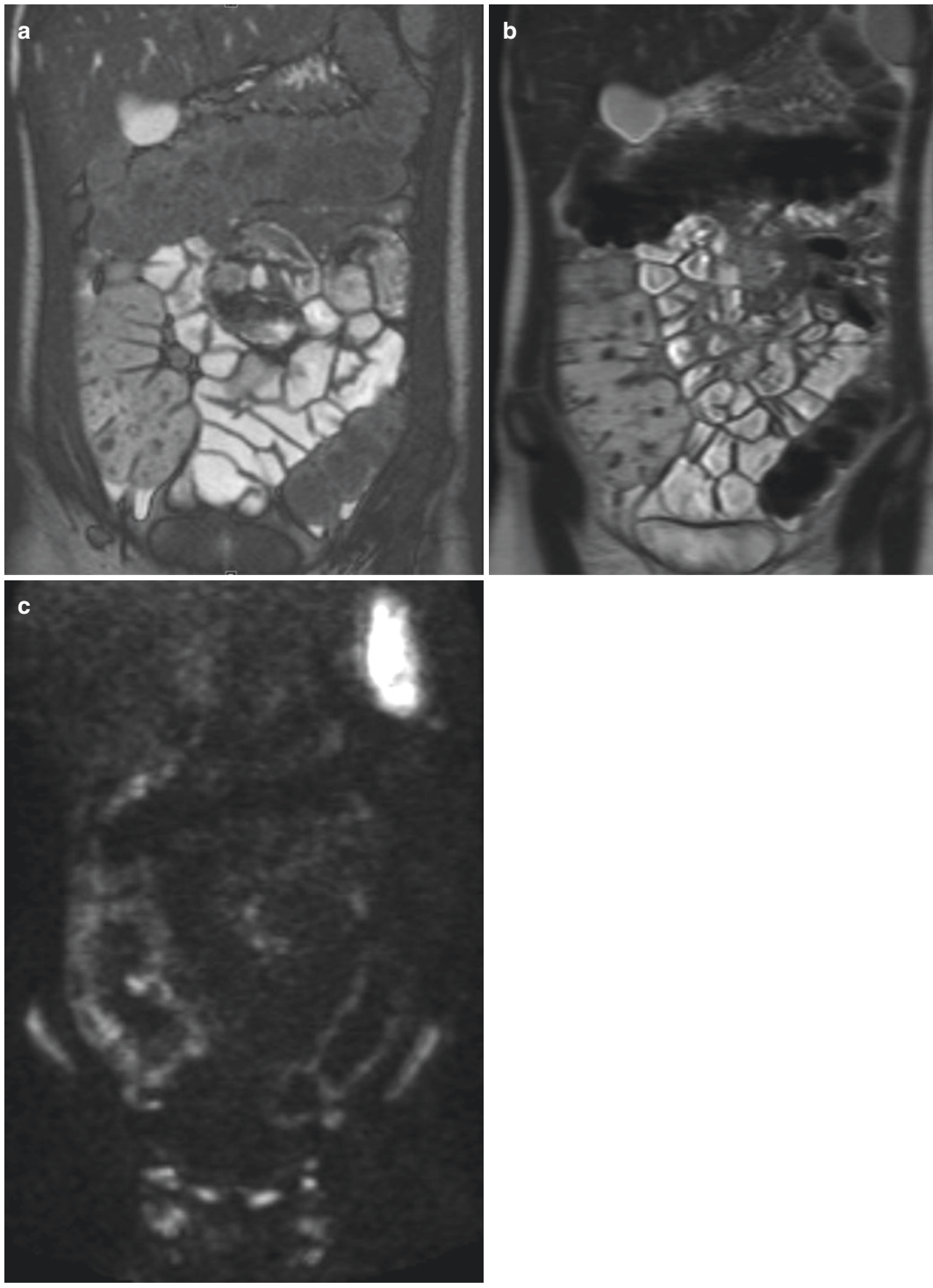

Fig. 12.7 Eleven-year-old girl who presents a light pancolitis on endoscopy (UC). (**a**) Coronal balanced turbo field echo (bTFE) sequence reveals a discrete thickening of the left colon with no evidence of thickening of the cecum. (**b**) Coronal T2-weighted turbo spin-echo (bTSE) sequence confirms the findings in (**a**). (**c**) DWI sequence (b1300) reveals abnormal bowel hypersignal. Early mucosal damage appears better depicted on diffusion

structure such as the psoas muscle. Active IBD results in restricted diffusion and increased mural T2 signal. This increased T2 signal is secondary to mural edema and inflammatory cell infiltration but can also be seen secondary to fat deposition seen in chronic strictures. Various contrast enhancement patterns may be seen after gadolinium injection including mucosal, layered mucosal and serosal, homogenous or predominantly serosal (Fig. 12.8). Correlation between imaging and surgical specimens histologically explored suggests increased enhancement the wall is positively correlated with disease chronicity, and the increased microvessels density commonly found in CD influences the rate of enhancement [49].

In addition, MR imaging is able to demonstrate additional findings in IBD including ulceration, pseudopolyps, and mural abscesses (typically bright on T2 weighted imaging and hypointense on T1 with ring enhancement following IV gadolinium administration).

Bowel affected by IBD has a variety of appearances depending on the disease chronicity and current level of activity. It may look fixed, dilated, exhibit pseudo-sacculations or become strictured.

The use of several sequences over the time course of the examination, and motility sequences are all useful in differentiating bowel wall collapsed with pseudo-thickening from true pathological bowel wall thickening. In this situation, the absence of injection of antiperistaltic agent is interesting.

MRI also provides a detailed evaluation of extramural findings including: fibrofatty proliferation, engorged mesenteric vessels supplying an inflamed bowel (the comb sign), fistula, abscess, and inflammatory lymphadenopathy.

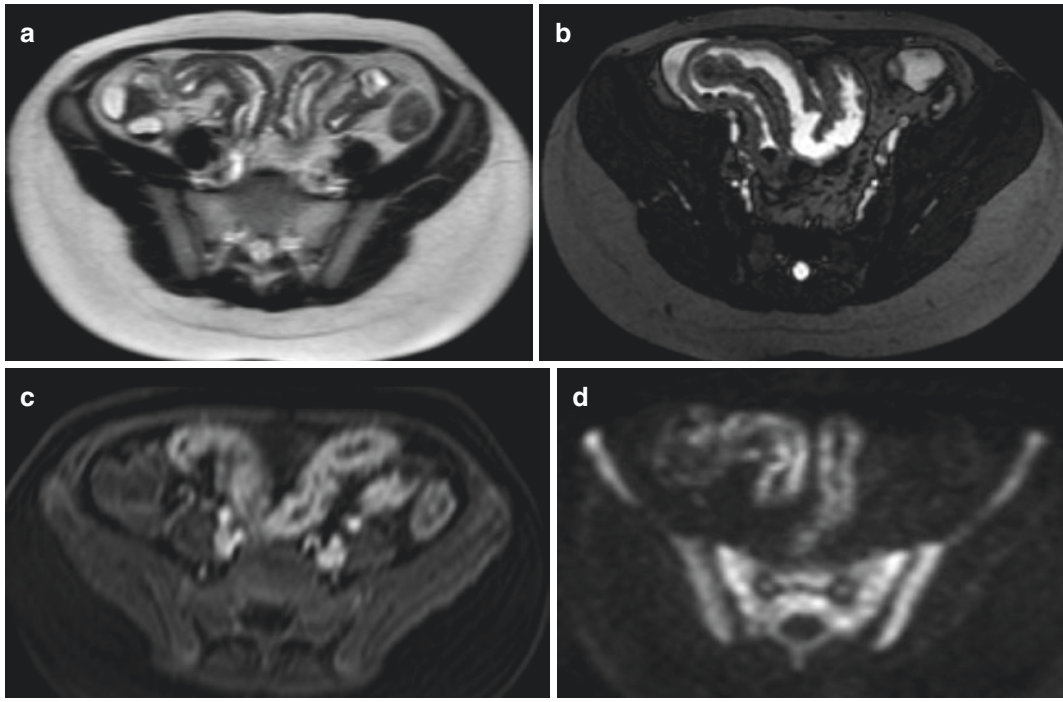

Fig. 12.8 Fourteen-year-old girl treated for ileal CD. Abnormal MR findings on different sequences. (**a**) Axial T2-weighted single-shot turbo spin-echo (SshSE) sequence demonstrating thickening of an ileal loop. (**b**) Axial balanced Turbo Field Echo (bTFE) sequence confirms the findings in (**a**). (**c**) Axial T1-weighted fat saturation after gadolinium injection sequence reveals marked enhancement of the thickened loop. (**d**) Axial DWI sequence (b1300) demonstrates an abnormal bowel hypersignal

12.3.2.4 Complications

Abscess, sinus tract, and fistula are typically found in CD and are infrequent in UC.

- *Stenosis*: Diagnosis is based on bowel thickening with associated upstream distension greater than 3 cm which is consistent across all sequences, particularly on the cine motility (Cine-MR) (Fig. 12.9).
- *Fistula and Sinus tracts*: These present as high T2 signal linear tracts usually with restricted diffusion and increased enhancement following IV gadolinium. The perineum can usually be included in the field of exploration, particularly in children, thereby allowing evaluation of perianal fistulas. In this regard, MRI holds a significant advantage over US (Fig. 12.10).
- *Abscess*: An abscess presents as a well-defined encapsulated lesion, frequently with heterogeneous hyperintense T2 signal, central restricted diffusion and low T1 signal with avid rim enhancement following gadolinium.

12.3.2.5 Disease Activity

MRE has higher accuracy for evaluating small bowel inflammation than colonic [43], particularly if the colon is not prepared and a water enema administered. One of the primary goals of imaging in IBD is to differentiate active inflammation from fibrotic disease. This is of paramount importance and has treatment implications: active disease may respond to medical treatment while symptomatic fibrosis typically requires surgical resection. The differentiation is, however, complicated by the fact that inflammation and fibrosis frequently co-exist in the same bowel segment [24, 50, 51]. A number of MRI activity scores have been developed and validated against a range of reference standards including colonoscopy and histopathology. For example, Rimola et al. [52] have described the Magnetic Resonance Index of Activity (MaRIA). Using inflammation scores from seven bowel segments from the rectum to the terminal ileum, the score quantifies disease activity by applying an equation to each segment as follows: 1.5 × maximum bowel wall thickness +0.02 × bowel wall relative contrast enhancement + 5 × bowel wall edema on T2-weighted imaging +10 × presence of ulceration. The overall summed score is highly correlated with the endoscopic Crohn Disease Endoscopic Index of Severity in adults. Steward et al. [53] developed an alternate score against a histopathological reference standard based on visual scoring of bowel wall thickness, T2 signal, contrast enhancement and inflammatory changes in the adjacent mesentery which has similar accuracy to the MaRIA score. The grading of mural T2 signal is common to most MRI inflammation grading scores, although Barkmeier et al. [51] failed to show an association of T2 signal with histological fibrosis or inflammation while Tielbeek reported that a higher T2 mural/CSF ratio was significantly associated with more histological inflammation as well as mild fibrostenosis [54]. In clinical practice, interpretation of MR derived disease activity is performed in conjunction with the patient's clinical data in order to predict patient outcome and optimize the therapeutic decision. A few MRI findings seem predictive of the need for surgery; perianal disease at baseline, fibrotic stenosis, and intra-abdominal fistulae at MRE [55].

More recently, Hordonneau et al. [56] have proposed a new scoring system, obviating the need for gadolinium administration by replacing evaluation of contrast enhancement with grading of diffusion weighted imaging: 1.321 × ADC (mm^2/s) + 1.646 × wall thickening (mm) + 8.306 × ulcers + 5.613 × edema + 5.039.

The utility of ADC values to grade disease activity, however, remains controversial and variable thresholds from 1.6 to 2.4×10^{-3} mm^2/s have been proposed to separate active from non-active disease [44]. Some data also suggests low ADC is found in fibrosis, confirmed using histology [27] (Fig. 12.11).

Due to the relative complexity of the MRI disease activity formulae, they are not usually routinely applied in clinical practice and are mainly used as research tools. Furthermore, use of ADC is not currently recommended; measurements are compromised by the small size of the bowel wall (risking inadvertent incorporation of luminal contents in the region of interest), low reproducibility of measurements between MRI-Units

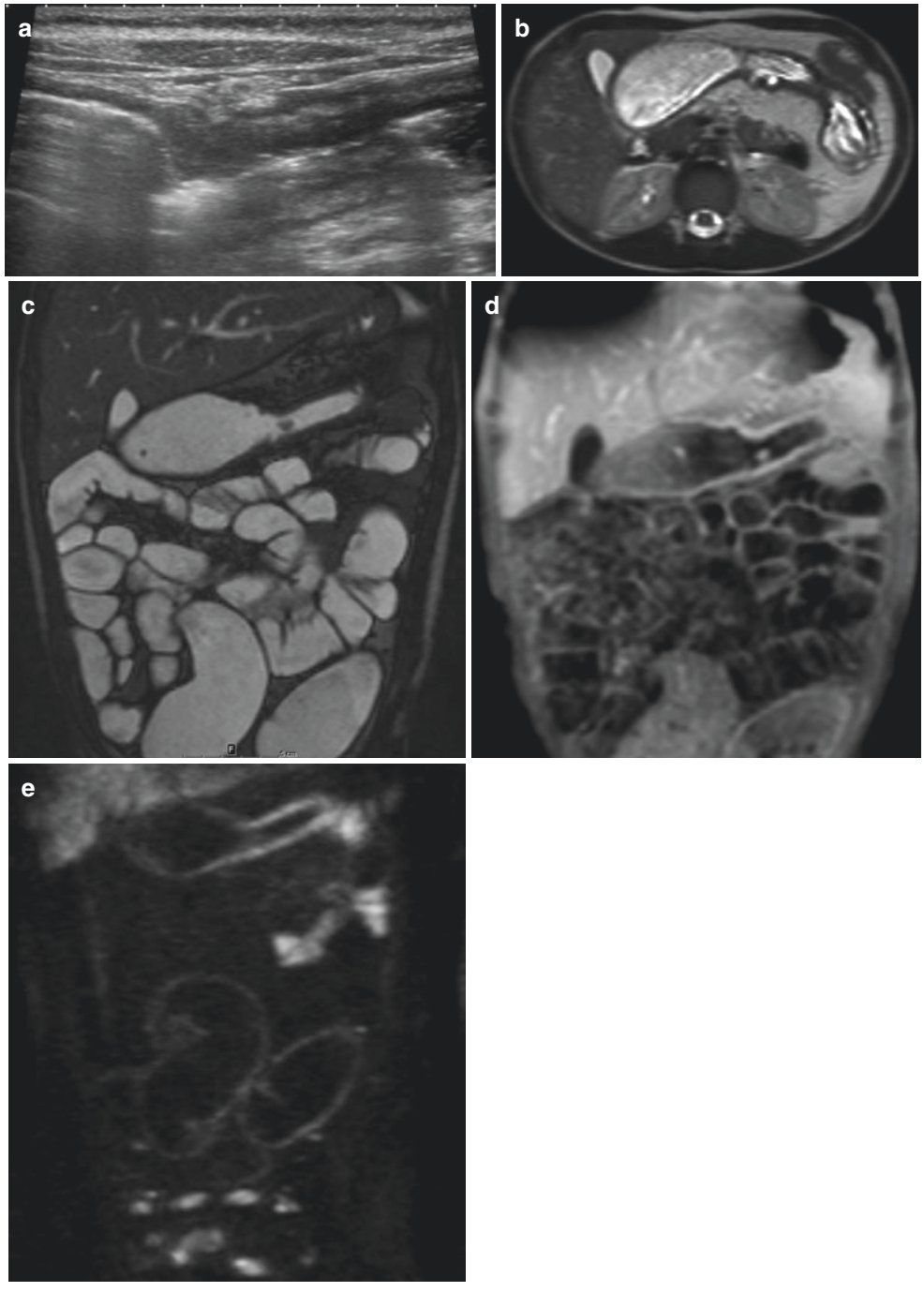

Fig. 12.9 Thirteen-year-old boy with a stenosis of the transverse colon during the evolution of a CD. (**a**) US scan shows a thickened transverse colon with a persistently compressed lumen. The right part of the transverse colon is largely distended by air and presents a normal bowel wall. (**b**) Axial T2-weighted single-shot turbo spin-echo (SshSE) sequence demonstrates a thickening of the left part of the transverse colon with two posterior ulcerations. The right part of the transverse colon is largely distended and presents a normal wall. (**c**) Coronal balanced Turbo Field Echo (bTFE) sequence confirms the findings in (**b**). (**d**) Coronal T1-weighted fat saturation sequence after gadolinium injection demonstrates enhancement of this thickened and stenotic loop as well as a discrete enhancement of the sigmoid colon. (**e**) Coronal DWI sequence (b1300) demonstrates an abnormal hypersignal in the transverse colon as well as in the wall of the sigmoid colon involved by CD

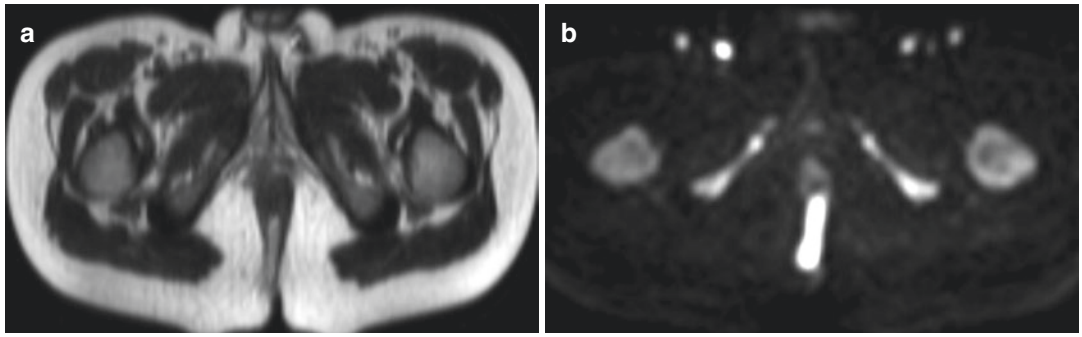

Fig. 12.10 Perineal fistula depicted during MRE in a 12-year-old girl with CD. (**a**) Axial T2-weighted single-shot turbo spin-echo (SshSE) sequence demonstrates a linear moderate hypersignal between the posterior wall of the rectum up to the adjacent skin. (**b**) Axial DWI sequence (b1300) demonstrates easily the intense hypersignal of the fistulous tract

and MRI- vendors, and non-standardization of b-values parameters [44].

12.3.3 Computed Tomography

In general, due to radiation exposure, the use of CT should be avoided in children when US is feasible (for example, in the non-obese patient) or when MR imaging is available. CT has a specific role in the pediatric patient with an acute abdomen: as diagnostic tool whenever neither US nor MR imaging is available, or as a guide to abscess drainage in collections not easily accessed using US guidance [9]. When used in this context, CT should be performed without distending the bowel with oral contrast, and a single phase after contrast (usually in the portal phase) covering the abdomen and pelvis should be acquired. Acquisition parameters should be adapted to the child's body weight as proposed by Donnelly et al. [57]. For example, in a child weighing between 27 to 36 kg, a tube current of 100 mA is usually sufficient while for a child weighing between 45.1 to 70 kg, the mA can be reasonably limited between 140 and 150 mA. Specific recommendations have been published in the pediatric literature and should be followed [58].

12.3.3.1 Positive Diagnosis [59]

In general, these mimic the ones described previously for US and MR Imaging.

In summary,

- Bowel wall thickening and/or increased contrast enhancement wall are the typical findings in IBD.
- Ulcerations are not usually visible on CT unless they are transmural and will appear as focal mucosal defects containing air or liquid.
- Sclerolipomatosis is well seen [29] in children as usually the volume of mesenteric fat is normally low. The density of diseased mesenteric fat is usually elevated (20–60 UH) due to the presence of associated edema and inflammatory cells.
- Engorged vasa recta within the mesenteric fat, perpendicular to the bowel surface (comb sign) can be seen.

12.3.3.2 Complications

CT traditionally has been considered as the reference for the detection of IBD related complications. However as detailed above, both US and MR imaging have similar diagnostic accuracy and remain the first-line test in pediatric practice when available.

- Abscess manifest as low attenuation lesions, which may be homogenous or heterogeneous, surrounded by a well-defined enhancing capsule.
- Stenosis present as a focally thickened bowel wall with upstream bowel dilatation, sometimes with semi-solid intra-luminal content (small bowel feces sign).

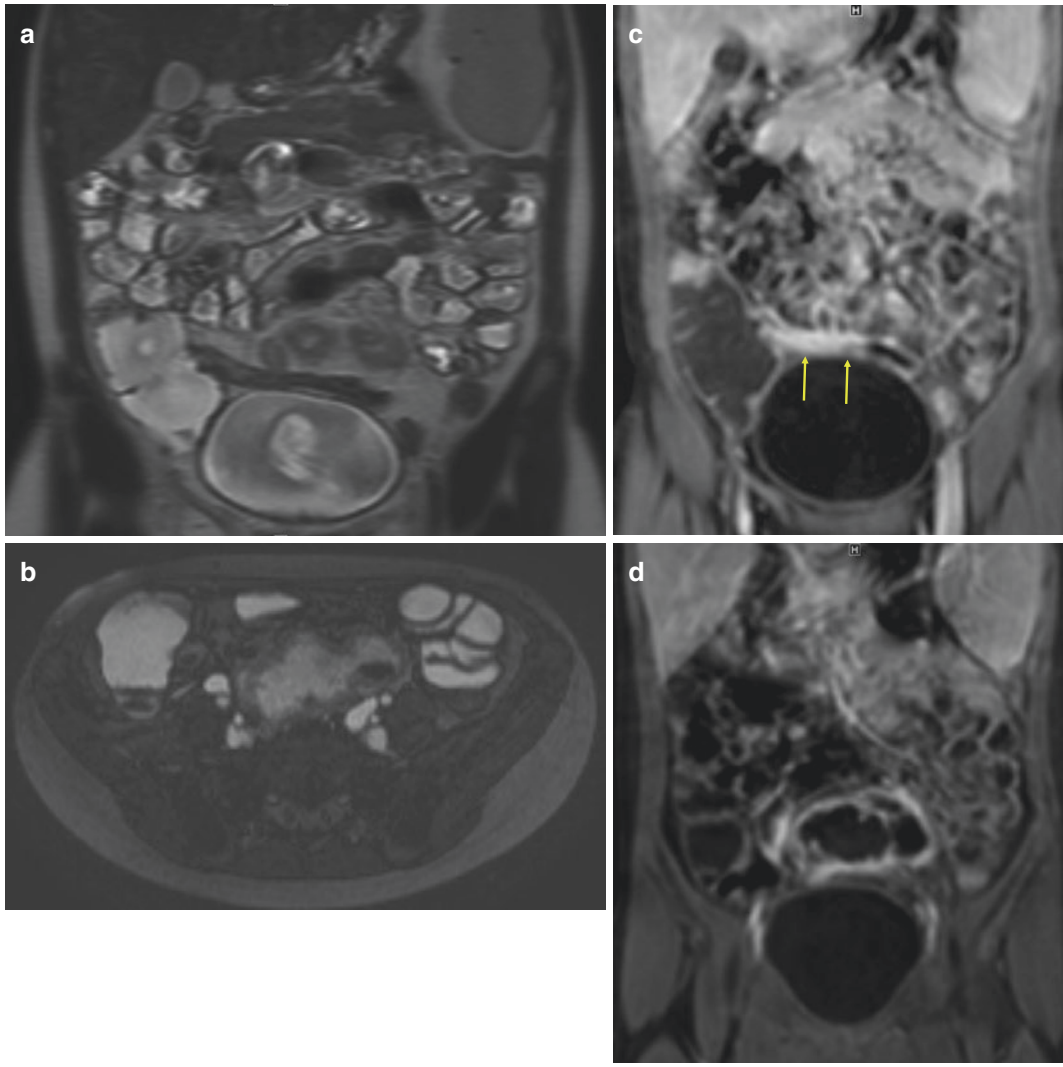

Fig. 12.11 Eleven-year-old boy with active ileal CD. A large abscess has developed adjacent to a strictured ileal loop. (**a**) Coronal T2-weighted single-shot turbo spin-echo (SshSE) sequence demonstrating a collapsed and rigid ileal loop with discrete thickening of its wall above the bladder. (**b**) Axial balanced Turbo Field Echo (bTFE) sequence shows a large abscess collection located immediately above and behind the abnormal loop. (**c**) Coronal T1-weighted fat saturation after gadolinium injection sequence reveals enhancement of this thickened and stenotic loop (*yellow arrows*). (**d**) Coronal T1-weighted fat saturation sequence after gadolinium injection reveals enhancement of the wall of the adjacent abscess. (**e**) Coronal DWI sequence (b1300) shows no abnormal hypersignal of the ileal loop (*yellow arrows*). This appearance would be in favor of a fibrostenotic segment. (**f**) Coronal DWI sequence (b1300) shows an intense hypersignal of the abscess

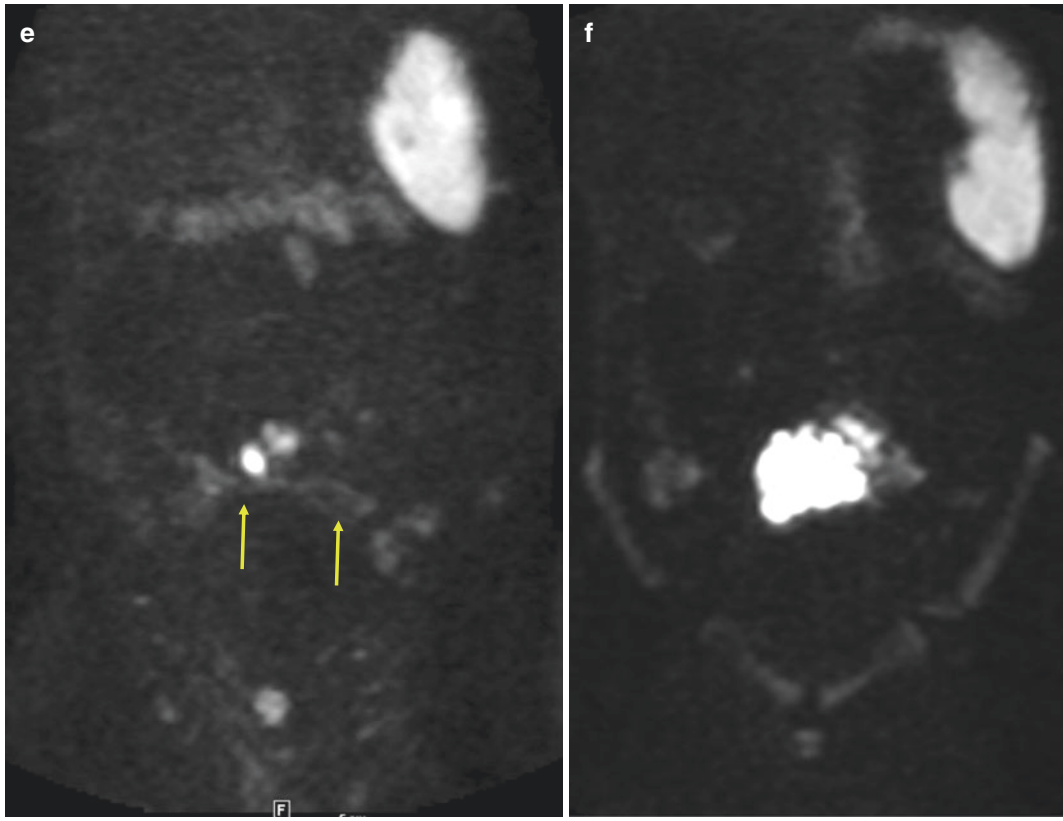

FIg. 12.11 (continued)

- Fistulae are seen as linear hypodense tracts between two bowel loops or between a bowel loop and another organ such as the skin and bladder.

12.4 Differential Diagnoses

In patients presenting acutely with a possible first diagnosis of IBD, there are several differential diagnoses that can mimic the imaging findings. Even in those with established IBD, it must be recognized that not all acute presentations are secondary to IBD, and alternative diagnosis may coexist. Two particular differential diagnoses that must be considered in all acute cases of IBD are:

- *Enteric infections*: including allergic colitis, eosinophilic gastroenteritis, and infantile primary immunodeficiency.
- *Appendicitis*: this diagnosis must be considered when thickening and hyperemia of the wall is limited to the appendix and the distal ileum is normal.

Conclusion

US is the modality of choice for initial exploration of acute presentations of pediatric IBD, either as potential first diagnosis or in those patients with established disease. Still, as noted above, the use of MRI is increasing, particularly using "rapid" protocols without IV contrast injection but with diffusion sequences. In appropriately trained hands, both US and MR-enterography (MRE) have high diagnostic accuracy to:

- Confirm the diagnosis,
- Phenotype the disease and in particular, describe the extent and define underlying activity and detect extraintestinal manifestations,
- Depict complications,
- Evaluate response to therapy

- Given the radiation exposure, the use of CT should be limited to acute diagnoses only when US and MR are not available, and to guide interventional procedures.

References

1. Paolantonio P, Ferrari R, Vecchietti F, et al. Current status of MR imaging in the evaluation of IBD in a pediatric population of patients. Eur J Radiol. 2009; 69:418–24.
2. Lazarev M, Huang C, Bitton A, et al. Relationship between proximal Crohn's disease location and disease behavior and surgery: a cross-sectional study of the IBD Genetics Consortium. Am J Gastroenterol. 2013; 108:106–12.
3. Auvin S, Molinie F, Gower-Rousseau C, et al. Incidence, clinical presentation and location at diagnosis of pediatric inflammatory bowel disease: a prospective population-based study in northern France (1988–1999). J Pediatr Gastroenterol Nutr. 2005;41: 49–55.
4. Levine A, Koletzko S, Turner D, et al. ESPGHAN revised Porto criteria for the diagnosis of inflammatory bowel disease in children and adolescents. J Pediatr Gastroenterol Nutr. 2014;58(6):795–806.
5. Kim SC, Ferry GD. Inflammatory bowel diseases in pediatric and adolescent patients: clinical, therapeutic, and psychosocial considerations. Gastroenterology. 2004;126:1550–60.
6. Aloi M, Lionetti P, Barabino A, SIGENP IBD Group, et al. Phenotype and disease course of early-onset pediatric inflammatory bowel disease. Inflamm Bowel Dis. 2014;20(4):597–605.
7. Shim JO, Seo JK. Very early-onset inflammatory bowel disease (IBD) in infancy is a different disease entity from adult-onset IBD; one form of interleukin-10 receptor mutations. J Hum Genet. 2014;59(6): 337–41.
8. Shin AR, Lee CK, Kim HJ, et al. Septic pylephlebitis as a rare complication of Crohn's disease. Korean J Gastroenterol. 2013;61(4):219–24.
9. Taylor SA, Avni F, Cronin CG, et al. The first joint ESGAR/ESPR consensus statement on the technical performance of cross-sectional small bowel and colonic imaging. Eur Radiol. 2016;27:2570–82.
10. Kljucevsek D, Vidmar D, Urlep D, et al. Dynamic contrast-enhanced ultrasound of the bowel wall with quantitative assessment of Crohn's disease activity in childhood. Radiol Oncol. 2016;50(4): 347–54.
11. Fufezan O, Asavoaie C, Tamas A, et al. Bowel elastography—a pilot study for developing an elastographic scoring system to evaluate disease activity in pediatric Crohn's disease. Med Ultrason. 2015;17(4): 422–30.
12. Serafin Z, Białecki M, Białecka A, et al. Contrast-enhanced ultrasound for detection of Crohn's disease activity: systematic review and meta-analysis. J Crohns Colitis. 2016;10(3):354–62.
13. Hiorns MP. Imaging of inflammatory bowel disease. How? Pediatr Radiol. 2008;38:S512–7.
14. Baud C, Saguintaah M, V,eyrac C, Couture A, Ferran JL, Barnéon G, et al. Sonographic diagnosis of colitis in children. Eur Radiol. 2004;14:2105–19.
15. Siegel M, Friedland J, Hildebolt C. Bowel wall thickening in children: differentiation with US. Radiology. 1997;203:631–5.
16. Calabrese E, Maaser C, Zorzi F, et al. Bowel ultrasonography in the management of Crohn's disease. a review with recommendations of an International Panel of Experts. Inflamm Bowel Dis. 2016;22(5): 1168–83.
17. Alison M, Kheniche A, Azoulay R, et al. Ultrasonography of Crohn disease in children. Pediatr Radiol. 2007;37:1071–82.
18. Bremner AR, Griffiths M, Argent J, et al. Sonographic evaluation of inflammatory bowel disease: a prospective, blinded, comparative study. Pediatr Radiol. 2006;36:947–53.
19. Magnano G, Granata C, Barabino A, et al. Polyethylene glycol and contrast-enhanced MRI of Crohn's disease in children: preliminary experience. Pediatr Radiol. 2003;33:385–91.
20. Ahmad TM, Greer ML, Walters TD, et al. Bowel sonography and MR enterography in children. Am J Roentgenol. 2016;206(1):173–81.
21. Dillman JR, Smith EA, Sanchez R, et al. Prospective cohort study of ultrasound-ultrasound and ultrasound-MR enterography agreement in the evaluation of pediatric small bowel Crohn disease. Pediatr Radiol. 2016;46(4):490–7.
22. Ripolles T, Martinez MJ, Morote V, et al. Appendiceal involvement in Crohn's disease: gray-scale sonography and color Doppler flow features. Am J Roentgenol. 2006;186:1071–8.
23. Maconi G, Radice E, Greco S. Bianchi Porro. Bowel ultrasound in Crohn's disease. Best Pract Res Clin Gastroenterol. 2006;20:93–112.
24. Rosenbaum DG, Conrad MA, Biko DM, et al. Ultrasound and MRI predictors of surgical bowel resection in pediatric Crohn disease. Pediatr Radiol. 2016;47:55–64.
25. Martinez MJ, Ripolles T, Paredes JM, Blanc E, Marti-Bonmati L. Assessment of the extension and the inflammatory activity in Crohn's disease: comparison of ultrasound and MRI. Abdom Imaging. 2009;34:141–8.
26. Spalinger J, Patriquin H, Miron MC, et al. Doppler US in patients with Crohn disease: vessel density in the diseased bowel reflects disease activity. Radiology. 2000;217:787–91.
27. Horsthuis K, Stokkers P, Stoker J. Detection of inflammatory bowel disease: diagnostic performance of cross-sectional imaging modalities. Abdom Imaging. 2008;33:407–16.
28. Pallotta N, Civitelli F, Di Nardo G, et al. Small intestine contrast ultrasonography in pediatric Crohn's disease. J Pediatr. 2013;163:778–84.

29. Civitelli F, Di Nardo G, Oliva S, et al. Ultrasonography of the colon in pediatric ulcerative colitis: a prospective, blind, comparative study with colonoscopy. J Pediatr. 2014;165(1):78–84.
30. Dillman JR, Smith EA, Khalatbari S, Strouse PJ. I.v. glucagon use in pediatric MR enterography: effect on image quality, length of examination, and patient tolerance. Am J Roentgenol. 2013;201(1): 185–9.
31. Maccioni F, Al Ansari N, Mazzamurro F, et al. Detection of Crohn disease lesions of the small and large bowel in pediatric patients: diagnostic value of MR enterography versus reference examinations. Am J Roentgenol. 2014;203:W533–42.
32. Cronin CG, Lohan DG, Mhuircheartaigh JN. MRI smallbowel follow-through: prone versus supine patient positioning for best small-bowel distension and lesion detection. Am J Roengenol. 2008;191: 502–6.
33. Leyendecker J, Bloomfeld R, DiSantis D, et al. MR enterography in the management of patients with Crohn disease. Radiographics. 2009;29:1827–46.
34. Maccioni F, Patak MA, Signore A. New frontiers of MRI in Crohn's disease: motility imaging, diffusion-weighted imaging, perfusion MRI, MR spectroscopy, molecular imaging, and hybrid imaging (PET/MRI). Abdom Imaging. 2012;37:974–82.
35. Dillman JR, Gadepalli S, Sroufe NS, et al. Equivocal pediatric appendicitis: unenhanced MR imaging protocol for nonsedated children-A clinical effectiveness study. Radiology. 2016;279(1):216–25.
36. Neubauer H, Pabst T, Dick A, et al. Small-bowel MRI in children and young adults with Crohn disease: retrospective head-to-head comparison of contrast-enhanced and diffusion-weighted MRI. Pediatr Radiol. 2013;43:103–14.
37. Oussalah A, Laurent V, Bruot O, et al. Diffusion-weighted magnetic resonance without bowel preparation for detecting colonic inflammation in inflammatory bowel disease. Gut. 2010;59:1056–65.
38. Kiryu S, Dodanuki K, Takao H, et al. Free-breathing diffusion-weighted imaging for the assessment of inflammatory activity in Crohn's disease. J Magn Reson Imaging. 2009;29:880–6.
39. Shenoy-Bhangle AS, Nimkin K, Aranson T, et al. Value of diffusion-weighted imaging when added to magnetic resonance enterographic evaluation of Crohn disease in children. Pediatr Radiol. 2016;46(1):34–42.
40. Seo N, Park SH, Kim KJ, et al. MR enterography for the evaluation of small-bowel inflammation in Crohn disease by using diffusion-weighted imaging without intravenous contrast material: a prospective noninferiority study. Radiology. 2016;278(3):762–72.
41. Sirin S, Kathemann S, Schweiger B, et al. Magnetic resonance colonography including diffusion-weighted imaging in children and adolescents with inflammatory bowel disease: do we really need intravenous contrast? Investig Radiol. 2015;50(1):32–9.
42. Dubron C, Avni F, Boutry N, et al. Prospective evaluation of free-breathing diffusion-weighted imaging for the detection of inflammatory bowel disease with MR enterography in childhood population. Br J Radiol. 2016;89(1060):20150840.
43. Oto A, Kayhan A, Williams JT, et al. Active Crohn's disease in the small bowel: evaluation by diffusion weighted imaging and quantitative dynamic contrast enhanced MR imaging. J Magn Reson Imaging. 2011;33:615–24.
44. Dohan A, Taylor S, Hoeffel C, et al. Diffusion-weighted MRI in Crohn's disease: current status and recommendations. J Magn Reson Imaging. 2016;44(6):1381–96.
45. Grand DJ, Guglielmo FF, Al-Hawary MM. MR enterography in Crohn's disease: current consensus on optimal imaging technique and future advances from the SAR Crohn's disease-focused panel. Abdom Imaging. 2015;40:953–96.
46. Park SH, Huh J, Park SH, et al. Diffusion-weighted MR enterography for evaluating Crohn's disease: effect of anti-peristaltic agent on the diagnosis of bowel inflammation. Eur Radiol. 2016;27: 2554–62.
47. Grand DJ, Beland MD, Machan JT, et al. Detection of Crohn's disease: comparison of CT and MR enterography without anti-peristaltic agents performed on the same day. Eur J Radiol. 2012;81:1735–41.
48. Day AS, Ledder O, Leach ST, et al. Crohn's and colitis in children and adolescents. World J Gastroenterol. 2012;18:5862–9.
49. Taylor SA, Punwani S, Rodriguez-Justo M, et al. Mural Crohn disease: correlation of dynamic contrast-enhanced MR imaging findings with angiogenesis and inflammation at histologic examination–pilot study. Radiology. 2009;251(2):369–79.
50. Punwani S, Rodriguez-Justo M, Bainbridge A, et al. Mural inflammation in Crohn disease: location-matched histologic validation of MR imaging features. Radiology. 2009;252:712–20.
51. Barkmeier DT, Dillman JR, Al-Hawary M, et al. MR enterography-histology comparison in resected pediatric small bowel Crohn disease strictures: can imaging predict fibrosis? Pediatr Radiol. 2016;46(4): 498–507.
52. Rimola J, Ordás I, Rodriguez S, et al. Magnetic resonance imaging for evaluation of Crohn's disease: validation of parameters of severity and quantitative index of activity. Inflamm Bowel Dis. 2011;17(8):1759–68.
53. Steward MJ, Punwani S, Proctor I, et al. Non-perforating small bowel Crohn's disease assessed by MRI enterography: derivation and histopathological validation of an MR-based activity index. Eur J Radiol. 2012;81(9):2080–8.
54. Tielbeek JA, Ziech ML, Li Z, et al. Evaluation of conventional, dynamic contrast enhanced and diffusion weighted MRI for quantitative Crohn's disease assessment with histopathology of surgical specimens. Eur Radiol. 2014;24:619–29.

55. Jauregui-Amezaga A, Rimola J, Ordas I, et al. Value of endoscopy and MRI for predicting intestinal surgery in patients with Crohn's disease in the era of biologics. Gut. 2015;64:1397–402.
56. Hordonneau C, Buisson A, Scanzi J, et al. Diffusion-weighted magnetic resonance imaging in ileocolonic Crohn's disease: validation of quantitative index of activity. Am J Gastroenterol. 2014;109(1):89–98.
57. Donnelly LF, Emery KH, Brody AS, et al. Minimizing radiation dose for pediatric body applications of single-detector helical CT: strategies at a large children's hospital. Am J Roentgenol. 2001;176(2): 303–6.
58. Toma P, Granata C, Magnano G, et al. CT and MRI of pediatric Crohn disease. Pediatr Radiol. 2007;37:1083–92.
59. d'Almeida M, Jose J, Oneto J, et al. Bowel wall thickening in children: CT findings. Radiographics. 2008; 28:727–46.

Acute Intestinal Intussusception

13

Alexia Dabadie and Philippe Petit

Contents

A. Dabadie • P. Petit (✉)
Department of Pediatric Imaging,
Hôpital Timone Enfants,
264 rue St Pierre, 13385 Marseille, Cedex 05, France
e-mail: adabadie@ap-hm.fr; ppetit@ap-hm.fr

13.1 Introduction

Acute intestinal intussusception (AII) represents a classic abdominal emergency in all (pediatric) hospitals. The persistent telescoping of bowel loops potentially compromises the flow within the blood vessels with the ultimate risks of wall ischemia and perforation.

Its frequency, compared to appendicitis, remains low but it represents the first cause of small bowel obstruction and the condition is potentially life threatening. Worldwide the mean incidence of this disease has been estimated to less than 1/10,000 children and to 1/1000 emergency departments admissions [1, 2]. Age at presentation ranges from a few weeks to adulthood but 75% occur before the age of 1 year [1, 2]. The rate seems to variate over time especially among children aged 3–5 months in whom the overall number of cases has markedly decreased the last years [3]. The male–female ratio is around 2–1 but important variations exist between ethnicities [4]. Classical symptoms include acute episode of abdominal pain with free intervals, vomiting, bloody stools, and palpable abdominal mass. Together, these four signs are present in less than 50% of patients and unexpected symptoms may be present as well. These include episodes of pallor and/or sweating, seizures, diarrhea, abdominal colic and distension or gastroenteritis.

The vast majority of intussusceptions are ileocolic. Their origin is multifactorial and still debated. Some authors have underlined a positive

F.E. Avni, P. Petit (eds.), *Imaging Acute Abdomen in Children*,
https://doi.org/10.1007/978-3-319-63700-6_13

association between the occurrence of AII and the previous use (<1 week) of drugs including antibiotics [5]. The hypertrophied lymphoid tissue located in the mucosa and submucosa of the terminal ileum is considered the trigger factor for this kind of intussusception. Symptomatic small bowel intussusceptions represent less than 2% of intussusceptions and may occur at any age since birth but they are more frequent in children older than 2 years [6]. Longer duration of symptoms, weight loss, familial history, and recurrent intussusceptions must alert the radiologist to the possible non-idiopathic nature of the AII. After treatment, the recurrence rate is around 10% and occurs either within the first hours or at distance from the first episode.

In some countries, even recently, mortality rate remains very high, up to 12% [7] due to late presentation to the hospital and a high frequency of peritonitis.

13.2 Diagnostic Role of Imaging

US has proved to be the imaging modality of choice in case of suspicion of AII. The US exploration should cover the whole abdomen and pelvis, first with a low frequency convex probe (3–6 MHz), with a high frequency linear probe (7–12 MHz) thereafter. US must fulfill the following tasks:

13.2.1 Ensure a Fast and Efficient Positive Diagnosis

- Ultrasound (US) has proved to be highly valuable for this purpose with a sensitivity of 98–100% and a specificity of 88–100% [8]. A plain radiograph of the abdomen is not performed anymore as long as US is available.
- Intussusception appears on high frequency US as a multilayered mass, which includes the receiving bowel loop (intussuscipiens) and the incarcerated one (intussusceptum) with their respective vascular supply within the mesentery. When a transverse US scan is performed at the top of the intussuscipiens, the intussusception has a typical target appearance. Lower on the intussuscipiens, this target pattern will contain various amounts of hyperechoic tissue corresponding to incarcerated fatty mesentery (Fig. 13.1a). On a sagittal section the different bowel layers and the mesentery will appear as a stratified mass composed of several parallel layers showing different echostructures (Fig. 13.1b).

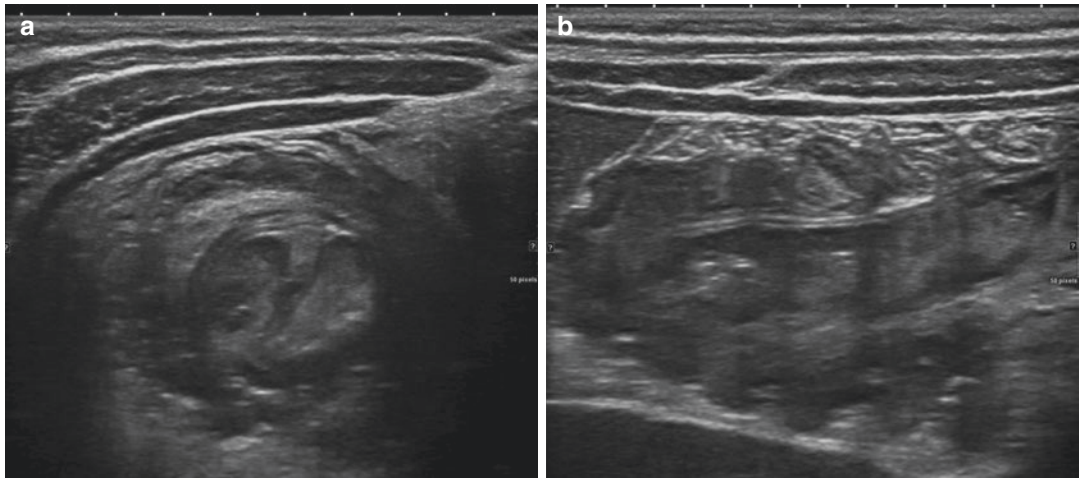

Fig. 13.1 Acute ileocolic intussusception in a 4-year-old-boy. (**a**) Transverse US section shows a target appearance (the crescent-in-doughnut sign). (**b**) Sagittal section demonstrated a multilayered structure giving the appearance of a sandwich

13.2.2 Rule Out Differential Diagnoses

- As previously mentioned, clinical signs can be quite confusing and AII may mimic different diseases including gastroenteritis, appendicitis, Meckel's diverticulitis, and any other causes of bowel obstruction. US is the examination of choice to differentiate accurately between these different entities. Noteworthy, in children with suspected but absent intussusception, the percentage of other intraabdominal diseases discovered by US has been reported ranging from 4% [9] to 16.7% [10].
- Intermittent intussusception: Transient intussusception is extremely frequent and is usually not responsible for the patient's clinical presentation. The small intestine and preferably the jejunum are mainly involved. It tends to occur in asymptomatic patients or in patients presenting GI viral infections. The loops involved are not thickened, their peristalsis is preserved and there are no signs of upstream bowel distension. The diameter of an ileoileal intussusception is inferior to 2.5 cm and its length is short, less than 3.5 cm [11] (Fig. 13.2). It disappears spontaneously or its position changes during the US examination. The prevalence of transient small bowel intussusception identified by CT with no clinical significance has been reported around 0.4% [12].
- False positive results include bowel volvulus secondary to malrotation and thickened bowel wall of any origin (inflammatory, infectious, tumoral, etc.).

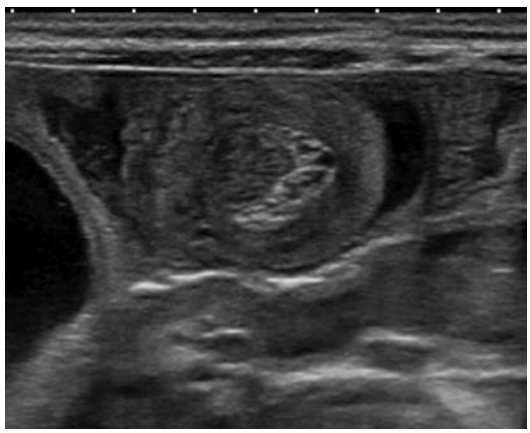

Fig. 13.2 Transient jejuno-jejunal intussusception incidentally discovered in a 1-year-old boy explored for UTI. The diameter of this intussusception on US is less than 2 cm. The thickness of the hyperechoic fat corresponding to the invaginated mesentery is similar to the one in Fig. 13.1. In these two cases, type of intussusception cannot be reliably differentiate on the inner fat core sign

13.2.3 Look For Evidence of Perforation

Bowel necrosis would lead to perforation and peritonitis but no descriptions of such abnormalities have been reported in pediatric practice either on US or on X-rays.

13.2.4 Identify the Type of Intussusception

For this purpose multiple US signs and measurements have been described.

- Diameter: It ranges from 0.8 to 4 cm. Below 2.5 cm, the likelihood of ileoileal intussusception (III) is high but ileocolic intussusceptions (ICI) diameter can be as small as 1.3 cm [13]. The mean diameter of an ileoileocolic (IICI) type is larger than that of an ICI but with a large overlap [14]. Therefore, the diameter alone cannot accurately differentiate between the different types of intussusceptions.
- Length: ICI is longer than an III; a length above 3.5 cm has been reported to be a strong independent predictor for the need of surgery [11].
- In theory, the number of bowel layers could help to differentiate between an III and an ICI from an IICI which by definition contains more bowel layers. Still, edematous infiltration of these layers induces the loss of their limits and subsequently they cannot be "counted" and distinguished one from another.
- Inner fat core (fat surrounding the vessel within the mesentery) has been reported to be

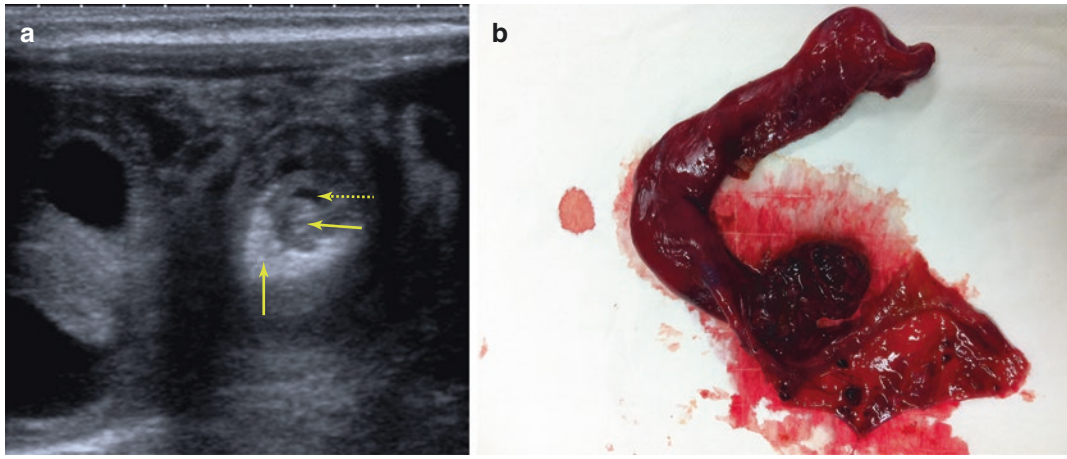

Fig. 13.3 Ileocolic intussusception in a 10-month-old-girl secondary to a Meckel's diverticulum: US appearances. (**a**) The tip of MD is slightly hyperechoic (*short yellow arrow*) with some anechoic fluid testifying associated bowel suffering (*dashed yellow arrow*). Hyperechoic mesenteric fat is present within the intussuscipiens (*long yellow arrow*). (**b**) Ischemic small bowel and associated ischemic MD were surgically removed

almost absent in III, thus its ratio with the thickness of the outer bowel wall (<1.0) is significantly different compared to ICI [13]. In our experience this sign does not appear highly specific (Figs. 13.1 and 13.2).

- Lymph nodes inside the lesion are much more frequent in ICI [13]. Peripheral enlarged lymph nodes are frequent but of no diagnostic value except when these enlarged nodes are rounded, frankly hypoechoic, and/or present with a disorganized vascularization, all features that must also raise the suspicion of lymphoma.
- Ascites is frequently present. Its volume is usually limited and of no help to differentiate the types of IIA.
- Abdominal location:
  - ICI are more likely to be located within the subhepatic area or the right lower quadrant.
  - Ileo-ileal spontaneous intussusceptions are preferably located in the paraumbilical area and in the left abdomen.
- Type of lead point [15]:
  - Primary Intussusception: It represents the most frequent form of AII which is either ileocolic or ileoileocolic. Most authors consider the so- called idiopathic or primary intussusception to be in fact related to hypertrophy of lymphoid tissue. Hypertrophied Peyer patches become entrapped and serve as lead point. Viral infections such as those caused by adenovirus, rotavirus, human herpes virus, CMV, and Epstein-Barr virus have all been reported to be associated with intussusceptions. However, the seasonal viral influence is not validated by large studies [16]. On the other hand, vaccination against rotavirus has been shown to be responsible for a slight increase in the incidence of intussusception with a more severe evolution [17]. For Hryhorczuk et al. [10] the overall sensitivity of US to detect intussusception was 97.9% and its specificity was 97.8%; the positive predictive value of the test was 86.6% and the negative predictive value was 99.7%. On daily practice, a junior resident on call with 6 months training in US should not miss this kind of intussusception.
  - Secondary Intussusceptions: They represent 1.5–12% of AII in children [18]. A majority involve the small bowel only. They can occur at any age but their incidence increases with age. Yet, they may occur in patients younger than 3 months [15]. Many but not all of them will require surgery. A long duration of symptoms, a known underlying disease, and recurrence are important clinical arguments to suspect a pathological lead point; however, the absence of these signs cannot exclude it [19].

- Meckel's diverticulum (MD): The inverted MD will induce an IICI. The presence of mesenteric fat at the tip or around the serosal surface of the intussusceptum is the clue for a US diagnosis. The location of the fat is different from the mesenteric fat which follows the associated invaginated small bowel (Fig. 13.3). This sign has been described as the double target sign [20]. Other findings include the presence within the intussuscipiens of a blind-ending segment of a thick-walled bowel; bowel which has lost its normal gut signature [21]; it may also appear as a thick-walled cystic mass [22].
- Duplication cyst: A duplication can be recognized when a cystic mass with a layered wall is present within the intussusception. In theory, the external hypoechoic layer, the muscularis mucosa, is in continuity with the equivalent one of the adjacent bowel loop; this finding being difficult to ascertain within the intussusceptum. The size of the cyst may help to differentiate it from a Meckel's diverticulum [22]. Spontaneous regressions have been documented [19].
- Intestinal tumors:
  - Polyps (familial polyposis, Peutz-Jeghers syndrome): on US, a polyp may have different patterns and is rarely recognized as such. A clue for diagnosis is the presence of central vessels (in the pedicle) which divides in a branching pattern within a focal mass visible within the intussusceptum [22] (Fig. 13.4).
  - Lymphoma may present as an intraluminal hypoechoic mass or a hypoechoic irregular thickened bowel wall. Chronicity of clinical symptoms

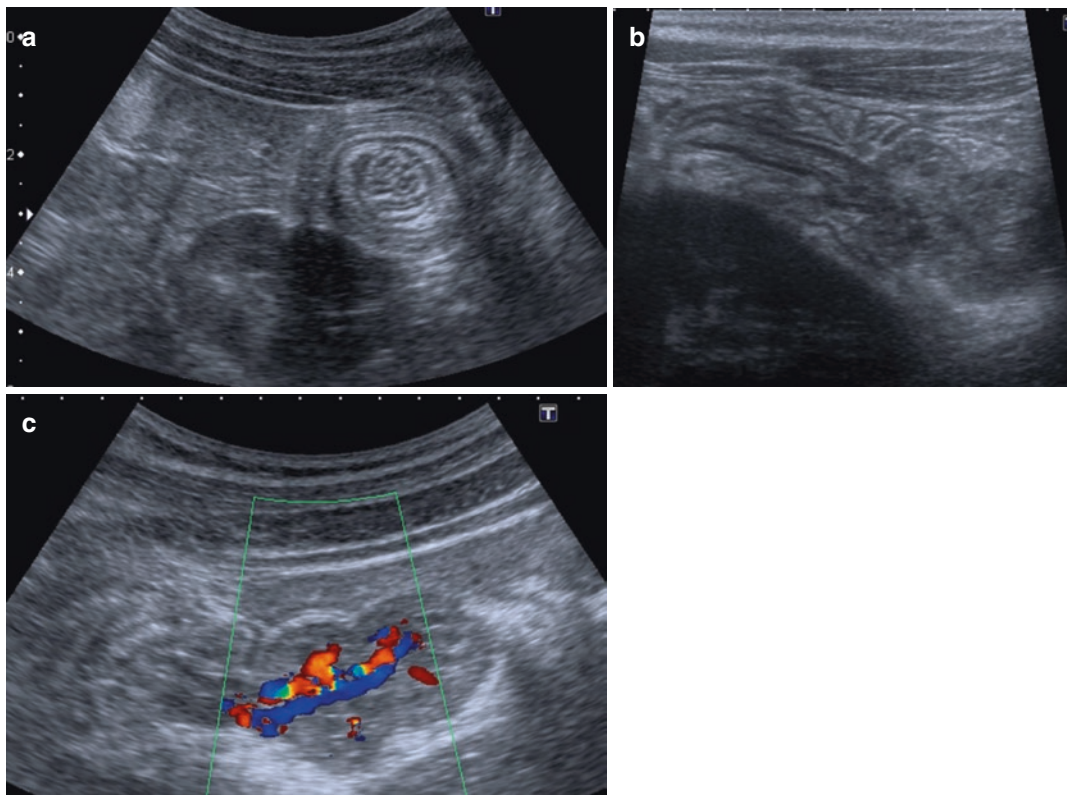

Fig. 13.4 Colo-colic intussusception secondary to a polyp in a 6-year-old boy: US appearance. (**a**) Typical target sign of an AII on a transverse scan. (**b**) Sagittal scan reveals a large pedunculated structure corresponding to a polyp. (**c**) Identification of the polyp is easier obtain when central vascularization is observed on color Doppler

and associated supplementary abnormal findings on US are of great help to propose this diagnosis [22].
  - Leiomyoma, lipoma, adenoma, Ewing's tumor are exceptionally involved and do not present typical US signature.
- Celiac disease: AII may develop in the course of such disease. It is limited to the small bowel and has a favorable prognosis with spontaneous healing. Dysmotility and mucosal inflammation are considered to be the lead points [23]:
- Postoperative: IIA was reported to account for 5–10% of postoperative bowel obstruction [15] and is supposed to be related to altered peristalsis. Most frequent abdominal surgeries involved are Ladd's procedures and retroperitoneal tumor resection. However, they may occur after non-abdominal surgery as well. AII commonly presents within the first 2 weeks after any surgery and involves exclusively the small bowel and on occasion multiple sites.
- Cystic fibrosis: Appendiceal mucocele, dysmotility, and thick inspissated feces may be responsible for intussusceptions.
- Henoch–Schönlein Purpura (See also Chap. 29): Intramural hemorrhage and edema within the bowel wall occur during this vasculitis and serve as lead points; the layered bowel wall structure is usually preserved [22]. Hyperemia on color Doppler is present within the wall of the intussusceptum. III is the type most frequently encountered still ICI and even colo-colic intussusceptions have been described [19]. Spontaneous resolution is the rule but exceptionally, perforation may occur [24]. Usually, AII is only one non-specific symptom of the disease which includes skin purpura, arthritis, renal involvement with the risk of renal failure, ureter and/or bladder thickening, scrotal involvement in boys and rarely cholecystitis, pancreatitis, muscular hemorrhagic infiltration, and neurological complications [25].
- Upper GI tubes: intussusception may develop secondary to the presence of a feeding tube or gastrostomy. Retrieval of the tube after disinflation of the inflated balloon is usually curative. In case of failure, surgery is required [15].
- On occasion, other lesions have been reported to be responsible for AII. The clinical context is sometimes helpful but the final diagnosis needs confirmation by means of biology or histology. This includes: ectopic pancreas, appendicitis, intestinal parasites, neutropenic colitis, Hirschsprung colitis, and foreign body.
- Waugh syndrome represents a rare association of ileocolic intussusception and malrotation. Less than 70 cases have been reported and reduction was successful only in a few cases [26].

13.2.5 Search For Signs Predicting Difficult Reduction

- Trapped peritoneal fluid between the incarcerated loop and the receiving one is observed in less than 15% of cases [27] and has been described as a highly predictive of bowel necrosis (Fig. 13.5) [28]. However, del-Pozo et al. have shown that 26% of such cases could still be reduced [27] and for Ntoulia et al. it has no impact on the reducibility [29].
- Absence or presence of flow on color Doppler in the intussusception is neither indicative of irreducibility nor for a risk of perforation. Kong et al. have shown that 31% of intussusceptions without detectable flow could be reduced by air enema in contrast to a 90% reduction rate when a flow was detectable [6]. On the other hand, color Doppler flow was present in all patients for whom reduction failed in Ntoulia's series [29].
- Thickening of the external bowel wall has a controversial role to predict reduction [30].
- Usually, intussusception limited to the small bowel is not candidate for radiological reduction because it may/will disappear spontaneously without interventional treatment.

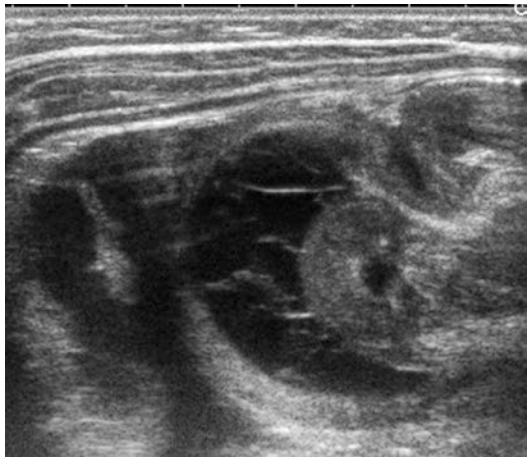

Fig. 13.5 US in a 1-year-old boy with AII: Trapped fluid with fibrinous septations is present around the intussusceptum. This ileal segment was necrotic at surgery

Furthermore, the presence of a lead point renders reduction more hazardous and surgery will be required. However, some authors have proposed to try to reduce them anyway if they are located close to the ileocecal valve even if a lead point has been identified, in order to facilitate subsequent surgery. This should not be attempted when there is evident or potential risk of perforation [19, 31]. The role of the ileocecal valve as a limiting factor in the success of pneumatic reduction in small bowel intussusceptum remains controversial [6, 31].

- IICI is more prone to present a lead point and is less easy to reduce [14].
- The distal location of the IIC intussusception, within the jejunum or proximal ileum, is definitively a risk of failure of reduction [29].

None of these US signs may fully predict failure of reduction.

13.3 The Therapeutic Role of Imaging [32, 33]

13.3.1 Indication

Taking into account the previous paragraph, all intussusceptions may potentially be treated radiologically. In practice, ICI and IICI are mainly concerned by such treatment.

13.3.2 Contraindications

Contraindications include any clinical sign of perforation and shock.

13.3.3 Temporary Non-Indication

Dehydration has to be corrected first and only thereafter the radiological reduction may be attempted.

13.3.4 Catheters

Twenty-two to twenty-four F catheters with no side holes are usually preferred. Foley balloon inflated outside the rectum and pressed against the anus might be used to reduce the enema leaks. We prefer to apply a manual compression on a wrapped catheter and to press the adjacent buttock than to tape the buttock together.

13.3.5 Methods

Direct confirmation and control of efficacy of reduction can be achieved either under fluoroscopy or under US control. Delivered doses with fluoroscopy vary significantly depending on the difficulty to succeed. Length of reduction is directly correlated with length of X-ray exposure. In practice, reduction starts by obtaining an AP plain film of the abdomen to serve as evidence of the degree of small bowel distension. This is of upmost importance, especially in case of air reduction, to ensure that small bowel loops distension is more significant at the end of the procedure, confirming the reduction. Reduction may also be achieved under US with the inconvenience to necessitate a second physician or a technician, one to perform the US while the second ensures the control of the enema.

13.3.6 Agents Used for Reduction

Advantages of *air* reduction include: no costs, less radiation exposure, easy to clean, less fecal peri-

toneal contamination in case of perforation. The main disadvantages of this technic include the absence of dedicated device allowing a continuous control of the colonic pressure and the potential risk of tension pneumoperitoneum. *Fluid* reduction may be obtained with either water, iodine or barium. The latter is more at risk of peritoneal complications in case of perforation. A recent meta-analysis of reduction with air shows better results than with liquid enema reduction [34].

13.3.7 Pressure

Low pressure attempt (60–80 mmHg) must be initially tested with an upper limit of 120 mmHg. The risk of perforation increases with increased pressure. A pressure of 120 mmHg is equivalent to 150 cm column of water or water soluble contrast material [35].

13.3.8 Associated Treatment

Neither sedation nor antalgic medication increases the success rate of the enema [36]. On the contrary, the use of sedation, suppressing the effect of the Valsalva maneuver, would increase the risk of perforation. Indeed, the Valsalva maneuver provides a protective effect against perforation, because external abdominal pressure decreases the transmural bowel pressure gradient [37, 38]. However, some authors claim a significant increase of reduction success under general anesthesia without increased rate of perforation [39, 40]. One major advantage of sedation is to suppress the child's anxiety and overall its pain.

13.3.9 Risk of Failure

Apart from the US findings already mentioned, duration of symptoms, visualization of contrast on X-rays within the intussuscipiens surrounding for few cm the intussusceptum are more likely to be associated with failure (Fig. 13.6).

13.3.10 Success of Treatment

In a meta-analysis, the success rate obtained whatever the technic used varies from 44 to 100% [33]. On average, the success rate should exceed 85%. Decrease in success rate is directly related to the length of symptomatology; the longer the symptoms, the less success of reduction. The use of repeated attempts (reports vary between 30 min and few hours) after the initial attempt has

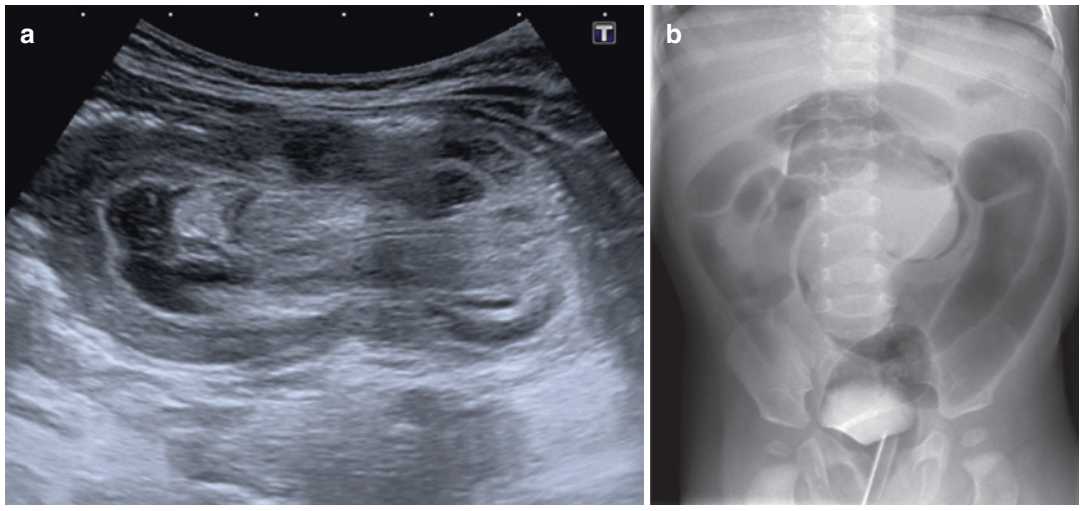

Fig. 13.6 Huge ileocolic intussusception in a 7-year-old boy. (**a**) Trapped fluid collection on US. (**b**) Attempt to air reduction was unsuccessful. Presence of air along an important segment of the intussusceptum is a risk factor of failure

shown increased success rate in enema reductions of intussusceptions [32, 36]. Delayed US control performed before a new attempt of reduction has also proved that the reduction may occur on its own. Contraindication to a repeat attempt reduction includes absence of partial reduction during the first attempt and signs of peritonitis or shock.

13.3.11 Doubtful Successful Reduction

Doubtful successful reduction, in the classic situation of ICI, should be suspected when the pneumatic insufflation shows no passage of air in the ileum or a passage without a complete reduction [41, 42]. Under these circumstances, US has a major role looking for the disappearance of the intussusception, the presence of an ileocecal valve edema explaining the absence of air reflux in the ileum and a thickened aerated terminal ileum (Fig. 13.7).

13.3.12 The Perforation Rate

The perforation rate must be kept under 1%. It can happen even at low pressure (60 mmHg). Either one of the intussusceptum or the intussuscipiens can perforate without sign of ischemia [33]. Perforation during air reduction may, if not recognized early enough, evolve towards a tension pneumoperitoneum. Enema needs to be stopped and the rectal tube freely opened. Abdominal decompression with direct puncture with an 18 G needle is possible but is rarely necessary [33].

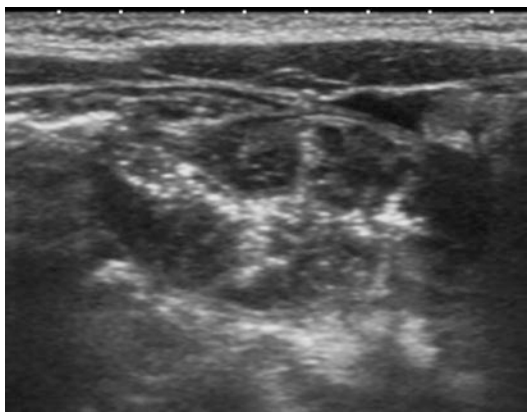

Fig. 13.7 Doubtful success of air reduction of an ileocolic intussusception. Fourteen-month-old boy. On US the terminal ileum is thickened and air is trapped in between the ileal folds (hyperechoic columns of bubbles). Absence of intussusception and presence of air in this bowel segment on US validate the successful air reduction

13.3.13 Recurrence Rate

Recurrence rate after reduction is reported in average to be as high as 10% [28, 33]. Most recurrences occur during the first 48 h post reduction and US confirms the diagnosis. A new attempt of reduction is usually performed. After three recurrences, a surgical procedure is necessary to look for local explanation including the presence of an undiagnosed lead point.

Conclusion

US is the method of choice to confirm or exclude the diagnosis of AII but also to identify its type and look for an associated lead point which will modify the therapeutic strategy. Multiple US criteria exist to predict difficulties for non-operative reduction. None of them is a contra-indication for a reduction attempt. Delayed treatment is the major risk factor for radiological reduction failure.

References

1. Jiang J, Jiang B, Parashar U, et al. Childhood intussusception: a literature review. PLoS One. 2013;8(7):e68482.
2. Huppertz HI, Soriano-Gabarró M, Grimprel E, et al. Intussusception among young children in Europe. Pediatr Infect Dis J. 2006;25(1 Suppl):S22–9.
3. Fischer TK, Bihrmann K, Perch M, et al. Intussusception in early childhood: a cohort study of 1.7 million children. Pediatrics. 2004;114(3):782–5.
4. World Health Organization, Initiative for Vaccine Research Department of vaccines and Biologicals. Acute intussusception in infants and children. Incidence, clinical presentation and management: a global perspective. WHO/V&B/02.19. 2002.
5. Vega García L, Fuentes-Leonarte V, Tenías JM, et al. Association between medication and intestinal intussusception in children: a case-crossover study. Pediatr Emerg Care. 2015;31(4):250–4.

6. Koh EPK, Chua JHY, Chui CH, Jacobsen AS. A report of 6 children with small bowel intussusception that required surgical intervention. J Pediatr Surg. 2006;41:817–20.
7. Bode CO. Presentation and management outcome of childhood intussusception in Lagos: a prospective study. Afr J Paediatr Surg. 2008;5(1):24–8.
8. del Pozo G, Albillos JC, Tejedor D, et al. Intussusception in children: current concepts in diagnosis and enema reduction. Radiographics. 1999;19(2): 299–319.
9. Pracros JP, Tran-Minh VA, Morin de Finfe CH, et al. Acute intestinal intussusception in children. Contribution of ultrasonography (145 cases). Ann Radiol. 1987;30(7):525–30.
10. Hryhorczuk AL, Strouse PJ. Validation of US as a first-line diagnostic test for assessment of pediatric ileocolic intussusception. Pediatr Radiol. 2009;39(10):1075–9.
11. Munden MM, Bruzzi JF, Coley BD, et al. Sonography of pediatric small-bowel intussusception: differentiating surgical from nonsurgical cases. Pediatr Imaging AJR. 2007;188:275–9.
12. Strouse PJ, DiPietro MA, Saez F. Transient small-bowel intussusception in children on CT. Pediatr Radiol. 2003;33(5):316–20.
13. Lioubashevsky N, Hiller N, Rozovsky K, et al. Ileocolic versus small-bowel intussusception in children: can US enable reliable differentiation? Radiology. 2013;269(1):266–71.
14. Peh WC, Khong PL, Lam C, et al. Ileoileocolic intussusception in children: diagnosis and significance. Br J Radiol. 1997;70(837):891–6.
15. Navarro O, Daneman A. Intussusception. Part 3: diagnosis and management of those with an identifiable or predisposing cause and those that reduce spontaneously. Pediatr Radiol. 2004;34(4):305–12.
16. Blanch AJ, Perel SB, Acworth JP. Paediatric intussusception: epidemiology and outcome. Emerg Med Australas. 2007;19(1):45–50.
17. Yih WK, Lieu TA, Kulldorff M, et al. Intussusception risk after rotavirus vaccination in U.S. infants. N Engl J Med. 2014;370(6):503–12.
18. Blakelock RT, Beasley SW. The clinical implications of non-idiopathic intussusception. Pediatr Surg Int. 1998;14:163–7.
19. Navarro O, Dugougeat F, Kornecki A, et al. The impact of imaging in the management of intussusception owing to pathologic lead points in children. A review of 43 cases. Pediatr Radiol. 2000;30(9):594–603.
20. Itagaki A, Uchida M, Ueki K, et al. Double target sign in ultrasonic diagnosis of intussuscepted Meckel diverticulum. Pediatr Radiol. 1991;21:148–9.
21. Daneman A, Myers M, Shuckett B, et al. Sonographic appearances of inverted Meckel diverticulum with intussusception. Pediatr Radiol. 1997;27(4): 295–8.
22. Zhang Y, Dong Q, Li SX, et al. Clinical and ultrasonographic features of secondary intussusception in children. Eur Radiol. 2016;26(12):4329–38.
23. Mushtaq N, Marven S, Walker J, et al. Small bowel intussusception in celiac disease. J Pediatr Surg. 1999;34(12):1833–5.
24. Couture A, Veyrac C, Baud C, et al. Evaluation of abdominal pain in Henoch-Schönlein syndrome by high frequency ultrasound. Pediatr Radiol. 1992;22(1):12–7.
25. Helbling R, Lava SA, Simonetti GD, et al. Gallbladder and pancreas in Henoch-Schönlein Purpura: review of the literature. J Pediatr Gastroenterol Nutr. 2016;62(3):457–61.
26. Al-Momani H. Waugh syndrome: a report of 7 patients and review of the published reports. Ann Saudi Med. 2014;34(6):527–31.
27. Del-Pozo G, Gonzalez-Spinola J, Gomez-Anson B. Trapped peritoneal fluid detected with US—relationship to reducibility and ischemia. Radiology. 1996;201:379–86.
28. Applegate KE. Intussusception in children: imaging choices. Semin Roentgenol. 2008;43(1):15–21.
29. Ntoulia A, Tharakan SJ, Reid JR, Mahboubi S. Failed intussusception reduction in children: correlation between radiologic, surgical, and pathologic findings. Am J Roentgenol. 2016;207(2):424–33.
30. Daneman A, Navarro O. Intussusception. Part 1: a review of diagnostic approaches. Pediatr Radiol. 2003;33(2):79–85.
31. Saxena AK, Seebacher U, Bernhardt C, et al. Small bowel intussusceptions: issues and controversies related to pneumatic reduction and surgical approach. Acta Paediatr. 2007;96(11):1651–4.
32. Stein-Wexler R, O'Connor R, Daldrup-Link H, et al. Current methods for reducing intussusception: survey results. Pediatr Radiol. 2015;45(5):667–74.
33. Daneman A, Navarro O. Intussusception. Part 2: an update on the evolution of management. Pediatr Radiol. 2004;34(2):97–108.
34. Sadigh G, Zou KH, Razavi SA, et al. Meta-analysis of air versus liquid enema for intussusception reduction in children. Am J Roentgenol. 2015;205(5): W542–9.
35. Kuta AJ, Benator RM. Intussusception: hydrostatic pressure equivalents for barium and meglumine sodium diatrizoate. Radiology. 1990;175(1):125–6.
36. Applegate KE. Intussusception in children: evidence-based diagnosis and treatment. Pediatr Radiol. 2009;39(Suppl 2):S140–3.
37. Shiels WE, Kirks DR, Keller GL, et al. John Caffey award. Colonic perforation by air and liquid enemas: comparison study in young pigs. Am J Roentgenol. 1993;160(5):931–5.
38. Kirks DR. Diagnosis and treatment of pediatric intussusception: how far should we push our radiologic techniques? Radiology. 1994;191:622–3.

39. Purenne E, Franchi-Abella S, Branchereau S, et al. General anesthesia for intussusception reduction by enema. Paediatr Anaesth. 2012;22(12):1211–5.
40. Ilivitzki A, Shtark LG, Arish K, et al. Deep sedation during pneumatic reduction of intussusception. Pediatr Radiol. 2012;42:562–5.
41. Hedlund GL, Johnson JF, Strife JL. Ileocolic intussusception: extensive reflux of air preceding pneumatic reduction. Radiology. 1990;174:187–9.
42. Murakami JW, Winters WD, Weinberger E, et al. Extensive reflux of air during enema for intussusception without reduction: case report. Can Assoc Radiol J. 1998;49(5):334–5.

Diseases of the Peritoneum, Mesentery, and Omentum

14

Fred E. Avni and Paul Humphries

Contents

F.E. Avni (✉)
Department of Pediatric Radiology,
Jeanne de Flandre Hospital, Av E Avinée 2,
59037 Lille-Cedex, France
e-mail: Freddy.Avni@Chru-Lille.fr

P. Humphries
University College London and Great Ormond Street Hospital for Children, London, UK

14.1 Definitions and Anatomy

The *peritoneum* is a thin serous membrane. The peritoneum that lines the abdominal wall is called the parietal peritoneum. The one that covers the viscera and organs is called the visceral peritoneum. Both consist of a single layer of simple cuboidal epithelium called a mesothelium. Serous fluid, approximatively 50–100 mL, is produced by the mesothelium and separates the parietal from the visceral peritoneum. The peritoneal cavity is a potential space closed in male patients, open in females as it communicates with the extraperitoneal space through the fallopian tubes, uterus, and vagina.

Folds of the peritoneum constitute ligaments and provide support to the various structures within the abdominal cavity.

A *mesentery* is a ligament composed of a double layer of peritoneum that covers the small bowel or parts of the colon and connects them to the posterior abdominal wall. The small bowel mesentery encloses the jejunum, ileum, and transverse colon (the so-called transverse meso-colon) and sigmoid (the so-called sigmoid-colon). The root of the small mesentery extends from the duodeno-jejunal flexure in the left upper quadrant to the ileocecal junction in the right lower quadrant. It contains the superior mesenteric artery and vein as well as their branches, lymph nodes, and fat. The transverse meso-colon joins the second part of the duodenum and head of the pancreas to the transverse colon. It contains the middle colic

F.E. Avni, P. Petit (eds.), *Imaging Acute Abdomen in Children*,
https://doi.org/10.1007/978-3-319-63700-6_14

artery and vein. The sigmoid mesocolon extends from the descending colon into the pelvic area containing sigmoidal and hemorrhoidal vessels.

An *omentum* is a ligament that joins the stomach to other structures. The lesser omentum joins the lesser curvature of the stomach to the liver as well as the duodenum to the liver. The greater omentum connects the greater curvature of the stomach to the transverse colon. The greater omentum is composed of four layers of peritoneum.

The peritoneal ligaments divide the peritoneum into two main compartments: the main cavity and the posterior lesser sac (communicating through the foramen of Winslow). The transverse mesocolon divides the peritoneal cavity into two further parts: supramesocolic (left and right) and inframesocolic (left and right) compartments. All the mesocolic spaces communicate between themselves [1–3].

14.2 Imaging

Diseases involving the peritoneum, mesentery, and omentum are numerous; they include among others, effusions and abscesses, consequences of intestinal malrotation and tumors. Many peritoneal diseases will be discovered during the work-up acute abdominal symptoms.

Ultrasound (US) will be the initial and preferred imaging method performed in order to evaluate peritoneal diseases in children, especially for the assessment of collections and tumors. It may also be used to guide drainage. Unfortunately, US does not provide global assessment of the abdominal and pelvic anatomy; cross sectional imaging will be necessary in complex or extensive diseases.

CT enables a much better evaluation of the peritoneal cavity and allows clearer differentiation between intra-, retro- and extra-peritoneal diseases. The main other advantages of CT are its availability, lack of operator dependency, and the short duration of the examination. As usual its use should be customized and cautiously adapted to the child and to the clinical indication. In order to adequately assess the peritoneum intravenous contrast should be used, in order to assess the degree of enhancement of the peritoneum and also to improve detection of tumor nodules.

Newer equipment reduces dramatically the amount of ionizing radiation.

MR imaging is and should be increasingly used to evaluate peritoneal diseases. Lack of ionizing radiation is a big advantage over CT. Yet, the technique may have a lower spatial resolution than CT, depending on the sequences employed. Other disadvantages are the duration of the examination, the need for sedation and motion artifacts and the relative reduced availability (particularly in the emergency setting outside normal working hours), newer sequences might reduce the time of acquisition of the images [1–4]. The need for Gadolinium chelates injection is considered by many as a limiting factor as well.

Plain film of the abdomen would be helpful to evaluate the distribution of the abdominal intestinal loops as well as to demonstrate evidence of perforation and extraintestinal air (as in abscesses). Abdominal calcifications will be easier to demonstrate.

Finally, an opacification of the upper GI tract could be of interest in selected cases of intestinal obstruction in relation with suspected malrotation,

14.3 Peritoneal Effusions

Small amount of free peritoneal fluid can be visualized in asymptomatic or even symptomatic children within the pelvis and around small bowel loops on US or on CT. As long as the fluid is echo-free and in small amounts, this should not be considered as abnormal. Noteworthy, the peritoneal mesothelium includes villosities and vesicles that secrete and reabsorb fluid. Therefore, the free fluid observed in small amounts can be related to rupture of mesothelial vesicles at the peritoneal surface; it can also result from the rupture of follicles in adolescent girls [5, 6]. Larger amounts of fluid effusions are abnormal and their origin should be evaluated based on clinical, biological, and imaging findings.

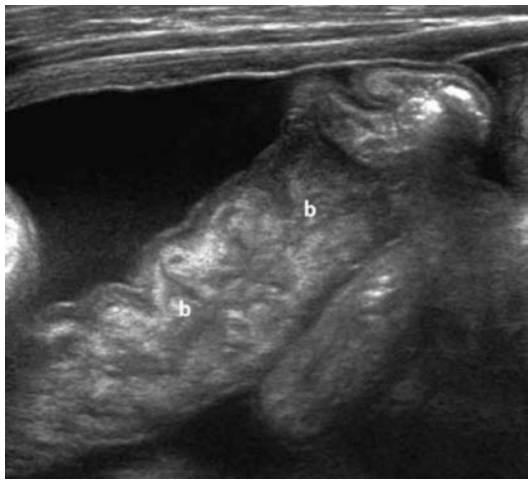

Fig. 14.1 Uncomplicated ascites (Case of Henoch–Schonlein Purpura). An echo-free fluid collection surrounds a bowel loop

14.3.1 Ascites (Uncomplicated)

Ascites (= significant amount of free peritoneal effusion) in an acute setting can be associated with numerous abnormal intraabdominal processes or with global organ failure. It is usually discovered during an US examination of the abdomen (Fig. 14.1). As mentioned, the finding of ascites must be correlated with the clinical and biological data [5–7].

Ascites can be encountered in or can be a sign of many different diseases (see the related chapters), among others:

- Liver diseases, associated or not with portal hypertension
- Intestinal obstructions and diseases (intussusception, gastroenteritis, midgut volvulus, meconium plug, etc.)
- Ovarian torsion
- Abdominal trauma in which ascites may indicate insult of an abdominal organ; the effusion may be somewhat echogenic due to the bloody content.
- Neoplasms: in this setting, the presence of ascites usually indicates metastatic spread of the disease.
- Systemic diseases such as Henoch–Schonlein syndrome or nephrotic syndromes (in relation with the hypoalbuminemia)
- Global organ failure as encountered in shock or heart failure
- Biloma corresponding to a collection of biliary fluid that may develop after (complicated) liver surgery or after hepatic trauma.
- Normal ventriculoperineal shunting
- Peritoneal dialysis (see below).

The US examination must investigate the entire abdominal cavity in order to provide clues as to the etiology of the ascites. Uncomplicated ascites usually appears as collections of echo free fluid without encapsulating wall and without septa (Fig. 14.1). It may collect at any part of the abdomen.

14.3.2 Particular Presentations of Ascites

14.3.2.1 Urinary Ascites

Ascites in relation with urinary tract leakage (usually post-obstruction) is a classical yet unusual finding as the urinary tract is retroperitoneal. Still, its presence within the peritoneum can be understood by leakage and rupture of the bladder (as in posterior urethral valves) or by a retrograde filling of the peritoneum through the uterus and fallopian tube when the urethra and vagina have a common opening. Furthermore, abdominal trauma may induce a communication between the retroperitoneum and the peritoneal cavity and explain the intraperitoneal presence of urinary ascites in case of trauma to the urinary tract.

14.3.2.2 Peritoneal Inclusion Pseudocysts

Peritoneal inclusion pseudocysts (PIP) correspond to fluid located in (abdomino-) pelvic compartments delineated by intestinal adhesions that can be related to previous (sometimes neonatal) surgery, endometriosis, or pelvic inflammatory diseases in adolescents (see also Chap. 24). They may contain accumulation of the fluid resulting from ruptured follicles (Fig. 14.2). PIP do not have a proper wall. Their size may be quite large (over 8–10 cm) and it may not always be possible to differentiate PIP from real ovarian cysts. Treatment includes puncture, sclerotherapy, or surgery [8].

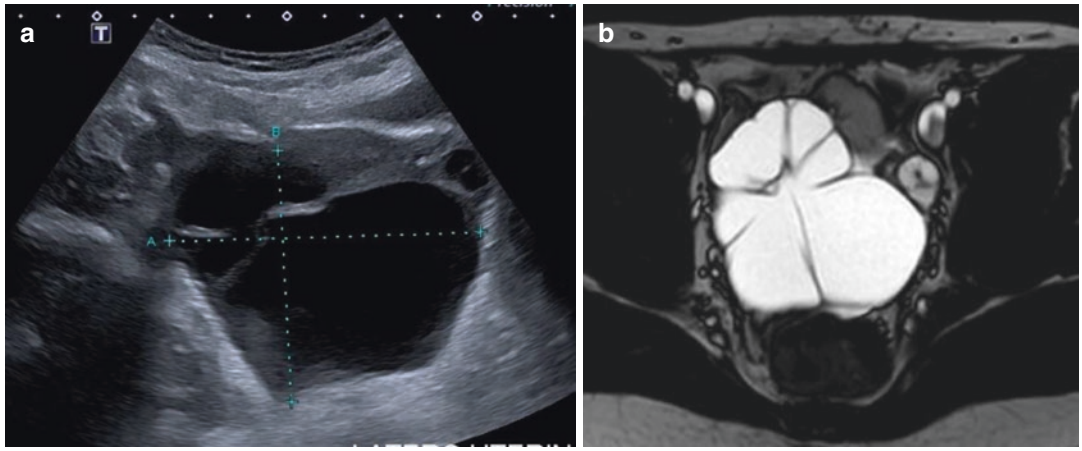

Fig. 14.2 Peritoneal inclusion cyst—10-year-old girl with a previous surgery for ovarian cystadenoma. (**a**) US: Transverse scan of the pelvis: a cystic septated mass (6 × 8 cm) is visualized behind the bladder (B); there is no apparent wall to the collection. (**b**) MR imaging: T2-weighted sequence; same cystic and septated appearance as on US

14.3.2.3 Cerebrospinal Fluid Pseudocysts

Intraabdominal cerebrospinal fluid (CSF) is an expected consequence of ventriculoperitoneal shunting. The fluid is usually distributed in the entire abdominal cavity in small volumes. Multiloculated, sometimes large, collections of CSF can develop when intestinal adhesions develop around the tip of the shunt catheter or around the shunt in its course within the abdominal wall (Fig. 14.3). The adhesions interfere with the normal drainage and may therefore induce uphill cerebral hypertension. These pseudocysts do not have a wall, still they may become infected and limited by a pseudo-wall representing inflammatory peripheral tissue from the omentum and bowel walls. Drainage under US control or surgery with replacement of the shunt may be necessary [9].

14.3.3 Peritonitis and Complicated Ascites

14.3.3.1 Secondary Peritonitis: So-called Peritonitis

Peritonitis corresponds to a diffuse inflammatory process involving parts or all of the peritoneum associated with complicated infected effusion. The most classical cause is appendicular peritonitis and abscess formation following a rupture of appendicitis (Fig. 14.4) (see Chap. 11). Infectious collections or abscesses may develop after rupture of Meckel's diverticulum or perforation of a bowel segment (Fig. 14.5). It can be a complication of any abdominal surgery. Collections/abscesses may also be associated with inflammatory bowel diseases. These infectious effusions may collect in single or multiple locations (communicating or not). Fistulae may develop between these abscesses and intestinal loops.

A meconium peritonitis is a particular peritonitis encountered in the neonatal period. It results from an in utero perforation of the bowel and spilling of the meconium in the abdominal cavity. It can organize as a meconium pseudocyst (see Chap. 5).

(Sclerosing) peritonitis is a complication of peritoneal dialysis; in such case, the peritoneum thickens and may calcify. The dialysis catheter will be visualized within it.

US is also able to detect abscesses; they appear as a relatively hypoechoic (sometimes septated) collection without evidence for peristalsis, without own wall but with peri-abscess inflammatory hypervascularized tissues (Figs. 14.4a and 14.5b). Some hyperechoic foci within the collection may represent air and anaerobic superinfection. In case of infection, the peritoneum, the mesentery, and the omentum may appear diffusely hyperechoic

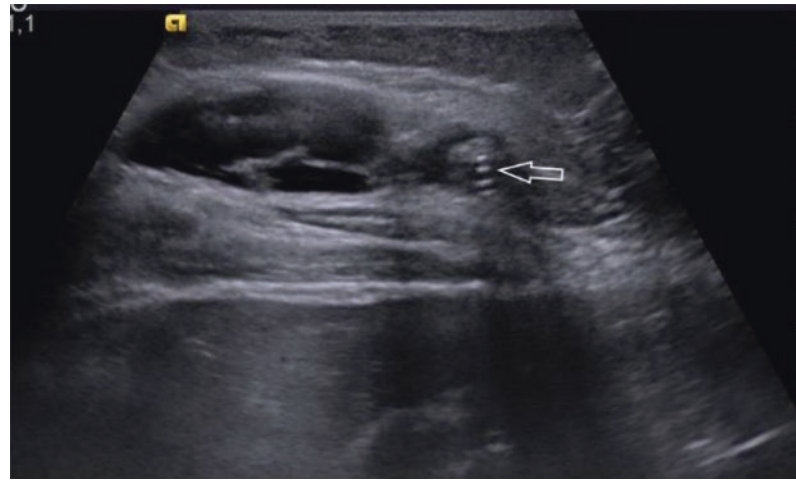

Fig. 14.3 Dysfunction of a ventriculo-peritoneal shunt (6-year-old boy) Ultrasound—Transverse scan of the abdominal wall. A collection of fluid is observed within the abdominal wall at the right of the shunt (*arrow*)

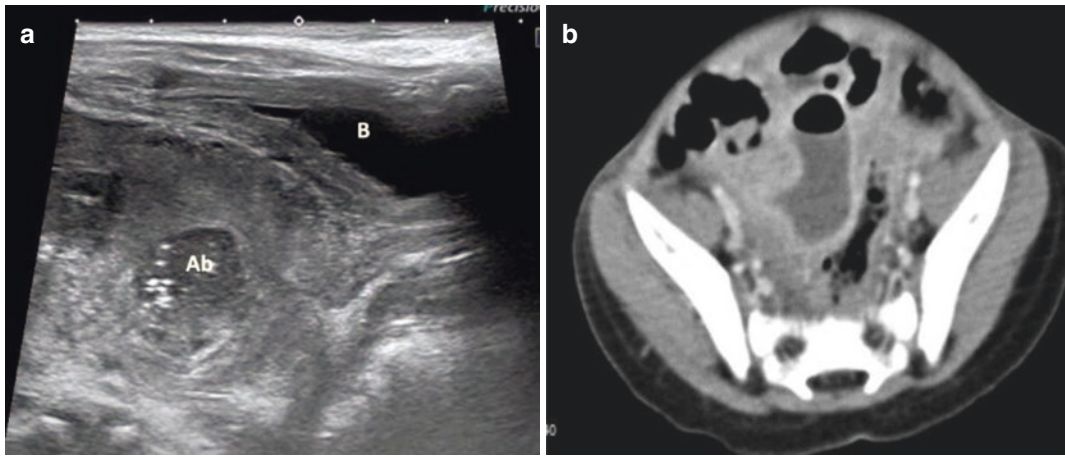

Fig. 14.4 Peritonitis and abscess following perforation of acute appendicitis (3-year-old girl). (**a**) US—Sagittal scan of the bladder. The rounded abscess contains heterogeneous material and is surrounded by thick inflammatory mesentery. (**b**) CE-CT confirms the US findings, the abscess (with an air/fluid level) and the inflammatory surrounding mesentery

(especially the mesentery). Some enlarged lymph nodes can be observed as well. This infectious hyperechogenicity must be differentiated from thickened and hyperechoic mesenteric fat as encountered in inflammatory bowel disease.

The potential extent and the number of collections is difficult to define by US alone and therefore, in acute clinical presentations as well as in cases with unfavorable evolution, a CE-CT may help to evaluate the entire peritoneum (Fig. 14.4b). MR imaging is surely accurate but is less easy to perform in an emergency setting mainly due to its lack of availability.

On CT, in case of peritonitis, the peritoneal sheets would enhance after contrast enhancement. CT is more accurate than US to establish the map and extent of the collections as well as the relation with the adjacent organs. It will also help to differentiate intraperitoneal from retro- or extraperitoneal collections. In case of posterior abdominal collection, a psoas abscess is a potential differential diagnosis to consider and will be easier to demonstrate on CT (and on MR imaging) [10–13].

US and CT may be performed to guide drainage of the collections if required.

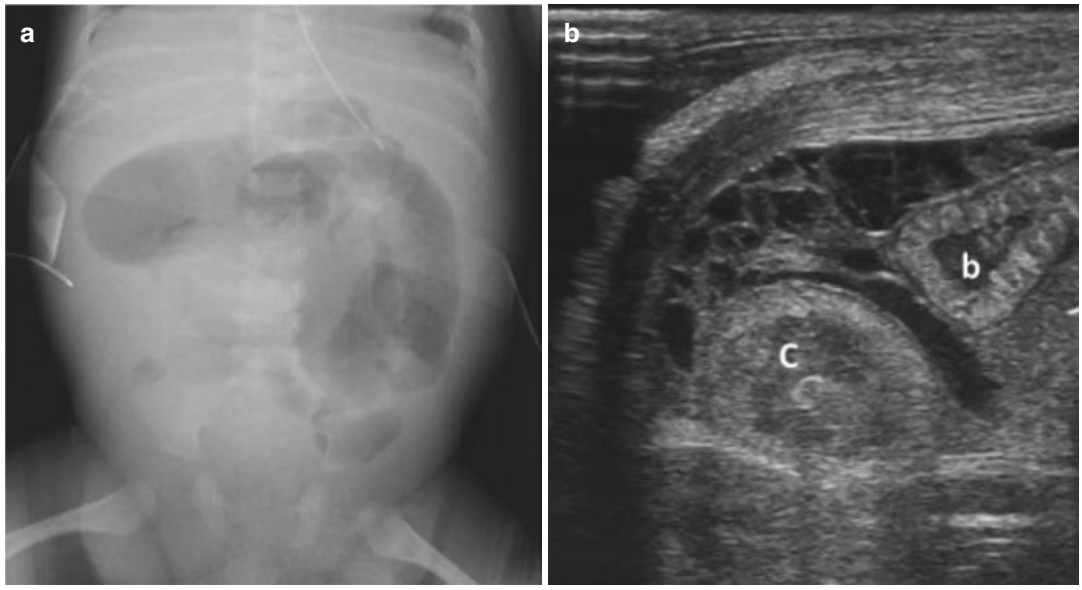

Fig. 14.5 Peritonitis following perforation of NEC in a premature. (**a**) Plain film of the abdomen confirming bowel (sub)obstruction and probable effusion. (**b**) US—Transverse scan—Septated collection in the right flank

14.3.3.2 Primitive Peritonitis

Primitive peritonitis (PP) is a rare disease usually related to pneumococcal infection. It may complicate cirrhosis, nephrotic syndrome or occur as an isolated disease. On US, the effusion appears echogenic, the bowel loops may be dilated but no obstruction will be demonstrated neither on US nor on CT or even during surgery (if performed). The diagnosis is confirmed by the culture of the effusion [14, 15].

14.3.3.3 Other Inflammatory and Infectious Mesenteric Processes

Mesenteric Lymphadenitis

Mesenteric lymphadenitis (ML) constitutes one of the main differential diagnoses to acute appendicitis; it should be suspected, on US examination, whenever enlarged lymph nodes measuring above 10 mm are visualized mainly in the ileocecal region. Like appendicitis, it is often associated with acute abdominal pain. In case of ML, other systemic symptoms can be present as well (signs of ENT infection, etc.). This diagnosis should be proposed cautiously only after that all other potential diagnoses of abdominal pain have been excluded. Furthermore, all differential diagnoses of enlarged abdominal lymph nodes must be considered especially Yersinia ileitis (Fig. 14.6), inflammatory bowel disease, or lymphoma. As indicated, evidence of an acute disease should be searched in and outside the abdominal cavity [16, 17].

Mesenteric Panniculitis

Mesenteric panniculitis (MP) is an extremely rare disease in children of unknown etiology and is characterized by chronic inflammation, fat necrosis, and fibrosis in the mesenteric adipose tissue. It occurs most commonly in the mesentery of the small intestine (90%) but can occur in any other site. Abdominal CT scan is the most effective diagnostic tool. Two signs are reported as typical: the "fat ring sign" reflecting preservation of fat around the vessels and a "tumoral pseudocapsule" separating normal from abnormal mesenteric fat. Thickening of the anterior peritoneal layer is also often present. When the panniculitis occurs in the RLQ, appendicitis is usually the suggested diagnosis.

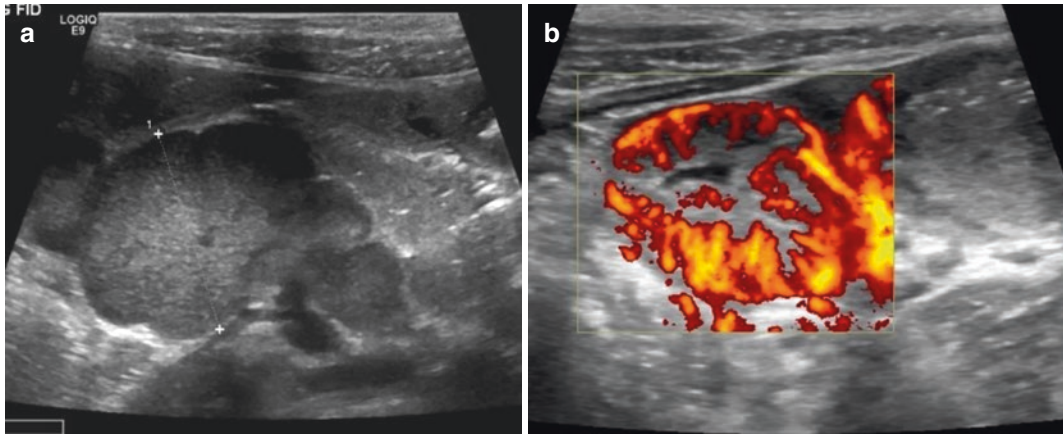

Fig. 14.6 Ileo-cecal Yersinia infection with associated lymphadenitis. (**a**) Lymphadenitis—US – Sagittal scan of the right iliac fossa displaying markedly enlarged lymph nodes. (**b**) Power-Doppler of the cecum showing thickening and hypervascularization

Surgical biopsy is usually necessary in order to ascertain the diagnosis.

The clinical course is usually favorable. Corticosteroids medications represent the preferred treatment [18, 19].

14.4 Ischemic Processes and Torsion

14.4.1 Omental Torsion and Infarcts

Primary omental torsion is an extremely rare cause of abdominal pain in children. It occurs when the omentum twists around its long axis causing edema and vascular compromise. Omental torsion can be primitive or secondary. Secondary omental torsion can be associated with tumors (Fig. 14.7), adhesions or hernia (see below). Segmental infarct may be an associated undistinguishable finding.

The underlying pathogenesis is unknown. Obesity is a favoring factor. The clinical symptoms commonly mimic those of appendicitis. It is mainly diagnosed during laparotomy.

On US, a painful superficial echogenic abdominal mass is visualized, anywhere but most commonly in the right flank or RLQ (Fig. 14.8a). On CT, without contrast injection, the omental fat may appear somewhat infiltrated with areas of mixed low attenuation areas and hyperattenuating streaks. The same pattern is observed after contrast injection (Fig. 14.8b). Similar findings can be visualized on MR imaging. The latter should be preferred when a tumor is suspected (Fig. 14.7b, c).

Surgical excision is the treatment of choice, especially when an underlying tumor is suspected [20].

14.4.2 Appendagitis

Epiploic appendagitis is a rarely reported cause of acute abdominal pain in children arising from inflammation of epiploic appendages that are distributed along the entire colon. Epiploic appendages may undergo torsion or thrombosis leading to ischemia and inflammation of the peripheral tissue, including the bowel wall, mesentery, and peritoneum. The most common location is the cecum, therefore, this rare diagnosis is usually misled as appendicitis. CT appears characteristic: oval to round fat attenuation lesion less than 5 cm diameter located on the antimesenteric side of the colon with surrounding inflammatory changes anterior to the colon (Fig. 14.9).

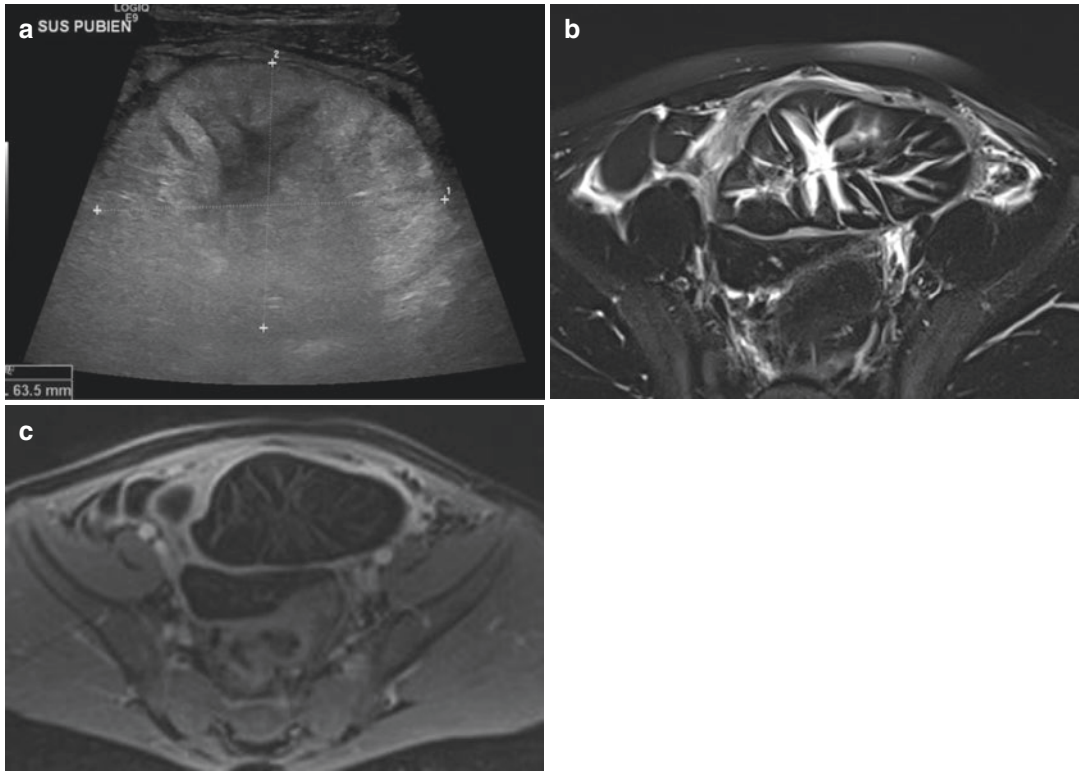

Fig. 14.7 Torsion of the greater omentum secondary to a giant lipoma (6-year-old boy). (**a**) US: A large (8 × 7 cm) echogenic mass occupies the pelvis. (**b**) MR imaging axial T2-weighted fat-sat confirming the fat content of the mass. (**c**) MR imaging axial T1 after Gd enhancement; lack of enhancement of the mass; an enhancement of the capsule is preserved

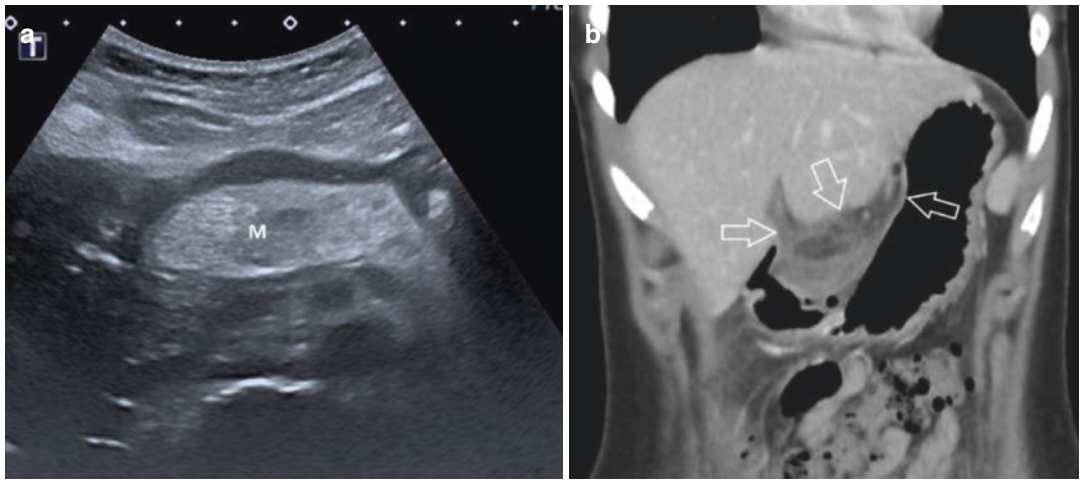

Fig. 14.8 Infarct of the lesser omentum in a 14-year-old teenage girl. (**a**) US Transverse scan of the epigastric area showing an oval hyperechoic mass. (**b**) CE-CT Venous phase; hypodense area below the margin of the liver surrounded by inflammatory reaction

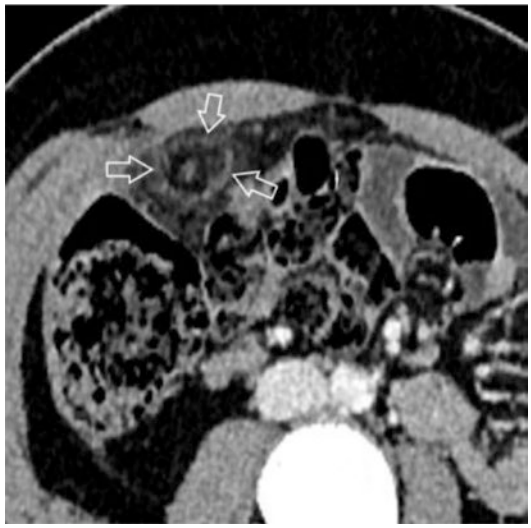

Fig. 14.9 Appendagitis in a 14-year-old girl—CE-CT. A round fat-containing lesion is visualized in the right flank. There is a central vessel, the lesion seems surrounded by a capsule and there is peripheral inflammatory reaction as well

The evolution is towards spontaneous resolution [21].

14.5 The Length of Mesentery and Malrotation [22–25] (See Also Chap. 9)

14.5.1 Normal Embryology

At 10 weeks gestation, the bowel re-enters the abdomen. The cephalad midgut (proximal small bowel) enters first and undergoes a third 90° counterclockwise rotation leading to the normal C loop duodenal pattern. The caudal midgut (distal ileum cecum and proximal colon) enter later and undergo additional 180° counterclockwise rotation. At this stage, the position of the cecum varies. Further elongation of the colon develops throughout the remainder of the gestation and postnatally. The second, third, and fourth portions of the duodenum are fixed in the retroperitoneum. The ligament of Treitz fixes the duodeno-jejunal junction. Descending and ascending colon mesenteries fuse with the retroperitoneum. The transverse mesocolon fuses partially with the greater omentum, the sigmoid mesocolon fuses with the retroperitoneum. The small bowel is fixed by a broad mesentery extending from the DJJ in the left upper abdomen to the ileocecal valve in the RLQ. The broad base of the mesentery stabilizes its position and prevents volvulus.

14.5.2 Abnormal Embryology

Arrest of the embryologic development may occur at any phase with variable consequences, leading to the different malrotation patterns. Early failure of rotation corresponds to the pattern of non-rotation (no further than the 90° first rotation). In such cases, the small bowel is located at the right and the colon at the left. Incomplete rotation represents a failure of the 180° counterclockwise rotation of the small bowel and the 180° rotation of the colon. The result abnormality is a spectrum from complete non-rotation to almost normal rotation. The risk for volvulus will vary with the degree of mesenteric attachment which might be difficult to directly assess with imaging. In reversed rotation, the duodenum rotates clockwise instead of counterclockwise. The duodenum becomes anterior to the SMA and the colon posterior. This may result in an internal hernia (and obstruction) (see below).

14.5.3 The Length of the Root of the Mesentery and the Risk of Volvulus

Normal rotation leads to a broad mesenteric root and no risk for volvulus. In case of non-rotation, the mesenteric root is wide and the risk of volvulus is low; still Ladd's band may cause obstruction. Incomplete rotation with the DJJ to the right of midline and a high positioned cecum are associated with a short mesenteric root predisposing to volvulus and Ladd's bands.

14.5.4 Imaging Rotation Anomalies (See Also Chaps. 7 and 9)

Imaging is unable to determine directly the length of the mesenteric root. It may demonstrate indirect features that allow to appreciate the type of

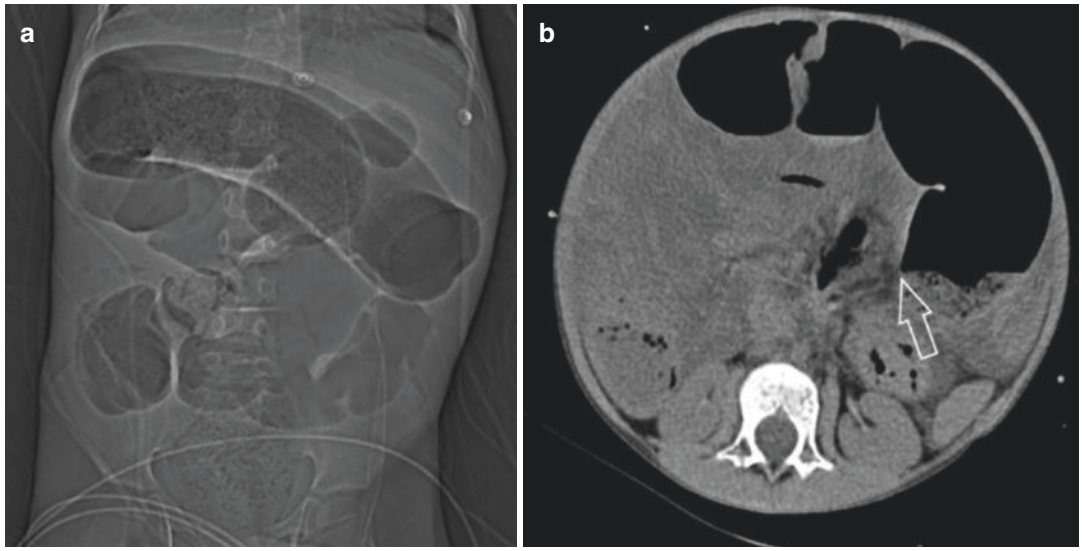

Fig. 14.10 Internal hernia. (**a**) Plain radiograph of the abdomen demonstrating an intestinal obstruction. (**b**) Unenhanced CT of the abdomen showing the area of herniation (*arrow*) with uphill dilatation. The sigmoid colon was the segment of digestive tract that was herniated

malrotation. UGI series represent the gold standard examination for this purpose as it may show exactly the position of the DJJ. Still the method does have some limitations.

US is very useful in the workup of an acute setting of intestinal obstruction as it is able to demonstrate the so-called whirlpool sign, so characteristic of midgut volvulus as consequence of an unstable malrotation.

To be noted, the screening and treatment of asymptomatic malrotation is still highly controversial [23, 24].

14.6 Internal Hernia

An internal hernia is defined as the protrusion of viscera through peritoneal mesenteric orifices. Internal hernias can be congenital or acquired. Internal hernia is classified according to their locations: para-duodenal, peri-cecal, transmesenteric, or inter-sigmoid hernias. The most common types in childhood are para-duodenal and trans-mesenteric hernias. They occur in two age groups, neonates and older children. Neonatal hernias tend to be trans-mesenteric whereas hernias in older children tend to be para-duodenal. Trans-mesenteric hernia is potentially associated with small bowel atresia, malrotation, and volvulus [25, 26].

UGI studies are able to suggest uncomplicated para-duodenal hernia whenever a poorly mobile cluster of intestinal loops is demonstrated on the left or right side of the vertebral spine. In some cases, the afferent and efferent bowel loops can be demonstrated. In case of obstruction, similar findings (afferent and efferent loops) can be observed on CT but with distension of the obstructed loops penetrating the hernia orifice (Fig. 14.10). Noteworthy, marked intestinal distension renders more difficult the demonstration of the hernia. The diagnosis of trans-mesenteric hernia is particularly challenging [25, 26].

14.7 Tumors

The peritoneum is characterized by its mesothelial layer. The mesentery and omentum have the same embryologic origin and consist of two or four layers of peritoneum. All contain connective tissue, blood vessels, lymphatics, nerves, and fat. Tumors may therefore arise from any structure or tissue. Intra-peritoneal tumors are usually very large at diagnosis.

Some tumors will be detected already in the fetus (see Chap. 5). For others, it will be an incidental finding during abdominal ultrasound. Yet, in the majority of patients, the tumor will be discovered following acute circumstances. Presenting symptoms are classically abdominal pain (80%), abdominal distension, abdominal mass (30–50%), nausea, vomiting, diarrhea, or peritonitis. Further complications include infection, hemorrhage, rupture, and torsion leading to volvulus. Due to their large size, it will usually be difficult to determine pre-operatively the precise origin and nature of the peritoneal tumors. The role of imaging will mostly be dedicated to define the internal content and the extent of the tumors as well as the relation of the tumors with adjacent organs and vessels. Imaging will usually provide features allowing to differentiate between peritoneal and retroperitoneal tumors. Mesenteric tumors should be differentiated from other intraperitoneal tumors (i.e., ovarian cysts).

US will be the first imaging modality performed and will be able to differentiate between cystic on non-cystic masses and demonstrate complications. The method will also be able to determine the degree of vascularization of the tumor and the suspicion of metastatic extension in case of suspected malignancy.

Cross-sectional imaging (preferably MR imaging, sometimes CT) will be necessary thereafter in order to further define the tumoral nature and extent [27, 28]. There are no firm recommendations for the types of sequences that should be used when using MR imaging to evaluate an intraabdominal mass lesion, however some general principles do apply. Firstly a high quality sequence with good anatomical detail is required, which necessitates cessation of motion, namely bulk body motion using sedation/general anesthesia; respiratory motion using navigator echo techniques to limit acquisition to end expiration; and suppressing bowel motion using spasmolytics. Isotropic thin section T2-weighted imaging is increasingly used for the purpose of anatomical definition (i.e., T2 SPACE, Siemens, Erlangan, Germany), which can then be reconstructed in any desired plane using 3D MPR software. Secondly it may be necessary to evaluate fat content of the lesion, which can be achieved using T1-weighted sequences both with and without fat suppression and in an opposed-phase imaging. This is most rapidly achieved using a four point DIXON technique, which provides images of fat, water, in phase and opposed phase with a very rapid acquisition. The third consideration is characterizing the mass and identifying more cellular areas that could be a target for biopsy, which is achieved using diffusion weighted imaging. It is recognized that restricted areas of diffusion correlate with more cellular areas and this can be used to guide biopsy and be reviewed at follow-up to assess treatment response, an area of current research. Finally, embryonal childhood tumors in general tend to enhance somewhat less than background normal tissue and hence post contrast fat suppressed T1-weighted imaging is also useful to define the borders between tumor and normal tissue and thus assist with surgical planning [29–31].

14.7.1 Cystic Tumors

A classification of peritoneal and retroperitoneal cystic masses based on the etiology and pathological features has been proposed by de Perrot et al. [32]. It includes

- Cysts of lymphatic origin (lymphatic cyst and lymphangioma)
- Cysts of mesothelial origin (simple mesothelial cyst, benign cystic mesothelioma and malignant cystic mesothelioma)
- Cysts of enteric origin (enteric cyst and enteric duplication)
- (Cysts of urogenital origin)
- Cystic teratoma
- Pseudocysts

In the peritoneum, mesenteric cysts, and other lymphatic malformations are the most common diagnoses to consider in case of very large cystic tumors.

The content of the mesenteric cyst can be chylous, serous, or hemorrhagic. The tumor appears uni- or multiloculated. Most mesenteric cysts are

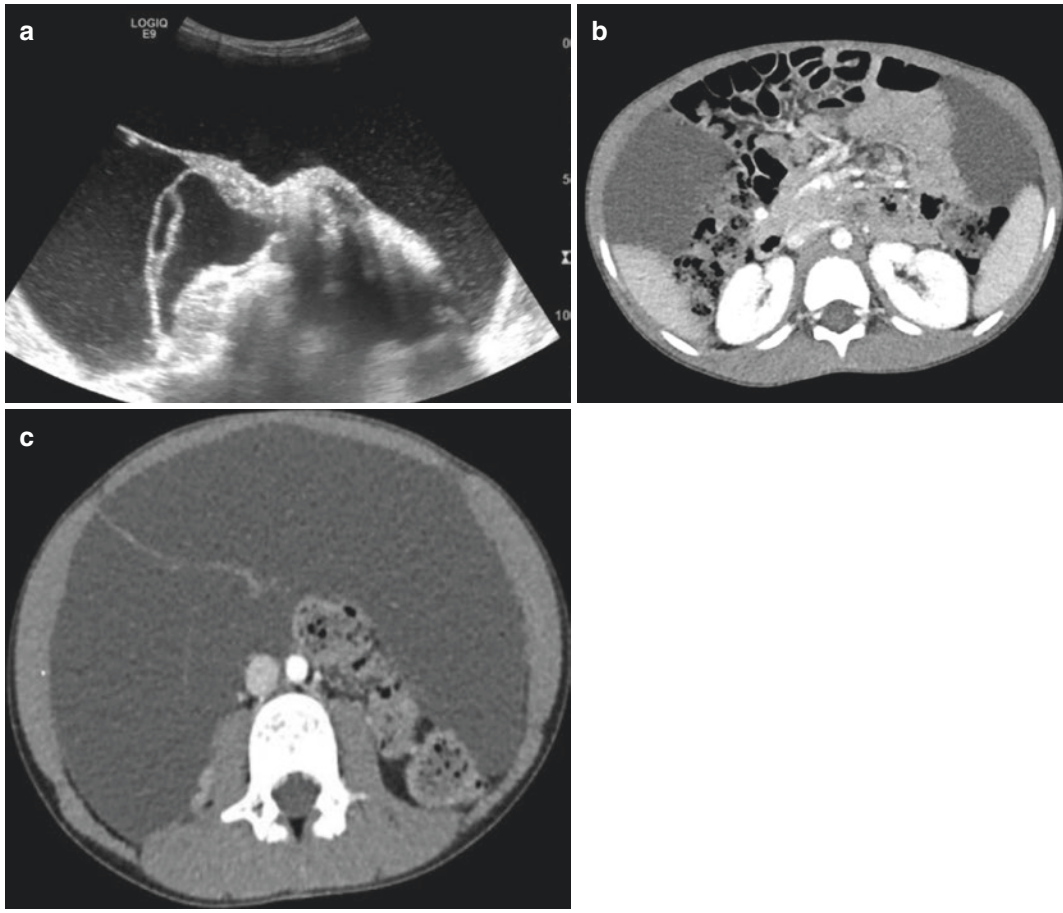

Fig. 14.11 Giant lymphatic malformation (lymphangioma). (**a**) US—A large part of the abdomen is occupied by a cystic mass with some septations. (**b**) CE-CT of the upper abdomen—The bowel loops are displaced towards the midline; the mass is limited upwards by the liver and spleen. (**c**) CE-CT of the lower abdomen: the mass occupies the entire abdomen; one septation is visible

located in the small bowel mesentery. Its content may appear echogenic due to complication (hemorrhage or infection). Around 3% of mesenteric cysts will present evidence of malignancy at histology.

Mesenteric lymphatic malformations may present as an isolated cystic (septated) mass. The may appear macro (Fig. 14.11) or microcystic (Fig. 14.12). The masses may grow very large before diagnosis. Due to the cystic content, lymphatic malformations may be misdiagnosed as ascites. The upper limit of the mass would help to differentiate between them. Ascites would fuse around the liver and spleen, whereas lymphangioma will be self-limited by the liver/spleen. Lymphatic malformations may also infiltrate the intestinal walls and be located very close to the mesenteric vessels, while some other lymphatic malformations will develop as multicentric and diffusely infiltrating masses (Figs. 14.11 and 14.12).

All these features would be important findings on imaging as they would influence the surgical approach [32–37].

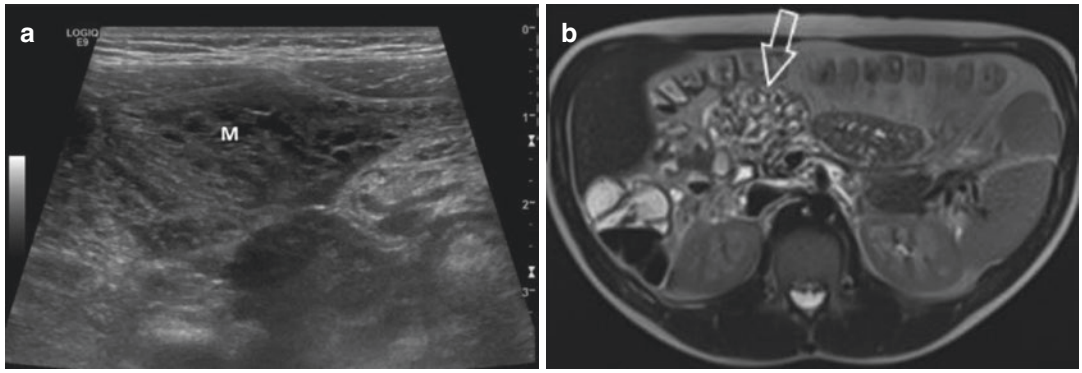

Fig. 14.12 Microcystic lymphangioma. (**a**) US—Transverse scan or the mid abdomen. A multiseptated microcystic mass occupies the anterior part of the abdomen. (**b**) MR imaging, T2-weighted sequence demonstrates a multicystic mass within the mesenteric fat, just below the transverse colon

14.7.2 Mixed and Solid Type Tumors

In case of abdominal solid or mixed type tumors, the classical renal or adrenal tumors must be considered first. Metastatic diseases extending to the peritoneum have to be considered thereafter as they are the most common peritoneal tumors. The primitive tumors leading to metastasis are more likely to be sarcoma.

Primary peritoneal tumors are rare; most are mesenchymal in origin (Table 14.1). They may grow and become very large before that symptoms appear. The tumors may appear as focal mass or diffuse disease.

Peritoneal tumors must be differentiated from tumors arising from the pelvis or the retroperitoneum mainly neuroblastoma, pelvic rhabdomyosarcoma, and ovarian (malignant) tumors. Unfortunately there are few characteristics that help to differentiate between all types of masses [(27).]

Some features of the "commonest" among primitive peritoneal masses can be underlined:

- *Inflammatory myofibroblastic tumor* may originate from any site but particularly in the lung, the mesentery, and omentum. It is considered as a neoplasm. The imaging findings are variable and nonspecific. The mass can induce intestinal obstruction [27].

Table 14.1 Peritoneal solid or mixed type tumors

Focal masses
– Inflammatory myoblastic tumor
– Castleman disease
– Mesenteric fibromatosis
– Lipoma
– Neurofibroma
– Mesenteric hemangioma
Diffuse disease
– Desmoplastic small round cell tumor
– Burkitt lymphoma
– Rhabdomyosarcoma
– Hemangiomatosis
– Diffuse microcystic lymphangioma/lymphatic disease

- *Extraosseous Ewing sarcoma* developing within the mesentery is a rare soft-tissue tumor that is part of the Ewing sarcoma family of tumors. They are characterized by their small round blue cells (on histology) and include osseous Ewing sarcoma, extraosseous Ewing sarcoma, primitive neuroectodermal tumor (PNET), and Askin tumor. These tumors appear similar to desmoplastic small round cell tumor. Immunohistochemical and genetic studies are necessary in order to differentiate between them.
- When developing within the peritoneum and mesentery, the tumors tend to grow rapidly, invade the bowel walls, and develop metastasis (Fig. 14.13). They also may induce compression of the urinary tract [27, 38].

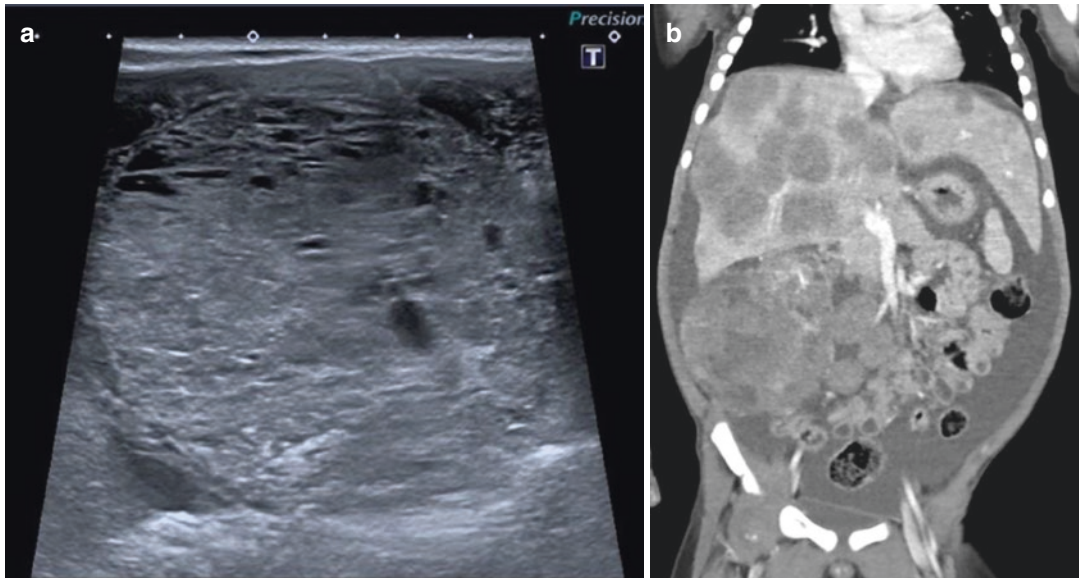

Fig. 14.13 Extraosseous Ewing's sarcoma 1-year-old boy. (**a**) US Transverse scan of the left flank—An echogenic microcystic mass is demonstrated. (**b**) CE-CT Frontal reformatted view. The lobulated mass enhances partially; there are liver metastases and ascites

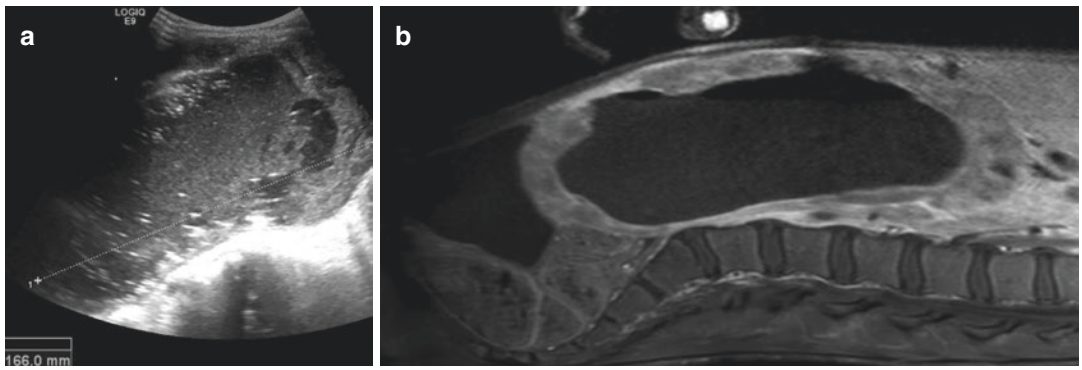

Fig. 14.14 Burkitt Lymphoma—Localized necrotic type in a 14-year-old boy. (**a**) US: sagittal scan; huge 16 cm abdominal mass with necrotic center. (**b**) MR imaging post Gd T1-Weighted sequence—Enhancement of the peripheral wall of the necrotic mass

– *Rhabdomyosarcoma (RMS)* of the omentum and mesentery represents a small percentage of RMS in children. The tumor appears lobulated and may spread in the entire omentum leading to a so-called omental "cake" which is best visualized on cross-sectional imaging. Primary peritoneal tumors must be differentiated from pelvic disease extending to the abdomen [27, 39].
– *(Sporadic) Burkitt lymphoma* is the most common form of non-Hodgkin lymphoma and the most common malignancy involving the mesentery and omentum. It is predominantly an extranodal disease. Masses (large solitary or multiple)

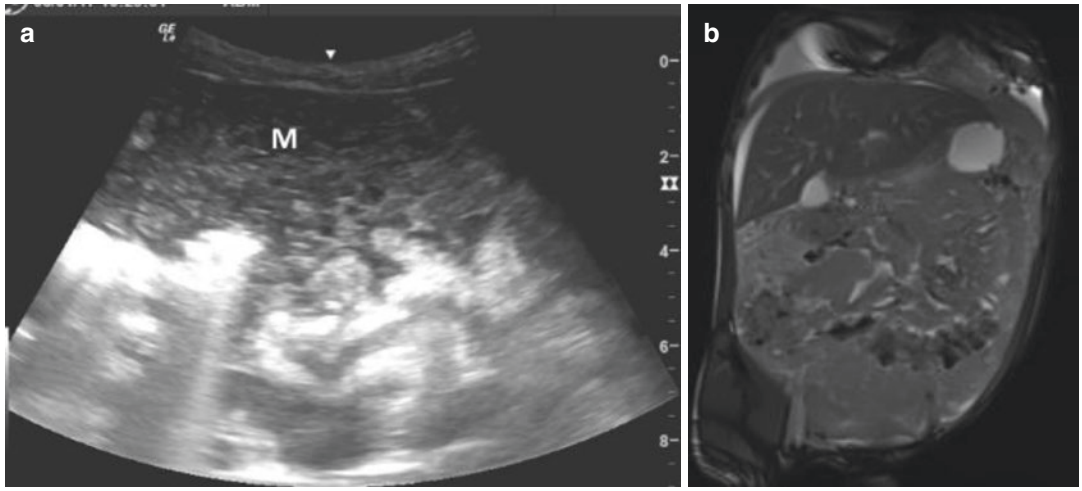

Fig. 14.15 Burkitt lymphoma diffuse type—7-year-old boy. (**a**) US—echogenic heterogeneous mass filling the anterior peritoneal space and displacing the bowel loops backwards. (**b**) MR imaging—T2-weighted sequence—Frontal view. The entire peritoneal cavity, especially in the pelvis (so-called "cake pattern"), is filled with tumor, the bowel loops are displaced to the midline. Note the presence of perihepatic ascites and pleural effusion

are found in 31–64%, most arise in the ileocecal region. Bowel involvement is frequent and the mural masses serve as lead points for intussusception. Central necrosis represents a typical finding on imaging as well as mesenteric vessel encasement (Fig. 14.14). Peritoneal seeding and ascites may develop (Fig. 14.15). Lesions may develop in the kidneys, ovaries, and breasts.

On US, the tumors will appear as hypoechoic (large) masses with central necrosis (Fig. 14.14a) or as diffuse peritoneal invasion ("peritoneal cake") (Fig. 14.15a). Bowel wall thickening or mural masses are best evaluated by CT or MR (Figs. 14.14b and 14.15b) imaging [27].

– *Infantile hemangioma* is high flow vascular neoplasm that may arise in any body site including the mesentery. They are rarely congenital and most develop during the first weeks of life. At US, infantile hemangioma appears as a localized mass or as diffuse thickening of the mesentery. Hypo- or echogenic patterns have been reported (Fig. 14.16a). The anatomical area involved appears highly hypervascularized containing large vessels, branches of the mesenteric vessels (Fig. 14.16a, b). Low resistance arterial waveforms are usually demonstrated at spectral Doppler. At CE-CT, enhancement is massive after contrast injection. At MR imaging, the masses may appear partially cystic and septated; enhancement is massive as well (Fig. 14.16c) [27, 40].
– *Lipoma* is rare in the mesentery but can be found anywhere. Lesions greater than 2 cm can cause abdominal pain, GI bleeding, intussusception, and bowel obstruction. Larger lipoma can twist around their vascular pedicle (Fig. 14.7), leading to ischemia and infarction. Imaging may show lesional or perilesional hemorrhage, surrounding inflammatory changes as edema and fat stranding. Torsion of a lipoma must be differentiated from omental torsion. The location should help for this differentiation [41].

Conclusions

Although rare mesenteric and omental pathologies should be considered in case of abdominal acute conditions especially, abscesses, tumors, and intestinal obstruction.

US first, CT and MR imaging thereafter should be used to differentiate between all potential diseases.

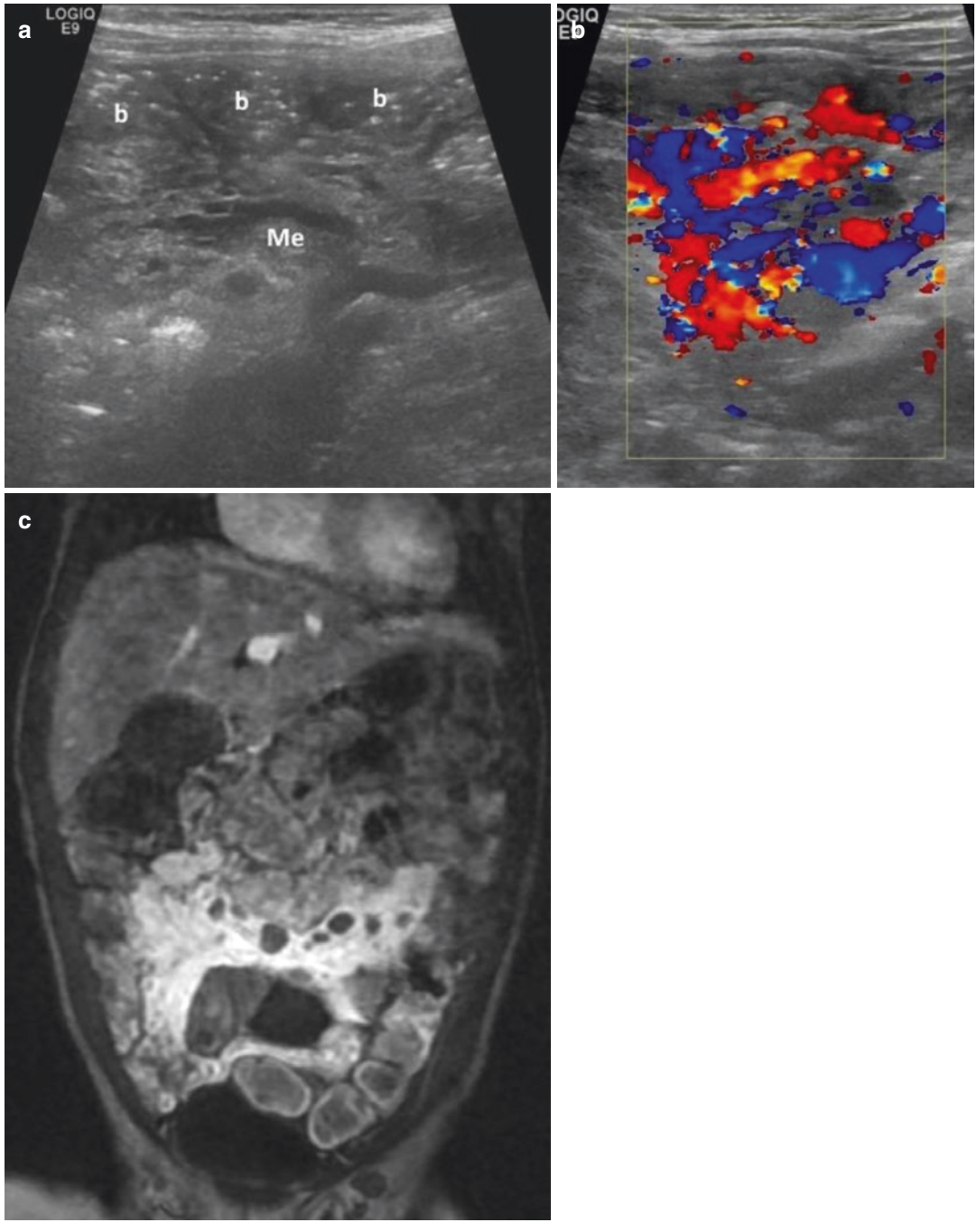

Fig. 14.16 Mesenteric hemangioma in a 2-year-old girl. (**a**) US—Mid-abdomen scan—thickened mesentery with large vessels. (**b**) Color Doppler—impressive hypervascularization. (**c**) MR imaging—T1-weighted post Gd—Important hypersignal of the mesentery. Signal voids due to enlarged vessels

References

1. Meyers AM. Clinical anatomy of the abdomen. In: Meyers MA, Charnsang C, Oliphant M, editors. Meyer's dynamic radiology of the abdomen. 6th ed. Berlin: Springer; 2011. p. 23–40.
2. Tirkes T, Sandrasegaran K, Patel AA, et al. Peritoneal and retroperitoneal anatomy and its relevance for cross sectional imaging. Radiographics. 2012;32:437–51.
3. Blackburn SC, Stanton MP. Anatomy and physiology of the peritoneum. Semin Pediatr Surgery. 2014;23:326–30.
4. Siegel MJ. Spleen and peritoneal cavity. In: Siegel MJ, editor. Pediatric sonography. 4th ed. Philadelphia, PA: Wolter Kluwer Health Publisher; 2011. p. 305–38.
5. Jecquier S, Jecquier JC, Hanquinet S. Intraperitoneal fluid in children: normal US findings depend on which scan head you use. Pediatr Radiol. 2003;33:86–91.
6. Beierle EA, Chen MK, Whalen TV, et al. Free fluid on abdominal CT scan after blunt trauma does not mandate exploratory laparotomy in children. J Pediatr Surg. 2000;35:990–2.
7. Sivit CJ. Significance of peritoneal fluid identified by US examination in children with acute abdominal pain. J Ultrasound Med. 1993;12:743–6.
8. Vallerie AM, Lerner JP, Wright JD, et al. Peritoneal inclusion cysts: a review. Obstet Gynecol Survey. 2009;63:321–4.
9. Kariyattil R, Steinbok P, Shingal A, et al. Ascites and abdominal pseudocysts following ventriculoperitoneal shunt surgery: variations of the same theme. J Neurosurgery. 2007;106:350–3.
10. Roach JP, Partrick DA, Bruny JL, et al. Complicated appendicitis in children: a clear role for drainage and delayed appendicectomy. Am J Surg. 2007;194:769–72.
11. Dinler G, Sensoy G, Helek D, et al. Tuberculous in children: report of nine patients and review of the literature. World J Gastroenterol. 2008;14:7235–9.
12. Tan FL, Loh D, Prabjakaran K. Sclerosing encapsulating peritonitis in a child secondary to peritoneal dialysis. J Pediatr Surg. 2005;40:e21–3.
13. Nam SH, Kim SC, Kim DY, et al. Experience with meconium peritonitis. J Pediatr Surg. 2007;42:1822–5.
14. Uncu N, Bulbul M, Yildiz N, et al. Primary peritonitis in children with nephrotic syndrome: results of a 5-year multicenter study. Eur J Pediatr. 2010;169:73–6.
15. Nielsen KR, Ejletsen T, El-Batran S, et al. A five-year survey of pneumococcal peritonitis in two Danish counties – incidence, diagnosis and clinical entities. Clin Microbiol Infect. 2003;9:738–40.
16. Toorenvliet B, Vellekoop A, Bakker R, et al. Clinical differentiation between acute appendicitis and acute mesenteric lymphadenitis in children. Eur J Pediatr Surg. 2011;21:120–3.
17. Kamarzyn B, Werner EA, Rejaie B, et al. Mesenteric lymph nodes in children: what is normal and what is abnormal. Pediatr Radiol. 2005;35:774–7.
18. Bae SH, Park SJ, Kim WS, et al. Mesenteric panniculitis in a thirteen old Korean boy treated with prednisolone: a case report. Pediatr Gastroenterol Hepatol Nutr. 2016;19:143–6.
19. Mavridis G, Livatidi E, Nikolaos B, et al. Primary omental torsion in children: ten year experience. Pediatr Surg. 2007;23:879–82.
20. Redmond P, Sawaya DE, Miller KH, et al. Epiploic appendagitis: a rare case of acute abdominal pain in children. Report of a case and review of the pediatric literature. Pediatr Emerg Care. 2015;31:717–9.
21. Savin T, Kurpios NA, Shyer AE, et al. On the growth and form of the gut. Nature. 2011;476:57–62.
22. Strouse PJ. Disorders of intestinal rotation and fixation (malrotation). Pediatr Radiol. 2004;34:837–51.
23. Marine MB, Karmazyn B. Imaging of malrotation in the neonate. Semin Ultrasound CT MRI. 2014;35:555–70.
24. Graziano K, Islam S, Dasgupta R, et al. Asymptomatic malrotation: diagnosis and surgical management: an APSA outcomes and evidence based practice committee systematic review. J Pediatr Surg. 2015;50:1783–90.
25. Tang V, Daneman A, Navarro OM, et al. Internal hernia in children: spectrum of clinical and imaging findings. Pediatr Radiol. 2011;41:1559–68.
26. Villalona GA, Diefenbach KA, Touloukian RJ. Congenital and acquired mesocolic hernias presenting with small bowel obstruction in childhood and adolescence. J Pediatr Surg. 2010;45:438–42.
27. Chung EM, Biko DM, Arzamendi AM, et al. Solid tumors of the peritoneum, omentum and mesentery in children: radiologic- pathologic correlation. Radiographics. 2015;35:521–46.
28. Chang TS, Ricketts R, Abramowsky CR, et al. Mesenteric cystic masses: a series of 21 pediatric cases and review of the literature. Fetal Pediatr Pathol. 2011;30:40–4.
29. Chavhan GB, Babyn P, Vasanawala SS. Abdominal MR imaging in children: motion compensation, sequence optimization and protocol organization. Radiographics. 2013;3:709–13.
30. Pokharel SS, Macura KJ, Kamel IR, et al. Current MR imaging lipid detection techniques for diagnosis of lesions in the abdomen and pelvis. Radiographics. 2013;33:681–702.
31. Humphries PD, Sebire NJ, Siegel MJ, et al. Tumors in pediatric patients at DW MR imaging: apparent diffusion coefficient and tumour cellularity. Radiology. 2007;245:848–54.

32. de Perrot M, Bründler M, Tösch M, et al. Mesenteric cysts; towards less confusion? Dig Surg. 2000;17:323–8.
33. Tan J, Tan K, Chew S. Mesenteric cysts: an institution experience over 14 years and review of the literature. World J Surg. 2009;33:1961–5.
34. Heaton TE, Liechty K. Postnatal management of prenatally diagnosed abdominal masses and anomalies. Prenat Diagn. 2008;28:656–66.
35. Oliveira C, Sacher P, Meuli M. Management of prenatally diagnosed abdominal lymphatic malformations. Eur J Pediatr Surg. 2010;20:302–6.
36. Kim S, Kim H, Lee C, et al. Clinical features of mesenteric malformation in children. J Pediatr Surgery. 2016;51:582–7.
37. Tuncer AA, Narci A, Dilek FH, et al. Benign cystic mesothelioma in a child: case report and review of the literature. Balkan Med J. 2016;33:232–4.
38. Shibuya S, Takamizawa S, Hatata T, et al. Extraosseous ewing sarcoma in the mesentery: the first report of cases in children. Pediatr Surg Int. 2015;31:995–9.
39. Leung RS, Calder A, Roebuck D. Embryonal rhabdomyosarcoma of the omentum. Pediatr Radiol. 2009;39:865–8.
40. Yang G, Li J, Jin H. Giant mesenteric hemangioma of cavernous and venous mixed type: a rare case report. BMC Surg. 2013;13:50.
41. Laguna BA, Iyer R, Rudzinski ER, et al. Torsion of a giant mesocolic lipoma in a child with Bannayan-Riley-Ruvalcaba. Pediatr Radiol. 2015;45:449–452.

Acute Hepato-Biliary Diseases in Children

15

Stéphanie Franchi-Abella and Danièle Pariente

Contents

15.1 Introduction

Acute hepato-biliary disorders may affect previously healthy children or children with known hepatopathy or other diseases. Acute presentation is variable usually nonspecific, associating: jaundice, abdominal pain, fever, nausea and vomiting, neurological impairment in case of hepatic encephalopathy or an abdominal mass. Biological tests will provide information regarding the severity of the disorder, its mechanisms (biliary obstruction versus hepatocyte disorders), the presence of infection, raised tumoral markers, etc.

Imaging has a key role to make the diagnosis of the disorders and associated abnormalities, to search for complications. It can be useful to guide treatment.

Interventional radiology plays a role in the management of some of these disorders.

15.2 Imaging Work-Up

Ultrasonography (US) with high-resolution transducers adding color- and pulsed-Doppler is the imaging modality of choice. The real time capacity of US associated with the high spatial resolution of this technic allows very high quality and detailed demonstration of the anatomical structures. The use of Doppler provides important information on hemodynamics.

Liver MR imaging is an important imaging modality for assessing both the liver parenchyma

S. Franchi-Abella (✉) • D. Pariente
Department of Paediatric Radiology, Hôpital Bicêtre-Hôpitaux Universitaires Paris-Sud – Assistance Publique Hôpitaux de Paris,
78 Rue Du General Leclerc, 94275 Le Kremlin-Bicêtre, France
e-mail: stephanie.franchi@aphp.fr; daniele.pariente@aphp.fr

F.E. Avni, P. Petit (eds.), *Imaging Acute Abdomen in Children*,
https://doi.org/10.1007/978-3-319-63700-6_15

and the biliary tract. The smallest coil available, adapted to the size of the abdomen of the child should be selected to increase spatial resolution. Baseline protocol including usual T2- and T1-weighted acquisitions in the axial plane should be performed. If the biliary tract anatomy needs to be assessed, 2D and 3D MR cholangio-pancreatography (MRCP) should be performed. Gadolinium injection is necessary for the characterization of liver masses or vascular disorders.

Computed Tomography (CT) is indicated in case of vascular disorders and for the work-up of tumors in order to confirm the diagnosis as well as for the vascular mapping before interventional radiology or surgery.

The aim of the examination is to evaluate [1]:

- The liver: size, margins, parenchyma (homogeneous/heterogeneous), presence of nodules,
- The biliary tract: dilatation of intrahepatic and/or extrahepatic bile ducts, aspect of the gallbladder (size, wall, content), etc.
- The vascular network: hepatic veins and inferior vena cava, main portal vein and portal branches, hepatic artery, ductus venosus.
- The signs of portal hypertension: demonstration of hepatofugal veins, patent ductus venosus after the age of 1 month, or patency of paraumbilical vein, thickened small omentum, splenomegaly.
- All other intraabdominal organs and vessels.

15.3 Classical Presentations on Imaging

15.3.1 Obstructive Cholestasis and Diseases of the Gallbladder and the Bile Ducts

15.3.1.1 Cholelithiasis

The usual acute presentation of cholelithiasis in children is jaundice with or without pain that progresses to symptoms similar to cholecystitis. Right upper quadrant pain with fever is common. Acute secondary pancreatitis is also possible.

Once considered rare, common bile duct stones have become more frequent in children because of the higher prevalence of obesity. There is a variety of known predisposing factors that are summarized in Table 15.1.

Abdominal US is the key examination as it will demonstrate easily bile ducts dilatation and the presence of stones or sludge in the gallbladder and in the bile ducts. The extrahepatic bile duct diameter varies with age from less than 1.5 mm before the age of 1 year to less than 3.5 mm in teenagers (Fig. 15.1).

When US is inconclusive because no stone is visible or when there is a suspicion of underlying biliary malformation (mostly pancreatico-biliary maljunction also called abnormally long common bilio-pancreatic duct), MRCP can be helpful; it may depict small stones localized at the end of the common bile duct and show the bilio-pancreatic duct that should measure less than 5 mm long (Figs. 15.1 and 15.2) [2].

As in adults, an endoscopic or surgical treatment is applied in symptomatic patients especially those having a predisposing factor.

15.3.1.2 Biliary Malformations-Choledochal Cyst

Biliary malformations may present acutely with abdominal pain, or evidence of pancreatitis and cholestasis. The most frequent malformation is probably the pancreaticobiliary maljunction (PBM) in which the pancreatic and the bile ducts join anatomically outside the duodenal wall with a

Table 15.1 Causes of gallstones in children

Causes of gallstones in childhood
• Hemolytic anemia
• Infection
• Dehydration
• Cirrhosis
• Cystic fibrosis
• Wilson's disease
• Crohn's disease and ileal resection
• Parenteral nutrition
• Drugs: furosemide and ceftriaxone
• Biliary tract obstruction (choledochal cyst, sclerosing cholangitis)
• Caroli's disease
• Obesity
• Familial history
• Metachromatic leukodystrophy

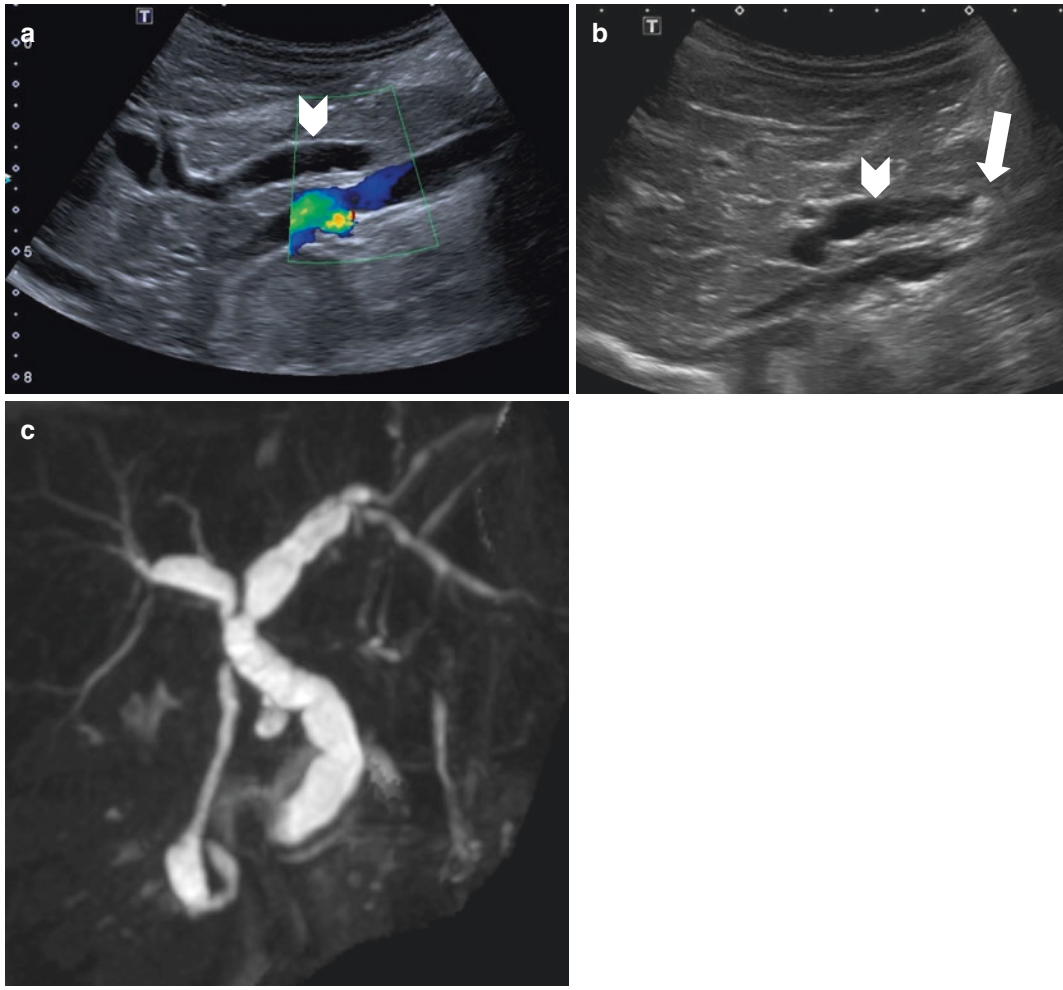

Fig. 15.1 Cholelithiasis. Seven-year-old girl presenting with acute abdominal pain and jaundice. (**a**) US shows a marked dilatation of intra an extra-hepatic bile ducts (*head-arrow*). (**b**) With a hyperechoic stone at the end of the common bile ducts (*arrow*). (**c**) After spontaneous migration of the stone in the bowel, MRCP performed to search for an underlying bilio-pancreatic malformation shows the normal aspect of the biliary tree and the bilio-pancreatic junction

common pancreatico-biliary duct measuring more than 6 mm. Therefore reciprocal reflux of bile and pancreatic juice occurs resulting in various complications: dilatation of extra-hepatic bile ducts (choledochal cyst) with or without obstruction, biliary stones, abdominal pain, pancreatitis and biliary or pancreatic cancers in older patients [3].

In most cases, the initial US will reveal variable degrees of extra- ± intrahepatic bile ducts dilatation, with or without stones as well as signs of pancreatitis. In some cases, PBM might be demonstrated with US. Still in most cases, MRCP is the key examination to confirm PBM (Fig. 15.2). Furthermore, this technique shows accurately the anatomy of bile ducts before surgery [2]. In doubtful cases, direct transhepatic puncture of the gallbladder can be performed and will allow direct opacification of the biliary tract and of the PBM. During the puncture, the level of amylase can be evaluated and confirm the diagnosis, as it is very elevated in the bile in most cases [4].

If the obstruction is complete or associated with infection or major pain, biliary drainage may be indicated prior to surgery (see Sect. 15.4.2). Surgery consists of complete resection of the extrahepatic bile duct and the gallbladder

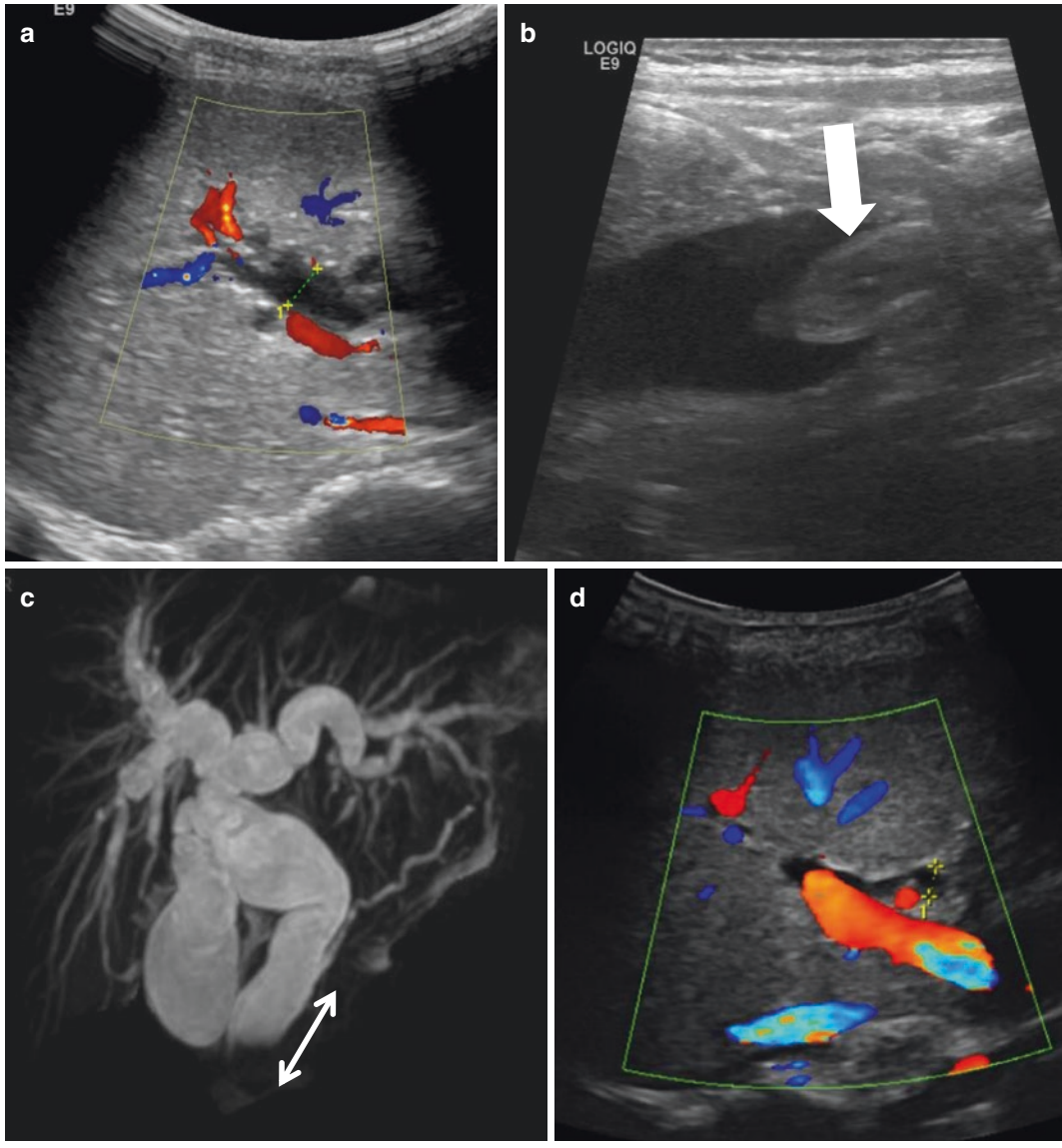

Fig. 15.2 Choledochal cyst. 2.5-year-old boy presenting with intense abdominal pain and jaundice. (**a**) US shows a marked dilatation of intrahepatic and extrahepatic bile ducts. (**b**) with sludge at the end of the common bile duct. There was a high suspicion of choledochal cyst with acute obstruction by the sludge (*arrow*). (**c**) MRCP confirms the diagnosis showing a pancreatico-biliary maljunction with an abnormally common bilio-pancreatic duct measuring 15 mm (*double arrow*). (**d**) Spontaneous resolution of the pain and the jaundice. (**d**) US control shows the dramatic decrease of the diameter of the common bile duct. Note that the dilatation of the choledochal cyst may be very mild in the absence of obstacle

with hepatico-jejunostomy. This surgery is also performed in order to prevent tumoral transformation. In most cases, the prognosis is good. Stenosis of the bilio-digestive anastomosis may happen; postoperative US follow-up is mandatory to detect postoperative bile ducts dilatation.

The main differential diagnosis of biliary tract malformation during childhood is cholelithiasis without underlying malformation (see15.3.1.1).

15.3.1.3 Varia: Extrinsic Compression, Cholangitis

In exceptional cases, initial imaging will reveal an intra-biliary tumor (rhabdomyosarcoma), an extrinsic compression by a mass (tumor, duodenal duplication, etc.) or diffuse abnormalities of the bile ducts that may reveal sclerosing cholangitis (especially in the context of inflammatory bowel disease, Langerhans cells histiocytosis, immunodeficiency disorders or autoimmune hepatitis, IgG4 syndrome) (Fig. 15.3). In case of sclerosing cholangitis, subsequent MRCP will be very useful to search for irregular dilatation of bile ducts and thickening of bile ducts. The prognosis is usually poor leading to biliary cirrhosis.

15.3.1.4 Gallbladder Abnormalities

Usually revealed by right upper quadrant pain, acute abnormality of the gallbladder is usually first confirmed on US.

Hydrops of the gallbladder consists in an acute distension without any mechanical obstruction of the cystic duct. On US, the gallbladder appears distended, with thin walls and anechoic content. It may be associated with numerous disorders such as scarlet fever, streptococcus, salmonella and Shigella infection, Kawasaki disease, leptospirosis, extensive burning, polyarteritis nodosa, familial paroxysmal polyseritis and prolonged parenteral nutrition. Spontaneous resolution is the usual outcome. Perforation is rare but may occur (Fig. 15.4).

Acute acalculous cholecystitis is usually revealed by abdominal pain of the right upper quadrant and fever. It is defined by the presence of a large gallbladder with at least two of the following three criteria on US: increased gallbladder wall thickening (>3.5–4 mm), pericholecystic fluid and the presence of sludge. It is the most frequent type of cholecystitis in children. It may develop in previously healthy and non-critically ill children. It is related in most cases to viral infection: hepatitis A virus (HAV) and Epstein Barr virus (EBV) hepatitis in most cases. The prognosis is good. Association with Kawasaki disease is also reported; the hepatobiliary involvement is associated with coronary artery disorders (see Sect. 15.3.2.5). Acalculous cholecystitis can develop also in critically ill children or post-surgery patients or be associated with severe bacterial infection. Conservative treatment is the rule. Percutaneous cholecystostomy can be proposed in selected cases. In very exceptional cases, rupture may happen (Fig. 15.4).

Thickening of the gallbladder wall may also be encountered in association with ascites, hypoalbuminemia, portal hypertension, and cardiac failure [5, 6].

15.3.2 Acute Hepatobiliary Disease

15.3.2.1 Acute Liver Failure

Acute liver failure is very rare in infants and children. Patients present with aspecific symptoms such as nausea, vomiting, weakness, anorexia, jaundice, pruritus, and fever. In severe cases, seizure and encephalopathy may develop.

The aims of imaging the liver must be to look for (Fig. 15.5):

- Signs of chronic liver disease that may suggest an underlying unknown disease,
- Involvement of other organs indicative of some specific diagnosis: for instance, enlarged lymph nodes suggestive of a hemopathy,
- Signs of portal hypertension such as persistent patent ductus venosus, thickened small omentum with or without direct visualization of the left gastric vein that may be enlarged with hepatofugal flow, hepatofugal portal flow, splenomegaly, etc. [1].

Whatever the etiology, common findings on imaging will be: enlarged liver, ascites and thickened gallbladder wall.

Usual etiologies and suggestive patterns on abdominal imaging are listed in Table 15.2 [7].

15.3.2.2 Infection

Liver infections are severe conditions that usually present acutely and may be fatal. Viral hepatitis is the most common diffuse infection of the liver in otherwise healthy children. Imaging plays a role in severe presentations or in complications. Bacterial liver infection may present as

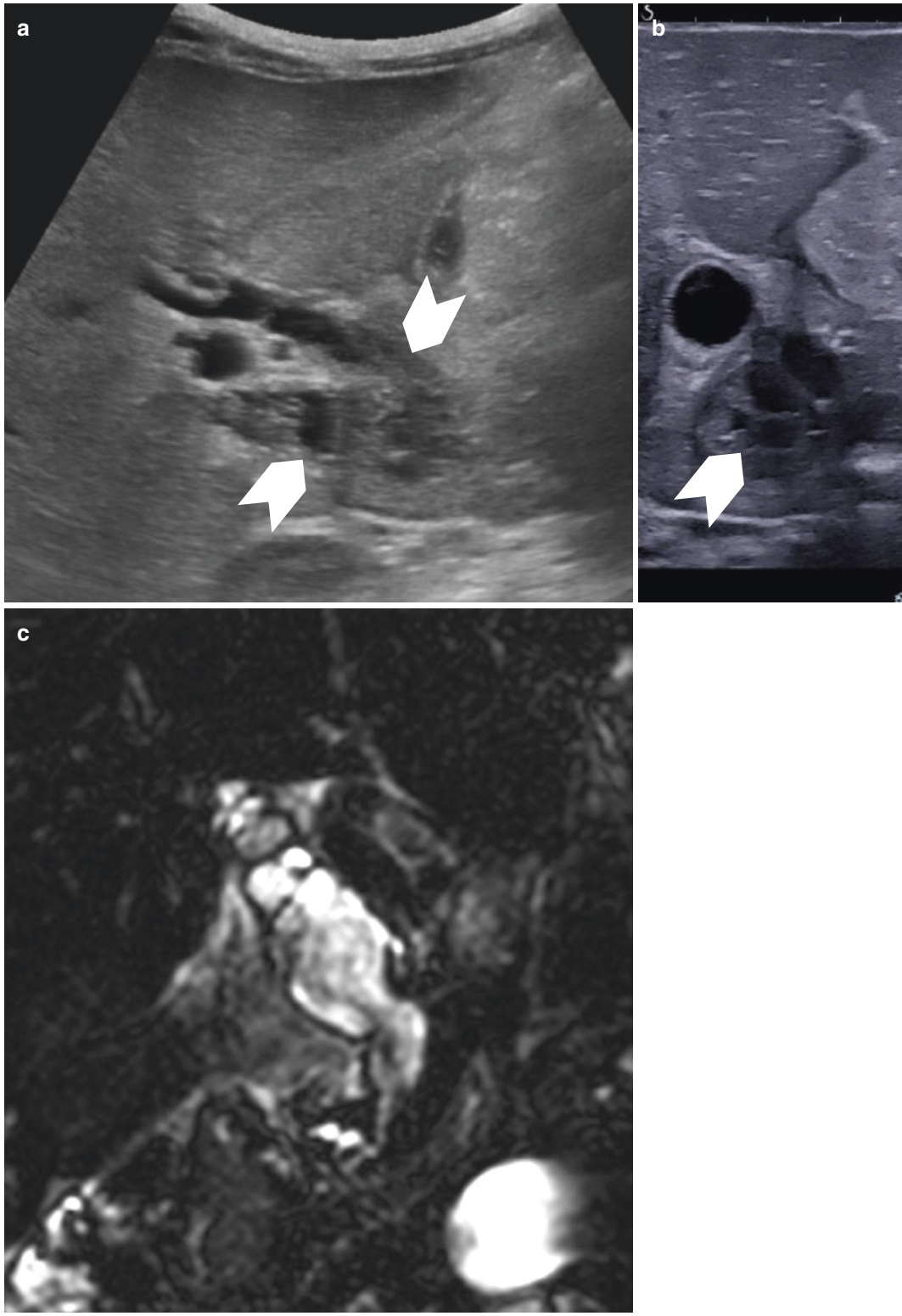

Fig. 15.3 Biliary rhabdomyosarcoma. Four-year-old boy presenting acute acholic stools and jaundice. (**a**) US shows the marked dilatation of intra and extrahepatic bile ducts with solid tissue (*arrows*) visible at the end of the common bile duct. (**b**) US shows the extension in the cystic duct as well (*arrow*). (**c**) MRCP shows the presence of abnormal tissue in the extrahepatic bile duct with a high signal intensity on T2-weighted imaging

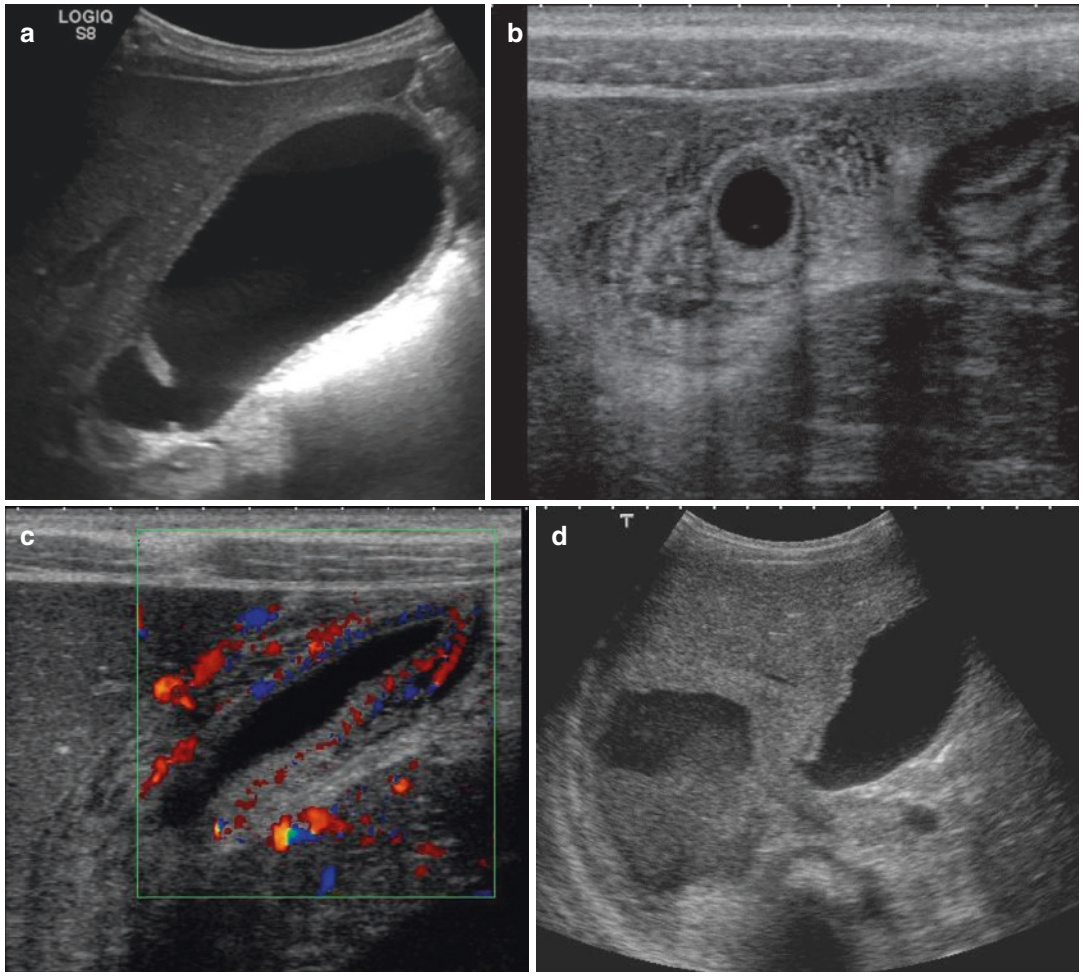

Fig. 15.4 Hydrocholecystis and acalculous acute cholecystitis, aspects on US. (**a**) Distended gallbladder with thin walls and anechoic content consistent with a hydrocholecystis associated with Kawasaki disease. (**b**) and (**c**) Thickened and hypervascularized gallbladder walls consistent with an acalculous acute cholecystitis in a context of autoimmune hepatitis. (**d**) Collection revealing the spontaneous perforation of hydrocholecystis associated with hepatitis A

pyogenic abscess, granulomatous disease or diffuse infection. Parasitic infections are also possible and may involve the biliary tree (ascariasis) or the parenchyma (echinococcosis or amebiasis). Immunocompromised patients are more susceptible to other infectious agents especially fungus. Imaging plays a key role in the early detection, characterization, and management of these severe conditions.

Viral Hepatitis

Most viral hepatitis in infants and children are caused by Hepatitis viruses or EBV. However a number of other viruses have been implicated in childhood hepatitis such as mumps, measles, Varicella zoster virus, herpes simplex virus, and cytomegalovirus.

The diagnosis relies on clinical data and biology.

Imaging can search for a cause of hepatic failure and for complications. US may show an enlarged heterogeneous liver with periportal hyperechogenicity related to peri-portal edema. The wall of the gallbladder may be thickened. Lymphadenopathies may be present along the hepatic pedicle (Fig. 15.4).

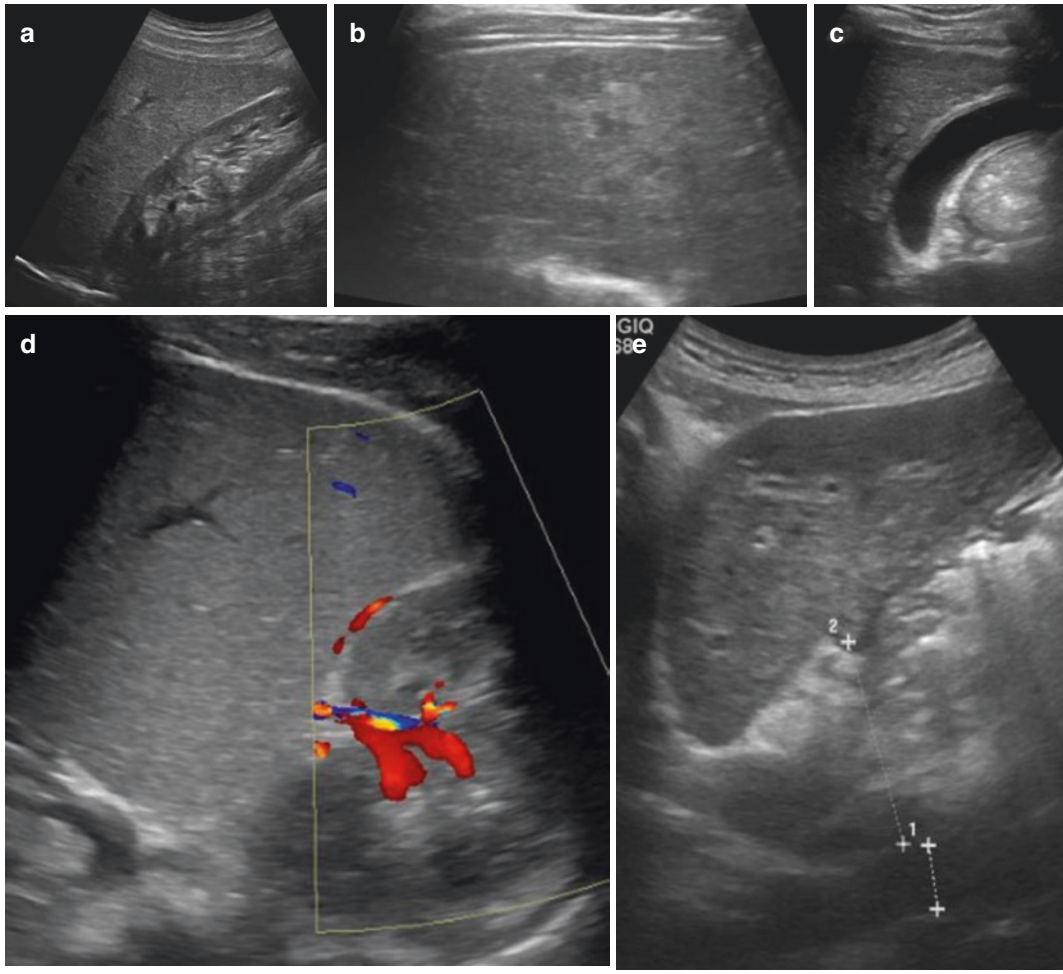

Fig. 15.5 Acute liver failure revealing underlying chronic liver disease (Wilson disease) in two different patients. (**a**) Examination with curvilinear probe shows a hyperechoic liver probably steatotic with normal size and regular margins. (**b**) High-resolution examination with high frequency probe shows that the parenchyma is heterogeneous. (**c**) Irregular margins of the liver clearly visible along the gallbladder. (**d**) Spontaneous spleno-renal shunts consistent with portal hypertension. (**e**) Thickened small omentum consistent with portal hypertension

CT or MR imaging should be performed in severe cases especially if liver transplantation is planned. They can show peri-portal hypodensity/hyperintensity on T2-weighted imaging and heterogeneous liver parenchyma. Sometimes the whole liver will appear hypointense on T1-weighted imaging and hyperintense on T2-weighted imaging [8].

Bacterial Infection

Liver Abscess

Pyogenic abscesses are rare in children. The pathogenesis of liver abscesses is multifactorial; they can result from ascending cholangitis, hematogenous dissemination from a gastrointestinal infection (via the portal vein) or from disseminated (via the hepatic artery), or through contiguous spread.

Hepatic abscesses have mainly been reported in immunocompromised children with chronic granulomatous disease, bone marrow transplant, immunosuppressive chemotherapy congenital or acquired immunodeficiency, or in children with intraabdominal infection. Yet, liver abscess can occur without any predisposing factor.

Clinical presentation is not specific but may include hepatomegaly with tenderness, fever

Table 15.2 causes of acute liver failure and suggestive patterns on imaging [7]

			Imaging suggestive patterns
Infants	Infectious	Hepatitis A, hepatitis B, NANB hepatitis, HSV	Acalculous cholecystitis
	Drugs and toxins	Acetaminophen, valproate, isoniazid	
	Metabolic	Hereditary fructose intolerance, mitochondrial disorders, tyrosinemia	Large kidneys
	Immune	Autoimmune hepatitis, macrophage activation syndrome, hemophagocytic syndrome	
	Abnormal perfusion	Congenital heart disease, myocarditis, severe asphyxia, vascular or anatomic abnormality	Dilatation of hepatic veins, obstruction of hepatic veins or portal veins, heterogeneity of liver parenchyma
	Other	Malignancy	Mass, lymph nodes, liver may be homogeneous
Children	Infectious	Acute viral hepatitis A/B, NANB hepatitis, EBV	Acalculous cholecystitis
	Drugs and toxins	Acetaminophen, valproate, isoniazid	
	Immune	Autoimmune hepatitis, macrophage activation syndrome, hemophagocytic syndrome	
	Abnormal perfusion	Budd-Chiari syndrome, congenital heart disease, myocarditis, severe asphyxia, vascular or anatomic abnormality	Stenosis or thrombosis of hepatic or portal veins Dilatation of portal vein Abnormal pulsed-Doppler pattern Signs of chronic liver disease
	Metabolic	Wilson's disease	Large gallbladder Sludge, stones
	Other	Malignancy, hyperthermia	Mass, lymph nodes may be homogeneous

(70–90% of patients) and biological signs of infection.

In most patients, the infection is usually polymicrobial aero- or anaerobic. Infective organisms are usually Staphylococcus aureus (50% of the cases), Streptococcus, Escherichia coli, Enterococcus faecalis, Klebsiella, Enterobacter, Pseudomonas organisms, and salmonellae [9].

Abdominal US is the first examination to perform and will show in most cases a solitary mass with variable patterns ranging from a well-defined, homogeneous, hypoechoic or fluid containing mass to a poorly defined, heterogeneous mass. Pleural effusion with lung condensation may be associated. On CE-CT, the typical aspect is the "double target sign" with a central low attenuation fluid-filled area surrounded by a high attenuation inner ring and a low-attenuation outer ring. The inner layer shows early contrast enhancement that persists on the delayed phase whereas the outer ring enhances only during the delayed phase.

On MR imaging, hepatic abscesses typically show central low T1-weighted and high T2-weighted signal intensity. The double target sign on T2-weighted appears as an isohypointense inner layer and a hyperintense outer layer. Enhancement is similar to the one observed on CT. Perilesional edema can appear as high signal intensity on T2-weighted. High intensity on DWI with decrease of apparent diffusion coefficient (ADC) is usually seen.

On dynamic CT and MR imaging, a transient, early, wedge shaped or circumferential segmental region of hepatic enhancement, which equilibrates in late phase, can be associated with liver

abscess and reflects perfusion disorders of the surrounding liver probably related to the compression or thrombosis of adjacent portal veins (Fig. 15.6) [8].

The different complementary examinations must search for an infection at the origin of or associated with the liver abscess. If no source is discovered, an underlying predisposing disorder such as immunodeficiency must be searched.

Gas can be present within the mass and may raise the possibility of a gastrointestinal fistula or anaerobic infection (Fig. 15.10).

Management of pyogenic liver abscesses includes antibiotic therapy and percutaneous drainage if the abscess is large enough (>5 cm) [10] (see Sect. 15.4.3).

Bacterial Granulomatosis Liver Disease

The most frequent bacterial granulomatosis liver disease is related to cat-scratch disease also called bartonellosis. It is an infection caused by Bartonella henselae that is introduced into human host through a scratch or a bite from a cat. Disseminated infection is seen in 5–10% of cases and may involve the liver, the spleen, the lymph nodes, the skeleton, and more rarely the brain. Patients may present with unexplained fever and bad general condition.

Hepatic bartonellosis is characterized by multiple necrotizing granulomas usually small (<3 cm), with or without splenomegaly.

The radiologic features are not specific, consisting of multiple hypoechoic micronodules on US, hypodense on CT and with hyperintensity on T2-weighted and hypointensity on T1-weighted on MR. Enhancement after contrast injection may be absent, may be homogeneous or with a rim enhancement (Fig. 15.7).

Association with similar nodules in the spleen and lymphadenopathies are suggestive of the diagnosis in immunocompetent children with no underlying disorder.

The diagnosis is suspected on the basis of the history of contact with a young cat and relies on serologic tests or PCR test or more rarely biopsy.

In most cases, spontaneous resolution is the rule with progressive disappearance of the nodule within 1–5 months. Residual hepatic and splenic calcifications can be observed.

Imaging features are not specific and may be encountered in sarcoidosis, some fungal affection, etc.

Parasitic Infection

Parasitic infections of the liver include parenchymal disorders with amebic abscesses or echinococ-

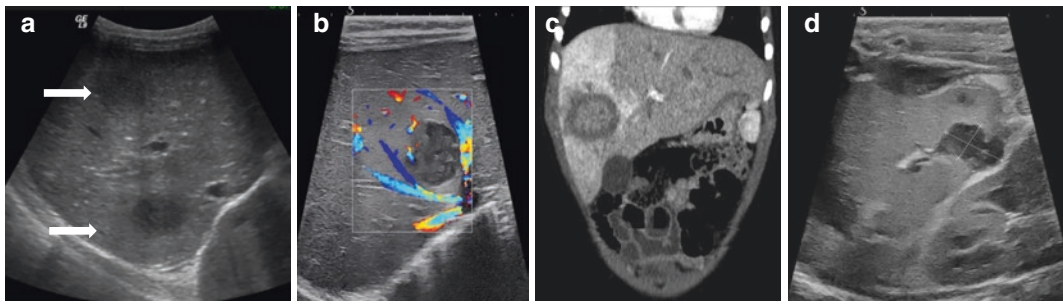

Fig. 15.6 Liver abscesses: 4-year-old girl presenting with acute abdominal pain and fever. (**a**) Initial US examination shows two hypoechoic rather well-defined hepatic nodules consistent with liver abscesses in the context. (**b**) Color Doppler demonstrates patency of the surrounding vessels. (**c**) CE-CT shows a well-defined isoattenuating central area with a hypoattenuating appearance of its peripheral wall (target-appearance). Note the associated wedge-shaped segmental region of hepatic enhancement, highly suggestive of liver abscess. Puncture and drainage of the largest abscess confirmed the diagnosis and showed the presence of Staphylococcus aureus. (**d**) US after direct puncture of one abscess that confirmed the diagnosis of liver abscesses with the presence of Staphylococcus aureus. Further investigation revealed chronic granulomatous disease

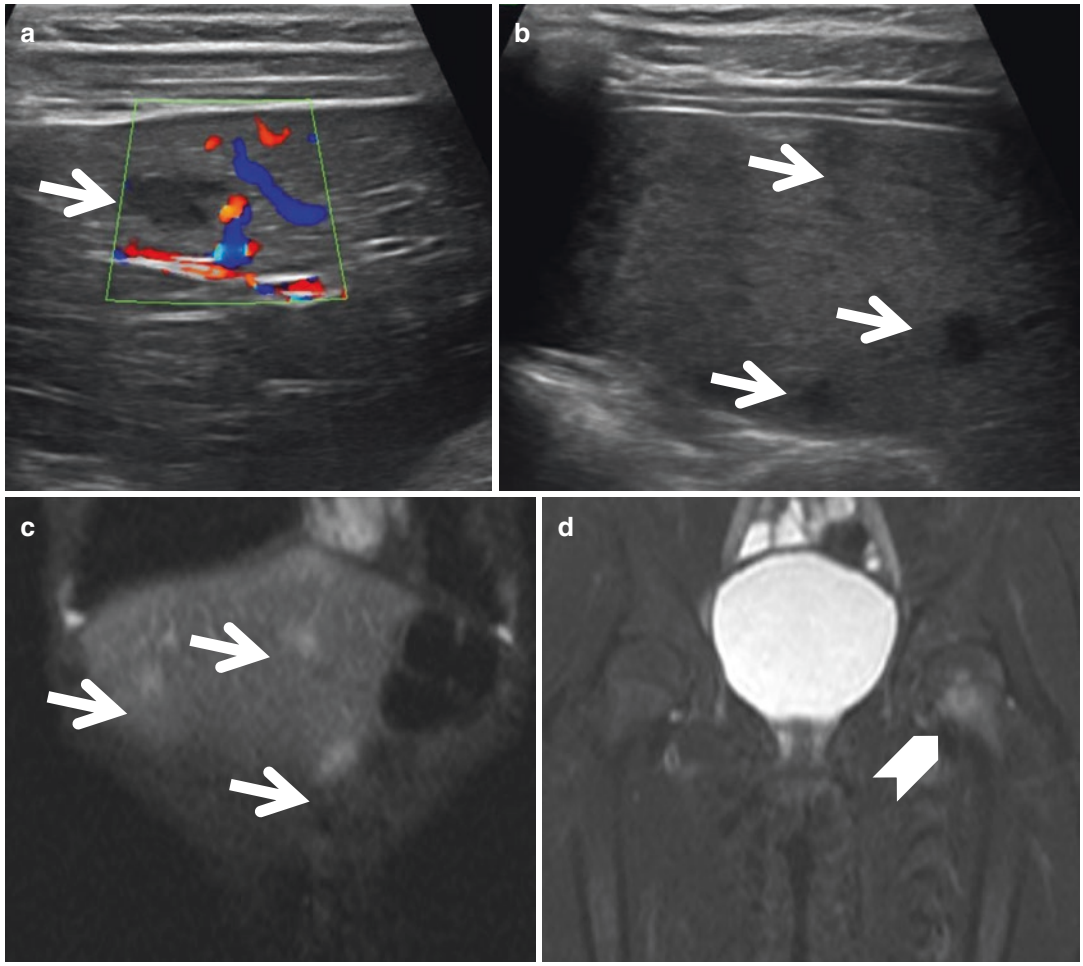

Fig. 15.7 Cat-scratch disease with hepato-splenic and bone involvement. Twelve-year-old girl with poor general state and fever for 3 weeks associated with bone pains. (**a**) Liver US shows multiple hypoechoic micronodules. (**b**) The same pattern is found in the spleen. (**c**) MRI shows hepatic micronodules with a hyperintensity on T2-weighted imaging. (**d**) There is also abnormal high signal intensities on T2-weighted imaging of the medulla of the left femoral neck. Cat scratch disease was confirmed with serology

cus infection and more rarely biliary involvement with Ascariasis and Distomatosis.

Entamoeba histolytica causes amebic liver abscess. This protozoan infection is endemic in Africa, Southeast Asia, Central and South America.

Patients usually present with right upper quadrant pain, fever, cough, and hepatomegaly.

At imaging, amebic abscess is usually solitary, unilocular with imaging features similar to pyogenic abscess. Intraabdominal extension of the liver abscess is possible [11].

Cystic echinococcosis (CE), also called hydatid cyst, is caused by Echinococcus granulosus. Human CE remains highly endemic in pastoral communities, particularly in regions of South America, the Mediterranean littoral, Eastern Europe, the Near and Middle East, East Africa, Central Asia, China, and Russia. Up to 80% patients have a single organ involved and a solitary cyst localized to the liver (4/5) or lungs (1/5).

The cyst may grow progressively or persist without changes for years. Clinical symptoms usually occur when the cyst compresses or ruptures into neighboring structures.

The diagnosis is based on clinical findings, imaging techniques, and serology. A definitive

diagnosis can be given by microscopic examination of the fluid and histology.

US examination has a key role for diagnosis and follow-up. A standardized classification proposed by the WHO-Informal Group on Echinococcosis (WHO-IWGE) allows a natural grouping of cysts into three relevant groups: active, transitional, and inactive, useful for management decision. Imaging features of hydatid cyst corresponds to the stage of cyst growth: unilocular, with daughter cysts, partially calcified or densely calcified. Biliary complications or rupture will be suspected on US.

CT and/or MR imaging with MRCP will give a precise mapping of the lesions and additional diagnostic criteria in doubtful cases. CT is the best exam to show calcifications that are highly suggestive for the diagnosis. MR imaging with MRCP will show biliary tract compression, distorsion or invasion by the mass [12] (Fig. 15.8).

Treatment indications are complex and are based on cyst characteristics, available medical/surgical expertise and equipment, and adherence of patients to long-term monitoring.

Management includes antiparasitic agents, percutaneous treatment, and surgery [12, 13] (see Sect. 15.4.3).

Parasitic infection such as Ascariasis and Fascioliasis may involve the liver and the biliary tree and present acutely with obstruction of the bile ducts leading to biliary colic, obstructive jaundice, or pancreatitis. US plays an important role in the diagnosis and the evaluation of complications. Ascariasis adult worms and flukes from fascioliasis can be directly seen in the bile ducts and the gallbladder; they would appear as non-shadowing, echogenic tubular structures sometimes with a longitudinal central echo-free line representing the gastrointestinal tract of the worm. Spontaneous movements of the worms are also visible. Hepatic fascioliasis manifests also

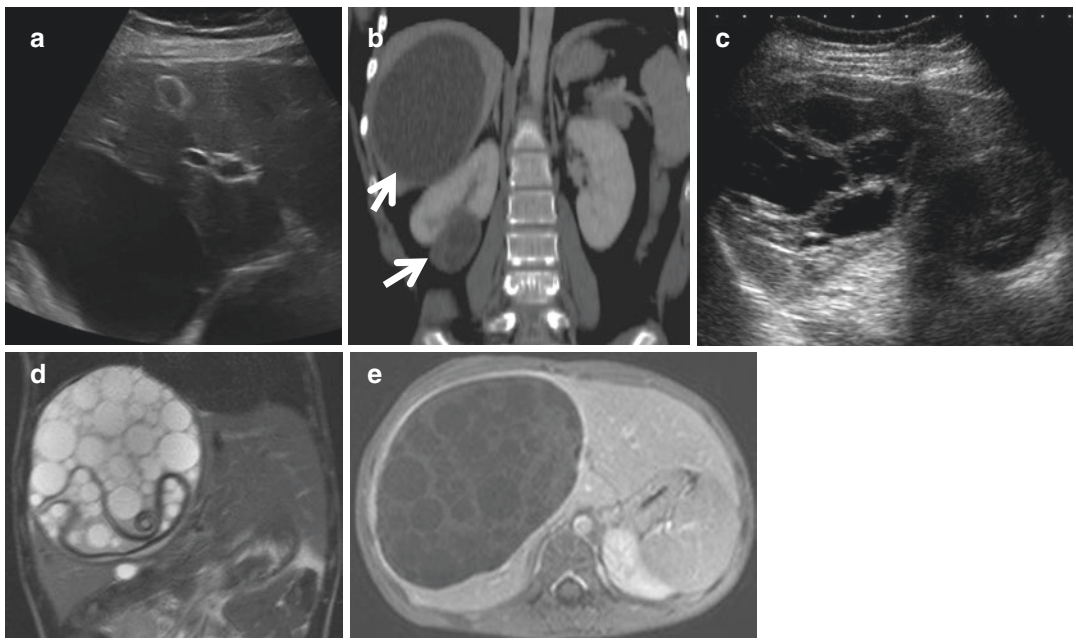

Fig. 15.8 Echinococcal cysts. Nine-year-old girl with abdominal pain (**a**–**c**). (**a**) Liver US shows a simple fluid-filled cysts. (**b**) On CE-CT both hepatic and renal lesions appear as simple fluid-filled cysts. (**c**) US performed after percutaneous treatment of the hepatic cyst shows the changes of aspect of the cyst that became multiseptated. In another child, (**d**, **e**). (**d**) MRI with T2-weighted image shows the typical aspect of multiple small daughter cysts within a large right cystic mass on T2-weighted-imaging. The degenerative membrane is visible with low signal intensity at the lower part of the cyst on the coronal view. (**e**) T1-weighted post Gadolinium image shows the fluid signal of this multilocular cyst. (Courtesy of Pr Petit)

with multiple microabscesses arranged in a characteristic tract like fashion, in the subscapular region of the liver. Large cystic lesions may also be observed [14].

Fungal Infection

Invasive fungal infection is a complication of prolonged neutropenia in immunocompromised patients with hematologic malignancies, in hematopoietic stem cell or solid-organ transplant recipients as well as in other immunosuppressed patients.

Early recognition of hepatic fungal infection is crucial to initiate therapy and avoid fatal complications in immunocompromised patients.

Candida aspergillus and Cryptococcus neoformans account for 80% of all fungal infections. Other opportunistic fungal pathogens include Histoplasmosis, Mucormycosis, Trichosporon, Blastoschizomyces, Fusarium, etc.

Hepatic candidiasis is a manifestation of disseminated candidiasis, frequently associated with spleen and/or renal localization.

US features of hepatosplenic candidiasis are described in four patterns: a "wheel-within-wheel" pattern with a hypoechoic nidus with hyperechoic inner ring and hypoechoic outer ring, a "bull's eye" with hyperechoic inner ring and hypoechoic outer ring, hypoechoic nodule which is the most common but least specific pattern, and echogenic focus of scar or calcification in the later stages of infection and indicating early resolution.

CT findings are not specific and include multiple foci of low attenuation of variable size (2–20 mm), with or without peripheral enhancement and calcifications. MR imaging may show more lesions than CT but with no specific aspect. Lesions appear hypointense on T1-weighted and markedly hyperintense on T2-weighted [8, 15] (Fig. 15.9).

Histoplasmosis is also a fungal infection that may involve the liver in immunocompromised patients. It is encountered especially in rivers valleys in central and South America, Africa, Asia, and Australia. Imaging patterns are very similar to that of Candidiasis and other fungal agents, including spleen involvement.

15.3.2.3 Liver Masses

Liver masses may be discovered in emergency conditions because of abdominal pain, abdominal enlargement, hemorrhage, and/or rupture with or without trauma, infection, and cardiac failure in hypervascularized tumors, etc.

The aims of imaging are:

- To show the pattern of the mass(es) (solid, cystic, mixed), its limits, its vascularization, and its location.
- To search for local-regional and general extension
- To search for signs of predisposing factors such as underlying chronic liver disease, involvement of other organs indicative of

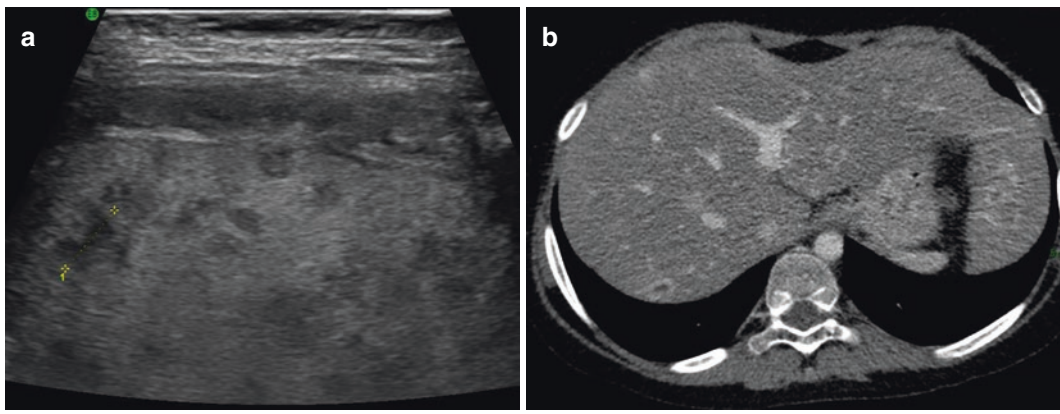

Fig. 15.9 Candidiasis in children treated for acute leukemia. (**a**) Multiple hypoechoic nodules on US exam. (**b**) On CE-CT hypodense liver nodules with thin rim enhancement (*arrows*)

some specific diagnosis: for instance, enlarged lymph nodes suggestive of hemopathy, adrenal gland mass (neuroblastoma), enlarged hyperechoic kidneys (tyrosinemia), etc.

According to the age, biological tests, aspects on imaging and associated disorders, a few differential diagnosis will be suggested (Fig. 15.10, Tables 15.3 and 15.4, [16, 17].

15.3.2.4 Vascular Disorders

Vascular disorders may present acutely. The symptoms will depend on the type of disorder: portal hypertension with gastrointestinal bleeding, ascites, cardiac failure, acute hepatic encephalopathy, etc.

Hepatic Vein and Portal Vein Thrombosis

Portal and hepatic venous thrombosis or stenosis are rare instances that can lead to portal hypertension. Children may present with ascites, mostly associated with hepatic veins thrombosis (Budd-Chiari syndrome), and/or gastrointestinal (GI) bleeding, the latter mostly related to portal vein thrombosis.

Liver transplantation is the first predisposing factor usually related to hepatic or portal venous anastomosis disorder. In other children, exceptional portal or hepatic venous thrombosis or stenosis will be mostly related to tumors, coagulation disorders, or infection. In some instances, the causative factor remains unclear.

Abdominal US-Doppler is the first line examination and will show the obstructed vessels, signs

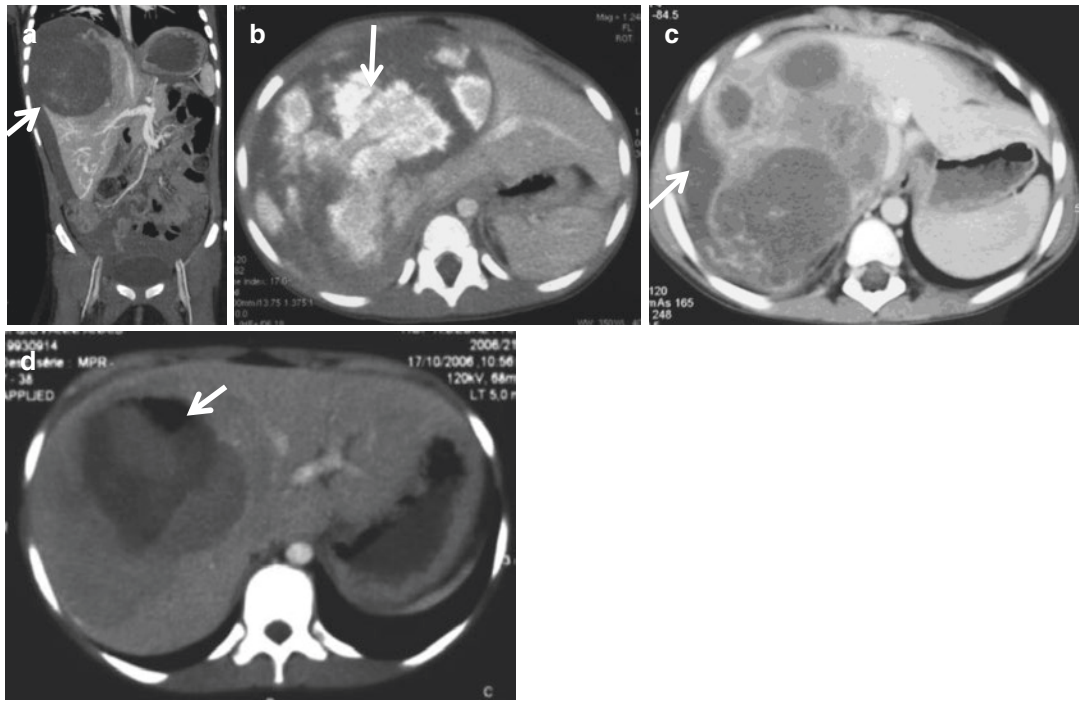

Fig. 15.10 Acute presentation of liver tumors: (**a**) 4-year-old girl presenting intense abdominal pain and deglobulization after a car accident. CE-CT shows a large hypoattenuation hepatic tumor with a large amount of intraperitoneal fluid in relation with the rupture of the tumor (*arrow*). Alpha-feto-protein level was 229,000 ng/mL confirming the suspicion of hepatoblastoma. (**b**) 4-year-old girl presenting with rapid and painful abdominal enlargement revealing on CE-CT a large hepatic tumor with strong arterial enhancement rather at the center of the tumor (*arrow*) in relation with an angiosarcoma. (**c**) 8-year-old girl presenting with abdominal pain. CE-CT shows the large rather necrotic mass of the right lobe with sub-capsular effusion (*arrow*) in relation with an undifferentiated embryonal sarcoma. (**d**) 12-year-old girl presenting with abdominal pain, pallor and fever after a trauma. Large hepatic mass containing gas (*arrow*) corresponding to a liver adenoma complicated with hemorrhage and infection (Salmonella)

Table 15.3 Hepatic mass: diagnostic orientation according to the imaging features and the context

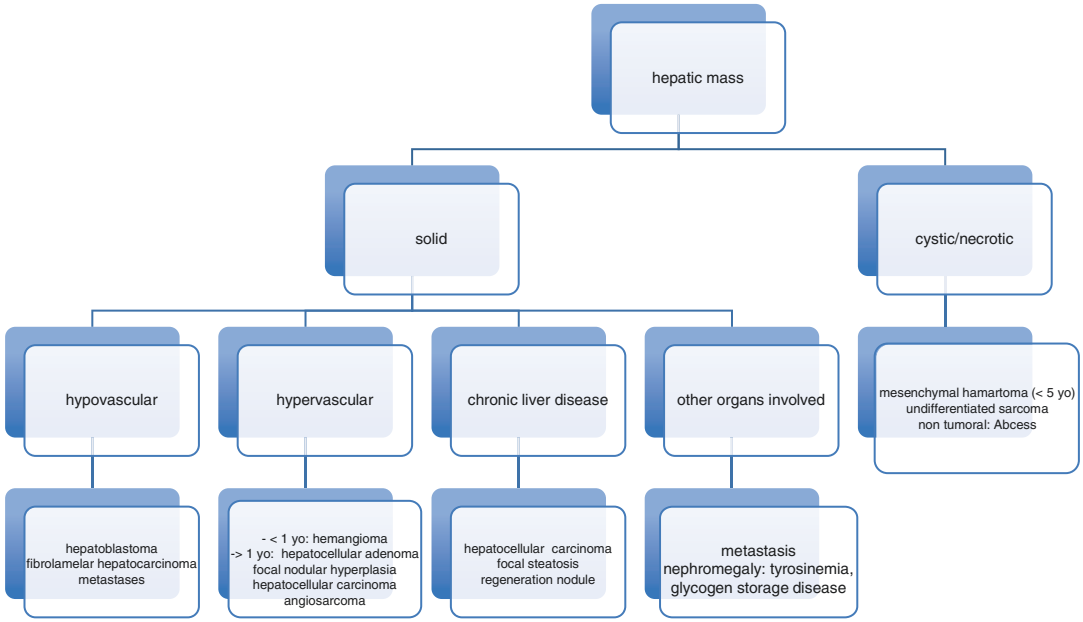

Table 15.4 Predisposing factors for liver tumors in children

Tumors	Predisposing factor
Hepatoblastoma	Beckwith-Wiedemann syndrome
	Familial colic polyposis
	Gardner syndrome
	Fetal alccolisation syndrome
	Very low birth weight
	Parents exposure to toxics
Hepatocellular carcinoma	Chronic viral hepatitis (HVB, HCV)
	Glycogen storage disease 1 and 3
	Tyrosinemia
	Progressive familial intrahepatic cholestasis (PFIC)
	Biliary atresia
	Alpha1-antitrypsine deficiency
	Hemochromatosis
	Congenital and acquired porto-systemic shunt
Hepatocellular adenoma	Glycogen storage disease 1 and 3
	Androgen therapy (Fanconi anemia)
	Heterozygote mutation of HNF1 alpha
	Congenital and acquired porto-systemic shunt
Focal nodular hyperplasia	Congenital and acquired porto-systemic shunt

of portal hypertension, and whenever possible the causative factor.

Abdominal Angio-MR imaging or Angio-CT will provide information for the vascular mapping and demonstrate additional anomalies (Fig. 15.11).

Arterio-Portal Fistula

Arterio-portal fistula may be congenital (with or without underlying Rendu Osler disease) or acquired after trauma or biopsy. According to the extension of the reverse flow in the portal system, it may lead to various grades of portal hypertension.

The diagnosis is ascertained using US-Color Doppler that will show a direct communication of the hepatic artery and the adjacent portal vein with or without an ectatic part. The Doppler study will show a reversed flow in the portal vein that can be arterialized with a demodulation of the flow in the feeding artery. In very severe cases, reverse portal flow can be observed in the extrahepatic portal veins and can be associated with severe portal hypertension (Fig. 15.12). In congenital forms, a spontaneous resolution has not been reported.

Rarely infantile liver hemangioma may present with arterioportal or porto-hepatic fistula, which

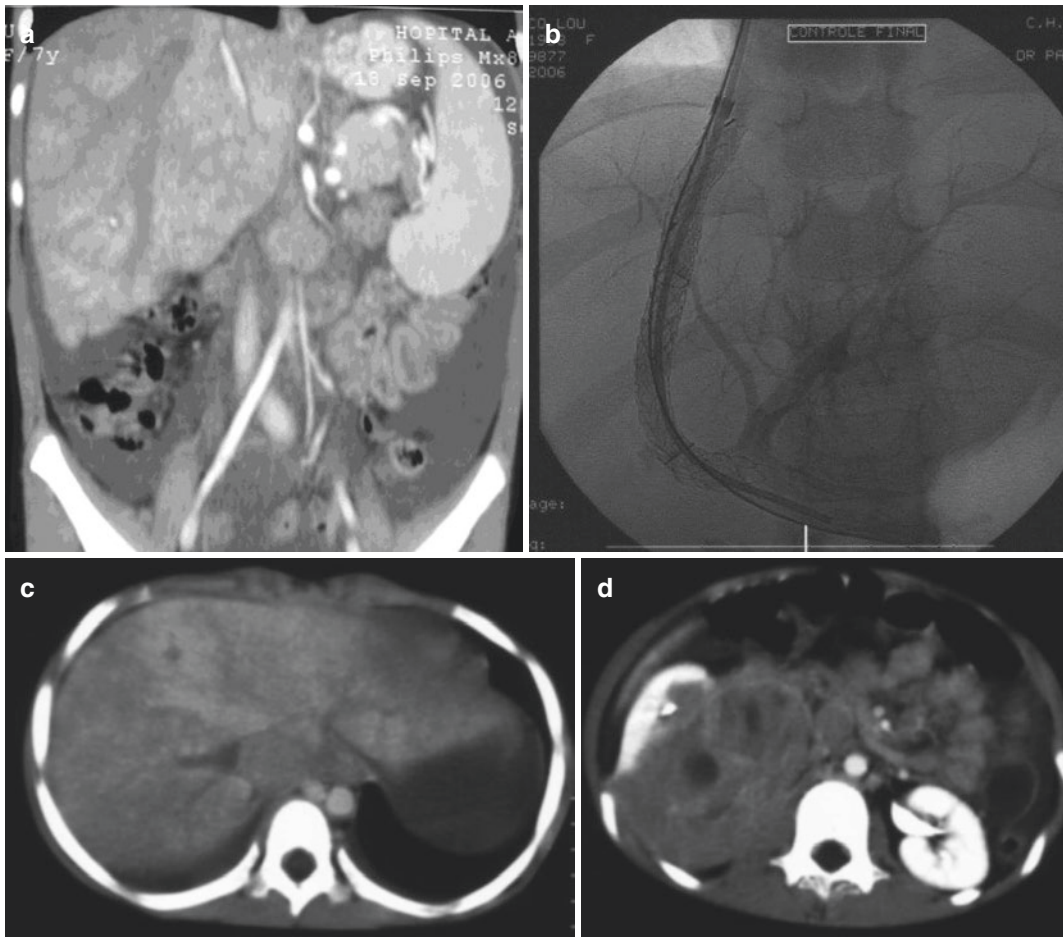

Fig. 15.11 Budd-Chiari syndrome. Ten-year-old girl presenting with abdominal pain and rapid abdominal enlargement (**a**, **b**). (**a**) CE-CT at the venous phase shows the heterogeneous enhancement of the liver with absence of opacification of the enlarged right hepatic vein that is thrombosed. Note the presence of ascites. (**b**) after failure of medical treatment and hepatic vein angioplasty, placement of a TIPSS allowed the resolution of portal hypertension. Essential thrombocythemia was found as a causative factor. Eight-year-old girl presenting acute abdominal pain (**c**, **d**). (**c**) CE-CT at the venous phase shows the heterogeneous enhancement of the liver with no enhancement of the hepatic veins and an enlarged thrombosed inferior vena cava. (**d**) The thrombosis of the IVC and the hepatic veins at the origin of the Budd-Chiari syndrome were caused by the spread of a tumoral thrombus from a nephroblastoma involving the right kidney

can close spontaneously. A potential progressive increase of portal hypertension will favor a therapeutic approach based on interventional radiology (see15.4.4.1). In arterio-portal fistula related to trauma or iatrogenic, a spontaneous resolution is possible and imaging follow-up is sufficient unless symptoms develop or unless the size of the fistula or pseudo-aneurysm increases; these unfavorable evolutions indicate the need for endovascular closure [2, 18, 19] (Fig. 15.12).

Congenital Porto-Systemic Shunts

Congenital porto-systemic shunts consist in abnormal communications between one or several systemic vein(s) and one or several portal vein(s). Patients may present acutely ill due to metabolic disorders such as hypoglycemia in newborns and infants and hyperammonemia at any age, cardiac failure, pulmonary hypertension, hypoxemia related to intrapulmonary arteriovenous shunt, liver tumor, etc.

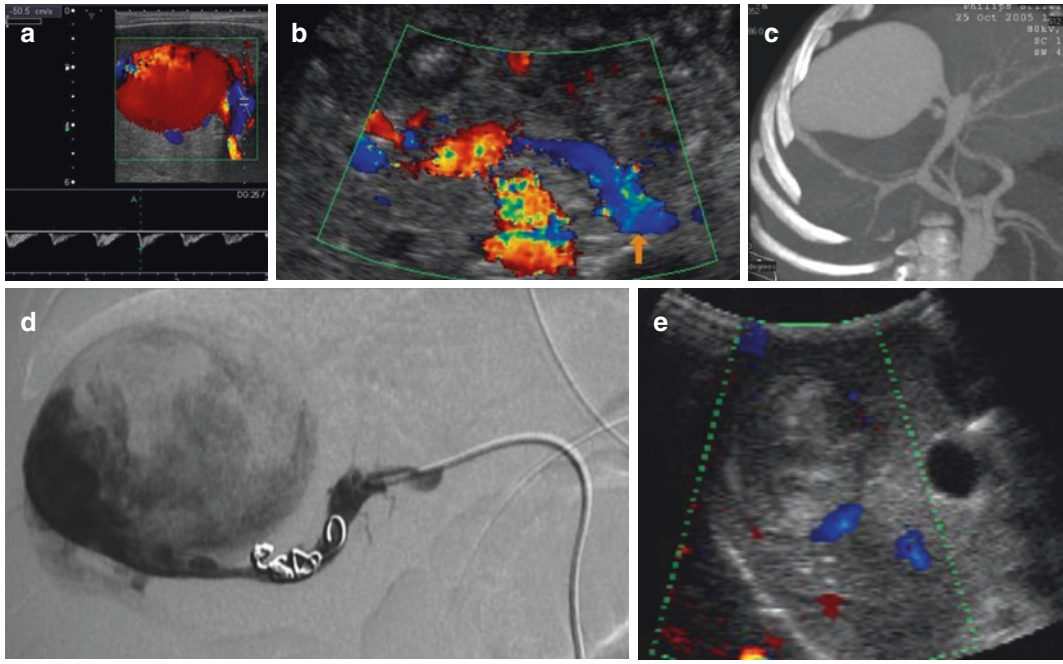

Fig. 15.12 Congenital arterio-portal fistula. Three-month-old boy presenting with recent difficulties for feeding, diarrhea, and blood in the stools. (**a**) US Doppler shows a large ectatic vascular lesion with reversed-flow and arterialization of the portal flow highly suggestive of an arterio-portal shunt. (**b**) Color-Doppler shows the reverse flow in the splenic vein in relation with severe portal hypertension secondary to the arterio-portal fistula. (**c**) CE-CT confirms the direct communication of the ectatic arterio-portal fistula fed by a left hepatic artery and drained by the two portal veins. (**d**) Embolization with coils of the left hepatic artery feeding the arterio-portal fistula was performed. (**e**) US examination performed immediately after arterial embolization showed the thrombosis of the malformation. The baby had a very good outcome with immediate and complete resolution of portal hypertension

The diagnosis is usually confirmed on US-Doppler that shows the abnormal communication between the systemic and the portal venous systems.

Depending on the clinical presentation, closure of the shunt may be rapidly necessary [20] (see Sect. 15.4.4.3).

15.3.2.5 Systemic Diseases with Hepatic Involvement (See Also Chap. 29)

A number of systemic diseases may involve the liver and biliary tree, especially Kawasaki disease, Henoch-Schönlein purpura, graft versus host disease (GVHD), and veno-occlusive disease (VOD) after hematopoietic stem cell transplantation.

Kawasaki syndrome is an acute febrile vasculitis that occurs predominantly in infants and young children. A major complication is the occurrence of coronary artery abnormalities potentially life-threatening. Acute abdominal presentation may be related to hepatobiliary manifestations that develop such as right upper quadrant pain or jaundice accompanied by persistent fever. In the absence of specific symptoms, the diagnosis of Kawasaki disease may be delayed increasing the risk for complications especially coronary arteries disorders. According to some studies, gallbladder abnormalities occur in 15% of the patients with Kawasaki disease and appear as wall thickening and/or gallbladder distension. Involvement of the gallbladder seems to be significantly associated with an increased risk of coronary involvement and resistance to intravenous immunoglobulin treatment (Fig. 15.4) [6]. When the patients become symptomatic, steroid therapy may be required.

Henoch-Schönlein purpura may be associated with hepato-biliary disorders in about 9% of the

cases according to Chao study reporting on 225 patients. US findings included hepatomegaly and thickened gallbladder wall [21].

After hematopoietic stem cell transplantation, hepato-biliary complications such as graft versus host disease (GVHD) and veno-occlusive disease (VOD) (also called sinusoidal obstruction syndrome) can lead to acute presentation and are life-threatening complications. Hepatic GVHD typically manifests as cholestatic jaundice and even liver failure. Biliary tract abnormalities on imaging include abnormal enhancement of the biliary tract, gallbladder thickening, dilatation of the common bile duct, pericholecystic fluid, and biliary sludge. VOD is related to the destruction of hepatic microvasculature after chemotherapy and/or radiation. It usually develops 1 week before to 3 weeks after cell transplantation and associates portal hypertension, jaundice, and painful hepatomegaly. Imaging features include hepatosplenomegaly, gallbladder wall thickening, ascites, and periportal infiltration. On Doppler study, the reported signs of VOD are: Resistivity Index of the hepatic artery greater than 0.75, to-and-fro or even hepatofugal portal flow, monophasic flow in the hepatic veins and even hepatofugal flow in the paraumbilical veins [22].

15.3.2.6 Liver Transplantation: Complications with Acute Presentation

Infection

At any time after liver transplantation, severe sepsis can be related to cholangitis. Imaging will search for biliary tract dilatation that can be related to biliary anastomosis stenosis. If the sepsis is severe and associated with biliary tract dilatation, percutaneous transhepatic cholangiography is indicated for drainage of the bile ducts and dilatation of the bilio-digestive or bilio-biliary stenosis (See Sect. 15.4.2).

In rare cases, diffuse cholangiopathy is present with multiple intrahepatic bile duct stenosis and dilatations. Irregularities of the bile ducts may be increased by acute cholangitis. Imaging will search for hepatic artery thrombosis or stenosis that can cause biliary ischemia and ischemic cholangiopathy [23].

Arterial and Hepatic or Portal Venous Thrombosis

Acute venous or arterial thrombosis may develop at any time after LT with abdominal pain, liver tests abnormalities, or even liver failure with diffuse necrosis of the liver graft. Diagnosis is achieved on US. An angio-CT is necessary in most cases to confirm the diagnosis.

In case of arterial thrombosis, if the diagnosis is confirmed during the acute phase of the thrombosis, the treatment is either surgical or radiological depending on the anatomy. If signs suggestive of parenchymal or biliary ischemia are already present at diagnosis, medical treatment with anticoagulation should be proposed. Follow-up will show the consequences of the thrombosis that can range from no complication to loss of the graft or even death in the absence of retransplantation. Ischemic cholangiopathy can develop several weeks or months after the arterial occlusion.

In case of hepatic venous obstruction, anticoagulation is usually the first step of treatment. If the diagnosis of stenosis is clear on imaging, attempt of angioplasty ± thrombectomy with either interventional radiology or surgery will be performed as soon as possible.

In case of portal venous obstruction, medical treatment with anticoagulation is usually the first step. If it fails, interventional radiology or surgery will be proposed to restore the portal vein patency (see Sect. 15.4.4) [23].

15.4 The Role of Interventional Radiology

In children, most procedures are performed under general anesthesia by interventional radiologists, mostly in specialized pediatric hepatology and liver surgery centers [23].

15.4.1 Liver Biopsy

In an emergency setting, liver biopsy is indicated in case of liver tumors or in case liver failure when it is not possible to obtain the diagnosis based on clinical and biological data.

Liver biopsy can be performed through interventional radiology either by percutaneous access or via transjugular approach in case of coagulation disorders or perihepatic ascites.

In all cases, continuous sonographic guidance is mandatory to avoid complications. A choice of route of access maintaining interposed normal liver, between the capsule and the target, is necessary to prevent hemorrhage and intraperitoneal contamination.

Percutaneous liver biopsy should be performed using 16 G biopsy needles. When more than one core is required, coaxial biopsy needle is needed [24].

Biopsy specimen will be fixed according to the pathologist's recommendations.

In exceptional intrabiliary tumors or masses, if biliary drainage is necessary, percutaneous transbiliary biopsy can be performed during the same procedure.

15.4.2 Biliary Interventions

In the context of emergency, biliary interventions will be indicated in biliary obstruction complicated by infection mostly after liver transplantation. In rare instances of rare malignant biliary obstruction, drainage of the biliary tree may be indicated when chemotherapeutic agents that are metabolized by the liver have to be given to the patient. In exceptional cases, biliary opacification can be necessary to confirm the diagnosis of bilio-pancreatic malformation.

Percutaneous transhepatic cholangiography (PTC) and percutaneous transhepatic transcholecystic cholangiography (PTTC), percutaneous biliary drainage, dilatation of biliary strictures are well-established techniques [23].

Transhepatic access is the rule and puncture is performed through hepatic parenchyma using US guidance.

In pediatric patients, the most common cause of benign biliary stenosis is liver transplantation. Biliary dilatation is usually performed using angioplasty-type balloon. Biliary drainage is necessary after dilatation. No consensus exists on the procedure [23].

15.4.3 Percutaneous Treatment of Hepatic Abscess

Percutaneous treatment of pyogenic abscesses either by aspiration or catheter drainage has become the preferred method for the management of liver abscess when antibiotherapy is not sufficient due to the large size of the abscess.

Catheter drainage appears to be safe and more effective than aspiration to allow a high success rate and a reduced time to obtain clinical relief if the lesion is larger than 5 cm diameter [10]. Catheters of 6 and 8 F in size are usually sufficient especially for intercostal access in young children.

When no fluid is obtained after puncture, biopsy is useful to confirm the diagnosis of abscess on histology and bacteriology studies.

15.4.4 Vascular Interventions

15.4.4.1 Arterial Interventions

The main pediatric indications for arterial interventions are:

- Arterial embolization in symptomatic hemangiomas in infants younger than 1 year and symptomatic arteriovenous fistulas (acquired or congenital);
- Dilatation of anastomotic stenosis or recanalization of hepatic artery after liver transplantation.

15.4.4.2 Portal Interventions

The management of portal hypertension especially after liver transplantation is the main indication of portal intervention. It can consist in portal vein angioplasty and/or recanalization, in embolization of varices in case of gastrointestinal bleeding with failure of medical and endoscopic management, placement of Transjugular Intrahepatic Porto-Systemic-Shunt (TIPSS) in exceptional cases of cirrhosis and Budd-Chiari syndrome.

Acute portal thrombosis is usually treated with anticoagulation therapy as a first step [23].

15.4.4.3 Hepatic Vein Interventions

Main indications of hepatic venous interventions in emergency concern liver recipients with hepatic vein or inferior vena cava stenosis or thrombosis. In very rare instance, Budd-Chiari may happen in children with native liver or closure of congenital porto-hepatic shunt may be necessary.

Budd-Chiari syndrome may present acutely and require treatment with interventional radiology when anticoagulation therapy fails to restore the patency of hepatic veins.

The first step treatment is angioplasty of hepatic vein(s) or IVC stenosis or obstruction, with or without placement of a stent. In case of failure of this treatment, placement of Transjugular Intrahepatic Porto-Systemic-Shunt (TIPSS) may be necessary (Fig. 15.11) [23].

Conclusion

Acute presentation of hepato-biliary disorders may be acute in a previously healthy child, can be associated with known or unknown underlying chronic liver or biliary disease, or be associated with systemic diseases.

Imaging has a key role for diagnosis of the disorders and associated abnormalities and complications and may be useful to guide treatment. Interventional radiology plays a role in the management of some of these diseases.

References

1. Pariente D, Franchi-Abella S. Paediatric chronic liver diseases: how to investigate and follow up? Role of imaging in the diagnosis of fibrosis. Pediatr Radiol. 2010;40(6):906–19.
2. Chavhan GB, Babyn PS, Manson D, Vidarsson L. Pediatric MR cholangiopancreatography: principles, technique, and clinical applications. Radiogr Rev Publ Radiol Soc N Am Inc. 2008;28(7):1951–62.
3. Kamisawa T, Kuruma S, Tabata T, Chiba K, Iwasaki S, Koizumi S, et al. Pancreaticobiliary maljunction and biliary cancer. J Gastroenterol. 2015;50(3):273–9.
4. Kamisawa T, Ando H, Hamada Y, Fujii H, Koshinaga T, Urushihara N, et al. Diagnostic criteria for pancreaticobiliary maljunction 2013. J Hepatobiliary Pancreat Sci. 2014;21(3):159–61.
5. Poddighe D, Tresoldi M, Licari A, Marseglia GL. Acalculous acute cholecystitis in previously healthy children: general overview and analysis of pediatric infectious cases. Int J Hepatol. 2015;2015:459608.
6. Yi DY, Kim JY, Choi EY, Choi JY, Yang HR. Hepatobiliary risk factors for clinical outcome of Kawasaki disease in children. BMC Pediatr. 2014;14:51.
7. Newland CD. Acute Liver Failure. Pediatr Ann. 2016;45(12):e433–8.
8. Bächler P, Baladron MJ, Menias C, Beddings I, Loch R, Zalaquett E, et al. Multimodality imaging of liver infections: differential diagnosis and potential pitfalls. Radiogr Rev Publ Radiol Soc N Am Inc. 2016;36(4):1001–23.
9. Brook I. Intra-abdominal, retroperitoneal, and visceral abscesses in children. Eur J Pediatr Surg Off J Austrian Assoc Pediatr Surg Al Z Kinderchir. 2004;14(4):265–73.
10. Dietrich CF, Lorentzen T, Appelbaum L, Buscarini E, Cantisani V, Correas JM, et al. EFSUMB guidelines on interventional ultrasound (INVUS), Part III – abdominal treatment procedures (Short Version). Ultraschall Med Stuttg Ger 1980. 2016;37(1):27–45.
11. Merten DF, Kirks DR. Amebic liver abscess in children: the role of diagnostic imaging. AJR Am J Roentgenol. 1984;143(6):1325–9.
12. Bulakçı M, Kartal MG, Yılmaz S, Yılmaz E, Yılmaz R, Şahin D, et al. Multimodality imaging in diagnosis and management of alveolar echinococcosis: an update. Diagn Interv Radiol Ank Turk. 2016;22(3):247–56.
13. Brunetti E, Kern P, Vuitton DA. Writing Panel for the WHO-IWGE. Expert consensus for the diagnosis and treatment of cystic and alveolar echinococcosis in humans. Acta Trop. 2010;114(1):1–16.
14. Lim JH, Kim SY, Park CM. Parasitic diseases of the biliary tract. AJR Am J Roentgenol. 2007;188(6):1596–603.
15. Castagnola E, Ruberto E, Guarino A. Gastrointestinal and liver infections in children undergoing antineoplastic chemotherapy in the years 2000. World J Gastroenterol. 2016;22(25):5853–66.
16. Adeyiga AO, Lee EY, Eisenberg RL. Focal hepatic masses in pediatric patients. AJR Am J Roentgenol. 2012;199(4):W422–40.
17. Franchi-Abella S, Branchereau S. Benign hepatocellular tumors in children: focal nodular hyperplasia and hepatocellular adenoma. Int J Hepatol. 2013;2013:215064.
18. Kumar A, Ahuja CK, Vyas S, Kalra N, Khandelwal N, Chawla Y, et al. Hepatic arteriovenous fistulae: role of interventional radiology. Dig Dis Sci. 2012;57(10):2703–12.
19. Teplisky D, Tincani EU, Lipsich J, Sierre S. Congenital arterioportal fistulas: radiological treatment and color Doppler US follow-up. Pediatr Radiol. 2012;42(11):1326–32.

20. Bernard O, Franchi-Abella S, Branchereau S, Pariente D, Gauthier F, Jacquemin E. Congenital portosystemic shunts in children: recognition, evaluation, and management. Semin Liver Dis. 2012;32(4):273–87.
21. Chao HC, Kong MS, Lin SJ. Hepatobiliary involvement of Henoch-Schönlein purpura in children. Acta Paediatr Taiwanica Taiwan Er Ke Yi Xue Hui Za Zhi. 2000;41(2):63–8.
22. Mahgerefteh SY, Sosna J, Bogot N, Shapira MY, Pappo O, Bloom AI. Radiologic imaging and intervention for gastrointestinal and hepatic complications of hematopoietic stem cell transplantation. Radiology. 2011;258(3):660–71.
23. Franchi-Abella S, Cahill AM, Barnacle AM, Pariente D, Roebuck DJ. Hepatobiliary intervention in children. Cardiovasc Intervent Radiol. 2014;37(1):37–54.
24. Dezsőfi A, Baumann U, Dhawan A, Durmaz O, Fischler B, Hadzic N, et al. Liver biopsy in children: position paper of the ESPGHAN Hepatology Committee. J Pediatr Gastroenterol Nutr. 2015;60(3):408–20.

Acute Pancreatitis (AP)

16

Alexia Dabadie and Philippe Petit

Contents

16.1 Introduction

Acute and reversible inflammation of the pancreatic gland in children is rare but its incidence increases [1–4]. In a review of pediatric patients, Benilfa et al. [5] report this pathology to be twice as frequent in girls as in boys with the youngest patient to be 1 week-old. Generally, though, age at presentation is likely to be above 5 years; more than 80% of children were older than 11-year-in Pant series [4].

- The etiologies are numerous [4, 6]; the most frequent are traumatic, idiopathic, biliary, congenital, multi-systemic diseases [i.e., lupus [7], hemolytic uremic syndrome [8, 9], Reye syndrome], drugs [L-asparaginase, valproic acid, steroids, sulfasalazine, acetaminophen, 6 mercaptopurine, etc.], and toxins [5, 10]. Post transplantation [11], viral infections, Henoch-Schönlein purpura, hereditary and metabolic causes (hyperlipidemia and hypercalcemia), worms (ascaris), or ectopic pancreas are less frequent. Acute onset of chronic pancreatitis includes cystic fibrosis, familial hereditary pancreatitis, juvenile tropical pancreatitis syndrome, and idiopathic fibrosing pancreatitis.
- Clinical symptoms are nonspecific, mainly, acute abdominal pain, abdominal distension, irritability, fever, and vomiting.
- The biological diagnosis is considered positive when serum amylase and lipase are three fold the normal values. However, up to 40% of children with AP have normal biological levels.

A. Dabadie • P. Petit (✉)
Department of Pediatric Imaging,
Hôpital Timone Enfants, 264 Rue St Pierre,
13385 Marseille Cedex 05, France
e-mail: adabadie@ap-hm.fr; ppetit@ap-hm.fr

F.E. Avni, P. Petit (eds.), *Imaging Acute Abdomen in Children*,
https://doi.org/10.1007/978-3-319-63700-6_16

– Recurrence occurs in 15 of 35% of cases [6]. They are principally related to pancreatic duct malformations or are idiopathic [5].
– Mortality is lower than in adults, still it has been reported in an old meta-analysis to be as high as 10% [5]. A more recent report that includes 371 children, from 2002 to 2012, describes a lower mortality (5%) [10].

16.2 Imaging Specificities

Imaging allows the diagnosis of pancreatitis, may search for its causes, assesses complications, and contributes to the follow-up.

A normal imaging exam, especially in the initial days of the disease, does not rule out the diagnosis of AP.

16.2.1 Ultrasound

US is usually the first imaging tool used to explore a vomiting and painful child. The whole abdomen and pelvis must be explored initially with a convex low frequency transducer then with a high frequency linear probe. In children, in most cases, the pancreas can be analyzed with an 8–12 MHz probe. However, visualization of the pancreatic gland may be impaired in AP by the associated paralytic ileus. Examining the patient in left lateral decubitus—using the left lobe of the liver as acoustic window—or in right lateral decubitus through the spleen will allow a more complete approach of the whole pancreas. US is also essential and contributes to the identification of the various causes of AP, to the diagnosis and follow-up of fluid collections, vessels morphology, and vessels patency. It will monitor the morphologic evolution of the pancreatic gland and the caliber of the pancreatic duct.

Contrast enhanced US has only been scarcely reported in children [12]. It has proved to be efficient for the diagnosis of AP including the analysis of the pancreatic parenchyma vascularization in adults [13].

US elastography in AP has been published in a population where only few children were included; further publications are needed to confirm the potential interest for pediatric practice [14].

Endoscopic US is less likely to be used in children as it is an invasive technique [15]. This exploration is mostly reserved for therapeutic purposes, especially for biliary stone extraction and pseudo-cyst drainage.

16.2.2 CT

A CT should not be systematically performed during AP. Based on the child's clinical condition, there might be specific indications but only a few days after the onset of the acute episode. Kandula et al. reported on a series of 87 children younger than 3 years. CT was performed in only 47% of the patients [8]. The role of CT is to define the pancreatic gland viability (edema vs necrosis), to look for the associated complications (infected or non-infected collections, venous thrombosis, duct obstruction) and whenever possible to define the cause of the AP. It allows a fast evaluation of the abdomen and pelvis. The first CT must be performed without and with contrast. Axial and coronal reconstructions are useful. Slice thickness must range from to 2 to 3 mm. Thanks to the short acquisition time and age of the patients, a sedation is rarely needed. Exposure parameters must be adapted to the patient's body weight. For instance, recommendations from the "Societé Francophone d'Imagerie Pédiatrique et Prénatale" for a 10-year-old child, 32 kg weight, propose a CTDI of 7 ± 3 mGy (35 cm abdomen exploration) (www.sfip-radiopediatrie.org).

16.2.3 MR Imaging

Thanks to the high contrast resolution of the parenchyma and its strong ability to analyze pancreatic and biliary ducts, MR imaging in general and MR cholangiopancreatography (MRCP) specifically are of great value. Examinations performed at 3 Tesla offer a better signal to noise than at 1.5 T as well as the ability to reduce acquisition time and to improve resolution but with increased susceptibility to artifacts [16].

The need for sedation, patient's movements related to pain, difficulties to install these fragile patients during the acute phase of the disease and the length of the study (25 min in average) are important limiting factors.

- MR protocol:
  - Breath-hold sequences with a limited number of slices can be used in patients over 6–7 years. In younger patients, respiratory triggering sequences are mandatory.
  - Negative oral agents: in the initial period of AP, their use is usually not necessary in fasting and/or vomiting patients.
  - Coils: multi-elements phased array or surface coils adapted to the child size are mandatory.
  - Sequences: Depending on the magnet used different protocols are proposed [17–19]. In practice, two types of sequences are needed.

    Pancreatic parenchyma sequences: the normal gland appears bright on T1-weighted and T1-weighted fat saturation. On T2-weighted, the normal gland is iso-signal to the adjacent normal liver. Injection of Gadolinium chelates allows to differentiate edematous reaction from necrosis (in the latter, there is no enhancement). Slice thickness varies from 2.5 to 4 mm.

    Ductal sequences: heavily T2-weighted sequences from 3D thin 0.4 mm slices to 2D thick (3–4 cm) multiplanar slices are used to obtain as much information as possible on the aspect of the pancreatic duct (caliber, continuity, content) and on its junction with the biliary duct. Peripancreatic fluid collections are also better visualized with these sequences.
- At distance of the acute episode: Secretin which increases the excretion of pancreatic juice provides interesting information for the morphologic and functional analysis of the pancreatic duct especially in case of suspected pancreatic duct rupture. However, the use of this product is not approved in many countries and is expensive (between 150 and 250 Euros).

16.3 Imaging Patterns

16.3.1 Positive Diagnosis of AP

Imaging for this specific purpose is not always necessary. Most AP are diagnosed based on clinical and biological data alone [9, 20].

There are wide physiological variations of the thickness of the different segments of the pancreas and therefore, a diagnosis based on measurements only has a low value. On the other hand, Chao et al. [21] have found a significant difference in the diameter of the pancreatic body between children with AP and age-matched controls. A bulky appearance with convex contours of the gland are important findings in favor of AP (Fig. 16.1). Inflammation is responsible for increased volume and/or heterogeneity of the peri-pancreatic fat. Injection of contrast allows to differentiate necrotic from viable parenchyma. Homogenous or heterogeneous fluid collections can be demonstrated. All adjacent vascular structures must be explored to exclude potential venous thrombosis or arterial aneurism.

16.3.1.1 On Ultrasound

Analysis of the pancreatic echotexture compared to the liver is usually not helpful for the diagnosis. During AP, the pancreas remains hypo or isoechoic or can even be hyperechoic. Chao et al. reported that a pancreatic duct larger than 1.5 mm in children between 1 and 6 years, larger than 1.9 mm at ages between 7 and 12 years, and larger than 2.2 mm at ages between 13 and 18 years was significantly associated with AP, mainly idiopathic [20]. However, the caliber of the pancreatic duct is also variable depending on the etiology (obstructive vs non-obstructive). The duct can be compressed by the swollen gland (Fig. 16.2) or distended, secondary to its obstruction or due to underlying chronic pancreatitis. Evaluation of the peri-pancreatic collections content (debris, gas bubbles, septations) is better demonstrated with US.

16.3.1.2 On CT

The main advantages of CT compared to US are to visualize accurately the entire gland whatever

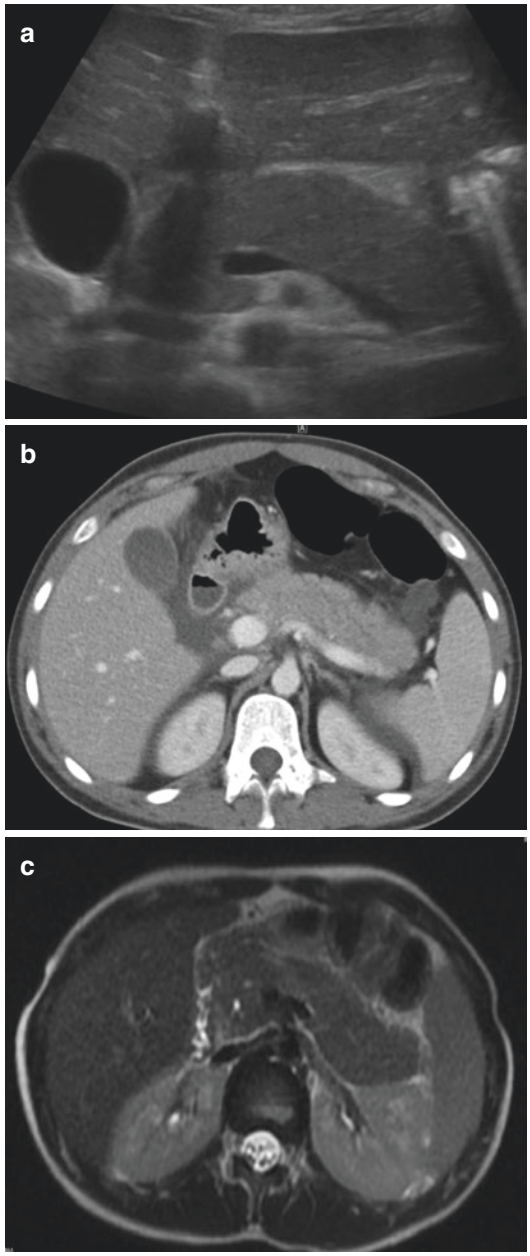

Fig. 16.1 Acute pancreatitis—Classic appearance on imaging of the pancreatic gland after the first days of edematous acute pancreatitis in different patients. (**a**) US transverse scan showing an enlarged pancreatic gland with convex contours. (**b**) CE-CT showing a swollen homogenous pancreatic gland with convex contours. Some effusion is visible. (**c**) MR imaging T2-weighted sequence showing an enlarged pancreatic gland with convex contours

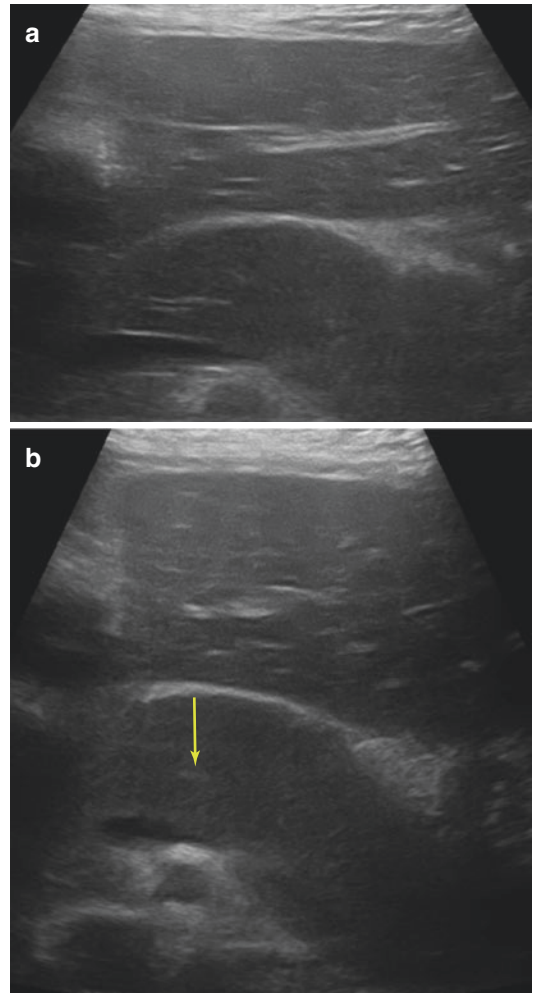

Fig. 16.2 Acute pancreatitis. Consequences on pancreatic duct. (**a**) The pancreatic duct is visible as two separate parallel lines in the pancreatic head. (**b**) It is compressed by the edematous gland at the junction between the isthmus and body of the pancreas (*yellow arrow*)

the bowel distension and to differentiate, thanks to contrast injection, edematous reaction from necrosis of the gland. Additional positive findings include enlargement either diffuse or focal, irregular and ill-defined contours of the gland, ductal distension, infiltration of the peripancreatic fat, thickening of the adjacent fascial planes, detection and analysis of the peripancreatic fluid collections (size, density, contains, wall) (Fig. 16.3).

16.3.1.3 On MR Imaging

MR exploration has the same advantages and ability to detect AP than CT without the inconvenience of ionizing radiation but with a longer time of examination as well as the need for sedation in patients younger than 5 years. Inflammation is responsible for a diffuse or focal loss of the normal T1-weighted hypersignal of the pancreatic gland and a heterogeneous appearance in T2-weighted sequences. Focal increased hyperintensity on T1 is present in case of hemorrhage. Gadolinium injection is not necessary to confirm the presence of an AP but allows the differentiation between viable pancreatic tissue and necrosis (Fig. 16.4).

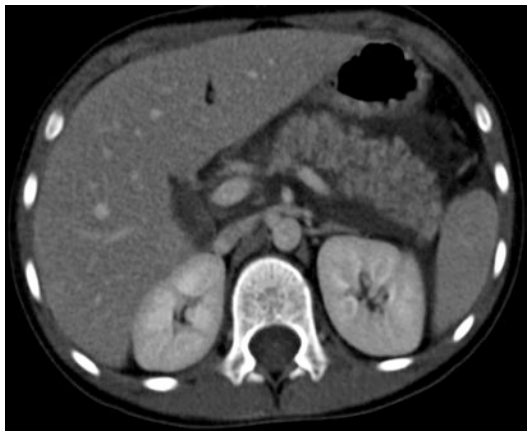

Fig. 16.3 Acute edematous pancreatitis on CE-CT: Homogenous swollen pancreatic gland with surrounding homogenous hypodense fluid collections

16.3.2 Positive Diagnosis of the Causes of AP

Determining the cause is mandatory in order to prevent recurrent episodes. Imaging plays an important role for this purpose and helps to define the therapeutic strategy. Some of the causes are obvious (known trauma), others must be searched carefully to be treated immediately (obstructive lithiasis) or at distance of the AP. Resolution of the pancreatic gland edema several days or weeks after the beginning of AP allows to appreciate more easily the presence of congenital duct malformations (common pancreato-biliary canal, pancreas divisum, etc.) or signs of chronic pancreatitis [19].

16.3.2.1 Trauma

Causes of traumatic AP include accidental, post-surgical, post-endoscopic, and non-accidental trauma. The latter will not display any specific finding on imaging but must be considered as

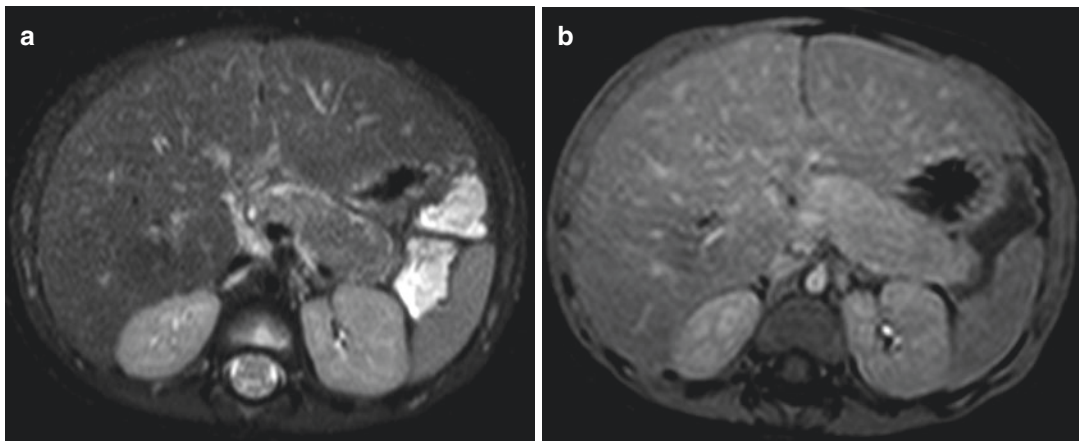

Fig. 16.4 Acute edematous pancreatitis on MR imaging in a 5-year-old child. (**a**) T2-weighted fat saturation sequence showing a homogenous swollen pancreatic gland. (**b**) T1 gadolinium fat saturation showing a homogenous swollen pancreatic gland

potential cause. Additional dedicated imaging explorations related to clinical symptoms and children's age must be performed (i.e., brain CT, skeletal survey) as required. In case of polytrauma, CT is the imaging of choice allowing a full work-up of all the organs. Rupture of pancreatic duct is an important issue which could be visualized either on CT or MR imaging (Fig. 16.5). This rupture must be treated, either surgically and/or endoscopically in order to restore duct continuity and suppress the enzymatic leak.

16.3.2.2 Biliary Lithiasis

Stones within the biliary tract appear on US hyperechoic with or without shadowing depending on their size and their content. On CT, the stones are either hyperdense or isodense. On MR imaging, they are better visualized on T2 sequences as hyposignal nodular structures in a dependent position. On T1-weighted sequences, depending on their composition, the signal can be highly variable (Fig. 16.6).

An underlying pathology is frequently associated, including congenital malformation of the bile ducts, hemoglobinopathies, parenteral nutrition, or short bowel syndrome.

16.3.2.3 Malformations

MRCP is the imaging technique of choice.

Pancreaticobiliary Junction Anomaly

A common biliopancreatic channel is defined by a junction of the common bile duct and the pancreatic duct outside the duodenal wall. Reflux of bile or stenosis of the pancreatic duct is responsible for the AP. US and MR imaging can demonstrate the anomalous junction within the head of the pancreas especially when the ducts are dilated [22] (Figs. 16.7 and 16.8).

Pancreas Divisum

Absence of fusion between the ventral and dorsal pancreatic anlages results in absence of connection between the dorsal Santorini canal and the ventral main pancreatic duct. The Santorini drains the body and tail of the pancreas and ends within the minor papillae (Fig. 16.9). This anomaly is more prone to provoke AP.

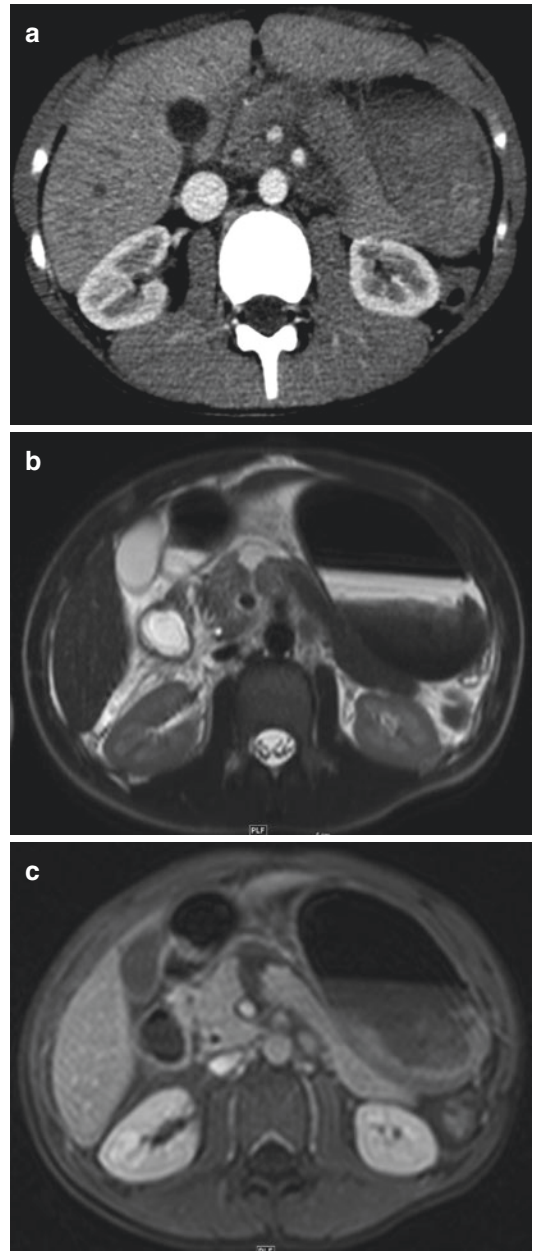

Fig. 16.5 Fracture of the pancreas in a 5-year-old boy. (**a**) CE-CT 3 mm cut reveals a hypodense fracture in the mid-body of the pancreas. (**b**) MR imaging T2-weighted FS: the contrast between normal pancreatic tissue and fracture is better seen on the 4 mm T2 FS. (**c**) MR imaging T1-weighted fat saturation postgadolinium injection

Duplication

Pancreatic duplication is a very rare malformation where the canal of the duplicated gland can be stenotic and responsible for AP. Imaging,

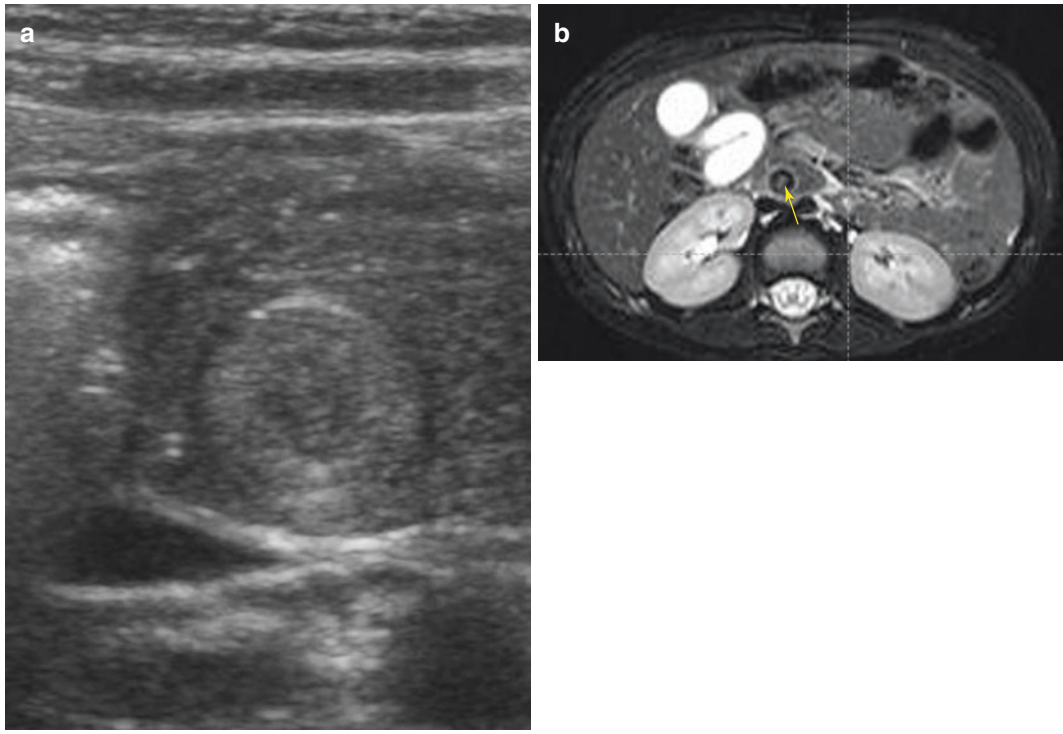

Fig. 16.6 Pancreatitis secondary to biliary lithiasis in a 7-year-old girl. (**a**) US: transverse scan through the head of the pancreas; the lithiasis appears as a hyperechoic pseudo-tumor with a large and layered structure with no posterior shadowing. (**b**) MR imaging T2- weighted sequence reveals a two layered hyposignal lesion within the distal common bile duct in the head of the pancreas

either CT (Fig. 16.10) or MR imaging allows to ascertain the diagnosis.

Annular Pancreas

This pathology can exceptionally be revealed by an AP. The visualization of pancreatic tissue around or on the right lateral side of the duodenum suggests the diagnosis. An abnormal pancreatic canal encircling the duodenum can also be demonstrated [23]. Lin et al. report [24] a review of 15 children with annular pancreas. In their series, 80% of patients presented associated malformations including malrotation (40%), intrinsic duodenal obstruction (33%), trisomy 21 (27%), and duodenal bands (27%).

16.3.2.4 Autoimmune Pancreatitis

Less than 30 cases of autoimmune pancreatitis have been published in children. Two types have been described. Type 2 is the most frequent in children and is associated with ulcerative colitis and a normal serum level of IgG4. It occurs in a younger population than in type 1. CT and MR imaging demonstrate a diffuse enlargement of the pancreatic gland, multifocal pancreatic duct narrowing, peripancreatic hypointense or hypodense rim, respectively, on MR imaging or CE-CT [25]. Other reported associated abnormalities include sclerosing cholangitis, renal mass or nephritis, retroperitoneal fibrosis, and submandibular masses. Rapid regression of imaging abnormalities under steroid therapy may confirm the etiological diagnosis.

16.3.3 Complications

Complications have been reported from 10 to 21% in small pediatric series [20, 26].

16.3.3.1 Acute Complications

Within 4 weeks after the beginning of the AP.

A new classification of the complications based on their presentation before and after

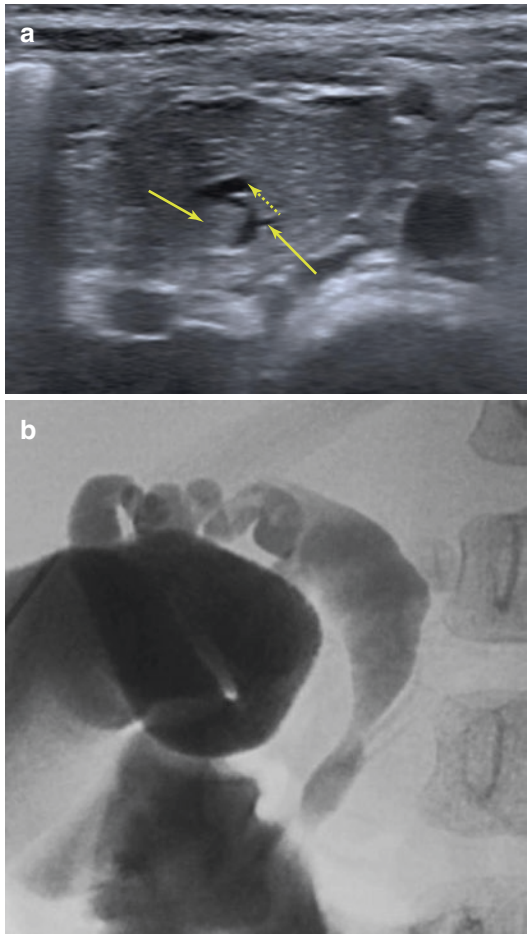

Fig. 16.7 Acute pancreatitis secondary to common biliopancreatic canal (CBPC) in a 3-year-old girl. (**a**) US: Small arrow and *small dashed arrow* show the pancreatic ducts (main and accessory) joining the dilated common bile duct within an enlarged head of pancreas; *large yellow arrow* points to a small associated lithiasis within the CBD. (**b**) Percutaneous cholecystography confirms the CBPC with two separate abnormal junctions of the main and accessory ducts within a choledochal cyst. Note the associated congenital cystic duct dilatation

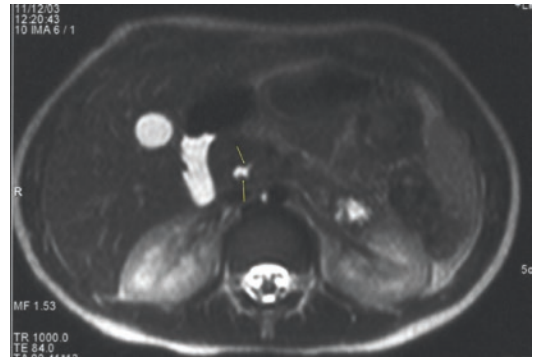

Fig. 16.8 MR imaging axial T2-weighted sequence on a 7-year-old boy with CBPC: The pancreatic and bile ducts jointo a CBPC (*small yellow arrow*) far from the ampulla, within the pancreatic head. *Small dashed arrow* reveals a lithiasis in hyposignal in a dependent position within the common bile duct

Fig. 16.9 Pancreas divisum on MRCP. Coronal reconstruction. The main pancreatic duct joins the minor papilla while the common bile duct with the ventral pancreatic canal joins the major papilla in the duodenum wall

1 week of the beginning of the AP is now in use in adults [27] but is not yet applied in pediatric practice.

Fluid Collections

Fluid collections present on imaging without a well-defined surrounding limit and with or without internal tissues. They are located close or at distance of the pancreatic bed.

Hemorrhage within or outside the gland is more likely to be associated with more severe evolution. Spontaneous hyperdensity on CT or hypersignal in T1 sequences on MR imaging are clues for their diagnosis.

Pancreatic Necrosis

Necrotizing pancreatitis is defined as a diffuse or focal well-limited non-enhanced pancreatic parenchyma involving more than 30% of the pancreatic gland or larger than 3 cm [28]. CT, MR imaging, and US after contrast injection are able

to demonstrate these non-vascularized heterogeneous pancreatic tissues (Fig. 16.11).

16.3.3.2 Late Complications

After 4 weeks of the onset of the AP.

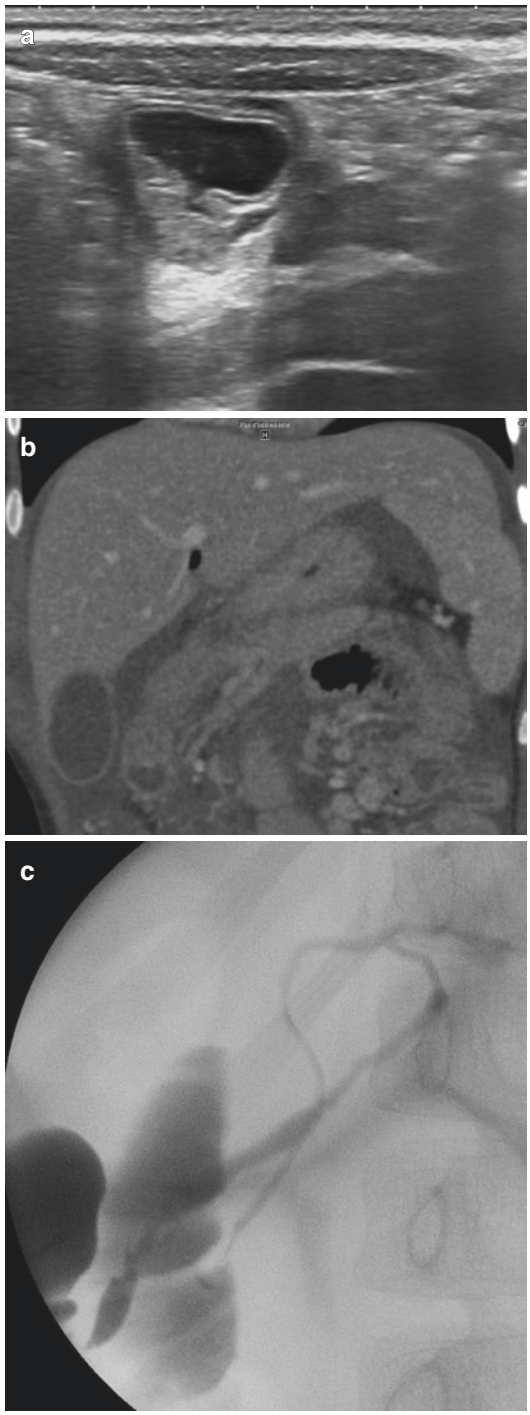

Fig. 16.10 Duplication cyst connected to an ectopic pancreas as cause of recurrent acute pancreatitis—6-year-old girl. (**a**) US transverse scan showing a cystic mass with layered wall. (**b**) CE-CT—Reformatted coronal view—visualizes an abnormal duct with thickened wall below the pancreatic gland. (**c**) Percutaneous opacification of the duplication prior to surgery confirms a complete duodenopancreatic duplication with a duplicated pancreatic duct starting from the duplication cyst and joining the main duct in the tail of the pancreas

Pseudocysts

Pseudocysts have been reported to develop in 10% up to 44% of patients [5, 9] depending on the AP etiology [20, 29, 30]. They are defined by the presence of a well-limited fluid collection without necrotic tissue (Fig. 16.12) and without endothelium lining. It is located close or at distance to the pancreas and may be responsible for:

- Portal veins compression and segmental portal hypertension,
- Arterial wall erosion and pseudo-aneurysm with a risk of acute hemorrhage,
- Bowel obstruction
- Sepsis: diagnosis of associated infection can be considered when an enhancing thickened wall is present.

Pseudocysts may regress spontaneously, fistulating into a hollow viscus; its persistence after 6 weeks and a size greater than 6 cm render

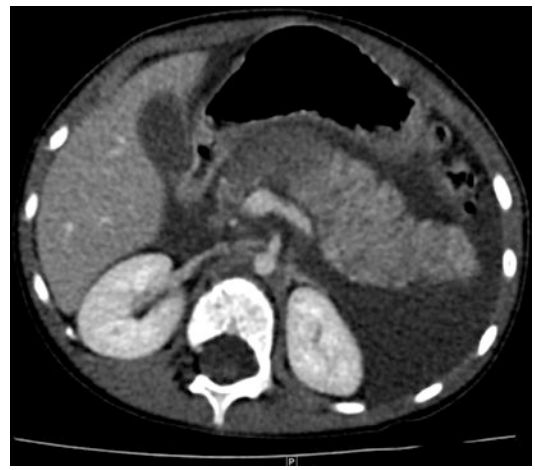

Fig. 16.11 Acute idiopathic pancreatitis in a 5-year-old boy. CE-CT displays pancreatic head necrosis and a collection around the tail

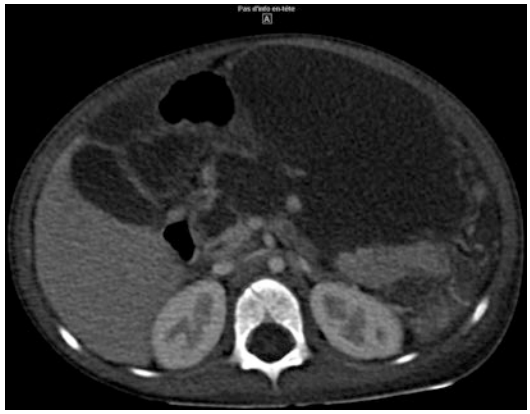

Fig. 16.12 Same patient than Fig. 16.11. CE-CT performed 4 weeks later at the same level than Fig. 16.11 shows destruction of the head and body of the pancreas and large well-limited pseudocyst which was drained endoscopically

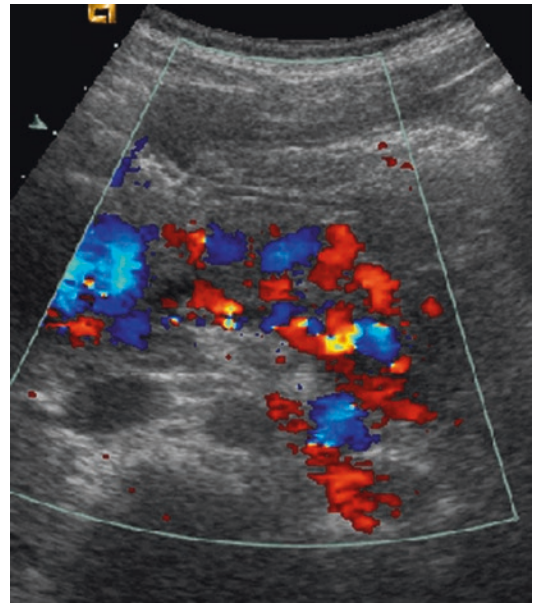

Fig. 16.13 Late complications of AP (12-year-old boy)—US color Doppler follow-up 4 weeks after acute pancreatitis reveals multiple collateral veins around the pancreatic gland secondary to splenic vein thrombosis

unlikely its resolution [31]. In the series of de Blaauw [30] on post traumatic AP, pseudocysts developed in 44% of cases; 17% among them needed a drainage (mean size 10 cm). Endoscopic cysto-enterostomy is the therapeutic method of choice. Percutaneous or surgical drainages are possible alternative methods when the endoscopic approach is not possible.

Infected Fluid Collections

Infected fluid collections or infected pseudocysts can be suspected on imaging when gas bubbles are visualized within the collection or in case of thick and inflammatory bowel wall. It must be differentiated from infected necrosis of the gland which would not be well limited. Puncture under imaging guidance is recommended to confirm infection that will need to be treated more aggressively either by large percutaneous drainage (abscess) or surgery (infected parenchymal necrosis).

Venous Compression

Stenosis secondary to pseudocyst compression or thrombosis of the portal system is diagnosed (Fig. 16.13), thanks to:

- Direct signs:
  - Reduction of the caliber of the vein compressed by a pseudocyst
  - Presence of a clot within the lumen
- Indirect signs:
  - Presence of collateral veins
  - Inversion on Doppler-US of the direction of the venous flow upstream to the obstruction.

Pseudoaneurysm

Pseudoaneurysm occurs secondary to the erosion of an artery wall by pancreatic enzymes. It presents as a sacciform channel communicating with the artery. The splenic artery is most frequently involved. It can be discovered during follow-up imaging or revealed during hemorrhage secondary to its rupture. CT is the examination of choice for diagnosis and therapeutic planning [32, 33].

Stricture of the Pancreatic Duct

A stricture may develop especially after trauma and lead to progressive chronic pancreatitis. MRCP is the imaging of choice to evaluate and to follow the consequences of this lesion.

16.3.4 Prognostic Role of Imaging

Severe pancreatitis is defined when one of the following features is present: death (sic), pancre-

atic surgery, acute renal or respiratory failure, severe gastrointestinal bleeding, shock during the initial admission, pseudocyst development [9]. More recent criteria have been proposed but are nowadays only applicable to adults [27].

Multiple scores using clinical and biological results have been used to assess the prognosis of AP (Ranson, APACHE II, Glasgow modified, DeBanto). The sensitivity of these tests is low and none of them have really proved to be useful in daily practice [18, 26, 34].

Baltazhar et al. [35] have developed almost 30 years ago, in adults, the CT Severity Index (CTSI) based on CT analysis of the pancreatic gland (enlargement and percentage of necrosis) and the presence, number, and aspects of adjacent fluid collections. A modified CTSI, taking into account the extra-pancreatic complications and simplifying the evaluation of the pancreatic necrosis has also been proposed but not been evaluated in children [36]. The CTSI has been shown to be a better predictor of acute severe pancreatitis than clinical scores in children [20, 26]. Interestingly enough, less than 35% of the children enrolled in these publications were explored by CT. The sensitivity of CTSI was 80% and its specificity varies between 76 and 86% [20, 26].

These results influence the therapeutic strategy (i.e., antibiotherapy, drainage, surgery) but the CTSI's benefit for the patient's final outcome remains unknown [37].

In summary, the clinical score appears useful during the initial first week of AP to assess the immediate child management. Imaging, guided by clinical and biological results, is more important after the first week especially to search for complications and to establish the need for follow-up.

However, as mentioned earlier, the need for CT examination in children remains limited during AP since most of the patients have a rapid favorable clinical outcome and because of the radiation risk. In the future, the use of contrast US and MR imaging with faster sequences will probably reduce even more the need for CT.

Conclusion

The place of imaging in children with acute pancreatitis differs from adults. The use of CT is not systematic. It is recommended for traumatic and/or severe pancreatitis. The prognostic role of imaging appears limited.

US and MR imaging are the major imaging procedures that are used to search for an etiology (lithiasis, malformations), to look for late complications (collections, segmental portal hypertension, pancreatic canal stenosis), and ensure their follow-up.

References

1. Nydegger A, Heine RG, Ranuh R, et al. Changing incidence of acute pancreatitis: 10-year experience at the Royal Children's hospital, Melbourne. J Gastroenterol Hepatol. 2007;22:1313–6.
2. Bai HX, Lowe ME, Husain SZ. What have we learned about acute pancreatitis in children? J Pediatr Gastroenterol Nutr. 2011;52:262–70.
3. Lopez MJ. The changing incidence of acute pancreatitis in children: a single-institution perspective. J Pediatr. 2002;140:622–4.
4. Pant C, Deshpande A, Olyaee M, et al. Epidemiology of acute pancreatitis in hospitalized children in the United States from 2000–2009. PLoS One. 2014;9:e95552.
5. Benifla M, Weizman Z. Acute pancreatitis in childhood—analysis of literature data. J Clin Gastroenterol. 2003;37:169–72.
6. Meyer A, Coffey MJ, Oliver MR, et al. Contrasts and comparisons between childhood and adult onset acute pancreatitis. Pancreatology. 2013;13(4):429–35.
7. Marques VL, Gormezano NW, Bonfá E, et al. Pancreatitis subtypes survey in 852 childhood-onset systemic lupus erythematosus patients. J Pediatr Gastroenterol Nutr. 2016;62(2):328–34.
8. Kandula L, Lowe ME. Etiology and outcome of acute pancreatitis in infants and toddlers. J Pediatr. 2008;152(1):106–10.
9. Lautz TB, Chin AC, Radhakrishnan J. Acute pancreatitis in children: spectrum of disease and predictors of severity. J Pediatr Surg. 2011;46(6):1144–9.
10. Guo Q, Li M, Chen Y, Hu H, Hu W. Predictors for mortality following acute pancreatitis in children. Pediatr Surg Int. 2014;30(11):1111–5.
11. Eghtesad B, Reyes JD, Ashrafi M, et al. Pancreatitis after liver transplantation in children: a single-center experience. Transplantation. 2003;75(2):190–3.
12. Valentino M, Galloni SS, Rimondi MR, et al. Contrast-enhanced ultrasound in non-operative management of pancreatic injury in childhood. Pediatr Radiol. 2006;36(6):558–60.
13. Cai D, Parajuly SS, Wang H, et al. Accuracy of contrast-enhanced ultrasound compared with conventional ultrasound in acute pancreatitis: diagnosis and complication monitoring. Exp Ther Med. 2016;12(5):3189–94.
14. Mateen MA, Muheet KA, Mohan RJ, et al. Evaluation of ultrasound based acoustic radiation force

impulse (ARFI) and eSie touch sonoelastography for diagnosis of inflammatory pancreatic diseases. JOP. 2012;13(1):36–44.
15. Darge K, Anupindi S. Pancreatitis and the role of US, MRCP and ERCP. Pediatr Radiol. 2009;39(Suppl 2):S153–7.
16. Almehdar A, Chavhan GB. MR cholangiopancreatography at 3.0 T in children: diagnostic quality and ability in assessment of common paediatric pancreatobiliary pathology. Br J Radiol. 2013;86(1025):20130036.
17. Chavhan GB, Babyn PS, Manson D, et al. Pediatric MR cholangiopancreatography: principles, technique, and clinical applications. Radiographics. 2008;28:1951–62.
18. Restrepo R, Hagerott HE, Kulkarni S, et al. Acute pancreatitis in pediatric patients: demographics, etiology, and diagnostic imaging. Am J Roentgenol. 2016;206(3):632–44.
19. Anupindi SA, Chauvin NA, Khwaja A, et al. Magnetic resonance imaging of pancreaticobiliary diseases in children: from technique to practice. Pediatr Radiol. 2016;46(6):778–90.
20. Fabre A, Petit P, Gaudart J, et al. Severity scores in children with acute pancreatitis. J Pediatr Gastroenterol Nutr. 2012;55:266–7.
21. Chao HC, Lin SJ, Kong MS, et al. Sonographic evaluation of the pancreatic duct in normal children and children with pancreatitis. J Ultrasound Med. 2000;19:757–63.
22. Chapuy S, Gorincour G, Roquelaure B, et al. Sonographic diagnosis of a common pancreaticobiliary channel in children. Pediatr Radiol. 2006; 36(12):1300–5.
23. Ohno Y, Kanematsu T. Annular pancreas causing localized recurrent pancreatitis in a child: report of a case. Surg Today. 2008;38(11):1052–5.
24. Lin YT, Chang MH, Hsu HY, Lai HS, Chen CC. A follow-up study of annular pancreas in infants and children (in Chinese). Zhonghua Min Guo Xiao Er Ke Yi Xue Hui Za Zhi. 1998;39:89–93.
25. Bolia R, Chong SY, Coleman L, MacGregor D, Hardikar W, Oliver MR. Autoimmune pancreatitis and IgG4 related disease in three children. ACG Case Rep J. 2016;3(4):e115.
26. Lautz TB, Turkel G, Radhakrishnan J, et al. Utility of the computed tomography severity index (Balthazar score) in children with acute pancreatitis. J Pediatr Surg. 2012;47:1185–91.
27. Thoeni RF. The revised Atlanta classification of acute pancreatitis: its importance for the radiologist and its effect on treatment. Radiology. 2012;262(3):751–64.
28. Banks PA, Freeman ML. Practice guidelines in acute pancreatitis. Am J Gastroenterol. 2006; 101:2379–400.
29. Bolia R, Srivastava A, Yachha SK, et al. Prevalence, natural history, and outcome of acute fluid collection and pseudocyst in children with acute pancreatitis. J Pediatr Gastroenterol Nutr. 2015;61(4):451–5.
30. De Blaauw I, Winkelhorst JT, Rieu PN, et al. Pancreatic injury in children: good outcome of nonoperative treatment. J Pediatr Surg. 2008;43(9):1640–3.
31. Yoder SM, Rothenberg S, Tsao K, et al. Laparoscopic treatment of pancreatic pseudocysts in children. J Laparoendosc Adv Surg Tech A. 2009;19(Suppl 1):S37–40.
32. Larsen CC, Laursen CB, Dalby K, Graumann O. Splenic artery pseudoaneurysm due to acute pancreatitis in a 6-year-old boy with acute lymphoblastic leukaemia treated with L-aspariginase. BMJ Case Rep. 2014;20:1–3.
33. Puri A, Acharya H, Tyagi S, Curian S, et al. Pseudoaneurysm of the radial branch of the splenic artery with pancreatic pseudocyst in a child with recurrent acute pancreatitis: treatment with endovascular stent graft and cystogastrostomy. J Pediatr Surg. 2012;47(5):1012–5.
34. Hashimoto N, Yotani N, Michihata N, Tang J, Sakai H, Ishiguro A. Efficacy of pediatric acute pancreatitis scores at a Japanese tertiary center. Pediatr Int. 2016;58(3):224–8.
35. Balthazar EJ, Robinson DL, Megibow AJ, et al. Acute pancreatitis: value of CT in establishing prognosis. Radiology. 1990;174:331–6.
36. Mortele KJ, Ip IK, Wu BU, et al. Acute pancreatitis: imaging utilization practices in an urban teaching hospital--analysis of trends with assessment of independent predictors in correlation with patient outcomes. Radiology. 2011;258(1):174–8.
37. Alhajeri A, Erwin S. Acute pancreatitis: value and impact of CT severity index. Abdom Imaging. 2008;33(1):18–20.

Acute Presentations of Splenic Diseases

17

Fred E. Avni and Catherine M. Owens

Contents

F.E. Avni (✉)
Department of Pediatric Imaging, Jeanne de Flandre Hospital, 59037 Lille-Cedex, France
e-mail: freddy.avni@chru-lille.fr

C.M. Owens
GOSH NHS Trust, London, UK

17.1 General Consideration

Splenic functions include immunologic surveillance, red blood cell breakdown, and splenic contraction for blood volume augmentation following hemorrhage.

A wide range of pathologic conditions can affect the spleen. Some of these processes cause isolated splenic disease, whereas others involve the spleen as part of a systemic illness. Imaging is playing an important role in diagnosis and characterization of these diseases especially in their acute settings [1].

US plays a central role for the evaluation of the spleen. The spleen is easily visualized and measured with curved probes. It will appear relatively and diffusely hypoechoic with a central vascular pedicle demonstrable on color Doppler. A more reticular pattern, potentially corresponding to white and red pulp, will be visualized using linear probes [2, 3].

On early phase of CE-CT, the spleen may appear heterogeneous as the contrast progresses distally. In newborns, there is a larger proportion of red pulp and therefore on MR imaging, the spleen tends to be hyposignal compared to the liver in T1 and T2-weighted sequences. After 1 year, the white pulp becomes larger. The spleen will then appear hyperintense compared to the muscles and hypointense to the liver on T1-weighted images. It will appear hypersignal to the liver on T2-Weighted sequences [4].

F.E. Avni, P. Petit (eds.), *Imaging Acute Abdomen in Children*,
https://doi.org/10.1007/978-3-319-63700-6_17

17.2 "Acute" Splenomegaly

Splenomegaly is defined as enlargement of the splenic longest diameter 2SD above the mean for the age. Splenomegaly can be an isolated sign at presentation or can occur associated with a variety of symptoms. The main causes of splenomegaly are listed in Table 17.1. US is usually the main imaging technique used to define splenomegaly (measuring its longest axis) (Fig. 17.1). The technique will also be able to determine any abnormal pattern associated: tumoral involvement, diffuse micro- or macronodular pattern, visibility of vascular collaterals, etc. As indicated by US findings or clinical condition, complementary MR imaging or CE-CT will be performed in order to confirm the splenic disease and provide further evidence of systemic (e.g., thoracoabdominal) disease [1–5].

Table 17.1 Causes of splenomegaly

Infection
Leukemia and lymphoma
Portal hypertension
Acute splenic sequestration in sickle cell anemia
Lymphoproliferative diseases
Collagenosis
Langerhans cell histiocytosis
Storage disorders
Congestive heart failure
Sarcoidosis

One of the most common noninfectious causes of splenomegaly is portal hypertension (see Chaps. 8 and 15) in relation with chronic hepatic disease and cirrhosis. The associated hepatic features will be demonstrated by US, color Doppler, and elastography as required. Sometimes, the splenomegaly will be the initial finding leading to the discovery of the portal hypertension.

Sickle cell disease may lead to acute splenic sequestration and splenomegaly due to trapping of large amount of blood. Hypovolemic shock can ensue. The diagnosis is based on clinical findings and imaging is rarely performed. Whenever performed, US may show heterogeneity of the splenic parenchyma and patency of splenic vessels on Doppler evaluation [6, 7].

Infiltration of the spleen secondary to malignant hematological diseases (leukemia and lymphoma—see also Chap. 27) is another classical cause of splenomegaly. The infiltration may be diffuse or nodular (Fig. 17.2a). The nodules usually appear hypoechoic and multiple. CT or preferably Pet-CT may demonstrate the extent of the disease and other organs involvement as well as adenomegaly (Fig. 17.2b). Noteworthy, leukemia and lymphoma may also lead to splenic infarcts and splenic rupture (see below) [1].

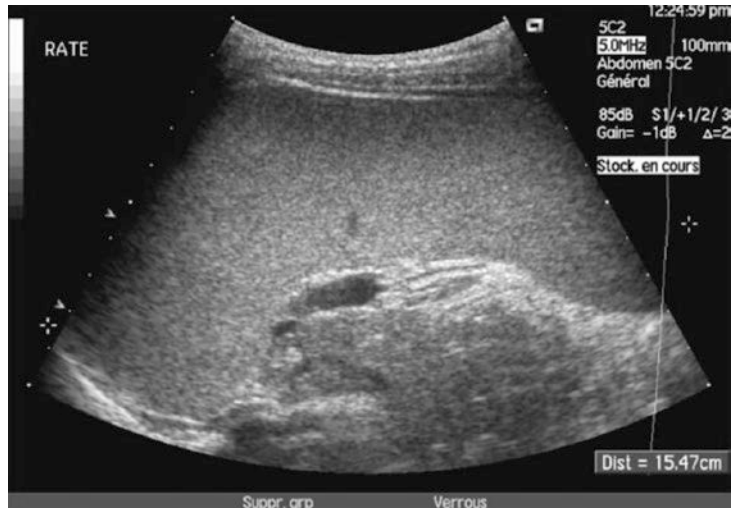

Fig. 17.1 Splenomegaly—US—Sagittal view of the *left flank* in a 7-year-old girl with acute leukemia. Massive homogeneous enlargement of the spleen measuring about 16 cm on its sagittal length

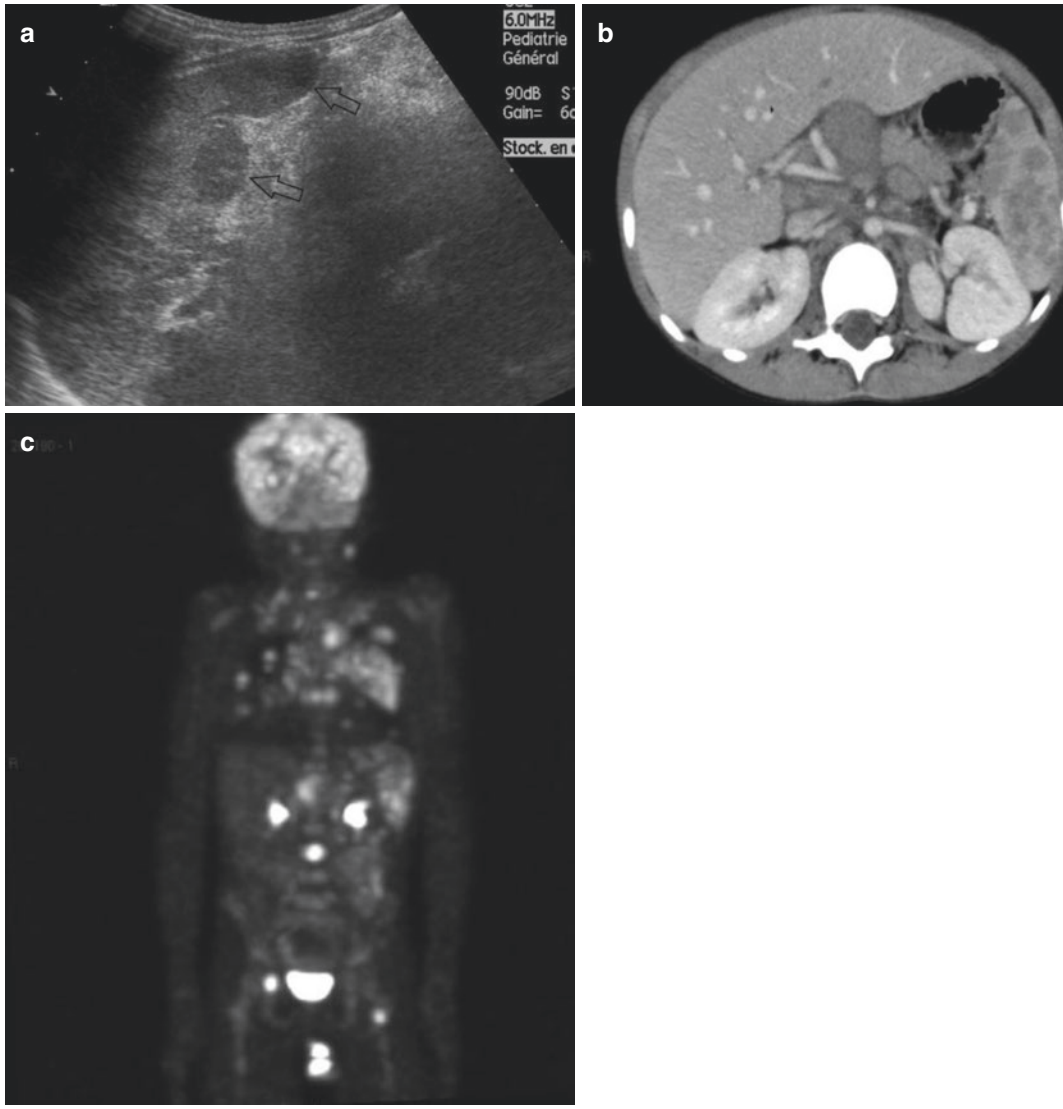

Fig. 17.2 Splenic involvement by lymphoma. (**a**) US—sagittal view of the *left upper abdomen* (13-year-old boy). The spleen, at its margin, appears nodular and hypoechoic (*arrows*). (**b**) CE-CT confirms the nodular involvement of the spleen and demonstrates multiple enlarged lymph nodes in the epigastric area. (**c**) PET scan demonstrates the whole body extension of the disease with multiple locations within the neck, chest, abdomen, and inguino-scrotal areas

Many other diseases may determine diffuse splenic involvement and multiple focal abnormalities (calcified or not). Most are infectious and related to bacterial, fungal, viral, and granulomatous infiltrate. Catch scratch fever (Fig. 17.3), TORCH, mycobacterium species, histoplasmosis, candidiasis, aspergillosis, and AIDS are potential agents. Previous history, clinical and biological data would help to differentiate between the potential causes. As for leukemia and lymphoma, US will detect the diffuse infiltration usually micronodular and patchy; whenever a systemic, more extensive disease is suspected, CT and/or MR imaging may be performed [1, 7, 8].

Splenic tumors may be detected due to their sudden enlargement secondary to intratumoral hemorrhage. Lymphatic malformations,

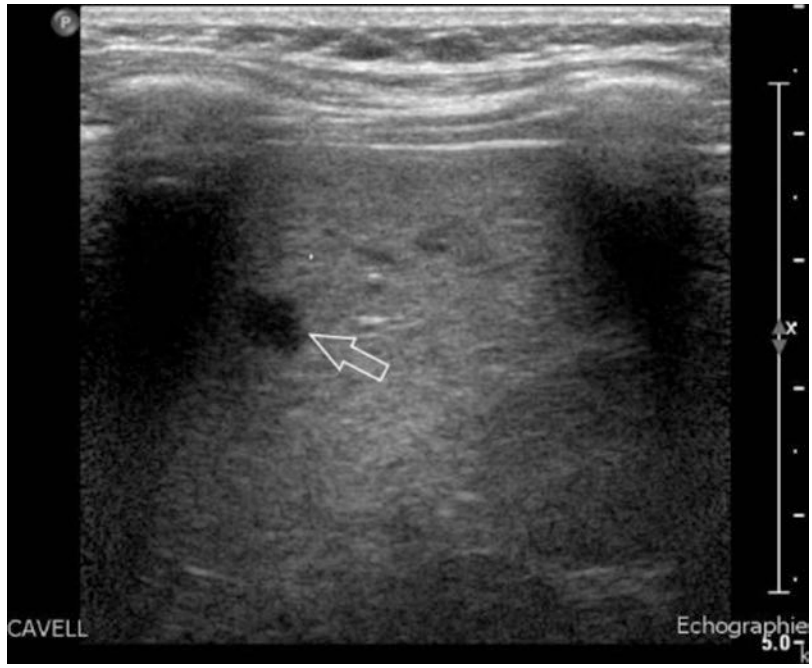

Fig. 17.3 Splenic involvement by Bartonellosis (Cat's scratch disease) in a 2-year-old girl with axillary enlarged lymph nodes. Ultrasound—Transverse scan of the spleen showing hypoechoic ill-defined small irregular nodule (*arrow*)

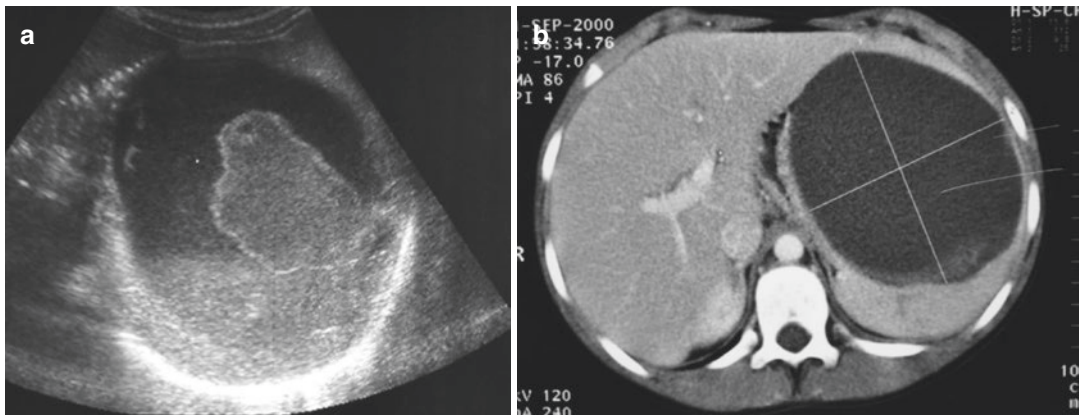

Fig. 17.4 Epidermoid cyst of the spleen that has suddenly enlarged in a 4-year-old boy. (**a**) US—Transverse scan—displays a large (6 cm) cystic mass with central echogenic content potentially corresponding to hemorrhage. (**b**) CE-CT displays the well-limited mass with some dependent hyper-densities

hemangioma, or angiosarcoma (Fig. 17.4) may typically bleed and determine acute "splenomegaly." CT or MR imaging will be helpful in demonstrating an underlying tumor and its complication as well as the potential diagnosis [9].

Finally, the finding of splenomegaly may lead to the discovery of some systemic and metabolic diseases such as Langerhans cell histiocytosis or Gaucher disease [1].

17.3 Infarcts and Vascular Disorders

Splenic infarcts can be caused by various conditions such as hemoglobinopathies, torsion, collagen vascular diseases, splenic artery aneurysm, infection, or portal hypertension. It can also be caused by surgical inadvertent ligation of the splenic artery. The appearance of

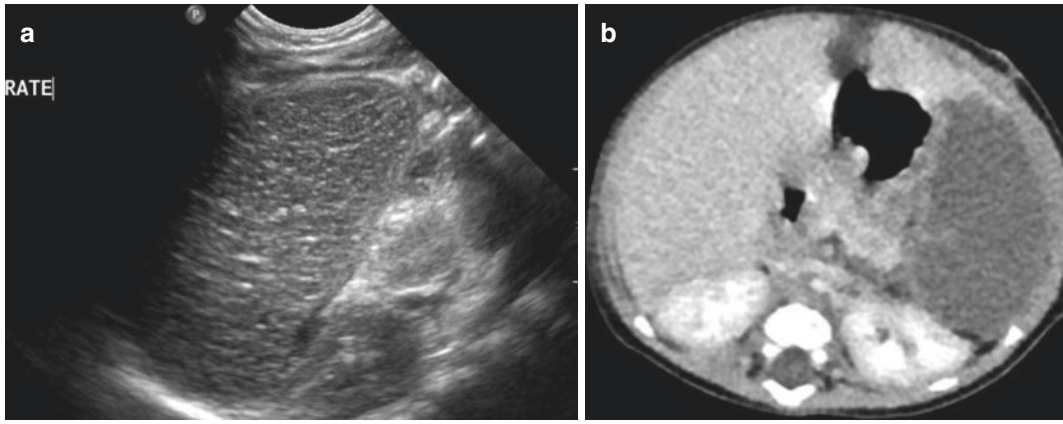

Fig. 17.5 Post-operative status for neuroblastoma; peri-operative inadvertent ligation of the splenic artery (2-year-old boy). (**a**) US—sagittal of the spleen. It displays a peculiar hypoechoic pattern. (**b**) CE-CT—Completely absent enhancement of the spleen

infarct depends on the time of the event and the extent of the infarcted area(s). In the acute phase, global infarction will determine edematous swelling of the spleen which will appear hypoechoic (Fig. 17.5a). The splenic parenchyma would appear more heterogeneous in case of more focused areas of infarcts such as in sickle cell disease. CT is the best imaging method to assess the degree of infarction (Fig. 17.5b). Infarcts will appear as non-enhancing areas. A subcapsular hematoma may be an associated finding.

Over time the infarcted area will tend to shrink with volume loss. Fibrosis or calcifications may develop [10–12].

Splenic artery aneurysm may develop secondary to trauma and pancreatitis. US with color Doppler is surely able to detect this vascular complication. Still, CT angiography should be performed whenever such anomaly is suspected in order to confirm the extent of traumatic lesions or the extent of pancreatic disease as well as to define the need of therapeutic embolization (see Chaps. 16 and 25) [13].

Splenic artery and vein thrombosis are rare conditions in children and usually related to pancreatitis (see Chap. 16). The thrombosis is best demonstrated by color Doppler US and confirmed by contrast-enhanced CT [1].

17.4 Splenic Rupture

17.4.1 Trauma (See Chap. 25)

The spleen is the intra-abdominal organ most vulnerable to trauma. There are varying degrees of splenic injuries which include lacerations, fracture, rupture, intrasplenic and subcapsular hematomas. US will always be the first imaging modality used in case of blunt abdominal trauma (as long as the clinical status of the patient is stabilized). Further evaluation will be decided upon the US findings and the clinical suspicion. Contrast-enhanced CT will be needed especially when active bleeding is suspected.

Since many years now, the majority of splenic injuries were managed non-surgically [1].

17.4.2 Non-traumatic Rupture and Hematoma of the Spleen

Non-traumatic rupture and hematoma of the spleen occurs most commonly in association with an infiltrative disease process such as malaria or infectious mononucleosis. Other causes include hemolytic anemia, pancreatitis, and hematologic malignancies. Rupture may be the initial presenting feature of mononucleosis or

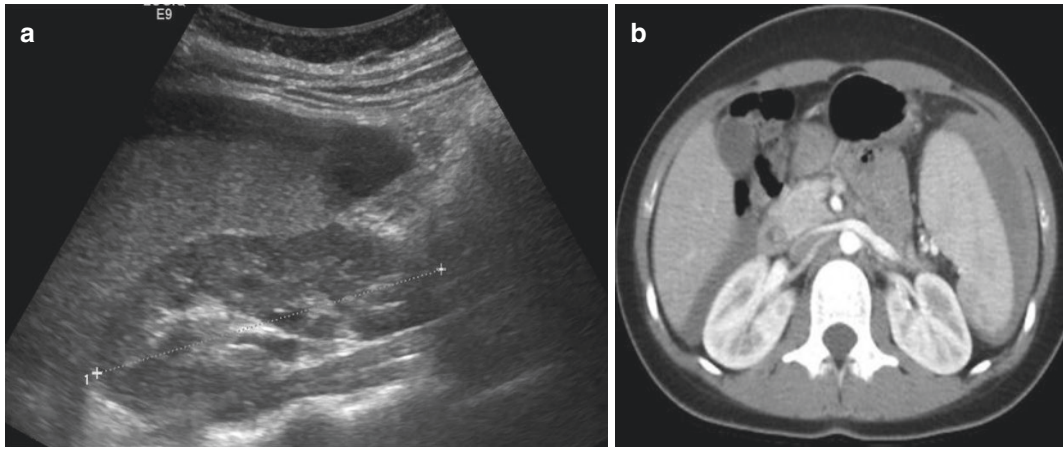

Fig. 17.6 Splenic rupture in a 16-year-old adolescent infected by EBV with acute onset of flank pain (it resolved spontaneously). (**a**) US of the *left upper abdomen* showing fluid around the spleen. *LK* = left kidney. (**b**) CE-CT confirms the peri-splenic fluid collection. There are some fluid around the liver as well

leukemia. Noteworthy, in case of mononucleosis rupture may occur during the 4–6 first weeks of the disease whereas in leukemia, the rupture may occur at any time at diagnosis, during therapy or at recurrence of the disease. Noteworthy, the rupture may occur on a normal size spleen. Thrombocytopenia and associated infectious processes are favoring features.

US will usually be the first imaging procedure performed. The initial findings may be misleading as subcapsular hemorrhage or intrasplenic rupture may at first appear echogenic and potentially missed. Rapidly, though, the echogenicity would decrease (Fig. 17.6a) and the detection will become easier; still, intrasplenic rupture/hematoma could be misinterpreted as due to a bleeding tumor. CE-CT may be useful to confirm the diagnosis and exclude an underlying tumor (Fig. 17.6b) [14, 15].

17.5 Torsion of (a Wandering) Spleen and Accessory Spleens

17.5.1 Torsion of the Spleen

The spleen is normally fixed in the left hypochondrium by the spleno-gastric and spleno-renal ligaments. A wandering spleen is characterized by excessive mobility and migration of the spleen from its normal position due to lack of fixation and to an unduly long splenic pedicle containing the splenic vessels. The condition can be observed in children as well as in adults. The long pedicle is predisposed to torsion. The risk of torsion being complete or partial splenic infarct.

The clinical presentation of uncomplicated wandering spleen can be asymptomatic and noted incidentally on imaging. Splenic torsion may be acute or chronic. Acute torsion may mimic appendicitis, twisted ovary, peritonitis, or intestinal obstruction.

A particular presentation is encountered whenever the twisted spleen pulls the stomach downwards and entails a gastric volvulus outlet obstruction. The pancreas may be trapped as well and bouts of pancreatitis increase the pain.

An abdominal mass can be palpated as well. Bouts of abdominal pain are the characteristics of chronic torsion.

Imaging plays an essential role for the diagnosis. Whatever imaging modality used, the clue to the diagnosis will be absence of the spleen in the left hypochondrium and presence of a “mass” in the abdomino-pelvic cavity (Fig. 17.7a). US with color Doppler can achieve this diagnosis demonstrating the ectopic spleen and the lack of vascularization. The distended stomach should not be overlooked as distended bowel loops.

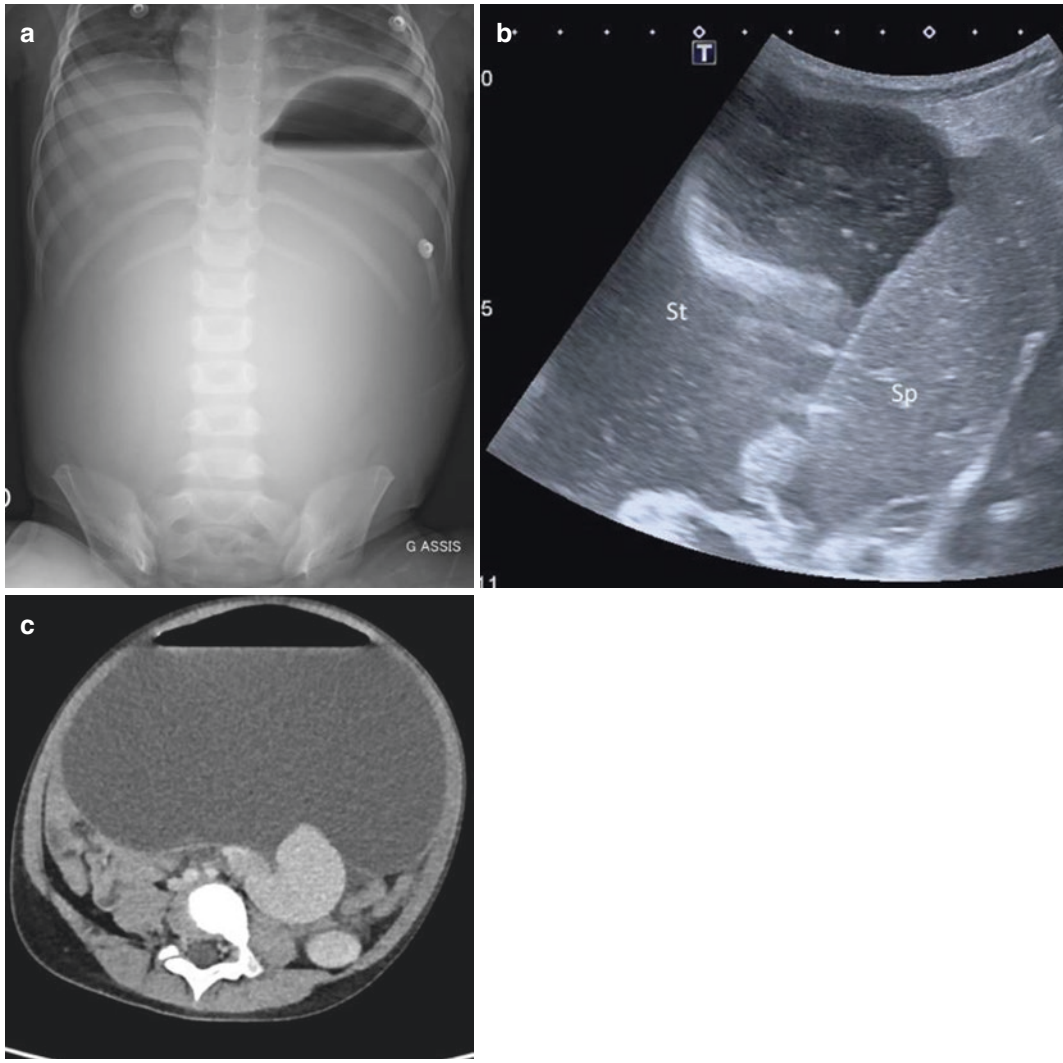

Fig. 17.7 Wandering spleen with subsequent gastric volvulus in a 2-year-old girl. (**a**) Plain radiograph of the abdomen showing an airless abdomen due to massive gastric obstruction and distension. (**b**) US of the *left flank*: the spleen (Sp) is located in the lower part of the *left flank* adjacent to the spine. The fluid-filled marked distended stomach (St) lies close to the spleen. (**c**) CE-CT of the lower abdomen showing that the parenchyma of the wandering spleen enhances confirming persistent perfusion. Markedly distended stomach that had been pulled and undergone torsion due to the migration of the spleen. (The child was operated and the spleen attached to the diaphragm; follow-up was uneventful)

The diagnosis is easier to achieve on CE-CT especially in order to define the degree of persistent vascularization of the spleen and to optimize surgery (Fig. 17.7b) (splenopexy vs splenectomy). CT may demonstrate more easily than US the twisted pedicle [16–18].

17.5.2 Torsion of Accessory Spleen

An accessory spleen is caused by the failure of splenic anlage to fuse during embryogenesis. Their sizes vary from few mm to several cm. Accessory spleens are usually located in the

vicinity of the splenic hilum but they may be located anywhere in the abdomen and in the left scrotum. The vascular pedicle of an accessory spleen is commonly related to the splenic hilum. Torsion and infarction of an accessory spleen may potentially occur but are very rare. Imaging may sometimes suggest the diagnosis. On US, the twisted accessory spleen would appear as a round hypoechoic mass close to the splenic hilum with no or little vascularization on color Doppler. The presence of another supplementary accessory spleen in the vicinity helps for the diagnosis [19].

Conclusion

The spleen may be involved a large panel of pathologies specific to the spleen or part of more global diseases. Imaging and especially US will demonstrate the splenic lesions. In selective cases, MR imaging and CE-CT may contribute to the global evaluation of the diseases.

References

1. Patterson A, Frush D, Donnely LF, et al. A pattern-oriented approach to splenic imaging in infants and children. Radiographics. 1999;19:1465–85.
2. Siegel MJ. The spleen and peritoneal cavity. In Siegel's Pediatric Sonography. 4th ed. Wolters Kluwer Publisher; 2011. pp 305–338.
3. Nemati M, Hajalioghli P, Jahed S, et al. Normal values of spleen length and volume: an US study in children. Ultrasound Med Biol. 2016;42:1771–8.
4. Elsayes KM, Narra VR, Mukundan G, et al. MR imaging of the spleen: spectrum of abnormalities. Radiographics. 2005;25:967–82.
5. Gale HI, Bobbitt CA, Setty BN, et al. Expected US appearance of the spleen in children and young adults with sickle cell disease. J Ultrasound Med. 2016;35:1735–45.
6. Lima da Silva Filho I, Severo Ribeiro G, Gomes Moura P, et al. Sickle cell disease: acute clinical manifestations in early childhood and molecular characteristics in a group of children in Rio de Janeiro. Rev Bras Hematol Hemoter. 2012;34:196–201.
7. Maritsi DN, Zarganis D, Metaxa Z, et al. Bartonella henselae infection: an uncommon mimicker of autoimmune disease. Case Rep Pediatr. 2013;2013. Article ID 726826:4.
8. Shrot S, Barkat G, Ben-Shlush A, et al. BCGitis and BCGosis in children with primary immunodeficiency – imaging characteristics. Pediatr Radiol. 2016;46:3237–45.
9. Abbott RM, Levy AD, Aguilera NS, et al. Primary vascular neoplasms of the spleen: radiologic-pathologic correlation. Radiographics. 2004;24:1137–63.
10. Unal E, Onur MR, Akpinar E, et al. Imaging findings of splenic emergencies: a pictorial review. Insights Imaging. 2016;7:215–22.
11. Naviglio S, Abate MV, Chinello M, et al. Splenic infarction in acute infectious mononucleosis. J Emerg Med. 2016;50:e11–3.
12. Khatib R, Rabah R, Sarnaik SA. The spleen in sickling disorders: an update. Pediatr Radiol. 2009;39:17–22.
13. Larsen CC, Laursen CB, Dalby K, et al. Splenic artery pseudo-aneurysm due to acute pancreatitis in a 6-year-old boy with ALL treated with L-asparaginase. BMJ Case Rep. 2014; doi:10.1136/bcr-2013-202298.
14. Athale UH, Kaste SC, Bodner SM, et al. Splenic rupture in children with hematologic malignancies. Cancer. 2000;88:480–90.
15. Bartlett A, Williams R, Hilton M, et al. Splenic rupture in infectious mononucleosis: a systematic review of published case reports injury. Int J Care Injured. 2016;47:531–8.
16. Lombardi R, Menchini L, Cornelli T, et al. Wandering spleen in children: a report of 3 cases and a brief literature review underlining the importance of diagnostic imaging. Pediatr Radiol. 2014;44:279–88.
17. Fiquet-Francois C, Belouadah M, Ludot H, et al. Wandering spleen in children: multicenter retrospective study. J Pediatr Surg. 2010;45:1519–24.
18. Sanchez R, Lobert P, Herman R, et al. Wandering spleen causing gastric outlet obstruction and pancreatitis. Pediatr Radiol. 2010;40(Suppl 1):S89–91.
19. Perez-Fontan FJ, Soler R, Santos M, et al. Accessory spleen torsion: US, CT and MR findings. Eur Radiol. 2001;11:509–12.

Part V

Any Age: The Uro-Genital Tract

Urinary Tract Infection

18

Pierre-Hugues Vivier and Adnan Hassani

Contents

P.-H. Vivier (✉)
Ramsay Générale de Santé, Hôpital Privé de l'Estuaire, Radiologie, 505 Rue Irène Joliot Curie, 76620 Le Havre, France

Service d'Imagerie Pédiatrique et Fœtale, CHU Charles Nicolle, 1 Rue de Germont, 76031 Rouen Cedex, France
e-mail: pierrehuguesvivier@yahoo.fr

A. Hassani

Service d'Imagerie Pédiatrique et Fœtale, CHU Charles Nicolle, 1 Rue de Germont, 76031 Rouen Cedex, France

18.1 Background

Urinary tract infection (UTI) in children is very common and depends on age and sex. UTI is more frequent in boys (3.7%) than in girls (2%) in the first year of life, with an increased risk in uncircumcised boys. Later, the incidence is greater in girls (3%) than in boys (1%) [1, 2].

In newborns, symptoms of UTI are often non-specific. Fever can be absent even in case of pyelonephritis. Vomiting, poor appetite, failure to thrive, diarrhea, jaundice, lethargy, and irritability can be the main symptoms. There is a higher risk of urosepsis in neonates than in children and adults [1, 2].

Up to 30% of infants and children experience recurrent infections during the first 6–12 months after an initial UTI [3, 4]. Recurrent UTI is at risk for renal scarring, poor renal growth, hypertension, preeclampsia, and in extreme cases impaired renal function. The goal of the imaging work-up is to detect complications in case of acute UTI but mainly to look for risk factors of recurrent UTI.

Bladder and bowel dysfunction is also a classical risk factor of UTI in toilet-trained children, especially in girls and should always be kept in mind, as it is at risk for recurrence and failure of anti-reflux treatment.

18.2 Diagnosis of UTI

The diagnosis of UTI is based on urine analysis. Urine sampling is of paramount importance.

F.E. Avni, P. Petit (eds.), *Imaging Acute Abdomen in Children*,
https://doi.org/10.1007/978-3-319-63700-6_18

18.2.1 Urine Sampling

Suprapubic bladder aspiration (SPA) is the most sensitive method to get an uncontaminated urine sample, and is considered as the standard method [5]. Its use requires US to ensure that the bladder is full enough to perform the puncture [6] that remains more painful than catheterization in infants <2 months [7]. However local anesthetics can be used topically to reduce pain [8].

Despite a higher rate of contamination, bladder catheterization is an acceptable alternative to SPA. Urine obtained through catheterization for culture has a sensitivity of 99%, compared with that obtained through SPA [5].

Although SPA and bladder catheterization are recommended in non-toilet trained children, plastic bags are still commonly used to avoid catheterization. Yet, bags are associated with a higher rate of contamination and false positive culture of 88% in case of a prevalence of UTI of 5% [5]. As a result plastic bags may be used to exclude UTI by using dipsticks but not for diagnostic purposes. Culture of urine collected from plastic bags would generate an unacceptable rate of false positive and would lead to treat patients without UTI with antibiotics, with additional costs such as ultrasound, and potentially VCUG which requires catheterization.

18.2.2 Dipstick

Urine dipstick is useful to exclude UTI in case of negativity for both leukocyte esterase and nitrites [9]. However, in case of positivity for either leukocyte esterase or nitrite, urine analysis and culture are necessary and have to be performed on a clean urine sampling (SPA or bladder catheterization).

18.2.3 Urinalysis and Culture

The diagnosis of UTI is made on the basis of quantitative urine culture in addition to pyuria. However, culture results require at least 24 h. Urinalysis can predict the results and enable presumptive therapy to be initiated before obtaining the definitive results of the culture.

Based on the 2011s guideline from the American Academy of Pediatrics, urine specimens have to be obtained only by invasive methods: SPA or urethral catheterization. Microscopy can be used to detect pyuria and/or bacteriuria. If a counting chamber is used, pyuria is considered significant in case of at least 10^4 WBC per mL. When pyuria is absent, a positive culture is generally considered as an asymptomatic bacteriuria.

At microscopy, the presence of bacteria in a fresh, Gram-stained specimen of uncentrifuged urine correlates with 10^5 CFUs per mL in culture [5].

The threshold for bacteriuria is the presence of at least 5×10^4 CFUs per mL of a single urinary pathogen [10].

18.3 How to Image Acute UTI

18.3.1 When to Image Acute UTI

Ristola et al. have shown that US performed after a first UTI in children aged 2–24 months with normal prenatal US was abnormal in 22% with dilatation of the urinary tract in 13% [11]. As a result a normal prenatal US does not preclude the need for US in this setting, and thus should be systematic.

US should be performed as soon as possible in neonates, in case of urosepsis, unusually severe clinical illness and poor response to therapy. In other cases, an early US during the acute phase may be misleading and should be avoided [5]. Animal studies demonstrate that Escherichia coli endotoxin can produce dilatation during acute infection, which could be confused with hydronephrosis, pyonephrosis, or obstruction [12]. Parenchymal edema during acute infection can alter the size and shape of the kidneys and their echogenicity. The presence of these abnormalities makes it inappropriate to consider US performed early during an acute infection to be a true baseline study that would be used for later comparison in the assessment of renal growth. US can be performed at least 10 days after initiating the antibiotherapy.

18.3.2 Ultrasound

US is the cornerstone of UTI imaging. It is easily accessible and provides relevant information, with no radiation exposure and with a low cost. It may confirm the diagnosis in case of doubtful pyelonephritis, but mainly it can identify risk factors and complications. The use of a linear high frequency probe is of utmost importance in neonates and young children to assess as good as possible the renal parenchyma, and especially its corticomedullary differentiation.

18.3.2.1 Signs of Pyelonephritis at US

US patterns of acute pyelonephritis (APN) include:

- Pelvic wall thickening (Fig. 18.1). It is sometimes improperly called pyelitis as US cannot differentiate a thickening related to a true pyelitis or to VUR. It may also more rarely correspond to a post-operative reaction or renal transplant rejection [13, 14]. Pelvic wall is considered thickened when it exceeds 0.8 mm [14].
- Peripelvic fat thickening with increased echogenicity and blurred boundaries [15] (Fig. 18.2).
- Focal or global parenchymal hyperechogenicity (Figs. 18.2, 18.3, and 18.4) due to nephritis, with loss of cortico-medullary differentiation.
- Focal or global renal swelling related to edema whether the nephritis is focal or involves the entire parenchyma. Axial views are more suitable than coronal ones to assess these changes [16] (Fig. 18.2). Substantial focal enlargement can sometimes produce a pseudo-tumoral appearance [17, 18] (Fig. 18.4).

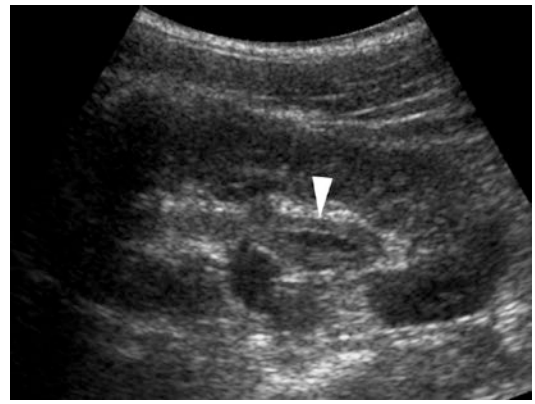

Fig. 18.1 Pelvic wall thickening (*arrowhead*)

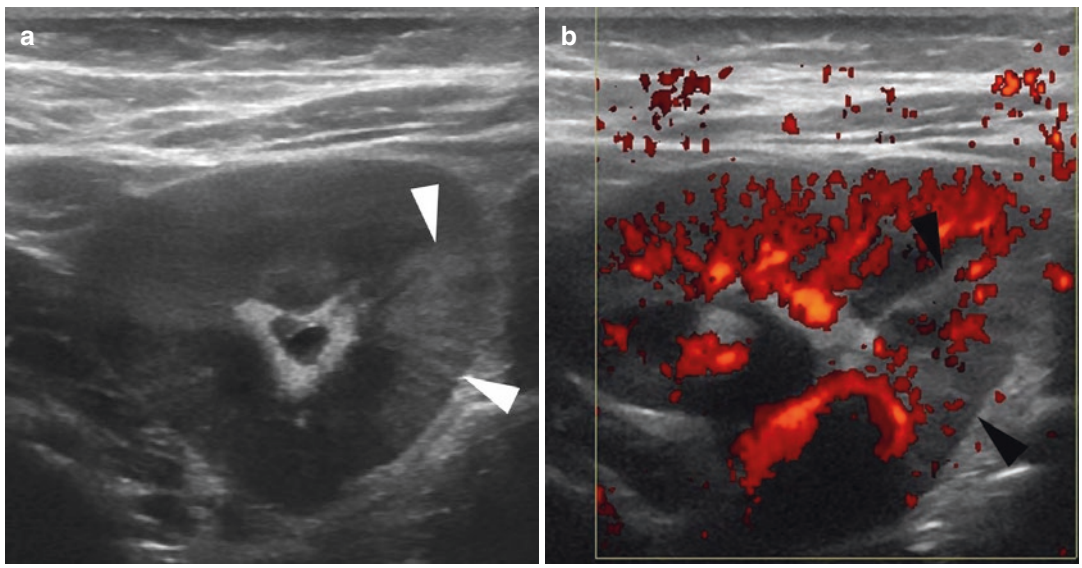

Fig. 18.2 Nephritis. Axial sonogram (**a**) demonstrates pelvic wall thickening, increased peripelvic fat thickening, and a focal nephritis: area of increased echogenicity (*white arrowheads*) with a striated pattern. Power Doppler image (**b**) shows diminished flow in the same area (*black arrowheads*)

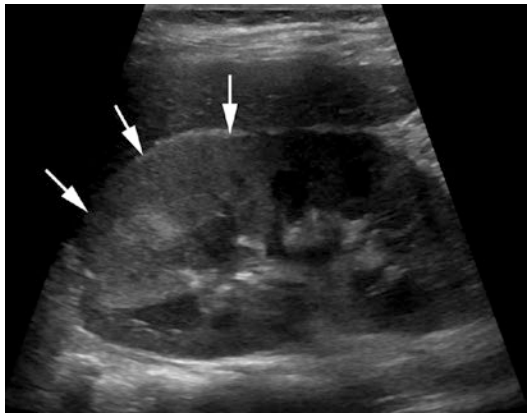

Fig. 18.3 Focal nephritis: increased echogenicity with loss of corticomedullary differentiation and parenchymal swelling

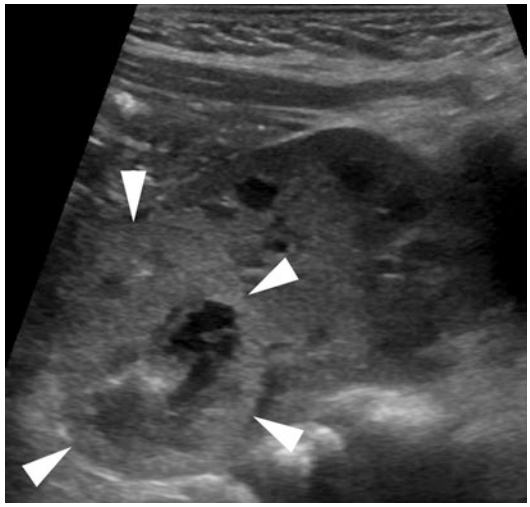

Fig. 18.4 Pseudotumoral pyelonephrits (*arrowheads*) with a small hypoechoic area corresponding to liquefaction (abscess)

– Focal or global decrease in renal parenchyma vascularization at color and Power Doppler due to inflammatory edema and ischemic lesions [19] (Fig. 18.2).

The sensitivity of gray-scale sonography for the diagnosis of renal inflammation is only 25–40% [20–22]. The additional use of color Doppler increases the sensitivity to 65v–75%, and with addition of power Doppler imaging, the sensitivity and specificity increase to 75% and 86% to 100%, respectively [20–23].

New renal ultrasensitive Doppler imaging techniques, also called micro-Doppler imaging, based on ultrafast plane wave imaging ("AngioPLUS") [24] or on advanced clutter suppression algorithms ("Superb Microvascular Imaging":SMI) [25, 26] might be of great interest to better assess renal parenchyma microvascularization [27]. These new Doppler techniques have not been evaluated in acute pyelonephritis yet.

18.3.2.2 Complications: Abscess and Pyohydronephrosis

A renal abscess is a necrotic cavity filled with purulent material that corresponds to a nephritis area that ultimately liquefies. Large abscesses require prompt percutaneous or surgical drainage. Most of abscesses are intra-parenchymal, and appear as a well-limited hypoechoic mass with or without thick walls (Fig. 18.5). It may contain septations and mobile debris and rarely highly echogenic foci corresponding to gas bubbles. There is no internal flow at Doppler imaging.

Pyohydronephrosis corresponds to the accumulation of purulent urine in a dilated kidney. It can be due to an obstructive uropathy, or less often secondary to calculi or stricture. This is a urologic emergency and requires prompt percutaneous or surgical drainage. It appears as mobile hypoechogenic debris echoes in the urine (Fig. 18.6), with or without a fluid–fluid level. Care should be taken when describing echogenic urine as false positive cases of pyohydronephrosis are commonly encountered using this sonographic description only. The term pyohydronephrosis should be used in case of severe clinical state at presentation or insufficient response to antibiotics after 48 h of antibiotics.

18.3.2.3 Risk Factors at US

The main interest of US is to identify an underlying uropathy that favors UTI; it corresponds generally to a pelvicalyceal dilatation or ureteral dilatation. Bladder diverticulum, ureterocele (Fig. 18.7), urachal diverticulum (Fig. 18.8), and dilatation of the upper part of the urethra should be screened as well. Urinary stones can be a risk factor for UTI (and a complication), especially in

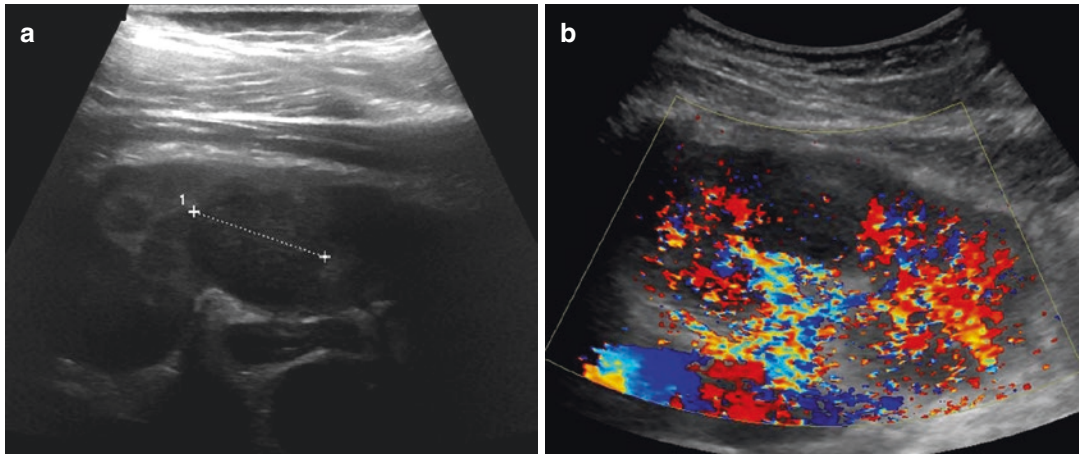

Fig. 18.5 Renal abscess. Longitudinal sonogram (**a**) shows a thickened pelvic wall with peripelvic fat hyperechogenicity along with a hypoechogenic round area (abscess). *Color Doppler* image (**b**) shows absence of internal flow in the abscess

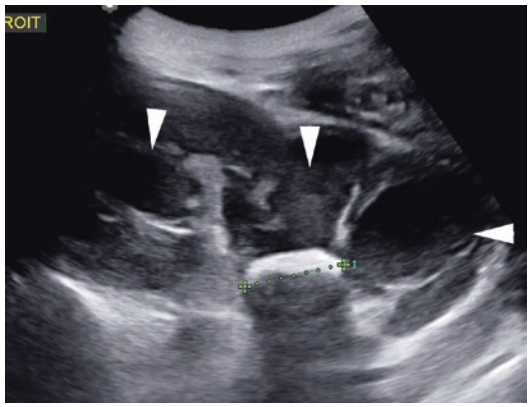

Fig. 18.6 Pyohydronephrosis. Calyces are dilated and filled with echogenic urine (*arrowheads*) with mobile debris with obstruction related to a pelvic stone

case of Proteus mirabilis infection. In the setting of UTI, upper tract dilatation in children is much more frequently related to a uropathy than an infected colitis nephritis.

Noteworthy, the ability of US to detect Grades I-V VUR is poor and varies according to different studies, with a sensitivity of 16–40% and negative predictive value of 25–86% [28–31].

It is well known that ureteral and pelvicalyceal dilatation may often be absent in case of high grade VUR (III–V). Also US is a poor predictor of high grade reflux with a sensitivity of 68–77% and a negative predictive value of 88–94% [32–34]. This high negative predictive value of normal US makes the diagnosis of high grade VUR unlikely for children with a first febrile UTI.

18.3.3 ^{99m}Tc-DMSA-Scintigraphy

^{99m}Tc- dimercaptosuccinic acid (DMSA) is still considered as the gold standard imaging method in detecting renal parenchymal involvement in patients diagnosed with acute pyelonephritis [35]. Approximately 40% of the administered dose accumulates in the distal tubular cells, providing a cortical study. Images are acquired 2–3 h after tracer injection, and APN areas appear as photopenic defects or exhibit a striated pattern. Due to its limited spatial resolution, ^{99m}Tc-DMSA scintigraphy cannot readily differentiate APN from chronic scarring or renal cyst. Moreover, scintigraphy has negative aspects including the need for intravenous access, high cost, and exposure to radiation: approximately 1 mSv regardless of the age of the child [36, 37]. As a result, its use is no longer recommended in daily practice as in case of APN [5]. However, it remains an excellent method to assess the renal parenchyma after recurrent APN to screen for renal scarring and to quantify the differential renal function.

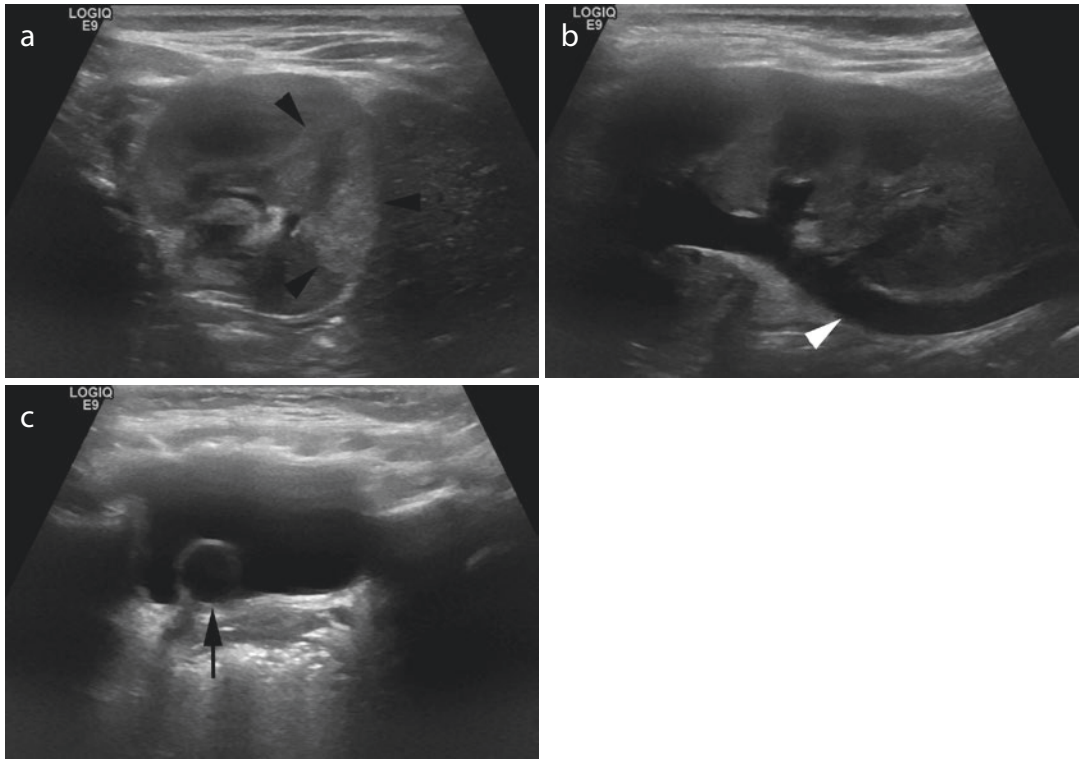

Fig. 18.7 Pyelonephritis associated with a single system ureterocele. Axial sonogram (**a**) shows a hyperechoic area with loss of corticomedullary area corresponding to a focal nephritis (*black arrowheads*). Longitudinal sonogram (**b**) demonstrates ureteral (*white arrowhead*) and pelvicalyceal dilatation. Axial sonogram on the bladder (**c**) shows a cystic structure within the posterior wall of the bladder corresponding to an ureterocele (*arrow*)

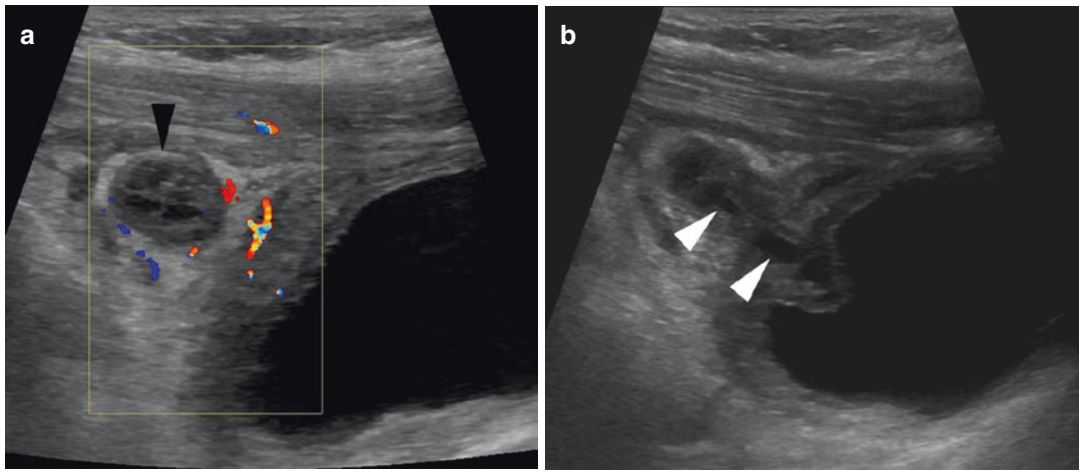

Fig. 18.8 UTI related to pyourachus. Para-sagittal sonogram (**a**) shows a heterogeneous and echogenic mass corresponding to a pyourachus (*black arrowhead*) just above the bladder with peripheral hyperechoic fat and inflammatory abnormal flow with *color Doppler*. Sagittal sonogram (**b**) depicts the fistulous tract (*white arrowheads*) extending from the pyourachus to the bladder dome

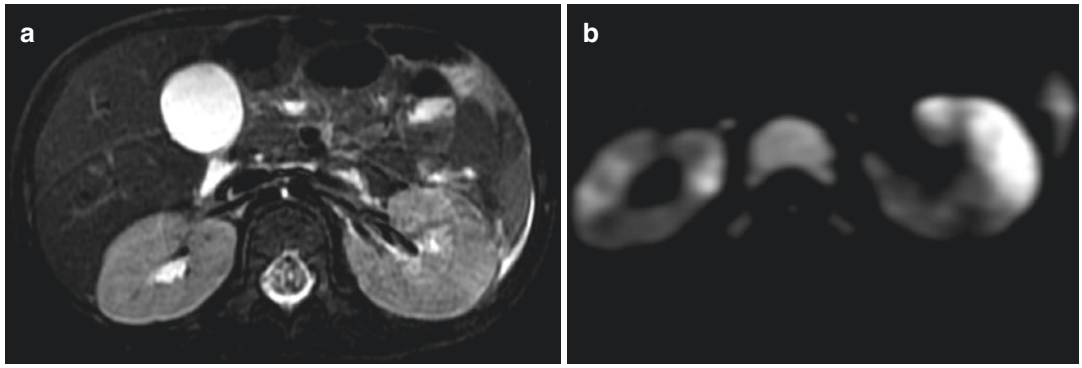

Fig. 18.9 Bilateral pyelonephritis at MR imaging. Axial T2-W image (**a**) shows an enlarged left kidney without salient signal anomaly. Axial DWI image (**b**) depicts multiple and bilateral areas of hyperintensities corresponding to nephritis areas

18.3.4 MR Imaging

MR imaging can show pyelonephritis without contrast using diffusion-weighted imaging (DWI) [38]. Nephritis appears hyperintense with restricted diffusion on apparent diffusion coefficient maps (Fig. 18.9). Moreover, the use of T2-weighted sequences provides an anatomic study that makes MR imaging an attractive imaging modality in this setting. The combination of axial and coronal oblique views of both sequences is optimal to ensure that diffusion anomalies are real and do not correspond to artifacts. T2-weighted images allow kidney length and renal pelvis measurements. Much better than scintigraphy, T2-weighted images can show abscesses (marked hyperintensities with hypointense rim) but also renal scarring or cortical cysts. It is noteworthy that areas of nephritis are often not visible on T2-weighted images, and when an anomaly is visible it appears as an hypo or hyperintense area [39]. The use of these different sequences makes this examination shorter than 15 min, without the need for intravenous puncture and contrast infusion. However, sedation remains necessary.

Indications for MR imaging can include a doubtful urine culture, antibiotic prescription before urinalysis or unfavorable clinical response after 48 h of antibiotics. Limitations for MR imaging is an age younger than 6–8 months as diffusion is known to be spontaneously reduced in this age group [40]. Another limitation is that the duration of the hypersignal on DWI images is unknown for the moment, and it is not possible to ensure that DWI anomalies do not correspond to a previous pyelonephritis in case of history of multiple UTI.

18.3.5 Computed Tomography

Computed tomography (CT) is sometimes used in case of doubtful or complicated pyelonephritis due to its easy access, fast acquisition time, and reduced need for sedation. It requires iodinated-contrast infusion (1–2 mL/kg) at the arterial or nephrographic phase. As US should be performed systematically before performing a CT, a single phase study is generally sufficient. Moreover, an unenhanced acquisition has a poor additional value and should be avoided. An abdominal exploration without irradiating the pelvis and gonads should be favored as much as possible, although the protocol should be tailored to each patient. Dedicated age-specific, weight-specific pediatric CT-protocols must be used. Imaging features include a round or wedge-shaped area of diminished attenuation (Fig. 18.10). Alternating pathological and nor-

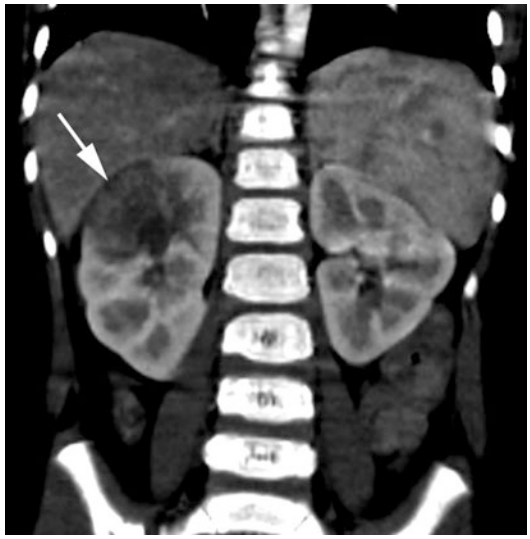

Fig. 18.10 Focal pyelonephritis at CT. Coronal image at a late arterial phase shows a wedge-shaped area of diminished attenuation at the *right upper pole* (*arrow*)

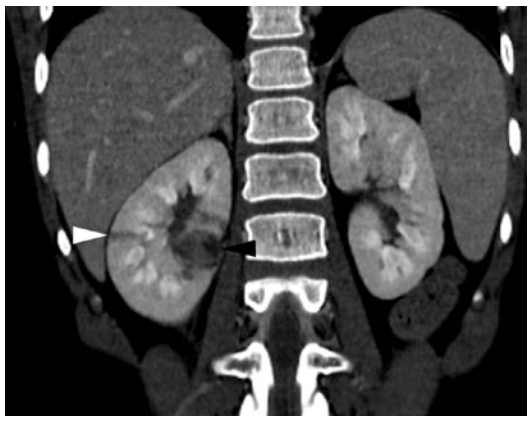

Fig. 18.11 Renal abscess at CT (Same patient as Fig. 18.5). Coronal image at nephrographic phase depicts a linear area of low attenuation nephritis (*white arrowhead*) and a round structure with lower attenuation areas corresponding to the early phase of an abscess (*black arrowhead*)

mal areas can generate a striated pattern. Abscesses appear as well-marginated hypodense cavities, with a lower attenuation than the adjacent nephritic area with or without a thick rim (Fig. 18.11). Ideally, CT should be performed only when MR imaging is not available or is not diagnostic enough.

18.3.6 Voiding Cystourethrography (VCUG) and Contrast-Enhanced Voiding Urosonography (ce-VUS)

The use of VCUG remains controversial. This examination is relatively invasive with potential side effects including dysuria, urinary retention, hematuria, and infection [41, 42]. Moreover, it exposes the patients to radiations. The radiation burden decreases regularly, thanks to the progressive replacement of screen film radiography by computed radiography and now by digital radiography. Sulieman et al. reported in 2016 measured doses in children explored by VCUG [43]. The mean entrance surface air kerma (ESAK) and range (mGy) corresponded to 2.2 ± 0.5 (0.8–9.2) in infants and young children (≤5 years) to 3.90 ± 0.6 [1–10] in adolescents.

A general trend has been to decrease dramatically the use of VCUG which was historically almost systematic after the first UTI in children. Its main goal is to diagnose vesicoureteric reflux. Thirty to forty percent of children investigated for UTI have VUR [28].

Historically, VUR was treated almost exclusively by open surgical reimplantation of the ureter. With the recognition that VUR often resolves spontaneously with time, the concept of antibiotic prophylaxis was introduced to prevent UTI while waiting for VUR resolution.

The efficiency of antibiotic prophylaxis has been a long-standing debate with inconsistent results. That is why the guideline issued by the American Academy of Pediatrics in 2011, based on a meta-analysis, did not recommend antibiotic prophylaxis in children without reflux or with grade I to grade IV reflux [5]. As a result, VCUG was not recommended systematically after the first UTI, but only in case of hydronephrosis, scarring or other findings that would suggest either high grade VUR or obstructive uropathy or in other atypical or complex clinical circumstances. VCUG should also be performed in case of febrile UTI recurrence.

Since this guideline, two prospective studies have confirmed that prophylaxis has a real impact. The Randomized Intervention for Children with

Vesicoureteral Reflux (RIVUR) study, a large multicenter, randomized placebo-controlled trial, involving 607 children between the ages of 2–71 months with grade I to grade IV reflux, showed that prophylaxis reduced the risk of recurrence of UTI by almost 50% [44]. However, the number of new renal scars was not different in this study.

Another large, multicenter clinical trial, the Swedish Reflux Trial, involved 203 children aged 1 to younger than 2 years with grade III–IV reflux also showed a reduction in recurrent UTIs in girls on antibiotic prophylaxis [45]. Based on these studies, the guidelines issued in 2015 by the European Association of Urology (EAU) and the European Society for Paediatric Urology (ESPU) recommended a more frequent use of VCUG than the American Guideline. The European guidelines recommend to perform VCUG in non-toilet trained children systematically in girls after the first UTI even in case of normal ultrasound and in boys younger than 1 year.

VUR depicted by VCUG is classically graded according to The International Reflux Study Group from grade I to V (Fig. 18.12).

If VUR is the most common anomaly in the setting of UTI, VCUG can show a range of other urinary tract abnormalities, including ureterocele (Fig. 18.13) or posterior urethral valves (Fig. 18.14).

VCUG may also suggest a dysfunctional voiding (Fig. 18.15), but radiological signs are not specific. In case of potential dysfunctional voiding, uroflowmetry should be performed.

ce-VUS is gaining more and more interest as it is a radiation free alternative to VCUG. It investigates the urinary tract with intravesical administration of contrast agent: the second generation corresponds to microbubbles of sulfur hexafluoride (Sonovue(R), Bracco, Milan, Italy). Thus, ce-VCUG requires bladder catheterization as VCUG, and shares the same side effects except radiation exposure. It makes it a very safe procedure [46, 47].

In comparison with VCUG, ce-VUS has a sensitivity of 85–100% and a specificity of 78–97% for reflux screening [48].

Numerous reports indicate that ce-VUS is a highly sensitive and specific method, which can in many cases replace VCUG. Diagnosis of urethral pathologies can be achieved by using transperineal and interscrotal approaches in boys [49].

18.3.7 Uroflowmetry

In case of UTI, bladder and bowel dysfunction (BBD) should always be considered in toilet-trained children (although not as an emergency procedure, but surely in order to prevent recurrences). BBD is a major risk for UTI recurrence and failure of VUR treatment.

BBD is often present in the presence of UTI regardless of the presence of VUR and is more frequent in girls. However, VUR and BBD are frequently associated: 34–70% of children referred for VUR have BBD [50]. The prevalence of BBD in children who experienced a first UTI and have VUR is as high as 54% [51]. Correction of lower urinary tract dysfunction is important to decrease the rate of UTI recurrence.

Embryological, anatomical, and functional interactions between bladder and bowel are well established. BBD may generate a myriad of lower urinary tract symptoms (LUTS), accompanied by bowel complaints, primarily constipation and/or encopresis, LUTS symptoms common to BBD include dysuria, urgency, urinary frequency, daytime incontinence, enuresis, dribbling, straining, voiding postponement, and urinary retention.

In addition to a clinical history and physical examination, voiding and bowel diaries are essential for the initial evaluation of BBD. If BBD is considered possible, uroflowmetry should be performed.

Uroflow studies consist of measuring the rate, volume voided, voiding time, post-void residual volume and examining the pattern during urination into a uroflowmeter. Post-void residual is also frequently measured. It is often and advantageously combined with electromyography (EMG) by use of skin patch electrodes evaluating the perineal muscles.

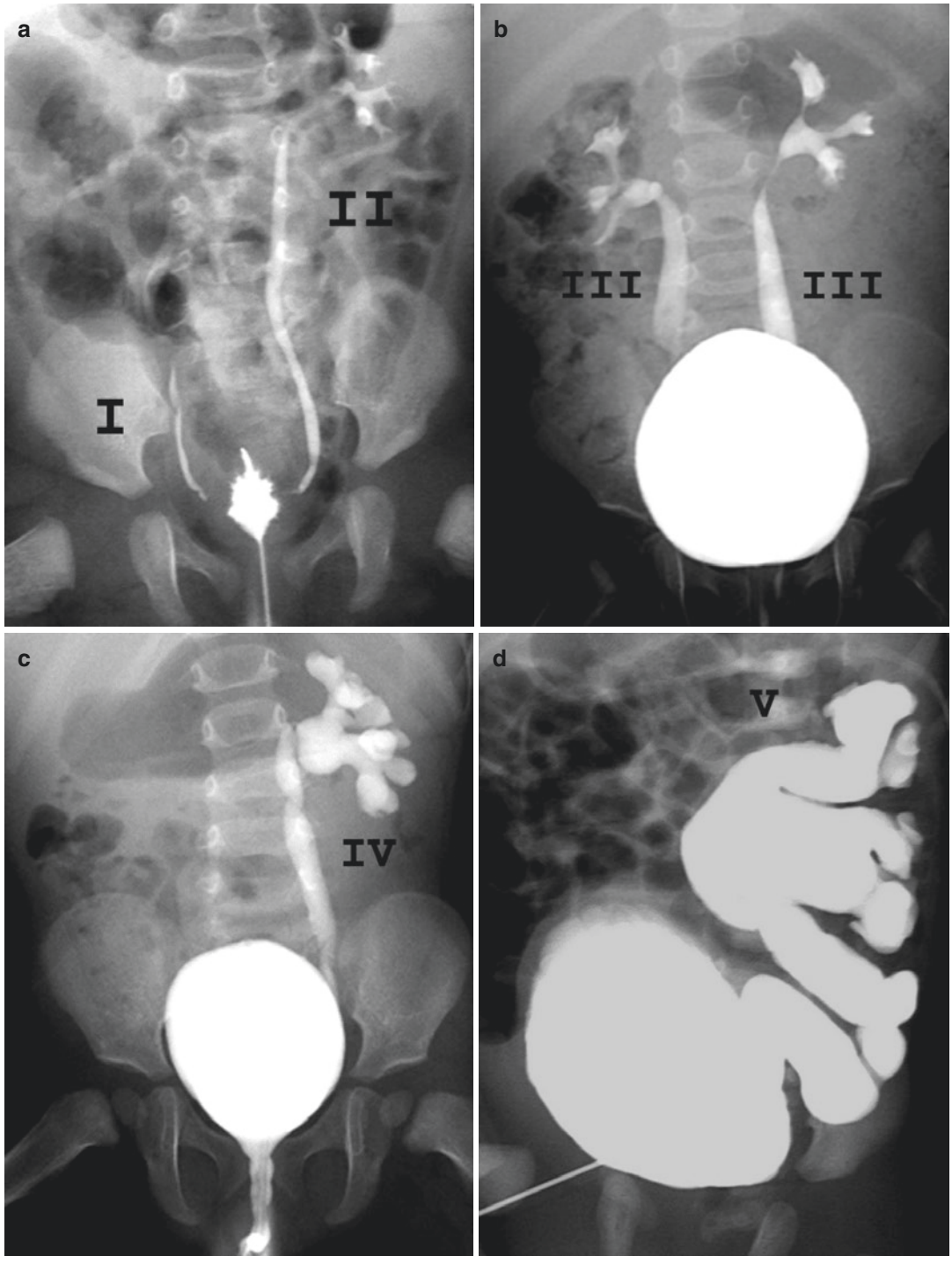

Fig. 18.12 Vesicoureteral reflux (VUR) at VCUG. VUR grading

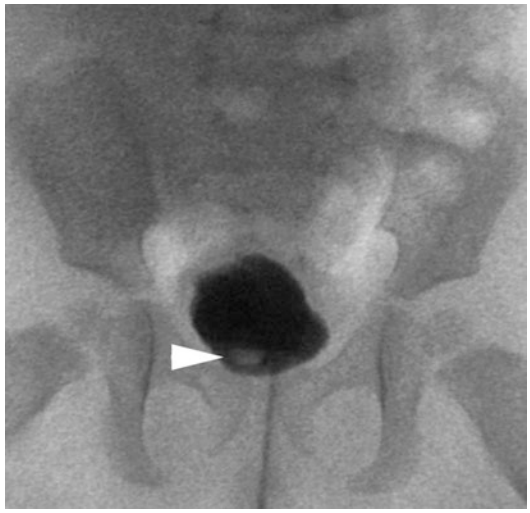

Fig. 18.13 Ureterocele at VCUG (Same patient as Fig. 18.7). Round lucency (*arrowhead*) at the right aspect of the trigone

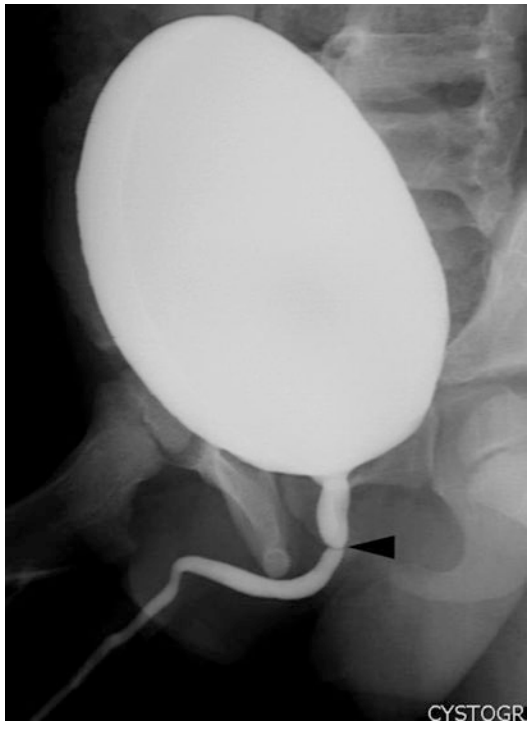

Fig. 18.14 Posterior urethral valves in a 10-year-old boy without upper tract dilatation. Slightly dilated proximal (*posterior*) urethra leading to abrupt narrowing (*arrowhead*) corresponding to a linear radiolucent band corresponding to the valves

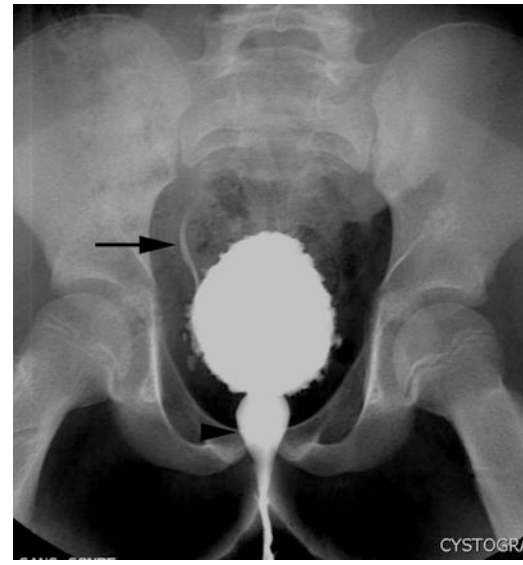

Fig. 18.15 Signs of dysfunctional voiding at VCUG. The micturating image shows a spinning top urethra (*arrow head*), with a trabeculated bladder wall and a *right* vesicoureteric reflux of grade I (*arrow*)

The advantage of combining EMG with uroflowmetry is the ability to appreciate synergy or dyssynergy between the bladder and the pelvic floor, i.e. external striated sphincter activity [52, 53].

Normal voiding occurs when the bladder outlet relaxes and the detrusor contracts. During a normal detrusor contraction with minimal intraurethral resistance, the normal flow curve is bell-shaped with a high maximum flow rate while the external sphincter relaxes with a poor electrical activity (Fig. 18.16).

Uroflowmetry combined with perineal EMG can show classically two kinds of curves suggestive of dysfunctional voiding (contraction of the urethral sphincter during voiding):

– a staccato-shaped curve (Fig. 18.17): this flow pattern is irregular and fluctuating throughout voiding but the flow is continuous, never reaching zero during voiding. This pattern suggests incoordination of the bladder and the sphincter with intermittent sphincter overactivity during voiding

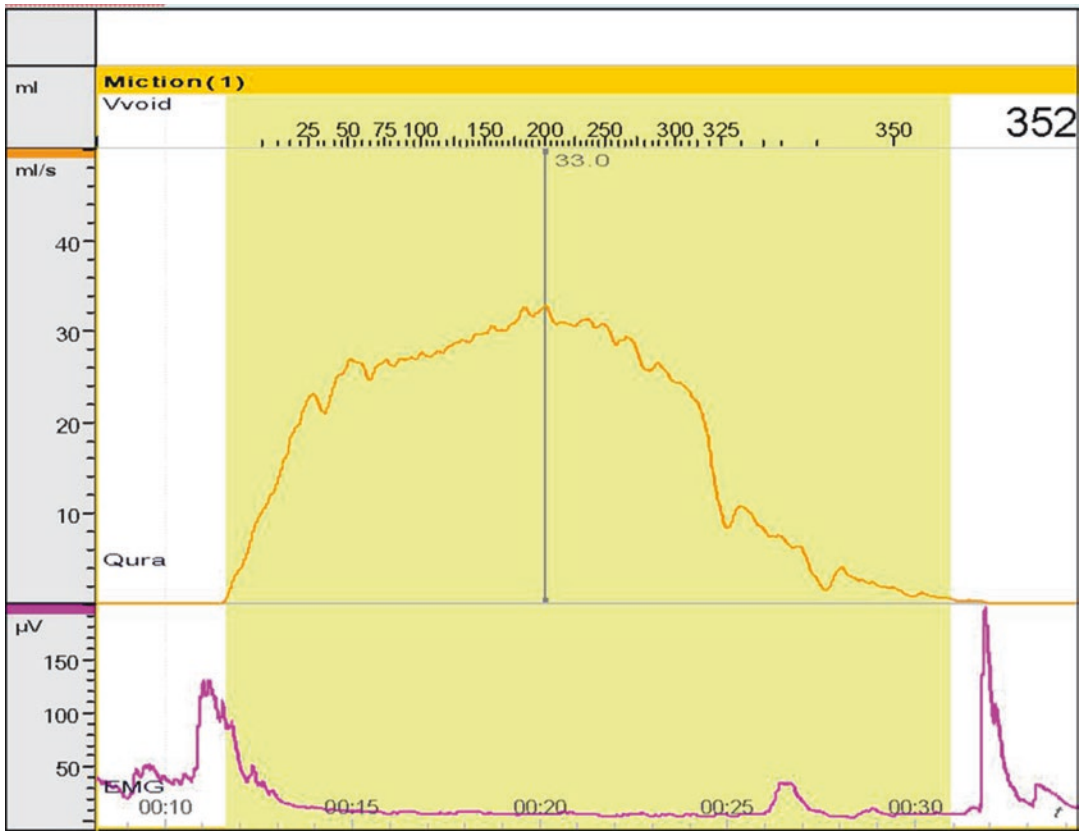

Fig. 18.16 Normal voiding at uroflowmetry combined with perineal electromyogram (EMG) in a 10-year-old girl: *bell-shaped* uroflow curve (*orange*) with poor EMG activity (*purple*) during voiding

– Interrupted-shaped curve: this flow will display discrete peaks with spikes similar to a staccato-shaped curve but unlike the latter pattern, there will be segments where zero flow with complete cessation between these peaks exists. This flow pattern suggests an underactive bladder. Each peak represents abdominal muscle straining creating the main force for urine evacuation. In between each strain, the flow ceases. It is possible this flow pattern can be seen with incoordination between the bladder and external urethral sphincter.

Uroflowmetry with perineal EMG is also useful to assess the efficiency of the treatment of BBD.

Conclusion

The first imaging modality in case of UTI in children remains US, which may potentially show signs of pyohydronephrosis. The use of a high-frequency-probe is of great value in infants and young children in this goal. It is an excellent exam for detecting dilatation of the urinary tract revealing a uropathy that may be at risk for UTI. Also it can show complications as pyelopyonephrosis or renal abscesses. When to perform VCUG remains a subject of debate, and recent guidelines are not in line. New imaging modalities are less invasive. Ce-VUS is replacing slowly VCUG due to its absence of radiation exposure. MRI is also replacing CT for the same reason. MRI has also the advantage of not requiring contrast injection by use of DWI.

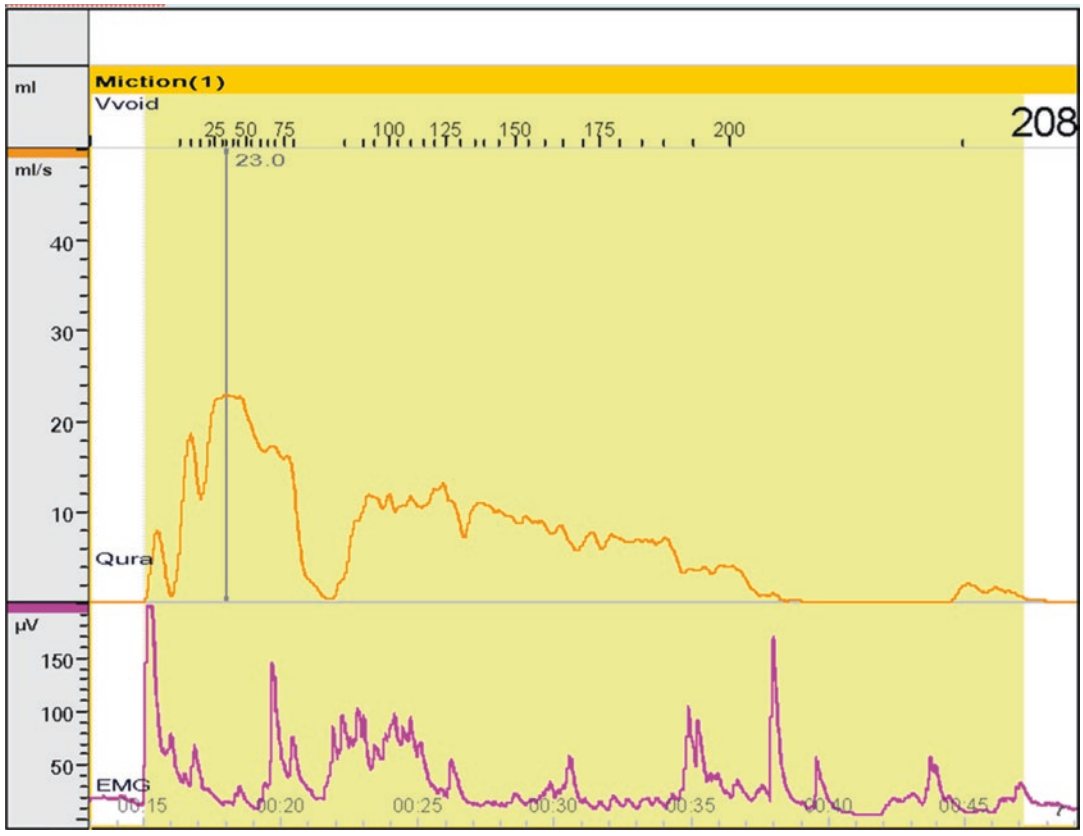

Fig. 18.17 Figure NORMAL. Dysfunctional voiding at uroflowmetry combined with perineal electromyogram (EMG) in a 10-year-old girl: *mixed pattern* of staccato and interrupted uroflow curve (*orange*) with abnormal electrical peaks at EMG (*purple*) during voiding

References

1. Kanellopoulos TA, Salakos C, Spiliopoulou I, Ellina A, Nikolakopoulou NM, Papanastasiou DA. First urinary tract infection in neonates, infants and young children: a comparative study. Pediatr Nephrol. 2006;21(8):1131–7.
2. Shaikh N, Morone NE, Bost JE, Farrell MH. Prevalence of urinary tract infection in childhood: a meta-analysis. Pediatr Infect Dis J. 2008;27(4):302–8.
3. Mangiarotti P, Pizzini C, Fanos V. Antibiotic prophylaxis in children with relapsing urinary tract infections: review. J Chemother. 2000;12(2):115–23.
4. Nuutinen M, Uhari M. Recurrence and follow-up after urinary tract infection under the age of 1 year. Pediatr Nephrol. 2001;16(1):69–72.
5. Roberts KB. Urinary tract infection: clinical practice guideline for the diagnosis and management of the initial UTI in febrile infants and children 2 to 24 months. Pediatrics. 2011;128(3):595–610.
6. Kiernan SC, Pinckert TL, Keszler M. Ultrasound guidance of suprapubic bladder aspiration in neonates. J Pediatr. 1993;123(5):789–91.
7. Kozer E, Rosenbloom E, Goldman D, Lavy G, Rosenfeld N, Goldman M. Pain in infants who are younger than 2 months during suprapubic aspiration and transurethral bladder catheterization: a randomized, controlled study. Pediatrics. 2006;118(1):e51–6.
8. Dutta S. Use of eutectic mixture of local anesthetics in children. Indian J Pediatr. 1999;66(5):707–15.
9. Whiting P, Westwood M, Bojke L, Palmer S, Richardson G, Cooper J, et al. Clinical effectiveness and cost-effectiveness of tests for the diagnosis and investigation of urinary tract infection in children: a systematic review and economic model. Health Technol Assess. 2006;10(36):iii-iv, xi-xiii, 1–154.
10. Hoberman A, Wald ER, Reynolds EA, Penchansky L, Charron M. Pyuria and bacteriuria in urine specimens obtained by catheter from young children with fever. J Pediatr. 1994;124(4):513–9.

11. Ristola MT, Hurme T. Consequences of following the new American Academy of Pediatrics guidelines for imaging children with urinary tract infection. Scand J Urol. 2015;49(5):419–23.
12. Roberts JA. Experimental pyelonephritis in the monkey. III. Pathophysiology of ureteral malfunction induced by bacteria. Investig Urol. 1975;13(2):117–20.
13. Alton DJ, LeQuesne GW, Gent R, Siegmann JW, Byard R. Sonographically demonstrated thickening of the renal pelvis in children. Pediatr Radiol. 1992;22(6):426–9.
14. Robben SG, Boesten M, Linmans J, Lequin MH, Nijman RM. Significance of thickening of the wall of the renal collecting system in children: an ultrasound study. Pediatr Radiol. 1999;29(10):736–40.
15. Dacher JN, Avni F, Francois A, Rypens F, Monroc M, Eurin D, et al. Renal sinus hyperechogenicity in acute pyelonephritis: description and pathological correlation. Pediatr Radiol. 1999;29(3):179–82.
16. Johansson B, Troell S, Berg U. Renal parenchymal volume during and after acute pyelonephritis measured by ultrasonography. Arch Dis Child. 1988;63(11):1309–14.
17. Hitzel A, Liard A, Vera P, Manrique A, Menard JF, Dacher JN. Color and power Doppler sonography versus DMSA scintigraphy in acute pyelonephritis and in prediction of renal scarring. J Nucl Med. 2002;43(1):27–32.
18. Malaki M, Jamshidi M, Ilkhchooyi F. Xanthogranulomatous pyelonephritis presenting with thrombocytopenia and renal mass. Urol Ann. 2012; 4(1):51–4.
19. Eggli KD, Eggli D. Color Doppler sonography in pyelonephritis. Pediatr Radiol. 1992;22(6):422–5.
20. Dacher JN, Pfister C, Monroc M, Eurin D, LeDosseur P. Power Doppler sonographic pattern of acute pyelonephritis in children: comparison with CT. AJR Am J Roentgenol. 1996;166(6):1451–5.
21. Lavocat MP, Granjon D, Allard D, Gay C, Freycon MT, Dubois F. Imaging of pyelonephritis. Pediatr Radiol. 1997;27(2):159–65.
22. Stogianni A, Nikolopoulos P, Oikonomou I, Gatzola M, Balaris V, Farmakiotis D, et al. Childhood acute pyelonephritis: comparison of power Doppler sonography and Tc-DMSA scintigraphy. Pediatr Radiol. 2007;37(7):685–90.
23. Winters WD. Power Doppler sonographic evaluation of acute pyelonephritis in children. J Ultrasound Med. 1996;15(2):91–6. quiz 7-8
24. Bercoff J, Montaldo G, Loupas T, Savery D, Meziere F, Fink M, et al. Ultrafast compound Doppler imaging: providing full blood flow characterization. IEEE Trans Ultrason Ferroelectr Freq Control. 2011;58(1):134–47.
25. Lee YS, Kim MJ, Han SW, Lee HS, Im YJ, Shin HJ, et al. Superb microvascular imaging for the detection of parenchymal perfusion in normal and undescended testes in young children. Eur J Radiol. 2016;85(3):649–56.
26. Machado P, Segal S, Lyshchik A, Forsberg F. A novel microvascular flow technique: initial results in thyroids. Ultrasound Q. 2016;32(1):67–74.
27. Correas JM, Anglicheau D, Joly D, Gennisson JL, Tanter M, Helenon O. Ultrasound-based imaging methods of the kidney-recent developments. Kidney Int. 2016;90(6):1199–210.
28. Hoberman A, Charron M, Hickey RW, Baskin M, Kearney DH, Wald ER. Imaging studies after a first febrile urinary tract infection in young children. N Engl J Med. 2003;348(3):195–202.
29. Massanyi EZ, Preece J, Gupta A, Lin SM, Wang MH. Utility of screening ultrasound after first febrile UTI among patients with clinically significant vesicoureteral reflux. Urology. 2013;82(4):905–9.
30. Nelson CP, Johnson EK, Logvinenko T, Chow JS. Ultrasound as a screening test for genitourinary anomalies in children with UTI. Pediatrics. 2014;133(3):e394–403.
31. Zamir G, Sakran W, Horowitz Y, Koren A, Miron D. Urinary tract infection: is there a need for routine renal ultrasonography? Arch Dis Child. 2004;89(5):466–8.
32. Hung TW, Tsai JD, Liao PF, Sheu JN. Role of renal ultrasonography in predicting vesicoureteral reflux and renal scarring in children hospitalized with a first febrile urinary tract infection. Pediatr Neonatol. 2016;57(2):113–9.
33. Preda I, Jodal U, Sixt R, Stokland E, Hansson S. Value of ultrasound in evaluation of infants with first urinary tract infection. J Urol. 2010;183(5):1984–8.
34. Tsai JD, Huang CT, Lin PY, Chang JH, Lee MD, Huang FY, et al. Screening high-grade vesicoureteral reflux in young infants with a febrile urinary tract infection. Pediatr Nephrol. 2012;27(6):955–63.
35. el Hajjar M, Launay S, Hossein-Foucher C, Foulard M, Robert Y. Power Doppler sonography and acute pyelonephritis in children: comparison with Tc-DMSA scintigraphy. Arch Pediatr. 2002;9(1):21–5.
36. Smith T, Evans K, Lythgoe MF, Anderson PJ, Gordon I. Radiation dosimetry of technetium-99m-DMSA in children. J Nucl Med. 1996;37(8):1336–42.
37. Vestergren E, Jacobsson L, Lind A, Sixt R, Mattsson S. Administered activity of 99Tcm-DMSA for kidney scintigraphy in children. Nucl Med Commun. 1998;19(7):695–701.
38. Vivier PH, Sallem A, Beurdeley M, Lim RP, Leroux J, Caudron J, et al. MRI and suspected acute pyelonephritis in children: comparison of diffusion-weighted imaging with gadolinium-enhanced T1-weighted imaging. Eur Radiol. 2014;24(1):19–25.
39. Faletti R, Cassinis MC, Fonio P, Grasso A, Battisti G, Bergamasco L, et al. Diffusion-weighted imaging and apparent diffusion coefficient values versus contrast-enhanced MR imaging in the identification and characterisation of acute pyelonephritis. Eur Radiol. 2013;23(12):3501–8.

40. Jones RA, Grattan-Smith JD. Age dependence of the renal apparent diffusion coefficient in children. Pediatr Radiol. 2003;33(12):850–4.
41. Cruickshank G. Urinary infection with micturating cystogram. Lancet. 1979;1(8111):332–3.
42. Zerin JM, Shulkin BL. Postprocedural symptoms in children who undergo imaging studies of the urinary tract: is it the contrast material or the catheter? Radiology. 1992;182(3):727–30.
43. Sulieman A, Babikir E, Alrihaima N, Alkhorayef M, Dalton A, Bradley D, et al. Radiation exposure in pediatric patients during micturating cystourethrography procedures. Appl Radiat Isot. 2016;117:36–41.
44. Hoberman A, Greenfield SP, Mattoo TK, Keren R, Mathews R, Pohl HG, et al. Antimicrobial prophylaxis for children with vesicoureteral reflux. N Engl J Med. 2014;370(25):2367–76.
45. Brandstrom P, Esbjorner E, Herthelius M, Swerkersson S, Jodal U, Hansson S. The Swedish reflux trial in children: III. Urinary tract infection pattern. J Urol. 2010;184(1):286–91.
46. Papadopoulou F, Ntoulia A, Siomou E, Darge K. Contrast-enhanced voiding urosonography with intravesical administration of a second-generation ultrasound contrast agent for diagnosis of vesicoureteral reflux: prospective evaluation of contrast safety in 1,010 children. Pediatr Radiol. 2014;44(6):719–28.
47. Darge K, Papadopoulou F, Ntoulia A, Bulas DI, Coley BD, Fordham LA, et al. Safety of contrast-enhanced ultrasound in children for non-cardiac applications: a review by the Society for Pediatric Radiology (SPR) and the International Contrast Ultrasound Society (ICUS). Pediatr Radiol. 2013;43(9):1063–73.
48. Darge K. Voiding urosonography with US contrast agents for the diagnosis of vesicoureteric reflux in children. II. Comparison with radiological examinations. Pediatr Radiol. 2008;38(1):54–63. quiz 126-7
49. Duran C, Valera A, Alguersuari A, Ballesteros E, Riera L, Martin C, et al. Voiding urosonography: the study of the urethra is no longer a limitation of the technique. Pediatr Radiol. 2009;39(2):124–31.
50. Koff SA, Wagner TT, Jayanthi VR. The relationship among dysfunctional elimination syndromes, primary vesicoureteral reflux and urinary tract infections in children. J Urol. 1998;160(3 Pt 2):1019–22.
51. Shaikh N, Hoberman A, Keren R, Gotman N, Docimo SG, Mathews R, et al. Recurrent urinary tract infections in children with bladder and bowel dysfunction. Pediatrics. 2016;137(1)
52. Van Batavia JP, Combs AJ, Hyun G, Bayer A, Medina-Kreppein D, Schlussel RN, et al. Simplifying the diagnosis of 4 common voiding conditions using uroflow/electromyography, electromyography lag time and voiding history. J Urol. 2011;186(4 Suppl):1721–6.
53. Wenske S, Combs AJ, Van Batavia JP, Glassberg KI. Can staccato and interrupted/fractionated uroflow patterns alone correctly identify the underlying lower urinary tract condition? J Urol. 2012;187(6):2188–93.

Imaging Urolithiasis and Their Complications

19

Fred E. Avni, R.-H. Priso, and Robert Novo

Contents

F.E. Avni (✉)
Department of Pediatric Imaging, Jeanne de Flandre Hospital, 59037 Lille-Cedex, France
e-mail: Freddy.Avni@chru-lille.fr

R.-H. Priso
Department of Pediatric Urology, Jeanne de Flandre Hospital, 59037 Lille-Cedex, France

R. Novo
Department of Pediatric Nephrology, Jeanne de Flandre Hospital, 59037 Lille-Cedex, France

19.1 Introduction

Urolithiasis occurs after a complex interaction of environment and heredity. Urinary crystals bind and precipitate when physical and biochemical conditions disturb the balance of stone promoting and inhibiting factors. Small urinary calculi may pass unnoticed, larger calculi may cause pain or obstruct the urinary tract. Although rarer than in adults, the prevalence of urolithiasis has been increasing these last years. The prevalence of urinary stones varies per region, country, and continent (1 in 1000 to 1 in 7500 hospital admissions in the United States). Stones are more commonly seen in Caucasian than in Afro-American children. Stones are mainly composed of calcium oxalate (75%), calcium phosphate (10%), struvite (10%), and uric acid (5%). Kidney stones (as well as nephrocalcinosis) are usually symptoms of a disease, not the disease itself.

The lithiasis may remain in the kidney or migrate. Smaller lithiasis tends to migrate unnoticed and larger stones induce obstructive colic. Vesical stones are more commonly seen in developing countries. Several symptoms will lead to the diagnosis of urolithiasis. Hematuria is encountered in 33–90% of children, pain (mainly in older children) in about 50%. UTI is frequently the presenting symptom in preschool-age children.

About 40% of children with urolithiasis have a positive family history and predisposing causes for urolithiasis can be recognized in 75% of

F.E. Avni, P. Petit (eds.), *Imaging Acute Abdomen in Children*,
https://doi.org/10.1007/978-3-319-63700-6_19

children and adolescents. Metabolic diseases include mainly hereditary hypercalciuria, cystinuria, hyperoxaluria, and hypercitrulinemia. Urinary tract infection used to be the leading cause of urolithiasis. Its rate has diminished in developed countries. Noteworthy, urolithiasis in infants has higher rates of recurrence, associated metabolic disease, infection, and congenital malformation than in older children or adolescents.

Obtaining a thorough medical history with a careful medical examination followed by appropriate imaging is mandatory for an early and correct diagnosis [1–5].

Acute presentations of urolithiasis will prompt treatment. Several options are presently available adapted to the type of lithiasis, its size, and complications. A medical expulsion therapy (MET) has been developed in recent years to solve the renal colic conservatively on the basis of outpatient follow-up. Yet, in some cases, interventional procedures (mainly extracorporeal shock wave lithotripsy—ESWL, ureteroscopy and percutaneous nephrolithotomy—PCNL) will be needed (see below). Imaging is always be part of the management in order to guide the procedures and to assess the success of the treatment. All the interventional procedures expose the patients to significant ionizing radiation directly related to the operating times. Techniques to minimize radiation during intervention and follow-up are essential applying the ALARA principles.

19.2 Diagnosis Imaging

Imaging techniques are used to exclude or confirm the presence of a lithiasis, to determine its size and location. In the setting of acute symptoms, the initial diagnosis testing has to demonstrate obstruction, stasis, infection or evidence for underlying metabolic disease. In children, this diagnosis relies mainly on ultrasound (US). Still, like in adults, there has been an increasing use of unenhanced CT scan especially in emergency departments [6–8]. MR imaging is presently not as useful in the emergency setting urolithiasis. Yet, it does provide additional information in case of complex urinary tract malformation [1–5].

19.2.1 Ultrasound

US has the advantage of being easily available, avoiding radiation and noninvasive. The technique depends on the examiner skills. Yet, US has and should have the first role for assessing the presence of a urolithiasis within the pelvicalyceal system as well as the consequences of the migration of the lithiasis. The examination should be performed under adequate hydration. Typically a urolithiasis appears as a hyperechoic focus with acoustic shadowing behind it (Fig. 19.1). Stones as small as 1.5–2 mm can be detected. Depending on their structure, not all urolithiasis will demonstrate this acoustic shadowing. In doubtful cases, color Doppler may be used to demonstrate the so-called typical "twinkle artifact" (Fig. 19.2), producing reverberating colors behind the stone. It should be noted that soft stones induced by medications such as indinavir, ceftriaxone, and sulfadiazine may be more difficult to identify.

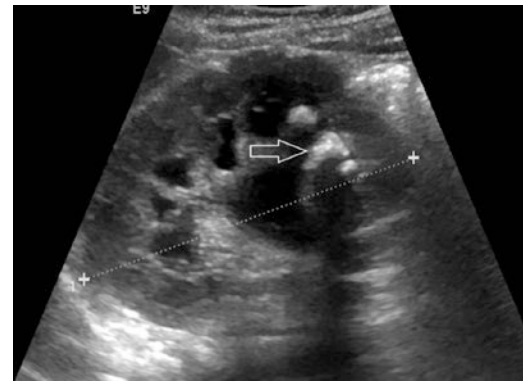

Fig. 19.1 US of a typical lithiasis. Sagittal scan of the left kidney demonstrating a hyperechoic lithiasis in the lower calices with acoustic shadowing (*arrow*). The pyelocaliceal system is dilated due to the migration of another lithiasis

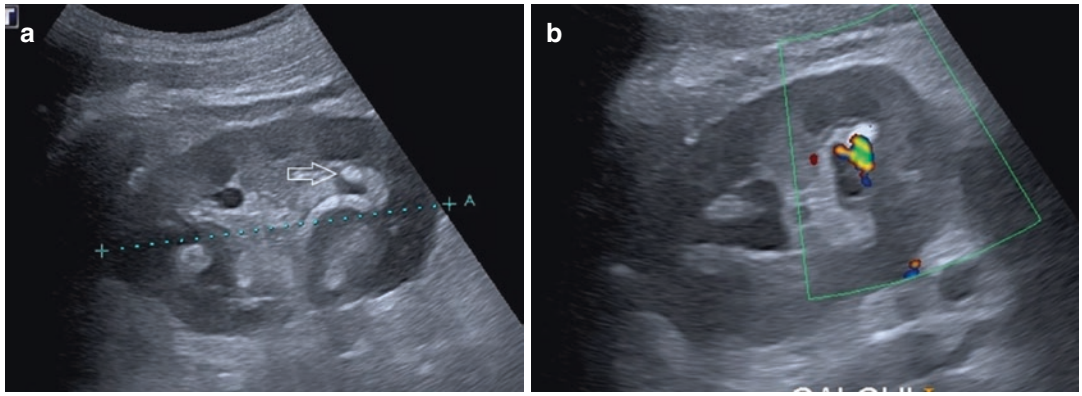

Fig. 19.2 US of a lithiasis without acoustic shadowing and the twinkle sign. (**a**) Sagittal scan of the kidney; there is a hyperechoic focus without shadowing (*arrow*). (**b**) Sagittal scan applying the color Doppler, the typical artifact is obvious

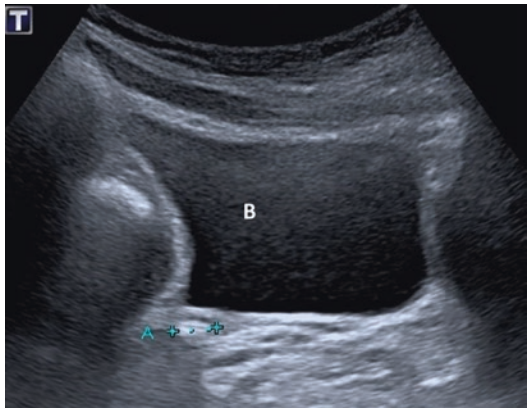

Fig. 19.3 Lithiasis at the UV junction. Case of a 10-year-old boy under chemotherapy for Hodgkin disease. US of the right UV junction demonstrating the lithiasis (*between the crosses*) *B* Bladder

US is able to demonstrate dilatation of the urinary tract secondary to obstruction (Fig. 19.1). The technique is highly accurate in demonstrating pyelo-ureteral junction obstructive stones or lithiasis obstructing the uretero-vesical junction (with a sufficiently full bladder) (Fig. 19.3). One should not hesitate to examine the patient both supine and prone in order to increase the detection of renal stones. In case of acute obstruction, the renal parenchyma may appear hyperechoic and swollen and on duplex Doppler analysis, the resistive index may rise close to 1. US may also demonstrate perirenal fluid indicating fornix rupture. Intrarenal staghorn calculus may be underdiagnosed in the absence of calyceal dilatation as they may appear linear with little acoustic shadowing (Fig. 19.4a). Lithiasis within the lumbar ureter may also be harder to demonstrate. Combining an abdominal radiograph (Fig. 19.4b) and US increases the sensitivity for detecting the stone. Lithiasis within the bladder is usually large and causes acoustic shadowing (Fig. 19.5); it should not be overlooked due to an empty bladder or due to the shadowing. Overall the sensitivity of US for detecting urolithiasis is estimated around 75% and its specificity around 100% compared to 95% and 98%, respectively, for CT.

Another important role for US will be to demonstrate an underlying metabolic disease. For this purpose, the liver should be examined as metabolic diseases may affect both the kidneys and the liver (e.g., tyrosinemia). In the kidneys, a metabolic disease should be suggested in case of recurrent (multiple) lithiasis or in case of nephrocalcinosis (Fig. 19.6) (see below). The latter is defined as calcium deposits within the renal medulla, cortex or both. In typical cases, the nephrocalcinosis will be located within the pyramids (Fig. 19.6) and

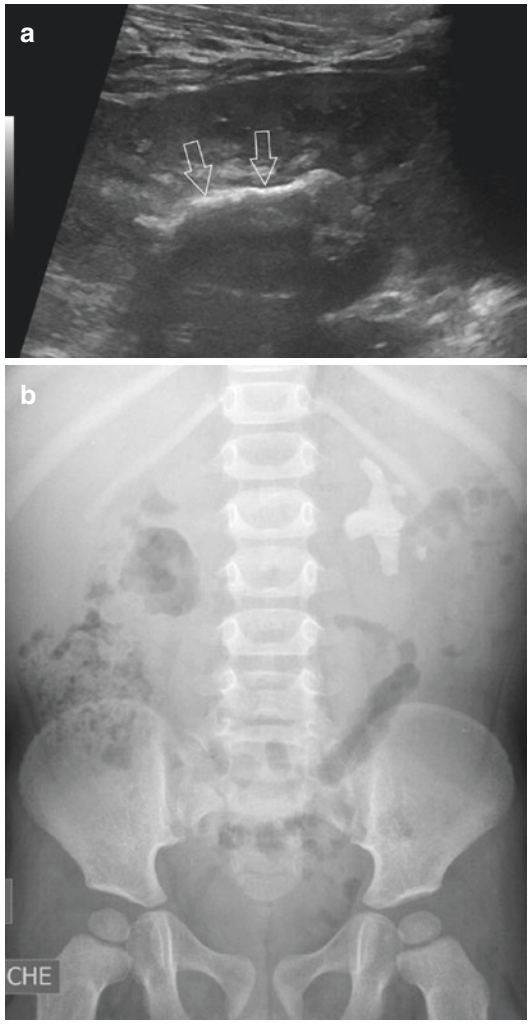

Fig. 19.4 Staghorn lithiasis—case of congenital cystinuria. (**a**) Sagittal scan of the left kidney. The staghorn urolithiasis appears as a long thick line with limited shadowing (*arrows*). (**b**) Plain radiograph of the abdomen demonstrating the calcified staghorn urolithiasis

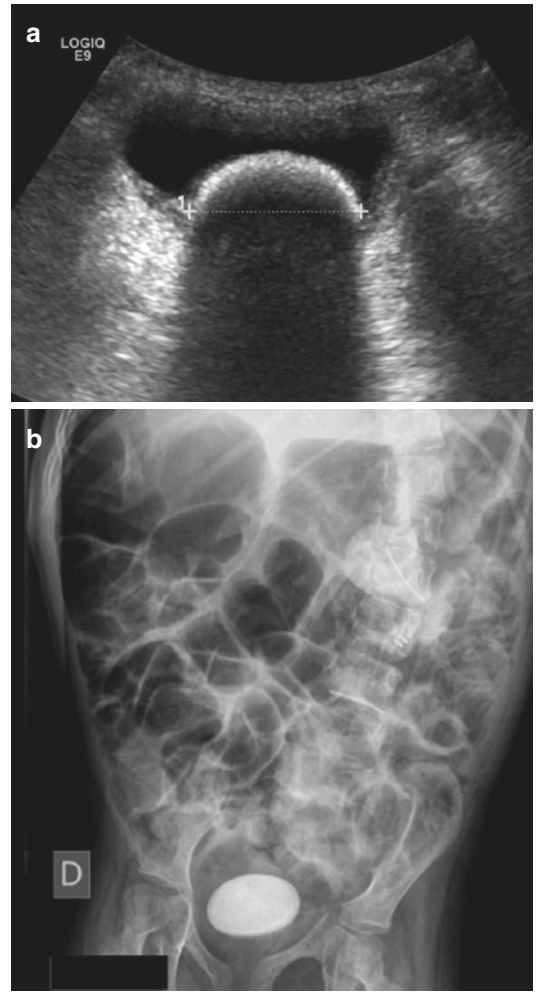

Fig. 19.5 Vesical lithiasis—case of 5-year-old disabled girl. (**a**) US demonstrating a large intravesical lithiasis (*between the crosses*) with acoustic shadowing. (**b**) Plain radiograph confirms the presence of a calcified lithiasis

induce a reversed cortico-medullary differentiation (hyperechoic medulla). In less typical cases, the nephrocalcinosis will be more subtle. Less usually, it will be diffused to both the renal cortex and medulla (e.g., oxalosis—see below) [5–8].

The use of US will also be important for the follow-up of any treatment (see below).

19.2.2 Conventional Radiology (KUB: Intravenous Urography) [7]

19.2.2.1 Kidney-Ureter-Bladder (Plain Radiograph of the Abdomen)

The KUB film can reveal radio-opaque stones (>90% of lithiasis in children) (Figs. 19.4b and 19.5b). Its specificity is 69%, its sensitivity is 82%. Calculi containing uric acid, cysteine, xanthine, or indinavir tend to be radiolucent. Another

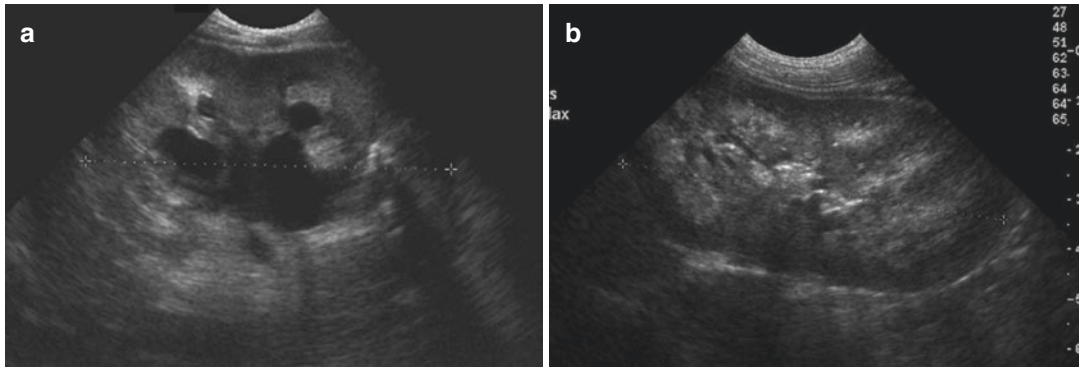

Fig. 19.6 Idiopathic hypercalciuria in a 3-year-old boy. (**a**) Dilatation of right kidney due to urolithiasis with hyperechoic medulla. (**b**) Left kidney with typical appearance of nephrocalcinosis due to the hypercalciuria

interest of KUB would be the visibility of some parts of the skeleton; the detection of some specific skeletal anomalies (signs of secondary hyperparathyroidism, osteoporosis, etc.) would orient towards metabolic diseases.

19.2.2.2 Intravenous Urography (IVU)

The use of IVU has greatly diminished. Nowadays, IVU will be used when a CT scan is not available and before therapeutic planning like lithotripsy in order to precisely localize the lithiasis especially in case of low density, poorly opaque stones. For this purpose, only a few films (1, 2, or) are sufficient at 10 or 15′ post injection of contrast. IVU is contraindicated in acute ureteral obstruction (risk of fornix rupture) and in case of renal failure.

19.2.3 CT

Nonenhanced CT (NE-CT) is the method with the highest sensitivity (91–100%) and specificity (91–100%) for the demonstration of urolithiasis. Density measurements of the lithiasis facilitate estimation of stone composition. The disadvantage of the method is the radiation burden (2.8–5.0 mSv) much higher than with a plain film of the abdomen. The use of CT scan has expanded during the last years especially in emergency departments and therefore one of the main issues will be to reduce this irradiation either by reducing the number of CTs or by optimizing the settings used for the examination. CT seems helpful in case of multiple locations or urolithiasis blocked in the lumbar segment of the ureter (Fig. 19.7a, b). Noteworthy, the couple "US + plain film of the abdomen" have somewhat lower success but usually provide sufficient information in comparison to NECT.

As mentioned, whenever a CT is performed, the settings should be optimized in order to maximize diagnostic sensitivity and minimize the dose by increasing the pitch and decreasing mA. The latter should be decreased around 80–100 mA. Even at such low mA, the sensitivity of CT for detecting urolithiasis is as high as 96% and its specificity around 95%. The mA settings should not be reduced further as the diagnostic accuracy might be decreased. Iterative reconstruction techniques should be favored since they produce images of similar diagnosis yield at lower doses. Further technical improvements will help to reduce the doses. To be noted, the use of dual energy CT improves the characterization of urolithiasis. The higher the Hounsfield units score on CT, the less likely the success of extracorporeal shock wave lithotripsy [6–10].

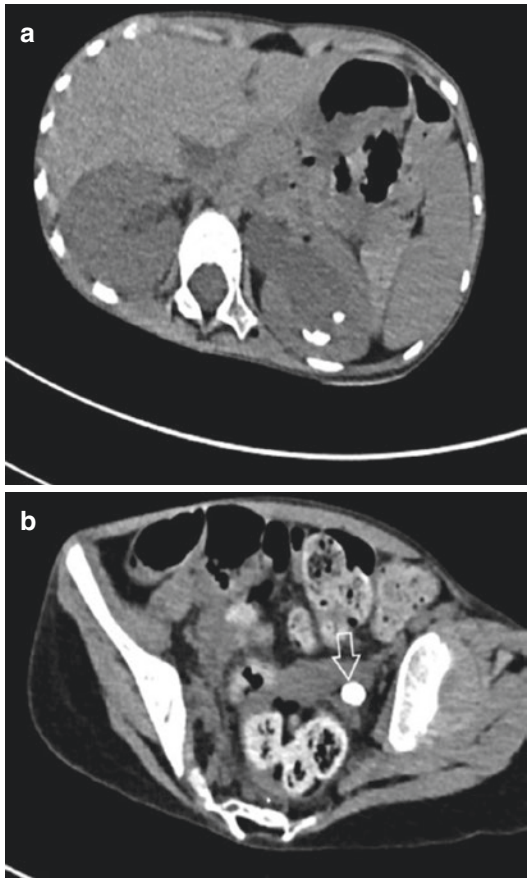

Fig. 19.7 Multiple left urolithiasis with obstructing left ureter lithiasis—Unenhanced CT work-up. (**a**) Axial view of the kidneys. The left pyelocaliceal system appears dilated with two lithiases in the dependent calices. (**b**) Axial view of the lower abdomen a large lithiasis is obvious

19.3 Urolithiasis and UTI [1, 2]

Urinary tract infections (UTI) are associated with an increased risk of developing urolithiasis especially when the UTI is due to Proteus, Klebsiella, pseudomonas, and enterococcus. These microorganisms induce a biochemical cascade that creates conditions to struvite stone formation. Struvite stones start small but may grow as staghorn calculi filling the entire pelvicalyceal system.

On imaging, the stone may be isolated without dilatation (Fig. 19.8). Still, more commonly, the infected urine (pyonephrosis) mixed with sludge

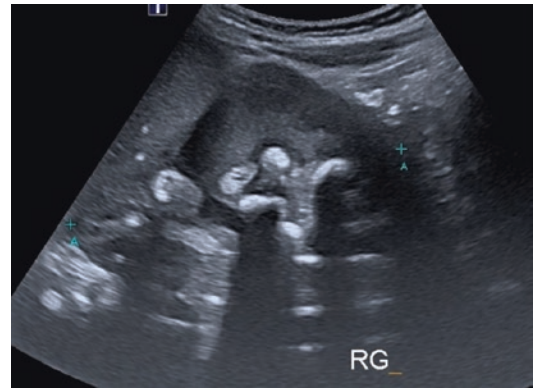

Fig. 19.8 Obstructing urolithiasis with APN. Sagittal scan of the left kidney (*between the crosses*); there are multiple lithiasis within the renal hilum; the renal parenchyma appears swollen and without CMD

and stones will provoke obstruction and dilatation of the urinary tract leading to acute symptoms [5].

Xanthogranulomatous pyelonephritis (XPN) probably represents the long-term consequences of the association of unrecognized UTI and urolithiasis. On imaging, XPN appears as a completely disorganized kidney with massive calcifications and sometimes a pseudotumoral pattern.

19.4 Some Specific Lithogenic Metabolic Diseases [5, 11–14]

As mentioned, when a urolithiasis is diagnosed, an underlying metabolic disease must be suspected in case of familial history, recurrent disease, bilateral diffuse lithiasis, associated nephrocalcinosis, and the demonstration of associated renal and liver disease. To be noted, some metabolic diseases may induce bilateral obstructive lithiasis and potentially acute renal failure.

– The majority of calculi in children (50%) are composed of calcium oxalate or calcium phosphate. The causes are variable. The most common cause is *idiopathic hypercalciuria*; the results and complications are similar: stone formation with subsequent complications (Fig. 19.6).

– *Idiopathic hyperuricosuria* is uncommon in children, relatively more frequent in neonates. Children with cyanotic congenital heart disease and hemolysis may develop uric acid stones. Lesch-Nyhan syndrome and type I glycogen storage disease are also associated with an excess of urate production. Both would rather develop nephrocalcinosis than urolithiasis.
– *Primary hyperoxaluria* type I and type II are autosomal recessive disorders. Oxalosis develops as calcium oxalate precipitates in multiple organs and joints. Oxalate precipitates in kidneys and impairs their function. The *neonatal form* appears as cortico-medullary nephrocalcinosis. Hepato-renal failure develops rapidly in infancy. In *older children*, hyperoxaluria is characterized by recurring oxalate of calcium urolithiasis and recurring renal colic episodes.
– *Cystinuria* is an autosomal recessive disorder of the renal tubular transport. Individuals affected have an excessive excretion of cysteine, arginine, lysine, and ornithine. Recurrent nephrolithiasis and their complications are the main clinical complications (Fig. 19.4).

19.5 Urolithiasis and Uropathies

Urinary tract dilatation leads to stasis that facilitates crystal formation. Once crystals are stationary in the urinary tract, they will grow and aggregate with consequently stone formation. 10–20% of patients with urolithiasis have an underlying urinary tract malformation. Ureteropelvic junction obstruction and primary megaureter account for the majority of cases. On imaging, the urinary tract will appear dilated facilitating the demonstration of the echogenic lithiasis [1–4].

19.6 Induced Urolithiasis

Several conditions may favor the development of lithiasis; to be mentioned, prolonged lying, some antibiotics, specific antimitotic (Fig. 19.3) or anti-viral medications have been shown to induce urolithiasis [15].

19.7 Monitoring of Treatment

The immediate management of nephrolithiasis depends upon the severity of the pain, and the presence of obstruction or infection. Urinary stones migrating within the renal collecting system can cause pain or infection in a partially or completely obstructed urinary tract. Pain is intense and requires immediate and effective care.

In some patients, outpatient medical management with oral analgesics and hydration is possible. However, in others, especially those with nausea, vomiting, and severe pain, hospitalization is required for parenteral fluid and pain medication.

Other indications for hospitalization include urinary obstruction, solitary kidney, and infection.

During its use, renal function should be monitored due to the risk of nephrotoxicity [16]. Because urinary tract infection is often present in children with nephrolithiasis, a urine culture should be obtained. If a urinary tract infection is diagnosed, appropriate antibiotic therapy should be initiated. The majority of stones less than 5 mm in diameter will pass spontaneously, even in small children [17].

During the acute phase, increasing urine flow will be guaranteed by oral or parenteral hydration in cases with severe vomiting, diarrhea, or lack of oral intake.

Regardless of the cause of urolithiasis, high fluid intake more than 1 ml/kg is important in preventing supersaturation of the urine and is thought to facilitate stone passage. More recently the concept of "medical expulsion therapy" has been introduced based on increased fluid intake and medication; furthermore, several studies have also demonstrated an increase in spontaneous stone passage in children treated with alpha-adrenergic blockers or calcium channel blockers [2, 18–20].

During this medical treatment, US can be performed to monitor the migration of the lithiasis and the resolving dilatation.

Urologic removal of stones may be required in patients with persisting severe pain that is refractory to analgesic therapy, or in those with obstruction or infection. In case of a lithiasis

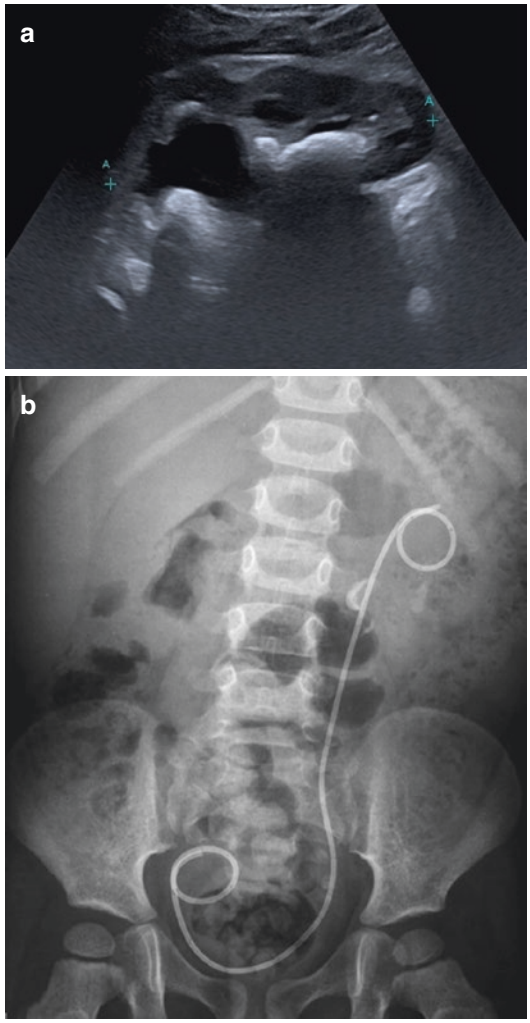

Fig. 19.9 Dilatation after ESWL. (**a**) US Sagittal scan of the left kidney demonstrating left dilatation and fragmented lithiasis. (**b**) Plain radiograph of the abdomen: a JJ stent has been previously introduced; fragments of the lithiasis are visible in the left lumbar area

stucked at the pyeloureteral junction or at the ureteropelvic junction with persistent colicky kidney, a JJ stent will be introduced (Fig. 19.9). This allows the bypass of urine from the renal pelvis to the bladder but also widens the ureter. This last point is important because a second procedure will allow to remove the stent and easy an ureteroscopy to catch the stone in an endoscopic basket (Dormia device). If the stone is too big an intraureteral lumen shock wave lithotripsy may be used.

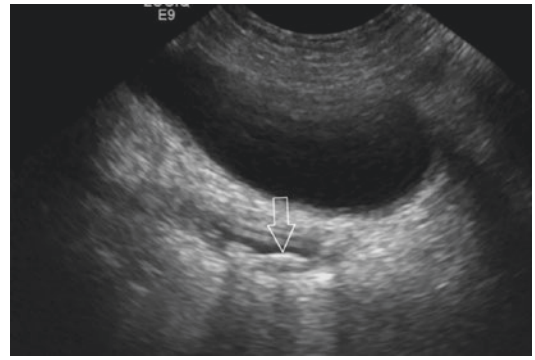

Fig. 19.10 Steinstrasse—Typical visualization of multiple tiny fragments in the lower ureter (*arrow*)

An obstructive lithiasis complicating a pyelonephritis is a surgical emergency. A ureteral stent and a bladder catheterization will be installed under proper antibiotherapy.

Bilateral urolithiasis with oligoanuria needs bilateral ureteral stent, as well and if not possible, a bilateral percutaneous nephrostomy. As soon as possible, an ESWL should be performed to break the stone (Figs. 19.9 and 19.10).

For rare cases of staghorn lithiasis, cystinuria stone not responding to ESWL, a PCNL (percutaneous nephrolithotripsy), or an open surgical stone extraction may be used.

To be noted, a lithiasis discovered in the kidney without any symptoms will be managed by the nephrologist (genetics, biochemical analysis) and the surgeon. A size >10 mm will be treated by ESWL (extracorporeal shock wave lithotripsy).

Imaging will be used to guide the urologic procedures and their complications. These can potentially correspond to hematoma post ESWL, obstruction of the urinary tract post- fragmentation of the lithiasis and migration and rarely infection. US will also be used to monitor the effects of treatment and demonstrate the typical "steinstrasse" corresponding to the fragmented stone (Fig. 19.10).

In the particular case of ESWL, the breaking of the lithiasis and the migration of the fragments may be difficult to follow by US alone. In such case, a plain radiograph of the abdomen may be useful as most lithiases are radiopaque and will be easily visualized (Fig. 19.9).

As mentioned before, all efforts should be made to reduce as much as possible the radiation burden associated with these urologic (potentially repeated) procedures.

Conclusion

Imaging has a major role for the diagnosis and follow-up of the complications of urolithiasis. The first lign examination is US followed as required by CT. US may demonstrate underlying anomalies such as uropathies or suggest metabolic diseases. The technique will be most helpful for the follow-up under appropriate therapy. CT (sometimes KUB) is more accurate than US for the demonstration of ureteric lithiasis and massive/staghorn calculi. Imaging (US) will also be necessary to follow the effects of treatment.

References

1. Van Batavia JP, Tasian GE. Clinical effectiveness in the diagnosis and acute management of pediatric nephrolithiasis. Int J Surg. 2016;36:698–704.
2. Hernandez JD, Ellison SE, Lendvay TS. Current trends, evaluationand management of pediatric urolithiasis. JAMA Pediatr. 2015;169:964–70.
3. Mohamed J, Riadh M, Abdellatif N. Urolithiasis in infants. Pediatr Surg Int. 2007;23:295–9.
4. Ristau BT, Dudley AG, Casella DP, et al. Tracking of radiation exposure in pediatric stone patients: the time is now. J Pediatr Urol. 2015;11:e1–8.
5. Hoppe B, Kemper MJ. Diagnostic examination of the child with urolithiasis or nephrocalcinosis. Pediatr Nephrol. 2010;25:403–13.
6. Johnson EK, Graham DA, Chow JS, et al. Nationwide emergency department imaging practices for pediatric urolithiasis patients; room for improvement. J Urol. 2014;192:200–6.
7. Strohmaier WL. Imaging in pediatric urolithiasis – what's the best choice. Transl Pediatr. 2015;4:36–40.
8. Colleran GC, Callahan MJ, Paltiel HJ, et al. Imaging in the diagnosis of pediatric urolithiasis. Pediatr Radiol. 2017;47:5.
9. Karmazyn B, Frush DP, Applegate K, et al. CT with a computed-simulated dose reduction for detection of pediatric nephron-urolithiasis: comparison of standard and reduced radiation dioses. AJR Am J Roentgenol. 2009;192:143–8.
10. Passerotti C, Chow JS, Silva A, et al. US versus CT for evaluating urolithiasis. J Urol. 2009;182:1829–34.
11. Copelovitch L. Urolithiasis in children. Pediatr Clin N Am. 2012;59:881–96.
12. Coward RJM, Peters CJ, Duffy PG, et al. Epidemiology of paediatric renal stone disese in the UK. Arch Dis Child. 2003;88:962–5.
13. Cochat P, Pichault V, Bacchetta J. Nephrolithiasis related to inborn meta bolic diseases. Pedaitr Nephrol. 2010;25:415–24.
14. Diallo O, Janssens F, Hall M, Avni F. Type 1 primary hyperoxaluria in pediatric patients: renal sonographic patterns. AJR Am J Roentgenol. 2004;183:1767–70.
15. Twombley K, Baum M, Gattineni J. Accidental and iatrogenic causes of acute kidney injury. Curr Opin Pediatr. 2011;23:208–14.
16. Penido MG, Tavares Mde S. Pediatric primary urolithiasis: symptoms, medical management and prevention strategies. World J Nephrol. 2015;4(4):444–54.
17. Kalorin CM, Zabinski A, Okpareke I, et al. Pediatric urinary stone disease--does age matter? J Urol. 2009;181:2267.
18. Tasian GE, Cost NG, Granberg CF, Pulido JE, Rivera M, Schwen Z, et al. Tamsulosin and the spontaneous passage of ureteral stones in children: a multi-institutional cohort study. J Urol. 2014;192:506–11.
19. Velázquez N, Zapata D, Wang H, et al. Medical expulsive therapy for pediatric urolithiasis: systematic review and meta-analysis. J Pediatr Urol. 2015;11(6):321–7.
20. Mokhless I, Zahran AR, Youssif M, et al. Tamsulosin for the management of distal ureteral stones in children: a prospective randomized study. J Pediatr Urol. 2012;8:544–8.

Acute Urinary Tract Obstruction and Urological Emergencies

20

Fred E. Avni and René-Hilaire Priso

Contents

20.1 Introduction

Acute urinary tract obstruction and urological emergencies are major concern even though they represent a small percentage of the overall incoming patients at the pediatric emergency room. A rapid assessment and management of the clinical condition is essential to preserve the renal function and bladder voiding. Prenatal data, any perinatal abnormalities discovered, the latest medical history, previous surgery, medications, the child's complaints, and the physical examination are all essential for a proper management and the first steps leading to specific management measures as required.

Oligo-anuria, flank pain, raised temperature, pyuria, and hematuria are the most frequent among symptoms that would orient towards an acute urological condition. This initial assessment must determine accurately the degree of emergency and the type of care required. Patients clinically unstable must be promptly addressed. For the others, imaging can be performed later after the clinical and biological evaluation in order to optimize its contribution. As usual, US is the first examination to be performed. Its first aim will be to determine the presence, the degree, and potentially the level of an obstruction. The main goal will be to differentiate pyelo-ureteral (and other upper urinary tract obstruction) from bladder outlet obstruction (and other lower urinary tract obstruction). US may also demonstrate urinary tract tumors.

F.E. Avni (✉)
Department of Pediatric Imaging, Jeanne de Flandre Hospital, 59037 Lille–Cedex, France
e-mail: Freddy.Avni@chru-lille.fr

R.-H. Priso
Department of Pediatric Urology, Jeanne de Flandre Hospital, 59037 Lille–Cedex, France

F.E. Avni, P. Petit (eds.), *Imaging Acute Abdomen in Children*,
https://doi.org/10.1007/978-3-319-63700-6_20

In the absence of urinary tract dilatation, acute nephropathies should be considered (refer to the Chaps. 6 and 21 detailing acute renal failure).

Importantly as well, imaging may orient towards extra-abdominal pathologies causing urological symptoms.

The imaging workup will be progressively adapted as needed by the clinical, biological, and sonographic findings. CT, MR imaging, plain film, and cystography may be used as complementary procedures as required [1–4].

20.2 Acute Upper Urinary Tract Obstruction

20.2.1 Congenital Uropathies

With the wide use of obstetrical US, most congenital urinary tract anomalies are detected during fetal life. These uropathies are then managed after birth (see Chap. 5). Marked dilatation requires a quick diagnosis and therefore imaging should be performed rapidly after birth.

Some uropathies may escape the antenatal diagnosis or may be under-evaluated due to neonatal physiological dehydration (Fig. 20.1). They will be discovered following an acute complication. Most of the time, there will be important flank pain with vomiting, urinary tract infection with fever (Fig. 20.2), repeated cystitis, urolithiasis, or a trauma (Fig. 20.3), all leading to the discovery of the underlying uropathy. Trauma as well may lead to the discovery of an unknown UPJ obstruction. Urolithiasis and urinary tract infection will more commonly be associated with congenital megaureters.

Ultrasound must be performed first and will most of the time demonstrate the (marked) UT dilatation (Fig. 20.1) as well as most of the complicating events. To be noted, the urinary tract dilatation may be intermittent and related to external compression, for instance, by a crossing vessel. Color Doppler ultrasound will be necessary to demonstrate the abnormal vessel (Fig. 20.4). MR angiography may be performed in doubtful cases [1–6].

In case of marked dilatation, whatever the cause, a nephrostomy (Fig. 20.1c) or a JJ stent placement may be necessary. An opacification of the urinary tract will then be performed in order to confirm the diagnosis. A DTPA or MAG3 scan will be performed subsequently to determine the remaining renal function. Then the most accurate treatment will be decided based on this workup.

20.2.2 Acquired Acute Urinary Tract Obstruction

Acquired acute urinary tract obstruction can result from various medical or surgical events.

They are most commonly urolithiasis, urinary tract infection, tumors, and post-surgical complications. Furthermore, unilateral obstruction on a single kidney or bilateral ureteral obstruction are major risk for kidneys function and should be managed promptly.

The role of imaging will be to confirm the UT obstruction and determine as much as possible the underlying cause.

20.2.2.1 Urolithiasis

Kidney stone disease affects equally boys and girls, accounting for 1:1000–1:7600 hospital admissions in the USA. UTI and genetic/metabolic diseases are the leading causes for their development in children (in western world countries). Flank pain with vomiting, hematuria, and UTI with or without fever are the main symptoms. The UT is most of the time dilated because of the obstruction. Imaging, especially US, will demonstrate the dilatation as well as the lithiasis (Fig. 20.5). A lithiasis stuck within the lumbar ureter is more easily demonstrated by CT than by US (See Chap. 19). Noteworthy, several medications are lithogenic and knowing the history of the disease and the various treatments is essential [7, 8].

20.2.2.2 UTI

UTI may lead to ureteral obstruction especially in cases of fungal infections (candidiasis) (see Chap. 18). Imaging, especially US will demonstrate the dilatation as well as echogenic urine corresponding

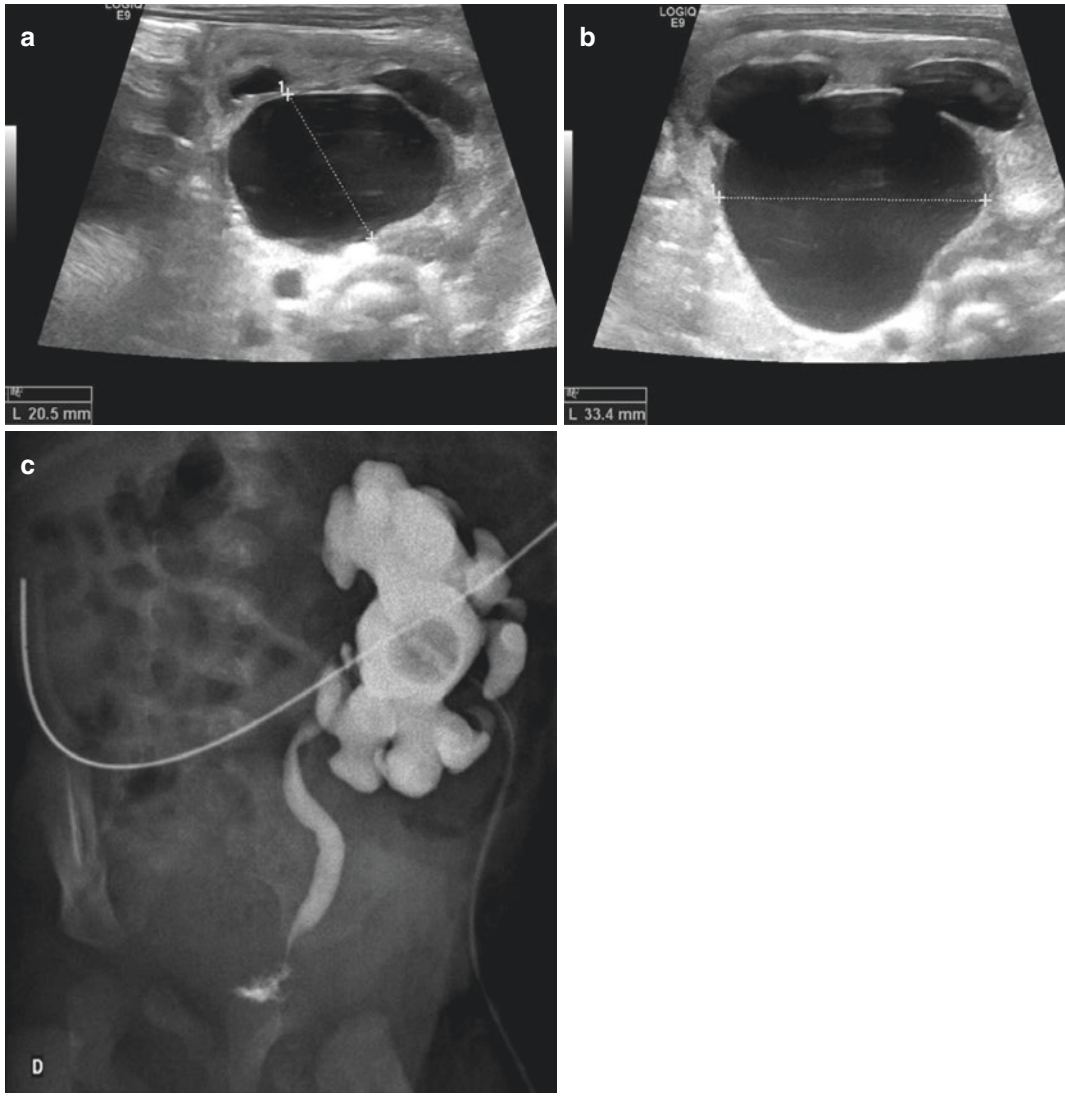

Fig. 20.1 Worsening UPJ obstruction. (**a**) US at birth: transverse scan of the dilated renal pelvis measuring 20 mm. (**b**) US at day 20: transverse scan; the dilatation has increased and the pelvis measures 33 mm. (**c**) Pyelography: opacification through the catheter of nephrostomy, confirming the UPJ obstruction

to pyonephrosis (Fig. 20.5) and thickening of the ureteral wall to be noted, as mentioned, the presence of an underlying congenital uropathy as well as the presence of urolithiasis increases the risk of ureteral obstruction [9, 10].

20.2.2.3 Neoplasms

Some benign neoplasms of the ureter such as fibro-epithelial polyps or ureteral webs may induce ureteral obstruction. More generally any large malignant pelvic tumor may invade the ureters or the posterior part of the bladder (see below) and determine uphill dilatation of the UT [11–13].

20.2.2.4 Post-Operative Obstruction and Complications

In case of marked urinary tract dilatation due to obstruction or to reflux, on the basis of clinical,

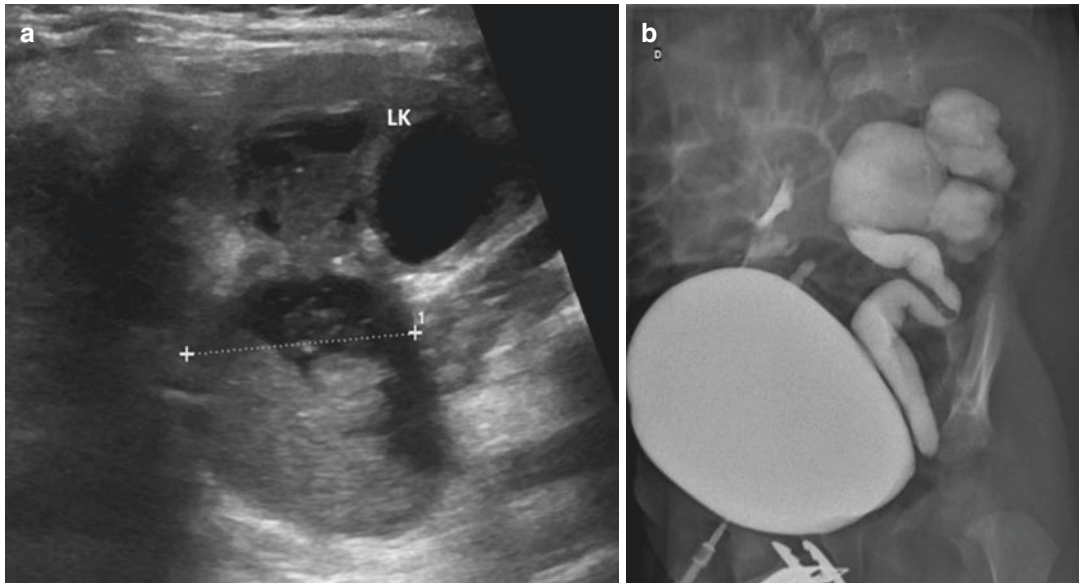

Fig. 20.2 Superinfection of a uropathy (at age 1 month). (**a**) US of the left kidney (LK)—transverse dilatation of pyelo-caliceal system. The urine appears echogenic (in the context of high fever, pyonephrosis is suspected). (**b**) VCUG performed after treatment demonstrated bilateral VUR; grade 4/5 on left and grade 2 on the right side

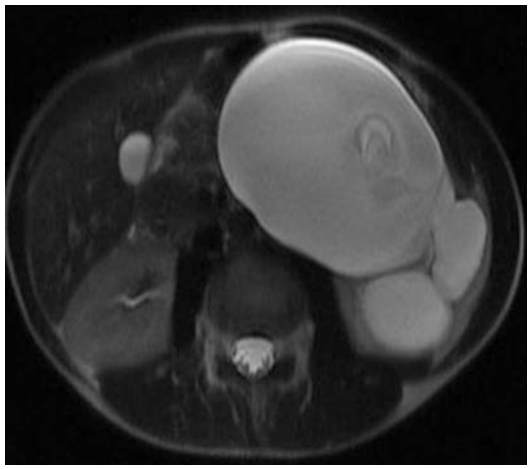

Fig. 20.3 Huge UPJ obstruction discovered after an abdominal trauma (US was performed first, not shown) in a 15 year-old patient. MR imaging T2-weighted sequence; huge pyelo-ureteral dilatation

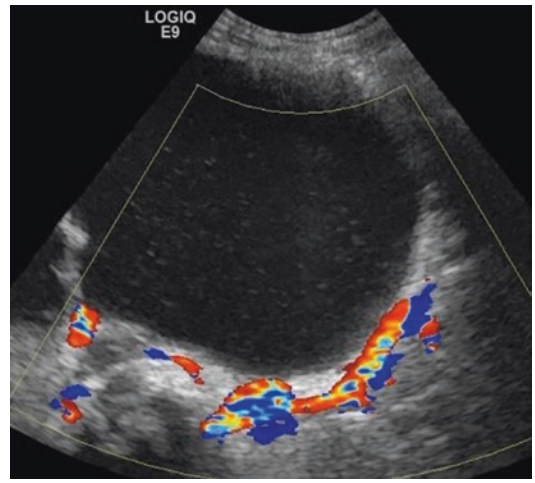

Fig. 20.4 Crossing vessels associated with UPJ obstruction in a 3-year-old boy. Color Doppler displays two crossing vessels, one artery and one vein, at the level of the dilated system

scintigraphy, and other imaging findings, surgery may be elected. A ureteral stent may or not be left after the procedure. US will be performed to assess post-operative follow-up. In most cases, the urinary tract dilatation will resolve progressively (in several weeks). A moderate persisting dilatation is acceptable and will be related to post-operative edema at the site of surgery (Fig. 20.6). This dilatation is transitory. In some other cases, hemorrhage (Fig. 20.7) or a hematoma may develop and induce pseudo-obstructive dilatation. The hematoma will appear as a collection of various

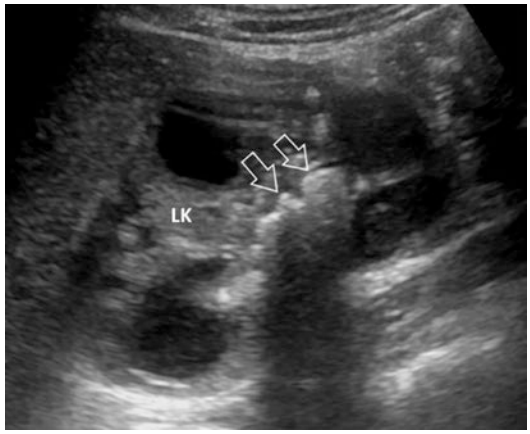

Fig. 20.5 Infection and urolithiasis in a patient with congenital cystinuria (16-year-old girl). US—sagittal scan of the left kidney (LK). Echogenic lithiasis is visible with the renal hilum (*Arrows*). Some calices are dilated and contain echogenic pus

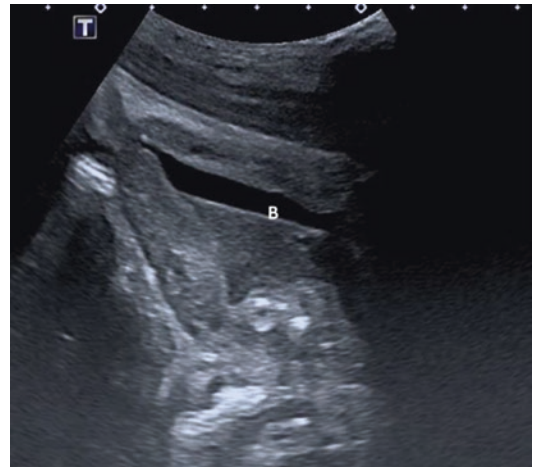

Fig. 20.7 Hematuria 2 days after ureteral reimplantation. US of the bladder (B); sagittal scan demonstrating a fluid/echogenic level corresponding to intravesical bleeding

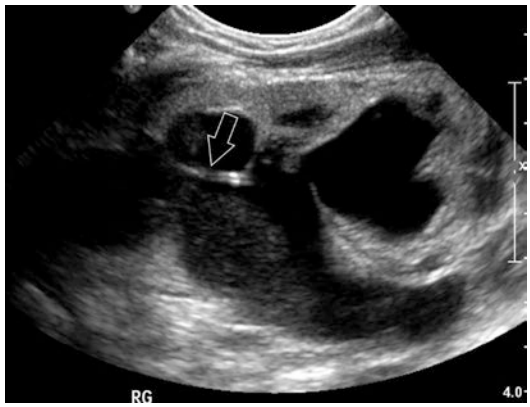

Fig. 20.6 One week post-operative UPJ obstruction. A JJ catheter is still present (*arrow*). Sagittal scan of the left kidney. Persisting dilatation. The urine appears echogenic possibly corresponding to blood

echogenicity around the site of anastomosis; with time this might resolve as well. Rarely, a leakage may occur at the site of operation with a urinoma (Fig. 20.8). A persisting or increasing dilatation with reduction of the renal function on renal scan is most of the time related to a postoperative stenosis. It will be treated with a JJ stent or a redo procedure [14, 15].

Finally, acute and delayed ureteral obstruction may occur after endoscopic treatment of vesicoureteral reflux by injections of hyaluronic polymer (Deflux®) (Fig. 20.8). The obstruction is usually transitory and due to associated edema at the site of injection. The incidence of real obstruction is evaluated between 1–6%. On US, the Deflux® appears as a hyperechoic nubbin located at the uretero-vesical junction (Fig. 20.8). There is no need for other imaging as US is sufficient to demonstrate post injection dilatation and the potential resolution with time [16, 17].

20.3 Acute Bladder Retention

Acute urinary retention is the inability to void despite the sense of bladder fullness or inability to void after 12–18 h with bladder distension. Acute urinary retention is rare in children; still many different causes can determine retention and some need urgent management [11, 18].

The workup should start by the age, gender, the medical history including prenatal history, neurological changes, voiding dysfunction, constipation, hematuria, and medications.

The clinical examination should focus on the palpation of an abdominal mass, the aspect of the external genitalia, a search for evidence of occult dysraphism; motor and sensory neurological exam and rectal continence must be checked as well.

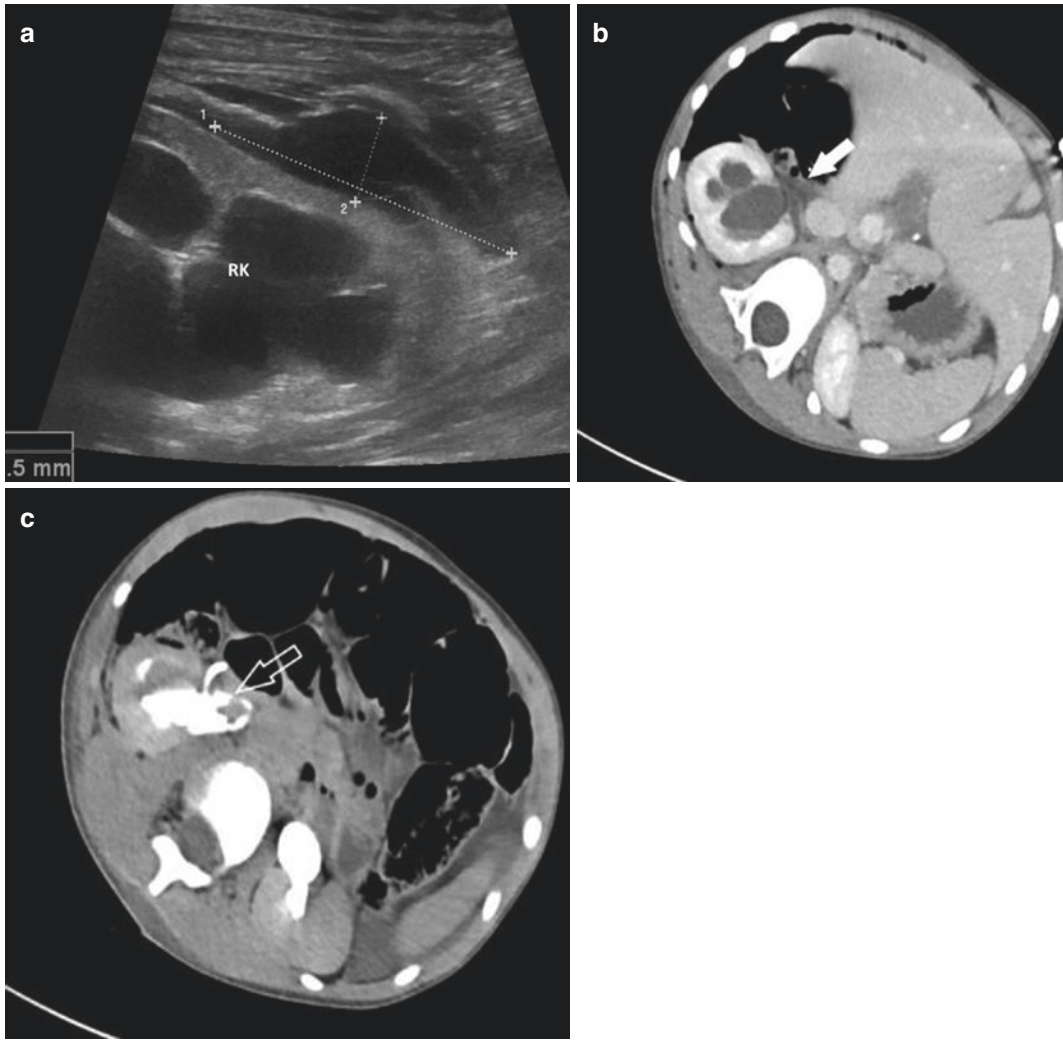

Fig. 20.8 Urine leakage after UPJ obstruction surgery. (**a**) US, transverse scan of the right kidney (RK) demonstrates a collection (*limited by the crosses*) around the right kidney. (**b**) CE-CT Early phase—A collection of fluid is visible at the level of the renal hilum (*arrow*). (**c**) CE-CT Late phase; a leaking of contrast is demonstrated (*arrow*)

Urinalysis and urine culture are mandatory.

The causes are various and include among others:

- Obstructive uropathies
- Urethral obstruction
- Voiding dysfunction
- "Mass" effect on the bladder
- Central or peripheral neurological disease
- Lithiasis
- UTI
- Medications
- Post-operative obstruction
- Local infection

US will always be the first imaging technique performed as it will confirm the bladder retention (size of the bladder, thickening of its wall, presence of diverticula) and the potential surrounding anomalies (ureterocele, polyp, abdomino-pelvis mass, etc.) causing the retention (Fig. 20.9).

If the cause is not determined by the US, complementary imaging especially MR imaging of the spine, voiding cysto-uretrogram (suprapubic), and endoscopy should be performed in accordance with the clinical findings.

20.3.1 Neurological Causes for Acute Bladder Retention

Neurological etiologies are the commonest cause for acute bladder retention. Tethered cord, trauma, transverse myelitis, Guillain-Barré syndrome, encephalitis, primary or metastatic neoplasms, and spina bifida surgery may all lead to urinary retention as first symptom. Therefore a detailed neurological examination must be performed in order to localize the level of the deficit. Furthermore, an MR imaging of the spine and cord will be the most appropriate imaging procedure [11, 18].

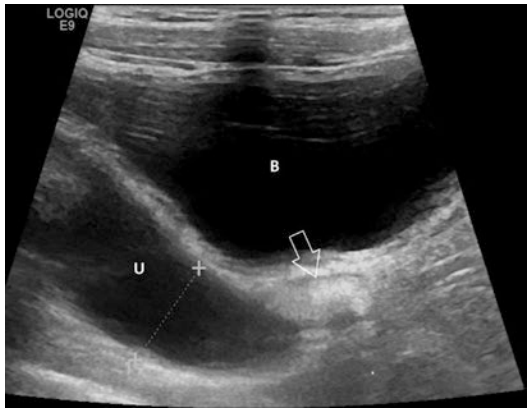

Fig. 20.9 Obstruction post Deflux. US—Sagittal scan through the right ureter. The ureter (U) appears dilated up the granuloma induced by the Deflux (*Arrow*). *B* bladder

20.3.2 Voiding Dysfunction

Infrequent voiding, lazy bladder, and the Hinman-Allen syndrome represent frequent causes of urinary retention. The etiology originates most probably from the avoidance of voiding or abnormal reflex contraction of the sphincters. Urodynamic studies will help to confirm the diagnosis.

20.3.3 Tumors

Any retroperitoneal mass may compress the bladder and induce bladder outlet obstruction. Among others, pelvic neuroblastoma, prostatic rhabdomyosarcoma, neurofibromatosis, or sacro-coccygeal teratoma (Fig. 20.10) may

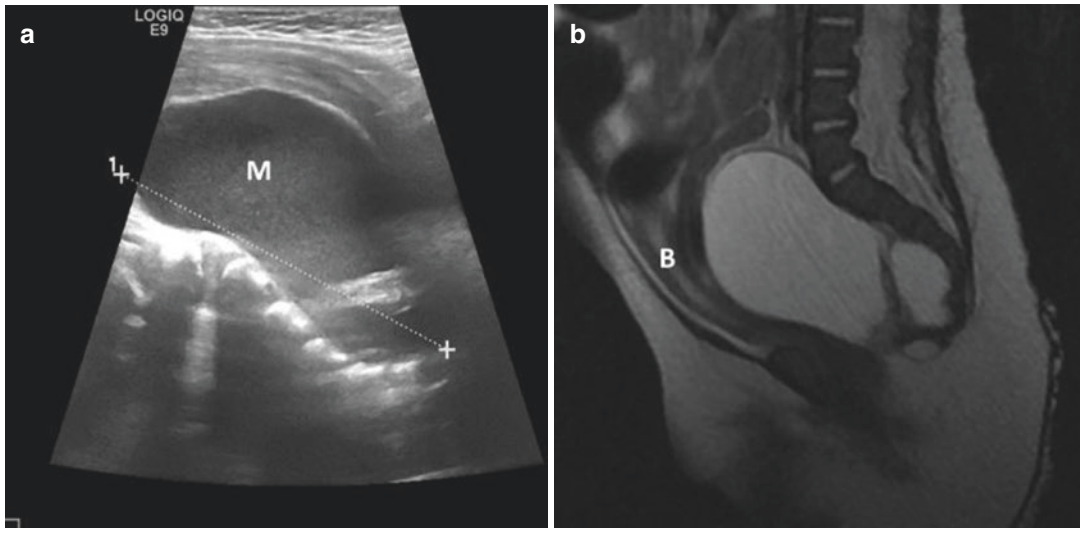

Fig. 20.10 Acute bladder retention secondary to sacro-coccygeal teratoma in a 3-month-old girl. (**a**) US, sagittal of the pelvis (the bladder had been emptied) demonstrating a large cystic septated mass (M) (6 cm between the crosses). (**b**) MR imaging T2 weighted sequence—the mass behind the empty bladder (B) occupies most of the pelvis

determine urinary retention. CT or MR imaging will be necessary to evaluate the tumor and its extent [11–13].

To be noted, abscesses (such as in appendiceal peritonitis), hematocolpos, and ovarian cysts may by their mass effect, induce urinary retention as well.

20.3.4 Urethral Causes

Posterior urethral valves, ureterocele (Fig. 20.11), urethral polyps, or dilatation of Cowper gland (Fig. 20.12) may induce bladder outlet obstruction. These conditions may be discovered at any age as, for instance, PUV are potentially detected in utero (and managed at birth—see Chap. 5) but may also be diagnosed in children or teenager boys. A VCUG will be essential to demonstrate the urethral anomalies [19, 20].

Circumcision, cure of hypospadias, urethral trauma may induce urethral stenosis that would determine obstruction. Suprapubic VCUG will confirm the stenosis.

20.3.5 Varia

Upper UTI and cystitis may result in urinary retention due to associated voiding dysfunction. Furthermore, infected phimosis, urethritis (Fig. 20.13), and cystitis are classical causes of urinary retention and are easily confirmed by local examination and urinalysis.

Massive constipation may sometimes be the clue of a bladder retention. This can be confirmed by a plain radiograph of the abdomen.

A bladder lithiasis may be obstructive. It can develop secondary to a long history of bladder catheter, CIC, or a foreign body in the bladder.

Finally various medications may induce bladder retention and therefore, a detailed history is

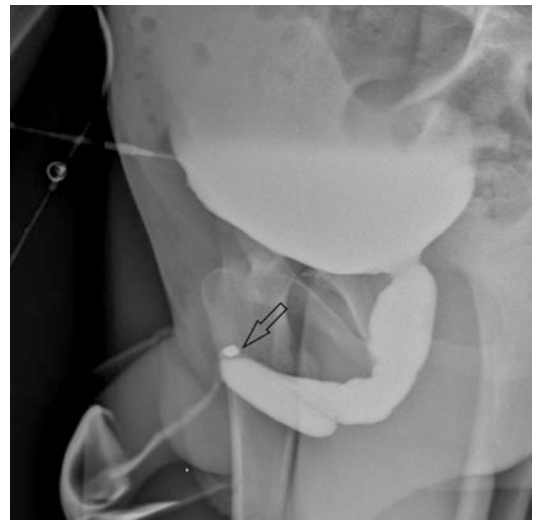

Fig. 20.12 Distended Cowper gland obstructing the urethra—VCUG view. The distended Cowper gland induces an uphill dilatation at its connection within the urethra

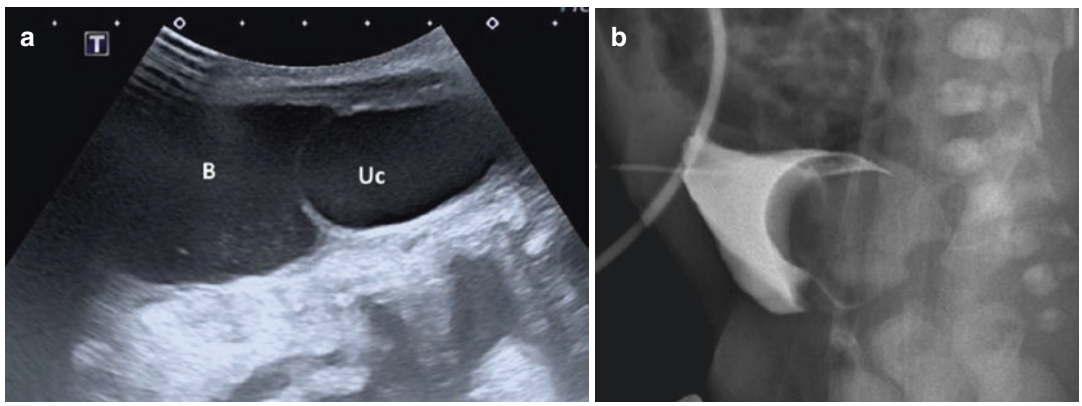

Fig. 20.11 Prolapsing ureterocele of a duplex system. (**a**) US, sagittal scan of the bladder (B); a large ureterocele (Uc) is visualized within the bladder. (**b**) VCUG: during micturition the ureterocele prolapses within the urethra and eventually creates a transient obstruction

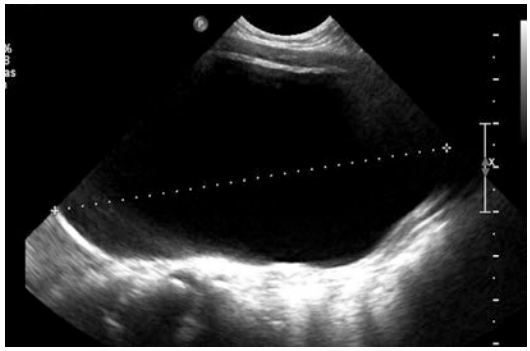

Fig. 20.13 Bladder retention due to urethritis (herpes infection). Sagittal scan of the markedly distended bladder

of upmost importance to find the origin of the retention. Antihistamines, morphinics, alpha-adrenergic agonists as well as neuroleptics may induce bladder retention [8, 21].

Conclusion

Acute urinary tract obstruction is an emergency. The renal function may be rapidly impaired with a blood fluid and electrolyte imbalance when the pathology is bilateral or involves a solitary kidney.

The management should be prompt: medical history, fluid and electrolyte balance, and an ultrasound are mandatory. A dilatation of the urinary tract means a rapid surgical procedure to relieve the obstructed kidney(s). Ureteral stent, bladder catheter, or a pyelostomy may be performed as well.

A renal dilatation may reveal a nephropathy. A hemodialysis or a peritoneal dialysis procedure will be carried on.

References

1. Lambert SM. Pediatric urological emergencies. Pediatr Clin N Am. 2012;59:965–76.
2. Shimada K, Matsumoto F, Kawagoe M. Urological emergencies in neonates with congenital hydronephrosis. Int J Urol. 2007;14:388–92.
3. Yilmaz E, Guney S. Giant hydronephrosis due to UPJ obstruction in a child: CT and MR appearance. Clin Imaging. 2002;26:125–8.
4. Yu M, Ma G, Ge Z, et al. Unilateral giant megaureter with renal dysplasia compressing controlateral ureter and causing bilateral hydronephrosis. BMC Urol. 2016;16:7.
5. Calder AD, Hiorns MP, Abhyankar A. CE-MR angiography for the detection of crossing renal vessels in children with symptomatic UPJO: comparison with operative findings. Pediatr Radiol. 2007;37:356–61.
6. Mitterberger M, Pingerra GM, Neururer R, et al. Comparison of CE-Color Doppler imaging, CT and MRI for the detection of crossing vessels in patients with UPJO. Eur Urol. 2008;53:1254–62.
7. Elsheemy MS, Shouman AM, Shoukry AL, et al. Ureteric stents vs percutaneous nephrostomy for initial urinary drainage in children with obstructive anuria and acute renal failure due to ureteric calculi: a prospective randomized study. BJU Int. 2015;115:473–9.
8. Shahrbaf FG, Assadi F. Drug induced renal disorders. J Renal Inj Prev. 2015;4:57–60.
9. Broadis E, Kronfli R, Flett ME, et al. Targeted top down approach for the investigation of UTI: a 10-year follow-up study in a cohort of 1000 children. J Pediatr Urol. 2016;12:39.e1–6.
10. Schilperoort JV, de Wall LL, Van der Horst HJ, et al. Anuria in a solitary kidney with candida bezoars managed conservatively. Eur J Pediatr. 2014;173:1623–5.
11. Nevo A, Mano R, Livine PM, et al. Urinary retention in children. Urology. 2014;84:1475–9.
12. Woo JR, Sisul D, Kaplan G, et al. Urologic outcomes of pediatric pelvic neuroblastoma presenting in acute urinary retention. Pediatr Hematol Oncol. 2013;30:662–7.
13. Bianchi D, Vespasiani G, Bove P. Acute kidney injury due to bilateral obstruction in children. World J Nephrol. 2014;3:182–92.
14. Dy GW, His RS, Holt SK, et al. National trends in secondary procedures following pediatric pyeloplasty. J Urol. 2016;195:1209–14.
15. Koyle MA, Butt H, Lorenzo A, et al. Prolonged urinary retention can and does occur after any type of ureteral reimplantation. Pediatr Surg Int. 2017;33:623.
16. Garcia-Aparicio L, Rodo J, Palazon P, et al. Acute and delayed vesico-ureteral obstruction after endoscopic treatment of primary VUR with dextranomer hyaluronic acid copolymer: why and how to manage. J Pediatr Surg. 2013;9:493–7.
17. Pagagiannopoulos D, Rosoklija I, Cheng E, et al. Delayed obstruction with asymptomatic loss of renal function after Deflux injection for VUR: a close look at a disturbing outcome. Urology. 2017;101:63.
18. Gatti JM, Perez-Brayfield M, Kirsch AJ, et al. Acute urinary tract retention in children. J Urol. 2001;165:918–21.
19. Donboklang L, Marbaniang E, KHongsni P. Lower UT obstruction in male children – a report of 3 cases. Med Ultrason. 2016;18:400–2.
20. Blast F, Rosch WH, Koen M, et al. Cowper's syringocele: a rare differential diagnosis of infravesical obstruction in boys and young adults. J Pediatr Urol. 2017;13:52.e1–5.
21. Bengtsson B, Woodon-Gorges SL, Poulain FR, et al. Urinary effects of morphine in preterm infants. Acta Paediatr. 2003;92:251–3.

Acute Renal Failure in Children

21

Fred E. Avni and Annie Lahoche

Contents

F.E. Avni (✉)
Department of Pediatric Imaging,
Jeanne de Flandre Hospital, Av Eugène Avinée, 2,
59037 Lille-Cedex, France
e-mail: Freddy.Avni@chru-lille.fr

A. Lahoche
Department of Pediatric Nephrology, Jeanne de Flandre Hospital, Lille-Cedex, France

21.1 General Considerations

21.1.1 Definition

Acute renal failure (ARF)—equally named "acute renal injury"—is classically defined as an abrupt and prolonged loss of renal function usually reversible in most cases. Several criteria are used to define the severity of the renal failure. Some are based on the need for renal replacement therapy, others are based on the serum creatinine level and volume of renal urine output. A recent classification, referred to as the pediatric RIFLE criteria, relies on the decrease of the GFR and of the urine output (stage 1 = renal risk, stage 2 = renal injury, stage 3 = renal injury, stage 4 = renal loss, and stage 5 = end stage and persistent failure over 3 months) [1, 2].

21.1.2 Epidemiology and Classification

Reported incidence rates usually refer to ARF in hospitalized patients. They vary markedly with respect to the population investigated and the geographical area considered. In the USA, the incidence of pediatric ARF, defined as need for renal replacement therapy, varies between 2 and 4 per 100,000 children aged <15 years. The incidence increases to 1–2% among critically ill patients and up to 82% among ventilated patients. In developing countries, an incidence around 9%

F.E. Avni, P. Petit (eds.), *Imaging Acute Abdomen in Children*,
https://doi.org/10.1007/978-3-319-63700-6_21

for non-critically ill and 36% for critically ill patients is reported.

ARF is usually classified according to pre-, intra-, and post-renal causes. *Prerenal ARF* predominantly includes states with reduced renal blood flow (secondary to hypovolemia, or cardiogenic shock, or a combination of these factors). *Intra-renal failure* includes glomerular, tubular, and interstitial diseases. Glomerulonephritis refers to a spectrum of diseases affecting the glomerular functional unit. Interstitial nephritis refers to sudden onset of RF resulting from an acute inflammatory process affecting both kidneys. Acute tubular and cortical necrosis result from tubulo-interstitial epithelial injury secondary to ischemia or to drug-induced nephropathy. Hemolytic and uremic syndrome (HUS) is the most common cause of ARF worldwide beyond the neonatal period and commonly affects preschool children. It accounts for 15–20% of pediatric ARF cases in developed countries and for 35% in developing countries. Post-renal ARF results from obstruction to the urinary from. The site of obstruction may occur from the tubule to the urethra. Most commonly the obstruction occurs at the uretero-pelvic junction due to congenital anomaly; still the obstruction can be secondary to inadvertent surgical ligation of ureter or compression from an abdomino-pelvic mass.

Noteworthy, the etiological spectrum of pediatric ARF has changed during the last years. The rate of secondary ARF due to surgical intervention, organ transplantation, drugs toxicity, and sepsis is increasing whereas the rates of primary renal disorders remain stable (acute glomerulonephritis, hemolytic and uremic syndrome, etc.). Pre-renal disorders have decreased. The rate of infectious diseases and intrarenal diseases remains stable in developing countries [1–6].

21.2 The Role of Imaging

In case of ARF, the primary role of imaging is to exclude post-renal obstructive causes by demonstrating bilateral urinary tract dilatation (unilateral in case of a single kidney). The examination will aim to demonstrate the degree and level of obstruction. Whenever a mass (or a mass effect) is demonstrated, complementary evaluation through MR imaging (preferably) or CT may be necessary in order to precise the diagnosis. The use of contrast material should be carefully evaluated in children with ARF in order to avoid worsen the renal impairment.

The next role for imaging would be to demonstrate an underlying disease that has favored the occurrence of an acute episode (urinary tract infection in case of congenital uropathies, obstructive urolithiasis in case of metabolic diseases, etc.).

A further role would be to orient towards acquired pathologies following surgery or secondary to some specific medications (see below).

The last challenge would be to find anomalies on imaging (mainly US) that may facilitate the diagnosis of renal (or pre-renal origin for the ARF). Unfortunately, in most cases, the only anomaly that will be detected will be parenchymal hyperechogenicity (as compared to the liver or to the spleen) (Fig. 21.1) associated or not with increased renal size (evaluated on the longest sagittal scan of the kidney), both being non-specific findings. The final diagnosis would be ascertained for many cases only through biopsy and histology. Still, this hyperechogenicity and the renal size can be used as markers for the follow-up of the disease. In a few specific diseases, the US examination will be more accurate (see below). Noteworthy,

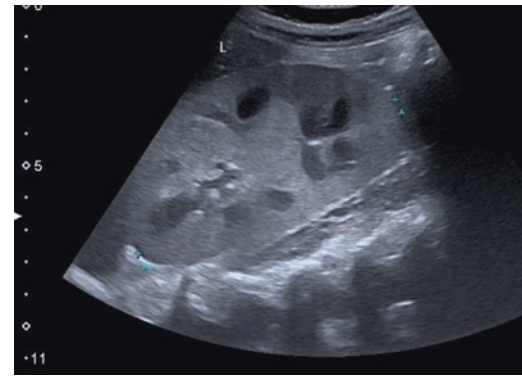

Fig. 21.1 Aspecific hyperechogenicity on US. Sagittal scan of the right kidney. The cortex is thick and hyperechoic (compared to the liver). Biopsy demonstrated evidence for acute tubular necrosis

Doppler (duplex and color) may help in some entities (HUS, renal vein thrombosis) to clarify or better assess the diagnosis. Norms for resistive Index (RI) are age dependent, higher, >0.8, in younger children, around 0.7 in older children [7–9].

Finally, US may be used to guide biopsies when the diagnosis remains unclear.

21.3 Ultrasound and Intrarenal ARF

As mentioned, ultrasound may demonstrate abnormal aspects in various renal (and pre-renal) ARF. In most cases, the findings will be aspecific confirming the renal insult but unable to determine a specific diagnosis. In a few cases, the changes will be more obvious enabling to orient and/or confirm a specific diagnosis.

21.3.1 Hemolytic and Uremic Syndrome (HUS)

HUS is characterized by microangiopathic hemolytic anemia, thrombocytopenia, and ARF. It is secondary to a specific strain of E. coli producing a Shiga-toxin. It is the most common cause of ARF in pre-school children. Five to 7 days after the ingestion of the toxin, gastro-intestinal symptoms occur. Among them, 5–15% of patients will develop symptoms of HUS. The key pathophysiological mechanism involves dissemination of the bacterial toxin to the renal microvasculature leading to swelling and apoptosis of endothelial cells. Occlusive thrombi develop in the renal arterioles and glomerular capillaries. Between 40–70% of children with HUS will become oligo-anuric necessitating renal replacement therapy. Thrombotic microangiopathy may also occur outside the kidneys and will affect the brain (10% of patients), the heart, or the pancreas. The digestive tract is almost always involved (especially the colon). Approximately 5–10% of HUS are not related to the shiga-toxin and appear as atypical HUS (aHUS). aHUS seems to be related to genetic mutations; it is characterized by recurrent bouts and more permanent kidney failure [1, 2].

On US, in both HUS and aHUS, during the acute oligo-anuric phase, the kidneys are slightly enlarged or remain within normal limits; the cortex becomes hyperechoic with increased corticomedullary differentiation (CMD)(Fig. 21.2a). On duplex Doppler, the diastolic flow disappears or even a reverse diastolic flow may appear (Fig. 21.2b). Noteworthy, the return of a diastolic flow is predictive of the resuming spontaneous diuresis (Fig. 21.2c).

US of the abdomen is able to demonstrate evidence for microangiopathic colitis through the thickening of the bowel wall and disappearance of the normal bowel wall stratification (Fig. 21.2d). In the appropriate clinical setting, swelling of the pancreas indicates pancreatitis and echogenic sludge in the gallbladder may indicate hemobilia (Fig. 21.2e). Cerebral MR imaging will be mandatory to evaluate the brain lesions in case of seizures [8–13].

Most cases of HUS (less for aHUS) return to normal. In some instances, renal growth will be impaired and hypertension will eventually develop [12].

21.3.2 Acute Glomerulonephritis and Acute Tubular Necrosis

Acute glomerulonephritis (AGN) refers to a disease affecting the glomerular functional unit. Inflammatory processes result in swelling of the glomerular epithelial cells. Immune deposits along the basement membrane are associated findings. AGN is classified by the type and site of deposits and according to associated underlying diseases. On US, the most usual finding is normal size kidney with increased echogenicity and "thickened" cortex. These features are nonspecific. Noteworthy, on color Doppler, the renal parenchyma may appear hypervascularized.

Acute tubular necrosis (ATN) may result from tubular epithelial injury resulting from vasomotor autoregulatory or drug induced mechanisms. The findings on US will be aspecific as well: mainly hyperechoic parenchyma (Fig. 21.1); still, due to the focused tubular insults, the pyramids may become small and irregular [1, 2, 8].

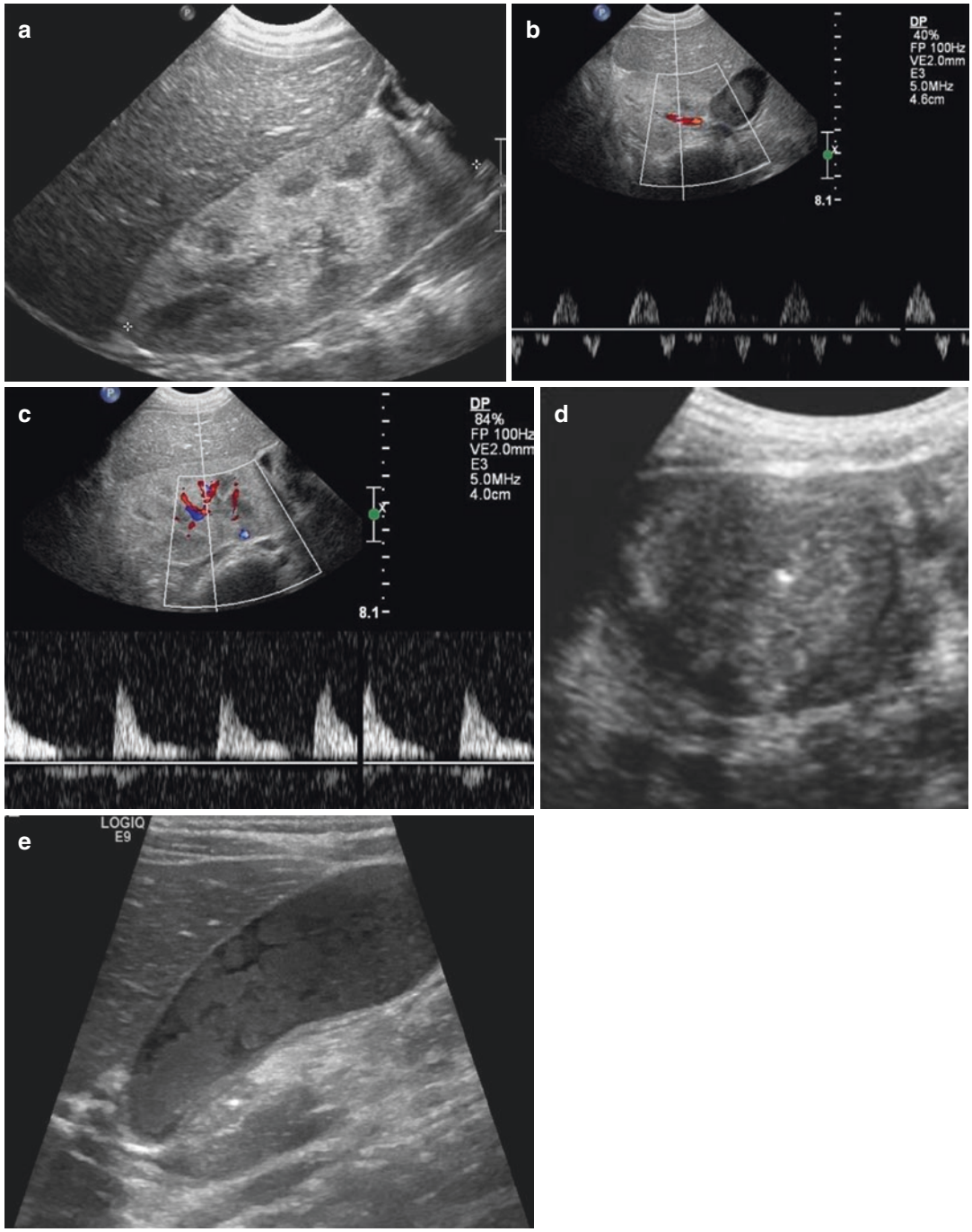

Fig. 21.2 Hemolytic and uremic syndrome (HUS)—US findings. (**a**) Examination obtained during the anuric/acute stage—Sagittal scan of the kidney (similar to the left one). The kidney is normal sized. The cortex appears hyperechoic with preserved CMD. (**b**) Duplex Doppler obtained during the acute stage. The spectrum demonstrates lack of normal diastolic flow. (**c**) Duplex Doppler obtained during the healing phase: the diastolic flow has resumed indicating that diuresis would restart. (**d**) Colitis observed during the acute phase—Transverse scan of a segment of the colon. The colonic wall appears globally echogenic with loss of the layered pattern (**e**) Hemobilia observed during the acute phase—Sagittal scan of the gallbladder that is enlarged and contains hyperechoic material.

21.3.3 Vasculitis and ARF (Henoch-Schonlein Purpura, Polyarteritis Nodosum, Kawasaki Disease)

Renal disease associated with vasculitis is variable and dependent on the size of the vessel involved in the inflammatory process. Large vessel involvement like in Takayasu arteritis would lead to renal artery stenosis and hypertension resulting in abnormal duplex Doppler profile. With smaller vessels involvement, the clinical presentation would more likely correspond to AGN [14].

Kawasaki disease is an acute, febrile vasculitis that predominantly develops in children less than 5 years. The disease has a striking predilection for the coronary arteries. In Kawasaki disease (KD), sterile pyuria is a common feature, occurring in 30–80% of patients and therefore a complete UTI workup including renal US, VCUG, and/or DMSA scan should be performed in such patients [14, 15].

Henoch-Schonlein purpura (HSP) is an immune mediated systemic vasculitis generally found in children. The clinical manifestations include purpura arthritis and abdominal pain. In about 50% of patients with HSP, the renal function is compromised due to nephritis resembling IgA nephritis with few US changes beside potential hyperechogenicity. Occasionally, the ureter may be affected resulting in ureteritis and ureteral obstruction [14, 16].

Polyarteritis nodosa (PN) is a necrotizing vasculitis associated with aneurysmal nodules along the walls of medium-sized muscular arteries; renal manifestations include hematuria, proteinuria, and hypertension. The kidneys appear patchy on DMSA scanning of the kidneys as well as on US. MR angiography may demonstrate renal and extrarenal aneurysms or stenosis on the medium size arteries. Angiography represents the gold standard examination for ascertaining the diagnosis [14].

21.3.4 Oncological Related Diseases and ARF (See Also Chap. 27)

Solid tumors like Wilms' tumors very rarely induce ARF unless the tumor is bilateral and involves the vessels. Renal involvement in malignant hemopathies, especially acute lymphoid leukemia, is more likely to compromise renal function. Leukemic infiltration of the kidneys occurs in 3–5% of patients at the time of diagnosis and can represent the initial finding of the disease. It occurs in 7–42% in the later stages of ALL. ARF in patients with hematological malignancies can present a major clinical problem; it develops as a result of a direct invasion by malignant cells determining obstruction of the ureters, renal artery or renal vein thrombosis. Other more indirect causes include AGN due to immunologic reactions, sepsis, hemolysis, and antileukemic therapy.

In cases with renal infiltration, on ultrasound, the kidneys could appear massively enlarged with heterogeneous patchy appearance of the renal parenchyma (Fig. 21.3a). Sometimes real nodules will be visualized that can be misinterpreted as primary tumors or renal lymphoma [17, 18]. Whenever necessary, MR imaging should ideally be performed to evaluate the renal involvement. Still, in an emergency setting a CT (Fig. 21.3b) can be performed with hyperhydration in order to prevent complications.

Once the chemotherapy has been started, ARF may develop due to the so-called "tumor lysis syndrome" or to urosepsis in immune-compromised patients related in particular to candidiasis. The latter may determine diffuse renal involvement with urinary sludge or fungus balls [19].

21.3.5 Congenital Metabolic Diseases

Various clinical and/or biological symptoms may lead to the discovery of metabolic diseases: failure to thrive, dehydration, signs of hepatic failure, or HT. In terms of renal failure several congenital metabolic entities will feature (A)RF (progressing into CRF) in the course of the disease. Tyrosinemia, primary oxalosis, and Bartter syndrome should be highlighted.

Hepato-renal tyrosinemia is a rare autosomal recessive disorder of tyrosine metabolism. Tyrosinemia affects liver and kidney function.

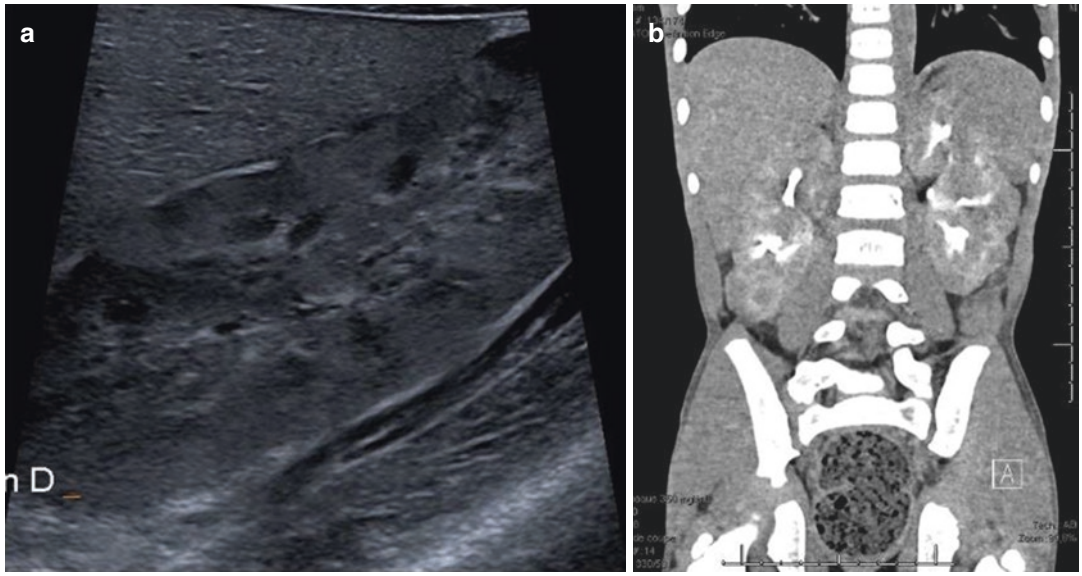

Fig. 21.3 Leukemic infiltration of the kidneys. (**a**) US Sagittal scan of the kidney. The kidney appears slightly enlarged. Its echogenicity appears inhomogeneous with diffuse poorly visible nodules. (**b**) CE-CT of the abdomen (performed to determine the extent of the disease): reformatted image showing irregular nodular enhancement of the renal parenchyma

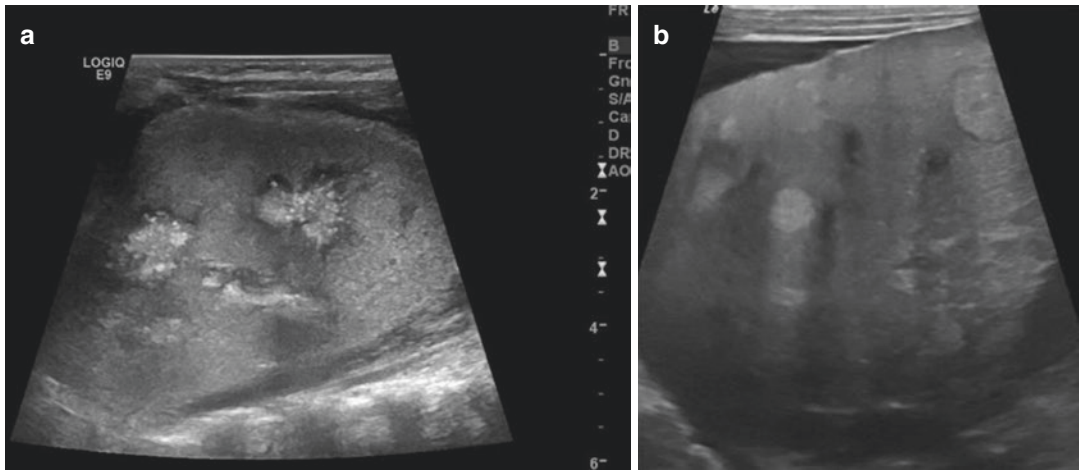

Fig. 21.4 Congenital tyrosinemia 2-year-old boy. (**a**) US of the kidney—Sagittal scan. Diffuse hyperechoic medulla corresponding to (bilateral nephrocalcinosis). (**b**) US of the liver—Sagittal scan through the right lobe. The liver parenchyma appears hyperreflective due to steatosis; there are several hyperechoic nodules corresponding to adenomas. Note the presence of perihepatic ascites

Hepatocellular carcinoma is a known long-term complication. On US, the association of hepatomegaly with steatosis and medullary nephrocalcinosis is suggestive of the disease (Fig. 21.4a). Hepatic nodules may develop corresponding to benign adenomas (Fig. 21.4b) [20].

Bartter syndrome is an inherited renal tubular disorder associated with hypokalemic alkalosis. In the course of the disease, ARF followed by CRF supervenes. On US, medullary nephrocalcinosis develops very rapidly during the first weeks or months after birth (Fig. 21.5) [21].

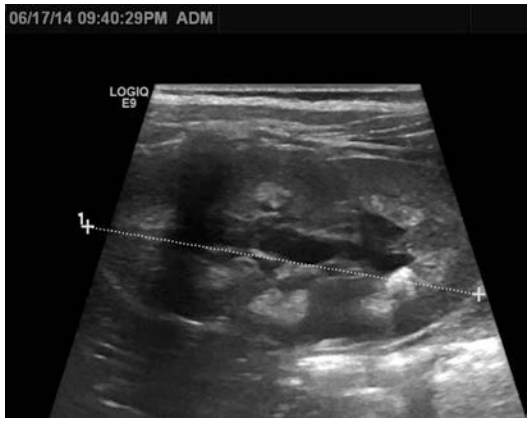

Fig. 21.5 Congenital Bartter syndrome in a 6-month-old infant. US of the right kidney (the baby is prone); the medulla appears hyperechoic; a urolithiasis has already developed at the lower pole

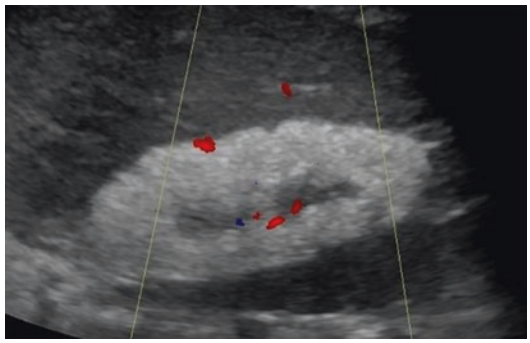

Fig. 21.6 Hyperoxaluria type I: US sagittal scan. Six-month-old infant with hepato-renal failure. Striking hyperechogenicity of the cortex; absent CMD

Primary oxalosis or primary hyperoxaluria type 1 is caused by a deficiency of the liver peroxisomal enzyme alanine glyoxylate–aminotransferase (AGT). When AGT activity is absent, glyoxylate is converted to oxalate which forms insoluble calcium salts that accumulate in the kidney and other organs. Individuals with HP type 1 are at risk for recurrent nephrolithiasis, nephrocalcinosis, and end stage renal disease. 20% of patients will develop the disease within the first 6 months of life while the majority will develop nephrolithiasis later in childhood or even in adulthood. On US, in the early forms, due to massive calcium deposits, the kidneys will appear highly and diffusely echogenic (Fig. 21.6). This appearance is characteristic of this form of the disease. For the rest, urolithiasis will develop and recur with secondary obstruction due to lithiasis migration [22].

21.3.6 Medications and Contrast Media Related ARF (See Also Chaps. 4, 5 and 6)

Several medications, including contrast media, have been reported to induce ARF. The mechanisms are various and complex. For some, the insult will be intrarenal while for others the medication will induce post renal obstruction. For some the effects will start in utero (maternal medications) for others, they will appear during childhood at the time of specific treatments.

In utero, insults by angiotensin-converting enzyme inhibitors and angiotensin II receptor blockers may induce renal tubular dysgenesis. Oligohydramnios develops progressively associated with the RF and neonatal death. NSAID may induce ATN while several other drugs may induce the formation of urolithiasis (see below). During childhood, no specific pattern will be observed on US unless post-renal obstruction occurs due to urolithiasis. In this perspective, two medications should be highlighted: ceftriaxone and melanine.

Ceftriaxone is a third generation cephalosporin that is widely used to treat various infections in children. About 33–67% of ceftriaxone is excreted unmetabolized in the urine while the remainder is eliminated through the biliary tract. Ceftriaxone at therapeutic doses can lead to the formation of biliary pseudolithiasis, nephrolithiasis, and bladder sludge and/or lithiasis. This lithiasis formation as well as secondary obstruction of the urinary tract will be demonstrated on US (Fig. 21.7a,b). The prognosis is favorable once the medication is stopped and the child sufficiently hydrated.

During the spring of 2008, an epidemic episode of urolithiasis was noted among children in China. This has been shown to be associated with consumption of melanine-contaminated powered formula. A few patients presented

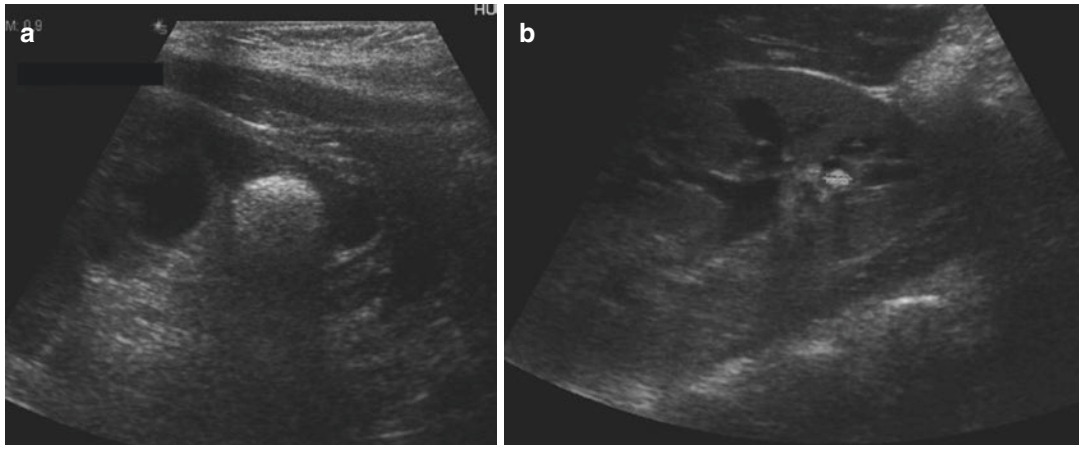

Fig. 21.7 Urinary tract obstruction and ARF due to lithogenic antibiotics (Ceftriaxone). (**a**) US—Transverse scan of the (empty) bladder: echogenic content with acoustic shadowing corresponding to sludge ball. (**b**) US—Sagittal scan of the kidney; a "lithiasis" (*between the crosses*) is visible within the pyelo-caliceal system

with ARF due to bilateral renal or ureteral calculi. The calculi ranged from 3–14 mm and showed little or no acoustic shadowing on US [6, 23–25].

21.3.7 Infection (See Also Chap. 18)

Sepsis and bilateral urinary tract infection (UTI) especially if associated with underlying chronic renal disease, congenital uropathies, or conditions reducing the patient defense mechanisms are able to further worsen renal function.

Ultrasound will be useful to demonstrate the underlying favoring condition and the potential consequences of the UTI (Fig. 21.8) [8].

21.3.8 Ischemia and Thrombosis (See Also Chaps. 4 and 6)

In children reduced flow to the kidney can result from hypovolemia, cardiac failure, and/or shock. These conditions potentially lead to pre-renal ARF. The kidney may appear hyperechoic on US and the RI increases. Some free fluid may collect in the perirenal third space.

Renal vein thrombosis usually occurs in prematurely born neonates and less frequently in full term neonates. Bilateral cases may be associated with ARF.

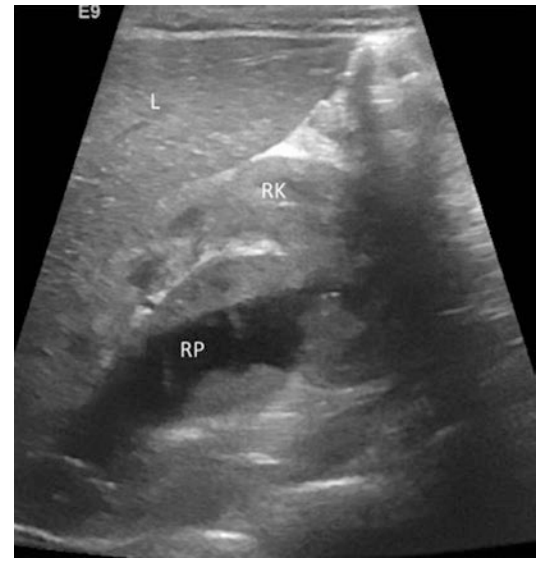

Fig. 21.8 Bilateral UT obstruction and ARF induced by UTI with massive pyonephrosis. Sagittal scan of the right kidney (RK). The pyelo-caliceal system (*RP* renal pelvis) is distended by thick pyonephrosis (pyonephrosis was bilateral). *L* Liver

21.4 Imaging and Post-Renal ARF

As mentioned above, one of the main roles of US in ARF is to demonstrate renal outflow obstruction, its second role is to demonstrate an underlying favoring anomaly or a complication of treatment.

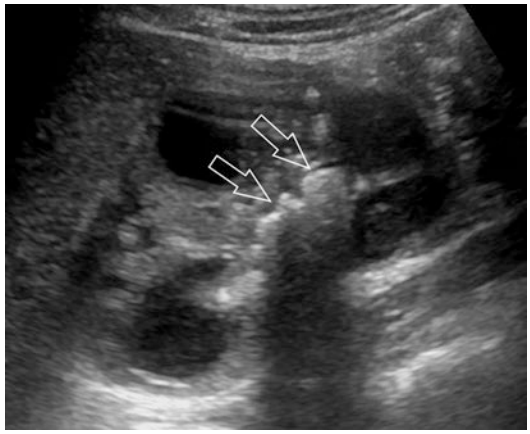

Fig. 21.9 Bilateral UT obstruction and AFR induced by bilateral urinary stones. Sagittal scan of the right kidney. The pyelo-caliceal system is obstructed by multiple lithiasis (*arrows*). (Lithiasis and obstruction were bilateral)

21.4.1 Bilateral Acquired Obstruction

Bilateral obstruction may develop secondary to pelvic compression by a pelvic tumor, by bilateral urolithiasis especially in the context of lithogenic metabolic disease (Fig. 21.9) (e.g., cystinuria, oxalosis, etc.) (see also chapter 19) or rarely by complications of UTI (fungus balls) (Fig. 21.8). US will demonstrate the dilatation of the urinary tract and the level of obstruction (Fig. 21.8). The presence of a mass will be demonstrated. Its nature and extension may be better determined by MR imaging and CT. The presence of urolithiasis is usually easy at the level of the kidneys, the uretero-vesical junction, or bladder. It might be more difficult when the lithiasis is located in the lumbar portion of the ureter. The presence of bilateral nephrocalcinosis would orient towards an underlying metabolic disease [8, 25–27].

21.4.2 The Single Functioning Kidney

The presence of a single (functioning) kidney renders it more vulnerable to acute insults. Acute obstruction secondary to surgical complications or to urolithiasis, severe trauma on a single functioning kidney may lead to ARF. Accurate diagnosis and appropriate rapid treatment are mandatory. Ultrasound will be the first line imaging and will solve most problems (Fig. 21.8). In complex cases, MR imaging or CT may be performed as rapid decisions depend on a precise evaluation [28] (Fig. 21.10).

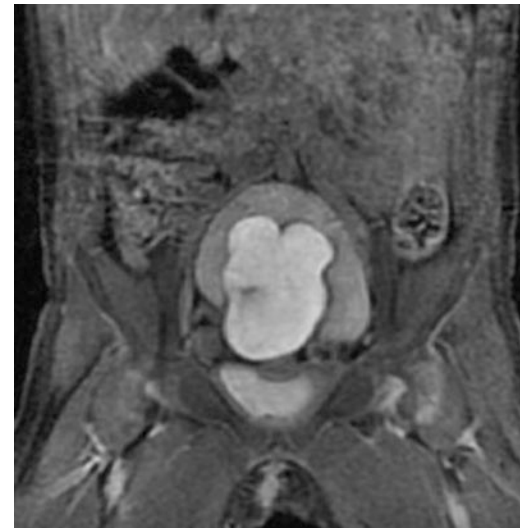

Fig. 21.10 UPJ obstruction in a single pelvic kidney—MR Imaging; frontal T1—Weighted sequence—Late acquisition

Conclusion

ARF in children is common, usually with good prognosis.

US is usually sufficient for the evaluation of the urinary tract. HUS is among the main cause; it is adequately followed by US.

Imaging is also important for the evaluation of post-renal obstruction.

References

1. Fichter A, Schaefer F. Acute kidney injury in children. In: Turner N, Lameire N, Goldsmith DJ, et al., editors. Oxford textbook of clinical nephrology. 4th ed. New York: Oxford University Press; 2016. p. 2024–37.
2. Plan V, Brophy PD, Fleming GM. Acute renal failure: prevention, causes and investigations. In: Geary DF, Schaefer F, editors. Comprehensive pediatric nephrology. Philadelphia: Mosby; 2008. p. 607–27.
3. Gheissari A, Mehrasa P, Merrikhi A, et al. Acute kidney injury: a pediatric experience over 10 years at a tertiary care center. J Nephropathol. 2012;1:101–18.

4. Goldstein SL. Acute kidney injury in children and its potential consequences in adulthood. Blood Purif. 2012;33:131–7.
5. Shah SR, Tunio SA, Arshad MH, et al. Acute kidney injury recognition and management: a review of the literature and current evidence. Glob J Health Sci. 2016;8:120–4.
6. Twombley K, Baum M, Gattineni J. Accidental and iatrogenic causes of acute kidney injury. Curr Opin Pediatr. 2011;23:208–14.
7. Faubel S, Patel NU, Lockhart ME, et al. Renal relevant radiology: use of US in patients with AKI. Clin J Am Soc Nephrol. 2014;9:382–94.
8. Riccabona M. Renal failure in neonates, infants and children: the role of US. Ultrasound Clin. 2006;1:457–69.
9. Schmidt IM, Main KM, Damgaard IN, et al. Kidney growth in 717 healthy children aged 0-18 months: a longitudinal cohort study. Pediatr Nephrol. 2004;19:992–1003.
10. Zerin JM, Blane CE. US assessment of renal length in children: a reappraisal. Pediatr Radiol. 1994;24:101–6.
11. Chavhan GB, Parra DA, Mann A, et al. Normal Doppler spectral waveform of major pediatric vessels: specific patterns. Radiographics. 2008;28:691–706.
12. Jenssen GR, Vold L. Hovland et al clinical features, therapeutic interventions and long term aspects of HUS in Norwegian children: a nationwide retrospective study from 1999-2008. BMC Infect Dis. 2016;16:285.
13. Scholbach TM. Changes of renal flow volume in the HUS – color Doppler US investigations. Pediatr Nephrol. 2001;16:644–7.
14. Dillon MJ, Eleftheriou D, Brogan PA. Medium-size-vessel vasculitis. Pediatr Nephrol. 2010;25:1641–52.
15. Watanabe T. Pyuria in patients with Kawasaki disease. World J Clin Pediatr. 2015;4:25–9.
16. Dalpiaz A, Schwamb R, Miao Y, et al. Urological manifestations of Henoch-Schonlein purpura: a review. Curr Urol. 2014;8:66–73.
17. Sherief LM, Azab SF, Zakaria MM, et al. Renal presentation in pediatric acute leukemia. Medicine. 2015;94(37):1–3.
18. Goyal S, Goyal A, Kolte S, et al. Disseminated renal Burkitt lymphoma with malignant inferior vena caval thrombosis in a child. Urology. 2016;95:180–3.
19. Hazouz S, Dafiri R. Renal candidal bezoar: case report and review of the literature. Arch Pediatr. 2014;21:70–2.
20. Mayorandan S, Meyer U, Gokcay G, et al. Cross sectional study of 168 patients with hepatorenal tyrosinemia and implications for clinical practice. Orphanet J Rare Dis. 2014;9:107.
21. Maruyama H, Shinno Y, Fujiwara K, et al. Nephrocalcinosis and placental findings in neonatal Bartter syndrome. AJP Rep. 2013;3:21–4.
22. Diallo O, Janssens F, Hall M, et al. AJR Am J Roentgenol. 2004;183:1767–70.
23. Hwang YJ, Hyun MC, Choi BS, et al. Acute kidney injury after using contrast during cardiac catheterization in children. J Korean Med Sci. 2014;29:1102–7.
24. Li N, Zhou X, Yuan J, et al. Ceftriaxone and ARF in children. Pediatrics. 2014;133:e97.
25. Shang P, Chang H, Yue ZJ, et al. Acute renal injury cause par the consumption of melanine-contaminated infant formula in 47 children: a multi-institutional experience in diagnosis, treatment and follow-up. Urol Res. 2012;40:293–8.
26. Gatti JM, Perez-Brayfield M, Kirsch AJ, et al. Acute urinary retention in children. J Urol. 2001;165:918–21.
27. Nalcacioglou H, Ozden E, Genc G, et al. An uncommon cause of acute kidney injury in young children: cystinuria. J Pediatr Urol. 2013;9:e58–63.
28. Choi MB, Kim JS, Seo JH, et al. Unilateral renal agenesis presenting with acute obstructive postrenal failure following administration of hydration fluid. Pediatr Int. 2006;48:420–2.

Complicated Urachal Remnants

22

Fred E. Avni

Contents

22.1 General Considerations

The urachus is a midline tubular structure that extends upwards from the dome of the bladder towards the umbilicus. It is a vestigial remnant of the connection between the early bladder and the fading allantois. The tubular urachus normally involutes before birth remaining as a fibrous band. Persistence of a (partially) patent urachus may give rise to various clinical problems in newborns, infants, children, and even adults. Congenital urachal anomalies may present under 4 different forms with variable percentages and consequences.

A first form, the commonest, is a completely patent urachus. It accounts for 50% of cases and is associated with several lower urinary tract anomalies, mainly the prune-belly syndrome and posterior urethral valves. The condition is easily recognized at birth due to urine leakage from the umbilicus. The patent urachus is visualized through retrograde voiding cystography. Management of this type of anomaly will be included in the global treatment of the underlying anomaly. A second anomaly, vesico-urachal diverticulum (3–5% of cases) will also be incidentally opacified during cystography. This anomaly lacks clinical significance. The two other congenital anomalies include an umbilical-urachal sinus (15%) and urachal cyst (30%). Part of the patients presenting these last 2 congenital anomalies will become symptomatic generally due to superinfection and enlargement of the urachus.

F.E. Avni
Department of Pediatric Imaging, Jeanne de Flandre Hospital, 59037 Lille–Cedex, France
e-mail: Freddy.Avni@chru-lille.fr

F.E. Avni, P. Petit (eds.), *Imaging Acute Abdomen in Children*,
https://doi.org/10.1007/978-3-319-63700-6_22

Because urachal remnant diseases are uncommon (1/7500 autopsies) and manifest with non-specific abdominal or urinary symptoms, pre-surgical diagnosis is not always achieved. Imaging techniques, presently US and CT, will have an important role for the characterization and the follow-up of complicated urachal remnants of the sinus and cyst types. MR imaging is infrequently used due to lack of availability and duration of examination but provides significant information; its use will surely increase especially with the potential contribution of DWI. US will also be essential for the differential diagnosis of other umbilical anomalies and for the demonstration of rare tumors developing within the urachus [1–9].

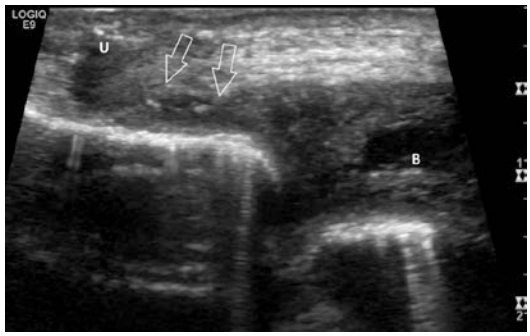

Fig. 22.1 Infected urachal remnant (sinus)—4-week-old baby boy. Sagittal scan on the midline. Thickening of the urachus (*arrows*) extending from the umbilicus (U) till the dome of the bladder (B)

22.2 Complicated Urachal Sinus

Urachal sinus consists of a blind dilatation of the urachus at the umbilical end. The main symptom of a complicated sinus would be a (recurrent) pus discharge through the umbilicus associated with the palpation of a thickened cord on the midline below the umbilicus. This is typically a pathology occurring in early life or infancy but it does occur at any age.

On US, the fibrous cord connecting the umbilicus to the bladder will appear hypoechoic and thickened with sometimes increased flow on color Doppler. The thickened urachus will measure 3–4 mm diameter or more. The thickening may involve the entire urachal remnant cord or more commonly the part below the umbilicus on a few cm (Figs. 22.1 and 22.2). Color Doppler will demonstrate the surrounding inflammation. No other imaging will usually be necessary.

The treatment will be mostly medical with antibiotics and the infection will resolve within a few weeks. The urachal remnant will return to a normal appearance. If necessary, the normalization can be followed up on US. As such no further treatment will be necessary [1, 7–10].

22.3 Complicated Urachal Cysts

A urachal cyst develops if the urachus remains patent in a localized segment somewhere between the umbilicus and the bladder. This occurs most

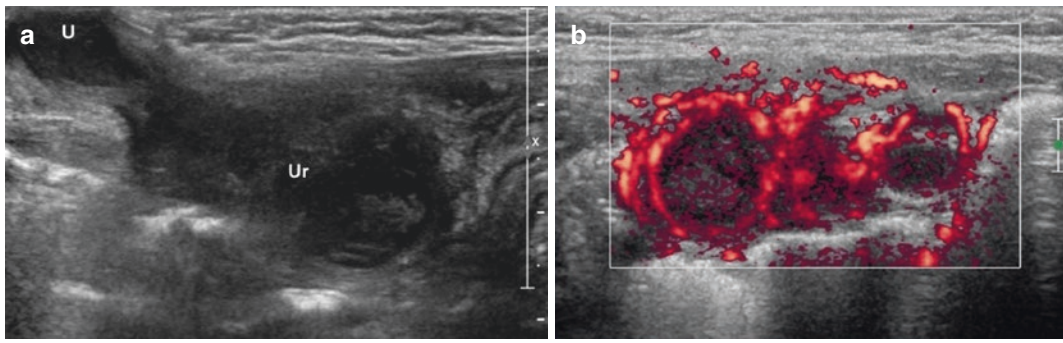

Fig. 22.2 Infected urachal remnant—2-year-old girl. (**a**) US Sagittal scan a loculated mass extends from the umbilicus (U) towards the bladder representing a urachal remnant (Ur) abscess. (**b**) Color Doppler US—transverse scan below the umbilicus—massive peri-abscess hypervasularization corresponding to inflammatory response

commonly in the lower third of the urachus. Urachal cysts may be detected incidentally in asymptomatic patients. They will become symptomatic due to their rapid enlargement generally secondary to infection. Clinically the patient will complain of abdominal fullness or pain; he/she may present with lower urinary symptoms in relation with a secondary cystitis.

A thin walled cyst with echo-free fluid content will be the usual appearance in incidental asymptomatic urachal cysts. The cyst being typically located on the midline, above the bladder. This particular type of congenital urachal remnant is a different entity from the urachal remnant that can appear as a nodular nubbin on the top of the bladder, within its wall. Especially, since this latter type of remnant may sometimes present a confusing protruding cystic appearance within the bladder [7, 8, 10].

Superinfected urachal cysts will manifest on US as a thick wall cystic mass with echogenic or heterogeneous content (Fig. 22.3a,b). The wall may appear hypervascularized on color Doppler as the surrounding tissues and the wall may become inflamed. Similar findings will be demonstrated on CE-CT or MR imaging (Fig. 22.3c–e). A thick wall cyst enhancing after contrast injection will be demonstrated. Inflamed surrounding tissues may show enhancement as well and determine irregular boundaries. Rarely the cyst may rupture rendering the diagnosis more difficult.

The differential diagnosis of an infected urachal sinus includes all potentially infected cysts of the abdomen especially those developing around the midline such as Meckel's diverticulum, mesenteric cyst, lymphangioma, or duplication cyst. A connecting tract from the cyst to the umbilicus (or to the bladder) is a clue for a urachal remnant [1].

The treatment is controversial. In young infants, it will be mainly medical; surgery being reserved for unfavorable evolution or recurrence. The treatment would more often be surgical in older children, as excision of the infected cyst is performed to prevent reinfection (30% of reinfection rate). Furthermore, some authors have reported the increased risk of tumoral development in unresected or incompletely resected urachal remnant (see below). As mentioned, this remains controversial [1, 3, 11, 12].

22.4 Other Umbilical Anomalies

Various other umbilical anomalies need to be considered whenever a urachal remnant is suspected. The pathologies may be self-limited to the umbilicus or the "tip of an iceberg," as part of the anomaly extends within the abdomen.

22.4.1 Localized Anomaly

Omphalitis is defined as erythema and edema of the umbilical region with or without discharge from the abdomen. An umbilical *granuloma* may develop after the cord separation when the epithelialization has been incomplete. The granulation tissue may overgrow and form a granuloma. Both entities do not require imaging and will be treated medically.

Rarely, an abscess may develop and masquerade as urachal remnant; imaging will demonstrate the limited localized lesion (Fig. 22.4).

22.4.2 Umbilical Anomaly as a Sign of a Deeper Intraabdominal Pathology

Umbilical discharge may be a common symptom to different entities. As mentioned already, it can correspond to the discharge of a patent or inflamed urachal remnant as well as associated with omphalitis. Another etiology for umbilical discharge or inflammation is *vitelline duct remnant*. Meckel's diverticulum is the most common type of vitelline duct remnant, but does not present usually umbilical symptoms (See also Chap. 11). On the contrary, a *patent vitelline duct* that represents only 2% of duct remnants does manifest with umbilical symptoms. In such condition, feces will appear in the umbilicus and will facilitate the diagnosis. Fistulography may be performed in case of uncertain diagnosis. It will show the connection to the digestive tract.

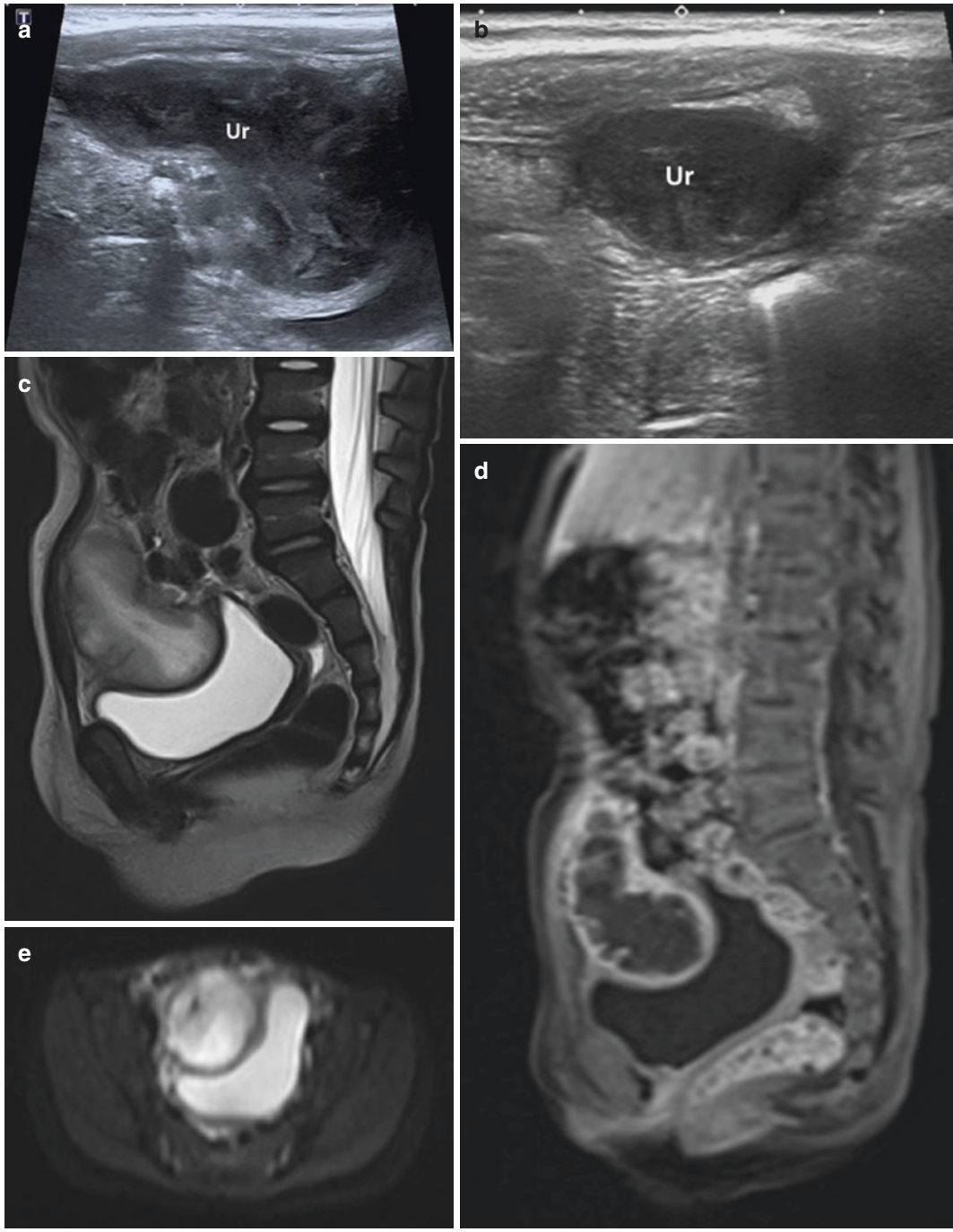

Fig. 22.3 Infected urachal cyst in a 5-year-old girl. (**a**) US—Sagittal scan showing a distended urachal remnant (Ur) cyst filled with echogenic material and extending from the bladder (B) towards the umbilicus. (**b**) US—Transverse scan below the umbilicus. The infected cyst appears round and located anteriorly just behind the abdominal wall (*Ur* urachal remnant cyst). (**c**) MR imaging—T2-weighted sequence—It demonstrates the infected cysts, lying on the dome of the bladder. (**d**) MR imaging—T1-weighted after Gd injection. Enhancement of the wall of the cyst and surrounding inflammatory tissues. (**e**) MR imaging DWI—Striking hypersignal of the abscess

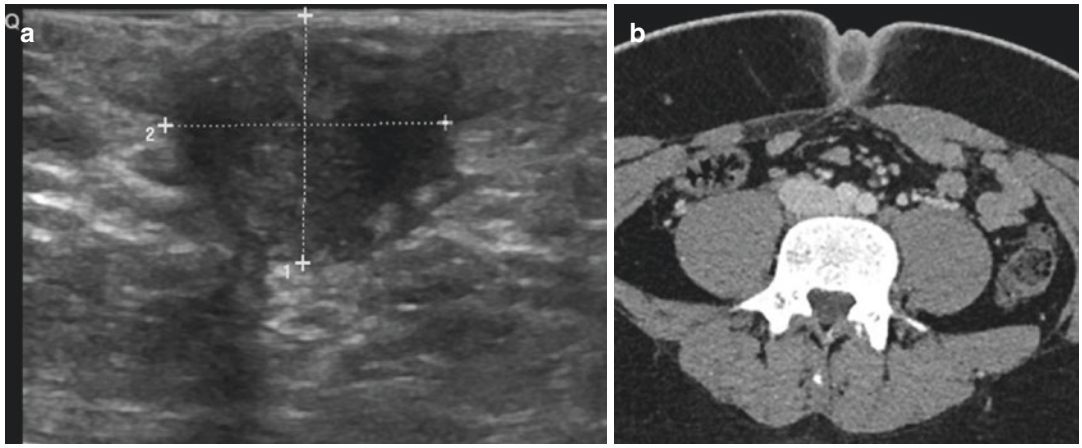

Fig. 22.4 Infected umbilical abscess—15-year-old adolescent. (**a**) US—Transverse scan at the umbilical level; a small collection (*between the crosses*) measuring 7x6 mm is visible with the umbilicus. (**b**) CE-CT confirms that the abscess is limited to the umbilicus without deep extension

Vitelline sinus or a vitelline cyst is also part of the panel of anomalies of vitelline duct remnants; they are also connected to the umbilicus; they may become infected and can cause umbilical inflammation. US may be performed to demonstrate the cyst type; the sinus may be more difficult to demonstrate. CT may be performed in ambiguous cases.

All symptomatic vitelline duct anomalies need to be excised.

An *umbilical hernia* develops when the umbilical ring fails to close after the cord separation. A protrusion will then appear at the umbilicus. It may contain just fat or some bowel loops. Umbilical hernia rarely incarcerates and the natural history is towards spontaneous resolution. Imaging is rarely necessary (see also Chap. 29) [4, 13].

22.5 Tumors Developing in Urachal Remnants

Very rarely urachal tumors develop in the urachus during childhood. Case reports of different types of tumors have been reported, both benign and malignant. Among others, benign teratoma, mucinous tumor, giant cell tumor, rhabdomyosarcoma (Fig. 22.5) or yolk sac tumor. Rupture of urachal tumors has been exceedingly rarely reported. Exceptionally as well, a tumor may develop within the umbilicus itself (e.g., duplication cyst) [12, 14–16].

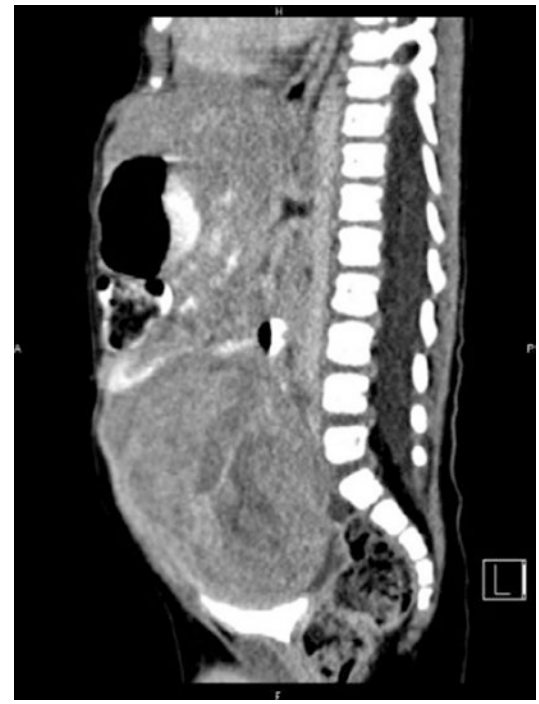

Fig. 22.5 Rhabdomyosarcoma developed in the dome of the bladder. CE-CT Reformatted sagittal scan; large oval solid type mass within the dome of the bladder (the urachal origin could not be definitively ascertained) (Courtesy N Rocourt MD)

Imaging rater CE-CT than US, or whenever available MR imaging will provide clues for the diagnosis of the tumoral nature of the mass rather than a complex inflamed urachal remnant. It will also help to determine the extension of the tumor.

Noteworthy, the relation between urachal remnants and carcinoma developing in adults is controversial. Urachal carcinoma accounts for few than 1% of bladder neoplasms (in adults). No convincing association has been established between urachal remnants in childhood and later urachal carcinoma. Therefore, it has been recommended that patients with asymptomatic umbilical remnants and patients under 1 year should not undergo surgical resection unless symptoms are recurrent [5, 12, 14–16].

Conclusion

Urachal remnants complications should always be included in the differential diagnosis of acute abdominal pain especially in young children. US is useful for their demonstration and for the differential diagnosis. CE-CT and MR imaging may provide additional information.

References

1. Yu J, Kim KW, Lee HL, et al. Urachal remnant diseases: spectrum of CT and US findings. Radiographics. 2001;21:451–61.
2. Choi YJ, Kim JM, Ahn SY, et al. Urachal anomalies in children: a single center experience. Yonsei Med J. 2006;47:782–6.
3. Naiditch JA, Radhakrishnan J, Chin AC. Current diagnosis and management of urachal anomalies. J Pediatr Surg. 2013;48:2148–52.
4. O'Donell KA, Glick PL, Caty MG. Pediatric umbilical problem. Pediatr Clin N Am. 1998;45:791–9.
5. Chouchan M, Cuckow P, Humphries PD. Utility of diffusion weighted imaging in the pre-surgical diagnosis of an infected urachal cyst. Pediatr Radiol. 2011;41:125–8.
6. Galati V, Donovan B, Ramji F, et al. Management of urachal remnants in early childhood. J Urol. 2008;180:1824–7.
7. Cilento BG, Bauer SB, Retik AB, et al. Urachal anomalies: defining the best diagnostic modality. Urology. 1998;52:120–2.
8. Widni EE, Hollwarth ME, Haxhija EQ. The impact of preoperative US on the correct diagnosis of urachal remnants in children. J Pediatr Surg. 2010;45:1433–7.
9. Copp HL, Wong IY, Krishnan C, et al. Clinical presentation and urachal remnant pathology: implications for treatment. J Urol. 2009;182:1921–4.
10. Metwalli ZA, Guillerman RP, Mehollin-Ray AR, et al. Imaging features of intravesical urachal cyst in children. Pediatr Radiol. 2013;43:978–82.
11. Stopak JK, Azarow KS, Abdessalam SF, et al. Trends in surgical management of urachal anomalies. J Pediatr Surg. 2015;50:1334–7.
12. Sato H, Furuta S, Tsuji S, et al. The current strategy for urachal remnants. Pediatr Surg Int. 2015;31:581–7.
13. Abdulhai SA, Glenn IC, Ponsky TA. Incarcerated pediatric hernias. Surg Clin N Am. 2016;97:129–45.
14. Gleason JM, Bowlin PR, Bagli DJ, et al. A comprehensive review of pediatric urachal anomalies and predictive analysis for adult urachal carcinoma. J Urol. 2015;193:632–6.
15. Sumer TL, Ramanathan S, Padura M. Urachal yolk sac tumor with rupture in a child. J Pediatr Hematol Oncol. 2017;39:e82–4.
16. Cheik-Helard A, Irtan S, Orbah D. Urachal RMS with poor outcome. J Pediatr Surg. 2015;50:1329–33.

Complications of Renal Graft

23

Audrey Aschero and Philippe Petit

Contents

23.1 Introduction

Approximately, nine children per million age-related population start renal replacement therapy each year worldwide [1]. All pediatric ages are interested. Renal dysplasia (congenital and acquired) and reflux nephropathy are the most frequent causes for pediatric end-stage renal disease in the youngest patients whereas focal glomerular sclerosis is more frequent in the oldest ones [2, 3]. The rate of success in pediatric renal transplantation has dramatically raised partly due to living donor grafts. Nowadays, acute rejection occurs in less than 15% of patients [4]. Five-year survival rate is above 80% with a significant drop at time of adolescence [5].

23.2 Imaging

US with Doppler (USD) is the imaging modality of choice to explore renal graft. USD is usually performed the same day or the day after transplantation and then repeated any time as required by clinical and/or biological data. Both convex and linear probes are useful. Contrast-enhanced US is a more invasive technique but its use must be considered whenever the Doppler perfusion analysis is inconclusive. The contribution of US elastography to evaluate parenchymal fibrosis is still debated [6–8].

When additional information are needed, MR Imaging is preferred to CE-CT and scintigraphy

A. Aschero • P. Petit (✉)
Department of Pediatric Imaging,
Hôpital Timone Enfants, 264 Rue St Pierre,
13385 Marseille Cedex 05, France
e-mail: aaschero@ap-hm.fr; ppetit@ap-hm.fr

F.E. Avni, P. Petit (eds.), *Imaging Acute Abdomen in Children*,
https://doi.org/10.1007/978-3-319-63700-6_23

as long as no sedation is needed. MR Imaging allows morphological and functional information without radiation burden with a lower cost than scintigraphy. Diffusion weighted imaging could detect acute renal transplant dysfunction [9]. The use of gadolinium macrocyclic products at the lowest possible dose is recommended to prevent risk of nephrogenic systemic fibrosis and to limit risk of accumulation of gadolinium within other tissues, especially the brain.

The use of scintigraphy (^{99m}TcMAG3) for the evaluation of the renal graft should be limited to children who need sedation.

23.3 Complications and Related Interventional Procedures [2, 10]

23.3.1 Vascular Complications

Vascular complications represent the most common cause of 1st-year-allograft lost (35%) and their reported incidence is up to 10%.

23.3.1.1 Arterial Thrombosis

Absence of flow within the main renal artery and the kidney parenchyma is easily detected on USD even before the clinical signs (reduction in urine excretion and raised creatinine level). During the immediate postoperative period this rare complication must be detected as fast as possible to avoid graft necrosis. Global infarction may display no parenchymal evidence on US but the kidney may appear globally hypoechoic. An anastomotic anomaly (dissection, kink) is the main cause of this complication. Surgical treatment is urgently required. Local thrombolysis is usually contra-indicated in the immediate post-operative period. Very severe acute rejection and hypercoagulablity status have to be considered as differential diagnoses. In doubtful cases, contrast-enhanced US would allow to exclude acute rejection, identifying poor residual highly resistive parenchymal flow. Thrombosis of more distal branches lead to segmental infarcts which appear as wedge shaped hypoechoic areas with perfusion defects on USD (Fig. 23.1). Parenchymal retraction will develop at distance of the acute event.

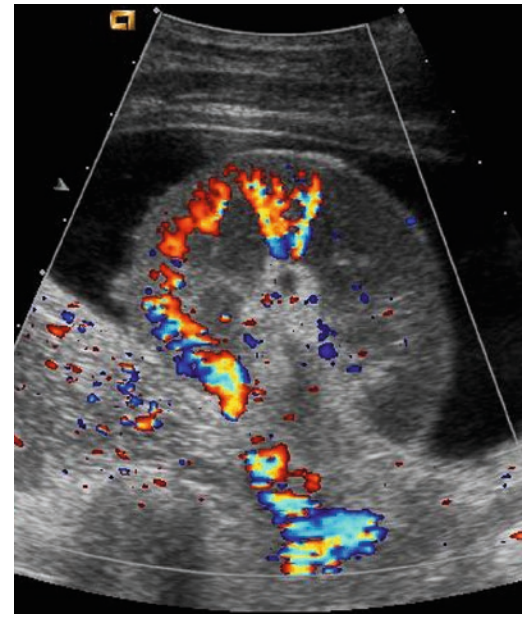

Fig. 23.1 Ten-year-old boy, USD follow-up of a kidney transplant. USD reveals segmental thrombosis with absence of peripheral flow of the lower pole of the graft surrounded by an anechoic fluid collection

Noteworthy, all these findings are nonspecific and may, for instance, be observed during an episode of acute pyelonephritis.

23.3.1.2 Arterial Stenosis

It is the most common vascular complication. It may appear at any time after transplantation. Most of them develop at the anastomotic site. End to end arterial anastomosis (with the internal iliac artery) is more prone to induce stenosis that end to side anastomosis (with the external iliac artery or with the aorta). A stenosis is considered hemodynamically significant when the arterial luminal narrowing is above 50%. USD may detect stenosis in the absence of clinical symptoms (bruits over the graft, hypertension, and increased creatinine level). Based upon the adult literature, direct signs include: a reduction in size of the main renal artery, a peak velocity in the main renal artery far above 2 m/s, marked turbulences with spectral broadening and vibration of the adjacent tissues but overall a renal/iliac arteries diameter ratio above 1.8 [11]. Indirect signs are also present especially for

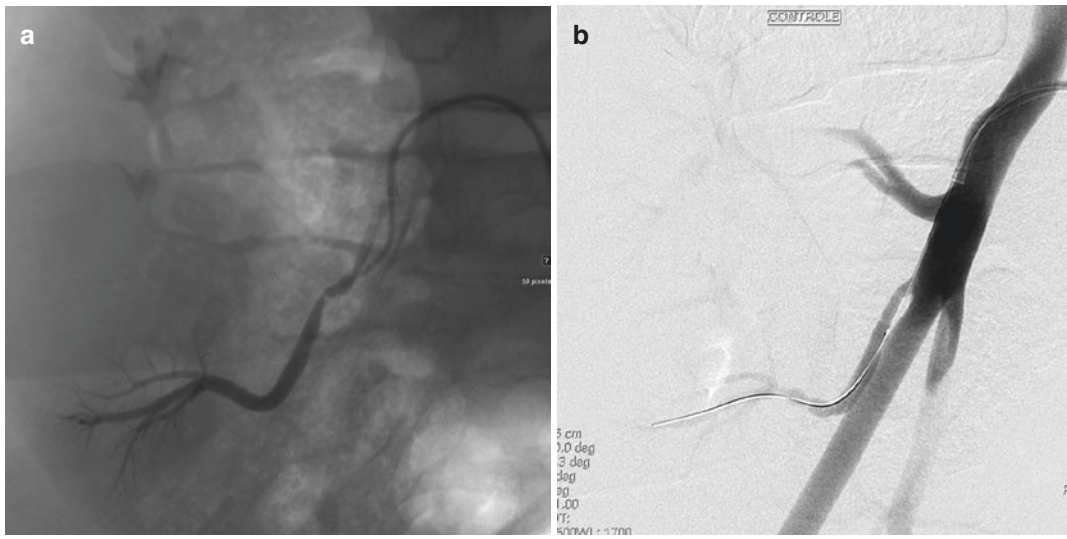

Fig. 23.2 Fifteen-year-old boy. USD follow-up of a kidney graft reveals a stenosis. (**a**) A severe stenosis of an accessory inferior artery is confirmed. (**b**) After angioplasty, disappearance of the stenosis

sever stenosis; they include small systolic amplitude and rounding of systolic peak (parvus), a prolonged systolic acceleration above 0.08 s (tardus) and a diminished resistive index (<0.56) obtained from interlobar or segmental arteries. 3D–Gadolinium MR angiography is preferred to the ionizing CE-CT in order to differentiate if necessary, stenosis from arterial kinking. Angioplasty is the treatment of choice for significant stenosis (Fig. 23.2).

23.3.1.3 Extra-Renal Pseudo-Aneurism

This very rare complication occurs at the anastomotic site; if unrecognized (by US), pseudoaneurysms carry a high risk of rupture with an associated high mortality rate.

23.3.1.4 Venous Thrombosis

This early complication may be suspected clinically in the presence of soft tissue swelling around the graft and/or ipsilateral lower extremity edema. Etiologies include anastomotic dysfunction and compression by fluid collections. Hypovolemia, hypercoagulability, and acute rejection are predisposing factors. On US, the main vein may look normal (fresh clots can be isoechoic or the main vein is not yet thrombosed) or contains echoic clots. On Doppler, there is no venous flow and the arterial flow is highly resistive or even presents with reversed diastolic flow. However, these arterial findings are non-specific and may be found in case of acute rejection, severe hydronephrosis, extrinsic graft compression [11]. Surgical thrombectomy is the only chance to save the graft during the first postoperative week while thrombolytic therapy can be attempted later.

23.3.1.5 Venous Stenosis

Venous stenosis may occur before thrombosis. Diminished diameter of the vein, turbulences, and increased speed within the vein on USD are the main findings.

23.3.2 Fluid and Pseudo-Fluid Collections

23.3.2.1 Hematoma

Hematoma the graft is a frequent finding in the postoperative days. It regresses within a few days. It appears as a hyper, isoechoic or heterogeneous fluid collection that progressively becomes anechoic. US may underevaluate the volume of this hematoma and the conclusions of US need to

be compared to perfusion Doppler and clinical findings [12].

23.3.2.2 Lymphocele

Lymphocele is also anechoic or may present some hyperechoic septations. In relation with the surgical dissection, it will appear relatively late after the transplantation. Percutaneous drainage with doxycycline injection is indicated in case of large persisting lymphocele; an estimated volume above 500 ml is reported as indication for surgery [13].

23.3.2.3 Urinoma

Urinoma looks quite similar to a lymphocele. The level of creatinine within the drained fluid (under US guidance) helps to differentiate these two entities. In case of doubt and in order to localize the leak, MR imaging with gadolinium injection is our preferred examination (vs CE-CT, scintigraphy or antegrade pyelography) under the condition of an acceptable renal function. Urine leaks are mostly located close to the vesicoureteral anastomosis but can also originate from the renal pelvis (surgical breach) or the ureter (ischemia).

23.3.2.4 Consequences

Large amounts of fluid may lead to parenchymal and/or excretory system compression and hypoperfusion and may become infected. The presence of gas within the collection and thickened hypervascularized wall around the collection are strong USD arguments for abscess formation. Urinoma secondary to small leak will be cured by JJ stent and drainage whereas other fluids collection will be drained under US guidance. Large urine leaks or large organized collections persisting despite drainage may require surgery.

23.4 Ureteral Stenosis

The site of ureteral anastomosis is the most frequent site of stenosis usually related to local surgical difficulties and poor ureteral blood supply. Ischemia may also responsible for stenosis at any level of the ureter and will usually be demonstrated at distance from the transplantation. US reveals progressive increasing dilatation. This

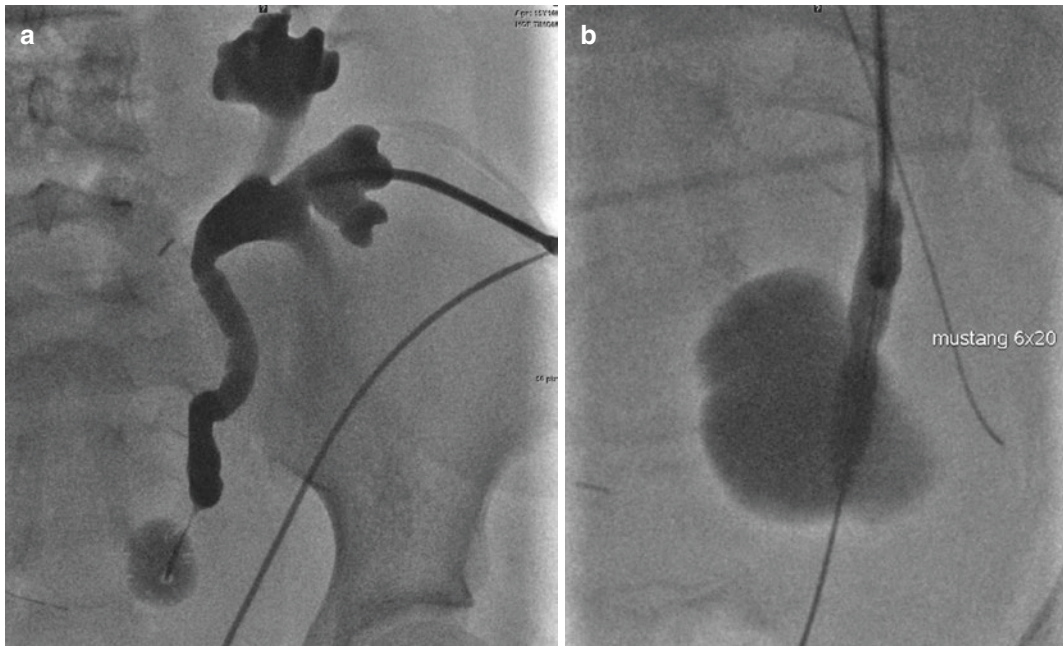

Fig. 23.3 Ureteral stenosis in a 10-year-old-boy. (**a**) Opacification through a nephrostomy drain visualizes a stenosis of the distal ureter with associated uretero-hydronephrosis. (**b**) The stenosis was treated by balloon dilatation

abnormal evolution should not be confused with a properly functioning transplant where the renal pelvis is slightly dilated, because of an increase in urine outflow and also due to the loss of ureteral tonicity after denervation. First treatment includes balloon dilatation of the stenosis and JJ stenting (Fig. 23.3). When this measure is unsuccessful surgical repair is required. The differential diagnosis of urinary tract obstruction due to stenosis includes obstruction secondary to blood clots, stones, and fungus balls, all frequent complications. To be noted, the typical symptoms of renal colic are absent due to denervation of the upper urinary tract.

23.5 Vesicoureteric Reflux

Vesicoureteric reflux may be seen up to 10% especially in children with prior bladder disability (neurologic bladder, posterior urethral valves, prune belly syndrome, etc.) [2]. Voiding cystography either with iodine or US with microbubbles confirms the diagnosis. Endoscopic treatment may be decided to suppress reflux.

23.6 Parenchymal Lesions

23.6.1 Pyelonephritis

Pyelonephritis is a frequent complication. Its diagnosis relies on fever and urine analysis. Thickening of the renal pelvis and ureter and echogenic material within these excretory cavities are frequent associated findings. The use of contrast-enhanced US may increase the accuracy of USD to identify pyelonephritis as a focal hypoechoic focal vascular defect.

23.6.2 Other Parenchymal Diseases

For other parenchymal diseases, USD can be normal or demonstrate findings that are neither specific nor sensitive. Loss of cortical medullary differentiation, swollen kidneys, and increased resistive index above 0.8 on duplex Doppler are common findings. Kidney biopsy is necessary to differentiate between the different types of rejection, acute tubular necrosis secondary to ischemic damage or nephrotoxicity related to immunosuppressive treatment (Cyclosporine, Tacrolimus). Chronic dysfunction appears as progressive reduction in the kidney volume, cortical thinning, increased cortical echogenicity, and mild hydronephrosis.

23.7 Renal Graft Biopsy Complications

23.7.1 Perirenal Hematomas

Perirenal hematoma are frequent, usually of limited size. Active bleeding during biopsy may be seen (Fig. 23.4); it is usually self-limited and embolization is rarely necessary.

23.7.2 Subcapsular Hematomas

Subcapsular hematoma are rare and generally of small size with no consequence on the graft function. They present as a crescent shaped

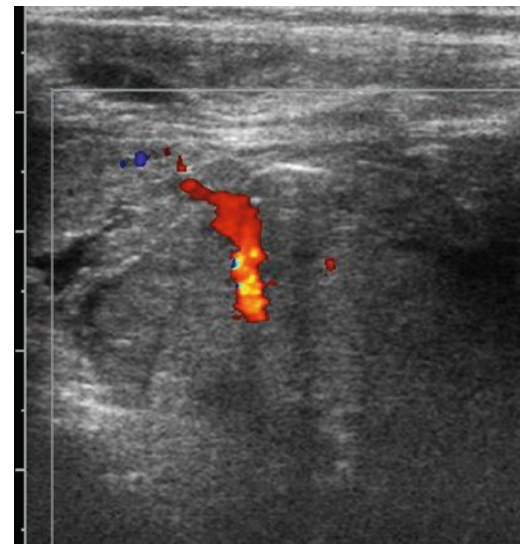

Fig. 23.4 USD appearance of an active bleeding during percutaneous kidney graft biopsy

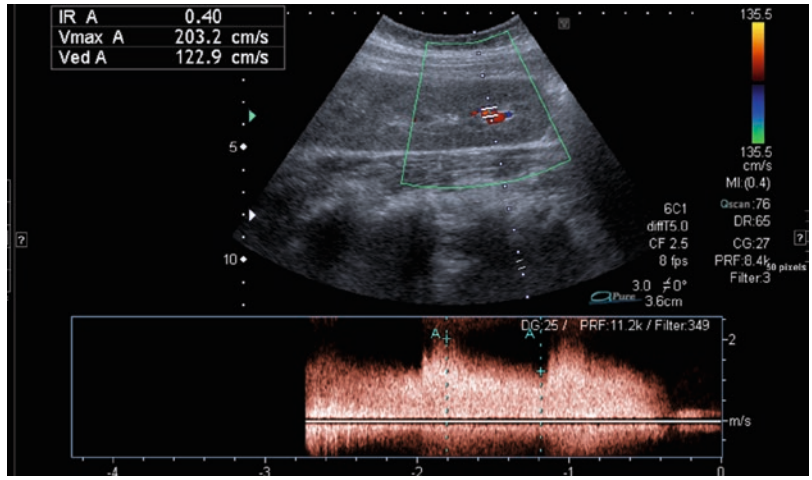

Fig. 23.5 Post kidney graft biopsy in a 13-year-old-boy. USD demonstrates a significant increased peripheral arterial flow with low resistive index revealing an arteriovenous fistula

collection, of various echotextures, compressing the underlying parenchyma. Large subcapsular hematoma may be responsible for hypertension and graft dysfunction [14]. In the latter, the subcapsular hematoma is associated with an increase resistive index on Doppler analysis. Percutaneous drainage or surgical capsulotomy must be considered.

23.7.3 Arteriovenous Peripheral Fistulas

Arteriovenous peripheral fistula are very frequent but close spontaneously within a few days in most cases. US Doppler reveals an increased flow in the feeding artery, increased velocity with turbulences within the fistula, decreased resistive index and arterialized flow within the draining vein (Fig. 23.5). Small fistula does not generate tissue vibration. Indication of embolization is limited due to kidney dysfunction secondary to renal ischemia (steal phenomenon), heart failure, or persistent hematuria.

23.7.4 Pseudoaneurysm

Pseudoaneurysm less frequent and appears as an anechoic structure highly vascularized. A size over 2 cm is an indication for embolization [15].

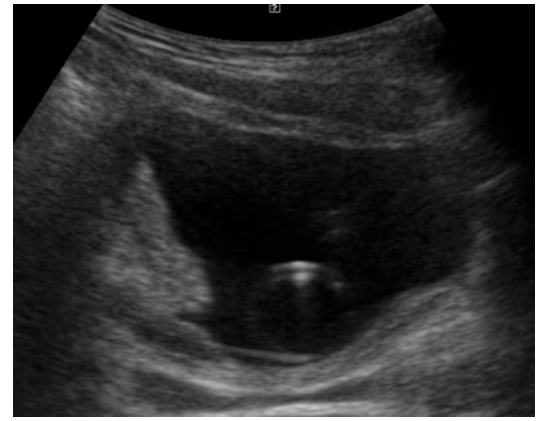

Fig. 23.6 US appearance of a focal infiltration of the bladder wall by BK Virus after kidney graft transplantation in a 12-year-old boy

23.8 Post-Transplant Lymphoproliferative Disorders

For Harambat et al. [1], they occur in 7.5% of patients and represent the main complication of renal transplantation in children increasing the risk of lethal outcome. Furthermore, an increased graft loss is observed during boyhood due to immunosuppressive drugs incompliance. Epstein-Barr virus is responsible for a dramatic increase in the rate of post transplantation lymphoma. BK Virus [16] and CMV have a great responsibility in the development of renal dysfunction (Fig. 23.6).

US is a major screening tool, looking for an enlarging graft, hypoechoic masses within the kidney graft, in its hilum as well as in the whole abdominal cavity. Biopsies under US guidance help to confirm the diagnosis. In case of proved lymphoma, cervical, chest, abdomen, and pelvis CE-CT is necessary to allow disease workup. Treatment will include cessation of immunotherapy, antiviral therapy, and chemotherapy.

Conclusion

- US-Doppler is the method of choice to follow renal graft and specially to analyze the kidney perfusion.
- Parenchymal USD findings are nonspecific.
- MR Imaging must be preferred when complementary imaging exploration is required. It allows morphologic and functional kidney evaluation.
- CE-CT has a limited role principally in case of lymphoproliferative disorder workup.

References

1. Harambat J, Ranchin B, Bertholet-Thomas A, et al. Long-term critical issues in pediatric renal transplant recipients: a single-center experience. Transpl Int. 2013;26:154–61.
2. Stanescu AL, Hryhorczuk AL, Chang PT, et al. Pediatric abdominal organ transplantation: current indications, techniques, and imaging findings. Radiol Clin N Am. 2016;54(2):281–302.
3. Shapiro R, Sarwal MM. Pediatric kidney transplantation. Pediatr Clin N Am. 2010;57:393–400.
4. United States Renal Data System. 2014 annual report. vol. 2. Pediatric end stage renal disease. 2014. [Chapter 7]. Available at: http://www.usrds.org/2014/view/v2_07.aspx.
5. Badet L, Matillon X, Codas R, et al. Pediatric kidney transplantation. Prog Urol. 2016;26(15):1045–52.
6. Yang C, Jin Y, Wu S, et al. Prediction of renal allograft acute rejection using a novel non-invasive model based on acoustic radiation force impulse. Ultrasound Med Biol. 2016;42(9):2167–79.
7. Lee J, Oh YT, Joo DJ, et al. Acoustic radiation force impulse measurement in renal transplantation: a prospective, longitudinal study with protocol biopsies. Medicine (Baltimore). 2015;94(39):e1590.
8. Nakao T, Ushigome H, Nakamura T, et al. Evaluation of renal allograft fibrosis by transient elastography (Fibro Scan). Transplant Proc. 2015;47(3):640–3.
9. Abou-El-Ghar ME, El-Diasty TA, El-Assmy AM, et al. Role of diffusion-weighted MRI in diagnosis of acute renal allograft dysfunction: a prospective preliminary study. Br J Radiol. 2012;85(1014):e206–11.
10. Nixon JN, Biyyam DR, Stanescu L, et al. Imaging of pediatric renal transplants and their complications: a pictorial review. Radiographics. 2013;33(5):1227–51.
11. Moreno CC, Mittal PK, Ghonge NP, et al. Imaging complications of renal transplantation. Radiol Clin N Am. 2016;54(2):235–49.
12. Fananapazir G, Rao R, Corwin MT, et al. Sonographic evaluation of clinically significant perigraft hematomas in kidney transplant recipients. Am J Roentgenol. 2015;205(4):802–6.
13. Król R, Kolonko A, Chudek J, et al. Did volume of lymphocele after kidney transplantation determine the choice of treatment modality? Transplant Proc. 2007;39(9):2740–3.
14. Machida J, Kitani K, Inadome A, et al. Subcapsular hematoma and hypertension following percutaneous needle biopsy of a transplanted kidney. Int J Urol. 1996;3:228–30.
15. Kolofousi C, Stefanidis K, Cokkinos DD, et al. Ultrasonographic features of kidney transplants and their complications: an imaging review. ISRN Radiol. 2013;2013:480862.
16. Dharnidharka VR, Cherikh WS, Abbott KC. An OPTN analysis of national registry data on treatment of BK virusallograft nephropathy in the United States. Transplantation. 2009;87:1019–26.

Imaging Emergency Pelvic Diseases in Girls

24

Pauline Verpillat, Jean-François Chateil, Chantal Durand, and Fred E. Avni

Contents

24.1 Introduction

In case of acute pain of the lower abdomen, appendicitis is logically the most frequent diagnosis considered (see Chap. 10) even in girls. Still, gynecological pathologies should not be overlooked as they encompass a spectrum of entities that may clinically express as acute pain or other acute symptoms (enlarging mass, bleeding or even shock) and can mimic appendicitis. Among gynecological diseases presenting "acutely", some entities may occur during the neonatal period (hydrocolpos due to imperforate hymen or torsion of an ovarian cyst—see Chap. 5); some occur at any age, while others are specific to the post-menarchal adolescent period such as hematocolpos, endometriosis and rupture of a hemorrhagic cyst or rarely extrauterine pregnancy (Table 24.1).

US is the imaging modality of choice and is often sufficient for an accurate diagnosis when coupled with the clinical and biologicals data. Before starting the examinations, the radiologist should rapidly discuss with the young patient and her parents; it should be rapidly clarified whether

P. Verpillat (✉) • F.E. Avni
Department of Pediatric Radiology, Jeanne de Flandre University Hospital, 59037 Lille, France
e-mail: pauline.verpillat@chru-lille.fr

J.-F. Chateil
Department of Pediatric Radiology, Pellegrin University Hospital, 33000 Bordeaux, France

C. Durand
Department of Pediatric Radiology, Grenoble University Hospital, 38700 Grenoble, France

F.E. Avni, P. Petit (eds.), *Imaging Acute Abdomen in Children*,
https://doi.org/10.1007/978-3-319-63700-6_24

Table 24.1 Pathologies according to age

Any age	Antenatal and newborns (cf Chap. 5)	Postmenarchal period
• Adnexal torsion • Infection of the pelvis	• Hydrocolpos • Hematocoplpos • Torsion or hemorrhage of an ovarian cyst	• Extrauterine pregnancy • Hematocolpos • Endometriosis • Hemorrhagic and rupture of functionnal cyst

the parents will remain in the room during the examination. Indeed, some intimate questions could be asked, particularly if a vaginal way is possible and necessary. The radiologist performing the US examination should be reassuring as much as possible especially when examining adolescent girls. He/She should explain the way the examination will be performed.

The transabdominal way is the only possibility in the young virgin girls. Transabdominal US has to be performed with a full bladder (1/2 L of any liquid 1 h before the examination) in order to obtain an acoustic window that would facilitate the visualization of the adnexa. The use of perfusion or diuretic medications may be discussed to accelerate the process, allowing keeping the stomach empty in case that surgery is an option. Vaginal US if performed, has to be decided in agreement with the patient and only if the abdominal way is insufficient to clarify the diagnosis. MR imaging can be a good alternative examination in such case.

24.2 Adnexal Torsion (AT)

24.2.1 Epidemiology—Physiopathology—Clinical Data

Pediatric isolated ovarian torsion or entire adnexal torsion accounts for approximately 15% of all cases of ovarian torsion. In children, up to 52% of cases of adnexal torsion (AT) occur between 9 and 14 years, with a median age of 11 years. Noteworthy, there are two peaks: one during the first year of life and the second around 12 years. Pediatric AT represents about 3% of patients with acute abdominal pain referred to an emergency department [1, 2].

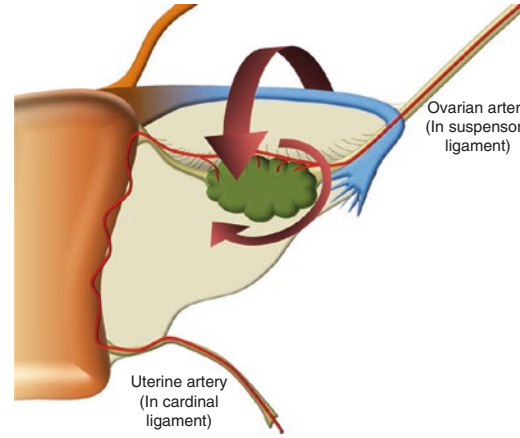

Fig. 24.1 Diagram defining the axis of torsion in true isolated ovarian (*small arrow*) and adnexal torsion (*large arrow*)

Whenever an AT progresses unrecognized, the ovarian blood supply becomes compromised, leading to tissue necrosis and potentially to a reduction of the reproductive capabilities of the patient. Therefore, timely diagnosis is crucial. Because the clinical presentation of AT may be nonspecific, preoperative diagnosis will potentially challenging.

AT is caused by partial or complete twisting of the ovary around its pedicle. True isolated ovarian torsion corresponds to a twisting of the ovary alone around the mesovarium. This form of torsion is rare. Global AT, including all adnexal components—ovary, fallopian tube and vascular pedicle - around the suspensory ligaments and the broad ligament is by far more common (Fig. 24.1). Rarely, an isolated torsion of the fallopian tube is also possible.

Torsion of the ovarian pedicle will first affect the lymphatic flow and only thereafter the venous flow, with subsequent stasis and thrombosis. This will result in progressive ovarian edema and enlargement. An interval of more than 10 h between initial symptoms and surgery is associated with high percentage of adnexal necrosis; still the actual duration of ischemia beyond which the damage is irreversible remains unknown [3].

AT occurs either in normal ovaries or in ovaries with an associated ovarian or para-ovarian mass. The mechanism of torsion in case of an associated

ovarian mass is probably related to the increased size and weight of the ovary that becomes pivotal to the torsion. The etiology of a torsion of an apparently normal ovary is less obvious. Possible explanations include excess meso-ovarium mobility, congenitally long pelvic ligaments, tubal spasm, or acute modifications in the intraabdominal pressure. For these reasons, the twist on healthy ovaries and their recurrence is more common in children than in adults as confirmed by Ashwal et al. who reported a higher rate of recurrent torsion in pre-menarchal patients [3, 8].

Neonatal (in girls younger than 1 month) AT is classical but rare, and its incidence is unknown. All aged considered, approximately 16% of pediatric cases occur in girls younger than 1 year. There are two potential mechanisms for adnexal torsion in neonates and infants. The prenatal migration of the ovaries from the abdomen to the pelvis indicates an increase in gonadal mobility. Alternatively, maternal-hormone-induced stimulation with resultant ovarian enlargement and cyst development could serve as a fulcrum for the torsion [8].

Pre-menarchal and post-menarchal girls with AT may or may not have an underlying anomaly. In large pediatric series, the incidence of an underlying ovarian pathology ranged from 51% to 84%. Whenever an underlying anomaly is present, it is more probably a benign tumor like a benign cystic teratoma, a follicular hemorrhagic cyst or a serous cystadenoma [4–7]. Malignant masses associated with torsion are extremely rare, accounting for 2% of cases only; this is possibly related to an invasion of the adjacent structures by the malignancy, with adhesions that limit the mobility of the adnexal structures.

Many studies indicate that the right ovary is more frequently involved [1, 9]. The lower rate of left torsion may be explained by the partial adhesion of the left adnexa to the mesosigmoid [4, 10, 11].

Abdominal pain, accompanied by nausea and vomiting, is the main clinical symptom [3, 9]. In case of classic ovarian torsion, pain is sudden and acute. The most common sign on physical examination is abdominal tenderness. The presence of fever is more common in children than in adults. Other symptoms or signs such as restlessness and a palpable pelvic mass are more frequently reported in childhood. Raised white cells count is associated with ovarian necrosis. Raised temperature is associated with more advanced cases and a higher risk of tissue necrosis [3, 9, 12, 13].

24.2.2 Imaging

As mentioned, transabdominal ultrasound is the preferred imaging modality in girls with pelvic pain and (clinically) suspected AT. CT and MR imaging are infrequently used, except in cases with misleading presentation or when sonography is inconclusive. A fairly filled bladder, serving as an acoustic window, is ideal in order to obtain diagnostic US images (Table 24.2).

24.2.2.1 Ultrasound Findings

On US, the demonstration *of an unilaterally enlarged ovary* is the most common finding in case of AT [1, 11, 14] (Fig. 24.2). Oltmann et al. [15] has reported that, in a pediatric population older than 1 year, the presence of a pelvic mass

Table 24.2 Imaging findings in typical form of adnexal torsion

All modality signs, but especially US findings	• Unilaterally enlarged ovary • Peripherally displaced follicles • Central stromal edema • Complex adnexal mass • Twist of the pedicle vessels ("whirlpool sign" or "nipple sign") • Medialization of the ovary • Displacement of the uterus of the midline • Free pelvic fluid • Thickened or enlarged fallopian tube.
Additional CT and MRI findings	• Lack of enhancement of the ovary after contrast injection • Twisted lombo-ovary pedicle
Specific addition of CT (if performed for another clinical suspicion)	• Differential diagnoses • Calcifications/fat in an adnexal germinal mass
Specific addition of MRI	• Anatomical characterization • Underlying adnexal mass • Evidence of necrosis and hemorrhagic infarction

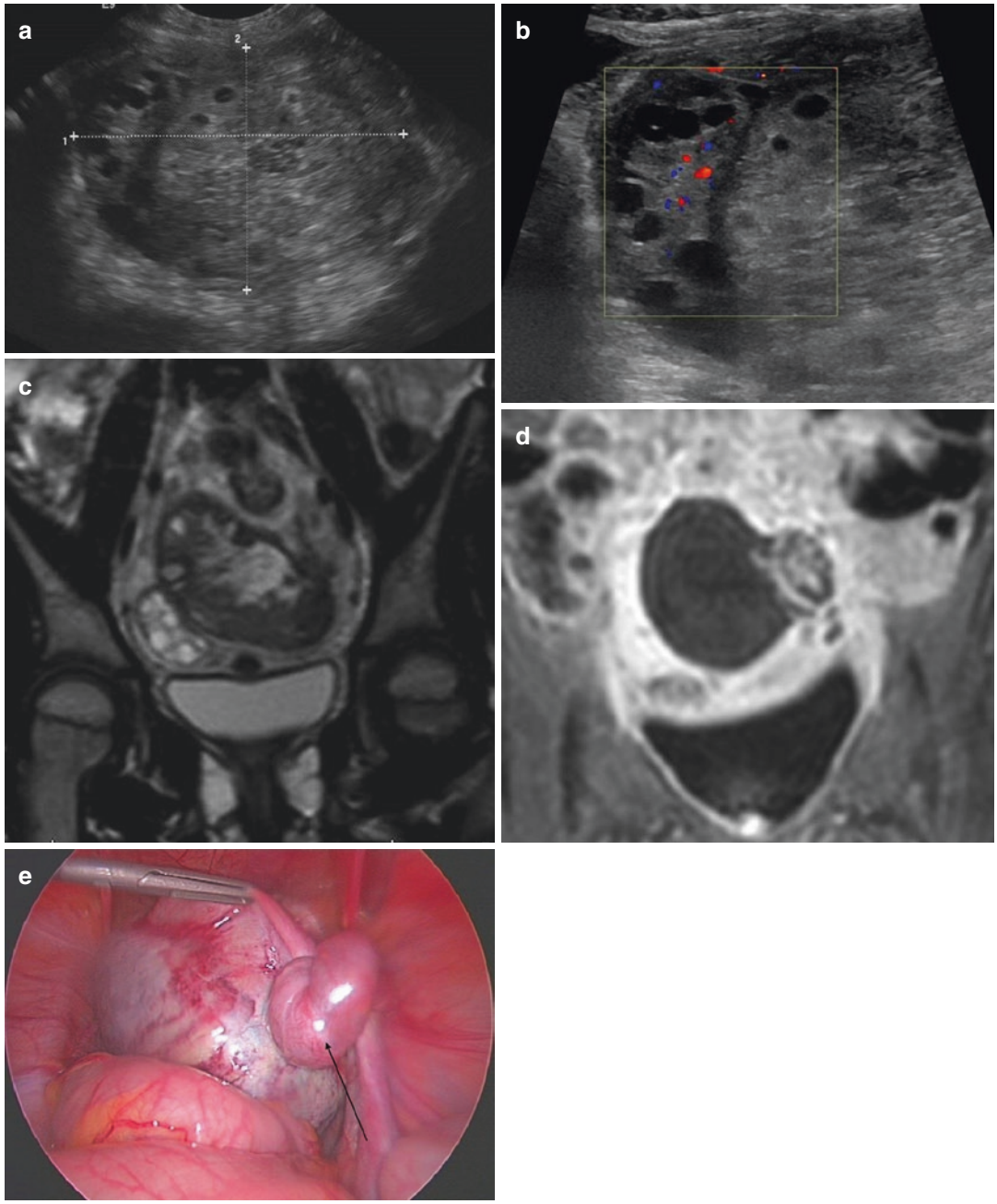

Fig. 24.2 Adnexal torsion in a 6 year-old girl. (**a**) Ultrasound Axial view: Significant increase in size of the left ovary which is medialized. The follicles are displaced peripherally. (**b**) Color Doppler US Axial view: Persisting vascularization on color Doppler (despite torsion). (**c**) MR imaging: Coronal T2-Weighted sequence: similar findings as in US. Significant asymmetry of size of the ovaries and medialization of the left adnexa. Note the central stromal edema visualized as a central hypersignal. (**d**) MR imaging: Coronal T1-Weighted sequence post Gd. Central lack of enhancement related to necrosis. US had shown persisting flow on Doppler. Whirl pool sign on the left side (**e**) Laparoscopic view showing the torsed adnexa (*arrow*)

larger than 5 cm diameter has the highest diagnostic sensitivity for the diagnosis of ovarian torsion. Servaes et al. have reported the interest of a volume ratio: the size of the twisted ovary was compared with that of the contralateral ovary; the median ratio between the twisted side and the normal side was 12. The median volume ratio was significantly greater (>20) when an adnexal mass was present [1]. The torsed adnexa determines the visualization (in up to 70% of cases) of a complex adnexal or abdomino-pelvic mass, that can predominantly be cystic, solid/echogenic or both [11, 16].

In addition to the ovarian enlargement, a peripheral displacement of the follicles secondary to stromal edema and venous congestion can be visualized in up to 70% of patients with AT [3, 17].

A *"whirlpool" sign or the "nipple" sign* has been reported in case of AT; it appears as a pseudo-mass of concentric stripes with a beaked center. This can also be visualized as an ellipsoid or tubular mass with internal heterogeneous echoes, depending on the plane of scanning. This sign corresponds to the torsion of the vascular pedicle, tubal structures and supporting ligaments. In a study by Lee et al., a twisted vascular pedicle was detected in 88% of cases of AT. When present, this finding is pathognomonic of AT [18].

Another potentially helpful sonographic sign is the *medialization of the adnexal structures* with sometimes a complete controlateral position of the twisted ovarian. As torsion occurs, the twisting of the adnexal structures adjacent to the broad ligament creates a centrifugal force that attracts the adnexal structures closer to the uterus [19].

The rates of the various US findings such as adnexal enlargement, adnexal edema, or ovarian or paraovarian cysts are reported similar between the pre- and the post-menarchal girls [13].

Ipsilateral deviation of the uterus (IDU) was found to be frequent in AT. This results from the displacement of the abnormal adnexa toward the midline with the broad ligament acting as a fulcrum pulling the uterus towards the affected side. The contralateral fallopian tube is straightened as well [20]. This sign is insufficient by itself. In the absence of supporting clinical and imaging findings of torsion, the identification of IDU in the routine clinical setting of an adnexal mass is not a strong predictor of AT.

Thickened or enlarged fallopian tube: fallopian tube torsion associated with a *hydrosalpinx* has been reported in approximately 9% of AT. Additional findings such as a thickened, echogenic fallopian wall and the presence of internal tubal debris or hemorrhage may render difficult the differentiaton between a fallopian tube torsion and hydro/pyosalpinx in relation with pelvic inflammatory disease. The clinical context and the search of a pelvis surgical history are essential for the differentiation.

In addition, free *pelvic fluid in the cul-de-sac* has been detected with US in up to 87% of cases of ovarian torsion [11, 16].

There are conflicting data regarding the utility of *Doppler evaluation* for the demonstration of vascular compromise in the setting of suspected AT. Evidence for ovarian torsion on color Doppler flow are highly variable and depend partially on the degree of vascular compromise.

The classic color Doppler sonographic sequence in adnexal torsion is first, the absence of venous flow followed by the absence of arterial flow. Noteworthy, the ovaries have a dual supply from both ovarian and uterine arteries, which can result in detection of arterial flow even when the ovary is found to be partially necrotic at surgery. Some authors have reported arterial or venous blood flow abnormalities in two-thirds of patients [4] while others report much higher rates [5, 21]. Conversely, in another study, 60% of patients with AT had normal color Doppler flow findings [11, 22]. Absence of Doppler flow does not occur in every case of AT and may occur only as a late finding [23]. So, the sensitivity of absent arterial flow can be as low as 40% [17]. However, some authors insist on a high negative predictive value [24].

Therefore, neither the presence nor the absence of Doppler flow can be used to definitively confirm or exclude torsion; still the degree of vascularization and the presence of flow might

be useful for predicting the viability of the ovary following detorsion. Fleischer et al. [25] have reported that the presence of central venous flow in a twisted ovary was associated with increased likelihood of ovarian viability post detorsion.

Noteworthy, in post-pubertal girls, hemorrhagic cysts can have a similar appearance to twisted ovaries [26]. Both entities may have a complex US appearance and a reduced or absent arterial flow. Large hemorrhagic cysts may be responsible of a mass effect on the adjacent ovarian tissue and on the blood flow.

If a AT on tumor is diagnosed by US, detorsion must be made in emergency by laparascopy after dosage of tumoral markers. MR imaging will be performed after surgery, to fully assess the mass.

24.2.2.2 MR Imaging and CT

In an acute clinical setting, after confirmatory US, no complementary examination should delay exploring laparoscopy.

When the diagnosis of AT is unclear, as in case of subacute or intermittent ovarian torsion, MR imaging can be useful to further delineate the anatomy, particularly in a preoperative setting. MR imaging can also characterize an underlying mass.

MR imaging protocol includes T2-Weighted sequences, T1-weighted fat-suppressed sequences to detect hemorrhage and fat in germinal masses, as well as T1-Weighted fat-suppressed post-contrast sequences. The latter are aimed to detect compromized vascular supply, which would suggest infarction or necrosis (Fig. 24.3).

As with US, an enlarged ovary is the most common finding on MR imaging [14]. It is more specific when it is associated with an edematous central stromal area and peripherally displaced follicles. This finding is best seen on T2-weighted sequences, appearing as a central hypersignal.

Performing CT is not recommended in the evaluation of suspected ovarian torsion in children, mainly because of ionizing radiation hazards and poor cost-efficiency when compared to US. It could be performed when the clinical presentation is unclear. Whenever performed, only a venous acquisition after contrast injection should be obtained. Noteworthy, a CT is useful as it can identify other causes of the acute pelvic symptoms such as appendicitis or urolithiasis, both may clinically mimic AT.

A further contribution of CT is its ability to demonstrate calcifications within germinal tumors.

CT and MR imaging were also found to be useful in delineating the twisted vascular pedicle, similarly to the sonographic whirpool sign (Fig. 24.2). The twisted lombo-ovarian pedicle can itself be visualized as inflamed and thickened.

A decreased or absent enhancement of the ovarian parenchyma after contrast injection confirms ovarian necrosis.

Further CT and MR imaging features include ascites, fallopian tube thickening, displacement of the uterus towards the twisted ovary, and change in position of the involved adnexa toward either the midline (medialization) or the contralateral side of the pelvis.

Finally, hemorrhagic infarct will appear as a T1 hypersignal and lack of enhancement.

24.2.3 Special Cases and Imaging Pitfalls

24.2.3.1 Isolated Torsion of a Fallopian Tube

Rarely, torsion can be limited to the Fallopian tube itself, leaving the ovary undamaged. The etiologies of fallopian tube torsion includes both intrinsic fallopian tube abnormalities and extrinsic causes like pelvic post-surgical or infectious adhesions, para-adnexal—para-tubal or para-ovarian—cysts, the latter are the most common cause for fallopian tube torsion in the pediatric population [27–29].

The clinical picture is the same as for a complete AT but it may be more subtle. Imaging may show tubal changes, such as dilated thick-walled tube or a pseudomass between the uterus and the ovary, whereas the ovary appears normal (Fig. 24.4). Tubal dilatation can be global or segmental with an

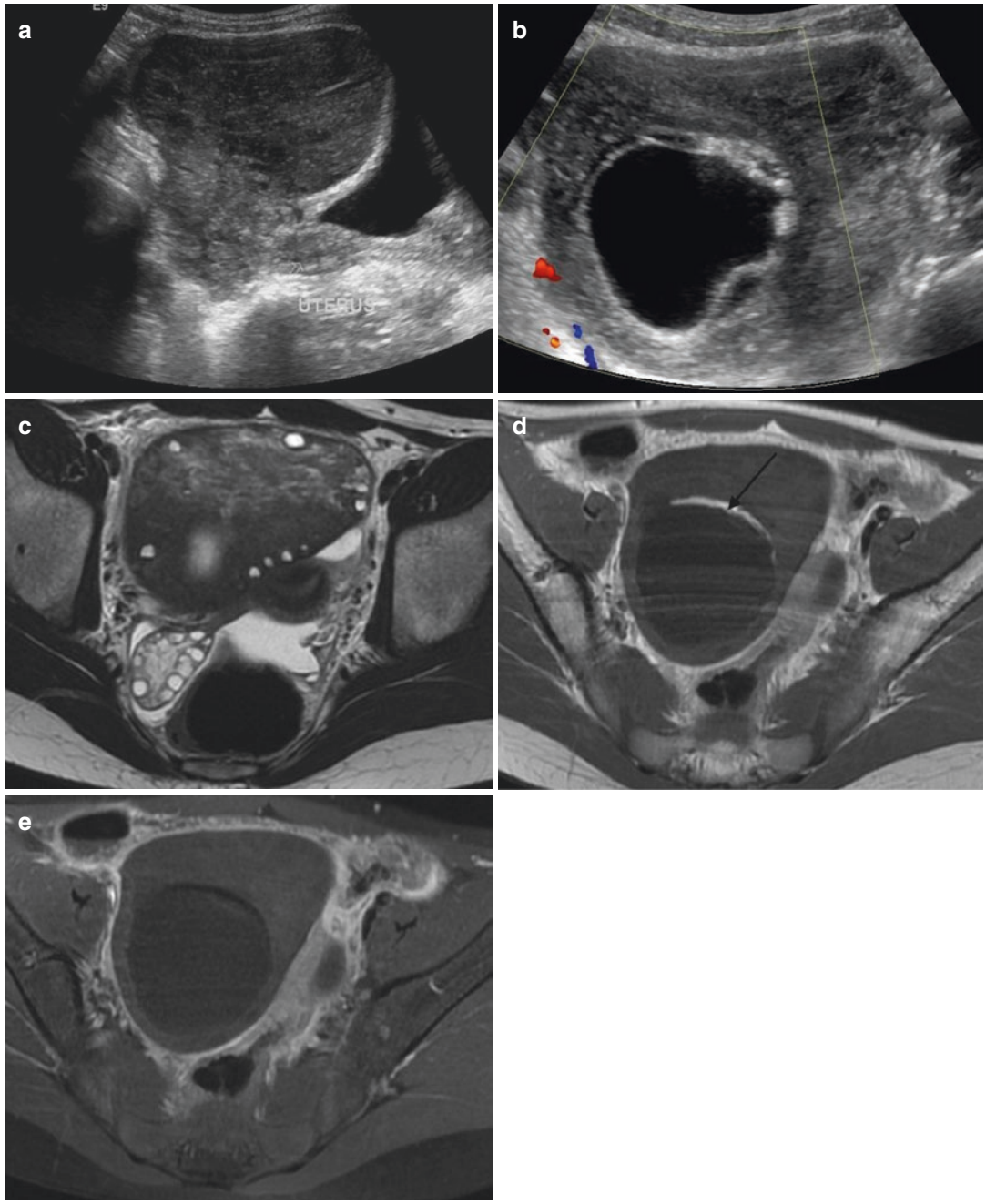

Fig. 24.3 Adnexal torsion in a 13 year-old girl with underlying benign cystic teratoma. (**a**) US Sagittal view: Large parauterine mass with follicles. (**b**) US Axial view: Central cystic component with a hyperechogenic crown. (**c**) MR imaging: Axial T2-Weighted sequence. Significant asymmetry of size of the ovaries and medialization of the left adnexa. Note the pelvic effusion and the displacement of the uterus off the midline. (**d**) MR imaging: Axial T1-Weighted post Gd. Lack of enhancement of the large twisted ovary with a central cystic area limited by a "fat component" (*arrow*) corresponding to a teratoma. (**e**) MR imaging: Axial T1-Weighted fat-saturated sequence. The fat component disappears confirming the diagnosis of teratoma

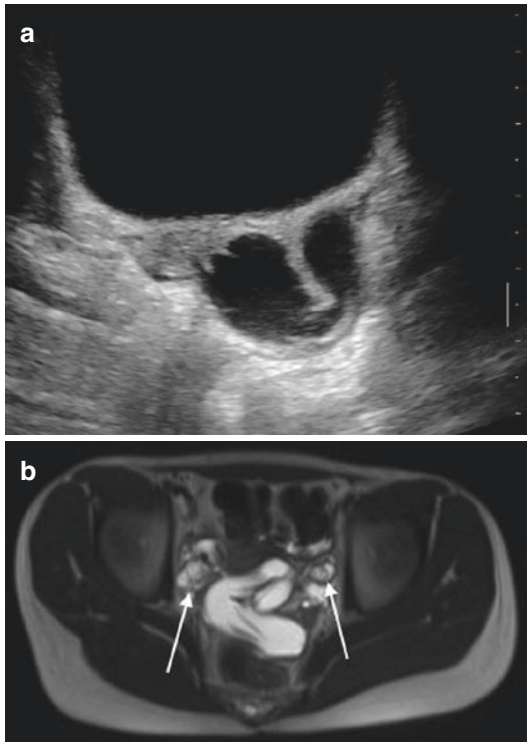

Fig. 24.4 Isolated left fallopian tube torsion in a 12 year-old girl, confirmed at laparoscopy. (**a**) US Axial view: Isolated tubal dilatation with presence of plicae tubariae ant thickening of tubal walls. (**b**) MR imaging: Axial T2-Weighted sequence. Two normal ovaries (*two arrows*) with isolated hydrosalpinx

appearance of a cyst. The visibility of plicae tubariae is useful and confirms the diagnosis of tubal dilatation. A paratubal or paraovarian mass is often associated as reported in the literature [30, 31]. The whirpool sign is difficult to detect.

MRI may be useful to establish the diagnosis. It is more specific when it is associated with hemorrhagic content in the fallopian tube, the whirlpool sign, lack of enhancement after contrast injection of the tube. MRI can also visualize an underlying mass like para tubal cyst [30, 31].

24.2.3.2 Recurrent or Asynchronous Adnexal Torsion

Asynchronous bilateral torsion is defined as torsion of both ovaries but at different periods; asynchronous torsion is rare, but can be devastating in terms of fertility especially if repeated oophorectomy has to be performed. The risk of recurrent ipsilateral or asynchronous contralateral AT is unknown, though estimated figures range from 2% to 5% [32] to as high as 10% in the absence of apparent ovarian disease [5]. It is likely that these patients have underlying anatomic variations that render them at increased risk of AT.

Though paratubal and paraovarian cysts are rare in adolescent females, the influence of postmenarchal hormonal stimulation on these tubal derivates could favor asynchronous AT [33].

24.2.3.3 Association with an Incarcerated Inguinal Hernia

The inclusion of an ovary in an inguinal hernia is "classic" and the diagnosis can be confirmed easily by US [34]. It is usually not painful; when uncomplicated, the treatment should not an emergent but a programmed surgery.

AT may occur within an indirect inguinal hernia that will become incarcerated. It occurs more often in pre-menarchal girls [13]. Merriman reviewed 71 cases of irreducible hernias in girls and report that 82% the hernias contained an ovary; 11 ovaries had twisted [35]. Very rarely the hernia may contain the fallopian tube and the uterus (Fig. 24.5). All these conditions require emergency treatment, usually surgery.

24.2.3.4 Context of Primary Hypothyroidism

Precocious puberty, large bilateral polycystic ovaries and premature menarche can develop in a context of severe hypothyroidism, facilitating a twist of the adnexa [36].

24.2.3.5 Uterine Torsion

Uterine torsion is considered exceedingly rare in children and very rare reports have been published. The diagnosis is rarely made preoperatively and necrosis of the uterus is a dramatic complication [37].

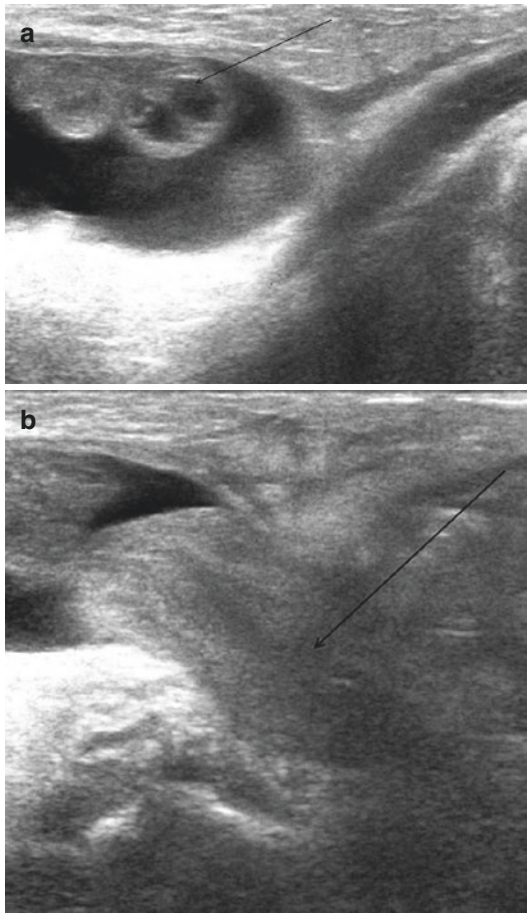

Fig. 24.5 Incarcerated ovary and uterus in an inguinal hernia. (**a**) US Axial view: Incarcerated ovary (*arrow*) with fluid in a inguinal hernia. (**b**) US Sagittal view: Uterus gets into the hernia (*arrow*)

24.2.4 Treatment

The exact duration of torsion that would lead to permanent ovarian necrosis is unknown. Surgery has to be performed as early as possible.

The question of a malignant tumor is rapidly raised when a mass is present. Surgery in emergency is mandatory to treat the torsion, but the tumor is not always removed at that time, allowing secondary biological and imaging work-up before deciding on the optimal treatment.

The best treatment of a confirmed AT is controversial. Over the past decade, multiple studies have demonstrated a partial preservation of ovarian function after a conservative approach, just untwisting the vascular pedicle; this even despite the necrotic appearance of the twisted ovary at surgery [38]. As the risk and clinical significance of secondary emboli is unproven and the risk of malignancy is low, ovarian conservation is currently the accepted management in girls with ovarian torsion.

Another debate is whether patients should undergo ovariopexy to prevent recurrent torsion. There are multiple case reports of adolescents with recurrent ipsilateral and contralateral torsion in normal-appearing ovaries that have been successfully treated via ovariopexy to the pelvic sidewall [39].

24.3 Hemorrhagic Cysts and Rupture of Functional Cysts

In the post-menarchal period, functional cysts are very common. There are two types of functional cysts: the follicular cyst and the luteal cyst. Both can get complicated by hemorrhage and rupture that can induce acute pain, most often in the second part of the cycle.

Noteworthy, a rupture or a hemorrhage of a functional cyst can be encountered in the perinatal period as well (see Chap. 5).

24.3.1 Physiopathology

A follicular cyst is the result from a dominant pre-ovulatory follicle whose size is increasing due to a continuous stimulation by gonadotropic hormones. The rate of discovery of "pure fluid containing cysts" on US examinations ranges between 13.7–20% [40, 41].

The corpus luteum operates like a cyclic physiological endocrine gland. Its normal size ranges between 15 and 25 mm. A cyst of the corpus luteum results from excessive intracystic bleeding. The US presentation of a corpus luteum and of a cyst of the corpus luteum is similar, only their size varies [42] (Fig. 24.6).

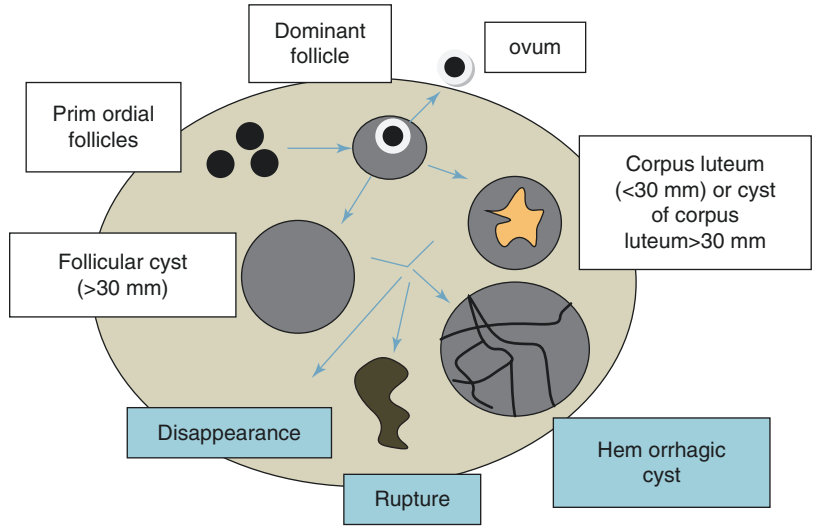

Fig. 24.6 Diagrammatic representation showing the relationship between the different physiological and pathological changes of the dominant follicle

24.3.2 Imaging

Functional cysts and their complications are clearly best imaged by US.

On US, a follicular cyst corresponds to an intra-ovarian unilocular cystic lesion larger than 3 cm but less than 8 cm diameter. This criterion of 3 cm allows to differentiate it from a simple physiological dominant follicle that would measure between 15 and 28 mm. The follicular cyst is usually anechoic containing pure fluid leading to posterior acoustic enhancement. The cyst wall is thin and can sometimes appear splitted due to the detachment of the granulosa cells layer. No atypical sign such as calcification or intracystic proliferation should be observed. A subtle vascularization of the wall of the cyst is typical of its functional character.

There is no absolute ultrasound criteria to differentiate an uncomplicated follicular cyst from some pure cystic ovarian tumors. Only US follow-up with a spontaneous regression of the cyst allows a retrospective confirmation of the functional nature of the cyst. A follicular cyst usually regresses spontaneously in 1–3 months. However, up to 35% of follicular cysts do persist ("persisting follicular cyst") over the 3 months period.

A cystic but heterogeneous structure measuring less than 25 mm, surrounded by a crown of peripheral hypervascularisation without internal vascularization is characteristic of a simple corpus luteum. It is unilocular and may present carved outlines. There is a typical peripheral vascularization [41]. A cyst of the corpus luteum is defined by a diameter larger than 30 mm with the same US characteristics.

Number of events may complicate the course of functional cysts: namely intracystic hemorrhage, cracking or breaking and AT; all conditions associated with acute abdominal pain. Intracystic bleeding may be responsible for the acute enlargement of these cysts with a very heterogeneous content. Multiple patterns exist; the most common being an aspect in so called "fishing net" corresponding to tracts of fibrin [43] (Figs. 24.7 and 24.8).

In cases of rupture, intraperitoneal effusion will appear usually limited to the pelvis but sometimes diffusing into the entire abdomen in case of vascular rupture. The cyst would then have disappeared or present a slumped appearance.

MR imaging can provide additional information in case of complex adnexal mass whenever there is a doubt on the presence of a solid tumoral component. MR imaging can also be more useful in evaluating atypical forms, especially in the absence of significant changes during follow-up ultrasound examinations.

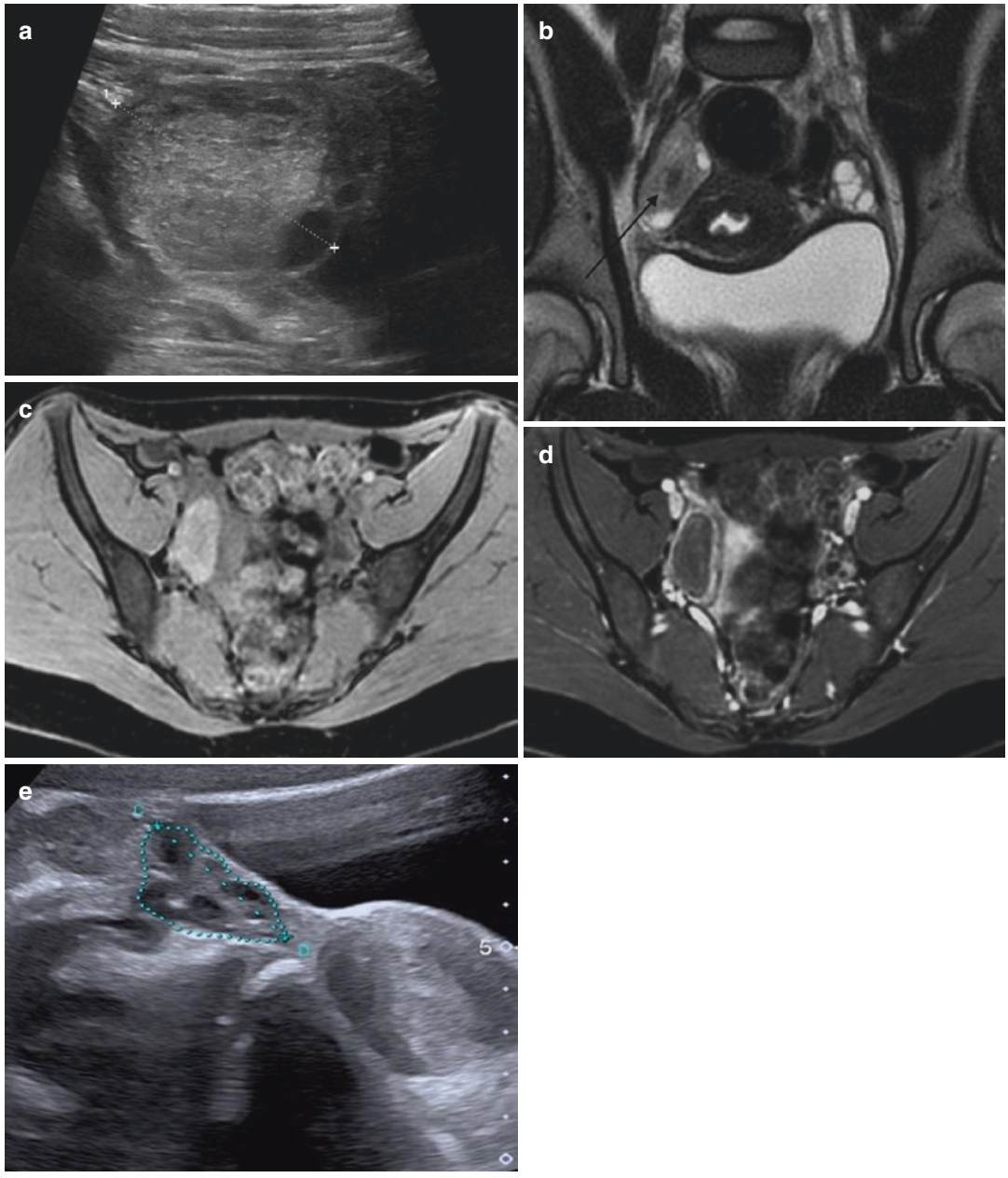

Fig. 24.7 Functional hemorrhagic cyst in a 14 year-old girl. (**a**) US Axial view: Hyperechoic cyst within the ovary. The echogenicity raises a doubt about a possible endometrioma justifying the realization of a MRI. (**b**) MR imaging: Coronal T2-Weighted sequence. Cyst with homogeneous high T2-W intensity (*arrow*). (**c**) MR imaging: Axial T1-Weighted fat-saturated sequence. Hypersignal of the cyst due to hemorrhagic content. (**d**) MR imaging: Sagittal T1-weighted fat-saturated post Gd sequence. Thin peripherical vascularization of the walls in connection with the functional character. (**e**) US Axial view: Normal size of the ovaries 3 months later

24.4 Hematocolpos

There are two circumstances beyond the neonatal period where a hematocolpos can be discovered:

- Painful primary amenorrhea without pubertal delay, frequently associated with a painful retention of the first menstruations
- Primary dysmenorrhea caused by the retention of menstruation in a one-eyed hemivagina in a context of uterine malformation

The role of imaging is to characterize the uterine malformation and its complications, to determine the optimal treatment and to check for associated urologic complications, which are present in 30–50% of cases. Other malformations can be discovered on this occasion like spinal or heart abnormalities [44].

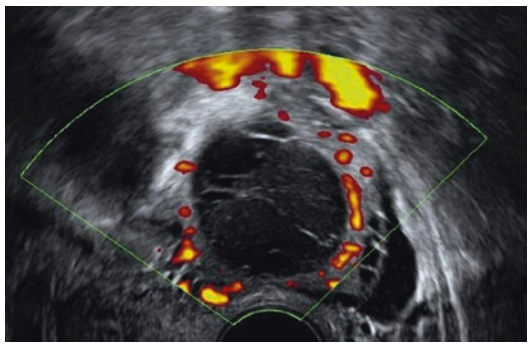

Fig. 24.8 Endocavitary US of a functional hemorrhagic cyst in a 16 year-old girl. Heterogeneus content resembling a "fishing net" with peripherical hypervacularization

24.4.1 Painful Primary Amenorrhea

24.4.1.1 Clinical Presentation

The incidence of "painful primary amenorrhea" is approximately 1/2000 young adolescents [45]. It is caused by a hymeneal imperforation in 90% of cases. More rarely, it results from a vaginal diaphragm or atresia [46].

Classical presentations include cyclic abdominal pain or presence of a pelvic mass corresponding to the retention of blood distending the obstructed vagina. The accumulated blood may compress the adjacent pelvic organs or vessels. Other atypical clinical presentations are possible such as back pain, constipation, urinary retention or urinary incontinence mimicking "cauda equina syndrome" [47, 48]. A dysuria or bilateral hydronephrosis is also possible. Finally, some cases of abscess and infection of the upper genital tract have been reported due to ascending infection in the colpos after spontaneous rupture of the hymen [49].

Surgery is the treatment of choice [46].

24.4.1.2 Imaging

Transabdominal US will show a centro-pelvic retrovesical collection with a fine echogenic content corresponding to the distended vagina with blood. The uterus can be seen on top of the collection (Fig. 24.9). The uterine cavity can be distended as well if a hematometria is associated. Peritoneal hematic effusion and a hematosalpynx are also possible.

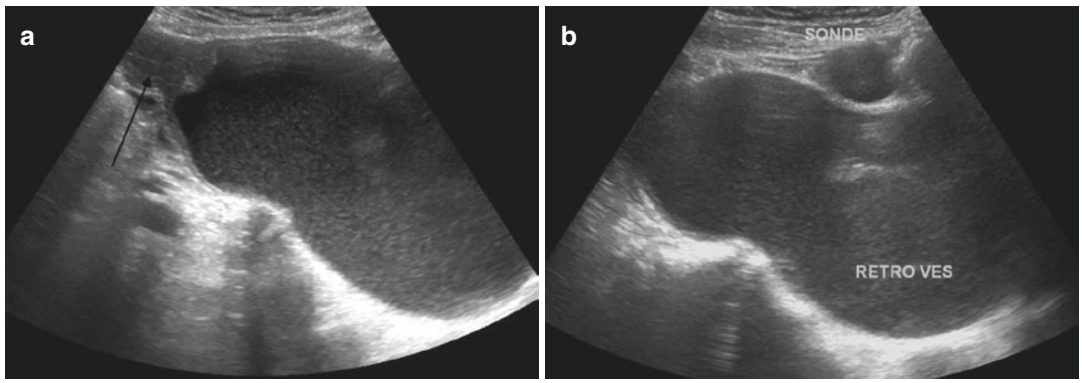

Fig. 24.9 Hematocolpos in a 13 year-old girl due to a hymeneal imperforation. Acute urinary retention. (**a**) US Sagittal view: Centro-pelvic retrovesical collection with a fine echogenic content. The uterus lies at the top of the collection (*arrow*). (**b**) US Axial view: Colpos behind the bladder

The aim of MR imaging will have to confirm the anomaly and to search for association with urogenital malformations (e.g. renal agenesis, multicystic dysplastic kidney) (Fig. 24.10).

24.4.2 Primary Dysmenorrhea Associated with Utero-Vaginal Malformations

24.4.2.1 Clinical Presentation

The association between dysmenorrhea and utero-vaginal malformations is classical and usually related to a bicornuate uterus with an one-eye hemi-uterus and hemi-vagina (Class U3 V2 or V3 in the ESHRE/ESGE classification) responsible of blood retention during menstruation; the menstruation from the other horn is normal and eliminated normally [50].

Müllerian malformations include a broad range of anomalies, resulting from the incomplete formation and/or differentiation of Müllerian ducts.

Bicornuate or didelphys (bicornuate and bicervix) uterus with obstructed hemivagina is the result of a lateral non-fusion of the Müllerian ducts with asymmetric obstruction (Fig. 24.11). These complete or incomplete forms correspond to 11% of uterine malformations.

Bicornuate uterus results from incomplete or partial fusion of the müllerian ducts. The duplicated endometrial cavity may be associated with cervix duplication (bicornuate bicollis) or without cervix duplication (bicornuate unicollis). If a longitudinal vaginal septum is also present (one-fourth of cases), a bicornuate bicollis uterus may be indistinguishable from a uterus didelphys. Uterus didelphys results from complete failure of müllerian duct fusion with duplication of the uterine horns, cervix, and proximal vagina.

Patients with hemivaginal obstruction can also present with dysmenorrhea secondary to endometriosis, infections, and pelvic adhesions attributed to retrograde menstrual flow from the obstructed side.

The obstructed unilateral vagina is an indication for vaginal septum resection.

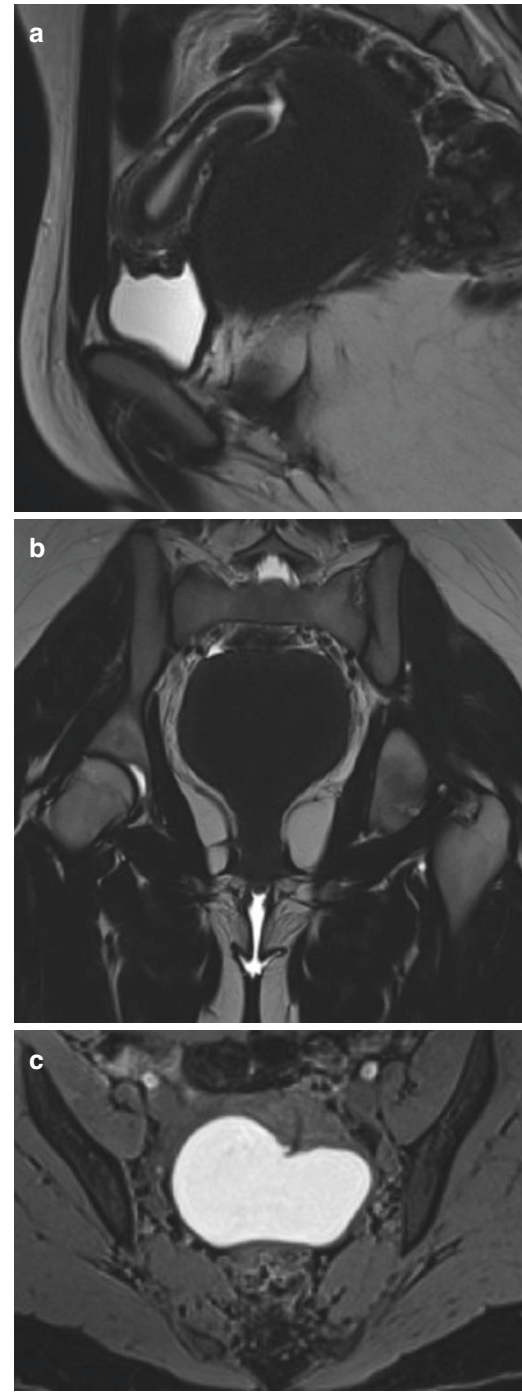

Fig. 24.10 Hematocolpos in a 14 year-old girl due to a lower vagina atresia. (**a**) MR imaging: Sagittal T2-Weighted sequence. Collection in the upper part of the vagina without retention associated in uterus. (**b**) MR imaging: Coronal T2-Weighted sequence. The colpos occupies the upper 2/3 of vagina. (**c**) MR imaging: Axial T1-weighted fat-saturated sequence. Hemorrhagic signal of the colpos

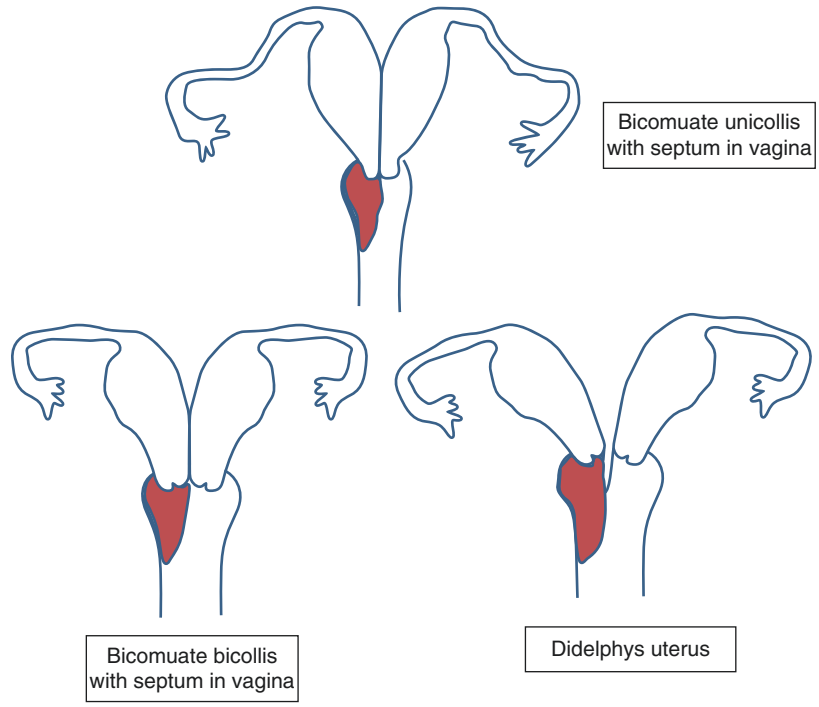

Fig. 24.11 Diagrammatic representation showing the different malformations responsible for colpos in case of primary dysmenorrhea

24.4.2.2 Imaging

The anatomy of the genital tract and the urinary tract must be analyzed in detail with the help of the different imaging modalities.

US Findings

The differentiation between uterus didelphys and bicornuate bicollis uterus is difficult on US. The common points are the presence of a uterine fundal cleft and a wide distance between the two horns. The best way to demonstrate the cleft is on a true coronal image oriented to the uterine fundus; this is easier to obtain on 3D US or on MR imaging. The two uterine cavities are noncommunicating. Visualization of the vaginal septum itself is difficult. Through the abdominal approach, a retro-vesical collection with fine echogenic content is seen. Through the vaginal approach (if possible), the probe can sometimes be introduced into the hemivagina along the hematocolpos if is not too large.

The obstructed uterine cavity can by distended by a hyperechogenic material corresponding to hematometria and the other will appear normal.

MR Imaging Findings (Fig. 24.12)

MR imaging is the modality of choice for the study of utero-vaginal anatomy [51], especially in virgin patients. The method should be performed after the acute event. As with US, MR imaging demonstrates two widely divergent uterine horns and two separate cervices. A fundal cleft greater than 1 cm has been reported to be 100% sensitive and specific as to the diagnosis of fusion anomalies (didelphys and bicornuate) [44]. Duplication or septation of the proximal vagina may be visualized at MR imaging in the coronal plane. The presence of a unilateral hemivaginal septum obstructing one of the uterine horns will cause that horn to be markedly distended from blood products, demonstrating high signal intensity at T1-weighted imaging.

Malformations of urinary tract like renal agenesis or like ectopic ureter are possible, typically at the same side of the vaginal obstruction. Noteworthy, diagnosing an obstructed vagina may be the opportunity to diagnose a Herlyn-Werner-Wunderlich syndrome (HWWS), which

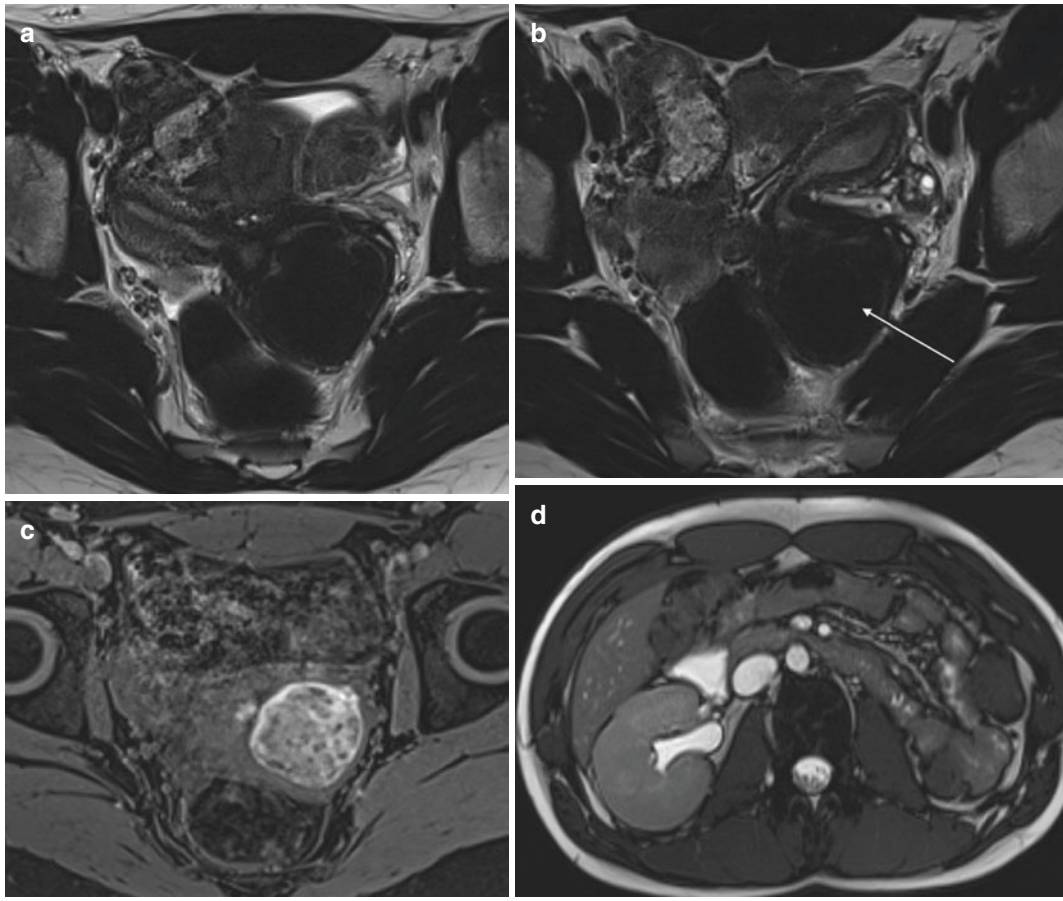

Fig. 24.12 Hematocolpos in a 14 year-old girl in context of primary dysmenorrhea. (**a**) MR imaging: Axial T2-Weighted sequence. Right hemi-cavity of a didelph uterus. (**b**) MR imaging: Axial T2-Weighted sequence. Left hemi-cavity of a dideplh uterus with blood retention in an obstructed hemivagina (*arrow*). (**c**) MR imaging: Axial T1-Weighted fat-saturated sequence. Hemorrhagic signal of the colpos. (**d**) MR imaging: Axial T2-Weighted Gradient Echo sequence. Left renal agenesis

is a rare malformation that includes uterus didelphys, obstructed hemivagina, and ipsilateral renal agenesis or severe dysplasia [52].

24.5 Endometriosis

24.5.1 Physiopathology

Endometriosis corresponds to the implantation of ectopic and functional endometrial tissue outside the uterine cavity. Based on the theory of reflux of menstruation, these findings are mainly encountered in the post-menarchal period. Endometriosis includes superficial peritoneal forms, adnexal forms (or endometrioma) and deep forms including adherences around the uterus and adnexa but also infiltrations of pelvic or extrapelvic organs.

Endometriosis is more likely to occur in adolescents who have a history of chronic pelvic pain or dysmenorrhea resistant to medical treatment. The exact prevalence of endometriosis among adolescents is unknown. Indeed, studies are difficult to finalize due to the biases of inclusion in adolescents with severe chronic pelvic pain, in which the surgery is rarely performed [53]. A recent report showed that among a group of patients with endometriosis (42,077 women

10–90 years); 0.05%, 1.93% and 6.1% of patients were in the 10–14, 15–19 and 20–24 year age groups respectively, suggesting that endometriosis is less likely to be diagnosed in girls under the age of 20 years [54]. Furthermore, it is estimated that the prevalence of endometriosis in adolescents ranges from 45% to 70% in those undergoing laparoscopy for chronic pelvic pain [55].

The main presentation of endometriosis in adolescents is ovarian endometriomas. Endometriosis is mostly discovered in early stages (I or II of American Society of Reproductive Medicine Stage) [56]. Endometriosis in teenagers is considered by most authors as a progressive disease; Chapron et al. have concluded that deep endometriosis occurring in adults has its roots in adolescence and that endometriosis that starts in teenage years will progress to deep infiltrating endometriosis at long term [57]. Risk factors for adolescent endometriosis include early menarche, positive familial history and obstructive malformation like Mullerian duct malformations resulting in increased retrograde menstruation [58].

24.5.1.1 Premenarchal Endometriosis

Some exceptional cases of endometrioma in premenarchal girls have been described [59, 60]. To explain these phenomena, focus has been put on genetic alterations or mutations that may start in utero and would affect Mullerian rests [61]. Furthermore, Bouquet de Jolinière et al. the presence of misplaced endometrial glands and embryonic duct remnants referring to the possible theory of involvement of Müllerian or Wolffian cell rests in the pathogenesis of endometriosis [62]. Recently, some authors formulated the hypothesis that perinatal uterine bleeding occurring in some newborns, which is routinely discounted as insignificant, may be a cause of pre-menarchal and adolescent endometriosis [63].

24.5.2 Clinical Signs and Acute Presentations

The most common symptoms in adolescent with endometriosis correspond to the classical association of dysmenorrhea and chronic pelvic pain, more likely to occur as non-cyclical pain, unlike for adult women [64]. Other symptoms include dyschezia, constipation, intestinal cramps, bladder pain and dyspareunia in sexually active teenagers.

Endometriosis is a common cause of school absenteeism [65]. The severity of the disease is not directly related to the degree of pain [66, 67]. More rarely endometriosis may be present by infection of the endometrioma or exceptionally as acute non gynecological symptoms like urinary tract obstruction or catamenial pneumothorax.

24.5.3 Imaging

The purpose of imaging will be to achieve a precise mapping of the lesions but also to search for associated uterine malformation that favor the development of early lesions. The most common presentation of endometriosis is the presence of endometriomas which correspond to adnexal location of endometriotic implants responsible for the development of hemorrhagic cysts. They are typically bilateral and multiple, features which strongly orient towards this diagnosis.

24.5.3.1 Ultrasound Findings

Transabdominal US examination must include not only the pelvis but the entire abdominal cavity as well as the kidneys.

The "typical" endometrioma is an unilocular cyst with homogeneous low-level echogenicity (ground glass echogenicity) of the cyst fluid [68]. Multilocular cyst contains no more than four loculles. The cyst can contain a papillary growth appearing like a parietal hyperechogenic spot but it should never present a detectable blood flow. When the endovaginal ultrasound exam is possible, more patients experience pain during the examination vs. those presenting other types of benign masses.

The typical locations of deep pelvic endometriosis are the torus uterinum, the utero-sacral ligaments, the rectovaginal septum, the vagina, the bladder and the rectosigmoid colon [69, 70]. When a location is very lateral in the parameter, the ureter can be occluded as well. Some cases of ureteral invasion by endometriosis have been described [71].

24.5.3.2 MR Imaging

MR imaging is the best noninvasive technique for assessing deep infiltrating endometriosis [72, 73]. Endometrioma presents a homogeneous

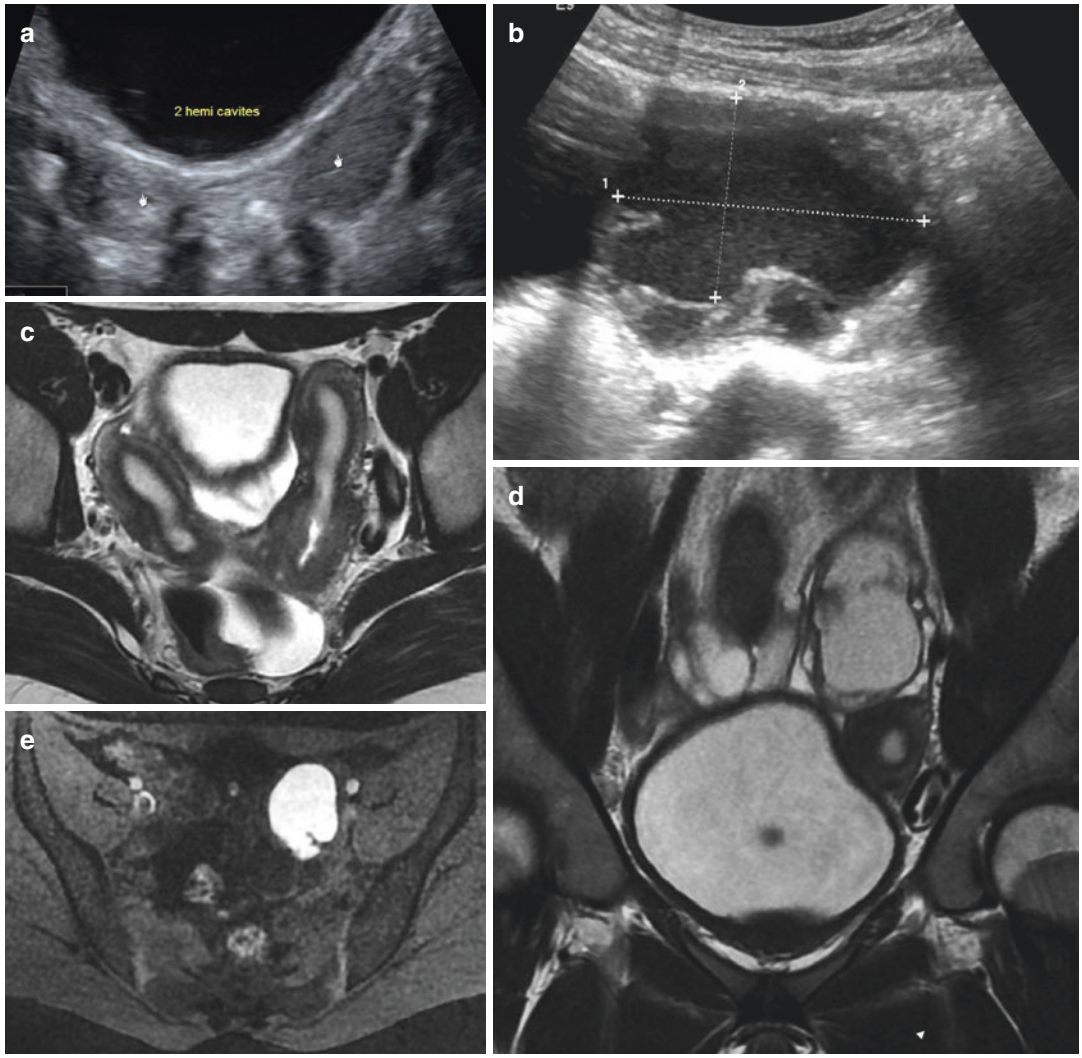

Fig. 24.13 Left endometrioma in a 15 year-old girl with didelphys uterus. (**a**) US Axial view: Two separate cavities behind the bladder (*heads of arrows*). (**b**) US Axial view: Unilocular cyst with homogeneous content (ground glass echogenicity) and polycyclic contours. (**c**) MR imaging: Axial T2-Weighted sequence. Uterus didelphys with complete separation of the uterine horns. (**d**) MR imaging: Coronal T2-Weighted sequence. Left ovarian cyst in relative hyposignal. (**e**) MR imaging: Axial T1-Weighted fat-saturated sequence. Homogeneous and intense hypersignal of the cyst

hyperintense T1-Weighted and a typical aspect of shading on T2-weighted without enhancement after injection (Fig. 24.13).

The diagnosis of deep infiltrating endometriosis is very rare and based on the combination of:

- Signal abnormalities [72]: hyperintense foci on T1-weighted or fat-suppression T1-weighted, corresponding to hemorrhagic foci and/or areas corresponding to fibrosis, hypointense on T2-weighted.
- Morphologic abnormalities. The organs can be displaced, reflecting the presence of adherences, typically like the medialization of the ovaries behind the uterus. All pelvic organs may be subject to thickening or to the presence of nodules with fibrous and/or hemorrhagic signal (Figs. 24.14 and 24.15).

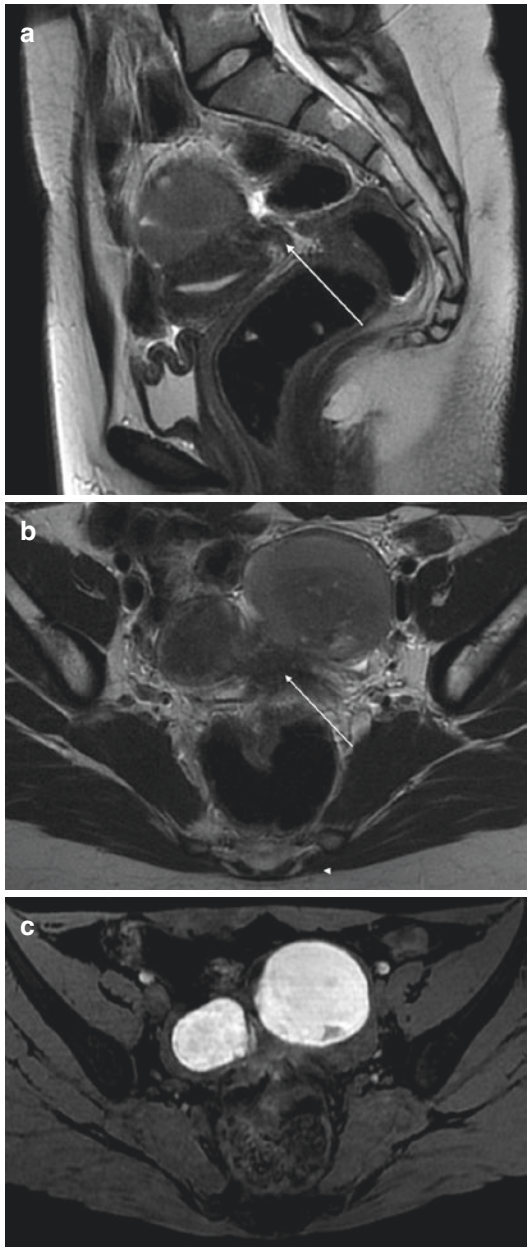

Fig. 24.14 Endometrioma and torus endometriosis in a 16 year-old girl. (**a**) MR imaging: Sagittal T2-Weighted sequence. Thickening of the torus (*arrow*) in hyposignal. (**b**) MR imaging: Axial T2-Weighted sequence. Thickening of the torus in hyposignal (*arrow*) and bilateral endometrioma in ovaries adjacent to posterior wall of the uterus. (**c**) MR imaging: Axial T1-weighted fat-saturated sequence. Homogeneous and intense hypersignal T1-W of the endometrioma

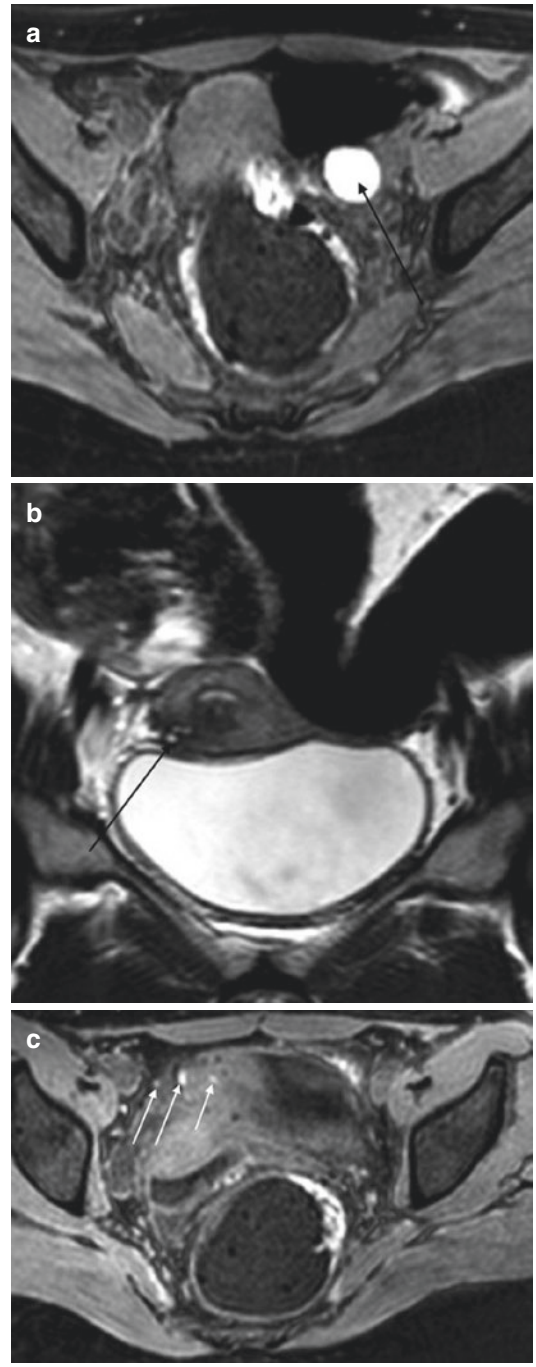

Fig. 24.15 Left endometrioma and bladder endometriosis in a 16 year-old girl. History of cyclical pain after resection of an one-eyed uterine horn. (**a**) MR imaging: Axial T1-Weighted fat-saturated sequence. Left ovarian cyst in homogeneous and intense hypersignal corresponding to an endometrioma (*arrow*). (**b**) MR imaging: Coronal T2-Weighted sequence. Thickening of the space between the uterus and bladder associated with hypersignal microcysts (*arrow*). (**c**) MR imaging: Axial T1-Weighted fat-saturated sequence. The hypersignal microcysts correpond to hemorrhagic foci (*arrows*)

Association with Mullerian Malformations

Although the exact cause of endometriosis is unknown, the theory of retrograde menstruation is supported by the finding of endometriosis in

females with obstructive genital tract anomalies [74, 75]. The major obstructive malformations are the hymen imperforation and the one-eyed hemivagina. However, the presence of endometrium in a rudimentary horn is an important finding and should be reported. Endometrial tissue in a non-communicating rudimentary horn can manifest clinically by pelvic pain caused by the increased prevalence of endometriosis due to retrograde flow of menses through the obstructed horn [76].

As mentioned above, Herlyn-Werner-Wunderlich syndrome (HWWS) is a rare malformation that involves uterus didelphys, obstructed hemivagina, and ipsilateral renal agenesis. Some authors have reported that patients with HWWS were more susceptible to pelvic endometriosis, and that all the ovarian endometriotic cysts were ipsilateral to the vaginal septum, which confirms the above mentioned hypothesis [77].

Patients suspected of having a Müllerian duct anomaly are often initially referred for pelvic ultrasonography. MR imaging provides additional information as to the demonstration of deep pelvic endometriosis. Both methods can be used to demonstrate associated urinary tract malformations (Fig. 24.13).

Atypical Location

In theory, endometriosis implant can settle anywhere in abdominal cavity and some exceptional case of juvenile catamenial pneumothorax have been described [78].

24.5.4 Treatment

Laparoscopy is still the gold standard for diagnosing endometriosis especially in those who have pelvic pain refractory to simple medical treatments.

24.6 Extra-Uterine Pregnancy

Abdominal pain is a common way to discover pregnancy in adolescents. The approach of the potential pregnant adolescent should be cautious. The presence of a third party chosen by the patient is desirable to provide psychological support. Although transvaginal ultrasound is possible, abdominal way should be performed first. In addition, the possibility of sexual abuse must be kept in mind and a careful questioning must be carried out. Once diagnosed, a multidisciplinary management is mandatory. This is beyond the scope of the chapter.

Extra uterine pregnancy (EUP), although rare, should be imperatively considered in any post-menarchal patient with acute pelvic pain even among young post-menarchal girls and a serum chorionic gonadotrophin level measurement should be obtained. A negative serum β- human chorionic gonadotropin (βHCG) result excludes the diagnosis of a living pregnancy.

A rapid diagnosis of EUP is essential because of the risk of important bleeding inside and outside the tube. EUP would occur in 0.5% of pregnancies in adolescent girls as compared with 1.5% of adults pregnancies [79].

The differential diagnosis as for any other pregnancy who presents with pain and bleeding in the first trimester includes normal early pregnancy, spontaneous abortion, missed abortion, molar pregnancy and ectopic pregnancy [80].

24.6.1 Physiopathology—Clinical Signs

The most common location of ectopic pregnancy is the fallopian tube, 75–80% in the ampullary portion, 10–20% in the isthmic portion, 2% in the interstitial portion or in the corneal region (Fig. 24.16). The primary goal of ultrasound is not to determine the exact location, but to identify a pregnancy outside the uterus.

The classic risk factors are rarely found in adolescents.

The classic triad of pain, bleeding and adnexal mass is present in about 45% of patients [80]. Even when the triad is present, a normal early pregnancy may still be the cause of symptoms.

24.6.2 Imaging

EUP is an US diagnosis that can be achieved through the abdominal approach but more easily by the intravaginal access. The sensitivity and specificity of transvaginal ultrasonography to

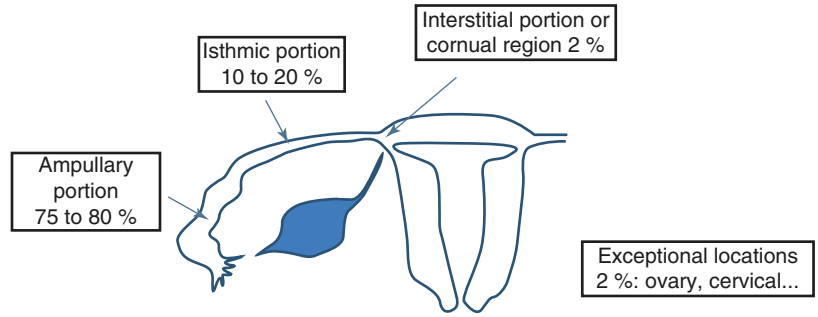

Fig. 24.16 Distribution of the different location of ectopic pregnancy

detect EUP are 90.9% and 99.9%, with positive and negative predictive values of 93.5% and 99.8%, respectively [81]. A positive β-hCG leads to the subsequent question: "Is there a gestational sac and where is it located?".

An intrauterine gestational sac should be seen by intravaginal sonography when the β-HCG level is greater than 1500 mIU/ml or by transabdominal sonography when the β-HCG level is greater than 2500 mIU/ml [82].

24.6.2.1 Directs Signs

The diagnosis can be ascertained when a *gestational sac with an embryonic pole or yolk sac* is identified outside the uterus, but this sign is found in only 10–20% of cases [80, 82, 83] (Fig. 24.17). Cardiac activity can be seen. However, more often, a *complex adnexal mass* separated from the ovary and his corpus luteum is visualized; it corresponds to a mix between a hematosalpinx and hyperechoic ring around the gestational sac. The Doppler signal around the ectopic sac corresponds to the reactional hypervascularization of the tubal walls.

24.6.2.2 Indirect Signs

- The absence of intrauterine gestational sac, is a major criteria and is contrasting with the *endometrial thickening*.
- In the adnexa, the most common findings is the *corpus luteum* which is a normal structure in pregnancy and which is located in the same side of the ectopic pregnancy in 85% of cases [84].
- *Free fluid and hemoperitoneum*.
- Ectopic pregnancies are often associated with a *intrauterine pseudo-sac* that can mimic a small gestational sac

In 15–20% of EUP, no sonographic sign will be visible at the first exam therefore, in case of

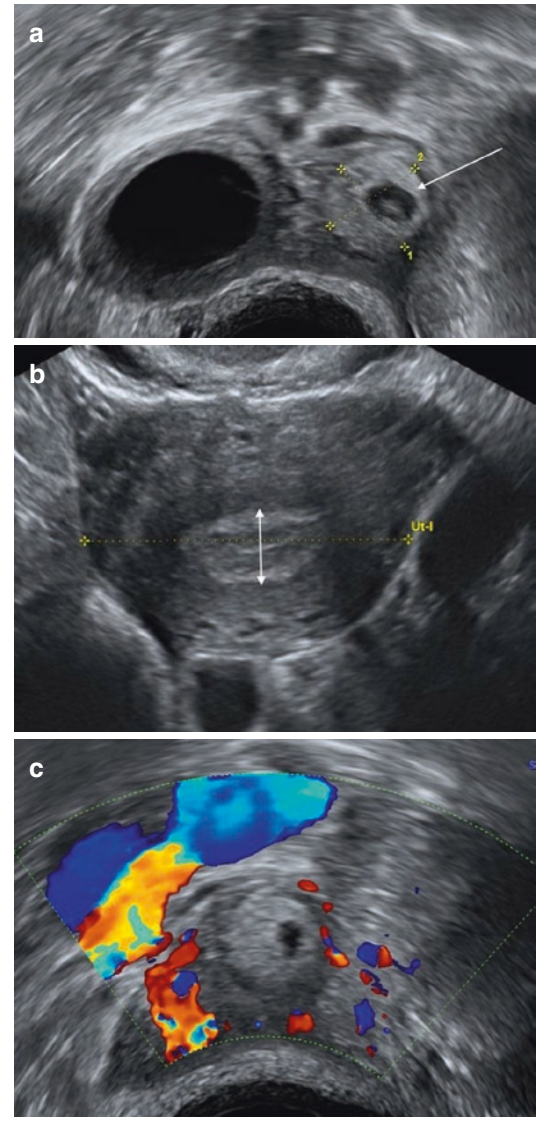

Fig. 24.17 Ectopic pregnancy in a 15 year-old girl. Endocavitary US. (**a**) US Axial view: Complex adnexal mass (*arrow*) separate from the ovary that contains a corpus luteum. Hyperechoic crown around the gestational sac. (**b**) US Axial view: Vacuity of uterine cavity which contrasts with an endometrial thickening. (**c**) Energy Doppler US: Reactional hypervacularization around the mass

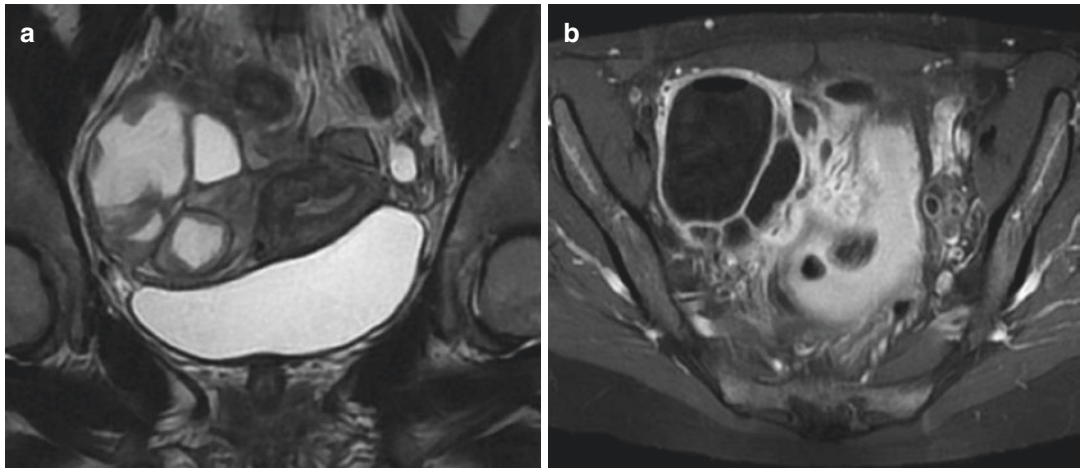

Fig. 24.18 Right tubo-ovarian abscess in a 18 year-old girl with Crohn disease. (**a**) MR imaging: Coronal T2-Weighted sequence. Tubo-ovarian abscess in contact with a terminal ileitis. (**b**) MR imaging: Axial T1-Weighted post-Gd fat-saturated sequence. Complex collections with thickened walls enhanced after the injection of a contrast

clinical doubt, the examination should be repeated 48–72 h after, unless real emergency situation [82].

MR imaging imaging has little indication for this diagnosis and should be reserved for unusual locations like pregnancy in a rudimentary horn, or angular development for example.

24.6.3 Treatment

The treatment can be medical or surgical depending on:

- Clinical signs
- Size of the gestational sac and hematosalpinx
- Presence of a hematoperineum
- Value of the β-HCG

24.7 Pelvic Inflammatory Disease

In young girls and teenagers, the differential diagnosis of acute abdominal pain along with fever, peritoneal signs and leukocytosis should include acute appendicitis, ovarian pathology, and pelvic inflammatory disease.

Salpingitis or inflammatory diseases of the pelvis in pre-pubertal and non-sexually active adolescents are rare since their main etiology is infection and germs ascending through sexual relations [85]. On the other hand, infection is possible by contiguity to a pelvic inflammatory digestive pathology. The main US finding is an adnexal mass with fluid, which is not specific.

Classically, tubo-ovarian abscess and pyosalpinx appear on imaging as complex collections with thick walls enhancing on CE-CT or MR imaging. This is eventually associated with inflammatory changes to adjacent bowel loops in case of IBD (inflammatory bowel disease) and pelvic effusion [86] (Fig. 24.18) (see also Chap. 12).

CT and MR imaging allow an overall assessment often required in pre-surgical evaluation. CT can also exclude appendicitis which is more common in this age group.

Conclusion

In young girls and adolescents, gynecologic diseases should always be kept in mind among the differential diagnosis of acute abdominal pain. Adnexal torsion should be considered first whatever the age of the patient. Adnexal torsion may occur with a completely normal ovary or will be associated with a benign tumor.

Ultrasound using the suprapubic approach is sufficient to achieve the diagnosis. MR imaging can be helpful in more complex situations, still its use should not delay treatment.

References

1. Servaes S, Zurakowski D, Laufer MR, Feins N, Chow JS. Sonographic findings of ovarian torsion in children. Pediatr Radiol. 2007;37(5):446–51.
2. Focseneanu MA, Omurtag K, Ratts VS, Merritt DF. The auto-amputated adnexa: a review of findings in a pediatric population. J Pediatr Adolesc Gynecol. 2013;26(6):305–13.
3. Ashwal E, Krissi H, Hiersch L, Less S, Eitan R, Peled Y. Presentation, diagnosis, and treatment of ovarian torsion in premenarchal girls. J Pediatr Adolesc Gynecol. 2015;28(6):526–9.
4. Beaunoyer M, Chapdelaine J, Bouchard S, Ouimet A. Asynchronous bilateral ovarian torsion. J Pediatr Surg. 2004;39(5):746–9.
5. Kokoska ER, Keller MS, Weber TR. Acute ovarian torsion in children. Am J Surg. 2000;180(6):462–5.
6. Cass DL, Hawkins E, Brandt ML, Chintagumpala M, Bloss RS, Milewicz AL, et al. Surgery for ovarian masses in infants, children, and adolescents: 102 consecutive patients treated in a 15-year period. J Pediatr Surg. 2001;36(5):693–9.
7. Aziz D, Davis V, Allen L, Langer JC. Ovarian torsion in children: is oophorectomy necessary? J Pediatr Surg. 2004;39(5):750–3.
8. Wang J-H, Wu D-H, Jin H, Wu Y-Z. Predominant etiology of adnexal torsion and ovarian outcome after detorsion in premenarchal girls. Eur J Pediatr Surg. 2010;20(5):298–301.
9. Rossi BV, Ference EH, Zurakowski D, Scholz S, Feins NR, Chow JS, et al. The clinical presentation and surgical management of adnexal torsion in the pediatric and adolescent population. J Pediatr Adolesc Gynecol. 2012;25(2):109–13.
10. Templeman C, Hertweck SP, Fallat ME. The clinical course of unresected ovarian torsion. J Pediatr Surg. 2000;35(9):1385–7.
11. Albayram F, Hamper UM. Ovarian and adnexal torsion: spectrum of sonographic findings with pathologic correlation. J Ultrasound Med. 2001;20(10): 1083–9.
12. Appelbaum H, Abraham C, Choi-Rosen J, Ackerman M. Key clinical predictors in the early diagnosis of adnexal torsion in children. J Pediatr Adolesc Gynecol. 2013;26(3):167–70.
13. Ashwal E, Hiersch L, Krissi H, Eitan R, Less S, Wiznitzer A, et al. Characteristics and management of ovarian torsion in premenarchal compared with postmenarchal patients. Obstet Gynecol. 2015; 126(3):514–20.
14. Duigenan S, Oliva E, Lee SI. Ovarian torsion: diagnostic features on CT and MRI with pathologic correlation. AJR Am J Roentgenol. 2012;198(2): W122–31.
15. Oltmann SC, Fischer A, Barber R, Huang R, Hicks B, Garcia N. Cannot exclude torsion--a 15-year review. J Pediatr Surg. 2009;44(6):1212–6. discussion 1217
16. Stark JE, Siegel MJ. Ovarian torsion in prepubertal and pubertal girls: sonographic findings. AJR Am J Roentgenol. 1994;163(6):1479–82.
17. Chang HC, Bhatt S, Dogra VS. Pearls and pitfalls in diagnosis of ovarian torsion. Radiographics. 2008;28(5):1355–68.
18. Lee EJ, Kwon HC, Joo HJ, Suh JH, Fleischer AC. Diagnosis of ovarian torsion with color Doppler sonography: depiction of twisted vascular pedicle. J Ultrasound Med. 1998;17(2):83–9.
19. Ngo A-V, Otjen JP, Parisi MT, Ferguson MR, Otto RK, Stanescu AL. Pediatric ovarian torsion: a pictorial review. Pediatr Radiol. 2015;45(12):1845–55.
20. Harmon JC, Binkovitz LA, Stephens J. Uterine position in adnexal torsion: specificity and sensitivity of ipsilateral deviation of the uterus. Pediatr Radiol. 2009;39(4):354–8.
21. Descargues G, Tinlot-Mauger F, Gravier A, Lemoine JP, Marpeau L. Adnexal torsion: a report on forty-five cases. Eur J Obstet Gynecol Reprod Biol. 2001;98(1):91–6.
22. Peña JE, Ufberg D, Cooney N, Denis AL. Usefulness of Doppler sonography in the diagnosis of ovarian torsion. Fertil Steril. 2000;73(5):1047–50.
23. Sasaki KJ, Miller CE. Adnexal torsion: review of the literature. J Minim Invasive Gynecol. 2014;21(2):196–202.
24. Naiditch JA, Barsness KA. The positive and negative predictive value of transabdominal color Doppler ultrasound for diagnosing ovarian torsion in pediatric patients. J Pediatr Surg. 2013;48(6):1283–7.
25. Fleischer AC, Stein SM, Cullinan JA, Warner MA. Color Doppler sonography of adnexal torsion. J Ultrasound Med. 1995;14(7):523–8.
26. Yoffe N, Bronshtein M, Brandes J, Blumenfeld Z. Hemorrhagic ovarian cyst detection by transvaginal sonography: the great imitator. Gynecol Endocrinol. 1991;5(2):123–9.
27. Harmon JC, Binkovitz LA, Binkovitz LE. Isolated fallopian tube torsion: sonographic and CT features. Pediatr Radiol. 2008;38(2):175–9.
28. Huchon C, Fauconnier A. Adnexal torsion: a literature review. Eur J Obstet Gynecol Reprod Biol. 2010;150(1):8–12.
29. Provansal M, Courbière B, Estrade J-P, Agostini A, Gamerre M. Isolated tubal torsion: about three cases. Gynecol Obstet Fertil. 2008;36(2):173–5.
30. Ormasa MCO, Hamouda ESM, Jung J. Isolated fallopian tube torsion with fimbrial cyst in a 10 year-old girl diagnosed by ultrasound: a case report. J Radiol Case Rep. 2015;9(12):29–36.
31. Sakuragi M, Kido A, Himoto Y, Onishi Y, Togashi K. MRI findings of isolated tubal torsions: case series of 12 patients: MRI findings suggesting isolated tubal torsions, correlating with surgical findings. Clin Imaging. 2017;41:28–32.
32. Celik A, Ergün O, Aldemir H, Ozcan C, Ozok G, Erdener A, et al. Long-term results of conservative management of adnexal torsion in children. J Pediatr Surg. 2005;40(4):704–8.

33. Thakore SS, Chun MJ, Fitzpatrick K. Recurrent ovarian torsion due to paratubal cysts in an adolescent female. J Pediatr Adolesc Gynecol. 2012;25(4):e85–7.
34. Hyun PM, Jung AY, Lee Y, Yang I, Yang DH, Hwang J-Y. CT and US findings of ovarian torsion within an incarcerated inguinal hernia. Emerg Radiol. 2015;22(1):91–4.
35. Merriman TE, Auldist AW. Ovarian torsion in inguinal hernias. Pediatr Surg Int. 2000;16(5–6):383–5.
36. Nandi-Munshi D, Tridgell A, Taplin CE. Acute ovarian torsion and primary hypothyroidism. Pediatrics. 2013;132(1):e233–8.
37. Grover S, Sharma Y, Mittal S. Uterine torsion: a missed diagnosis in young girls? J Pediatr Adolesc Gynecol. 2009;22(1):e5–8.
38. Oelsner G, Shashar D. Adnexal torsion. Clin Obstet Gynecol. 2006;49(3):459–63.
39. Dolgin SE, Lublin M, Shlasko E. Maximizing ovarian salvage when treating idiopathic adnexal torsion. J Pediatr Surg. 2000;35(4):624–6.
40. Ekerhovd E, Wienerroith H, Staudach A, Granberg S. Preoperative assessment of unilocular adnexal cysts by transvaginal ultrasonography: a comparison between ultrasonographic morphologic imaging and histopathologic diagnosis. Am J Obstet Gynecol. 2001;184(2):48–54.
41. Pascual MA, Hereter L, Tresserra F, Carreras O, Ubeda A, Dexeus S. Transvaginal sonographic appearance of functional ovarian cysts. Hum Reprod. 1997;12(6):1246–9.
42. Bazot M, Dechoux-Vodovar S, Morel A, Jarboui L, Thomassin-Naggara I. Ovaires: variations physiologiques et pathologies fonctionelles. EMC - Radiologie et imagerie médicale - section urogenital gynecol obstet 2014;9(4):1.
43. Okai T, Kobayashi K, Ryo E, Kagawa H, Kozuma S, Taketani Y. Transvaginal sonographic appearance of hemorrhagic functional ovarian cysts and their spontaneous regression. Int J Gynaecol Obstet. 1994;44(1):47–52.
44. Behr SC, Courtier JL, Qayyum A. Imaging of müllerian duct anomalies. Radiographics. 2012;32(6):E233–50.
45. Sakalkale R, Samarakkody U. Familial occurrence of imperforate hymen. J Pediatr Adolesc Gynecol. 2005;18(6):427–9.
46. Makris GM, Macchiella D, Vaidakis D, Chrelias C, Battista MJ, Siristatidis C. Abdominal tumor in a 14-year-old adolescent: imperforate hymen, resulting in hematocolpos-a case report and review of the literature. Case Rep Obstet Gynecol. 2015;2015:429740.
47. Gyimadu A, Sayal B, Guven S, Gunalp GS. Hematocolpos causing severe urinary retention in an adolescent girl with imperforate hymen: an uncommon presentation. Arch Gynecol Obstet. 2009;280(3):461–3.
48. Löllgen RM, Sabo J, Mettler A, Liniger B, Berger S. Unique presentation of hematometrocolpos mimicking cauda equina syndrome: severe back pain and urinary incontinence in an adolescent girl. J Emerg Med. 2016;51(2):e19–23.
49. Ho JW, Angstetra D, Loong R, Fleming T. Tuboovarian abscess as primary presentation for imperforate hymen. Case Rep Obstet Gynecol. 2014;2014:142039.
50. Grimbizis GF, Gordts S, Di Spiezio SA, Brucker S, De Angelis C, Gergolet M, et al. The ESHRE/ESGE consensus on the classification of female genital tract congenital anomalies. Hum Reprod. 2013;28(8):2032–44.
51. Troiano RN, McCarthy SM. Mullerian duct anomalies: imaging and clinical issues. Radiology. 2004;233(1):19–34.
52. Hall-Craggs MA, Williams CE, Pattison SH, Kirkham AP, Creighton SM. Mayer-Rokitansky-Kuster-Hauser syndrome: diagnosis with MR imaging. Radiology. 2013;269(3):787–92.
53. Sarıdoğan E. Adolescent endometriosis. Eur J Obstet Gynecol Reprod Biol. 2016;209:46–9.
54. Haas D, Chvatal R, Reichert B, Renner S, Shebl O, Binder H, et al. Endometriosis: a premenopausal disease? Age pattern in 42,079 patients with endometriosis. Arch Gynecol Obstet. 2012;286(3):667–70.
55. Vicino M, Parazzini F, Cipriani S, Frontino G. Endometriosis in young women: the experience of GISE. J Pediatr Adolesc Gynecol. 2010;23(4):223–5.
56. Janssen EB, Rijkers ACM, Hoppenbrouwers K, Meuleman C, D'Hooghe TM. Prevalence of endometriosis diagnosed by laparoscopy in adolescents with dysmenorrhea or chronic pelvic pain: a systematic review. Hum Reprod Update. 2013;19(5):570–82.
57. Chapron C, Lafay-Pillet M-C, Monceau E, Borghese B, Ngô C, Souza C, et al. Questioning patients about their adolescent history can identify markers associated with deep infiltrating endometriosis. Fertil Steril. 2011;95(3):877–81.
58. Ragab A, Shams M, Badawy A, Alsammani MA. Prevalence of endometriosis among adolescent school girls with severe dysmenorrhea: a cross sectional prospective study. Int J Health Sci. 2015;9(3):273–81.
59. Gogacz M, Sarzyński M, Napierała R, Sierocińska-Sawa J, Semczuk A. Ovarian endometrioma in an 11-year-old girl before menarche: a case study with literature review. J Pediatr Adolesc Gynecol. 2012;25(1):e5–7.
60. Ebert AD, Fuhr N, David M, Schneppel L, Papadopoulos T. Histological confirmation of endometriosis in a 9-year-old girl suffering from unexplained cyclic pelvic pain since her eighth year of life. Gynecol Obstet Investig. 2009;67(3):158–61.
61. Gargett CE, Schwab KE, Brosens JJ, Puttemans P, Benagiano G, Brosens I. Potential role of endometrial stem/progenitor cells in the pathogenesis of early-onset endometriosis. Mol Hum Reprod. 2014;20(7):591–8.

62. Bouquet de Jolinière J, Ayoubi JM, Lesec G, Validire P, Goguin A, Gianaroli L, et al. Identification of displaced endometrial glands and embryonic duct remnants in female fetal reproductive tract: possible pathogenetic role in endometriotic and pelvic neoplastic processes. Front Physiol. 2012;3:444.
63. Brosens I, Benagiano G. Is neonatal uterine bleeding involved in the pathogenesis of endometriosis as a source of stem cells? Fertil Steril. 2013;100(3):622–3.
64. Audebert A, Lecointre L, Afors K, Koch A, Wattiez A, Akladios C. Adolescent endometriosis: report of a series of 55 cases with a focus on clinical presentation and long-term issues. J Minim Invasive Gynecol. 2015;22(5):834–40.
65. Abbas S, Ihle P, Köster I, Schubert I. Prevalence and incidence of diagnosed endometriosis and risk of endometriosis in patients with endometriosis-related symptoms: findings from a statutory health insurance-based cohort in Germany. Eur J Obstet Gynecol Reprod Biol. 2012;160(1):79–83.
66. Dun EC, Kho KA, Morozov VV, Kearney S, Zurawin JL, Nezhat CH. Endometriosis in adolescents. J Soc Laparoendosc Surg. 2015;19(2):e2015.00019.
67. Gordts S, Puttemans P, Gordts S, Brosens I. Ovarian endometrioma in the adolescent: a plea for early-stage diagnosis and full surgical treatment. Gynecol Surg. 2015;12(1):21–30.
68. Van Holsbeke C, Van Calster B, Guerriero S, Savelli L, Paladini D, Lissoni AA, et al. Endometriomas: their ultrasound characteristics. Ultrasound Obstet Gynecol. 2010;35(6):730–40.
69. Bazot M, Thomassin I, Hourani R, Cortez A, Darai E. Diagnostic accuracy of transvaginal sonography for deep pelvic endometriosis. Ultrasound Obstet Gynecol. 2004;24(2):180–5.
70. Bazot M, Lafont C, Rouzier R, Roseau G, Thomassin-Naggara I, Daraï E. Diagnostic accuracy of physical examination, transvaginal sonography, rectal endoscopic sonography, and magnetic resonance imaging to diagnose deep infiltrating endometriosis. Fertil Steril. 2009;92(6):1825–33.
71. Lakhi N, Dun EC, Nezhat CH. Hematoureter due to endometriosis. Fertil Steril. 2014;101(6):e37.
72. Bazot M, Darai E, Hourani R, Thomassin I, Cortez A, Uzan S, et al. Deep pelvic endometriosis: MR imaging for diagnosis and prediction of extension of disease. Radiology. 2004;232(2):379–89.
73. Kinkel K, Chapron C, Balleyguier C, Fritel X, Dubuisson JB, Moreau JF. Magnetic resonance imaging characteristics of deep endometriosis. Hum Reprod. 1999;14(4):1080–6.
74. Silveira SA, Laufer MR. Persistence of endometriosis after correction of an obstructed reproductive tract anomaly. J Pediatr Adolesc Gynecol. 2013;26(4):e93–4.
75. Brosens I, Gargett CE, Guo S-W, Puttemans P, Gordts S, Brosens JJ, et al. Origins and progression of adolescent endometriosis. Reprod Sci. 2016;23:1282.
76. Uğur M, Turan C, Mungan T, Kuşçu E, Senöz S, Ağiş HT, et al. Endometriosis in association with müllerian anomalies. Gynecol Obstet Investig. 1995;40(4):261–4.
77. Tong J, Zhu L, Chen N, Lang J. Endometriosis in association with Herlyn-Werner-Wunderlich syndrome. Fertil Steril. 2014;102(3):790–4.
78. Inoue T, Chida M, Inaba H, Tamura M, Kobayashi S, Sado T. Juvenile catamenial pneumothorax: institutional report and review. J Cardiothorac Surg. 2015;10:83.
79. Ammerman S, Shafer MA, Snyder D. Ectopic pregnancy in adolescents: a clinical review for pediatricians. J Pediatr. 1990;117(5):677–86.
80. Levine D. Ectopic pregnancy. Radiology. 2007;245(2):385–97.
81. Condous G, Okaro E, Khalid A, Lu C, Van Huffel S, Timmerman D, et al. The accuracy of transvaginal ultrasonography for the diagnosis of ectopic pregnancy prior to surgery. Hum Reprod. 2005;20(5):1404–9.
82. Ardaens Y, Bouyer J, Madelenat P. Prise en charge de la grossesse extrautérine. Recommandations pour la pratique clinique. du CNGOF. 2003.
83. Perriera L, Reeves MF. Ultrasound criteria for diagnosis of early pregnancy failure and ectopic pregnancy. Semin Reprod Med. 2008;26(5):373–82.
84. Bonde AA, Korngold EK, Foster BR, Fung AW, Sohaey R, Pettersson DR, et al. Radiological appearances of corpus luteum cysts and their imaging mimics. Abdom Radiol (NY). 2016;41:2270.
85. Kielly M, Jamieson MA. Pelvic inflammatory disease in virginal adolescent females without tubo-ovarian abscess. J Pediatr Adolesc Gynecol. 2014;27(1):5–7.
86. Kim MY, Rha SE, Oh SN, Jung SE, Lee YJ, Kim YS, et al. MR imaging findings of hydrosalpinx: a comprehensive review. Radiographics. 2009;29(2):495–507.

Part VI

Any Age: General Overviews

Abdominal Trauma

25

Kathia Chaumoitre and Philippe Petit

Contents

25.1 Introduction

25.1.1 Epidemiology

Injury is the number 1 killer of children younger than 18 years [1]. Abdominal trauma occurs in up to 8% of children and abdominal injury is responsible for 9% of all post-traumatic deaths [2].

The vast majority of abdominal trauma in children are blunt trauma (more than 90%) with falls and motor vehicle collisions as main circumstances.

The mechanism of trauma is similar to adults with some physiologic differences. Children have smaller blood vessels and high vasoconstrictive response that make non-operative management possible in the vast majority of cases.

25.1.2 Biomechanics, Pediatric Specificities

The increased mobility of solid intraabdominal organs combined with a weaker abdominal wall are specific to pediatric patients.

K. Chaumoitre (✉)
Department of Pediatric Imaging, Hopital Nord, Chemin des Bourrellys, Marseille 13015, France
e-mail: kathia.chaumoitre@ap-hm.fr

P. Petit
Department of Pediatric Radiology, Timone Enfants, 264 rue St Pierre, 13385 Marseille Cedex 05, France

F.E. Avni, P. Petit (eds.), *Imaging Acute Abdomen in Children*,
https://doi.org/10.1007/978-3-319-63700-6_25

In children, the belts (scapular and pelvic) and the rib cage are poorly developed. Adiposity is low and its distribution differs from that of adults. The musculature of the abdominal wall is poorly developed as well. All these elements explain the low absorption of energy with direct impacts on the abdominal organs (liver, spleen, kidneys). On the other hand, the plasticity of the pelvic belt explains the low rate of pelvic fractures in children. The organs most frequently injured are the spleen, the liver, the kidneys, and the pancreas. All together they combine the great majority of the lesions. The other sites represent less than 1% of the lesions each with, in order of frequency, the small intestine, duodenum, colon, stomach and root of the mesentery [3].

The clinical examination for abdominal trauma in children may be misleading. The management is less standardized than in adults and will vary according to the habits of the emergency center in which the patient will be received [4]. The treatment of abdominal trauma is mainly conservative.

The abdomen is involved in 25% of cases of multiple trauma in children. Multiple trauma is mainly due to road accidents or falls.

The criteria for the severity of trauma in children are as follows [5]:

- Falls
  - >10 feet or two to three times the height of the child
- High-risk auto crash
  - intrusion, including roof: >12 inch occupant site; >18 inch any site
- Ejection (partial or complete) from automobile
  - death in same passenger compartment
- Vehicle telemetry data consistent with a high risk for injury;
  - automobile versus pedestrian/bicyclist thrown, run over, or with significant (>20 mph) impact; or
- Motorcycle crash >20 mph

In addition to severe trauma, which is usually managed in specialized centers, isolated abdominal trauma is very frequent, mostly mild. The etiologies are varied, often related to the practice of sport or outdoor activities (horseback riding, bicycling…). Their management is less codified and can be done in centers without wide experience in pediatric care with the risk of a maximalist management with systematic CE-CT (while US should be the first—and last—step in a mild trauma without signs of severity (no hemodynamic consequences)).

In case of blunt trauma, children considered to be at low risk of serious injury can be distinguished by the following clinical criteria [6, 7]:

- No evidence of abdominal wall trauma or seat belt sign
- Glasgow Coma Scale score > 13
- No abdominal tenderness
- No evidence of thoracic wall trauma
- No complaints of abdominal pain
- No decreased breath sounds
- No history of vomiting after the injury

25.2 Imaging

In children, due to reduced blood volume, even minor abdominal trauma, is susceptible to sudden hemodynamic decompensation. The placement of a venous line before any imaging exploration is therefore advised. Hemodynamic monitoring will be performed in case of hemodynamic instability or multiple trauma.

25.2.1 Plain Films

In case of isolated abdominal trauma, in a conscious child, no radiography is recommended. In case of multiple trauma or severe abdominal trauma with hemodynamic instability, a A-P chest X-ray and a A-P pelvis X-ray should be performed as soon as the patient is admitted, especially in older children that may be traumatized with high energy in a public road accident (2 wheels, pedestrians) or in case of falls of high height.

Compared to adults, in case of blunt abdominal trauma, associated pneumothorax is rarer in

children, especially because of the plasticity of the ribs that may distort but without fracturing.

25.2.2 US

25.2.2.1 US + Doppler: The First Step

Ultrasound is the first-line examination for abdominal trauma. Its efficiency for the diagnosis of a hemoperitoneum is well known but, even with an experienced operator, traumatic visceral lesions may be underestimated (compared with CE-CT). The trauma-induced parenchymal abnormalities are more difficult to see if the initial US is performed very early after the trauma. This is due to the initial isoechoic or slightly hyperechoic appearance of the parenchymal tears and hematoma.

In case of isolated abdominal trauma in a stable child, US + Doppler should be as complete as possible as it will probably be the only examination performed. There should be an analysis of the echotexture and vascularization of all the solid organs using a convex probe first and a linear probe thereafter. An analysis of the bowel wall is mandatory to search for a thickening or a hematoma in relation with the area the impact. It will also be necessary to observe any sign case of infiltration of the mesenteries or of the peritoneal fat. Apart from the search for a hemoperitoneum in all the usual recesses (Morrison space, parieto-colic gutters, pouch of Douglas…), it will also be necessary to look for a pneumoperitoneum specifically in all superficial area, including above the left hepatic lobe within the ligamentum teres or in the perisplenic space (Fig. 25.1).

Peritoneal effusion in various amounts and echogenicities may be observed after abdominal trauma; still isolated peritoneal effusion of low abundance may be physiological (found in one abdominal US out of 5 without any trauma). In case of trauma, it will also be necessary to look for associated pleural and/or a pericardial effusion. The negative predictive value of a complete abdominal US is excellent and US can be the only examination performed if it is normal with a reassuring clinical examination and a monitoring of 12–24 h [8].

Conversely, if the complete abdominal US is abnormal or if an optimal evaluation is not possible due to the child's movements or instability, this first examination will be completed by a CE-CT.

In case of severe trauma or multiple trauma, US will be performed at the patient's bed in the crash room (FAST echo) and will be limited to the rapid search for effusions (hemoperitoneum, hemothorax, hemopericardium) before the CE-CT.

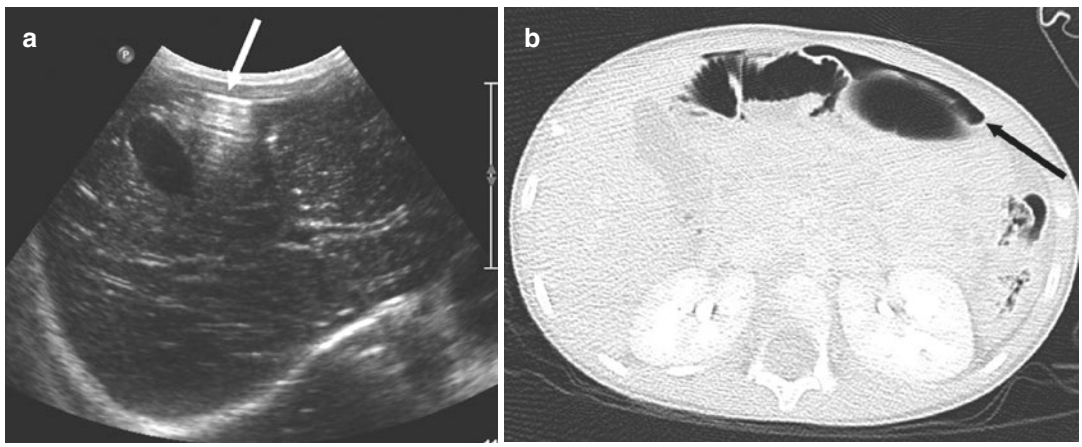

Fig. 25.1 Four year old girl, Pedestrian hit by a car. (**a**) US transverse scan: pneumoperitoneum above the liver (*white arrow*). (**b**) CT with contrast: pneumoperitoneum confirmed (*black arrow*). Left colic perforation was found at surgery

25.2.2.2 Is there a Place for Contrast-Enhanced US (CEUS)?

Because of concern over medical ionizing radiation exposure of children, contrast-enhanced ultrasound (CEUS) has generated recent interest as an ionizing radiation-free alternative to CT or MR imaging. CEUS has received approval for pediatric hepatic use but remains off-label for a range of other applications especially abdominal trauma [9].

The safety and the tolerability of this contrast agent have been well demonstrated in adults and a recent retrospective analysis in children concludes that pediatric CEUS is a safe and potentially cost-effective imaging modality [10].

In the context of abdominal trauma, the child has often already a venous line which simplifies the use of CEUS routinely. Experienced teams estimate that CEUS in isolated abdominal trauma of low energy can replace CE-CT as an initial examination when it is normal [11]. The addition of contrast would be a significant improvement to visualize lacerations, hematomas as well as possible vascular lesions (false aneurysms) and may avoid control CE-CT.

Apart from the acute phase, CEUS could also be used in the follow-up of traumatic lesions diagnosed by CE-CT. Currently the follow up is widely based on US-Doppler.

As long as these products do not have an administrative authorization for their use in abdominal trauma, it is necessary to have a written parental consent before their use. Another point that can slow the use of these products is their cost.

25.2.3 CE-CT

25.2.3.1 Still Mandatory

At the CT suite, the child has to be accompanied by an emergency physician or a senior pediatric intensivist or at least a pediatrician and a peripheral venous line must have been placed. Since the hemodynamics of a child are potentially very unstable, it is essential that the child has pulse and blood pressure monitoring. Installing on the scanner table is a crucial time. It is necessary to move the child with precaution, remove from the field of exploration all the metallic structures to avoid artifacts (ECG cables, electrodes…) (Fig. 25.2). The scan protocol should be chosen according to the weight of the child and the severity of the trauma (whole bodyscan, abdominal or thoracoabdominal acquisition).

A negative CT has a strong negative predictive value allowing a very early return home or even no hospitalization [12]. However, the impact of

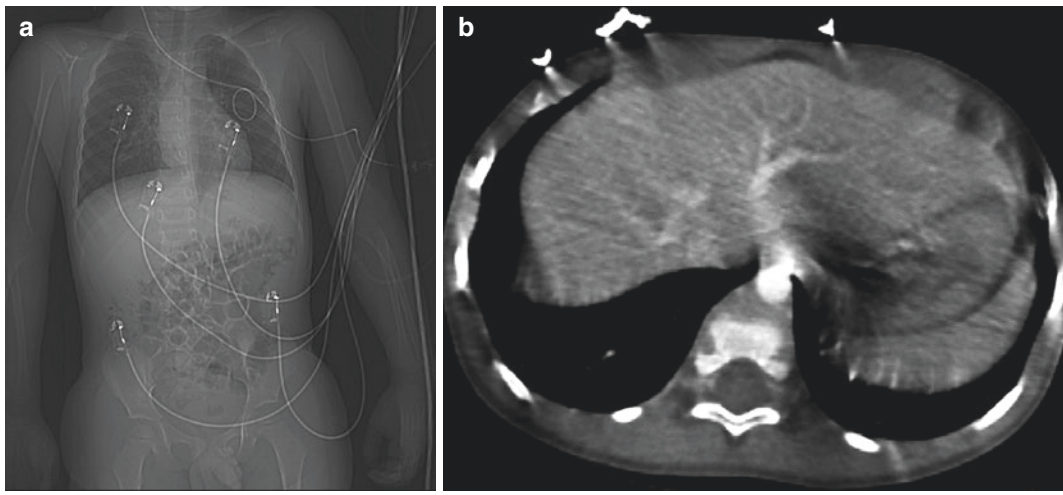

Fig. 25.2 Four year old girl. (**a**) Scout view: incorrect placement on CT table. (**b**) CT with contrast: liver and abdominal wall artefacts due to the multiple metallic cables on the field of view

CT on the management is not always linked to the clinical status, but overall this examination allows a precise initial assessment of solid organs lesions as well as a conservative treatment. To be noted, the performance of CT for the detection off bowel and/or mesenteric lesions is lower than for solid organs.

Not uncommonly, children are transferred from a non-specialized pediatric center after an initial CE-CT. It is important to review these CT preferably by pediatric radiologists; this second interpretation can find discrepancies in more than 10% of cases including lesions not described or an increase in the severity of lesions [13].

25.2.3.2 Protocols to Optimize Quality with a ALARA Dose

It is of upmost importance that the pediatric exploration protocols remain recorded in the CT and can easily be adapted to the child's weight in order to remain in the recommended doses:

- Until 10 kg: CTDIvol (mGy): 4 (±2)
- From 10 to 20 kg: CTDIvol (mGy): 5 (±3)
- From 20 to 35 kg: CTDIvol (mGy): 6 (±3)

Regarding the amount of iodine contrast media:

- Until 25 kg: 2 cc iodine contrast media/kg
- From 25 to 50 kg: 1.5 cc iodine contrast media/kg
- Beyond 50 kg: adult amount

Oral contrast is not useful, characteristics for detecting intra-abdominal injury are similar between CE-CT with and without oral contrast [14].

Injection Protocols

In adult patients suspected of having multiple trauma, it has been demonstrated that an unhanced abdomino-pelvic acquisition in addition to acquisition with contrast injection does not improve detection of traumatic lesions of the liver, spleen, kidneys or adrenal glands, nor the detection of intra- or retroperitoneal effusion; it does increase the dose [15]. In children, this issue is still controversial without consensus; still, it seems logical to limit the exposure to ionizing radiation by proposing an abdominal exploration directly with contrast media.

In children under 25 kg, the circulatory flow is rapid and an acquisition after injection with a start at 50 s after the start of the injection renders possible to have a good quality mixed arterial and venous phase.

In older child, in particular in the case of severe trauma, an arterial phase followed by a venous phase can be considered. It is also possible to carry out a protocol with multiphase injections: injecting one third of the iodine quantity and then waiting 30 s before injecting the remaining two thirds of iodinated contrast agent and start the acquisition 30 s after the beginning of the second injection. This renders possible to obtain on the same helix a good arterial and venous acquisition and to perform an abdominal CT with reasonable radiation doses.

In case of renal lesion or pelvic fracture, a further delayed acquisition (excretory phase) is recommended (5 min after IV injection). The goal is to search for urinoma (calices, pelvis or ureteral rupture) and/or bladder leakage. This should be performed with a low-dose protocol. Indeed, a clear decrease of the KV and the mAs is possible while keeping a good visualization of the iodine contrast in the urinary tract.

CE-CT of a traumatized child requires rules of good practice with precautions to avoid unnecessary radiation exposure or uninterpretable examination due to technical errors.

The current speed of scanners has dramatically reduced the need for sedation.

25.2.4 MR Imaging

25.2.4.1 Useful for the Follow-Up

MR imaging is very useful for monitoring abdominal trauma due to its performance and lack of ionizing radiation. It will surely have indications for the follow up of severe trauma (liver, spleen, kidneys) instead of CE-CT, in children who are old enough to avoid sedation (Fig. 25.3). In case of kidney trauma, MR urography will be performed allowing both the morphological and

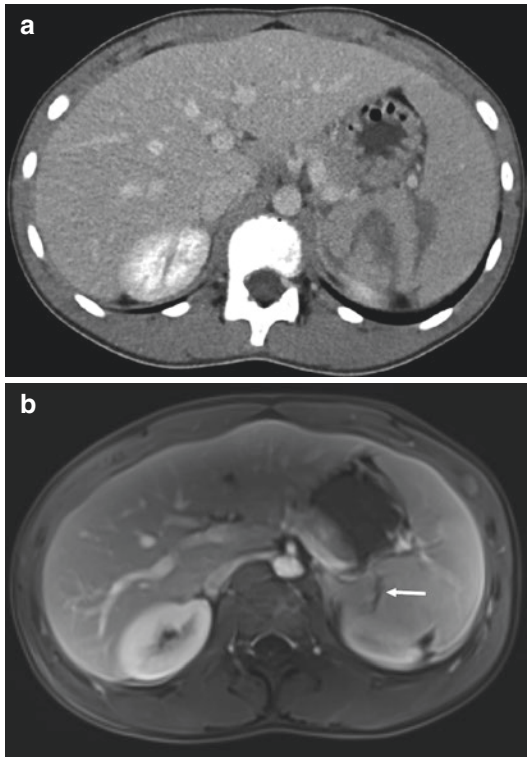

Fig. 25.3 Fourteen year old boy. (**a**) CT with contrast: Grade III splenic trauma. (**b**) MR with contrast: Long term follow-up by MRI to avoid ionizing radiation with rapid gradient echo T1 weighted sequence with gadolinium a linear parenchymal sequelae (*white arrow*)

split renal function assessment [16]. MR cholangio-pancreatography is useful in some acute or delayed complications of liver or pancreatic trauma, in order to demonstrate bile duct injuries and estimate the origin of "collections" (bilomas or pancreatic cysts).

25.2.4.2 Instead of CT in the Future?

The use of MR imaging as first step for acute trauma is still limited because of the length of the examination, the need for child cooperation or sedation, and the difficulty to explore the whole body in case of severe trauma unlike CE-CT.

Despite all these limitations, the development of rapid abdominal sequences of about 10 s makes it possible to use MR imaging as a first-line exploration in the next future in addition to ultrasound, avoiding ionizing radiation.

25.3 Liver and Biliary Tract Trauma

Liver and biliary tract trauma occur essentially secondary to blunt trauma with mechanisms of deceleration or contusion. They are encountered in 10–30% of these patients. In more than 70% of patients, the lesions induced do not provoke symptoms and can be managed conservatively.

25.3.1 Diagnosis

Imaging aspects of liver trauma are the same in children as for adults. The initial diagnosis is made on CE-CT. It will depict accurately any hepatic laceration appearing as a hypodense area, with variable shapes. When the laceration reaches the capsular surface and breaks the capsule, there is an associated hemoperitoneum (Fig. 25.4). Subcapsular hematoma typically compresses the lateral margin of the hepatic parenchyma. The demonstration of active bleeding will influence the prognosis and has to be searched actively [17].

Conservative treatment is possible thanks to close follow-up by US with Doppler looking for acute or delayed vascular or biliary complications. AAST classification of liver injury is presented in Table 25.1.

25.3.2 Evolution

Vascular or biliary complications are present in about 10% of cases.

Vascular complications include hemorrhage, hemobilia, arteriovenous fistula and pseudo-aneurysm, portal vein thrombosis, portal vein stenosis, Budd Chiari. They usually occur around day 15 and may progress asymptomatically or become complicated (hemorrhagic shock or portal hypertension). Their diagnosis is based on US with Doppler and CE-CT. Their treatment is conservative with the possibility of an endovascular treatment.

Biliary complications include fistulas, bilhemia, biloma, bilioperitoneum and stenosis of the biliary tract. The bilomas are present in 2–12% of hepatic trauma and their frequency increases with the severity of the trauma. Their

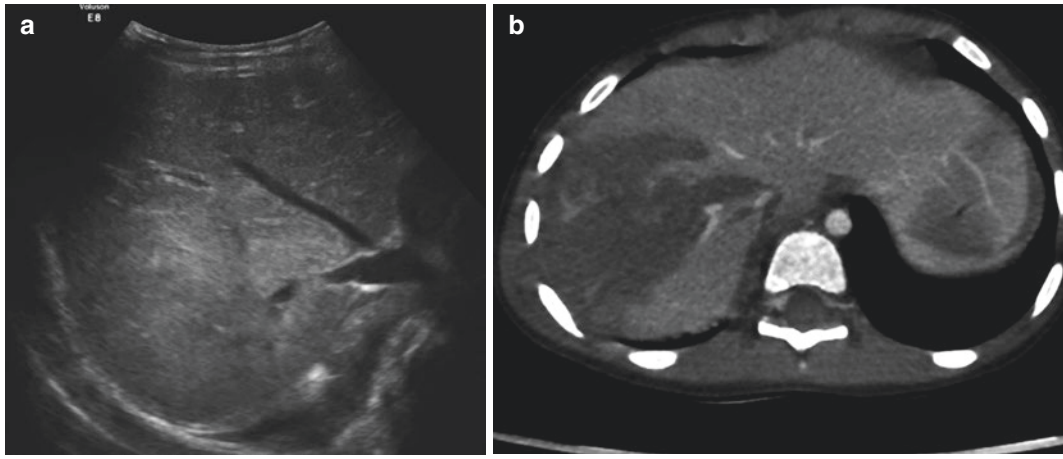

Fig. 25.4 Five year old girl. Auto crash. (**a**) US transverse scan: Initial US only shows heterogeneous right liver lobe. (**b**) CT with contrast: CE-CT shows grade IV liver lesion

Table 25.1 AAST classification of liver injury (N.b. advance one grade for multiple injuries up to grade III)

Grade I	Hematoma: subcapsular, <10% surface area Laceration: capsular tear, <1 cm parenchymal depth
Grade II	Hematoma: subcapsular, 10–50% surface area Hematoma: intraparenchymal <10 cm diameter Laceration: capsular tear 1–3 cm parenchymal depth, <10 cm length
Grade III	Hematoma: subcapsular, >50% surface area of ruptured subcapsular or parenchymal hematoma Hematoma: intraparenchymal >10 cm or expanding Laceration: capsular tear >3 cm parenchymal depth
Grade IV	Laceration: parenchymal disruption involving 25–75% hepatic lobe or involves 1–3 Couinaud segments
Grade V	Laceration: parenchymal disruption involving >75% of hepatic lobe or involves >3 Couinaud segments (within one lobe) Vascular: juxtahepatic venous injuries (retrohepatic vena cava/central major hepatic veins)
Grade VI	Vascular: hepatic artery avulsion

discovery is delayed from day 15 to sometimes several years after the trauma and this is the first diagnosis to be evoked in case of any post-traumatic collection (Fig. 25.5). Spontaneous regression is usual for small bilomas (<3 cm); in case of persisting collection, percutaneous puncture, drainage or endoscopic surgery can be performed. The bilomas can become infected and also favor the development of pseudo-aneurysms. Bilio-peritoneum should be considered whenever an intraperitoneal effusion with stable hemoglobin is demonstrated. It conveys an infectious risk. The management by peritoneal drain and biliary prosthesis (endoscopically) is based on the "stent and drain" concept, which achieves satisfactory results in 90% of cases [18, 19]. Biliary stenosis is exceptional. It is secondary to direct trauma or traumatic pancreatitis. It exposes to the risk of cirrhosis. Diagnosis is based on US, MR cholangiography and endoscopic retrograde cholangiopancreatography (ERCP) (Fig. 25.5). It may be treated by drainage, balloon dilation and endoprosthesis.

25.4 Splenic Trauma

In children, the spleen is one of the organs most frequently affected by abdominal trauma (about 20% of splenic involvement). The mean age is 10 years and the M/F sex ratio is 2/1. The spleen is the most vascularized organ of the body [17].

Because of the plasticity of the pediatric rib cage, rib fractures are rare, and severe parenchymal injuries may be present in the absence of rib fracture. The child's splenic capsule is stronger than that of an adult. Splenic traumas are isolated in 50% of cases and their treatment is conservative in more than 95% of cases.

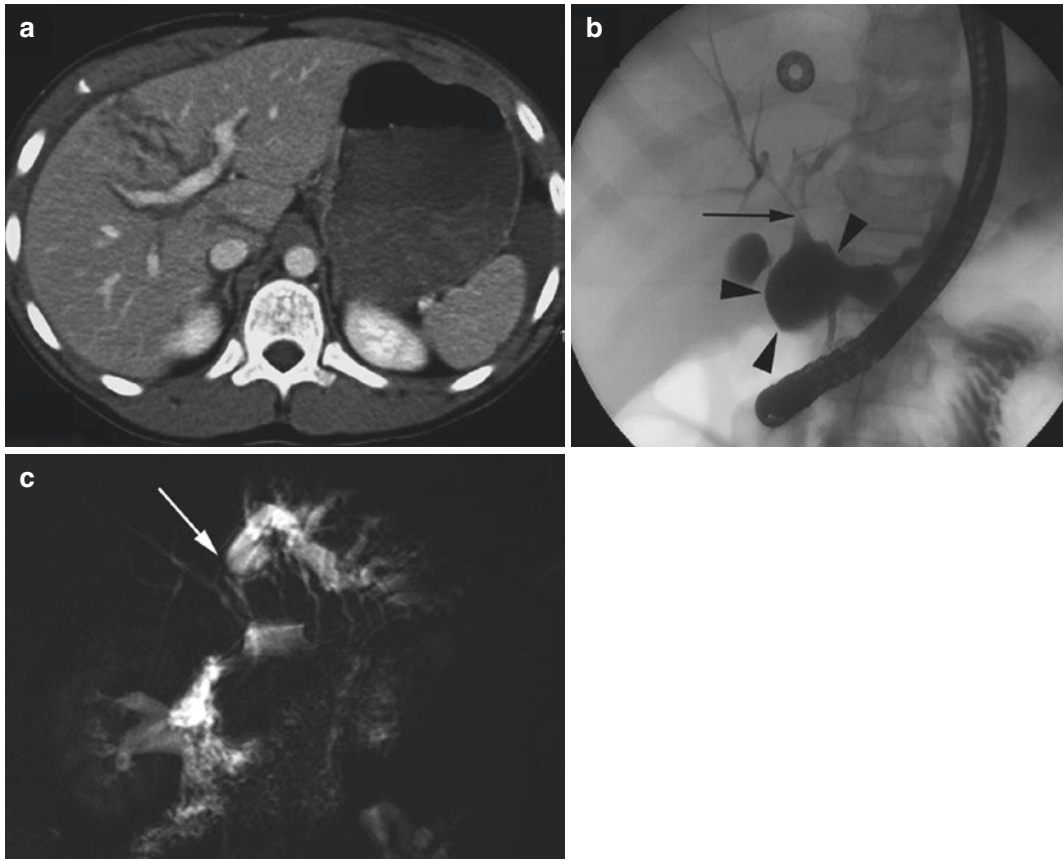

Fig. 25.5 Thirteen year old boy, Auto crash. (**a**) Initial CT with contrast: liver fracture (grade III) against portal bifurcation. (**b**) Endoscopy: follow-up demonstrates fluid effusion (*black arrow heads*) in relation with biliary duct rupture (*black arrow*), later treated by stent. (**c**) MR cholangiography without contrast shows a post-traumatic stenosis (*white arrow*) with dilation of left biliary tract, 2 months after trauma

25.4.1 Diagnosis

Excluding multiple trauma, splenic trauma can be suspected during the initial US examination in the presence of a hemoperitoneum and a heterogeneous appearance of the spleen. The study of the spleen with a superficial probe is essential as well as the use of color Doppler. One of the indirect signs of splenic trauma is a globular aspect of the spleen with loss of visualization of its hilum. The more recent the trauma, the more discrete and even absent the US signs might be (Fig. 25.6). US usually underestimates the importance of splenic lesions. CEUS is very useful to depict traumatic spleen injury (Fig. 25.7).

In the case of a positive US, if the child is hemodynamically stable, CE-CT will confirm the lesions but above all will look for signs of severity (active bleeding in free peritoneum) and associated lesions. The sensitivity and specificity of CT in the detection of splenic injury is close to 100%. Splenic lesions are best displayed in the venous phase, and are usually represented by lacerations [17]. The presence of congenital clefts can lead to misinterpretation and false-positive patients. These congenital clefts have regular and homogeneous well-defined limits whereas the lacerations would appear more irregular.

In case of hemodynamic shock, FAST echo will be the only exam performed before surgical management.

The use of AAST grades for spleen trauma is not always easy with poor inter-observer reproducibility of this classification [20] (Table 25.2).

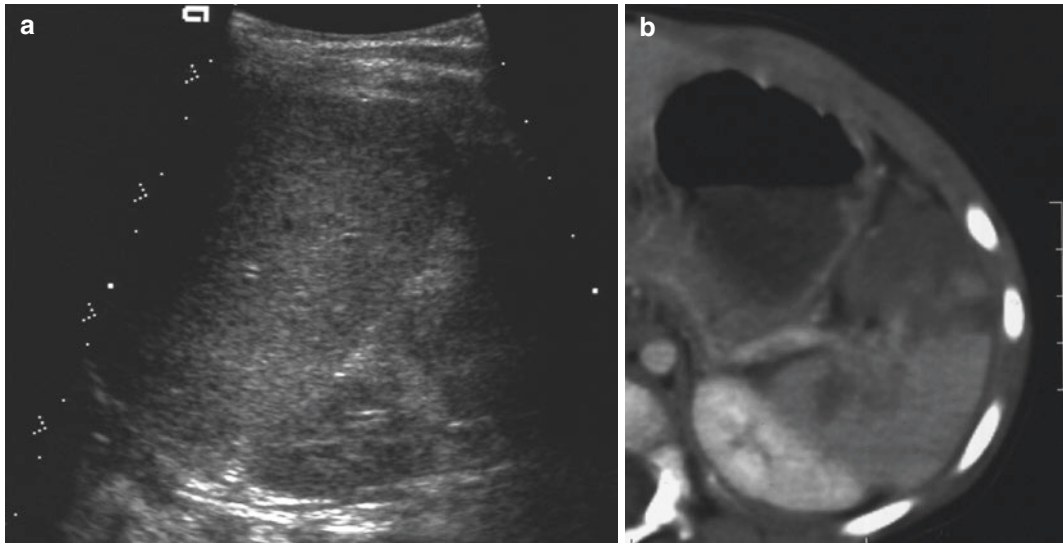

Fig. 25.6 Two year old girl. Direct abdominal trauma by the fall of a supermarket trolley. (**a**) US longitudinal scan: heterogeneous spleen with no visualization of the hilum. (**b**) CT with contrast: spleen injury under estimated by US

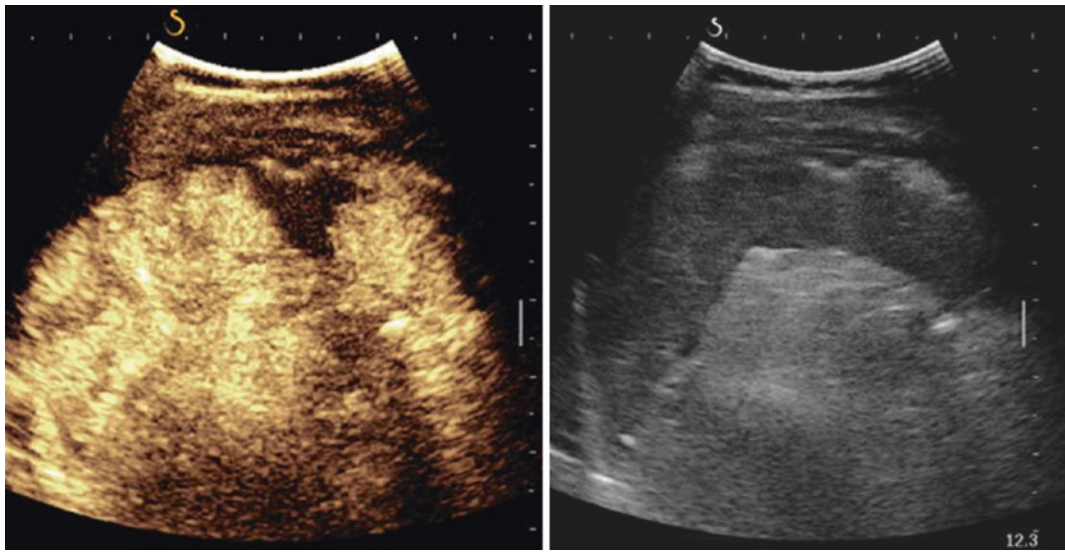

Fig. 25.7 Five year old boy with direct left flank trauma. CEUS perfectly shows spleen fracture while spleen seems to be normal on conventional US (Courtoisie Pr Delabrousse)

25.4.2 Evolution

Long-term complications of conservative management are very rare (<1%) in contrast to early complications, which can occur in up to 15% [21] and mostly affect the older child.

It is therefore necessary to perform an early US follow-up with Doppler to look for these complications:

- Secondary hemorrhage (between days 4 to 10)
- Cysts (between days 10 to 30)
- Pseudo aneurysms
- delayed splenic bleeding are exceptional in children [22].

The time table of follow-up varies according to the teams and the grade of severity. In case of severe liver trauma, US follow-up can be: US at

Table 25.2 AAST classification of splenic injury (N.b. advance one grade for multiple injuries up to grade III)

Grade I	*Subcapsular hematoma* <10% of surface area Capsular laceration <1 cm depth
Grade II	*Subcapsular hematoma* 10–50% of surface area Intraparenchymal hematoma <5 cm in diameter Laceration 1–3 cm in depth not involving trabecular vessels
Grade III	Subcapsular hematoma >50% of surface area or expanding Intraparenchymal hematoma >5 cm or expanding Laceration >3 cm in depth or involving trabecular vessels Ruptured subcapsular or parenchymal hematoma
Grade IV	Laceration involving segmental or hilar vessels with major devascularization (>25% of spleen)
Grade V	Shattered spleen Hilar vascular injury with splenic devascularization

day 0, day 2, day 7, day of discharge and day 30. This follow-up US examinations should control the disappearance of the hemoperitoneum before day 7 signing the absence of active bleeding as well as the analysis of the spleen; it must include a color Doppler study in order to look for a possible pseudo-aneurysm. Some teams highlight the performance of CEUS [23]. These pseudo aneurysms are not so rare when searched systematically. Most of these pseudo aneurysms thrombose spontaneously after a few days but if they persist, embolization can be proposed (Fig. 25.8).

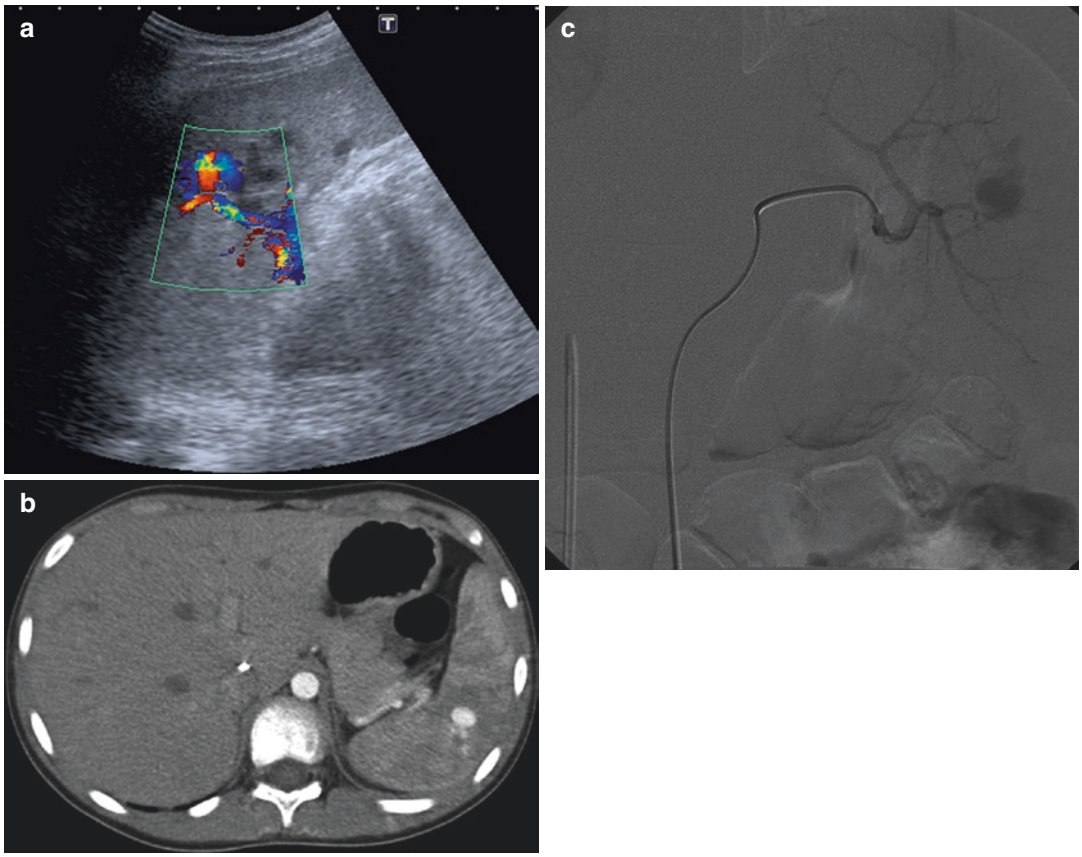

Fig. 25.8 Ten year old boy. Splenic trauma. (**a**) Control US with Doppler shows pseudo aneurism at day 10. (**b**) CT with contrast (arterial phase) confirmed the vascular lesion. (**c**) Arteriography: the pseudo aneurism was treated by embolization

Table 25.3 AAST classification of kidney injury (N.b. advance one grade for bilateral injuries up to grade III)

Grade I	Contusion or non-enlarging subcapsular perirenal hematoma, and no laceration
Grade II	Superficial laceration <1 cm depth and does not involve the collecting system (no evidence of urine extravasation), non-expanding perirenal hematoma confined to retroperitoneum
Grade III	Laceration >1 cm without extension into the renal pelvis or collecting system (no evidence of urine extravasation)
Grade IV	Laceration extends to renal pelvis or urinary extravasation Vascular: injury to main renal artery or vein with contained hemorrhage Segmental infarctions without associated lacerations Expanding subcapsular hematomas compressing the kidney
Grade V	Shattered kidney Avulsion of renal hilum: devascularization of a kidney due to hilar injury Ureteropelvic avulsions Complete laceration or thrombus of the main renal artery or vein

25.5 Renal and Urinary Tract Trauma

Blunt renal trauma in children is rare but more common than in adults but renal trauma are related to blunt trauma in over 90% of patients. High grade renal injury are 50% more frequent in children [24]. Indeed, the kidney of the child is proportionally larger, more mobile and more exposed because it is lower, below the costal margin than in adults; it is surrounded by less fat and by a weaker muscular wall. Associated visceral lesions are more frequent than in adults (40% of cases).

There is no correlation between the severity of the lesions and the importance, existence or absence of macroscopic or microscopic hematuria [25]. AAST classification of kidney injury is presented in Table 25.3.

Adrenal trauma in children is very rare but possible especially in case of severe trauma (falls from heights). Usually, a traumatic adrenal lesion is unilateral (>90%) and involves the right adrenal gland (85%). The diagnostic is made by CE-CT that demonstrates its association with liver, spleen or kidneys injuries [26].

25.5.1 Diagnosis

The aims of Imaging are to assess the extent of kidney damage, to guide therapeutic decisions, to investigate associated lesions, and to demonstrate sequelae.

US with Doppler is the first examination. It is sufficient when it is normal and the monitoring will be clinical [27].

CE-CT is the gold standard examination. It will be systematically performed if US is abnormal. It allows a complete assessment of the parenchymal lesions, the urinary tract (including delayed acquisition, 5 min post-IV) and of the vessels (Fig. 25.10). CE-CT is more accurate than US for staging. It allows a complete assessment of the all potential associated lesions (60% in the severe forms [28]). Delayed phase acquisition is fundamental looking for urine extravasation; this phase must be performed with a low dose protocol to limit the delivered dose.

Interventional radiology is reserved for cases where an endovascular treatment is considered (embolization of fistula, stent in post-traumatic dissections).

25.5.2 Evolution and Prognosis

Minor lesions have a very good prognosis and do not require monitoring. The lesions occurring on pre-existing renal disease always appear serious. More than half of patients with grade III lesions or more will experience sequelae (parenchymal atrophy, loss of renal function) [28]. Follow-up is essential for these patients (scintigraphy or MR urography, biology, blood pressure). Pedicular lesions, about 10% of cases, have a very poor prognosis, correlated with the diagnosis delay.

Late complications of severe forms include delayed hemorrhage, hematuria, urinomas, renal cysts, high blood pressure and impaired renal function. These severe forms require prolonged follow-up 3–4 months until a complete healing is demonstrated. Post-traumatic hypertension is exceptional but not negligible in severe forms (about 7–10%) [28].

The loss of function after severe renal trauma can be evaluated by renal scintigraphy or by functional

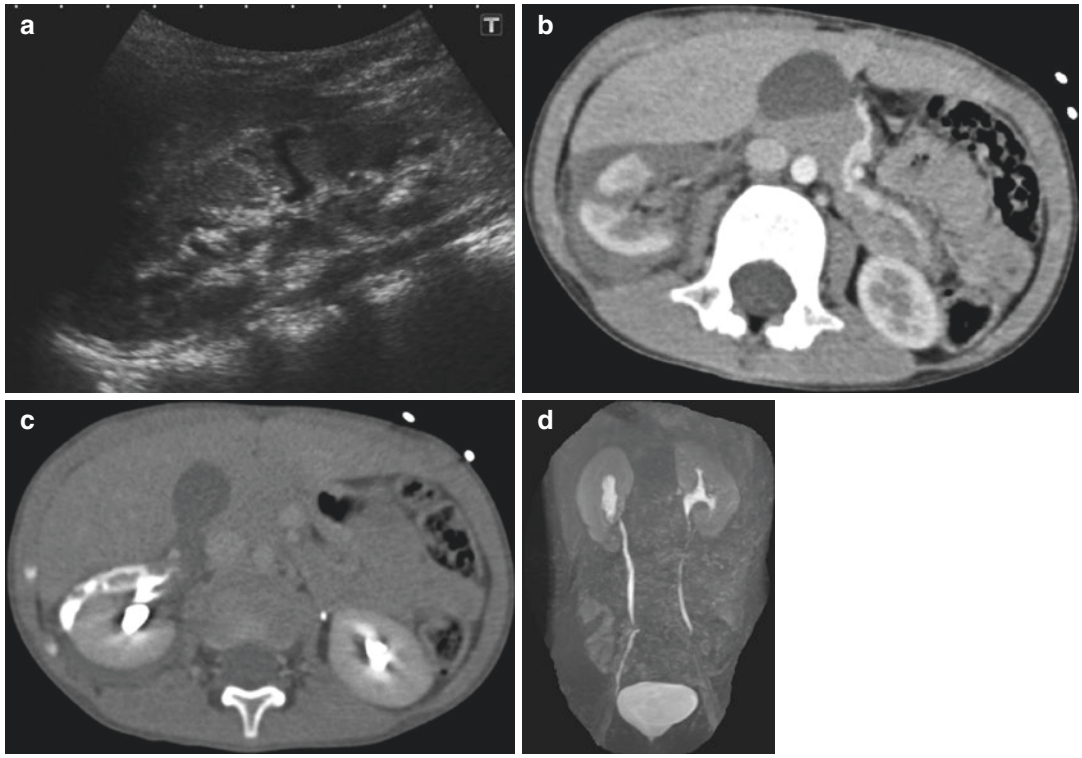

Fig. 25.9 Five year old boy. (**a**) Initial US shows fracture of the right kidney. (**b**) CT with contrast (arterial phase): complex fracture of the right kidney. (**c**) CT with contrast (delayed phase): urinoma. (**d**) Functional MR urography (3 months after trauma) shows normal excretion on gadolinium T1 weighted image. Split renal function was 45% for the right kidney

MR urography [29]. Dynamic CE-MR urography allows morphological assessment and measurement of split renal function and is useful in children who do not require sedation [30] (Fig. 25.9).

Conservative approach is accepted [31] except in cases with active hemorrhage requiring urgent surgery and in case of pedicular lesions where the treatment is quite controversial (surgical or endovascular treatment) [32, 33].

25.6 Duodenum and Pancreatic Trauma

Blunt pancreatic trauma is rare (<0.5%). Most treatments (75%) are non-operative. Morbidity and mortality rates are high (respectively 25% and 5%). Specific traumas are related to bike injuries and struck injuries [34].

The trauma mechanism is mostly due to direct compression of the pancreas against he spine causing transection of the body [35].

25.6.1 Diagnosis

The initial diagnosis is difficult, often delayed, fortunately without a significant increase in morbidity and mortality [3].

Raised amylase is one of the clues for the diagnosis. Trauma is one of the leading causes of pancreatitis in children.

In case of minor injury, there are limited findings on the initial CE-CT (normal aspect of the pancreas or slight edema). In case of pancreatic transection, the accuracy of CE-CT is close to 80% (Fig. 25.10).

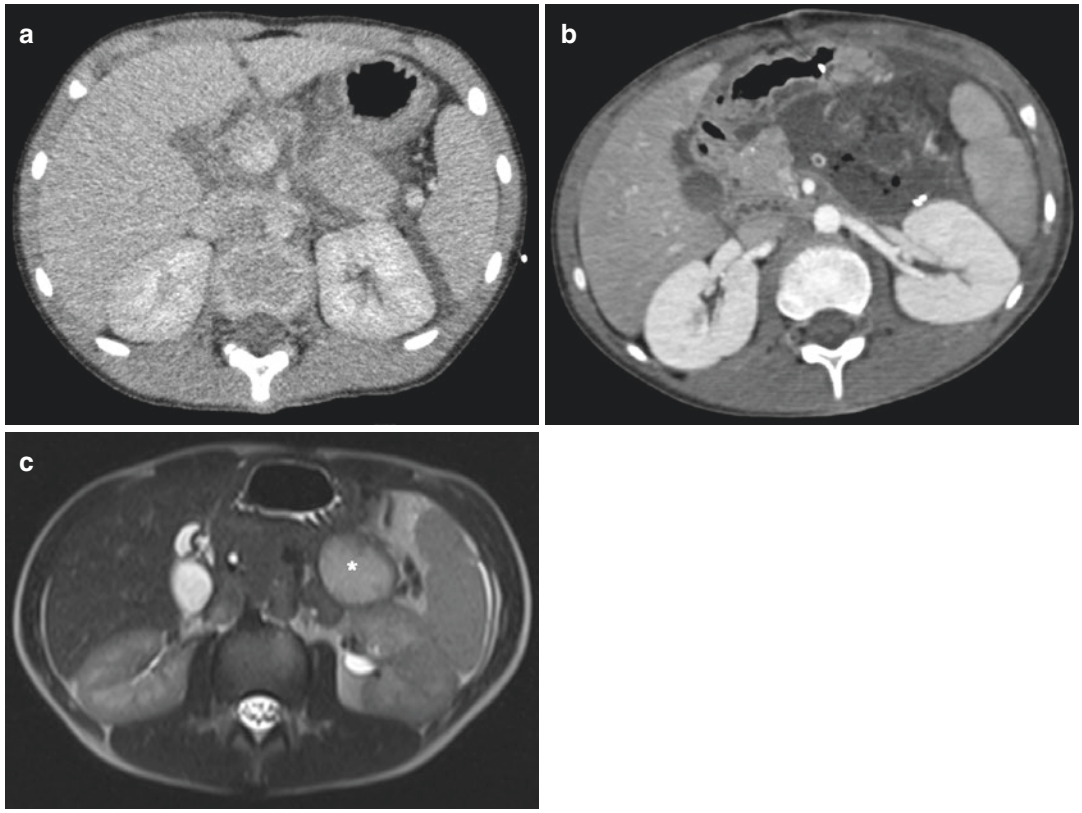

Fig. 25.10 Twelve year old girl. Epigastric trauma. (**a**) Initial CT with contrast done in a non-pediatric center with wrong protocol (too high kV, too low mAS) showing pancreatic transection treated by surgery. (**b**) Control CT with contrast indicated by post traumatic and post-operative severe pancreatitis. (**c**) Long term follow-up by MRI T2 weighted sequences showing residual pancreatic cyst (*)

In case of raised amylase and normal initial CE-CT, a control CT could be performed if US is still inconclusive.

25.6.2 Evolution

Conservative treatment is preferred unless there is an associated bowel perforation whose repair will often be surgical.

MRCP or ERCP are the gold standard for demonstrating damage of the pancreatic duct. One of the most important complications after pancreatic damage is the development of a pseudocyst secondary to the rupture of the pancreatic canal or one of secondary canals [35]. US will allow the follow-up.

The large pseudocysts can be treated by US guided puncture, external drainage, internal drainage by cysto-gastrostomy. Rupture of the pancreatic canal can be treated by endoscopic prosthesis or surgery.

25.7 Mesenteric and Bowel Trauma

Isolated bowel lesions are difficult to diagnose. Sensitivity and specificity of CE-CT are about 55% and 90% respectively.

CE-CT shows specific and non-specific signs. Specific signs include the tear of the bowel wall and the presence of pneumoperitoneum or retropneumoperitoneum (Fig. 25.11). The bowel wall

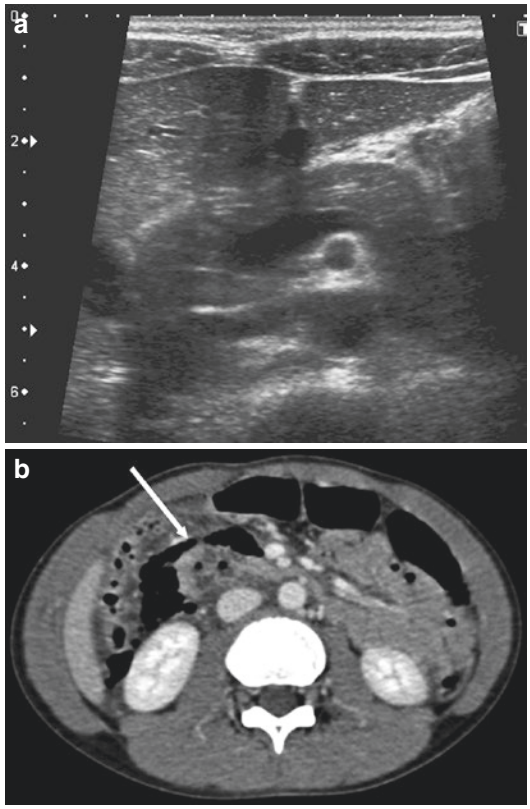

Fig. 25.11 Seven year old boy. Bike injury with direct epigastric trauma by the handlebar. (**a**) Initial US shows only a moderate fluid effusion without pancreatic anomaly. (**b**) CT with contrast: done because of the abdominal pain with abdominal contracture. It shows duodenum perforation (D2-D3) (*white arrow*)

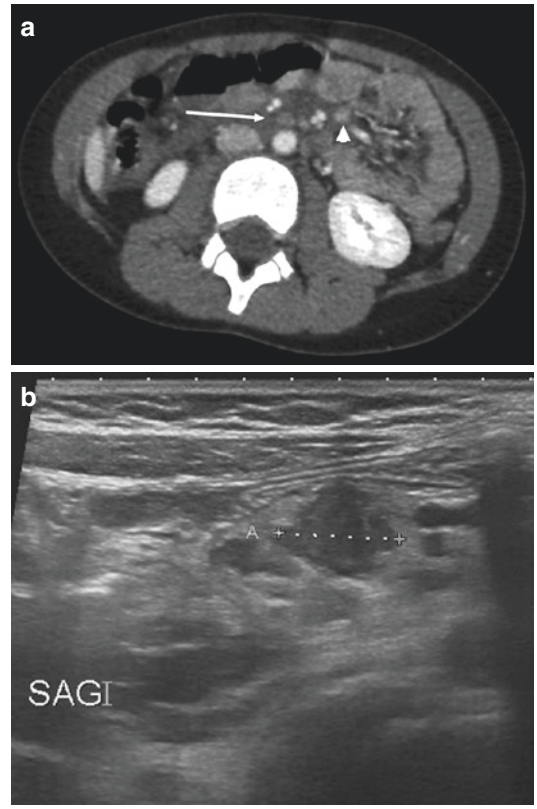

Fig. 25.12 Six year old girl. Epigastric trauma with normal initial US but abdominal contracture. (**a**) CT with contrast shows mesenteric infiltration (*white arrow*) with a little active bleeding (*white arrow head*). (**b**) Control US shows mesenteric hematoma treated conservatory with success

thickening is not a specific sign. The complete rupture of the bowel wall occurs most commonly in the mid to distal part of the small intestine [17].

CE-CT can also show mesenteric hematoma with or without active bleeding (Fig. 25.12).

In children less than 3 years, the diagnosis of a bowel hematoma in a questionable traumatic context should raise the possibility of non-accidental trauma (NAT), especially in case of duodenal hematoma. NAT can also cause visceral lesions or hematomas of the abdominal wall [36].

25.8 Pelvic Trauma

The pelvis of the child has an important plasticity due to the numerous growth plates. Pelvic fractures are therefore much rarer in children, around 1% compared to 4–5% in adults [37]. The main cause is pedestrian hit by a car. These are usually severe traumas with significant (5%) mortality, mostly related to the associated lesions (brain, liver, spleen).

The diagnosis of lesions will be made by CE-CT with particular attention for active bleeding on contact.

25.9 Non-Accidental Abdominal Trauma

Abdominal injuries in NAT are rare. There are rarely isolated and asymptomatic; they are usually part of multiple trauma. The patients are usually under the age of 3. The most frequently encountered lesions in this context are bowel

(duodenal hematomas, perforations), liver, splenic and pancreatic lesions (contusion or transection) [38].

When evaluating children with a history of blunt abdominal trauma caused by a fall, suspicion for NAT is warranted if the child is younger than 5 years, has a hollow viscus, pancreatic, and/or severe head injury and has a high ISS (Injury Severity Score) [39].

In case of suspicion of NAT, the clinical examination must be as complete as possible looking for abdominal pain but also skin hematomas. If the clinical examination is negative, the systematic realization of an abdominal US or CT is not justified.

25.10 Seat Belt Syndrome

The seat belt syndrome associates all the lesions due to high energy shock involving belted patients. Infrequent and improper use of appropriate belt restraints in children has led to high risks for injury in this population. Outside the context of the accident (violent shock with belted child), the clinical examination is essential in the search for cutaneous lesions. Seat belt sign was defined as a continuous area of erythema, ecchymosis, or abrasion across the abdomen secondary to a seat belt restraint. The horizontal part of the seat belt, in children, is often located against the hypochondria. The abdominal lesions due to the seat belt are liver injuries around the fixed point represented by the falciform ligament, intestinal and mesenteric lesions, as well as pancreatico-duodenal injuries [40]. A sudden deceleration produces hyperflexion of the lumbar spine over the fulcrum of the lap-belt with specific spine injuries (Chance fractures) [41].

It is useful, in case of seat belt syndrome, to perform a spinal MRI if the child presents pain on clinical examination. This exploration is not urgent as long as the child is hospitalized, at rest, and can be performed once the visceral lesions have been controlled.

25.11 Focus on Interventional Radiology in Pediatric Trauma

Embolization in case of pediatric trauma is uncommon in pediatric abdominal trauma (less than 3% in an American epidemiologic study) [42]. The cases are mostly related to splenic trauma and more rarely to kidney or pelvis trauma in older children [43]. Endovascular treatment of false aneurysms (spleen, liver) may be proposed in some cases of early complications. Interventional radiology requires trained teams and equipment suitable for children under 25 kg. Older children or teenagers can be managed as would adult patients. The indications of interventional radiology in children remain less well codified than in adults with a case-by-case discussion between surgeons and radiologists according to technical platforms and skills. The more conservative surgical management of abdominal trauma in children compared to adults is also found in interventional radiology with a greater tendency to a close monitoring and rather less invasive act, particularly in cases of contrast medium extravasation often regressive spontaneously in children [44, 45]. The use of CEUS can be very useful in the follow-up of the pseudoaneurysms which are relatively frequent when systematically searched by US (day 5 to 10) but rarely symptomatic. They majority regresses spontaneously (95% of spontaneous regression in a series of 101 cases with only 5 embolizations [23]).

Apart from embolization, interventional radiology may be useful in certain complications requiring drainage (biloma, urinoma), but much less frequently than in adults.

In case of renal pedicle damage, endovascular stenting - whose long-term permeability is unknown - or surgical treatment, is possible in the acute phase. Noteworthy, the prognosis itself is related to the duration of ischemia. The preservation of renal function is exceptional. The prognosis of these lesions remains very reserved [46].

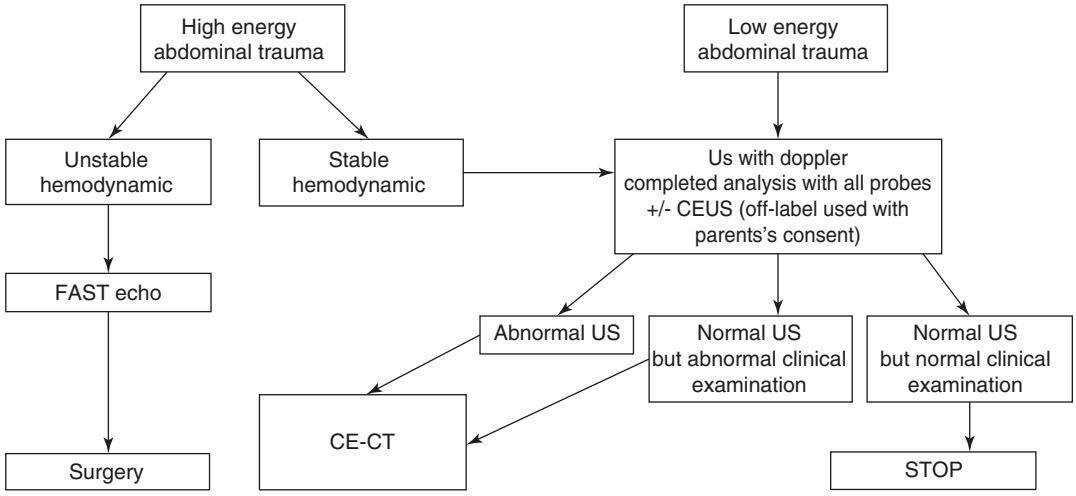

Fig. 25.13 Imaging management algorithm

The majority of isolated urinomas disappears spontaneously and requires no treatment. In case of symptomatic voluminous urinomas (with fever or pain) percutaneous drainage alone or associated with a nephrostomy or ureteral stenting (to decrease the urine supply) provides the complete resolution of persistent urine leakage [47]. The percutaneous drainage of the kidney ± of the collection is carried out under US guidance, usually under sedation with drain left in place for about 1 week. The ureteral catheter or nephrostomy generally stays in place for a longer period of time, depending on the type of urinary tract lesion.

25.12 Algorithms of Imaging Management

It is essential to have CT protocols dedicated to pediatrics and it is important to have algorithms for the management of children with abdominal trauma [48, 49] (Fig. 25.13).

Conclusion

Blunt abdominal trauma is a major but often unrecognized cause of death in children. Imaging plays a vital role in the early detection of abdominal trauma. Imaging management depends on the hemodynamic status and vital parameters. Abdominal US is the first step and may be sufficient if no anomaly is found. CEUS, even off-label, is a promising tool for the diagnosis and follow-up. CE- CT, performed selectively with dedicated pediatric protocols, has a high sensitivity and high negative predictive value. Non-operative management is generally safe in children with potential interventional radiology procedures in few cases. Follow-up is based on US and MR imaging to avoid ionizing radiations.

References

1. Muniz A. Evaluation and management of pediatric abdominal trauma. Pediatr Emerg Med Pract. 2008;5:32.
2. Holmes JF, Sokolove PE, Brant WE, Palchak MJ, Vance CW, Owings JT, Kuppermann N. Identification of children with intra-abdominal injuries after blunt trauma. Ann Emerg Med. 2002;39:500–9.
3. Canty TG Sr, Canty TG Jr, Brown C. Injuries of the gastrointestinal tract from blunt trauma in children: a 12-year experience at a designated pediatric trauma center. J Trauma. 1999;46:234–40.
4. Safavi A, Skarsgard ED, Rhee P, Zangbar B, Kulvatunyou N, Tang A, O'Keeffe T, Friese RS, Joseph B. Trauma center variation in the management of pediatric patients with blunt abdominal solid organ injury: a national trauma data bank analysis. J Pediatr Surg. 2016;51:499–502.

5. Morbidity and Mortality Weekly Report (MMWR). Centers for Disease Control and Prevention (CDC). Recommendations and reports. 2012. Vol. 61. P. 1.
6. Mahajan P, Kuppermann N, Tunik M, Yen K, Atabaki SM, Lee LK, Ellison AM, Bonsu BK, Olsen CS, Cook L, Kwok MY, Lillis K, Holmes JF, Intra-abdominal Injury Study Group of the Pediatric Emergency Care Applied Research Network (PECARN). Comparison of clinician suspicion versus a clinical prediction rule in identifying children at risk for intra-abdominal injuries after blunt torso trauma. Acad Emerg Med. 2015;22:1034–41.
7. Acker SN, Stewart CL, Roosevelt GE, Partrick DA, Moore EE, Bensard DD. When is it safe to forgo abdominal CT in blunt-injured children? Surgery. 2015;158:408–12.
8. Sirlin CB, Brown MA, Andrade-Barreto OA, Deutsch R, Fortlage DA, Hoyt DB, Casola G. Blunt abdominal trauma: clinical value of negative screening US scans. Radiology. 2004;230:661–8.
9. Rafailidis V, Deganello A, Watson T, Sidhu PS, Sellars ME. Enhancing the role of paediatric ultrasound with microbubbles: a review of intravenous applications. Br J Radiol. 2017;90:20160556.
10. Yusuf GT, Sellars ME, Deganello A, Cosgrove DO, Sidhu PS. Retrospective analysis of the safety and cost implications of Pediatric contrast-enhanced ultrasound at a single center. AJR Am J Roentgenol. 2017;208:446–52.
11. Sessa B, Trinci M, Ianniello S, Menichini G, Galluzzo M, Miele V. Blunt abdominal trauma: role of contrast-enhanced ultrasound (CEUS) in the detection and staging of abdominal traumatic lesions compared to US and CE-MDCT. Radiol Med. 2015;120:180–9.
12. Braungart S, Beattie T, Midgley P, Powis M. Implications of a negative abdominal CT in the management of pediatric blunt abdominal trauma. J Pediatr Surg. 2017;52:293–8.
13. Onwubiko C, Mooney DP. The value of official reinterpretation of trauma computed tomography scans from referring hospitals. J Pediatr Surg. 2016;51:486–9.
14. Ellison AM, Quayle KS, Bonsu B, Garcia M, Blumberg S, Rogers A, Wootton-Gorges SL, Kerrey BT, Cook LJ, Cooper A, Kuppermann N, Holmes JF, Pediatric Emergency Care Applied Research Network (PECARN), Pediatric Emergency Care Applied Research Network PECARN. Use of oral contrast for abdominal computed tomography in children with blunt torso trauma. Ann Emerg Med. 2015;66:107–114.e4.
15. Naulet P, Wassel J, Gervaise A, Blum A. Evaluation of the value of abdominopelvic acquisition without contrast injection when performing a whole body CT scan in a patient who may have multiple trauma. Diagn Interv Imaging. 2013;94(4):410–7.
16. Darge K, Higgins M, Hwang TJ, Delgado J, Shukla A, Bellah R. Magnetic resonance and computed tomography in pediatric urology: an imaging overview for current and future daily practice. Radiol Clin N Am. 2013;51:583–98.
17. Miele V, Piccolo CL, Trinci M, Galluzzo M, Ianniello S, Brunese L. Diagnostic imaging of blunt abdominal trauma in pediatric patients. Radiol Med. 2016;121:409–30.
18. Sharif K, Pimpalwar AP, John P, Johnson K, Donnell S, Ville D, De Goyet J. Benefits of early diagnosis and preemptive treatment of biliary tract complications after major blunt liver trauma in children. J Pediatr Surg. 2002;37:1287–92.
19. Castagnatti M, Houben C, Patel S, Devlin J, Harrison P, Karani J, Heaton N, Davenport M. Minimally invasive management of bile leaks after blunt liver trauma in children. J Pediatr Surg. 2006;41:1539–44.
20. Leschied JR, Mazza MB, Davenport M, Chong ST, Smith EA, Hoff CN, Ladino-Torres MF, Khalatbari S, Ehrlich PF, Dillman JR. Inter-radiologist agreement for CT scoring of pediatric splenic injuries and effect on an established clinical practice guideline. Pediatr Radiol. 2016;46:229–36.
21. Dobremez E, Lefevre Y, Harper L, Rebouissoux L, Lavrand F, Bondonny JM, Vergnes P. Complications occurring during conservative management of splenic trauma in children. Eur J Pediatr Surg. 2006;16:166–70.
22. Davies DA, Fecteau A, Himidan S, Mikrogianakis A, Wales PW. What's the incidence of delayed splenic bleeding in children after blunt trauma? An institutional experience and review of the literature. J Trauma. 2009;67:573–7.
23. Durkin N, Deganello A, Sellars ME, Sidhu PS, Davenport M, Makin E. Post-traumatic liver and splenic pseudoaneurysms in children: diagnosis, management, and follow-up screening using contrast enhanced ultrasound (CEUS). J Pediatr Surg. 2016;51:289–92.
24. Kurtz MP, Eswara JR, Vetter JM, Nelson CP, Brandes SB. Blunt abdominal trauma from motor vehicle collisions from 2007 to 2011: renal injury probability and severity in children versus adults. J Urol. 2016;197:906–10.
25. Nguyen MM, Das S. Pediatric renal trauma. Urology. 2002;59(5):762–6.
26. Aydogdu B, Okur MH, Arslan S, Arslan MS, Zeytun H, Basuguy E, Icer M, Goya C, Uygun I, Cigdem MK, Onen A, Otcu S. The adrenal gland: an organ neglected in pediatric trauma cases. Urol J. 2016;13(6): 2916–9.
27. Pietrera P, Badachi Y, Liard A, Dacher JN. Ultrasound for initial evaluation of post-traumatic renal lesions in children. J Radiol. 2001;82:833–8.
28. Delarue A, Merrot T, Fahkro A, Alessandrini P, Guys JM. Major renal injuries in children: the real incidence of kidney loss. J Pediatr Surg. 2002;37:1446–50.
29. Gouli JC, Merrot T, Kalfa N, Faure A, Chaumoitre K, Galifer RB, Alessandrini P. Outcome of severe closed kidney injuries in children. Prog Urol. 2012;22: 58–62.

30. Cerwinka WH, Kirsch AJ. Magnetic resonance urography in pediatric urology. Curr Opin Urol. 2010;20:323–9.
31. Margenthaler JA, Weber TR, Keller MS. Blunt renal trauma in children: experience with conservative management at a pediatric trauma center. J Trauma. 2002;52(5):928–32.
32. Halachmi S, Chait P, Hodapp J, Bgli DG, McLorie GA, Khoury AE, Farhat W. Renal pseudoaneurysm after blunt renal trauma in a pediatric patient: management by angiographic embolization. Urology. 2003;61:224.
33. Lin WC, Lin CH. The role of interventional radiology for pediatric blunt renal trauma. Ital J Pediatr. 2015;41:76.
34. Englum BR, Gulack BC, Rice HE, Scarborough JE, Adibe OO. Management of blunt pancreatic trauma in children: review of the National Trauma Data Bank. J Pediatr Surg. 2016;51:1526–31.
35. Bosboom D, Braam AW, Blickman JG, Wijnen RM. The role of imaging studies in pancreatic injury due to blunt abdominal trauma in children. Eur J Radiol. 2006;59:3–7.
36. Maguire SA, Upadhyaya M, Evans A, Mann MK, Haroon MM, Tempest V, Lumb RC, Kemp AM. A systematic review of abusive visceral injuries in childhood--their range and recognition. Child Abuse Negl. 2013;37:430–45.
37. Swaid F, Peleg K, Alfici R, Olsha O, Givon A, Kessel B, Israel Trauma Group. A comparison study of pelvic fractures and associated abdominal injuries between pediatric and adult blunt trauma patients. J Pediatr Surg. 2017;52:386–9.
38. Sheybani EF, Gonzalez-Araiza G, Kousari YM, Hulett RL, Menias CO. Pediatric nonaccidental abdominal trauma: what the radiologist should know. Radiographics. 2014;34:139–53.
39. Carter KW, Moulton SL. Pediatric abdominal injury patterns caused by "falls": a comparison between nonaccidental and accidental trauma. J Pediatr Surg. 2016;51:326–8.
40. Borgialli DA, Ellison AM, Ehrlich P, Bonsu B, Menaker J, Wisner DH, Atabaki S, Olsen CS, Sokolove PE, Lillis K, Kuppermann N, Holmes JF, Pediatric Emergency Care Applied Research Network (PECARN). Association between the seat belt sign and intra-abdominal injuries in children with blunt torso trauma in motor vehicle collisions. Acad Emerg Med. 2014;21:1240–8.
41. de Gauzy JS, Jouve JL, Violas P, Guillaume JM, Coutié AS, Chaumoitre K, Launay F, Bollini G, Cahuzac JP, Accadbled F. Classification of chance fracture in children using magnetic resonance imaging. Spine. 2007;32:E89–92.
42. Fenton SJ, Sandoval KN, Stevens AM, Scaife ER. The use of angiography in pediatric blunt abdominal trauma patients. J Trauma Acute Care Surg. 2016;81:261–5.
43. Kiankhooy A, Sartorelli KH, Vane DW, Bhave AD. Angiographic embolization is safe and effective therapy for blunt abdominal solid organ injury in children. J Trauma. 2010;68:526–31.
44. Cloutier DR, Baird TB, Gormley P, McCarten KM, Bussey JG, Luks FI. Pediatric splenic injuries with a contrast blush: successful nonoperative management without angiography and embolization. J Pediatr Surg. 2004;39:969–71.
45. Ingram MC, Siddharthan RV, Morris AD, Hill SJ, Travers CD, McKracken CE, Heiss KF, Raval MV, Santore MT. Hepatic and splenic blush on computed tomography in children following blunt abdominal trauma: is intervention necessary? J Trauma Acute Care Surg. 2016;81:266–70.
46. Merrot T, Portier F, Galinier P, Paul JL, Chaumoitre K, Moscovici J, Panuel M, Alessandrini P. Trauma of the renal pedicle in children. Report of 2 cases of late revascularization with endovascular prosthesis. Prog Urol. 2000;10:277–81.
47. Russell RS, Gomelsky A, McMahon DR, Andrews D, Nasrallah PF. Management of grade IV renal injury in children. J Urol. 2001;166(3):1049–50.
48. van Schuppen J, Olthof DC, Wilde JC, Beenen LF, van Rijn RR, Goslings JC. Diagnostic accuracy of a step-up imaging strategy in pediatric patients with blunt abdominal trauma. Eur J Radiol. 2014;83:206–11.
49. Fallon SC, Delemos D, Akinkuotu A, Christopher D, Naik-Mathuria BJ. The use of an institutional pediatric abdominal trauma protocol improves resource use. J Trauma Acute Care Surg. 2016;80:57–63.

Foreign Bodies

26

Alexia Dabadie and Philippe Petit

Contents

26.1 Introduction

Ingested gastro-intestinal foreign bodies (FB) represent the vast majority of abdominal and pelvic FB while self-introduced urinary and genital tract FB and lost material during surgery are only scarcely reported.

FB ingestion is a current cause of pediatric emergency consultation. More than 100000 FB have been reported to be ingested per year in the USA [1]. It is of upmost importance to differentiate ingestion from aspiration, the latter being associated with the risk of acute death. In doubtful situation, an expiratory chest AP X-ray is needed. If the clinical suspicion is high and even when the chest X-ray is normal a fibroscopy is warranted.

Starting already at the age of a few months, every child may be potentially affected by ingestion of a FB with a peak incidence between 6 months and 4 years. Older children, especially those with psychiatric or neurologic impairment may also be affected including impaired judgment for the ingested substance. Child abuse must be considered [2] in case of uncommon presentation but even in classical situations [3].

Most of the ingested FB will be symptom free. Only 1% of all ingested foreign bodies will result in perforation [4]. Between 50% and 90% of foreign objects pass spontaneously through the digestive tract, 10–20% require endoscopic removal, and less than 1% require surgical removal [1]. However, depending on the location within the abdomen and of the size and the nature

A. Dabadie • P. Petit (✉)
Department of Pediatric and Prenatal Imaging,
Hôpital Timone Enfants,
264 Rue St Pierre, 13385 Marseille Cedex 05, France
e-mail: adabadie@ap-hm.fr; ppetit@ap-hm.fr

F.E. Avni, P. Petit (eds.), *Imaging Acute Abdomen in Children*,
https://doi.org/10.1007/978-3-319-63700-6_26

of the FB, immediate or delayed abdominal symptoms and/or complications may occur. Although the morbidity associated with such ingestions is low (0.1%), when complications do occur the mortality has been reported as high as 1500 deaths per year in the United States [4].

26.2 Ingested Foreign Body: Clinical and Imaging Presentations

26.2.1 At the Time of Ingestion

At the time of ingestion, the presentation can be variable from symptom free to substernal pain, swallowing difficulties, vomiting, rarely hematemesis or respiratory distress.

- FB can be blocked within the esophagus (crico-pharyngeus muscle, at the level of the aortic arch, lower sphincter), the pylorus or the duodenum. The lower third of the esophagus represents the least frequent location.
- AP fluoroscopic views of the chest, including the cervico-thoracic junction, and of the abdomen are needed. If the FB is not seen or not clearly identified (Fig. 26.1), then dedicated plain radiographs with several focused views centered on the suspected area are required. These images will allow to localize and characterize the type and number of radio-opaque FB. A lateral view is needed to confirm the exact position when the FB is located above the carina (Fig. 26.2). The visualization on X-rays of the FB depends on its own density and on the contrast generated by its adjacent surroundings. Plastics are not visible but non-leaded glass can be visible due to its density [5]. Except for thin aluminum FB, all metals are visible on X-rays.

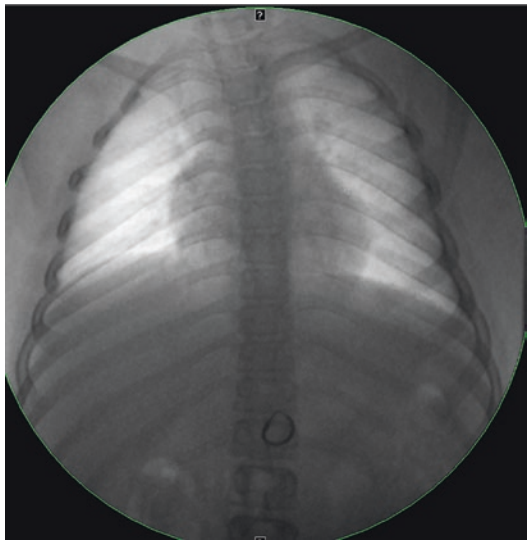

Fig. 26.1 Seven-year-old girl who has swallowed her mother's earring that is easily recognized on this AP fluoroscopic view. There is no need for a plain radiograph

The decision to remove the FB is based on its type, shape, nature, and its progression.

- Ingested coins, which are the most frequent FB, within the lower esophagus will pass through the stomach in the majority of cases. Those that are impacted will need extraction [1].
- Absorbed cells, especially the button-cell types, may produce micro currents and cause digestive wall liquefaction necrosis and thermal lesions (Fig. 26.3).
- Sharp objects increase the risk of gastric perforation from 1% to 35% [6]

Sharp objects and button-cells need to be removed either endoscopically if accessible or surgically.

26.2.2 Delayed Presentation

The longer the FB remains, the higher the risk of release by the FB of toxic substances (lead, cadmium, mercury, silver, zinc, manganese, cadmium, lithium, sulfur oxide, copper, brass, or steel) [7]. Furthermore, the longer the FB is fixed, the higher the risk of ulceration by compression [8]. Associated structural abnormalities of the lower third of the esophagus (strictures, rings, fundoplication), inflammatory conditions (reflux esophagitis, eosinophilic esophagitis), and motor dysfunction (achalasia) render higher the risk of no progression [8].

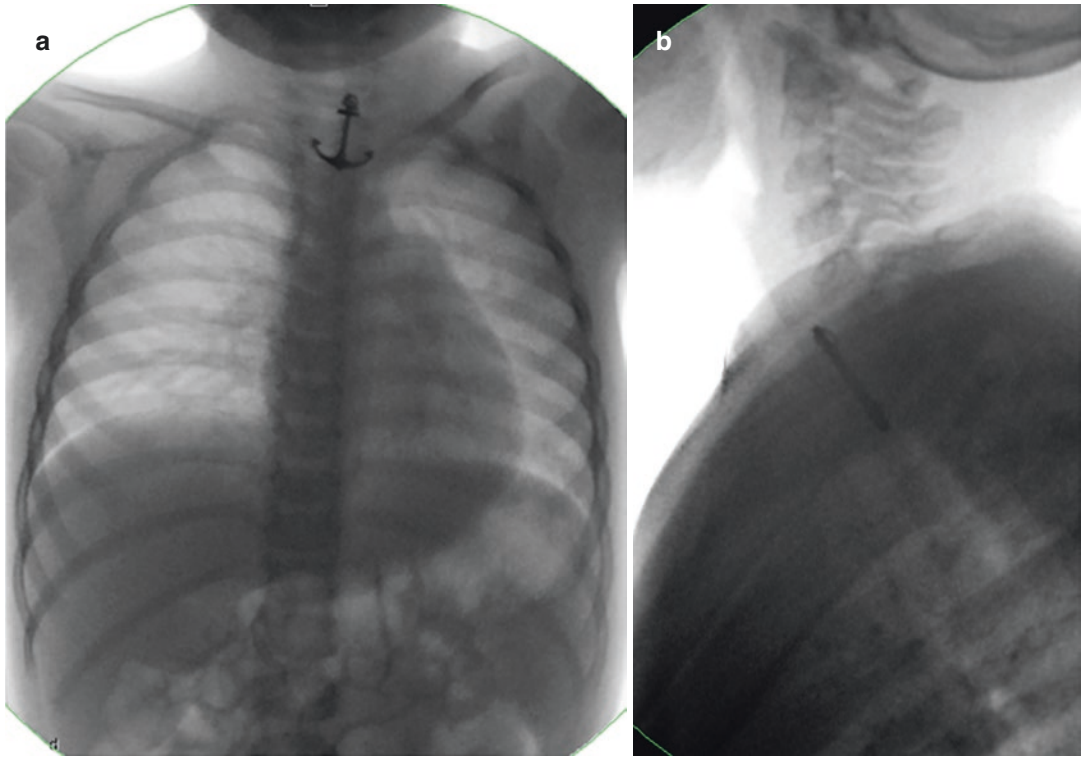

Fig. 26.2 Two-year-old girl ingestion of a small anchor well identified in the upper third of the esophagus: Fluoroscopic views. (**a**) AP fluoroscopic view. (**b**) Lateral fluoroscopic view

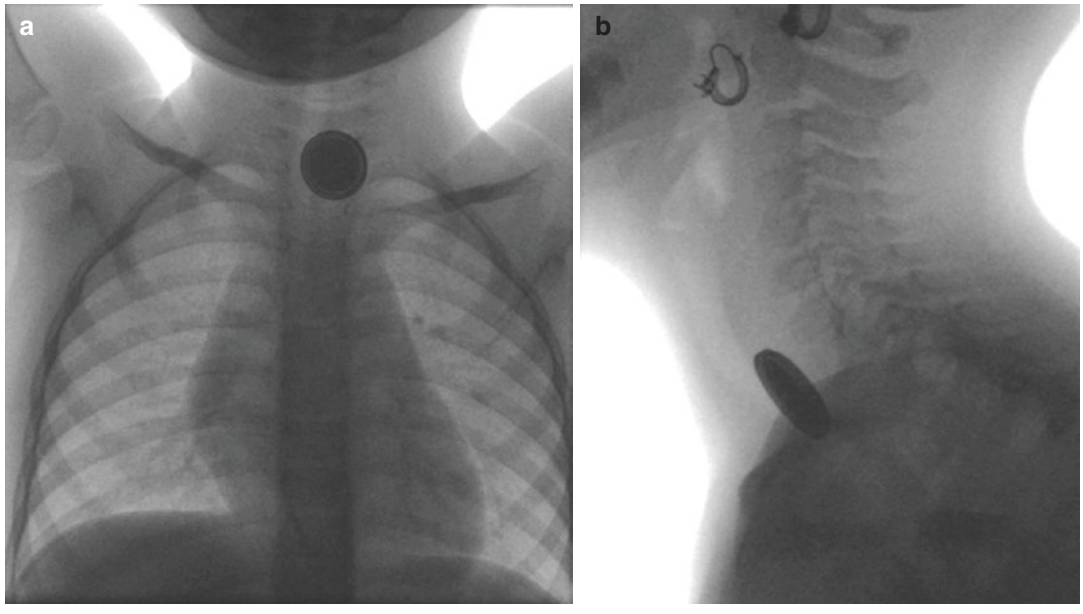

Fig. 26.3 Ingestion of button cell battery in an 8-year-old girl. Endoscopy revealed a small posterior ulceration. Fluoroscopic views allowing recognition of the nature and the location of the FB. (**a**) AP fluoroscopic view. (**b**) Lateral fluoroscopic view

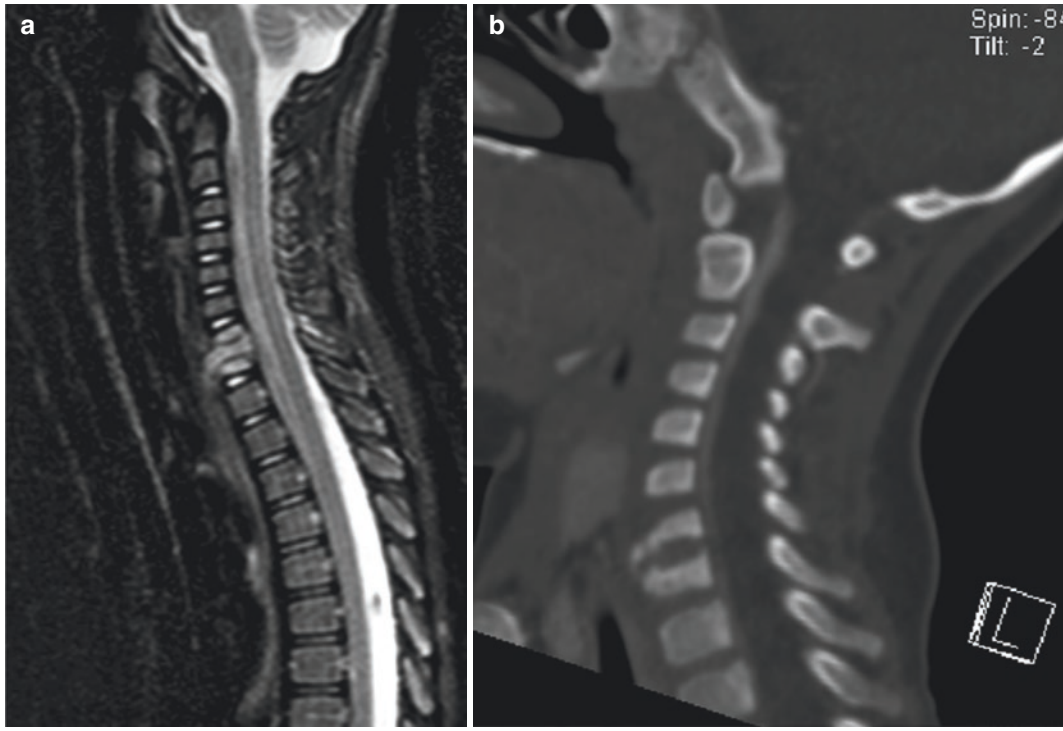

Fig. 26.4 Late complication of ingested FB—Same patient as in Fig. 26.3. Two months later the patient presented with unexplained neck stiffness. (**a**) MR imaging sagittal T2-weighted sequence: Chronic spondylodiscitis C7-Th1. (**b**) Sagittal reformatted CT: Chronic spondylodiscitis with anterior bone bridging

In this context of delayed presentation, the FB ingestion is either unrecognized or the symptoms occur during follow-up or even after its retrieval (Fig. 26.4). Within the abdominal cavity, the clinical symptoms are related to obstruction, perforation, or infection. In case of such clinical presentation, abdominal US is the examination of choice and should be completed by an AP plain film of the abdomen looking for radio-opaque FB.

- Esophagus, stomach and duodenum:
  - Substernal pain is classically related to mucosal esophageal ulceration and should be managed rapidly by endoscopy [8].
  - Exceptional deaths related to vasculo-esophageal fistulas induced by ingested button batteries have been reported. As a rule, all ingested batteries must beneficiate from an endoscopy. In case of severe endoscopic lesion, the option of further thoracic imaging must be considered in order to evaluate the peri-esophageal damage [9].
  - Gastric obstruction may be related to various large FB including different types of bezoars (lactobezoar, phytobezoar, trichobezoar, medication induced bezoar, mixed-food bezoar). Their US appearance varies demonstrating most commonly an overdistended stomach, in a patient supposedly npo, with a heterogeneous content that may appear too well organized and sometimes acoustic shadowing. Surgical treatment is often required to remove the bezoar.

    Lactobezoar is a compact mass made of undigested milk and gastric secretion occurring in neonates. Prematurity, immaturity of gastric motility, discontinuous enteral feeding, treatment for gastro-esophageal reflux and milk with high casein concentration are predisposing factors. Gastric perforation may occur [10]

    Other bezoars occur later in childhood and are related to psychiatric or neurological disabilities. A specific entity, the Rapunzel

syndrome, includes a gastric trichobezoar extending far below the stomach up to the small intestine [11]; CT is recommended whenever such a pathology is suspected.

– Persistence within the stomach even of a non-aggressive FB over 3 weeks will need extraction. On the other hand, flat cell-button may be responsible for electric and toxic burns, ulceration by compression, and general toxicity if their content is released. These risks increase in FB staying for more than 48 h in the stomach. Endoscopic removal is required if the patient is symptomatic or if fragmentation of the battery occurs. Follow-up plain films of the abdomen is recommended to evaluate progression.
– Duodenal loop is a classic location prone to block long ingested FB.

• Below the duodenum:
  – Obstruction: The ileo-cecal valve represents a natural obstacle to any kind of FB. Rarely magnets can also cause bowel obstruction, which may lead to volvulus [12, 13]. In this context, the association of abdominal plain film and US are the most adapted imaging explorations.
  – Perforation:

    Earth magnets are typically made of iron, boron, and neodymium and are 5–10 times more powerful than traditional magnets [1]. When multiple, they may lead to perforation or bowel fistula when located on two adjacent bowel loops (Fig. 26.5). In case of suggestive clinical signs, rapid surgical removal is mandatory to suppress the risk of perforation.

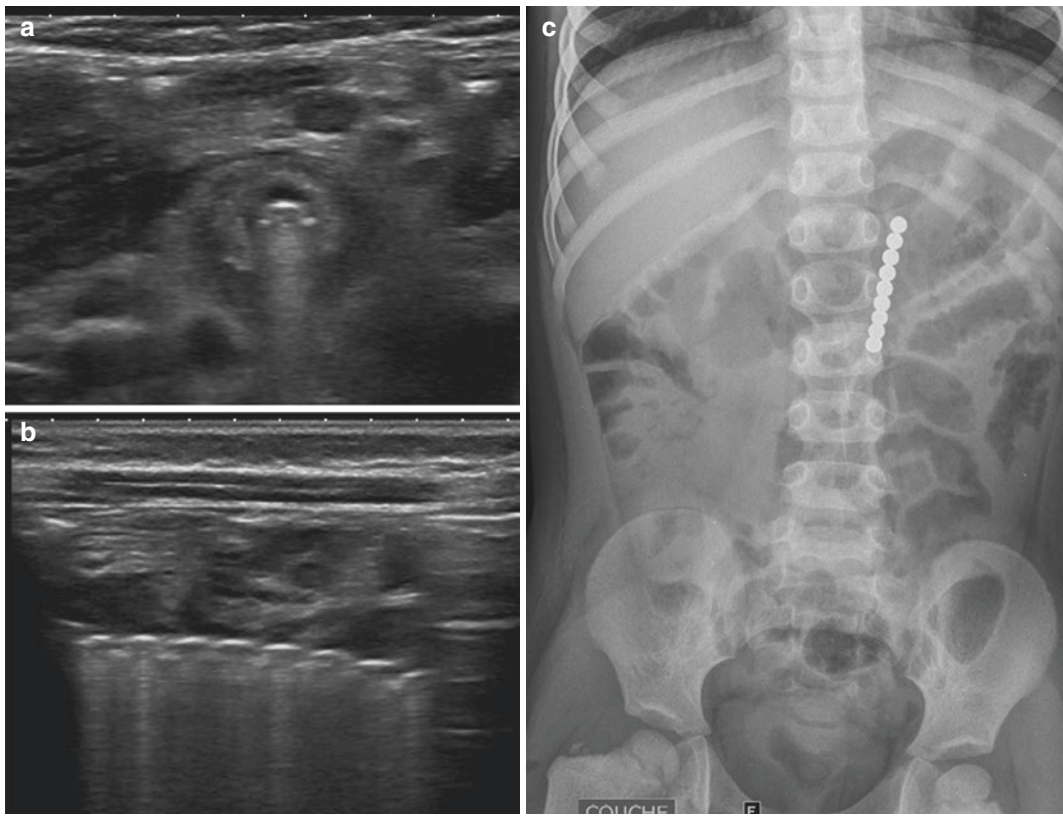

Fig. 26.5 Ingestion of magnets in a three-year-old girl who complained of persisting abdominal pain and vomiting. (**a**) US transverse scan demonstrating a thickened small bowel loop containing echogenic material. (**b**) US sagittal scan, the FB extends outside the bowel lumen. (**c**) Plain film of the abdomen identifies multiple magnets which were removed under coelioscopy. A small perforation of two adjacent loops compressed by the magnets was present

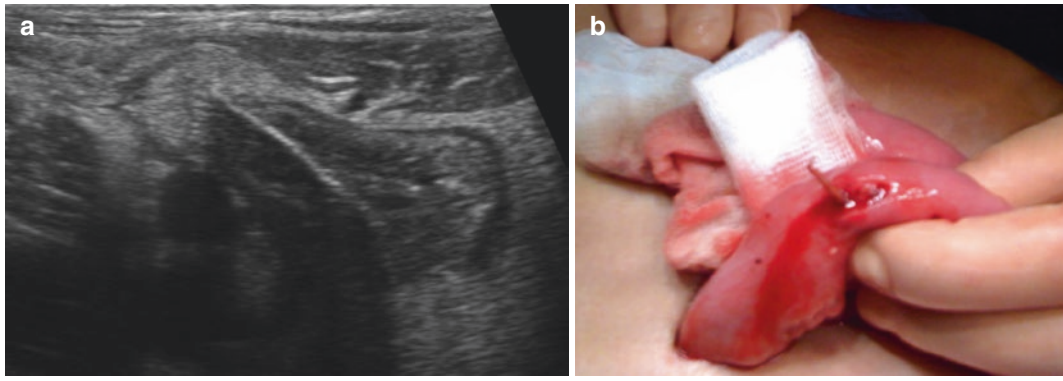

Fig. 26.6 Eight-year-old boy suspected of appendicitis. (**a**) US revealed a sharp attenuating foreign body transfixiating the small bowel wall with adjacent peritoneal reaction. (**b**) Surgery confirms the bowel perforation by a toothpick

Sharp FB, radio-opaque or not, may be responsible for perforation and secondary peritonitis.

Battery cells are rarely responsible for small or large bowel perforation by electric burns. Their transit time is generally too fast to generate such lesion.

US is most useful as it may demonstrate the FB itself (Fig. 26.6) as well as its consequences such as thickened bowel loop, adjacent increased echogenic fat, and eventually extraluminal gas bubbles. If the FB potentially contains metal, a plain film is also helpful (Fig. 26.7).

Interestingly enough, a perforation due to a FB has been described without peritonitis [14].

– Infection:

FB within a Meckel's diverticulum or within the appendix may be responsible for an acute infection. Depending on the local radiological expertise such diagnosis can either be achieved by US, MR imaging, or CT.

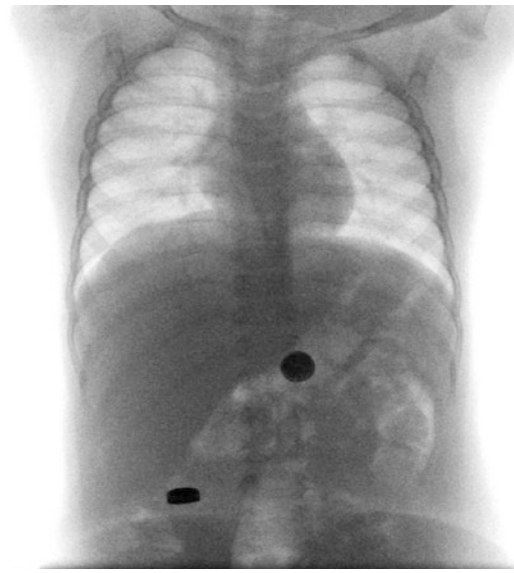

Fig. 26.7 One-year-old boy who has just ingested a flat cell battery. Fluoroscopic AP view of the chest and the abdomen reveals the presence of 2 batteries; the first one is in projection of the stomach, the second is located more distally in projection of the right iliac fossa

26.3 Genital Foreign Body: Clinical and Imaging Presentations

Prepubertal vaginal discharge associated or not with local sepsis or urinary tract infection [15] need to be investigated clinically as well as with US. US has been proven efficient for the visualization of vaginal FB. It will appear with variable echotextures and patterns with or without posterior acoustic shadowing (Fig. 26.8). Indentation of the posterior bladder wall is a frequent associated sign [16]. Child sexual abuse must be considered in the differential diagnosis. Vaginal foreign bodies are responsible for as much as 10% of all pediatric vaginitis.

26.4 Urinary Foreign Body: Clinical and Imaging Presentations

Urinary tract infection has been reported to be associated with self-introduced urethral or vesical FB [17]. Girls are more prone to be involved due to the shortness of the urethra. Associated clinical findings include hematuria, dysuria, and increased frequency of micturition. US and plain films will permit to achieve the diagnosis.

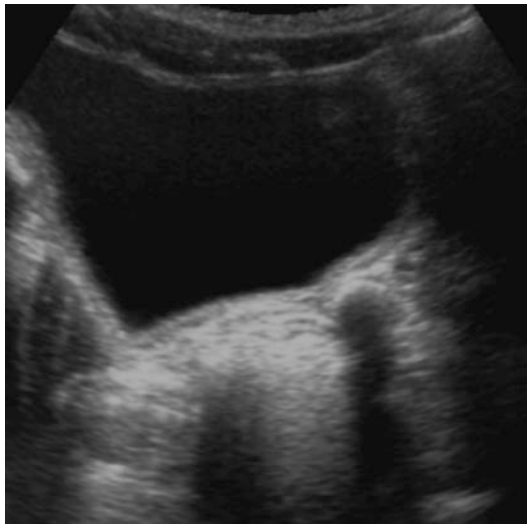

Fig. 26.8 Four-year-old girl presenting with malodorous vaginal discharge. US reveals a small hyperechoic foreign body with posterior shadowing corresponding to a small plastic toy

26.5 Lost Surgical Foreign Body: Clinical and Imaging Presentations

Retained post-surgical foreign bodies are infrequently encountered. Their real frequency is unknown. Most of them correspond to surgical sponge or pledget (so-called gossypibomas or textiloma). Symptoms may appear from a few days to a few years postoperatively or even be discovered incidentally. Pain, fever, compression of the adjacent structures are the main symptoms. Fistulization to the skin, to a hollow viscus, through the diaphragm or in the bladder are rare presentations [18]. Diagnosis on imaging may be obvious on plain films when the lost FB contains some metal. Since a few years, metallic markers are included in the surgical gauzes and are easily recognized on plain radiographs and other imaging. Older textilomas are more difficult to diagnose. They present on US as an important shadowing structure with or without gas bubbles or calcifications trapped within the fibers; rarely they present as cystic like structures with a thick wall and wavy internal echos. The CT presentation is also variable. Textiloma may present like a non-enhancing mass containing or not gas or calcifications (Fig. 26.9) or as a cystic structure with a calcified rim containing serpiginous non-enhancing material. It can present a thick enhancing wall. Lost FB can be mistaken for tumoral lesions. Only a few articles have reported their

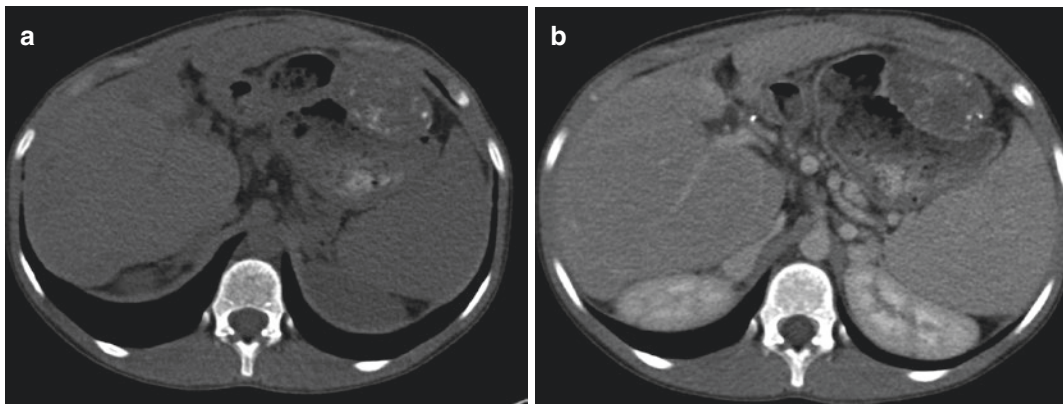

Fig. 26.9 Incidental textiloma in a 12-year-old girl operated 10 years ago for a porto-enterocystostomy for biliary atresia. CT workup before liver graft transplant (**a**) Plain CT reveals a mass with peripheral calcification adjacent to the stomach. (**b**) CE-CT portal phase demonstrates no enhancement of this lesion

MR imaging appearance, none in the pediatric literature. The lesions display a peripheral hyposignal rim on T1 and T2 weighted sequences that enhances after gadolinium injection and presents irregular contours of its inner surface. The content appears hyposignal on T2-weighted sequence [19]. Abscess and tumor are the main differential diagnoses.

Conclusion

- FB are mostly ingested. They are radiopaque and easily diagnosed on fluoroscopy at the time of presentation. When they are not clearly identified or localized, multiple view radiographs are needed.
- FB may have also other origins including: self-inflicted, post-surgical, and abuse.
- Acute abdominal complications may reveal FB. US examination is usually the primary imaging exam to be performed to identify non-radiopaque FB and to look for complications.

References

1. Wright CC, Closson FT. Updates in pediatric gastrointestinal foreign bodies. Pediatr Clin N Am. 2013;60(5):1221–39.
2. Gromb S, Lazarini HJ. An unusual case of sexual assault on an infant: an intraperitoneal candle in a 20-month-old girl. Forensic Sci Int. 1998;94:15–8.
3. Wadhera R, Kalra V, Gulati SP, et al. Child abuse: multiple foreign bodies in gastrointestinal tract. Int J Pediatr Otorhinolaryngol. 2013;77(2):287–9.
4. Kircher MF, Milla S, Callahan MJ. Ingestion of magnetic foreign bodies causing multiple bowel perforations. Pediatr Radiol. 2007;37:933–6.
5. Tseng HJ, Hanna TN, Shuaib W, et al. Imaging foreign bodies: ingested, aspirated, and inserted. Ann Emerg Med. 2015;66(6):570–82.
6. Kay M, Wyllie R. Pediatric foreign bodies and their management. Curr Gastroenterol Rep. 2005;7:212–8.
7. Pugmire BS, Lim R, Avery LL. Review of ingested and aspirated foreign bodies in children and their clinical significance for radiologists. Radiographics. 2015;35(5):1528–38.
8. Denney W, Ahmad N, Dillard B, et al. Children will eat the strangest things: a 10-year retrospective analysis of foreign body and caustic ingestions from a single academic center. Pediatr Emerg Care. 2012;28(8):731–4.
9. Pugmire BS, Lin TK, Pentiuk S, de Alarcon A, Hart CK, Trout AT. Imaging button battery ingestions and insertions in children: a 15-year single-center review. Pediatr Radiol. 2017;47(2):178–85.
10. Heinz-Erian P, Gassner I, Klein-Franke A, et al. Gastric lactobezoar - a rare disorder? Orphanet J Rare Dis. 2012;7:3.
11. Fallon SC, Slater BJ, Larimer EL, et al. The surgical management of Rapunzel syndrome: a case series and literature review. J Pediatr Surg. 2013;48(4):830–4.
12. Nui A, Hirama T, Katsuramaki T, et al. An intestinal volvulus caused by multiple magnet ingestion: an unexpected risk in children. J Pediatr Surg. 2005;40:e9–11.
13. Hernández Anselmi E, Gutiérrez San Román C, Barrios Fontoba JE, et al. Intestinal perforation caused by magnetic toys. J Pediatr Surg. 2007;42(3):E13–6.
14. Klein K, Pegoli W Jr, Lee YH. Transluminal migration of ingested foreign body without peritonitis. J Pediatr Surg. 2012;47(4):788–91.
15. Neulander EZ, Tiktinsky A, Romanowsky I, et al. Urinary tract infection as a single presenting sign of multiple vaginal foreign bodies: case report and review of the literature. J Pediatr Adolesc Gynecol. 2010;23(1):e31–3.
16. Caspi B, Zalel Y, Katz Z, Appelman Z, et al. The role of sonography in the detection of vaginal foreign bodies in young girls: the bladder indentation sign. Pediatr Radiol. 1995;25(Suppl 1):S60–1.
17. Fath Elbab TK, Abdelhamid AM, Galal EM, et al. Management of intravesical self-inflicted sharp objects in children: 10-year single-center experience. J Pediatr Urol. 2016;12(2):97.e1–5.
18. Manzella A, Filho PB, Albuquerque E, et al. Imaging of gossypibomas: pictorial review. AJR Am J Roentgenol. 2009;193(6 Suppl):S94–101.
19. Kim CK, Park BK, Ha H. Gossypiboma in abdomen and pelvis: MRI findings in four patients. AJR Am J Roentgenol. 2007;189:814–7.

27 Acute Abdominal Presentations of Neoplasia and Malignant Hemopathies

Anne M.J.B. Smets, Nathalie Rocourt, Eline E. Deurloo, and Elisa Amzallag-Bellenger

Contents

Abbreviations

ADC	Apparent diffusion coefficient
AFP	Alpha fetoprotein
AHT	Arterial hypertension
AII	Acute intestinal intussusception
ALL	Acute lymphoblastic leukemia
BP RMS	Bladder prostate rhabdomyosarcoma
CE-CT	Contrast-enhanced computed tomography
COG	Children's oncology group
CRC	Colorectal carcinoma
CT	Computed tomography
DWI	Diffusion weighted imaging
ERCP	Endoscopic retrograde cholangiopancreatography
FAP	Familial adenomatous polyposis
GI	Gastrointestinal
HCC	Hepatocellular carcinoma
HSCT	Hematopoietic stem cell transplantation
HSOS	Hepatic sinusoidal obstruction syndrome
IBD	Inflammatory bowel disease
MIBG	Metaiodobenzylguanidine
MRI	Magnetic resonance imaging

A.M.J.B. Smets (✉) • E.E. Deurloo
Department of Radiology, Academic Medical Center, Meibergdreef 9, 1105 AZ Amsterdam, The Netherlands
e-mail: a.m.smets@amc.uva.nl

N. Rocourt
Imagerie Médicale, Centre de Lutte Contre le Cancer Oscar Lambret, Avenue Combemale, BP 307 Lille, France

E. Amzallag-Bellenger
Department of Pediatric Imaging, Jeanne de Flandre Hospital, CHRU Lille, Av. Eugène Avinée 2, 59037 Lille-Cedex, France

F.E. Avni, P. Petit (eds.), *Imaging Acute Abdomen in Children*,
https://doi.org/10.1007/978-3-319-63700-6_27

MRTK	Malignant rhabdoid tumor of the kidney
PNET	Primitive neuroectodermal tumor
PTC	Percutaneous transhepatic cholangiography
RMS	Rhabdomyosarcoma
US	Ultrasonography
VOD	Veno-occlusive disease
WT	Wilms' tumor

27.1 Introduction

Children with an abdominal neoplasm or a malignant hemopathy may present with acute abdominal symptoms at any time during the course of their disease. The symptoms may be the first manifestation of cancer, they can be related to the subsequent therapy and may occur when there is progression or recurrence.

The most frequent abdominal symptom is pain. An abdominal mass may cause intense discomfort or pain due to its space-occupying nature. Poor intake and certain drugs such as vincristine, amitriptyline, and opioids may lead to constipation, accompanied by severe abdominal pain and opioids are known to cause paralytic ileus.

In many situations, the radiologist has a first-line role in the investigation of the origin of these symptoms and in the detection of possible health- or even life-threatening situations. A rapid and complete diagnosis is the aim of this emergency imaging in order to start adequate treatment in a timely manner. In this chapter, the most common acute abdominal manifestations and iatrogenic and non-iatrogenic complications of abdominal tumors and malignant hemopathies are discussed.

27.2 Rupture and Hemorrhage

27.2.1 Wilms' Tumor

Nephroblastoma or Wilms' tumor (WT), the most common pediatric renal tumor [1], is known for its propensity to bleed or rupture. Tumor rupture may occur spontaneously, during a surgical procedure or after minor abdominal trauma. This is why it is recommended to handle the tumor with care during clinical palpation and during surgery. The incidence of emergency surgery for preoperative tumor rupture has been estimated at 1.8% [2]. Clinical signs and symptoms are acute abdominal pain and a sudden drop in hemoglobin levels but tumor rupture is reported to be clinically silent in 33% of patients [3]. Intraperitoneal rupture is a diagnostic challenge for both the clinician and the radiologist, because it is a major risk factor for abdominal recurrence [4]. Demonstrating tumor rupture with imaging is a difficult matter. US is the first imaging test performed in a context of abdominal symptoms and it will confirm the presence of a renal tumor. Interruption of the tumor pseudo-capsula and ill-defined margins is suspicious for tumor rupture (Fig. 27.1a). The presence of ascites beyond the cul-de-sac, irrespective of attenuation, was reported to be the most useful indicator of tumor rupture on CE-CT in a study by Khanna et al. [5]. It has to be noted that an isolated small amount of fluid in the lowest part of the peritoneal cavity is frequently observed at diagnosis in patients with WT: this is not a reliable sign of intraperitoneal rupture since it can also be due to an inflammatory peritoneal reaction or to inferior vena cava compression or thrombosis. Retroperitoneal tumor rupture appears as intratumoral, subcapsular, or perirenal hemorrhage [3, 6] (Fig. 27.1b). Hemoperitoneum and/or intraperitoneal implants imply intraperitoneal dissemination [7]. In a study by the Children's Oncology Group (COG), the diagnostic performance of CT and MRI for abdominal staging in children with renal tumors was compared: preoperative tumor rupture was accurately classified by CT in 85.4% (70/82) and by MRI in 91.5% (75/82) of patients. Tumor rupture was present in only two patients in this cohort [8]. Whole abdominal radiotherapy is indicated when there is diffuse intra-abdominal tumor spread or gross preoperative or intraoperative rupture. This is an important burden for a young child; hence, the diagnosis of rupture should be weighed with care, as radiological findings are often equivocal. Ultimately, the post-nephrectomy pathology findings will determine the postoperative treatment.

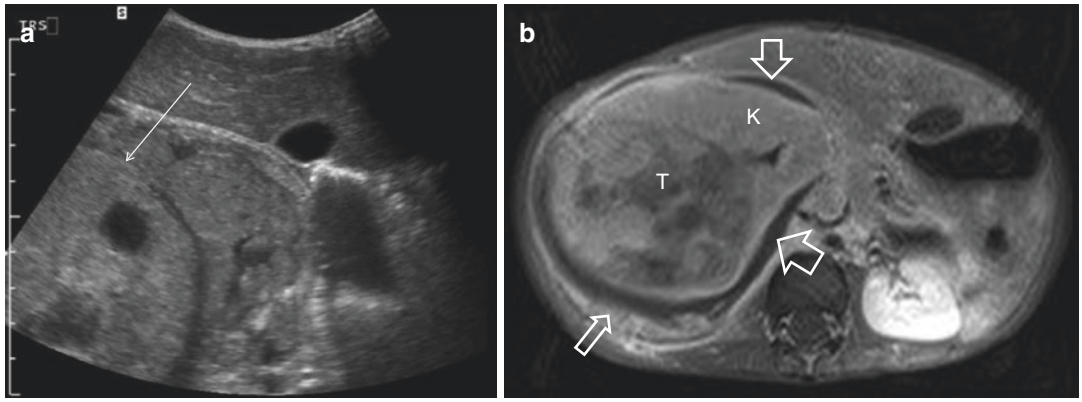

Fig. 27.1 A 2-year-old girl presenting with abdominal pain and low hemoglobin levels. (**a**) US shows a solid intrarenal tumor. The tumor has invade the renal pseudo-capsule locally (*white arrow*) (**b**) MR imaging: T1 fat sat post-Gd shows a subcapsular hematoma (*open arrows*) surrounding the right kidney (K) and the intrarenal tumor (T) (**b**). Pathology report after nephrectomy confirmed Wilms tumor with invasion of the pseudocapsula but no signs of intraperitoneal rupture

27.2.2 Spleen

Non-traumatic splenic rupture is a rare complication of hematological malignancies in children. A retrospective study found an incidence of 0.55% in a cohort of children with leukemia and lymphoma between 1991 and 1997 [9]. It may be the presenting symptom of leukemia but may also occur during treatment or recurrence. The mechanism is not totally understood and different etiologies have been suggested in the literature: splenic enlargement, leukemic infiltration of the splenic capsule, splenic infarction leading to hemorrhage of the capsule, leukemia-associated coagulopathy, and erosion or occlusion of blood vessels secondary to a fungal infection [9–13]. The signs and symptoms of non-traumatic splenic rupture are non-specific. Abdominal pain of varying intensity and location is a consistent symptom. US, the first-line imaging test, easily performed at bed-side, can identify peri-splenic and peritoneal effusion (hemorrhage), and subcapsular hemorrhage as a crescent collection at the convex border of the spleen [14]. In an emergency setting, CE-CT is usually the next diagnostic step [15–17]. The spleen being a vital organ in the protection against infection, non-operative management of splenic rupture in a stable trauma patient is considered the standard of care unless of course, the patient is hemodynamically unstable [18] (see also Chap. 17).

27.3 Gastro-intestinal Tract

Obstruction and inflammation of the gastrointestinal (GI) tract may occur acutely in a child with a malignancy. An abdominal tumor may be responsible for intestinal obstruction through compression, secondary intussusception, or direct tumoral invasion.

27.3.1 Intestinal Obstruction

Any abdominal tumor may compress the intestine and cause obstruction but Burkitt's lymphoma in particular is known for its close relation to the intestinal tract. Burkitt's lymphoma, a type of non-Hodgkin-lymphoma, is most frequently located in the abdomen. In 25% of cases the tumor is situated at the ileocecal junction, especially in children under 16 years, most likely because of the high concentration of lymphoid tissue in the terminal ileum [19, 20]. The typical clinical presentation is that of abdominal pain and/or a mass in the right lower quadrant. On imaging studies, the intestinal wall may appear locally thickened and hypoechoic and the intestinal wall structure may appear unclear [22] (Fig. 27.2a, b). Ascites is often present. Burkitt's lymphoma is a rare but well-known pathological lead point

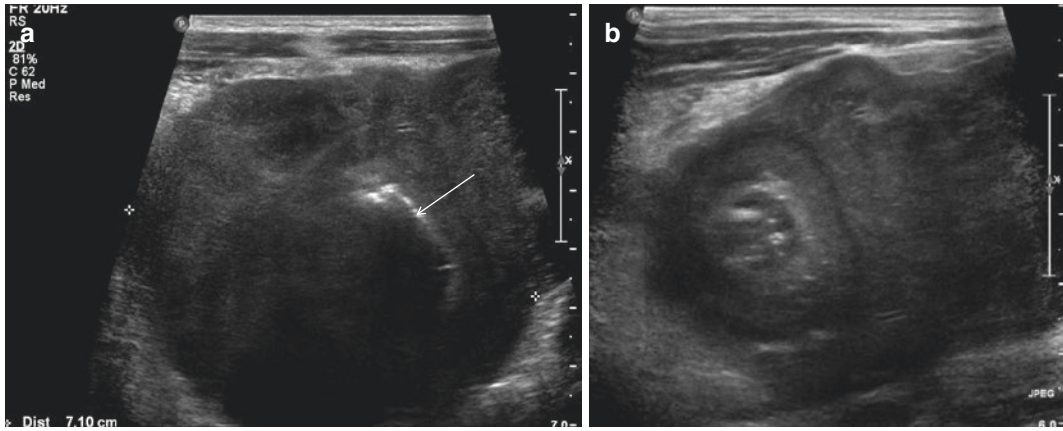

Fig. 27.2 A 7-year-old boy with severe and increasing intermittent abdominal pain and constipation since 4 weeks. US shows a large solid mass surrounding a bowel loop (*arrow*) (**a**), and a thickened and hypoechoic bowel wall up to 1 cm (**b**). The child was diagnosed with Burkitt's lymphoma

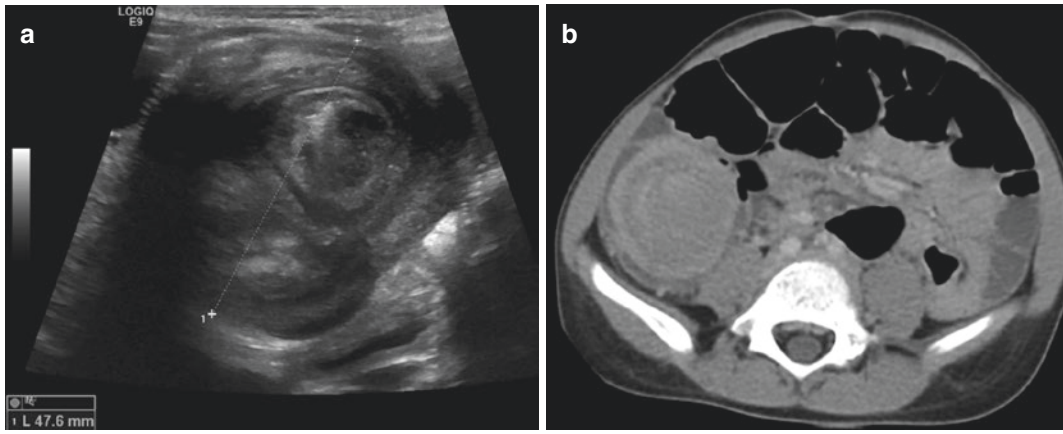

Fig. 27.3 A 5-year-old boy with right abdominal pain since 1 week. At US (**a**) an intestinal intussusception was found with a hypoechoic lobulated solid mass as leading point. (**b**) CE-CT displays an intussusception with an intraluminal mass. Pathology examination confirmed Burkitt's lymphoma

for acute intestinal intussusception (AII) and abdominal pain may be related to that complication. A history of weight loss and a longer duration of symptoms (abdominal pain, vomiting, and intestinal bleeding) are important clinical indications of lymphoma [21]. A lobulated (hypoechoic on US) mass is seen in the intussusceptum (Fig. 27.3a, b); At the end of a therapeutic enema, a mass will typically persist.

Colorectal carcinoma (CRC) is the most common primary GI tumor in children and adolescents, although extremely rare (1% of pediatric neoplasms) [22]. Presenting symptoms are abdominal pain, often cramping, bowel movement changes, rectal bleeding, nausea and/or vomiting, weight loss, and sometimes acute bowel obstruction [23]. The lack of specificity of the symptoms and the low diagnostic suspicion for cancer in children and particularly this type of cancer, frequently account for a delay in diagnosis. The poorer prognosis in young patients is related to this diagnostic delay as well as to the high incidence of poorly differentiated aggressive tumors. Children more frequently present with a more advanced stage (stage 3 and 4) and frequently have nodal involvement at diagnosis

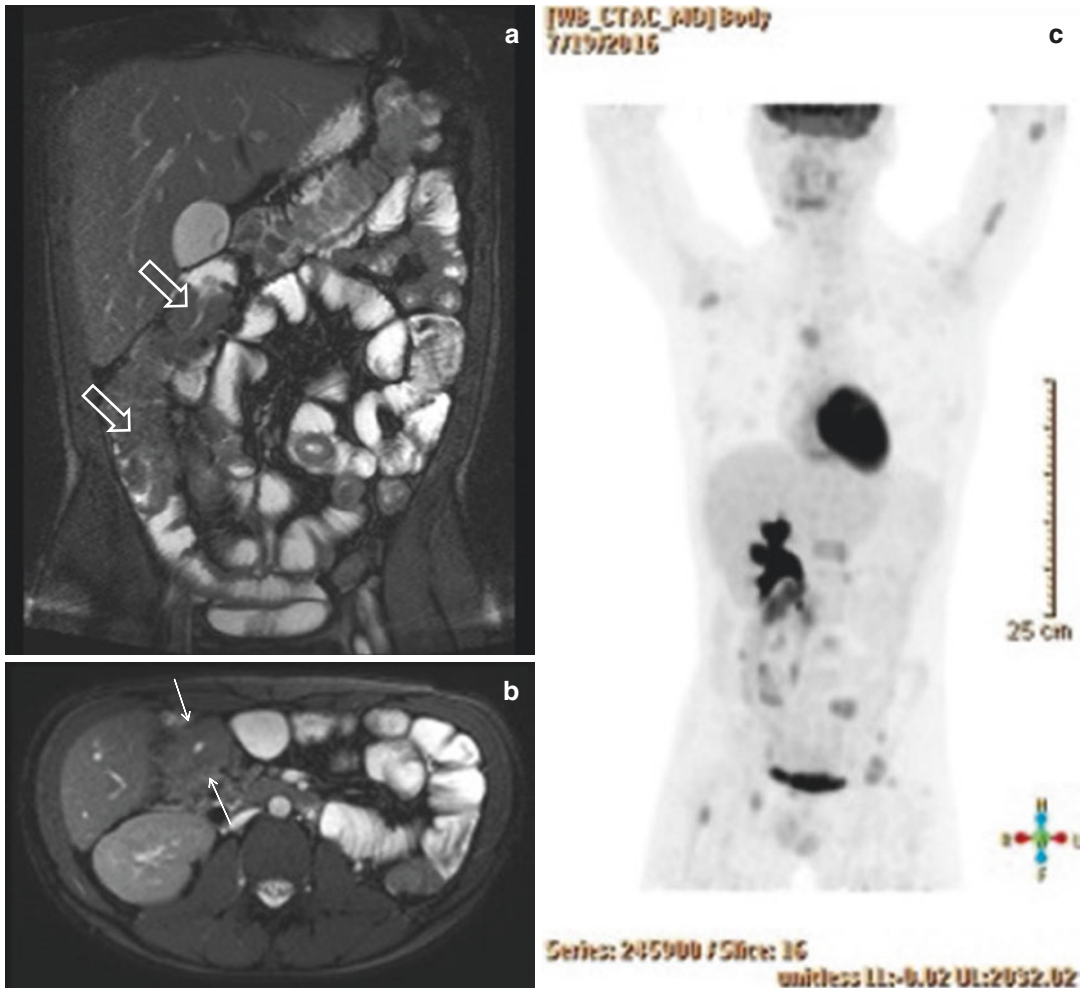

Fig. 27.4 This 16-year-old boy was referred for suspicion of IBD. He had a history of bowel movement changes, abdominal pain, and a weight loss of 17 kg in a period of 8 weeks. Coronal (**a**) and axial (**b**) T2-weighted images show a circumferential mass in the ascending and transverse colon (*arrows*). Workup with PET-CT (**c**) demonstrates multiple bone, peritoneal, and lymph node metastases from a primary colorectal carcinoma

compared to adults [23, 24]. Predisposing factors like familial adenomatous polyposis (FAP), inflammatory bowel disease (IBD), and Peutz-Jeghers syndrome are reported in only 10–30% [25]. The same genes and genetic pathways are found as in adult patients but overall the cancer biology is more aggressive [26]. Features of CRC on CT and MRI include focal or circumferential bowel wall thickening and luminal narrowing [27] (Fig. 27.4a–c). The final diagnosis is established with endoscopy and surgical biopsy or resection and histopathology examination.

27.3.2 GI Infection and Inflammation

Neutropenic colitis or typhlitis is a necrotizing infection occurring almost only in cancer patients. It is related to prolonged granulocytopenia and therefore most commonly encountered in patients with acute leukemia although any patient with neutropenia is at risk. In pediatric oncology patients, the reported incidence is between 0.5–6.7% and children above 16 years seem more prone to develop typhlitis [28, 29]. It is characterized by a classical triad of abdominal pain, fever

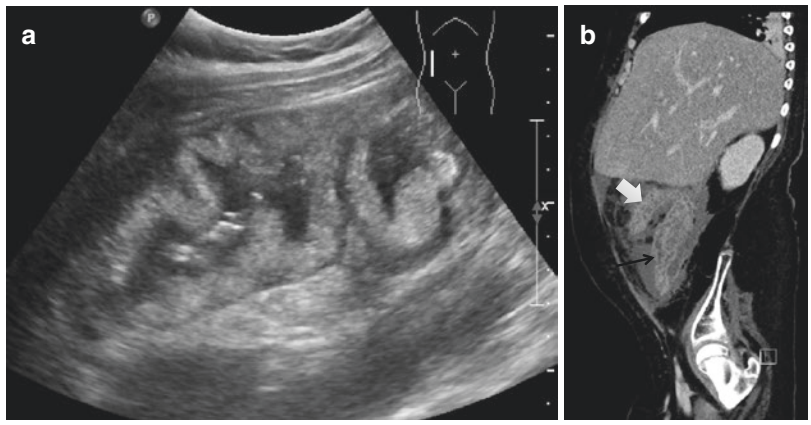

Fig. 27.5 During recurrence of AML, this 16-year-old girl developed typhlitis. On US, the ascending colon shows a thickened wall up to 1 cm (**a**). Another case of severe typhlitis in a 12-year-old girl with pre-B-ALL: the bowel wall of the entire colon and the terminal ileum was hypodense and thickened. Sagittal reconstruction (**b**) of CE-CT showing part of the ascending (*black arrow*) and part of the transverse colon (*white arrow*)

(although fever may be absent in the early stage of this complication), and neutropenia, and the diagnosis is confirmed by thickening of the bowel wall (≥3 mm) on imaging studies (Fig. 27.5a). Other common symptoms are abdominal tenderness, often localized in the right iliac fossa, vomiting, nausea, and constipation. The cecum and right colon are classically involved but McCarville et al. found the transverse colon and descending colon or rectum to be involved in 40% of a cohort of pediatric cancer patients [28] (Fig. 27.5b). Bowel wall thickness can be evaluated very accurately with high frequency US transducers, hence it is a reliable technique for detecting typhlitis. The treatment of choice is medical, with broad-spectrum antibiotics, granulocyte colony-stimulating factor, and total parenteral nutrition [30]. Surgery is required when typhlitis is complicated by perforation, uncontrolled sepsis, and GI bleeding [31]. In the latter, an interventional radiology procedure can also be attempted [32].

27.4 Liver, Biliary Tract, and Pancreas

27.4.1 Biliary Obstruction

Imaging is required whenever a mechanical obstruction needs to be excluded as a cause for jaundice (see Chap. 15). The most common cause of neoplastic biliary obstruction in childhood is embryonal rhabdomyosarcoma (RMS) of the biliary tree, accounting for 1% of all RMS [33]. It is a very rare tumor occurring in young children (median age 3 years) that obstructs the biliary system and usually presents with isolated jaundice [33, 34]. The tumor may arise in the liver parenchyma, in all parts of the biliary tree or within a choledochal cyst [35–38]. Differentiation from a choledochal cyst may at times be an issue: several case reports describe a biliary RMS mistaken for a choledochal cyst, which is a much more common cause of jaundice in a young child [39, 40]. With imaging, an intraductal mass is seen as well as the associated dilatation of the intrahepatic bile ducts (Fig. 27.6a, b). The enhancement pattern on CT is variable. On MRI, the tumor is usually predominantly hypointense on T1-weighted images and shows intense but inhomogeneous contrast enhancement [41]. The tumor is hyperintense on T2-weighted images and shows diffusion restriction (Fig. 27.6c–g). MR cholangiography can be performed in the same session. At percutaneous transhepatic cholangiography (PTC) and endoscopic retrograde cholangiopancreatography (ERCP), the ductal tumor is shown as filling defects with or without obstruction of the extrahepatic bile ducts (Fig. 27.6h) [35, 42].

The most common primary liver tumor in older children, hepatocellular carcinoma (HCC), very rarely presents with jaundice. Primary pancreatic tumors seldom present with jaundice but certain tumors that may invade the pancreas such as PNET, sarcoma or Burkitt's lymphoma may cause obstructive jaundice [43, 44] (Fig. 27.7a, b).

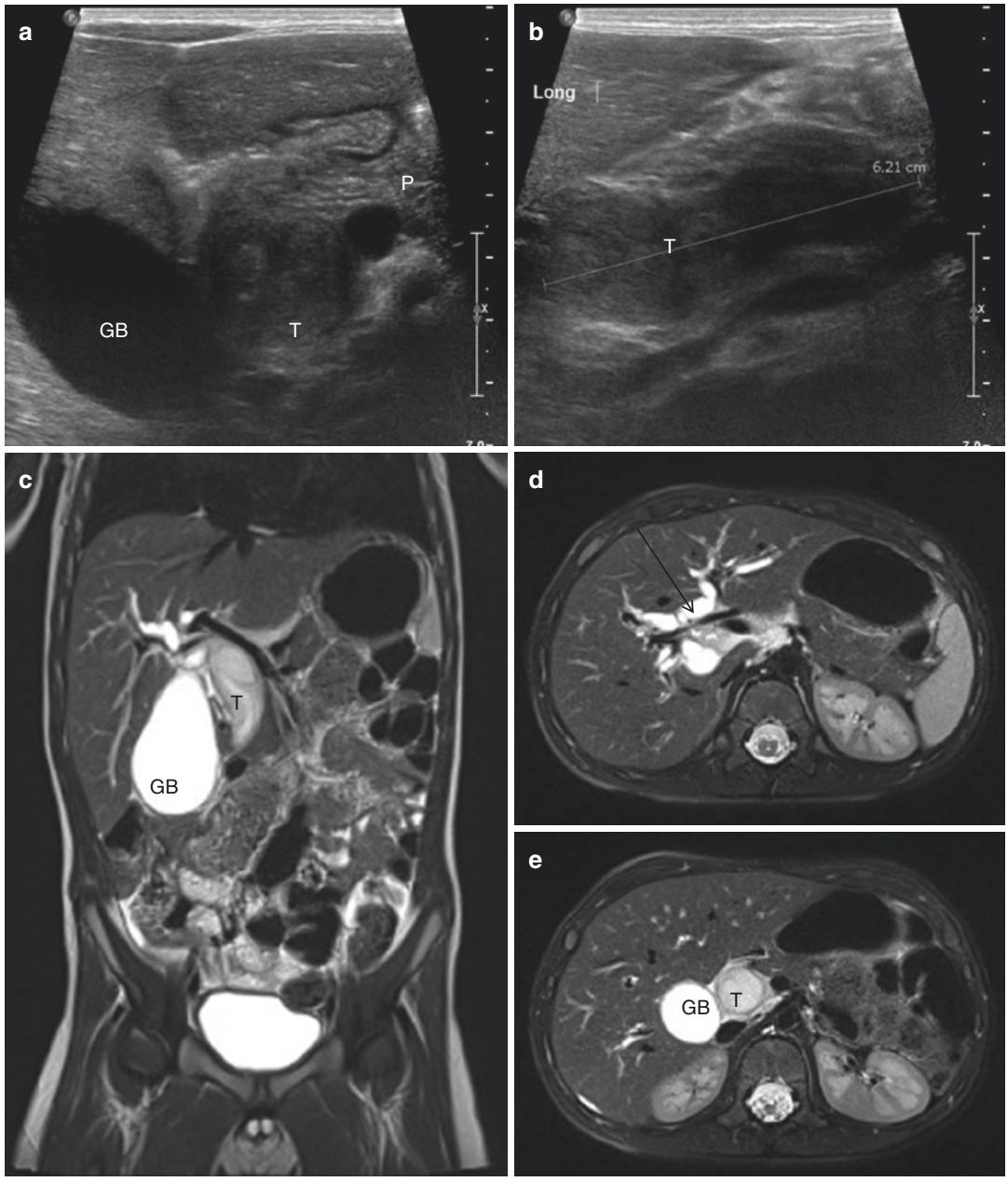

Fig. 27.6 This 3-year-old boy presented with progressive jaundice since 5 days. Axial (**a**) and sagittal (**b**) abdominal US and coronal (**c**) and axial (**d**, **e**) fat saturated T2-weighted MRI show a mass (T) in the distal choledochal duct (gall bladder (GB) and pancreas (P)) with secondary dilatation of the intrahepatic biliary ducts (*black arrow*). On diffusion-weighted images (*b* value = 800 s/mm^2) (**f**) and apparent diffusion coefficient (ADC) map (**g**) there is diffusion restriction in the tumor. ERCP shows filling defects in the choledochal duct (**h**)

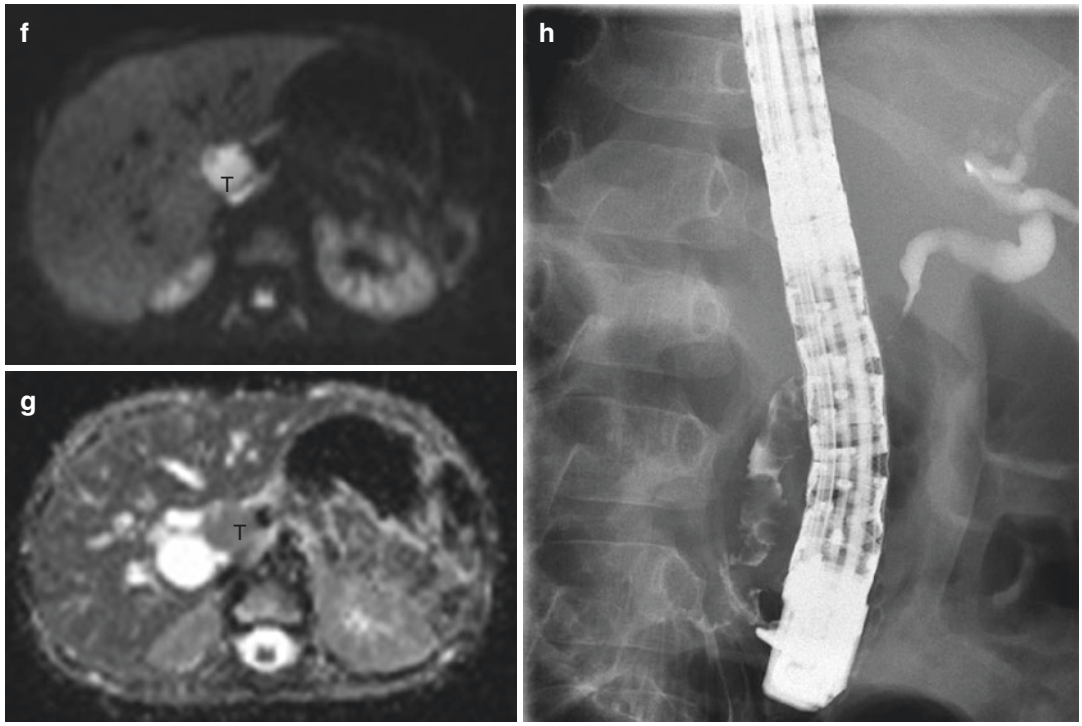

Fig. 27.6 (continued)

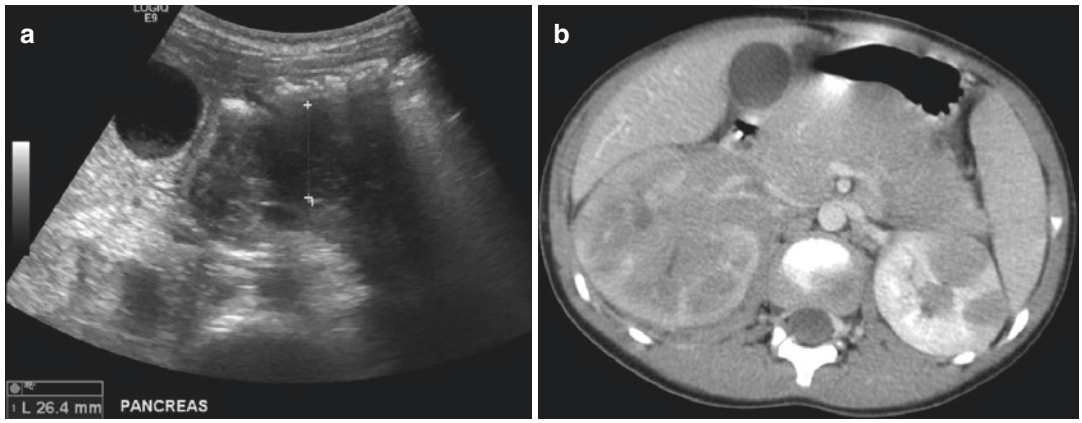

Fig. 27.7 A 5-year-old boy presented with anorexia, weight loss, and jaundice. (**a**) US shows an enlarged hypoechoic pancreas. (**b**) CE-CT shows infiltration of the pancreas and multiple nodules in the kidneys. Burkitt's lymphoma was diagnosed on renal biopsy

27.4.2 Veno-Occlusive Disease/ Hepatic Sinusoidal Obstruction Syndrome

Veno-occlusive disease (VOD), currently also known as hepatic sinusoidal obstruction syndrome (HSOS), is a serious, potentially life-threatening complication. It most commonly occurs after high dose chemotherapy in a context of hematopoietic stem cell transplantation (HSCT), with an incidence of 10–20% in children [45]. A milder form that usually resolves spontaneously occurs less frequently in patients receiving conventional chemotherapy [46–48]. Hepatic venous microvasculature is damaged and obliterated which leads to decreased liver outflow, causing portal hypertension.

Clinically, patients present with weight gain, fluid retention and ascites, painful hepatomegaly and jaundice. Laboratory findings are nonspecific. A reliable predictive diagnostic test is still lacking although according to recent publications, an increase in maximum systolic velocity of the hepatic artery and an increase in liver stiffness evaluated by transient elastography might be early findings of VOD in children [49–51].

27.4.3 Massive Hepatomegaly

Primary and secondary malignancies are uncommon causes of hepatomegaly in neonates and children. They may present as a life-threatening condition with respiratory distress and require an emergency workup and subsequent treatment. Cellular infiltration as a cause of hepatomegaly can be due to primary malignant tumors of the liver, mainly hepatoblastoma and HCC or metastatic disease. Hepatoblastoma is the most frequent malignant liver tumor of young children. The patients are younger than 5 years of age in 90% of the patients. Hepatoblastoma is usually solitary but in 20% of patients it is multifocal. HCC is the most frequent primary hepatic tumor of older children and adolescents. Primary hepatic malignancies in children usually present with progressive abdominal distension, hepatomegaly, or with an asymptomatic abdominal mass [34]. Alpha-fetoprotein (AFP) is strongly elevated in 90% of patients with hepatoblastoma, which makes it a very useful marker.

Diffuse metastatic infiltration can be seen in leukemia, lymphoma, and neuroblastoma. Liver infiltration is common in an advanced stage of neuroblastoma (stage 4) but is also part of a particular phenotype, stage 4S, with a favorable outcome and a usually spontaneously regressing small primary tumor. (Criteria necessary to meet with this particular stage are age below 1 year, dissemination limited to skin, liver, and/or bone marrow (and involvement of less than 10% of total nucleated cells) and metaiodobenzylguanidine (MIBG) scan negative for bone marrow [52]. Hepatomegaly, which is at times extensive, is often the presenting symptom. On US the liver contains multiple round isoechoic tumors surrounded by a hypoechoic rim (Fig. 27.8a) and on MRI the liver shows nodular infiltration (Fig. 27.8c–e). The metastases tend to hypoenhance compared to the liver parenchyma on CE-CT and post-Gd MRI. The primary tumor is usually small, sometimes calcified (Fig. 27.8b). Urine should be tested for elevated catecholamine levels and if necessary a MIBG-scan must be performed, to confirm neuroblastoma. In infants, on occasion, diffuse hepatic hemangiomatosis may mimic metastatic infiltration from neuroblastoma. A decreasing diameter of the abdominal aorta below the celiac trunk and a large hepatic artery are suggestive of

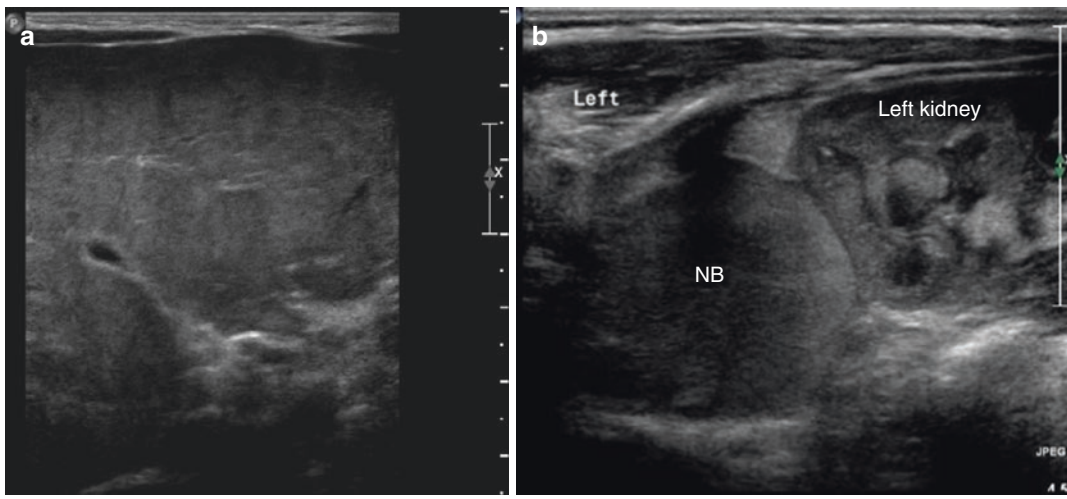

Fig. 27.8 Two-month-old infant with progressive abdominal distention and hepatomegaly. On US an enlarged liver is seen with heterogeneous liver parenchyma (**a**). There is a primary neuroblastoma (NB) of 2.5 cm in the left adrenal gland (**b**). T1- (**c**) and T2-weighted (**d**) axial and coronal T2-weighted (**e**) MRI shows hepatomegaly and diffuse nodular infiltration of the parenchyma and the primary tumor (NB) in the left adrenal gland

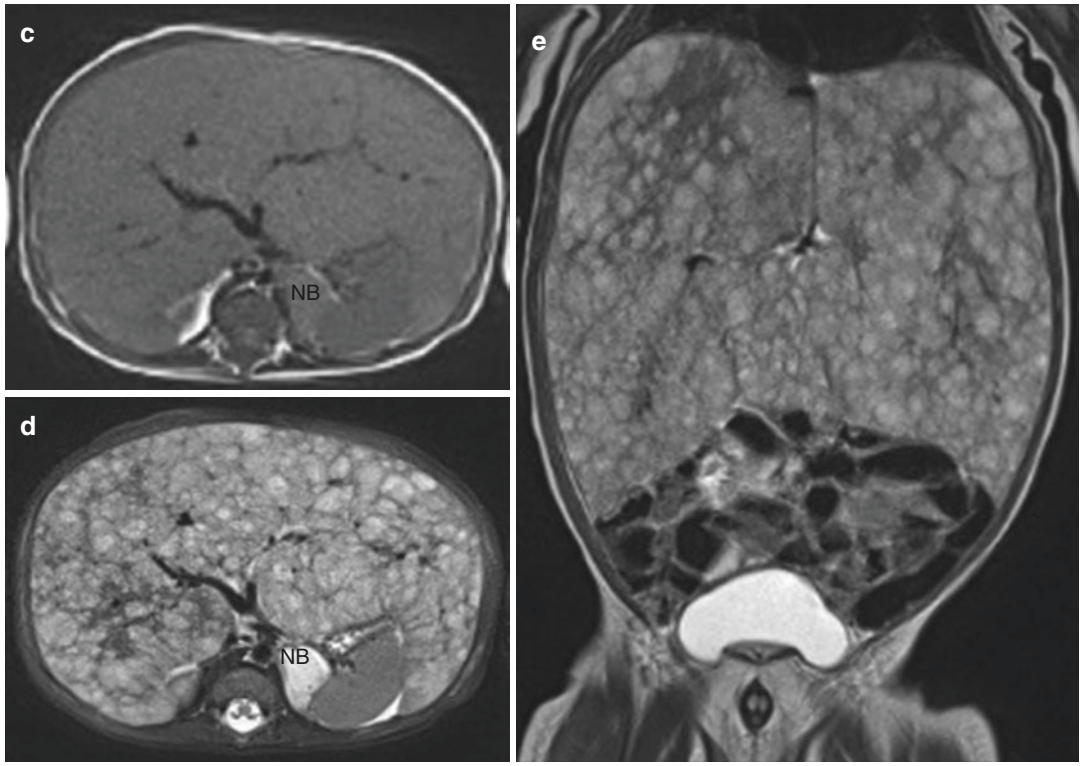

Fig. 27.8 (continued)

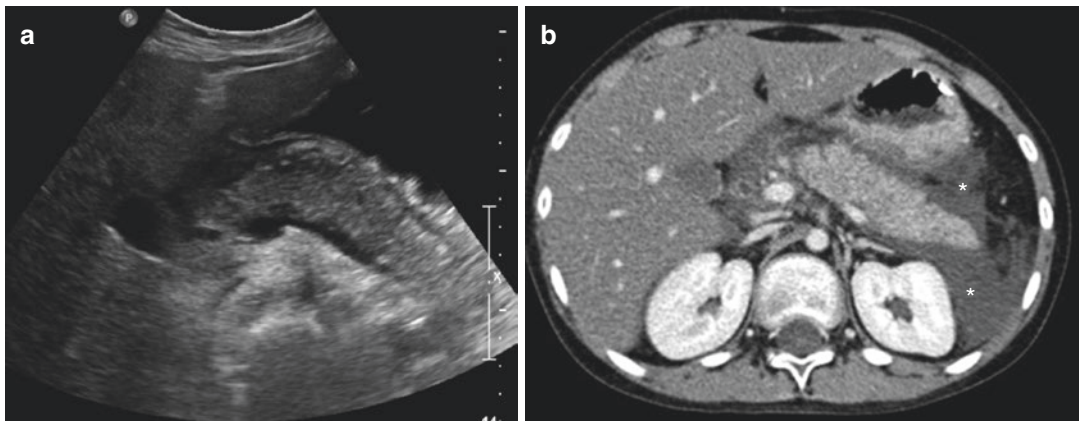

Fig. 27.9 During treatment with L-asparaginase for ALL, this 12-year-old boy developed acute pancreatitis. On US (**a**) and CE-CT (**b**) the pancreas is diffusely enlarged and there is intra- and retroperitoneal free fluid (*)

infantile liver hemangiomas as well as the hyperenhancing pattern (see also Chaps. 8 and 15).

27.4.4 Pancreatitis

A large number of chemotherapeutic drugs may induce pancreatitis in children. The drugs used in the treatment of acute lymphoblastic leukemia, doxorubicin, vincristine, prednisolone, and L-asparaginase in particular are known to cause pancreatitis [53]. L-asparaginase may even lead to severe necrotic pancreatitis [54]. Diffuse enlargement of the pancreas as well as peripancreatic fat streaking and fluid collections is seen on all imaging modalities (Fig. 27.9a, b).

High blood levels of amylase and lipase confirm the diagnosis. Burkitt's lymphoma very rarely presents with pancreatitis [44].

27.5 Genitourinary System

Genitourinary (GU) symptoms can be caused by a tumor, primarily or secondarily and may also be seen as side effects of oncologic therapy.

27.5.1 Urinary Retention

Whenever there is a decrease or absence of micturition in a child, it should be determined whether the cause is pre-renal, renal, or postrenal (see also Chaps. 6, 20, and 21). Large abdominal or pelvic tumors may cause urinary retention due to postrenal compression at the level of the ureters or the bladder and intrinsic tumors may obstruct the urethra (Fig. 27.10a, b). The most common intrinsic tumor of the lower urinary tract in the first 2 decades of life—with a peak incidence around 3 years and another peak during adolescence—is RMS. When a RMS arises from the bladder or the prostate, it is called a bladder-prostate (BP) RMS, because it usually infiltrates both structures. In girls both bladder and vagina may be infiltrated simultaneously. In BP RMS, the tumor frequently causes bladder outlet obstruction and urinary retention, which can be accompanied by obstipation, tenesmus, and urinary symptoms like dysuria, pollakiuria, and rarely hematuria. After initial US has discovered a bladder mass, MRI is the next step in the imaging workup. BP RMS shows nonspecific low signal intensity on T1-weighted and high signal on T2-weighted images and enhances heterogeneously (Fig. 27.11a–e). Heterogeneity may be due to intratumoral hemorrhage [55]. It is at times impossible to differentiate infiltration of the bladder wall from hypertrophy due to bladder outlet obstruction.

Certain types of abdominal tumors, particularly neuroblastoma, but also lymphoma and rhabdomyosarcoma, may invade the spinal canal, compress the spinal cord, and lead to neurological symptoms such as urinary retention (Fig. 27.12a, b).

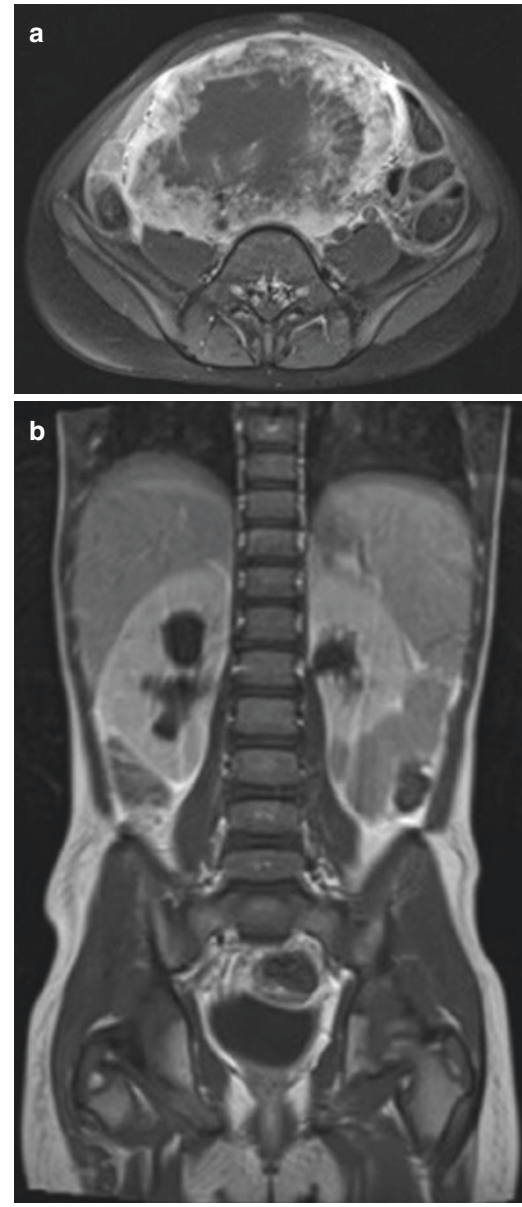

Fig. 27.10 Supravesical rhabdomyosarcoma in a 4-year-old boy. T1-weighted MRI post-Gd shows an enhancing tumor with central necrosis (**a**). The close relationship of the tumor with the ureters causes bilateral hydronephrosis (**b**)

27.5.2 Hypertension

Hypertension can be related to pain and anxiety, medication (corticosteroids, cyclosporine A, amphotericin) or fluid overload. It can also be due to renal artery or renal parenchyma compression or stretching by a mass with subsequent increase of renin production.

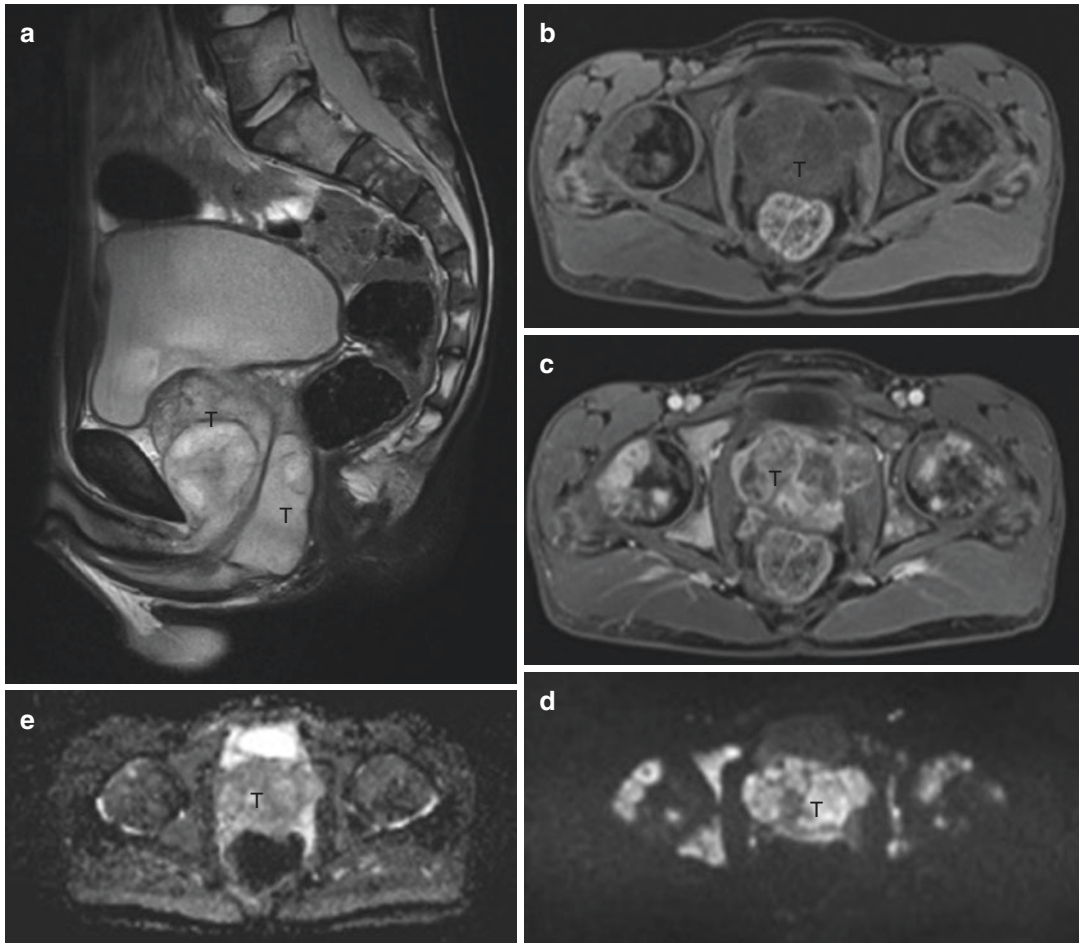

Fig. 27.11 This 16-year-old boy presented with acute urinary retention. There is a lobulated tumor (T) within the prostate, hyperintense on T2-weighted (**a**), hypointense on fat saturated T1-weighted (**b**) and heterogeneously enhancing on post-Gd T1-weighted images (**c**). The tumor shows heterogeneous diffusion restriction on diffusion-weighted images (b value = 1000 s/mm^2) (**d**) and apparent diffusion coefficient (ADC) map (**e**). Bone metastases of this alveolar rhabdomyosarcoma are visible in the pelvic bones, femora, and lumbosacral spine (hyperintense areas in the skeleton on Figs. 27.10a–d)

In 10–27% of the patients with neuroblastoma, hypertension is a presenting symptom due to the vasoconstrictive catecholamines secreted by the tumor and/or to tumoral compression of the renal artery, which stimulates the renin-aldosterone system [56]. Abdominal US is part of the workup for pediatric arterial hypertension, in order to exclude a renal tumor or a neuroblastoma that will be confirmed by CE-CT or MR imaging (Fig. 27.13).

27.5.3 Hematuria

Hemorrhagic cystitis can be a complication of cancer treatment. It is caused by damage to the bladder transitional epithelium and to the vessels by toxins, drugs (like cyclophosphamide and ifosfamide), radiation, and infection [31, 57]. Sometimes, hematuria is the presenting symptom of a tumor of the urinary tract. The most frequent renal tumor of infancy, WT, is reported to present

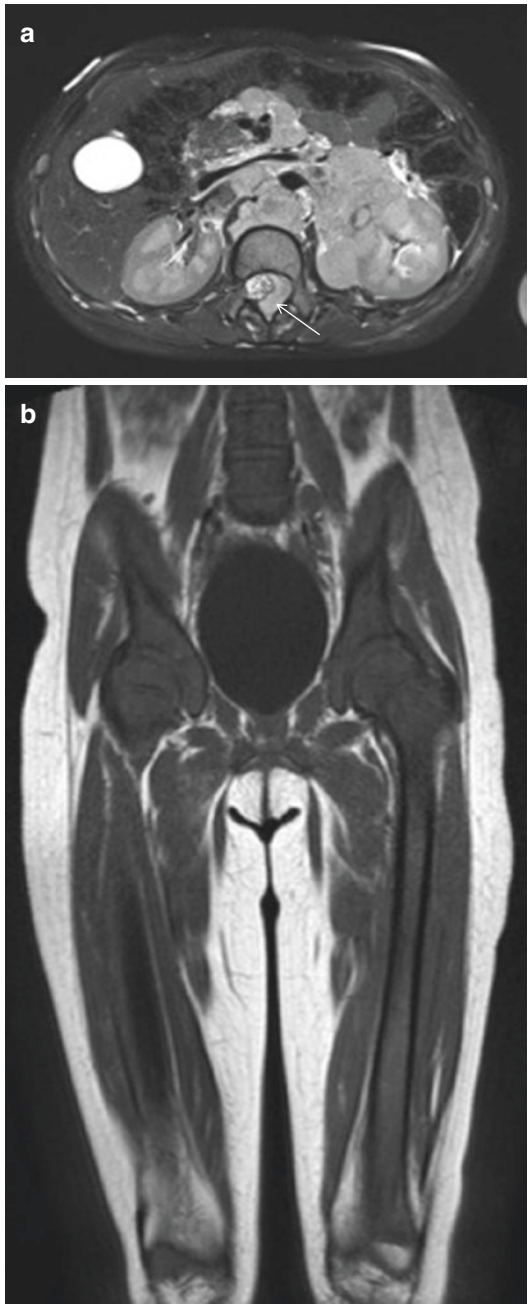

Fig. 27.12 A 4-year-old girl presenting with acute urinary retention. (**a**) On this fat saturated T2-weighted image a lobulated neuroblastoma with an intraspinal component (*white arrow*) is shown. (**b**) On this coronal T1-weighted image of pelvis and femora, the bone marrow is diffusely hypointense due to tumoral infiltration

with microscopic hematuria in 25% of cases. Macroscopic hematuria seldom occurs and is usually related to invasion of the renal pelvis

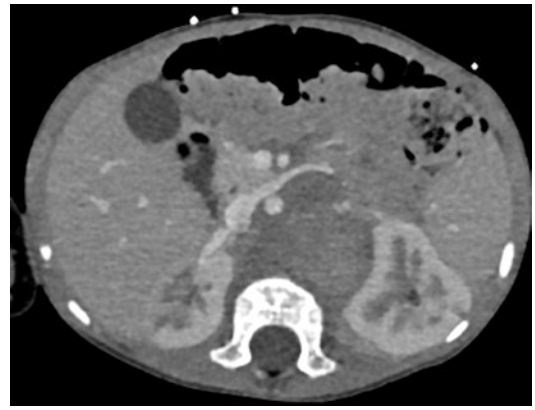

Fig. 27.13 This 22-month-old boy was admitted for arterial hypertension. On ultrasound, an adrenal mass was found (not shown). CE-CT shows a solid hypoenhancing left adrenal mass. It crosses the midline and stretches the right renal vessels causing impaired enhancement of the right kidney

[58]. Malignant rhabdoid tumor of the kidney (MRTK) is a rare, aggressive renal tumor occurring in young infants. Microscopic hematuria is present much more frequently (75.9%) [59], possibly because MRTK develops more centrally and close to the renal pelvis whereas WT is more often situated in the peripheral renal parenchyma. There are no reliable and constant features that are helpful in differentiating MRTK from WT although MRTK should always be considered in children younger than 2 years old, when the tumor contains linear calcifications and particularly when metastases are present at diagnosis [60] (Fig. 27.14a–c).

RMS is the most frequent bladder tumor in children. Although in most cases a BP RMS presents with bladder outlet obstruction, urinary symptoms, mimicking cystitis and hematuria may occasionally be more prominent. Persistent hematuria without a context of infection or trauma should always be investigated with US of the urinary tract. The bladder should be reasonably filled and if necessary, it can also be examined with a perineal approach. Bladder wall thickening, diffuse or focal should be further analyzed. Mobilization of the patient and color Doppler can be of help to differentiate debris or a blood clot from a tumor. MRI is the next step in the imaging workup.

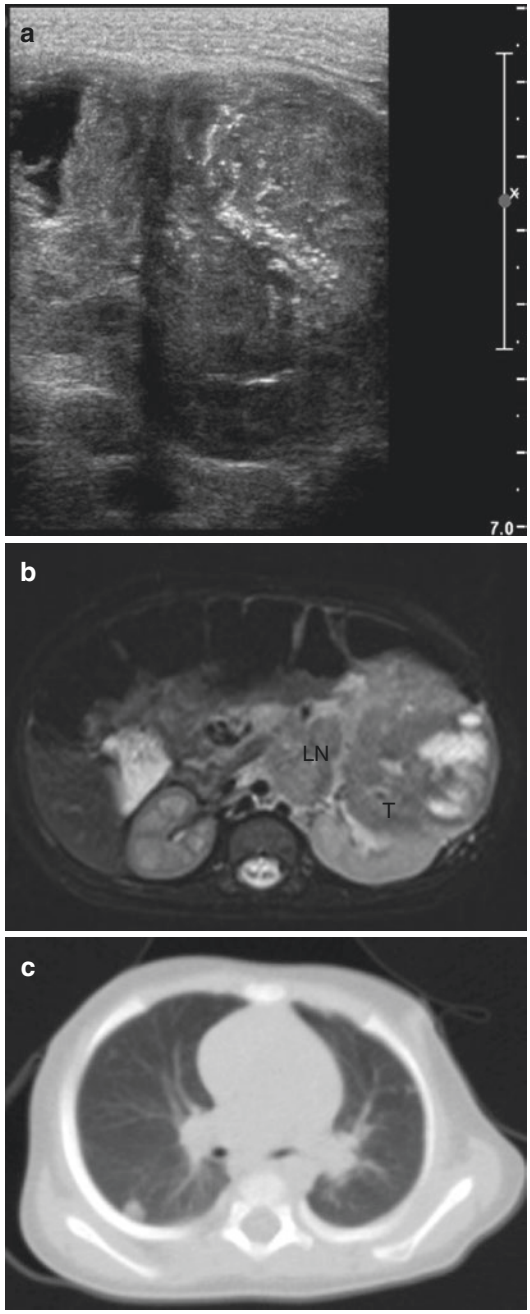

Fig. 27.14 A 5-month-old girl presented with a palpable mass in the left flank and an episode of macroscopic hematuria. US shows a solid left renal mass containing linear calcifications (**a**). On fat saturated T2-weighted MRI the tumor (T) shows a close relation to the left renal pelvis and several large lymph around the renal hilum (LN) (**b**). Lung metastases were present at diagnosis (**c**). The child also had a synchronic brain tumor (not shown). Pathology examination revealed a malignant rhabdoid tumor of the kidney

27.5.4 Ovarian Torsion
(See Also Chap. 24)

The incidence of an ovarian torsion related to underlying ovarian abnormalities in children is reported to be 27–48%. Ovarian cysts and teratomas and more rarely cystadenoma are the most commonly encountered lesions [61, 62]. A review of the literature indicates that in children underlying malignancies occur with an incidence of 1.8%, and consist mainly of germ cell tumors [62] (Fig. 27.15a–c). The main presenting symptoms of ovarian torsion are abdominal pain, nausea, vomiting, and fever. US is the primary imaging test to be performed. In a study by Servaes et al. [61], it appeared that the likelihood of an underlying ovarian mass increased with increasing volume ratio: a volume ratio greater than 20 yielded a probability of the patient having an ovarian mass of 70%. If the volume ratio was 20 or less, the probability that the torsed ovary was otherwise normal was approximately 90%. Regardless of an ovarian mass, ovarian torsion is a surgical emergency.

Conclusion

Imaging plays a major role in the detection of abdominal tumors and the abdominal manifestations of malignant hemopathies. At diagnosis and during the course of cancer treatment, patients may present with acute abdominal symptoms related to the tumor, to complications of the disease and/or the treatment and to a recurrence. It is important for radiologists examining children to know about these presenting symptoms and complications.

- WT is prone to hemorrhage and rupture and it should be carefully handled at examination.
- Splenic rupture is a rare complication of leukemia and lymphoma in children.
- Abdominal Burkitt's lymphoma is often related to the intestinal tract and can cause primary intestinal obstruction and secondary obstruction due to intussusception.
- Neutropenic colitis or typhlitis is a serious complication in neutropenic patients, especially patients with ALL.

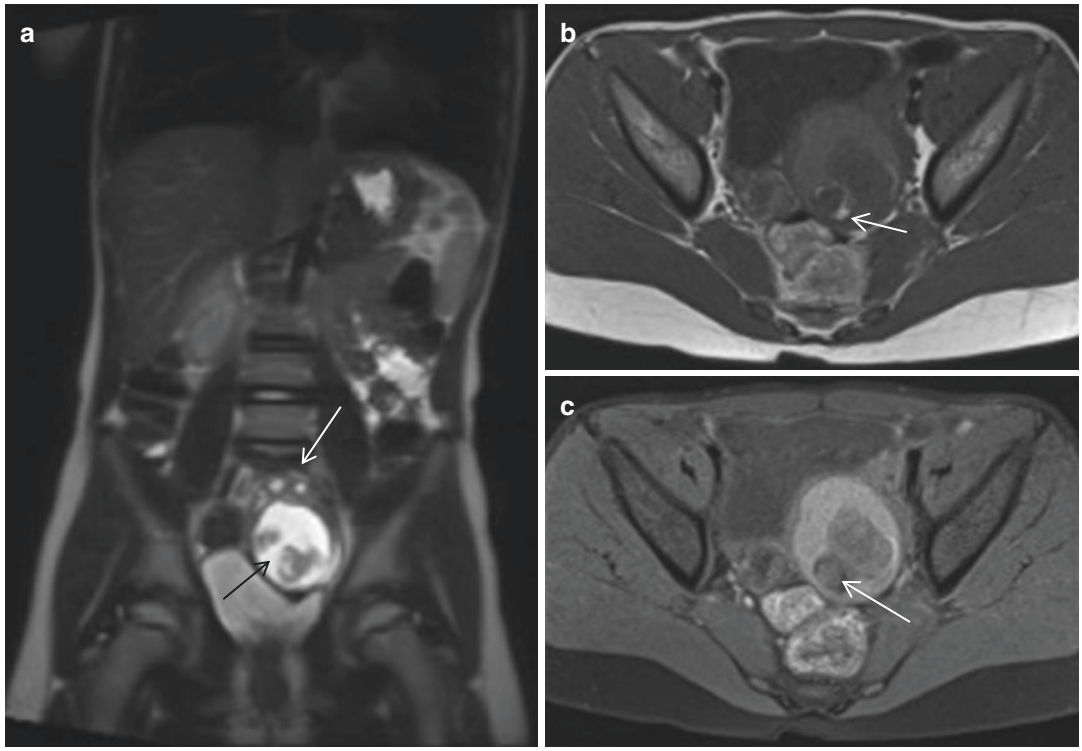

Fig. 27.15 Ovarian torsion with an underlying tumor in an 8-year-old girl with a short history of cyclic cramping abdominal pain and vomiting. On coronal T2-weighted MRI the left ovary is shown, it is enlarged and there is a string-of-pearls configuration of the follicles, indicating torsion (*white arrow*). The ovary carries is a well-circumscribed rounded tumor containing fluid and solid components (**a**). T1-weighted images without (**b**) and with (**c**) fat suppression show a fatty component within the tumor (*arrows*). Pathology examination confirmed the diagnosis of mature teratoma

- The most common neoplastic cause of isolated jaundice in children is RMS of the biliary tract. It may be mistaken for a choledochal cyst.
- An iatrogenic hepatic complication of chemotherapy, especially high dose chemotherapy, is VOD.
- Massive hepatomegaly may be caused by a primary hepatic tumor or by metastatic infiltration; in infants and young children neuroblastoma is the main cause.
- Pancreatitis is a well-known complication of specific chemotherapeutic drugs such as L-asparaginase.
- Urinary retention can result from tumoral obstruction, extrinsic or intrinsic or can be due to spinal cord compression from an intraspinal tumor component.
- Renal tumors and neuroblastoma may cause AHT due to renal compression or stretching of the renal artery; high catecholamine levels may also be a causative factor.
- Hematuria may be a sign of a tumor of the urinary tract. MRTK is in most cases associated with macroscopic hematuria. Oncologic treatment may cause hemorrhagic cystitis.
- Very rarely, a malignancy is the underlying cause of ovarian torsion in a child or adolescent.

References

1. Geller E, Kochan PS. Renal neoplasms of childhood. Radiol Clin N Am. 2011;49(4):689–709. vi
2. Godzinski J, et al. Primary nephrectomy for emergency: a rare event in the International Society of Paediatric Oncology Nephroblastoma Trial and Study no. 9. Eur J Pediatr Surg. 2001;11(1):36–9.
3. Brisse HJ, et al. Preoperative Wilms tumor rupture: a retrospective study of 57 patients. Cancer. 2008;113(1):202–13.
4. Shamberger RC, et al. Surgery-related factors and local recurrence of Wilms tumor in National Wilms Tumor Study 4. Ann Surg. 1999;229(2):292–7.
5. Khanna G, et al. Detection of preoperative Wilms tumor rupture with CT: a report from the Children's Oncology Group. Radiology. 2013;266(2):610–7.
6. Byerly D, Coley B, Ruymann F. Perirenal hemorrhage as first presentation of Wilms tumor. Pediatr Radiol. 2006;36(7):714–7.
7. Slasky BS, et al. CT appearances of involvement of the peritoneum, mesentery and omentum in Wilms' tumor. Pediatr Radiol. 1997;27(1):14–7.
8. Servaes S, et al. Comparison of diagnostic performance of CT and MRI for abdominal staging of pediatric renal tumors: a report from the Children's Oncology Group. Pediatr Radiol. 2015;45(2):166–72.
9. Athale UH, et al. Splenic rupture in children with hematologic malignancies. Cancer. 2000;88(2):480–90.
10. Knoblich R. Pathologic (so-called spontaneous) rupture of spleen in leukemia and lymphoma. Mich Med. 1966;65(2):105–10.
11. Bauer TW, Haskins GE, Armitage JO. Splenic rupture in patients with hematologic malignancies. Cancer. 1981;48(12):2729–33.
12. Shih LY, Su IJ. Chronic myeloid leukemia: manifesting as spontaneous splenic rupture and terminating in megakaryoblastic transformation. Med Pediatr Oncol. 1987;15(1):31–7.
13. Gorg C, et al. Spontaneous splenic rupture in acute myeloid leukemia: sonographic follow-up study. Bildgebung. 1994;61(1):37–9.
14. Gorg C, et al. Spontaneous rupture of the spleen: ultrasound patterns, diagnosis and follow-up. Br J Radiol. 2003;76(910):704–11.
15. Tonolini M, Bianco R. Nontraumatic splenic emergencies: cross-sectional imaging findings and triage. Emerg Radiol. 2013;20(4):323–32.
16. Gardner RV, et al. Splenic artery embolization as emergency treatment of splenic rupture in a child with T-cell acute lymphocytic leukemia having t(8;14) translocation. Med Pediatr Oncol. 2003;41(5):492–3.
17. Catalano O, et al. Real-time, contrast-specific sonography imaging of acute splenic disorders: a pictorial review. Emerg Radiol. 2004;11(1):15–21.
18. Stephenson JT, DuBois JJ. Nonoperative management of spontaneous splenic rupture in infectious mononucleosis: a case report and review of the literature. Pediatrics. 2007;120(2):e432–5.
19. Biko DM, et al. Childhood Burkitt lymphoma: abdominal and pelvic imaging findings. AJR Am J Roentgenol. 2009;192(5):1304–15.
20. Molyneux EM, et al. Burkitt's lymphoma. Lancet. 2012;379(9822):1234–44.
21. Navarro O, et al. The impact of imaging in the management of intussusception owing to pathologic lead points in children. A review of 43 cases. Pediatr Radiol. 2000;30(9):594–603.
22. Rao BN, et al. Colon carcinoma in children and adolescents. A review of 30 cases. Cancer. 1985;55(6):1322–6.
23. LaQuaglia MP, et al. Prognostic factors and outcome in patients 21 years and under with colorectal carcinoma. J Pediatr Surg. 1992;27(8):1085–9. discussion 1089-90
24. Poles GC, et al. Colorectal carcinoma in pediatric patients: a comparison with adult tumors, treatment and outcomes from the National Cancer Database. J Pediatr Surg. 2016;51(7):1061–6.
25. Hubbard JM, Grothey A. Adolescent and young adult colorectal cancer. J Natl Compr Cancer Netw. 2013;11(10):1219–25.
26. Khan SA, et al. Colorectal cancer in the very young: a comparative study of tumor markers, pathology and survival in early onset and adult onset patients. J Pediatr Surg. 2016;51(11):1812–7.
27. Horton KM, Abrams RA, Fishman EK. Spiral CT of colon cancer: imaging features and role in management. Radiographics. 2000;20(2):419–30.
28. McCarville MB, et al. Typhlitis in childhood cancer. Cancer. 2005;104(2):380–7.
29. Mullassery D, et al. Diagnosis, incidence, and outcomes of suspected typhlitis in oncology patients--experience in a tertiary pediatric surgical center in the United Kingdom. J Pediatr Surg. 2009;44(2):381–5.
30. Sundell N, et al. Management of neutropenic enterocolitis in children with cancer. Acta Paediatr. 2012;101(3):308–12.
31. Chui CH. Surgical management of complications of multimodal therapy. Pediatr Blood Cancer. 2012;59(2):405–9.
32. de Lijster MS, et al. Embolisation for caecal bleeding in a child with typhlitis. Pediatr Radiol. 2015;45(2):283–5.
33. Ruymann FB, et al. Rhabdomyosarcoma of the biliary tree in childhood. A report from the Intergroup Rhabdomyosarcoma Study. Cancer. 1985;56(3):575–81.
34. Chung EM, et al. From the archives of the AFIP: pediatric liver masses: radiologic-pathologic correlation. Part 2. Malignant tumors. Radiographics. 2011;31(2):483–507.
35. Linstedt-Hilden M, Brambs HJ. Two different manifestations of botryoid sarcoma (embryonal rhabdomyosarcoma) of the biliary tree. Bildgebung. 1994;61(1):40–3.
36. Mihara S, et al. Botryoid rhabdomyosarcoma of the gallbladder in a child. Cancer. 1982;49(4):812–8.

37. Caty MG, Oldham KT, Prochownik EV. Embryonal rhabdomyosarcoma of the ampulla of Vater with long-term survival following pancreaticoduodenectomy. J Pediatr Surg. 1990;25(12):1256–8.
38. Patil KK, et al. Embryonal rhabdomyosarcoma within a choledochal cyst. Can Assoc Radiol J. 1992;43(2):145–8.
39. Ali S, Russo MA, Margraf L. Biliary rhabdomyoscarcoma mimicking choledochal cyst. J Gastrointestin Liver Dis. 2009;18(1):95–7.
40. Tireli GA, et al. Embryonal rhabdomyosarcoma of the common bile duct mimicking choledochal cyst. J Hepato-Biliary-Pancreat Surg. 2005;12(3):263–5.
41. Roebuck DJ, et al. Hepatobiliary rhabdomyosarcoma in children: diagnostic radiology. Pediatr Radiol. 1998;28(2):101–8.
42. Cannon PM, Legge DA, O'Donnell B. The use of percutaneous transhepatic cholangiography in a case of embryonal rhabdomyosarcoma. Br J Radiol. 1979;52(616):326–7.
43. Chung EM, Travis MD, Conran RM. Pancreatic tumors in children: radiologic-pathologic correlation. Radiographics. 2006;26(4):1211–38.
44. Amodio J, Brodsky JE. Pediatric Burkitt lymphoma presenting as acute pancreatitis: MRI characteristics. Pediatr Radiol. 2010;40(5):770–2.
45. Cesaro S, et al. A prospective survey on incidence, risk factors and therapy of hepatic veno-occlusive disease in children after hematopoietic stem cell transplantation. Haematologica. 2005;90(10):1396–404.
46. Mohty M, et al. Sinusoidal obstruction syndrome/veno-occlusive disease: current situation and perspectives-a position statement from the European Society for Blood and Marrow Transplantation (EBMT). Bone Marrow Transplant. 2015;50(6):781–9.
47. Choi A, et al. Severe hepatic sinusoidal obstruction syndrome in a child receiving vincristine, actinomycin-D, and cyclophosphamide for rhabdomyosarcoma: successful treatment with defibrotide. Cancer Res Treat. 2016;48(4):1443–7.
48. Cesaro S, et al. Veno-occlusive disease in pediatric patients affected by Wilms tumor. Pediatr Blood Cancer. 2011;57(2):258–61.
49. McCarville MB, et al. Hepatic veno-occlusive disease in children undergoing bone-marrow transplantation: usefulness of sonographic findings. Pediatr Radiol. 2001;31(2):102–5.
50. Kaya N, et al. The diagnostic value of hepatic arterial velocity in venoocclusive disease after pediatric hematopoietic stem cell transplantation. J Pediatr Hematol Oncol. 2017;39:249.
51. Colecchia A, et al. Usefulness of liver stiffness measurement in predicting hepatic veno-occlusive disease development in patients who undergo HSCT. Bone Marrow Transplant. 2017;52(3):494–7.
52. Brodeur GM, et al. Revisions of the international criteria for neuroblastoma diagnosis, staging, and response to treatment. J Clin Oncol. 1993;11(8):1466–77.
53. Raja RA, et al. Serial ultrasound monitoring for early recognition of asparaginase associated pancreatitis in children with acute lymphoblastic leukemia. Pediatr Hematol Oncol. 2015;32(7):474–81.
54. Top PC, et al. L-asparaginase-induced severe necrotizing pancreatitis successfully treated with percutaneous drainage. Pediatr Blood Cancer. 2005;44(1):95–7.
55. Agrons GA, et al. From the archives of the AFIP. Genitourinary rhabdomyosarcoma in children: radiologic-pathologic correlation. Radiographics. 1997;17(4):919–37.
56. Madre C, et al. Hypertension in childhood cancer: a frequent complication of certain tumor sites. J Pediatr Hematol Oncol. 2006;28(10):659–64.
57. McCarville MB, et al. Imaging findings of hemorrhagic cystitis in pediatric oncology patients. Pediatr Radiol. 2000;30(3):131–8.
58. Lonergan GJ, et al. Nephrogenic rests, nephroblastomatosis, and associated lesions of the kidney. Radiographics. 1998;18(4):947–68.
59. Amar AM, et al. Clinical presentation of rhabdoid tumors of the kidney. J Pediatr Hematol Oncol. 2001;23(2):105–8.
60. Brennan B, Stiller C, Bourdeaut F. Extracranial rhabdoid tumours: what we have learned so far and future directions. Lancet Oncol. 2013;14(8):e329–36.
61. Servaes S, et al. Sonographic findings of ovarian torsion in children. Pediatr Radiol. 2007;37(5):446–51.
62. Oltmann SC, et al. Pediatric ovarian malignancy presenting as ovarian torsion: incidence and relevance. J Pediatr Surg. 2010;45(1):135–9.

Acute (Abdominal) Presentations of Non-malignant Hemopathies

28

Elisa Amzallag-Bellenger, Anne Smets, and Fred E. Avni

Contents

28.1 Introduction

Acute (abdominal) presentations of non-malignant hemopathies are often managed by the clinician (vaso-occlusive crisis in sickle cell disease), complications of analgesic medicine (bladder retention or fecaloma). In certain specific cases (biliary or splenic complications), imaging will be helpful. US is usually the first and often the only imaging procedure to be performed. CT or MR imaging has to be performed when there is clinical doubt or when US is inconclusive. The management of borderline hemopathies such as Langerhans cell histiocytosis (LCH) depends on the complications and imaging will be adapted to the clinical presentation.

28.2 Acute Presentation of Non-malignant (Congenital) Hemopathies

Congenital non-malignant hemopathies include sickle cell disease, thalassemia (most common type, 5% of the world population), spherocytosis, and deficit in G6PD [1]. The main biological consequence of all these diseases is hemolytic anemia resulting either in extravascular or in both intra- and extravascular destruction of red cells. Sickle cell disease affects many organs (brain, eyes, bone, lungs, etc.). In the abdomen, the kidneys (e.g., papillary necrosis), the liver and biliary tract (jaundice, lithiasis), the bowel (ileus),

E. Amzallag-Bellenger (✉) • F.E. Avni
Department of Pediatric Imaging,
Jeanne de Flandre Hospital, CHRU Lille,
Av Eugène Avinée 2, 59037 Lille-Cedex, France
e-mail: elisa.bellenger@chru-lille.fr

A. Smets
Department of Radiology, Academic Medical Center,
Meibergdreef 9, 1105 AZ Amsterdam, The Netherlands

F.E. Avni, P. Petit (eds.), *Imaging Acute Abdomen in Children*,
https://doi.org/10.1007/978-3-319-63700-6_28

and the spleen (splenic sequestration, infarct, autosplenectomy, etc.) can be affected and patients may present with acute symptoms.

The clinical expression of the diseases is most variable. Hepato-splenomegaly is the most common symptom. Hemolytic anemia can induce biliary lithiasis. Furthermore, jaundice and splenomegaly are the main findings in spherocytosis and sickle cell disease.

28.2.1 Biliary Complications

Biliary lithiasis is rare in children (around 0.20%) (see also Chap. 15) [2]. Their main etiology (75%) is hemolytic anemia associated with congenital hemopathies. Furthermore, 50% of patients with congenital hemopathies develop biliary lithiasis [2]. In these congenital hemopathies, the level of non-conjugated bilirubin is increased and precipitates to form first sludge and subsequently lithiasis (typically black pigmented lithiasis) [2]. Symptoms related to the biliary stones vary according to the age of the patients. In infants, the main symptom is jaundice related to migration of the stone, in older children vomiting is the most common finding and in adolescents, right hypochondrium pain along with high temperature and jaundice will in most cases be the prominent findings.

US will usually be sufficient to demonstrate the lithiasis and the potential complications such as migration of lithiasis and obstructive cholecystitis (Fig. 28.1).

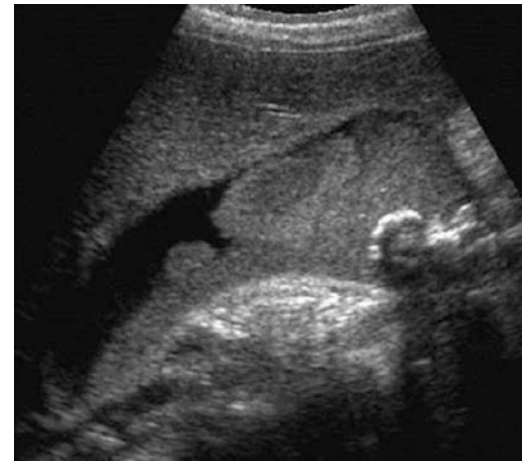

Fig. 28.1 Ten-year-old boy with sickle cell disease and right hypochondrium pain. US shows a distended gallbladder with lithiasis and sludge

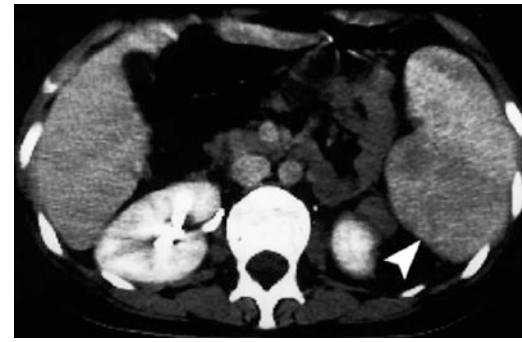

Fig. 28.2 Five-year-old boy with sickle cell disease and left hypochondrium pain. Axial CE-CT showing heterogeneous enhancement of the spleen corresponding to splenic infarction (*arrowhead*)

28.2.2 Splenic Complications

In all congenital hemopathies, the spleen traps the abnormal red blood cells and tries to eliminate them. This splenic overload will lead to splenomegaly, a classical finding in the early course of the disease. It may develop acutely, leading to the so-called "acute splenic sequestration crisis" (ASSC), usually seen in infants and young children. ASSC is characterized by sudden onset of anemia, massive splenomegaly, and abdominal pain. The clinical presentation is usually straightforward and no imaging is necessary.

The spleen may also be affected by successive episodes of infarction progressively leading to atrophy of the spleen and eventually to autosplenectomy [3]. On US, the parenchyma of the infarcted spleen appears heterogeneous with alternating hypo- and hyperechoic areas. The atrophied spleen appears small with irregular contours and it may calcify (see Chap. 17).

Whenever US is inconclusive or contradicts clinical symptoms, a CE-CT can help to demonstrate the infarcted areas (Fig. 28.2) and vascular complications.

28.2.3 Digestive Symptoms: Paralytic Ileus

Sickle cell disease may induce episodes of vaso-occlusive crisis and hemolysis by sicklemic micro-

vascular occlusion. These phenomena may affect any organ or vessel. Paralytic ileus or pseudoobstruction is a rare complication of sickle cell disease. Symptoms are non-specific: functional occlusion with distended bowel loops and vomiting. The treatment is medical and imaging is generally not necessary, beside a plain radiograph of the abdomen to exclude mechanical obstruction [4].

28.3 Langerhans Cell Histiocytosis

LCH is a systemic proliferative disorder characterized by clusters of Langerhans cells organized as granulomas. LCH is generally considered as a benign disease but chemotherapy is the main part of treatment. The most common manifestation of LCH is skeletal involvement. Extra-osseous disease is less frequent and indicates a more aggressive disease. Abdominal involvement corresponds to 40% of extra-osseous disease. In the abdomen LCH affects mainly the hepatobiliary and GI tract.

The liver itself is involved in 15–20% cases and this involvement is considered a feature of poor prognosis [5]. Children present with abdominal pain and rarely jaundice. Imaging may demonstrate the various stages of the involvement.

In the granulomatous and proliferative stage, periportal edema appears hypoechoic on US, hypodense on CT, and hypointense on T1- and T2- weighted MR imaging. Cholangitis, resulting from a direct invasion of the biliary tract will show as irregular biliary ducts, alternating dilatation, and stenosis. It may evolve towards sclerosing cholangitis.

During the xanthomatous stage of the disease, hyperechoic hepatic nodules are visualized with US, which will appear as hypodense nodules on CT and nodules enhancing after Gadolinium injection. Finally, during the fibrous stage, portal hypertension will develop [6].

The disease may also affect the digestive tract (from one extremity to the other) but clinical symptoms (abdominal pain, vomiting, diarrhea, intestinal obstruction, etc.) and imaging features are non-specific. Features of the involvement include thickening of the bowel wall, free peritoneal fluid, infiltration of the mesenteric fat, and mucosal enhancement on CT and MR Imaging. In the context of LCH, the diagnosis of intestinal involvement must be part of the differential diagnosis, which also includes IBD and GI infections [6].

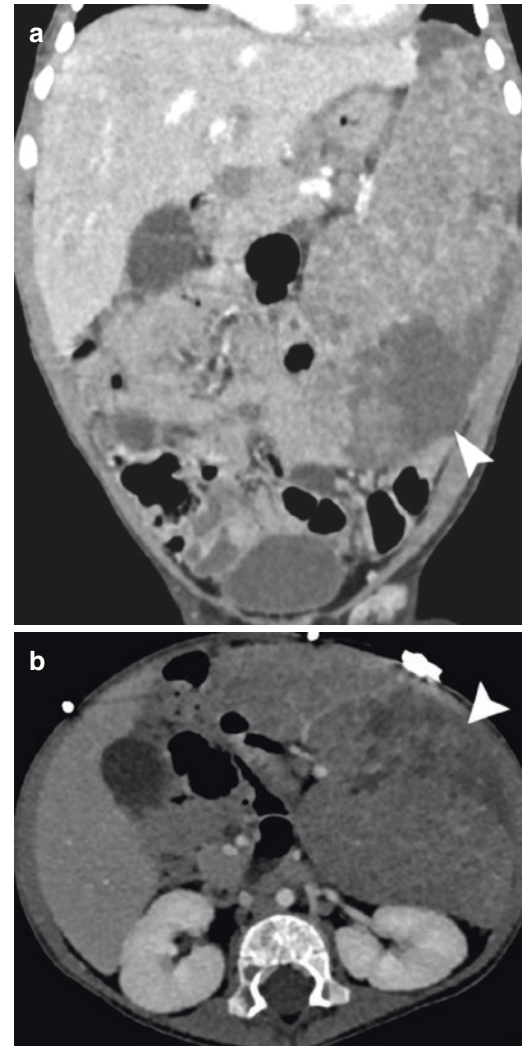

Fig. 28.3 Two-year-old girl with left abdominal pain. Bone lesions had been diagnosed previously. (**a**) Coronal CT image. (**b**) Axial CE-CT showing massive splenomegaly with heterogeneous enhancement corresponding to splenic infarction (*arrowhead*). Diagnosis of LCH was made on bone biopsy

The spleen is also commonly involved by LCH and splenomegaly is present in over 60% of cases. The splenic parenchyma may appear homogeneous or show multiple nodules [5]. Massive splenomegaly with infarcts is a rare but classic complication (Fig. 28.3) [7].

Conclusion

Acute (abdominal) presentations of non-malignant hemopathies rarely necessitate emergency imaging. Abdominal US is the first-line imaging that will display the classical biliary and splenic complications in these patients.

References

1. Noronha SA. Acquired and congenital hemolytic anemia. Pediatr Rev. 2016;37(6):235–46.
2. Poffenberger CM, Gausche-Hill M, Ngai S, Myers A, Renslo R. Cholelithiasis and its complications in children and adolescents: update and case discussion. Pediatr Emerg Care. 2012;28(1):68–76. quiz 77-8
3. Gale HI, Bobbitt CA, Setty BN, et al. Expected sonographic appearance of the spleen in children and young adults with sickle cell disease: an update. J Ultrasound Med. 2016;35(8):1735–45.
4. Khosla A, Ponsky TA. Acute colonic pseudoobstruction in a child with sickle cell disease treated with neostigmine. J Pediatr Surg. 2008;43(12):2281–4.
5. Zaveri J, La Q, Yarmish G, Neuman J. More than just Langerhans cell histiocytosis: a radiologic review of histiocytic disorders. Radiographics. 2014;34(7):2008–24.
6. De Souza Maciel Rocha Horvat N, Coelho CR, Roza LC, et al. Spectrum of abdominal imaging findings in histiocytic disorders. Abdom Imaging. 2015;40(7):2738–46.
7. Natsume H, Yamaguchi T, Ohsawa J, et al. Splenic infarction in Letterer-Siwe disease. Pediatr Int. 2005;47(3):329–32.

Acute Abdominal Presentation of Systemic Diseases and Vasculitis

29

Catherine Desvignes and Philippe Petit

Contents

29.1 Systemic Diseases

Systemic diseases represent a group of autoimmune diseases which may present in children acute abdominal symptoms. These symptoms are either due to the disease itself or are secondary to the side effects of the treatment.

29.1.1 Systemic Lupus Erythematosus

In children, during the evolution of the disease, abdominal symptoms have been reported to be present in as much as 19% of patients. The median age at the time of initial gastrointestinal symptoms is 12 years with a female–male ratio from 4 to 6:1. Abdominal pain is the most frequent symptom (present in 87% of patients) followed, in decreasing frequency, by vomiting, diarrhea, dysphagia, acute surgical abdomen, and intestinal hemorrhage. Very rarely, these various symptoms may reveal the disease. They are mostly related to direct lupic involvement (e.g., ascites, pseudo-obstruction, and pancreatitis) and more rarely to treatment-induced events or to infection [1, 2]. Spontaneous splenic rupture is an exceptional event that may reveal the disease as well [3]. In Richer's publication [2], 3 children with acute surgical abdomen underwent a laparotomy before that the correct diagnosis of lupus was obtained. US and CT were respectively performed in 67% and 15% of cases and are non-specific of the entity [1]. A marked increase of

C. Desvignes • P. Petit (✉)
Department of Pediatric Imaging,
Hôpital Timone Enfants, 264 Rue St Pierre,
13385 Marseille Cedex 05, France
e-mail: cdesvignes@ap-hm.fr; ppetit@ap-hm.fr

F.E. Avni, P. Petit (eds.), *Imaging Acute Abdomen in Children*,
https://doi.org/10.1007/978-3-319-63700-6_29

erythrocyte sedimentation rate associated with a normal or moderately elevated C-reactive protein are valuable clues to suspect systemic lupus erythematosus (SLE). Most symptoms resolve under a combination of corticoids and cyclophosphamides.

29.1.2 Behçet's Disease

The abdominal symptoms in children have been reported to occur in as much as 40% of patients [4]. Gastro-intestinal symptoms are frequent and consist mainly in isolated abdominal pain and discomfort. Bleeding and perforation are very rare. The ileum and the colon are the digestive sites most commonly involved. MR Imaging has been used in adults and is able to reveal bowel wall thickening, hyperemia, mesenteric infiltration, ulcerative lesions, and abscess formation [5].

29.1.3 Mediterranean Fever

This hereditary auto-inflammatory disorder is characterized by acute bouts of fever and serosal inflammation (peritoneum, pleura, and synovium) and is significantly associated with ethnicity (Turks, Arabs, Armenians, and Sephardic Jews). Disease onset is usually prior to 20 years in 90% of cases; furthermore, in 60% of cases, the age at onset is below 10 years. The disease may even already develop after the first year of life [6]. Abdominal pain results from inflammation of the peritoneal surface and can mimic a surgical acute abdomen. Associated hematuria can be present. Mechanical bowel obstruction may occur, due to recurrent accumulation of exudative fluid as well as encapsulated peritonitis. The most important complication is renal failure due to amyloidosis. The diagnosis is clinical, based on the association of an appropriate ethnic origin, with recurrent symptoms and fever accompanied by serositis ongoing for 1–4 days. Leukocytosis is present, and C-reactive protein is elevated. The findings on imaging are non-specific and include ascites, hepatomegaly, splenomegaly, lymphadenopathy, focal peritonitis, bowel obstruction, and peritoneal cyst [7]. The role of imaging, especially US, is to rule out any other pathology which will need surgical treatment.

29.1.4 Systemic Juvenile Idiopathic Arthritis

This subset includes as much as 15% of all juvenile idiopathic arthritis and may present extra-articular features including peritoneal serositis and hepatosplenomegaly [8].

29.2 Vasculitis

Vasculitis represents a group of diseases affecting different size arteries and their related organs. Depending on the type of vasculitis, pediatric patients present with some specific complications potentially different from adults.

29.2.1 Henoch-Schönlein Purpura

It is the most frequent pediatric vasculitis accounting for half of all childhood vasculitis [9]. On histology, the small vessels are affected without granulomatous wall reaction; this feature differentiates Henoch-Schönlein purpura (HSP) from Churg-Strauss syndrome and granulomatosis with polyangiitis (Wegener granulomatosis). IgA immune deposits are present in the wall of the arteries and in the renal glomeruli. Ninety percent of the cases occur before the age of 10 years and the peak at diagnosis is 7 years ± 3 years. There is a slight male predominance. The etiology remains unknown but infectious agents, insect bites, vaccinations, and drugs are suspected to act as triggering agents. Most cases are revealed during the winter. The disease usually lasts for 1–4 weeks. The most classical manifestations of HSP include non-thrombocytopenic purpura (Fig. 29.1), arthritis and arthralgia, glomerulonephritis, and gastrointestinal symptoms. To note: the GI symptoms may be the first diagnostic manifestation and can be recognized on imaging; abdominal pain may precede the skin lesions from 1 to 10 days [10] in 14–36% of cases [11]. High frequency ultrasound is the imaging procedure of choice to explore these patients. Abdominal involvement has been reported to occur in 50–75% of patients. Acute abdominal pain is the most frequent clinical sign

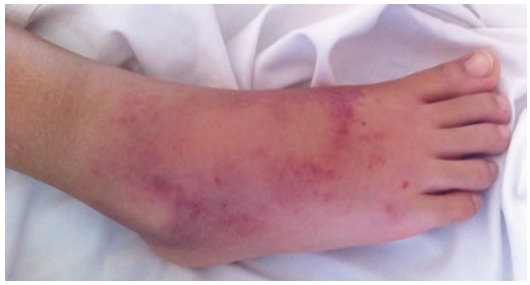

Fig. 29.1 Twelve-year-old girl who presents typical cutaneous lesions of HSP

and can be due (in decreasing frequency) to the following etiologies:

- Hemorrhage (Fig. 29.2) and/or edema of the bowel wall: they are mainly located within the small bowel and the duodenum. Thickening may be subtle or marked. Associated parietal hyperemia on color Doppler is frequent (Figs. 29.3 and 29.4). Spontaneous resolution without complication is the rule. Exceptional secondary perforations have been reported [11].

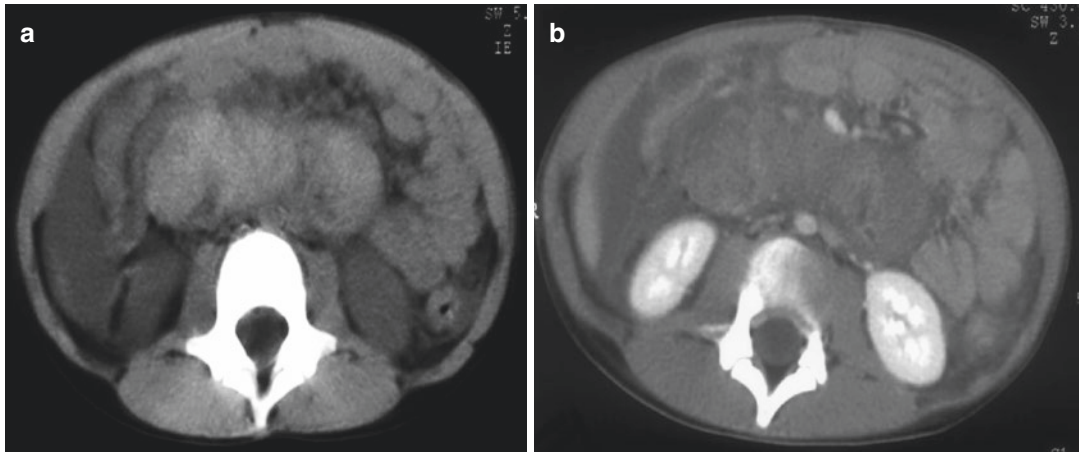

Fig. 29.2 Seven-year-old-girl presenting acute abdominal pain and vomiting. HSP revealed by a hematoma of the wall of third duodenum. (**a**) CT without contrast showing dense mural thickening of the third duodenum. (**b**) CE-CT showing absence of enhancement of this thickened wall

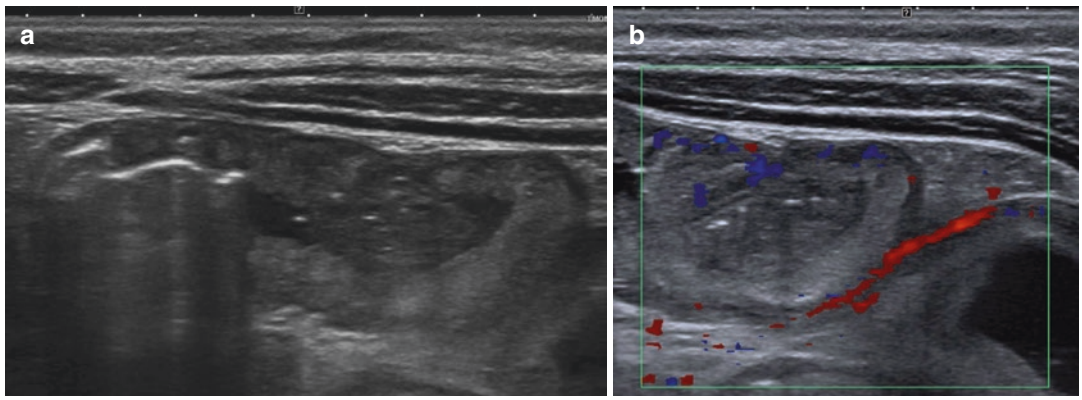

Fig. 29.3 HSP: US findings in a 5-year-old patient. (**a**) US Transverse scan of the jejunum demonstrates important thickening with loss of the bowel signature. (**b**) Color Doppler of the thickened bowel showing hyperhemia of jejunal loops

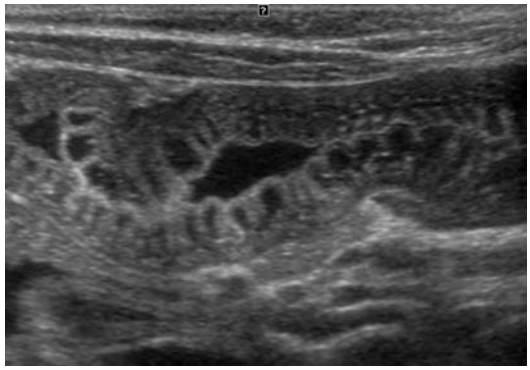

Fig. 29.4 HSP: Jejunal involvement in a 6-year-old girl. US—Sagittal scan of the left flank. Important thickening of the bowel but preservation of the "bowel signature"

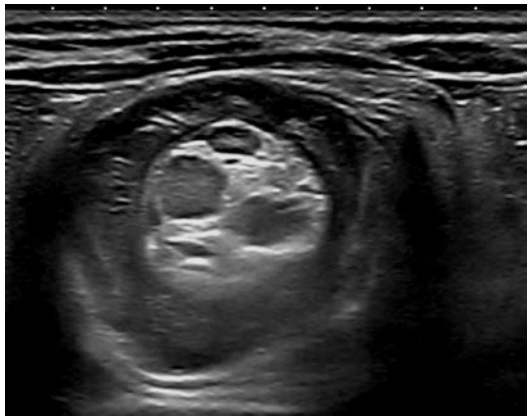

Fig. 29.5 HSP—Large ileo-colic intussusception visualized on US—Transverse scan of a 5-year-old boy. This intussusception could not be reduced radiologically

- Intussusception: Intramural hemorrhage and edema within the bowel wall occur during this vasculitis and serve as leading point; the layered bowel wall structure is usually maintained. Hyperemia on Doppler is present within the wall of the intussusceptum. Most intussusceptions involve the small bowel but ileo-colic intussusception (Fig. 29.5) and even colo-colic intussusceptions have been described [12]. The overall incidence ranges from 1.3% to 13.6% [11]. Spontaneous resolution is the commonest evolution. Persisting ilieo-ileo-colic intussusception can be treated by reduction under radiological guidance but with particular care [12]. Exceptionally, spontaneous perforation may occur [13].

Other abdomen and pelvis abnormalities include:

- Renal involvement (hematuria, proteinuria) occurs in 30–80% of cases mostly within the first months after the onset of symptoms. A risk of renal failure exists but is reported with variable percentages [10]: On US, the kidney can be normal or enlarged. The echogenicity of the renal parenchyma may also be normal or diffusely increased.
- Ureteral and/or bladder thickening (Fig. 29.6). Exceptionally ureteral thickening may result in severe obstruction.
- Scrotal thickening and inflammation of the adjacent structures [14] is frequently associated.
- Other extremely unusual clinical presentations include:
  - Pancreatitis, cholecystitis [15]
  - Late ileal stricture, gastrointestinal hemorrhage, entero-enteral fistulae, appendicitis, anterior abdominal wall hematoma [11].

29.2.2 Kawasaki Disease

It is the second most frequent vasculitis in children (25%). It occurs typically before the age of 5 years with a slight male predominance. Medium and small arteries are involved [9]. Typical US imaging findings include coronary artery aneurisms. During the acute phase of disease, fever, unilateral cervical lymph nodes, skin lesions, and non-specific abdominal symptoms may be present. The latter include abdominal pain, hydrops of the gallbladder (Fig. 29.7), ascites, intestinal pseudo-obstruction, focal colitis, bowel infarction, and bowel stricture secondary to ischemia [16]. Abdominal imaging may help earlier recognition of the disease before the development of coronary aneurisms (see also Chap. 21).

29.2.3 Takayasu Arteritis

Takayasu arteritis is the third most frequent childhood arteritis and involves typically the large arteries. The mean age at diagnosis is 13 years

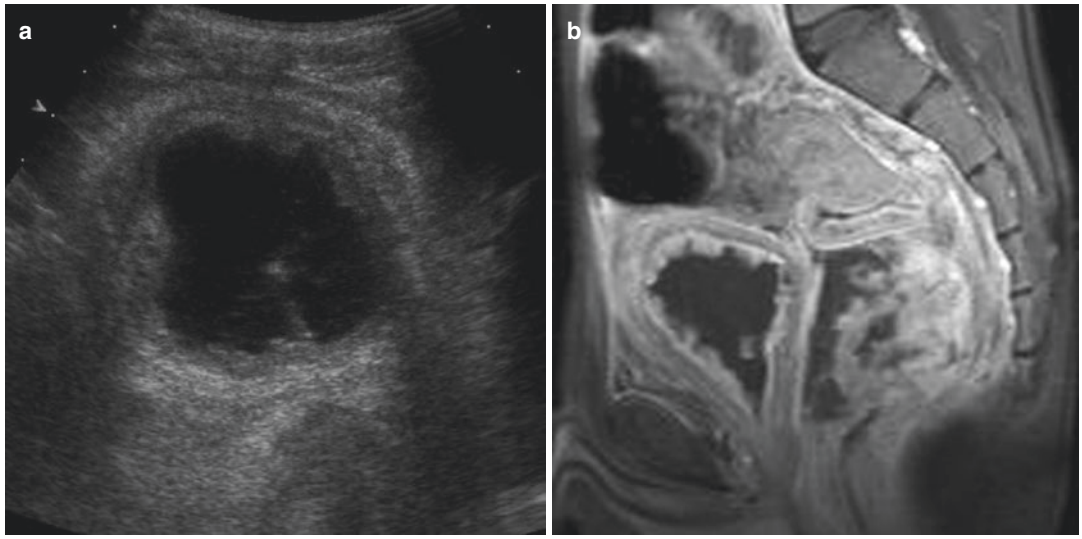

Fig. 29.6 HSP in a 12-year-old-boy with involvement of the bladder. (**a**) US: sagittal scan; marked irregular thickening of the bladder wall. (**b**) MR imaging T1-weighted sequence after gadolinium injection demonstrates the thickening of the bladder wall that involves mainly the endothelium

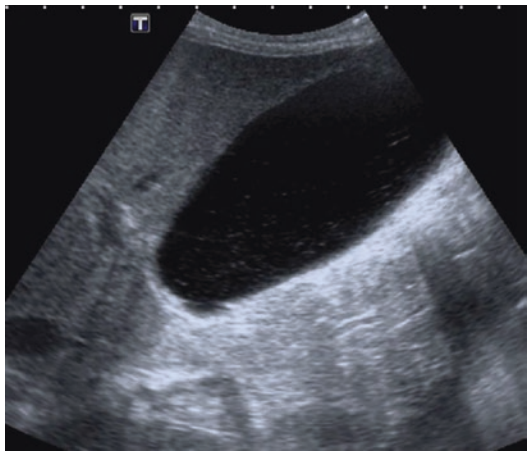

Fig. 29.7 Hydrops of the gallbladder in a 6-year-old girl with Kawasaki disease. US: sagittal scan; marked enlargement of the gallbladder with thin regular wall and anechoic content

with a female predominance; the youngest case reported was a 6-month-old [17]. Initial clinical presentation includes headache, prolonged fever, and weight loss. Later, the evolution of the disease results in various symptoms including claudication, abdominal angina, diminished vascular pulsations, and hypertension [9]. Renal artery involvement with renal hypertension is the most common manifestation at presentation. It occurs in 66–93% of children [18]. Direct and indirect signs (parvus-tardus) of stenosis can be depicted in US-Doppler. However, due to their ability to evaluate accurately all thoracic and abdominal arterial vessels, preferably MR imaging or CE-CT is recommended. Edema, thickening as well as enhancement of the arterial wall are major findings. Early treatment will prevent irreversible damages. Stenosis and thrombosis with the development of collaterals and aneurysms represent the potential evolution of the early features.

29.2.4 Polyarteritis Nodosa

This vasculitis causes necrotizing inflammation in small and medium-sized arteries and its presentation may overlap with Kawasaki disease. Association with Mediterranean fever has been reported as well as hepatitis viral B triggering. Children are rarely affected, in average around 9 years [19]. Clinical manifestations before 1 year of age are exceptional [20]. There is no sex predilection. Clinical manifestations are multisystemic; the skin and peripheral nerves are most frequently involved. Depending of the subtype of

polyarteritis nodosa (PAN), the gastrointestinal manifestations are variable and reported in about 17% of patients [19]. They are related to infarctions (abdominal cramping), rupture of aneurisms (hemorrhage) or obstruction and may reveal the disease [20, 21]. These aneurisms typically affect the renal, mesenteric, or hepatic arteries. Renal involvement (severe hypertension, renal failure) is frequent and is indicator of poor prognosis. Due to the size of the involved arteries, angiography is recommended in case of clinical suspicion.

Conclusion

- Abdominal symptoms may reveal complex systemic diseases or vasculitis. Imaging is not specific for systemic disease but plays a key role for a complete evaluation and characterization of the vasculitis in children.
- US-Doppler is the first line exploration in case of an acute abdomen.
- MR imaging is the exploration of choice in case of medium or large vessels vasculitis.
- Diagnostic angiography is the imaging modality of choice in case of suspicion of polyarteritis nodosa.

References

1. Richer O, Ulinski T, Lemelle I, et al. Abdominal manifestations in childhood-onset systemic lupus erythematosus. Ann Rheum Dis. 2007;66(2):174–8.
2. Bader-Meunier B, Armengaud JB, Haddad E, et al. Initial presentation of childhood-onset systemic lupus erythematosus: a French multicenter study. J Pediatr. 2005;146(5):648–53.
3. Tolaymat A, Mousily FA, Haafiz AB, et al. Spontaneous rupture of the spleen in a patient with systemic lupus erythematosus. J Rheumatol. 1995;22:2344–5.
4. Koné-Paut I. Behçet's disease in children, an overview. Pediatr Rheumatol Online J. 2016;14(1):10.
5. You JK, Kim MJ, Park S, et al. Intestinal Behçet's disease: breath-hold MR imaging. Abdom Imaging. 2001;26(3):309–14.
6. Sarı I, Birlik M, Kasifoğlu T. Familial Mediterranean fever: an updated review. Eur J Rheumatol. 2014;1(1):21–33.
7. Aharoni D, Hiller N, Hadas-Halpern I. Familial Mediterranean fever: abdominal imaging findings in 139 patients and review of the literature. Abdom Imaging. 2000;25(3):297–300.
8. Jain D, Aggarwal HK, Rao A, et al. Macrophage activation syndrome in a patient with systemic onset of the juvenile idiopathic arthritis. Reumatologia. 2016;54(1):42–7.
9. Khanna G, Sargar K, Baszis KW. Pediatric vasculitis: recognizing multisystemic manifestations at body imaging. Radiographics. 2015;35(3):849–65.
10. Calviño MC, Llorca J, García-Porrúa C, et al. Henoch-Schönlein purpura in children from northwestern Spain: a 20-year epidemiologic and clinical study. Medicine (Baltimore). 2001;80(5):279–90.
11. Choong CK, Beasley SW. Intra-abdominal manifestations of Henoch-Schönlein purpura. J Paediatr Child Health. 1998;34(5):405–9.
12. Navarro O, Dugougeat F, Kornecki A, et al. The impact of imaging in the management of intussusception owing to pathologic lead points in children. A review of 43 cases. Pediatr Radiol. 2000;30(9):594–603.
13. Couture A, Veyrac C, Baud C, et al. Evaluation of abdominal pain in Henoch-Schönlein syndrome by high frequency ultrasound. Pediatr Radiol. 1992;22(1):12–7.
14. Ben-Sira L, Laor T. Severe scrotal pain in boys with Henoch- Schönlein purpura: incidence and sonography. Pediatr Radiol. 2000;30(2):125–8.
15. Helbling R, Lava SA, Simonetti GD, et al. Gallbladder and pancreas in Henoch-Schönlein purpura: review of the literature. J Pediatr Gastroenterol Nutr. 2016;62(3):457–61.
16. Akikusa JD, Laxer RM, Friedman JN. Intestinal pseudoobstruction in Kawasaki disease. Pediatrics. 2004;113(5):e504–6.
17. Brunner J, Feldman BM, Tyrrell PN, et al. Takayasu arteritis in children and adolescents. Rheumatology. 2010;49:1806–14.
18. McCulloch M, Andronikou S, Goddard E, et al. Angiographic features of 26 children with Takayasu's arteritis. Pediatr Radiol. 2003;33(4):230–5.
19. Ozen S, Anton J, Arisoy N, et al. Juvenile polyarteritis: results of a multicenter survey of 110 children. J Pediatr. 2004;145(4):517–22.
20. Gomes RC, Marques VL, Cavalcante EG, et al. Severe intestinal involvement as initial manifestation of systemic childhood polyarteritis nodosa: report of two cases. J Pediatr Surg. 2013;48(2):425–8.
21. Venuta A, Ceccarelli PL, Biondini D, et al. Jejunal obstruction as initial presentation of polyarteritis nodosa in a 13-month-old boy. J Pediatr Surg. 2011;46(7):E27–9.

At the Boundaries of the Abdominal Cavity

30

Fred E. Avni, Nathalie Boutry, and Philippe Petit

Contents

30.1 General Considerations

When a child presents with acute or subacute abdominal symptoms a series of differential diagnoses are considered and they have been described in the various chapters of our book.

Once all these diagnoses have been excluded, one should keep in mind the possibilities of diseases at the boundaries of the abdominal cavity (or even further) that may mimic an abdominal origin.

As known and classically, a pneumonia can be discovered following the workup of abdominal pain, conversely abdominal diseases may induce pulmonary symptoms.

Among the other diagnoses, several musculoskeletal diseases can express acute abdominal symptoms and conversely abdominal diseases may induce by vicinity muscular symptoms.

Finally, some diseases of the abdomen may develop and extend outside of the abdominal cavity through congenital or acquired openings leading to potentially complicated hernias.

30.2 The Relations Between Thoracic and Abdominal Symptoms

As mentioned, a pneumonia can be discovered during the workup of abdominal pain; for instance, the pneumonia can be visualized incidentally in the lower thoracic areas on the plain

F.E. Avni (✉) • N. Boutry
Department of Pediatric Imaging, Jeanne de Flandre Hospital, 59037 Lille–Cedex, France
e-mail: Freddy.Avni@chru-lille.fr

P. Petit
Department of Pediatric Imaging,
Hôpital Timone Enfants, 264 Rue St Pierre,
13385 Marseille Cedex 05, France
e-mail: ppetit@ap-hm.fr

F.E. Avni, P. Petit (eds.), *Imaging Acute Abdomen in Children*,
https://doi.org/10.1007/978-3-319-63700-6_30

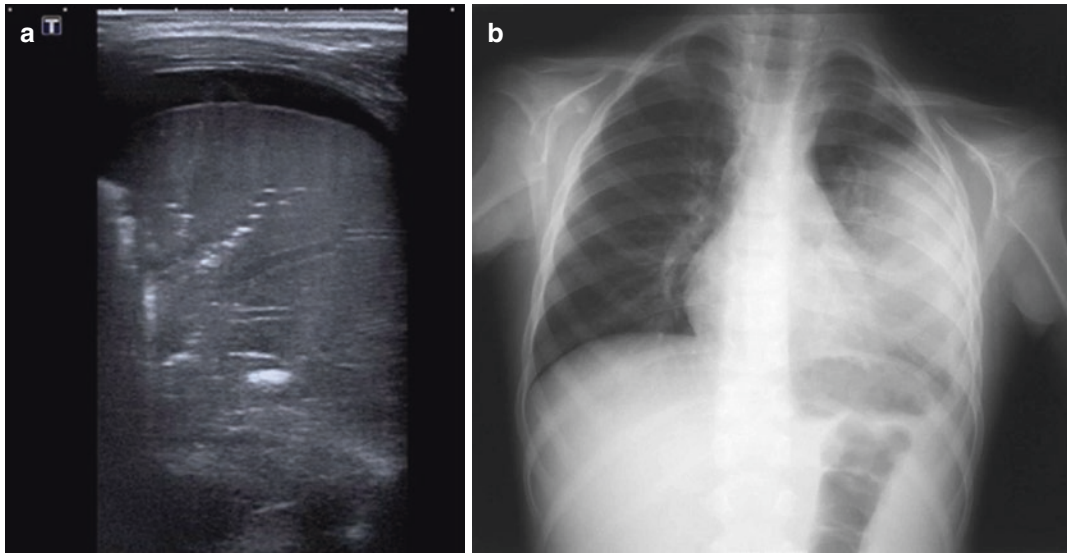

Fig. 30.1 Pneumonia masquerading as abdominal pain in a 7-year-old girl. (**a**) US of the left upper quadrant, above the diaphragm; hypoventilation of the left lung basis with pleural effusion suggesting pneumonia. (**b**) Chest radiograph confirms a massive pleuro-pneumopathy

film of the abdomen. Clearly, a lower lobe pneumonia must be searched after a negative US exploration of a febrile patient presenting with acute abdominal symptoms (Fig. 30.1) [1].

On the other hand, a diaphragmatic paralysis and lower lobes hypoventilation (Fig. 30.2a) may be induced by sub-diaphragmatic abscesses following perforation of a retro-hepatic appendicitis (Fig. 30.2) or as a sub-diaphragmatic complication of a pancreatitis. Therefore, in ambiguous cases, an US of the diaphragm or CT in ambiguous cases (Fig. 30.2b) should be performed to search for sub-diaphragmatic collections and establish their origin [2].

Furthermore, intrathoracic hernia of abdominal organs may determine thoracic and/or abdominal symptoms (see below).

30.3 The Relation Between Abdominal and Musculoskeletal Diseases

A psoas abscess is a typical disease where symptoms may mimic abdominal disease; clearly, a right psoas abscess may mimic an appendicitis. Psoas abscesses are rare in children and therefore rarely considered. They are mainly encountered in two age groups. A first peak is observed in neonates or infants where it can be isolated or combined with a septic arthritis (entity beyond the scope of this chapter) [3, 4]. A second peak is observed in adolescents (and adults) where it usually develops by contiguous spread from a diseased gastrointestinal tract most frequently involved by Crohn disease (see also Chap. 12). In case of isolated ilio-psoas abscess, US will demonstrate a collection (Fig. 30.3a) and raise the suspicion of an abscess but the technique will not be able to define the exact location and extent. In some cases, the technique will be able to demonstrate the close relation (and fistula) between the psoas and the diseased small bowel segment. The abscess as well as the surrounding digestive anomalies will be better evaluated by musculoskeletal MR imaging (Fig. 30.3b) and MR-enterography sequences. Whenever MR imaging is not available, a CT with and without contrast enhancement is also able to accurately define the anomalies and demonstrate the musculoskeletal involvement, the abscess as well as the associated digestive tract anomalies [5, 6].

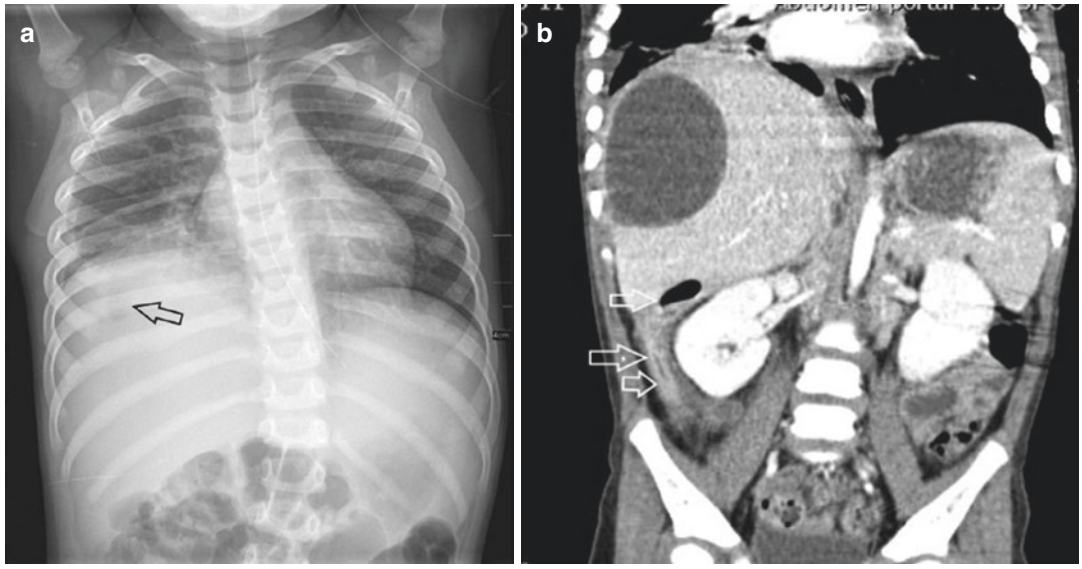

Fig. 30.2 Sub-diaphragmatic abscess masquerading as right pleuro-pneumopathy in a 2-year-old boy. (**a**) Chest radiograph demonstrates hypoventilation and pleural effusion of the right basis. A small air bubble is superimposed to the liver. (**b**) CE-CT—Reformatted frontal view (US had shown a perihepatic heterogeneous mass suggesting an abscess) confirms the perihepatic abscess and shows the perforated appendix with an air bubble below the liver (*arrows*)

Finally, psoas abscesses may also develop as a result from spondylodiscitis (especially from tuberculous infection) that may present with abdominal symptoms probably due to secondary peritoneal inflammation [7].

The treatment of the psoas abscess will depend upon its size, its nature (bacteria vs mycobacteria), and symptoms induced. Antibiotherapy and abscess drainage under imaging guidance can first be attempted. Surgery will be reserved to recurrence or to cases with unfavorable evolution.

Finally, spinal surgery can induce a postoperative ileus. This ileus may rarely reveal related acute pancreatitis [8].

30.4 Hernias

Hernias may develop in various parts within and at the limits of the peritoneal cavity, their origin may be congenital or acquired (see also Chap. 14). Some will be silent while others will present with acute symptoms. The use of imaging will be adapted to the type of hernia and its complications.

30.4.1 Hernias Through the Diaphragmatic Openings

There are variable openings through the diaphragm that may lead to intrathoracic hernia of abdominal viscera with potential acute abdominal symptoms.

30.4.1.1 Diaphragmatic Hernia

Congenital diaphragmatic hernia through the posterior Bochdalek orifice is the commonest type. This particular hernia is amenable to antenatal diagnosis and postnatal management. Postnatally, symptoms are mainly related to lung hypoplasia and pulmonary hypertension. This malformation is beyond the scope of the present book [9].

30.4.1.2 Hiatal Hernia

(See Also Chaps. 5 and 7)

A hiatal hernia corresponds to the herniation through the esophageal orifice into the mediastinum of the esophagogastric junction including a part or with the entire stomach. Very rarely other organs (liver, colon, etc.) may be included in the hernia.

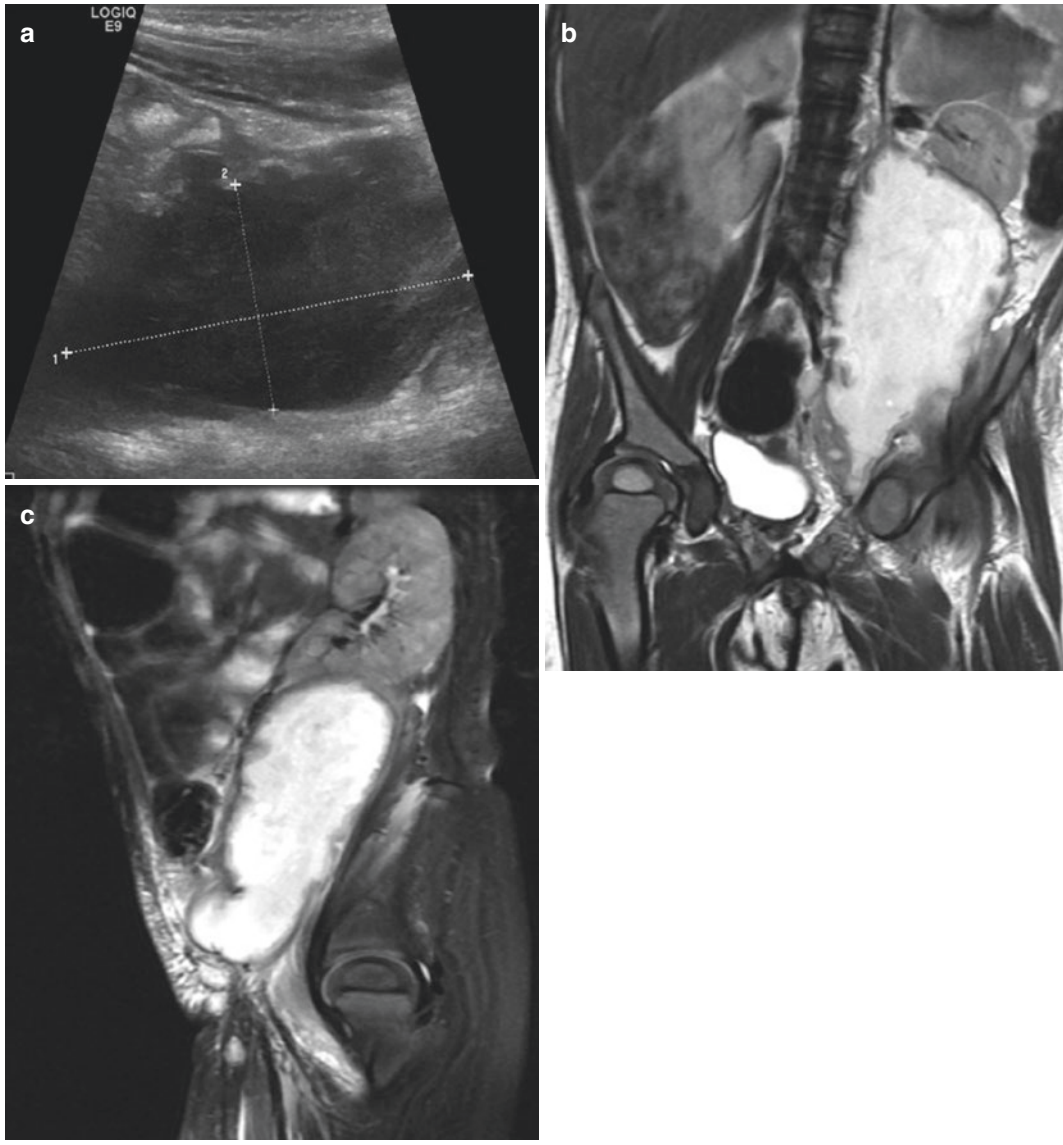

Fig. 30.3 Psoas-iliac abscess in a 2-year-old girl with acute abdominal symptoms (its origin could not be defined). (**a**) US—Sagittal scan of the left flank demonstrates a large oblong hypoechoic mass. The technique was not able to define its exact location. (**b**) MR imaging T2-weighted sequence—Frontal view—Inverted pyramidal collection below the left kidney with inflammatory reaction in the right hip area. The mass displaces the bladder to the right. (**c**) MR imaging T2-weighted sequence—parasagittal view. The collection is clearly located within the psoas-iliac muscle. There is an inflammatory reaction extending to the abdominal wall anteriorly and to the left hip muscles

There are three types of hernias: sliding hernia, paraesophageal hernia, or hernia associated with a congenital short esophagus. Hiatal hernias may be congenital or acquired. They most often determine mild to moderate symptoms related to gastroesophageal reflux and potentially failure to thrive. More dramatic symptoms such as acute vomiting may occur following an organo-axial volvulus of the herniated stomach with obstruction of the upper digestive tract. Cautious upper GI opacification with diluted barium can be performed to define the precise anatomy and the site of obstruction [9–11].

The treatment is surgical.

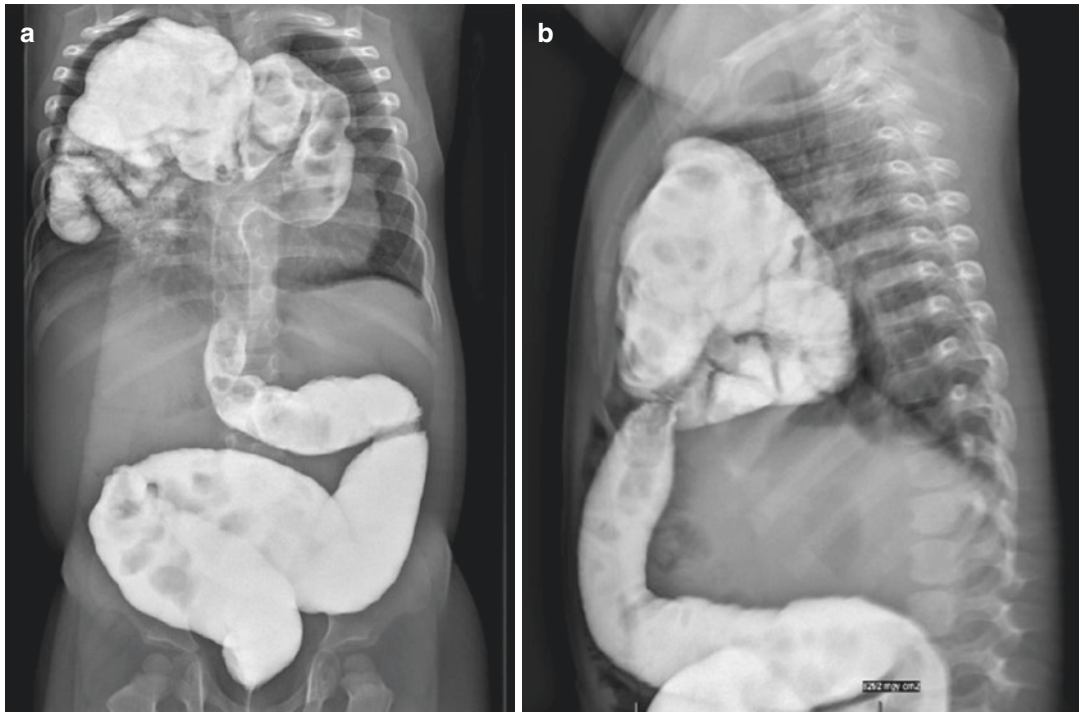

Fig. 30.4 Morgagni-Larey hernia—Infant 6 months, failure to thrive and vomiting. (**a**) Contrast enema—Frontal view—A large part of the colon and of the small bowel lies within the chest. (**b**) Contrast enema—Lateral view—The hernia is located anteriorly in the chest

30.4.1.3 Hernia through the Foramen of Morgagni (Also Named Larey)

The foramens of Morgagni (or Larey) are located anteriorly. They extend from the sternum medially towards the 8th rib laterally. The hernia is right sided in 90% of cases. It can be bilateral. The colon is the commonest organ herniated (Fig. 30.4); small bowel loops, the spleen, the liver, and the omentum can be herniated as well. The hernia can cause chronic respiratory symptoms and in rare cases abdominal acute symptoms due to intestinal (sub) obstruction [12, 13].

The repair of the foramen has to be surgical.

30.4.1.4 Acquired Hernias and Acute Abdominal Symptoms

A diaphragmatic orifice can develop due to trauma or as complication of surgery. In such circumstances, any abdominal organ may herniate within the chest and become obstructed (e.g., stomach, colon, small bowel, etc.) [14].

30.4.2 Inguinal Hernia (See Also Chap. 9)

Inguinal hernias are frequent anomalies in neonates and infants; they result from the patency of the peritoneo-scrotal canal. Hernias are more common on the right side and among boys. The hernia contains most commonly epiploic fat or bowel loops. In most cases, the hernias are asymptomatic and clinical follow-up will be sufficient. In some cases, the herniated intestinal loops may become incarcerated and determine acute obstruction necessitating manual or surgical resolution.

US of the inguino-scrotal canal will easily demonstrate the hernia, its content and potential complications such as intestinal obstruction. The technique will allow to differentiate hernia from other diagnosis such as hydrocele (diffuse peritesticular fluid), spermatic cysts (suspended cystic collection), or tumors (e.g., teratoma). In girls, it may demonstrate the presence within the hernia of a normal or of twisted ovary. A full US exami-

nation of the abdomen and pelvis US will determine the degree of associated bowel damage.

In case of doubt, a plain radiograph of the abdomen will confirm the degree of obstruction [15–19].

30.4.3 Umbilical Hernia and Other Parietal Hernias

Umbilical hernias are best evaluated by clinical examination and in most cases no imaging is necessary. Still, imaging may provide additional information in doubtful cases, whenever an unusual complication occurs or whenever an underlying mass is suspected (abscess, urachal cyst or mesenteric cyst, etc.) (see also Chap. 22). In such cases US will usually be sufficient to determine the associated anomaly [19, 20].

Other congenital or acquired parietal hernias are rare in children. Their rate might increase following laparoscopic surgery. Of interest is the Spigelian hernia which occurs through slit-like defects in the anterior abdominal wall adjacent to the semilunar line. Symptoms are mainly related to pain and to a palpable mass in relation with herniated bowel or fat (Fig. 30.5) [19, 21].

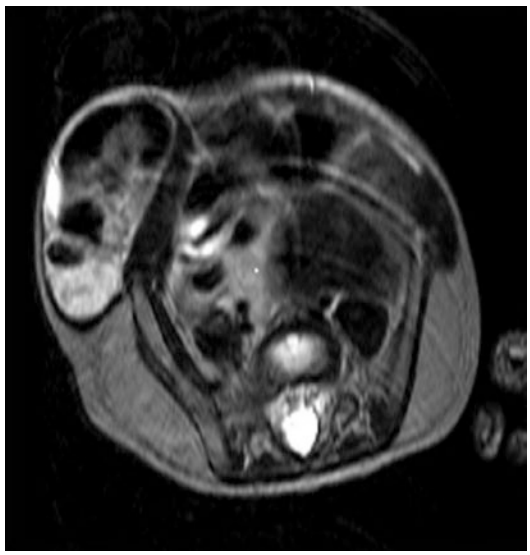

Fig. 30.5 Spigelian hernia—6-month-old infant with increasing lateral hernia—MR imaging; T2-weighted sequence—Axial view. A lateral hernia containing bowel loops can be visualized at the right side

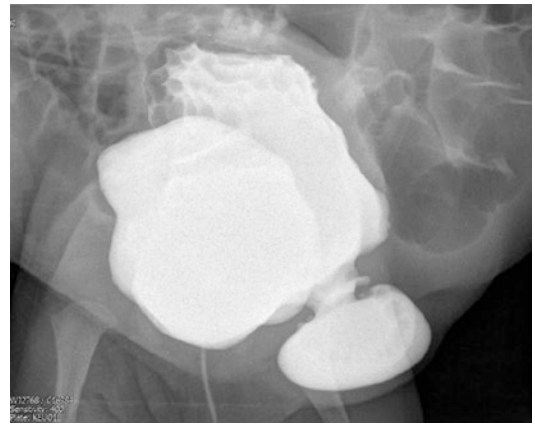

Fig. 30.6 Bladder "ears" hernia—VCUG in a newborn with prune belly syndrome. The bladder appears large and lobulated. A diverticulum extends towards the left inguinal canal

30.4.4 Ureteral and Vesical Hernias

Segments of the urinary tract are exceptionally involved in hernia. The bladder or the ureters may be included in inguinal hernia. The ureters may herniate through the sciatic orifices and get obstructed. US will demonstrate easily the relation between the hernia and the urinary tract. Whenever useful, VCUG (Fig. 30.6) or MR urography will offer a 3D evaluation of the relationship between the ureter and the adjacent structures [22, 23].

Conclusion

The boundaries of the abdomen should not be forgotten as etiology for abdominal symptoms either because when complications occur, the extra-abdominal organs may induce abdominal symptoms or because abdominal organs may be herniated outside of the abdominal cavity and develop complications.

References

1. Janssens LJ, Voorhoeve PG, van den Wildenberg FJ, et al. Acute abdominal pain in children caused by pneumonia. Ned Tijdschr Geneeskd. 2016;160:D533.
2. Galvan-Montano A, Flores-Nava G, Suarez-Roa ML, Salazar-Herrera MC, et al. Subhepatic appendicitis with subdiaphragmatic abscess in a pediatric patient

without malrotation: case report. Cir Cir. 2010; 78:79–81.
3. Wang E, Ma L, Edmonds EW, Zhao Q, et al. Psoas abscess with associated septic arthritis of the hip in infants. J Pediatr Surg. 2010;45:2440–3.
4. Horiuchi A, Kameoka K, Kuwabara J, et al. Neonatal iliopsoas abscess. Pediatric Int. 2012;54:712.
5. Charalampopoulos A, Macheras A, Charalabopoulos A, et al. Iliopsoas abscesses: diagnosis, aetiology and therapeutic approach in 5 patients with a literature review. Scand J Gastroenterol. 2009;44:594–5.
6. Martin I, Serra I, Manosa M, et al. Psoas abscess as a complication of Crohn's disease: report of 3 cases and literature review. Gastroenterol Hepatol. 2009;32:557–61.
7. Schwischuk LE. Vomiting, diarrhea and – oh! oh! what is that? Pediatr Emerg Care. 2004;20:54–6.
8. El Bouyousfi M, Leveque C, Miladi L, Irtan S, Hamza J, Oualha M. Acute pancreatitis following scoliosis surgery: description and clinical course in 14 adolescents. Eur Spine J. 2016;25(10):3316–23.
9. Chavhan GB, Babyn P, Cohen RA, et al. Multimodality imaging of the pediatric diaphragm: anatomy and pathologic conditions. Radiographics. 2010;30:1797–817.
10. Yousef Y, Lemoine C, St-Vil D, et al. Congenital paraesophageal hernia: the Montreal experience. J Pediatr Surg. 2015;50:1462–6.
11. Rai B, Ahmed R, Amer N, et al. Paraesophageal hiatus hernia in an 8 month-old infant with organoaxial volvulus of the stomach. BMJ Case Rep. 2014;2014:bcr2014204385. doi:10.1136/bcr-2014-204385.
12. Al-Salem AH. Congenital hernia of Morgagni in infants and children. J Pediatr Surg. 2007;42:1539–43.
13. Al-Salem AH, Zamakhshary M, Al Mohaidly M, et al. Congenital Morgagni's hernia: a national multicenter study. J Pediatr Surg. 2014;49:503–7.
14. Alper B, Vargun R, Kologlu MB, Fitoz S, Suskan E, Dindar H. Late presentation of a traumatic rupture of the diaphragm with gastric volvulus in a child: report of a case. Surg Today. 2007;37(10):874–7.
15. Taghavi K, Geneta VP, Mirjalili SA. The pediatric inguinal canal: systematic review of the embryology and surface anatomy. Clin Anat. 2016;29:204–10.
16. Sameshima YT, Yamanari NG, Silva MA, et al. The challenging US inguinal canal evaluation in neonates and children an update of differential diagnoses. Pediatr Radiol. 2016;47:461–72.
17. Hyun PM, Jung AY, Lee Y, et al. CT and US findings of ovarian torsion within an incarcerated hernia. Emerg Radiol. 2015;22:1–9.
18. Bhosale PR, Patnana M, Viswanathan C, et al. The inguinal canal: anatomy and imaging features of common and uncommon masses. Radiographics. 2008;28:819–35.
19. Abduhai SA, Glenn IC, Ponsky TA, et al. Incarcerated hernia in children. Surg Clin N Am. 2017;97:129–45.
20. O'Donnell KA, Glick PL, Caty MG. Pediatric umbilical problems. Pediatr Clin N Am. 1998;45:791–9.
21. Spinelli C, Strambi S, Pucci V, et al. Spigelian hernia in a 14 year-old girl. Eur J Pediatr Surg Rep. 2014;2:58–62.
22. Handu AT, Garge S, Peters NJ, et al. Undiagnosed uretero-inguinal hernia with solitary kidney in a child with ureteric injury durig herniotomy. J Pediatr Surg. 2012;47:799–802.
23. Arat A, Haliloglu M. Ureteral-sciatic hernia in a child demonstrated by voiding cystography. J Urol. 1998;160:157–8.